

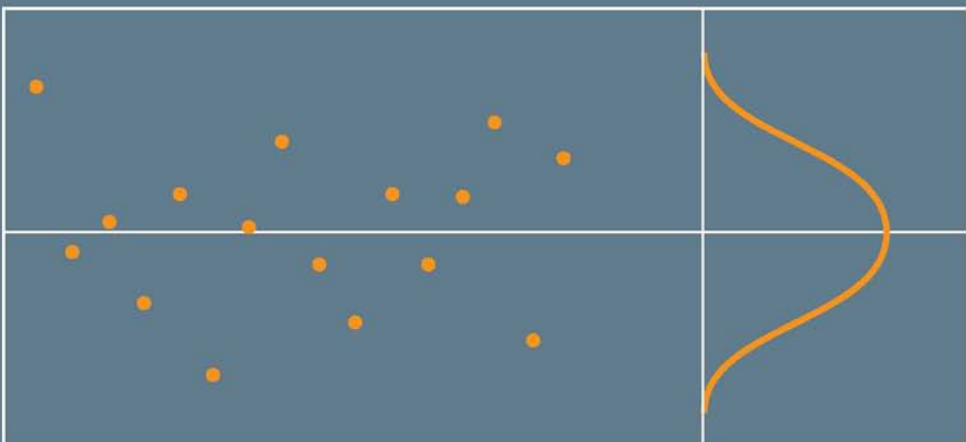
RICHARD S. FIGLIOLA

DONALD E. BEASLEY

Theory and Design for

MECHANICAL MEASUREMENTS

FIFTH EDITION



Theory and Design for Mechanical Measurements

Fifth Edition

Richard S. Figliola

Clemson University

Donald E. Beasley

Clemson University



John Wiley & Sons, Inc.

ACQUISITIONS EDITOR	Linda Ratts
PRODUCTION EDITOR	Anna Melhorn
PRODUCTION SERVICES MANAGER	Dorothy Sinclair
SENIOR MEDIA EDITOR	Tom Kulesa
SENIOR MARKETING MANAGER	Christopher Ruel
SENIOR DESIGNER	Wendy Lai

This book was set in 10/12 Times Roman by Thomson Digital and printed and bound by RR Donnelley,
The cover was printed by RR Donnelley.

This book is printed on acid free paper. ☺

Founded in 1807, John Wiley & Sons, Inc. has been a valued source of knowledge and understanding for more than 200 years, helping people around the world meet their needs and fulfill their aspirations. Our company is built on a foundation of principles that include responsibility to the communities we serve and where we live and work. In 2008, we launched a Corporate Citizenship Initiative, a global effort to address the environmental, social, economic, and ethical challenges we face in our business. Among the issues we are addressing are carbon impact, paper specifications and procurement, ethical conduct within our business and among our vendors, and community and charitable support. For more information, please visit our website: www.wiley.com/go/citizenship.

Copyright © 2011 John Wiley & Sons, Inc. All rights reserved.

No part of this publication may be reproduced, stored in a retrieval system or transmitted in any form or by any means, electronic, mechanical, photocopying, recording, scanning, or otherwise, except as permitted under Sections 107 or 108 of the 1976 United States Copyright Act, without either the prior written permission of the Publisher, or authorization through payment of the appropriate per-copy fee to the Copyright Clearance Center, Inc., 222 Rosewood Drive, Danvers, MA 01923, (978)750-8400, fax (978)750-4470 or on the web at www.copyright.com. Requests to the Publisher for permission should be addressed to the Permissions Department, John Wiley & Sons, Inc., 111 River Street, Hoboken, NJ 07030-5774, (201)748-6011, fax (201)748-6008, or online at <http://www.wiley.com/go/permissions>.

Evaluation copies are provided to qualified academics and professionals for review purposes only, for use in their courses during the next academic year. These copies are licensed and may not be sold or transferred to a third party. Upon completion of the review period, please return the evaluation copy to Wiley. Return instructions and a free of charge return shipping label are available at www.wiley.com/go/returnlabel. Outside of the United States, please contact your local representative.

Printed in the United States of America
10 9 8 7 6 5 4 3 2 1

Preface

We are pleased to offer this 5th edition of *Theory and Design for Mechanical Measurements*. This text provides a well-founded background in the theory of engineering measurements. Integrated throughout are the necessary elements for the design of measurement systems and measurement test plans, with an emphasis on the role of statistics and uncertainty analyses in design. The measurements field is very broad, but through careful selection of the topical coverage we establish the physical principles and practical techniques for many engineering applications while keeping page count and text cost manageable. Our aim is not to offer a manual for instrument construction and assembly. Instead, we develop the conceptual design framework for selecting and specifying equipment and test procedures and for interpreting test results, which we feel are necessary and common bases for the practice of test engineering. The text is appropriate for undergraduate and graduate level study in engineering, but is also suitably advanced and oriented to serve as a reference source for professional practitioners. The pedagogical approach invites independent study or use in related fields requiring an understanding of instrumentation and measurements.

The organization of the text develops from our view that certain aspects of measurements can be generalized, such as test plan design, signal analysis and reconstruction, and measurement system response. Topics such as statistics and uncertainty analysis require a basic development of principles but are then best illustrated by integrating these topics throughout the text material. Other aspects are better treated in the context of the measurement of a specific physical quantity, such as strain or temperature.

PEDAGOGICAL TOOLS TO AID LEARNING

In this textbook:

- Each chapter begins by defining a set of **learning outcomes**.
- The text develops an **intuitive understanding** of measurement concepts with its focus on test system modeling, test plan design, and uncertainty analysis.
- Each chapter includes carefully constructed **example problems** that illustrate new material and problems that build on prior material.
- Each example makes use of a **KNOWN, FIND, SOLVE** approach as an organizational aid to a problem's solution. This methodology for problem solutions helps new users to link words and concepts with symbols and equations. Many problems contain **COMMENTS** that expand on the solution, provide a proper context for application of the principle, or offer design application insight.
- **End-of-Chapter practice problems** are included for each chapter to exercise new concepts.
 - Practice problems range from those focused on concept development, to building of advanced skills, to open-ended design applications.
 - With each chapter, we have added new practice problems but have substantially “refreshed” many problems from previous editions.
 - We provide a detailed Instructors Manual for instructors who have adopted the book. We have carefully reviewed the solutions in this edition to minimize typographical and arithmetical errors. The manual is available on-line at the Wiley Instructor's website.
 - Answers to selected problems will be posted on the Wiley website.
- Use of the software in problem solving allows in-depth exploration of key concepts that would be prohibitively time consuming otherwise. The text includes on-line access to **interactive software** of

focused examples based on software using National Instruments Labview® for exploring some of the text concepts, while retaining our previous efforts using Matlab®. The Labview programs are available as executables so they can be run directly without a Labview license. The software is available on both the Wiley Student and Instructor's websites.

NEW TO THIS 5TH EDITION

With this 5th edition, we have new or expanded material on a number of topics. As highlights:

- We introduce Monte Carlo simulation methods in Chapter 4 and tie their use with uncertainty estimations in Chapter 5.
- Treatment of uncertainty analysis in Chapter 5 has been updated to include changes in test standards methodology relative to ASME PTC 19.1 Test Uncertainty and the International Standards Organization (ISO) Guide to Uncertainty in Measurements. These changes have been carried into the other chapters both in language and in example problems. Where we deviate from the methodology of the Standards, we do so for pedagogical reasons.
 - Discussion has been added on using rectangular (uniform) distributions in uncertainty estimation.
 - The treatment of non-symmetric uncertainty intervals and methods for treating correlated errors in Chapter 5 has been expanded and revisited in other chapters.
 - We have updated our symbol usage for closer consistency with the standards.
- We have added a section presenting image acquisition and processing using digital techniques in Chapter 7.
- We have changed our presentation of pressure transmission line effects to make better use of the lumped parameter methods of Chapter 3 that engineering students are familiar with, including discussion of the ideal elements of inertance, resistance, and compliance.
- We have revised our treatment of Butterworth filters, including added coverage, in Chapter 6.
- We have added an introduction to the analysis of strain gauge data to compute principal stresses in Chapter 11.

SUGGESTED COURSE COVERAGE

To aid in course preparation, Chapters 1 through 5 provide an introduction to measurement theory with statistics and uncertainty analysis, Chapters 6 and 7 provide a broad treatment of analog and digital sampling methods, and Chapters 8 through 12 are instrumentation focused.

Many users report to us that they use different course structures, so many that it makes a preferred order of topical presentation difficult to anticipate. To accommodate this, we have written the text in a manner that allows any instructor to customize the order of material presentation. While the material of Chapters 4 and 5 are integrated throughout the text and should be taught in sequence, the other chapters tend to stand on their own. The text is flexible and can be used in a variety of course structures at both the undergraduate and graduate levels.

For a complete measurements course, we recommend the study of Chapters 1 through 7 with use of the remaining chapters as appropriate. For a lab-course sequence, we recommend using chapters as they best illustrate the course exercises while building complete coverage over the several lab courses normally within a curriculum. The manner of the text allows it to be a resource for a lab-only course with minimal lecture. Over the years, we have used it in several forums, as well as professional development courses, and simply rearrange material and emphasis to suit the audience and objective.

We express our sincerest appreciation to the students, teachers, and engineers who have used our earlier editions. We are indebted to the many who have written us with their constructive comments and encouragement.

*Richard S. Figliola
Donald E. Beasley
Clemson, South Carolina*

Contents

1 Basic Concepts of Measurement Methods 1

1.1	Introduction	1
1.2	General Measurement System	2
1.3	Experimental Test Plan	6
1.4	Calibration	15
1.5	Standards	23
1.6	Presenting Data	30
1.7	Summary	31
References		31
Nomenclature		32
Problems		32

2 Static and Dynamic Characteristics of Signals 41

2.1	Introduction	41
2.2	Input/Output Signal Concepts	41
2.3	Signal Analysis	46
2.4	Signal Amplitude And Frequency	49
2.5	Fourier Transform and The Frequency Spectrum	63
2.6	Summary	71
References		71
Suggested Reading		71
Nomenclature		72
Problems		72

3 Measurement System Behavior 79

3.1	Introduction	79
3.2	General Model for a Measurement System	79
3.3	Special Cases of the General System Model	83
3.4	Transfer Functions	104
3.5	Phase Linearity	106
3.6	Multiple-Function Inputs	107
3.7	Coupled Systems	109
3.8	Summary	111
References		111
Nomenclature		111
Problems		112

4 Probability and Statistics 118

4.1	Introduction	118
4.2	Statistical Measurement Theory	119
4.3	Describing the Behavior of a Population	125
4.4	Statistics of Finite-Sized Data Sets	129
4.5	Chi-Squared Distribution	135
4.6	Regression Analysis	139
4.7	Data Outlier Detection	147
4.8	Number of Measurements Required	148
4.9	Monte Carlo Simulations	150
4.10	Summary	152
	References	152
	Nomenclature	153
	Problems	153

5 Uncertainty Analysis 161

5.1	Introduction	161
5.2	Measurement Errors	162
5.3	Design-Stage Uncertainty Analysis	164
5.4	Identifying Error Sources	168
5.5	Systematic and Random Errors	170
5.6	Uncertainty Analysis: Error Propagation	172
5.7	Advanced-Stage Uncertainty Analysis	176
5.8	Multiple-Measurement Uncertainty Analysis	182
5.9	Correction for Correlated Errors	195
5.10	Nonsymmetrical Systematic Uncertainty Interval	197
5.11	Summary	198
	References	199
	Nomenclature	199
	Problems	200

6 Analog Electrical Devices and Measurements 209

6.1	Introduction	209
6.2	Analog Devices: Current Measurements	210
6.3	Analog Devices: Voltage Measurements	214
6.4	Analog Devices: Resistance Measurements	219
6.5	Loading Errors and Impedance Matching	226
6.6	Analog Signal Conditioning: Amplifiers	230
6.7	Analog Signal Conditioning: Special-Purpose Circuits	234
6.8	Analog Signal Conditioning: Filters	239
6.9	Grounds, Shielding, and Connecting Wires	250
6.10	Summary	252
	References	253
	Nomenclature	253
	Problems	254

7 Sampling, Digital Devices, and Data Acquisition 260

7.1	Introduction	260
7.2	Sampling Concepts	261
7.3	Digital Devices: Bits and Words	269
7.4	Transmitting Digital Numbers: High and Low Signals	271
7.5	Voltage Measurements	271
7.6	Data-Acquisition Systems	283
7.7	Data-Acquisition System Components	284
7.8	Analog Input-Output Communication	288
7.9	Digital Input-Output Communication	293
7.10	Digital Image Acquisition and Processing	299
7.11	Summary	303
	References	303
	Suggested Reading	304
	Nomenclature	304
	Problems	305

8 Temperature Measurements 309

8.1	Introduction	309
8.2	Temperature Standards and Definition	310
8.3	Thermometry Based on Thermal Expansion	313
8.4	Electrical Resistance Thermometry	315
8.5	Thermoelectric Temperature Measurement	330
8.6	Radiative Temperature Measurements	351
8.7	Physical Errors in Temperature Measurement	356
8.8	Summary	365
	References	365
	Nomenclature	366
	Problems	367

9 Pressure and Velocity Measurements 375

9.1	Introduction	375
9.2	Pressure Concepts	375
9.3	Pressure Reference Instruments	378
9.4	Pressure Transducers	386
9.5	Pressure Transducer Calibration	392
9.6	Pressure Measurements in Moving Fluids	396
9.7	Modeling Pressure and Fluid Systems	400
9.8	Design and Installation: Transmission Effects	401
9.9	Fluid Velocity Measuring Systems	405
9.10	Summary	415
	References	416
	Nomenclature	417
	Problems	417

10 Flow Measurements 423

10.1	Introduction	423
10.2	Historical Background	423
10.3	Flow Rate Concepts	424
10.4	Volume Flow Rate Through Velocity Determination	425
10.5	Pressure Differential Meters	427
10.6	Insertion Volume Flow Meters	446
10.7	Mass Flow Meters	454
10.8	Flow Meter Calibration and Standards	459
10.9	Estimating Standard Flow Rate	460
10.10	Summary	461
	References	461
	Nomenclature	462
	Problems	462

11 Strain Measurement 466

11.1	Introduction	466
11.2	Stress and Strain	466
11.3	Resistance Strain Gauges	469
11.4	Strain Gauge Electrical Circuits	476
11.5	Practical Considerations for Strain Measurement	479
11.6	Apparent Strain and Temperature Compensation	482
11.7	Optical Strain Measuring Techniques	492
11.8	Summary	497
	References	498
	Nomenclature	498
	Problems	499

12 Mechatronics: Sensors, Actuators, and Controls 504

12.1	Introduction	504
12.2	Sensors	504
12.3	Actuators	534
12.4	Controls	540
12.5	Summary	557
	Nomenclature	558
	References	558
	Problems	559

Appendix A A Guide for Technical Writing 563

A Guide For Technical Writing	563
References	568

Appendix B Property Data and Conversion Factors 569

Appendix C Laplace Transform Basics 576

C.1 Final Value Theorem	577
C.2 Laplace Transform Pairs	577
References	577

Glossary 578

Index 585

Chapter 1

Basic Concepts of Measurement Methods

1.1 INTRODUCTION

We make measurements every day. Consider the common measurements illustrated in Figure 1.1. We routinely read the temperature of an outdoor thermometer to choose appropriate clothing for the day. We expect to have exactly 10 gallons or liters of fuel added to our tank when that volume is indicated on a fuel pump. And we expect measuring cups to yield correct quantities of ingredients in cooking. We put little thought into the selection of instruments for these routine measurements. After all, the direct use of the data is clear to us, the type of instruments and techniques are familiar to us, and the outcome of these measurements is not important enough to merit much attention to features like improved accuracy or alternative methods. But when the stakes become greater, the selection of measurement equipment and techniques and the interpretation of the measured data can demand considerable attention. Just contemplate how you might verify that a new engine is built as designed and meets the power and emissions performance specifications required.

But first things first. The objective in any measurement is to answer a question. So we take measurements to establish the value or the tendency of some variable, the results of which are specifically targeted to answer our question. The information acquired is based on the output of the measurement device or system. There are important issues to be addressed to ensure that the output of the measurement device is a reliable indication of the true value of the measured variable. In addition, we must address the following important questions:

1. How can a measurement or test plan be devised so that the measurement provides the unambiguous information we seek?
2. How can a measurement system be used so that the engineer can easily interpret the measured data and be confident in their meaning?

There are procedures that address these measurement questions.

At the onset, we want to stress that the subject of this text is real-life oriented. Specifying a measurement system and measurement procedures represents an open-ended design problem whose outcome will not have one particular solution. That means there may be several approaches to solving a measurement problem, and some will be better than others. This text emphasizes accepted procedures for analyzing a measurement problem to assist in the selection of equipment,

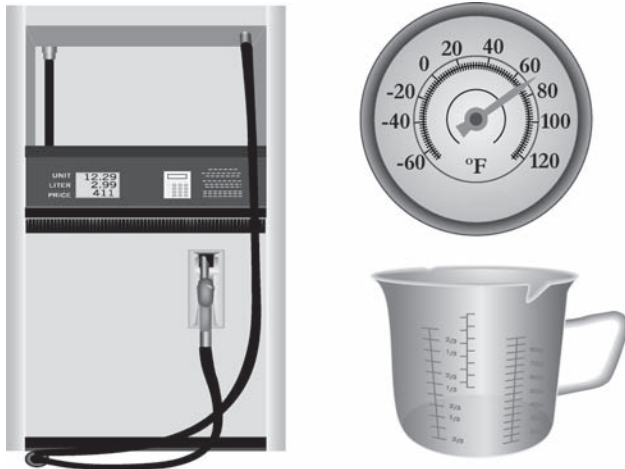


Figure 1.1 Common devices that involve measurements.

methodology, and data analysis to meet the design objectives. Perhaps more than in any other technical field, the approach taken in measurement design and the outcome achieved will often depend on the attention and experience of the designer.

Upon completion of this chapter, the reader will be able to

- identify the major components of a general measurement system, and state the function of each,
- develop an experimental test plan,
- distinguish between random and systematic errors,
- describe and define the various error types,
- define a standard and distinguish among primary, secondary, and transfer standards, and
- clearly delineate defined and derived dimensions in various unit systems.

1.2 GENERAL MEASUREMENT SYSTEM

A *measurement*¹ is an act of assigning a specific value to a physical variable. That physical variable is the *measured variable*. A measurement system is a tool used for quantifying the measured variable. As such, a measurement system is used to extend the abilities of the human senses that, while they can detect and recognize different degrees of roughness, length, sound, color, and smell, are limited and relative; they are not very adept at assigning specific values to sensed variables.

A system is composed of components that work together to accomplish a specific objective. We begin by describing the components that make up a measurement system, using specific examples. Then we will generalize to a model of the generic measurement system.

¹There are many new engineering measurement terms introduced. A glossary of the italicized terms is located in the back of the text for your reference.

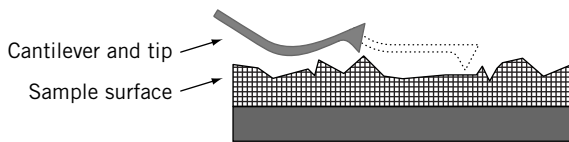


Figure 1.2 Sensor stage of an atomic-force microscope.

Sensor and Transducer

An increasingly important area of scientific inquiry is the characteristics of matter at the nanoscale. Suppose we want to measure the profile of a surface at a nanometer scale. We discover that a small (very small) cantilever beam placed near the surface is deflected by atomic forces. Let's assume for now that they are repulsive forces. If this cantilever is translated over the surface, the cantilever will deflect, indicating the height of the surface. This concept is illustrated in Figure 1.2; the device is called an atomic force microscope. The cantilever beam is a *sensor*, a physical element that employs some natural phenomenon, in this case deflection under the action of a force, to sense the variable being measured, in this case the height of the surface.

So, we have a sensor to measure at the nanometer scale. But we have no means of getting an output from the sensor that we can record. Suppose that the upper surface of the cantilever is reflective, and we shine a laser onto the upper surface, as shown in Figure 1.3. The movement of the cantilever will deflect the laser. Employing a number of light sensors, also shown in Figure 1.3, the deflection of the laser can be sensed and that deflection corresponds to the height of the surface. Together the laser and the light sensors (photodiodes) form the transducer component of the measurement system. A transducer converts the sensed information into a detectable signal. The signal might be mechanical, electrical, optical, or may take any other form that can be meaningfully recorded.

We should note that sensor selection, placement, and installation are particularly important to ensure that the sensor output accurately reflects the measurement objective. The familiar phrase

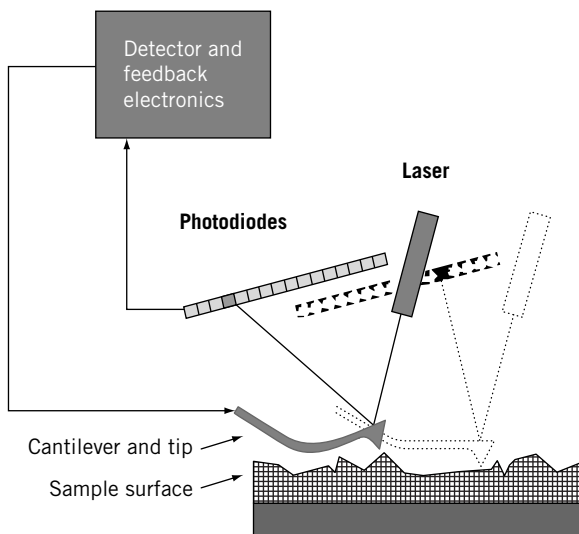


Figure 1.3 Atomic-force microscope with sensor and transducer stages.

associated with hot days, “100°F in the shade” implies a specific sensor placement. Accordingly, the interpretation of all information passed through and indicated by the system depends on what is actually sensed by the sensor. For example, the interpretation of the output of a medical thermometer depends on where its sensor is placed.

Output Stage

The goal of a measurement system is to convert the sensed information into a form that can be easily quantified. Consider a familiar example, the liquid-in-glass bulb thermometer. The liquid contained within the bulb on the common bulb thermometer of Figure 1.4 exchanges energy with its surroundings until the two are in thermal equilibrium. At that point they are at the same temperature. This energy exchange is the input signal to this measurement system. The phenomenon of thermal expansion of the liquid results in its movement up and down the stem, forming an output signal from which we determine temperature. The liquid in the bulb acts as the sensor. By forcing the expanding liquid into a narrow capillary, this measurement system transforms thermal information into a mechanical displacement. Hence, the bulb’s internal capillary design acts as a transducer.

The *output stage* indicates or records the value measured. This might be a simple readout display, a marked scale, or even a recording device such as a computer disk drive. The readout scale of the bulb thermometer in Figure 1.4 serves as the output stage of that measurement system.

It is worth noting that the term “transducer” is also often used in reference to a packaged device, which may contain a sensor, transducer, and even some signal conditioning elements. While such terminology is not true to our presentation, the context in which the term is used prevents ambiguity.

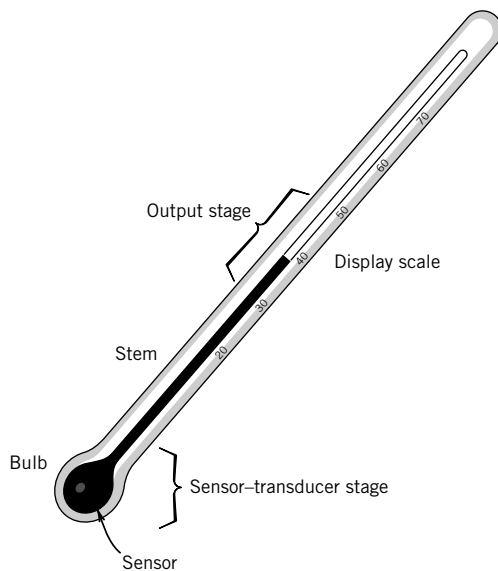


Figure 1.4 Components of bulb thermometer equivalent to sensor, transducer, and output stages.

General Template for a Measurement System

A general template for a measurement system is illustrated in Figure 1.5. Basically such a system consists of part or all of four general stages: (1) sensor-transducer stage, (2) signal-conditioning stage, (3) output stage, and (4) feedback-control stage. These stages form the bridge between the input to the measurement system and the system output, a quantity that is used to infer the value of the physical variable measured. We discuss later how the relationship between the input information, as acquired by the sensor, and the system output is established by a calibration. We have already discussed the sensor-transducer stage, so let's move on to the signal-conditioning stage.

The *signal-conditioning stage* takes the transducer signal and modifies it to a desired magnitude. This optional intermediate stage might be used to perform tasks such as increasing the magnitude of the signal by amplification, removing portions of the signal through some filtering technique, or providing mechanical or optical linkage between the transducer and the output stage. For example, the translational displacement of a mechanic's caliper (sensor) is often converted into a rotational displacement of a pointer. This stage can consist of one or more devices, which are often connected in series. For example, the diameter of the thermometer capillary relative to the bulb volume (see Fig. 1.4) determines how far up the stem the liquid moves with increasing temperature. It "conditions" the signal by amplifying the liquid displacement.

In those measurement systems involved in process control, a fourth stage, the *feedback-control stage*, contains a controller that interprets the measured signal and makes a decision regarding the control of the process. This decision results in a signal that changes the process parameter that affects the magnitude of the sensed variable. In simple controllers, this decision is based on the magnitude of the signal of the sensed variable, usually whether it exceeds some high or low set point, a value set by the system operator. For example, a simple measurement system with control stage is a household furnace thermostat. The operator fixes the set point for temperature on the thermostat display, and the furnace is activated as the local temperature at the thermostat, as determined by the

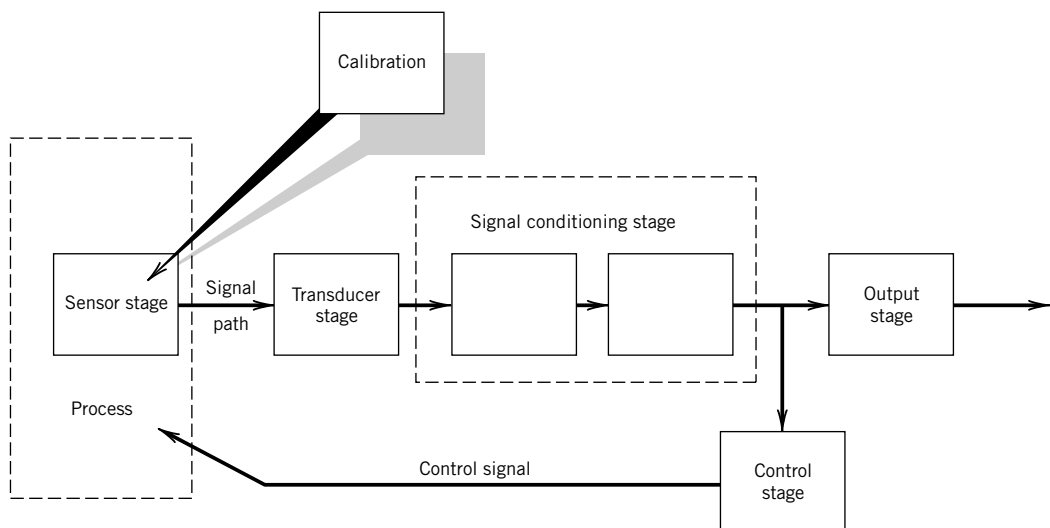


Figure 1.5 Components of a general measurement system.

sensor within the device, rises or falls above or below the set point. In a more sophisticated controller, a signal from a measurement system can be used as an input to an “expert system” controller that, through an artificial intelligence algorithm, determines the optimum set conditions for the process. *Mechatronics* deals with the interfacing of mechanical and electrical components with microprocessors, controllers, and measurements. We will discuss some features of mechatronic systems in detail in Chapter 12.

1.3 EXPERIMENTAL TEST PLAN

An experimental test serves to answer a question, so the test should be designed and executed to answer that question and that question alone. This is not so easy to do. Let’s consider an example.

Suppose you want to design a test to answer the question, “What is the fuel use of my new car?” What might be your test plan? In a test plan, you identify the variables that you will measure, but you also need to look closely at other variables that will influence the result. Two important variables to measure would be distance and fuel volume consumption. Obviously, the accuracy of the odometer will affect the distance measurement, and the way you fill your tank will affect your estimate of the fuel volume. But what other variables might influence your results? If your intended question is to estimate the average fuel usage to expect over the course of ownership, then the driving route you choose would play a big role in the results and is a variable. Only highway driving will impose a different trend on the results than only city driving, so if you do both you might want to randomize your route by using various types of driving conditions. If more than one driver uses the car, then the driver becomes a variable because each individual drives somewhat differently. Certainly weather and road conditions influence the results, and you might want to consider this in your plan. So we see that the utility of the measured data is very much impacted by variables beyond the primary ones measured. In developing your test, the question you propose to answer will be a factor in developing your test plan, and you should be careful in defining that question so as to meet your objective.

Imagine how your test conduct would need to be different if you were interested instead in providing values used to advertise the expected average fuel use of a model of car. Also, you need to consider just how good an answer you need. Is 2 liters per 100 kilometers or 1 mile per gallon close enough? If not, then the test might require much tighter controls. Lastly, as a concomitant check, you might compare your answer with information provided by the manufacturer or independent agency to make sure your answer seems reasonable. Interestingly, this one example contains all the same elements of any sophisticated test. If you can conceptualize the factors influencing this test and how you will plan around them, then you are on track to handle almost any test. Before we move into the details of measurements, we focus here on some important concepts germane to all measurements and tests.

Experimental design involves itself with developing a measurement test plan. A test plan draws from the following three steps:²

- 1. Parameter design plan.** Determine the test objective and identify the process variables and parameters and a means for their control. Ask: “What question am I trying to answer? What needs to be measured?” “What variables and parameters will affect my results?”

²These three strategies are similar to the bases for certain design methods used in engineering system design (1).

- 2. System and tolerance design plan.** Select a measurement technique, equipment, and test procedure based on some preconceived tolerance limits for error.³ Ask: “In what ways can I do the measurement and how good do the results need to be to answer my question?”
- 3. Data reduction design plan.** Plan how to analyze, present, and use the anticipated data. Ask: “How will I interpret the resulting data? How will I use the data to answer my question? How good is my answer? Does my answer make sense?”

Going through all three steps in the test plan before any measurements are taken is a useful habit for a successful engineer. Often, step 3 will force you to reconsider steps 1 and 2! In this section, we focus on the concepts related to step 1 but will discuss and stress all three throughout the text.

Variables

Once we define the question that we want the test to answer, the next step is to identify the relevant process parameters and variables. Variables are entities that influence the test. In addition to the targeted measured variable, there may be other variables pertinent to the measured process that will affect the outcome. All known process variables should be evaluated for any possible cause-and-effect relationships. If a change in one variable will not affect the value of some other variable, the two are considered independent of each other. A variable that can be changed independently of other variables is known as an *independent variable*. A variable that is affected by changes in one or more other variables is known as a *dependent variable*. Normally, the variable that we measure depends on the value of the variables that control the process. A variable may be continuous, in that its value is able to change in a continuous manner, such as stress under a changing load or temperature in a room, or it may be discrete in that it takes on discrete values or can be quantified in a discrete way, such as the value of the role of dice or a test run by a single operator.

The *control* of variables is important. A variable is controlled if it can be held at a constant value or at some prescribed condition during a measurement. Complete control of a variable would imply that it can be held to an exact prescribed value. Such complete control of a variable is not usually possible. We use the adjective “controlled” to refer to a variable that can be held as prescribed, at least in a nominal sense. The cause-and-effect relationship between the independent variables and the dependent variable is found by controlling the values of the independent variables while measuring the dependent variable.

Variables that are not or cannot be controlled during measurement but that affect the value of the variable measured are called *extraneous variables*. Their influence can confuse the clear relation between cause and effect in a measurement. Would not the driving style affect the fuel consumption of a car? Then unless controlled, this influence will affect the result. Extraneous variables can introduce differences in repeated measurements of the same measured variable taken under seemingly identical operating conditions. They can also impose a false trend onto the behavior of that variable. The effects due to extraneous variables can take the form of signals superimposed onto the measured signal with such forms as noise and drift.

³ The tolerance design plan strategy used in this text draws on uncertainty analysis, a form of sensitivity analysis. Sensitivity methods are common in design optimization.

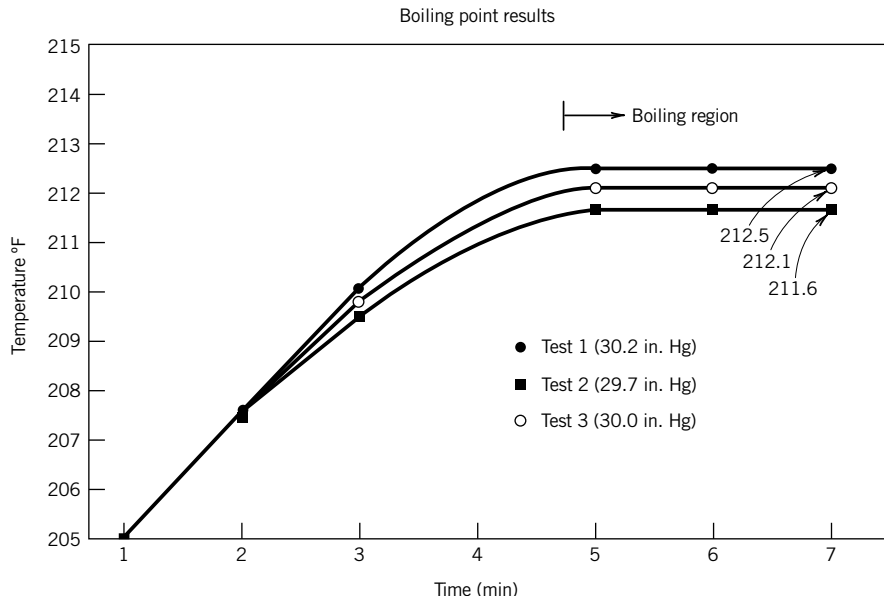


Figure 1.6 Results of a boiling point test for water.

Consider a thermodynamics experiment to establish the boiling point of water. The apparatus for measuring the boiling point might yield the results shown in Figure 1.6 for three test runs conducted on separate days. Notice the different outcome for each test.

Why should the data from three seemingly identical tests show such different results?

Suppose we determine that the measurement system accuracy accounts for only 0.1°F of the test data scatter. So another plausible contributing factor is the effect of an extraneous variable. Indeed, a close examination of the test data shows a measured variation in the barometric pressure, which would affect the boiling temperature. The pressure variation is consistent with the trend seen in the boiling point data. Because the local barometric pressure was not controlled (i.e., it was not held fixed between the tests), the pressure acted as an extraneous variable adding to the differences in outcomes between the test runs. *Control important variables or be prepared to solve a puzzle!*

Parameters

In this text, we define a *parameter* as a functional grouping of variables. For example, a moment of inertia or a Reynolds number has its value determined from the values of a grouping of variables. A parameter that has an effect on the behavior of the measured variable is called a *control parameter*. Available methods for establishing control parameters based on known process variables include similarity and dimensional analysis techniques and physical laws (2–4). A parameter is controlled if its value can be maintained during a set of measurements.

As an example, the flow rate, Q , developed by a fan depends on rotational speed, n , and the diameter, d , of the fan. A control parameter for this group of three variables, found by similarity methods, is the fan flow coefficient, $C_1 = Q/nd^3$. For a given fan, d is fixed (and therefore controlled), and if speed is somehow controlled, the fan flow rate associated with that speed can be measured and the flow coefficient can be determined.

Noise and Interference

Just how extraneous variables affect measured data can be delineated into noise and interference. *Noise* is a random variation of the value of the measured signal as a consequence of the variation of the extraneous variables. Noise increases data scatter. *Interference* imposes undesirable deterministic trends on the measured value. Any uncontrolled influence that causes the signal or test outcome to behave in a manner different from its true behavior is interference.

A common interference in electrical instruments comes from an AC power source and is seen as a sinusoidal wave superimposed onto the measured signal path. Hum and acoustic feedback in public address and audio systems are ready examples of interference effects that are superimposed onto a desirable signal. Sometimes the interference is obvious. But if the period of the interference is longer than the period over which the measurement is made, the false trend may go unnoticed. So we want either to control the source of interference or to break up its trend.

Consider the effects of noise and interference on the signal, $y(t) = 2 + \sin 2\pi t$. As shown in Figure 1.7, noise adds to the scatter of the signal. Through statistical techniques and other means, we can sift through the noise to get at the desirable signal information. But interference imposes a trend onto the signal. The measurement plan should be devised to break up such trends so that they appear as random variations in the data set. Although this will increase the scatter in the measured values of a data set, noise can be handled by statistics. It is far more important to eliminate false trends in the data set.

With this discussion in mind, recall the boiling point example earlier. Barometric pressure caused interference in each individual test. The barometric pressure did not change over the conduct of any one test. But we could discern the effect only because we showed the results of several tests taken over a period for which the value of this uncontrolled variable did change. This is a form of randomization in that as barometric pressure changed between tests, its effect was entered into the data set. Randomization methods are available that can be easily incorporated into the measurement

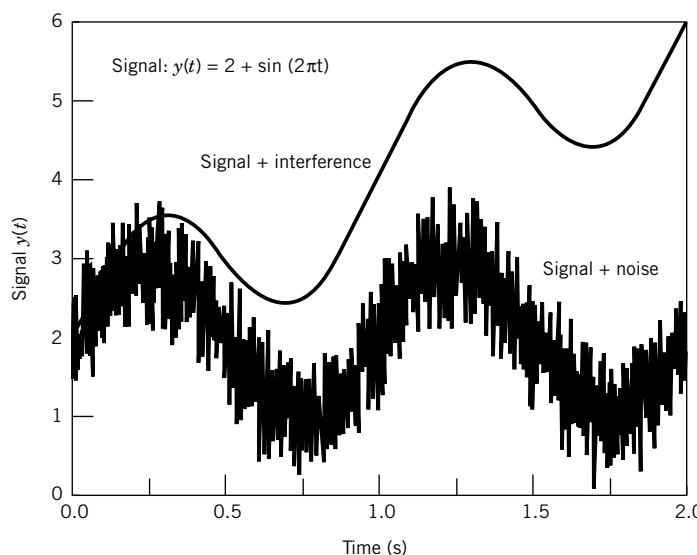


Figure 1.7 Effects of noise and interference superimposed on the signal $y(t) = 2 + \sin 2\pi t$.

plan and will minimize or eliminate interference trends. Several methods are discussed in the paragraphs that follow.

Random Tests

Recall our car fuel-usage example in which the question is: “What fuel usage should I expect from this car?” Let y be the fuel use, which depends on x_a , fuel volume consumption, and x_b , distance traveled. We determine y by varying these two variables (that is, we drive the car). But the test result can be affected by discrete extraneous variables such as the route, driver, weather, and road conditions. For example, driving only on interstate highways would impose a false (untypical) trend on our intended average fuel estimate, so we could drive on different types of roads to break up this trend. This approach introduces a random test strategy.

In general, consider the situation in which the dependent variable, y , is a function of several independent variables, x_a, x_b, \dots . However, the measurement of y can also be influenced by several extraneous variables, z_j , where $j = 1, 2, \dots$, such that $y = f(x_a, x_b, \dots; z_j)$. To find the dependence of y on the independent variables, they are varied in a controlled manner. Although the influence of the z_j variables on these tests cannot be eliminated, the possibility of their introducing a false trend on y can be minimized by a proper test strategy. Randomization is one such strategy.

Randomization

We define a *random test* by a measurement matrix that sets a random order to the change in the value of the independent variable applied. The effect of the random order on the results of the test is termed *randomization*. Trends normally introduced by the coupling of a relatively slow and uncontrolled variation in the extraneous variables with a sequential application in values of the independent variable applied will be broken up. This type of plan is effective for the local control of extraneous variables that change in a continuous manner. Consider Examples 1.1 and 1.2.

Discrete extraneous variables are treated a little differently. The use of different instruments, different test operators, and different test operating conditions are examples of discrete extraneous variables that can affect the outcome of a measurement. Randomizing a test matrix to minimize discrete influences can be done efficiently through the use of experimental design using random blocks. A block consists of a data set of the measured variable in which the controlled variable is varied but the extraneous variable is fixed. The extraneous variable is varied between blocks. This enables some amount of local control over the discrete extraneous variable. In the fuel-usage example, we might consider several blocks, each comprised of a different driver (extraneous variable) driving similar routes, and averaging the results. In the example of Figure 1.6, if we cannot control the barometric pressure in the test, then the imposed strategy of using several tests (blocks) under different values of barometric pressure breaks up the interference effect found in a single test. Many strategies for randomized blocks exist, as do advanced statistical methods for data analysis (5–8). In any event, a random test is useful to assess the influence of an uncontrolled variable. Consider Examples 1.3 and 1.4.

Example 1.1

In the pressure calibration system shown in Figure 1.8, a sensor–transducer is exposed to a known pressure, p . The transducer, powered by an external supply, converts the sensed signal into a voltage that is measured by a voltmeter. The measurement approach is to control the applied

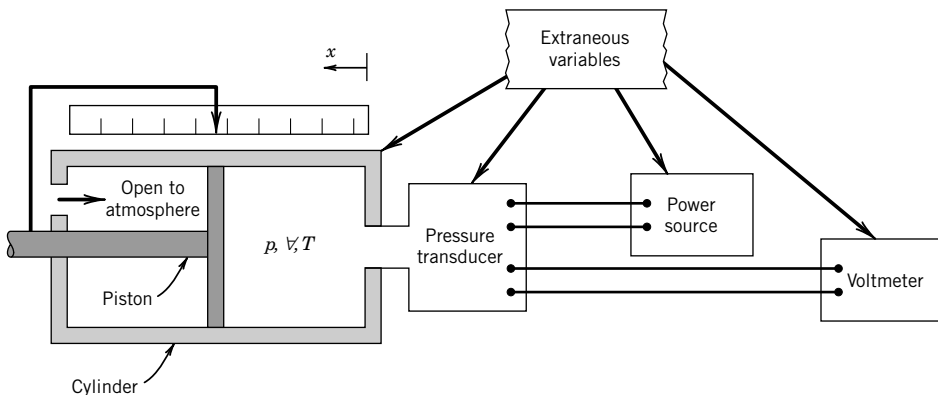


Figure 1.8 Pressure calibration system.

pressure by the measured displacement of a piston that is used to compress a gas contained within the piston-cylinder chamber. The gas chosen closely obeys the ideal gas law. Hence, piston displacement, x , which sets the chamber volume, $\forall = (x \times \text{area})$, is easily related to chamber pressure. Identify the independent and dependent variables in the calibration and possible extraneous variables.

KNOWN Pressure calibration system of Figure 1.8.

FIND Independent, dependent, and extraneous variables.

SOLUTION The control parameter for this problem can be formed from the ideal gas law: $p\forall/T = \text{constant}$, where T is the gas temperature. An independent variable in the calibration is the piston displacement that sets the volume. This variable can be controlled by locking the piston into position. From the ideal gas law, gas pressure will also be dependent on temperature, and therefore temperature is also an independent variable. However, T and \forall are not in themselves independent according to the control parameter. Since volume is to be varied through variation of piston displacement, T and \forall can be controlled provided a mechanism is incorporated into the scheme to maintain a constant gas temperature within the chamber. This will also maintain chamber area constant, a relevant factor in controlling the volume. In that way, the applied variations in \forall will be the only effect on pressure, as desired. The dependent variable is the chamber gas pressure. The pressure sensor is exposed to the chamber gas pressure and, hence, this is the pressure it senses. Examples of likely extraneous variables would include noise effects due to the room temperature, z_1 , and line voltage variations, z_2 , which would affect the excitation voltage from the power supply and the performance of the voltmeter. Connecting wires between devices will act as an antenna and possibly will introduce interference, z_3 , superimposed onto the electrical signal, an effect that can be reduced by proper electrical shielding. This list is not exhaustive but illustrative. Hence,

$$p = f(\forall, T; z_1, z_2, z_3), \text{ where } \forall = f_1(x, T).$$

COMMENT Even though we might try to keep the gas temperature constant, even slight variations in the gas temperature would affect the volume and pressure and, hence, will act as an additional extraneous variable!

Example 1.2

Develop a test matrix that will minimize the interference effects of any extraneous variables in Example 1.1.

KNOWN $p = f(\forall, T; z_1, z_2, z_3)$, where $\forall = f_1(x; T)$. Control variable \forall is changed. Dependent variable p is measured.

FIND Randomize possible effects of extraneous variables.

SOLUTION Part of our test strategy is to vary volume, control gas temperature, and measure pressure. An important feature of all test plans is a strategy that minimizes the superposition of false trends onto the data set by the extraneous variables. Since z_1 , z_2 , and z_3 and any inability to hold the gas temperature constant are continuous extraneous variables, their influence on p can be randomized by a random test. This entails shuffling the order by which \forall is applied. Say that we pick six values of volume, $\forall_1, \forall_2, \forall_3, \forall_4, \forall_5$, and \forall_6 , where the subscripts correspond to an increasing sequential order of the respective values of volume. Any random order will do fine. One possibility, found by using the random function features of a hand-held calculator, is

$$\forall_2 \forall_5 \forall_1 \forall_4 \forall_6 \forall_3$$

If we perform our measurements in a random order, interference trends will be broken up.

Example 1.3

The manufacture of a particular composite material requires mixing a percentage by weight of binder with resin to produce a gel. The gel is used to impregnate a fiber to produce the composite material in a manual process called the lay-up. The strength, σ , of the finished material depends on the percent binder in the gel. However, the strength may also be lay-up operator dependent. Formulate a test matrix by which the strength to percent binder-gel ratio under production conditions can be established.

KNOWN $\sigma = f(\text{binder}; \text{operator})$

ASSUMPTION Strength is affected only by binder and operator.

FIND Test matrix to randomize effects of operator.

SOLUTION The dependent variable, σ , is to be tested against the independent variable, percent binder-gel ratio. The operator is an extraneous variable in actual production. As a simple test, we could test the relationship between three binder-gel ratios, A , B , and C , and measure strength. We could also choose three typical operators (z_1 , z_2 , and z_3) to produce N separate composite test samples for each of the three binder-gel ratios. This gives the three-block test pattern:

Block					
1	z_1 :	A	B	C	
2	z_2 :	A	B	C	
3	z_3 :	A	B	C	

In the analysis of the test, all of these data can be combined. The results of each block will include each operator's influence as a variation. We can assume that the order used within each block is unimportant. But if only the data from one operator are considered, the results may show a trend consistent with the lay-up technique of that operator. The test matrix above will randomize the influence of any one operator on the strength test results by introducing the influence of several operators.

Example 1.4

Suppose following lay-up, the composite material of Example 1.3 is allowed to cure at a controlled but elevated temperature. We wish to develop a relationship between the binder–gel ratio and the cure temperature and strength. Develop a suitable test matrix.

KNOWN $\sigma = f(\text{binder, temperature, operator})$

ASSUMPTION Strength is affected only by binder, temperature, and operator.

FIND Test matrix to randomize effect of operator.

SOLUTION We develop a simple matrix to test for the dependence of composite strength on the independent variables of binder–gel ratio and cure temperature. We could proceed as in Example 1.3 and set up three randomized blocks for ratio and three for temperature for a total of 18 separate tests. Suppose instead we choose three temperatures, T_1 , T_2 , and T_3 , along with three binder–gel ratios, A , B , and C , and three operators, z_1 , z_2 , and z_3 , and set up a 3×3 test matrix representing a single randomized block. If we organize the block such that no operator runs the same test combination more than once, we randomize the influence of any one operator on a particular binder–gel ratio, temperature test.

	z_1	z_2	z_3
A	T_1	T_2	T_3
B	T_2	T_3	T_1
C	T_3	T_1	T_2

COMMENT The suggested test matrix not only randomizes the extraneous variable, it has reduced the number of tests by one-half over the direct use of three blocks for ratio and for temperature. However, either approach is fine. The above matrix is referred to as a Latin square (5–8).

If we wanted to include our ability to control the independent variables in the test data variations, we could duplicate the Latin-square test several times to build up a significant database.

Replication and Repetition

In general, the estimated value of a measured variable improves with the number of measurements. For example, a bearing manufacturer would obtain a better estimate of the mean diameter and the variation in the diameters of a batch of bearings by measuring many bearings rather than just a few.

Repeated measurements made during any single test run or on a single batch are called *repetitions*. Repetition helps to quantify the variation in a measured variable as it occurs during any one test or batch while the operating conditions are held under nominal control. However, repetition will not permit an assessment of how precisely the operating conditions can be set.

If the bearing manufacturer was interested in how closely bearing mean diameter was controlled in day-in and day-out operations with a particular machine or test operator, duplicate tests run on different days would be needed. An independent duplication of a set of measurements using similar operating conditions is referred to as a *replication*. Replication allows for quantifying the variation in a measured variable as it occurs between different tests, each having the same nominal values of operating conditions.

Finally, if the bearing manufacturer were interested in how closely bearing mean diameter was controlled when using different machines or different machine operators, duplicate tests using these different configurations holds the answer. Here, replication provides a means to randomize the interference effects of the different bearing machines or operators.

Replication allows us to assess the control of setting the operating conditions, that is, the ability to reset the conditions to some desired value. Ultimately, replication provides the means to estimate control over the procedure used.

Example 1.5

Consider a room furnace thermostat. Set to some temperature, we can make repeated measurements (repetition) of room temperature and come to a conclusion about the average value and the variation in room temperature at that particular thermostat setting. Repetition allows us to estimate the variation in this measured variable. This repetition permits an assessment of how well we can maintain (control) the operating condition.

Now suppose we change the set temperature to some arbitrary value but sometime later return it to the original setting and duplicate the measurements. The two sets of test data are replications of each other. We might find that the average temperature in the second test differs from the first. The different averages suggest something about our ability to set and control the temperature in the room. Replication permits the assessment of how well we can duplicate a set of conditions.

Concomitant Methods

Is my test working? What value of result should I expect? To help answer these, a good strategy is to incorporate *concomitant methods* in a measurement plan. The goal is to obtain two or more estimates for the result, each based on a different method, which can be compared as a check for agreement. This may affect the experimental design in that additional variables may need to be measured. Or the different method could be an analysis that estimates an expected value of the measurement. For example, suppose we want to establish the volume of a cylindrical rod of known material. We could simply measure the diameter and length of the rod to compute this. Alternatively, we could measure the weight of the rod and compute volume based on the specific weight of the material. The second method complements the first and provides an important check on the adequacy of the first estimate.

1.4 CALIBRATION

A *calibration* applies a known input value to a measurement system for the purpose of observing the system output value. It establishes the relationship between the input and output values. The known value used for the calibration is called the *standard*.

Static Calibration

The most common type of calibration is known as a static calibration. In this procedure, a known value is input to the system under calibration and the system output is recorded. The term “static” implies that the values of the variables involved remain constant; that is, they do not vary with time or space. In static calibrations, only the magnitudes of the known input and the measured output are important.

By applying a range of known input values and by observing the system output values, a direct calibration curve can be developed for the measurement system. On such a curve the input, x , is plotted on the abscissa against the measured output, y , on the ordinate, such as indicated in Figure 1.9. In a calibration the input value is usually a controlled independent variable, while the measured output value is the dependent variable of the calibration.

The static calibration curve describes the static input–output relationship for a measurement system and forms the logic by which the indicated output can be interpreted during an actual measurement. For example, the calibration curve is the basis for fixing the output display scale on a measurement system, such as that of Figure 1.4. Alternatively, a calibration curve can be used as part of developing a functional relationship, an equation known as a correlation, between input and output. A correlation will have the form $y = f(x)$ and is determined by applying physical reasoning and curve fitting techniques to the calibration curve. The correlation can then be used in later measurements to ascertain the unknown input value based on the output value, the value indicated by the measurement system.

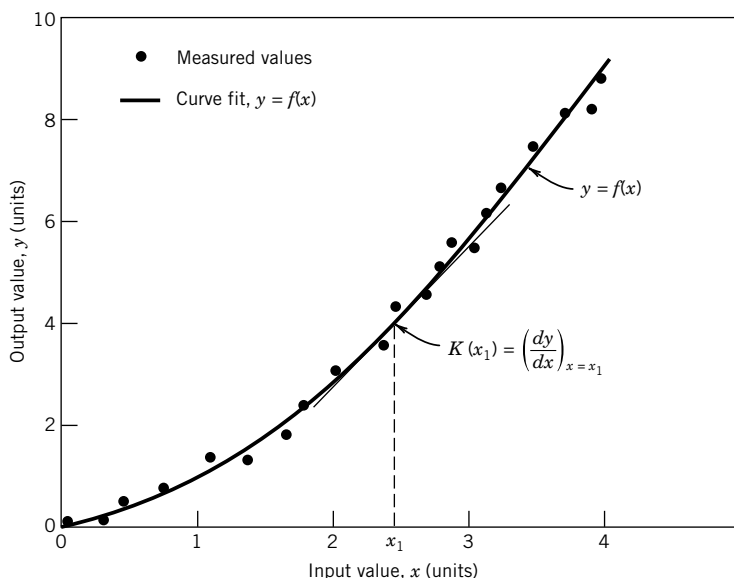


Figure 1.9 Representative static calibration curve.

Dynamic Calibration

When the variables of interest are time (or space) dependent and such varying information is sought, we need dynamic information. In a broad sense, dynamic variables are time (or space) dependent in both their magnitude and frequency content. A *dynamic calibration* determines the relationship between an input of known dynamic behavior and the measurement system output. Usually, such calibrations involve applying either a sinusoidal signal or a step change as the known input signal. The dynamic nature of signals and measurement systems is explored fully in Chapter 3.

Static Sensitivity

The slope of a static calibration curve provides the static sensitivity⁴ of the measurement system. As depicted graphically in the calibration curve of Figure 1.9, the static sensitivity, K , at any particular static input value, say x_1 , is evaluated by

$$K = K(x_1) = \left(\frac{dy}{dx} \right)_{x=x_1} \quad (1.1)$$

where K is a function of x . The static sensitivity is a measure relating the change in the indicated output associated with a given change in a static input.

Range

A calibration applies known inputs ranging from the minimum to the maximum values for which the measurement system is to be used. These limits define the operating *range* of the system. The input operating range is defined as extending from x_{\min} to x_{\max} . The input operating range may be expressed in terms of the difference of the limits as

$$r_i = x_{\max} - x_{\min} \quad (1.2)$$

This is equivalent to specifying the output operating range from y_{\min} to y_{\max} . The output span or full-scale operating range (FSO) is expressed as

$$r_o = y_{\max} - y_{\min} \quad (1.3)$$

It is important to avoid extrapolation beyond the range of known calibration during measurement since the behavior of the measurement system is uncharted in these regions. As such, the range of calibration should be carefully selected.

Resolution

The *resolution* represents the smallest increment in the measured value that can be discerned. In terms of a measurement system, it is quantified by the smallest scale increment or least count (least significant digit) of the output readout indicator.

⁴ Some texts refer to this as the *static gain*.

Accuracy and Error

The exact value of a variable is called the *true value*. The value of the variables as indicated by a measurement system is called the *measured value*. The *accuracy* of a measurement refers to the closeness of agreement between the measured value and the true value. But the true value is rarely known exactly, and various influences, called errors, have an effect on both of these values. So the concept of the accuracy of a measurement is a qualitative one.

An appropriate approach to stating this closeness of agreement is to identify the measurement errors and to quantify them by the value of their associated uncertainties, where an uncertainty is the estimated range of value of an error. We define an *error*, e , as the difference between the measured value and the true value, that is

$$e = \text{Measured value} - \text{True value} \quad (1.4)$$

While the true value is rarely known exactly, Equation 1.4 serves as a reference definition. Errors exist and they have a magnitude as given by Equation 1.4. The concept is something we discuss next and then develop extensively in Chapter 5.

Often an estimate for the value of error is based on a reference value used during the instrument's calibration as a surrogate for the true value. A relative error based on this reference value is estimated by

$$A = \frac{|e|}{\text{Reference value}} \times 100 \quad (1.5)$$

A few vendors may still refer to this term as the “relative accuracy.”

A special form of a calibration curve is the *deviation plot*, such as shown in Figure 1.10. Such a curve plots the error or deviation between a reference or expected value, y' , and the measured value, y , versus the measured value. Deviation curves are extremely useful when the differences between the reference and the measured value are too small to suggest possible trends on direct calibration plots. As an example, a deviation plot of the calibration of a temperature-sensing thermocouple is

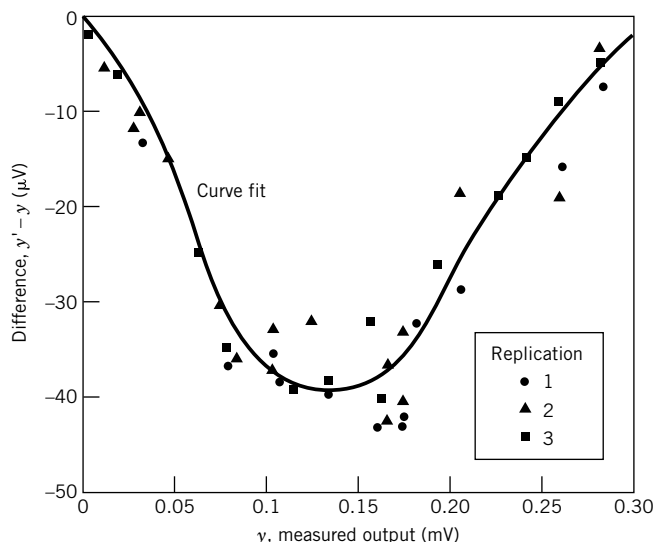


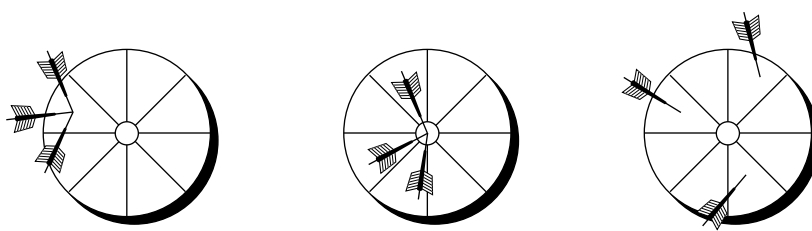
Figure 1.10 Calibration curve in the form of a deviation plot for a temperature sensor.

given in Figure 1.10. The voltage output during calibration is compared with the expected values obtained from reference tables. The trend of the errors can be correlated, as shown by the curve fit. We see the maximum errors are two orders of magnitude smaller than the measured values, but we also see that the errors are smallest at either limit of the measuring range. We also see that the error varies in magnitude. The range over which it varies is the uncertainty in the measurement.

Random and Systematic Errors and Uncertainty

Errors are effects that cause a measured value to differ from its true value. *Random error* causes a random variation in measured values found during repeated measurements of a variable. *Systematic error* causes an offset between the mean value of the data set and its true value. Both random and systematic errors affect a system's accuracy.

The concept of accuracy and the effects of systematic and random errors in instruments and measurement systems can be illustrated by the throw of darts. Consider the dart boards in Figure 1.11 where the goal will be to throw the darts into the bull's-eye. For this analogy, the bull's-eye can represent the true value and each throw can represent a measured value. In Figure 1.11a, the thrower displays good repeatability (i.e., a small effect from random error) in that each throw repeatedly hits the same spot on the board, but the thrower is not accurate in that the dart misses the bull's-eye each time. We see that a small amount of random error is not a complete measure of the accuracy of this thrower. The error in each throw can be computed from the distance between the bull's-eye and each dart. The average value of the error gives an estimate of the systematic error in the throws. This thrower has an offset to the left of the target. If the effect of this systematic error could be reduced, then this thrower's accuracy would improve. In Figure 1.11b, the thrower displays a high accuracy, hitting the bull's-eye on each throw. Both scatter and offset are near zero. High accuracy must imply a small influence of both the random and systematic errors as shown. In Figure 1.11c, the thrower does not show good accuracy, with errant throws scattered around the board. Each throw contains a different amount of error. While an estimate of the systematic error is the average of the errors in the throws, the estimate of the random error is related to the varying amount of error in the throws, a value that can be estimated using statistical methods. The estimates in the random and systematic errors of the thrower can be computed using the statistical methods that are discussed in Chapter 4 or the methods of comparison discussed in Chapter 5.



(a) High repeatability gives low random error but no direct indication of accuracy.

(b) High accuracy means low random and systematic errors.

(c) Systematic and random errors lead to poor accuracy.

Figure 1.11 Throws of a dart: illustration of random and systematic errors and accuracy.

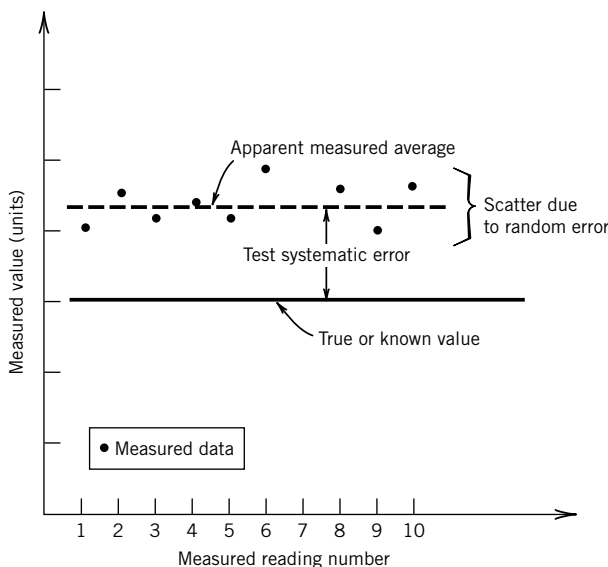


Figure 1.12 Effects of random and systematic errors on calibration readings.

Suppose we used a measurement system to measure a variable whose value was kept constant and known almost exactly, as in a calibration. For example, 10 independent measurements are made with the results as shown in Figure 1.12. The variations in the measurements, the observed scatter in the data, would be related to the random error associated with the measurement of the variable. This scatter is mainly due to (1) the measurement system and the measurement method, and (2) any uncontrolled variations in the variable. However, the offset between the apparent average of the readings and the true value would provide a measure of the systematic error to be expected from this measurement system.

Uncertainty

The *uncertainty* is a numerical estimate of the possible range of the error in a measurement. In any measurement, the error is not known exactly since the true value is rarely known exactly. But based on available information, the operator might feel confident that the error is within certain bounds, a plus or minus range of the indicated reading. This is the assigned uncertainty. Uncertainty is brought about by all of the errors that are present in the measurement system—its calibration, the data set statistics, and the measurement technique. Individual errors are properties of the instruments, the test method, the analysis, and the measurement system. Uncertainty is a property of the test result. In Figure 1.12, we see that we might assign an estimate to the random error, that is, the random uncertainty, based on the data scatter. The systematic uncertainty might be based on a comparison against a concomitant method. A method of estimating the overall uncertainty in the test result is treated in detail in Chapter 5.

The uncertainty values assigned to an instrument or measurement system specification are usually the result of several interacting random and systematic errors inherent to the measurement system, the calibration procedure, and the standard used to provide the known value. An example of the errors affecting an instrument is given for a typical pressure transducer in Table 1.1. The value assigned to each error is the uncertainty.

Table 1.1 Manufacturer's Specifications: Typical Pressure Transducer

Operation	
Input range	0–1000 cm H ₂ O
Excitation	±15 V DC
Output range	0–5 V
Performance	
Linearity error	±0.5% FSO
Hysteresis error	Less than ±0.15% FSO
Sensitivity error	±0.25% of reading
Thermal sensitivity error	±0.02%/°C of reading
Thermal zero drift	±0.02%/°C FSO
Temperature range	0–50 °C

FSO, full-scale operating range.

Sequential Test

A *sequential test* applies a sequential variation in the input value over the desired input range. This may be accomplished by increasing the input value (upscale direction) or by decreasing the input value (downscale direction) over the full input range.

Hysteresis

The sequential test is an effective diagnostic technique for identifying and quantifying hysteresis error in a measurement system. *Hysteresis error* refers to differences between an upscale sequential test and a downscale sequential test. The hysteresis error of the system is estimated by its uncertainty $u_h = (y)_{\text{upscale}} - (y)_{\text{downscale}}$. The effect of hysteresis in a sequential test calibration curve is illustrated in Figure 1.13a. Hysteresis is usually specified for a measurement system in terms of the maximum hysteresis error as a percentage of full-scale output range, r_o ,

$$\% u_{h_{\max}} = \frac{u_{h_{\max}}}{r_o} \times 100 \quad (1.6)$$

such as the value indicated in Table 1.1. Hysteresis occurs when the output of a measurement system is dependent on the previous value indicated by the system. Such dependencies can be brought about through some realistic system limitations such as friction or viscous damping in moving parts or residual charge in electrical components. Some hysteresis is normal for any system and affects the repeatability of the system.

Random Test

A *random test* applies a random order in the values of a known input over the intended calibration range. The random application of input tends to reduce the impact of interference. It breaks up hysteresis effects and observation errors. It ensures that each application of input value is independent of the previous. As such, it reduces calibration systematic error, converting it to random error. Generally, such a random variation in input value will more closely simulate the actual measurement situation.

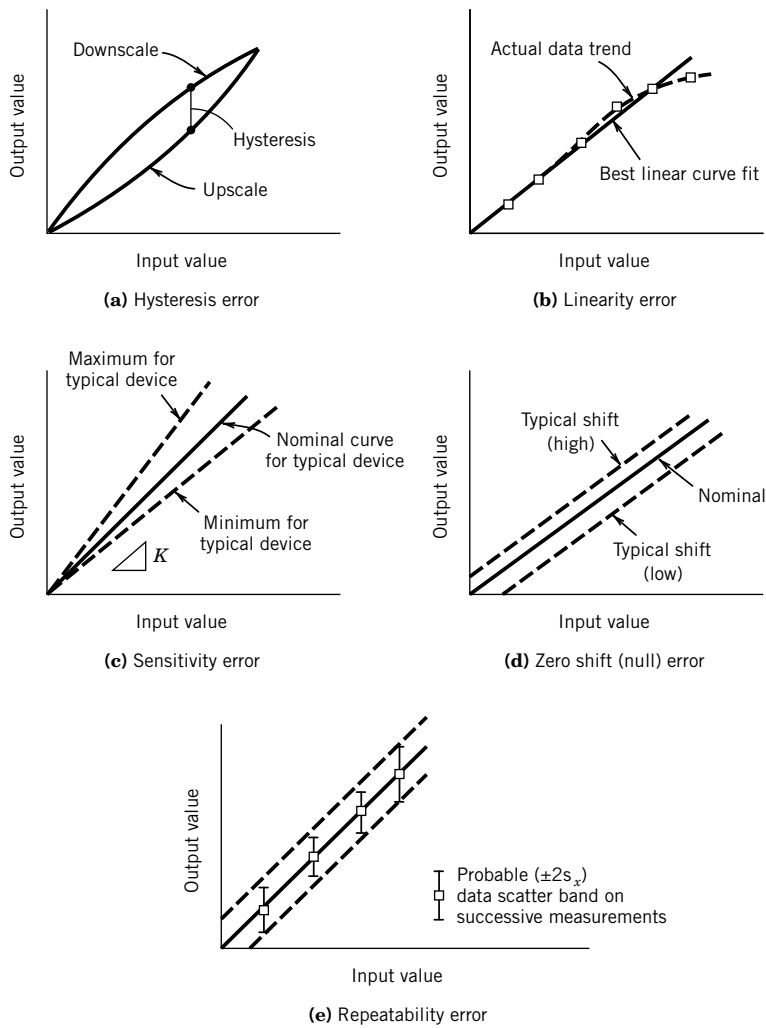


Figure 1.13 Examples of some common elements of instrument error.
(a) Hysteresis error.
(b) Linearity error.
(c) Sensitivity error.
(d) Zero shift (null) error.
(e) Repeatability error.

A random test provides an important diagnostic for the delineation of several measurement system performance characteristics based on a set of random calibration test data. In particular, linearity error, sensitivity error, zero error, and instrument repeatability error, as illustrated in Figure 1.13b–e, can be quantified from a static random test calibration.

Linearity Error

Many instruments are designed to achieve a linear relationship between the applied static input and indicated output values. Such a linear static calibration curve would have the general form

$$y_L(x) = a_0 + a_1 x \quad (1.7)$$

where the curve fit $y_L(x)$ provides a predicted output value based on a linear relation between x and y . However, in real systems, truly linear behavior is only approximately achieved. As a result,

measurement device specifications usually provide a statement as to the expected linearity of the static calibration curve for the device. The relationship between $y_L(x)$ and measured value $y(x)$ is a measure of the nonlinear behavior of a system:

$$u_L(x) = y(x) - y_L(x) \quad (1.8)$$

where $u_L(x)$ is a measure of the *linearity error* that arises in describing the actual system behavior by Equation 1.7. Such behavior is illustrated in Figure 1.13b in which a linear curve has been fit through a calibration data set. For a measurement system that is essentially linear in behavior, the extent of possible nonlinearity in a measurement device is often specified in terms of the maximum expected linearity error as a percentage of full-scale output range, r_o ,

$$\%u_{L_{\max}} = \frac{u_{L_{\max}}}{r_o} \times 100 \quad (1.9)$$

This is how the linearity error for the pressure transducer in Table 1.1 was estimated. Statistical methods of quantifying data scatter about a line or curve fit are discussed in Chapter 4.

Sensitivity and Zero Errors

The scatter in the data measured during a calibration affects the precision in predicting the slope of the calibration curve. As shown for the linear calibration curve in Figure 1.13c, in which the zero intercept is fixed, the scatter in the data about the curve fit are random errors. The *sensitivity error*, u_K , is a statistical measure of the random error in the estimate of the slope of the calibration curve (we discuss the statistical estimate further in Chapter 4). The static sensitivity of a device is also temperature dependent, and this is often specified. In Table 1.1, the sensitivity error reflects calibration results at a constant reference ambient temperature, whereas the thermal sensitivity error was found by calibration at different temperatures.

If the zero intercept is not fixed but the sensitivity is constant, then a drift in the zero intercept introduces a vertical shift of the calibration curve, as shown in Figure 1.13d. This shift is known as the *zero error* with uncertainty, u_z . Zero error can usually be reduced by periodically adjusting the output from the measurement system under a zero input condition. However, some random variation in the zero intercept is common, particularly with electronic and digital equipment subjected to temperature variations (e.g., thermal zero drift in Table 1.1).

Instrument Repeatability

The ability of a measurement system to indicate the same value on repeated but independent application of the same input provides a measure of the instrument *repeatability*. Specific claims of repeatability are based on multiple calibration tests (replication) performed within a given lab on the particular unit. Repeatability, as shown in Figure 1.13e, is based on a statistical measure (developed in Chapter 4) called the standard deviation, s_x , a measure of the variation in the output for a given input. The value claimed is usually in terms of the maximum expected error as a percentage of full-scale output range:

$$\%u_{R_{\max}} = \frac{2s_x}{r_o} \times 100 \quad (1.10)$$

The instrument repeatability reflects only the variations found under controlled calibration conditions.

Reproducibility

The term “reproducibility,” when reported in instrument specifications, refers to the closeness of agreement in results obtained from duplicate tests carried out under similar conditions of measurement. As with repeatability, the uncertainty is based on statistical measures. Manufacturer claims of instrument reproducibility must be based on multiple tests (replication) performed in different labs on a single unit or model of instrument.

Instrument Precision

The term “instrument precision,” when reported in instrument specifications, refers to a random uncertainty based on the results of separate repeatability tests. Manufacturer claims of instrument precision must be based on multiple tests (replication) performed on different units of the same manufacture, either performed in the same lab (same-lab precision) or, preferably, performed in different labs (between-lab precision).

Overall Instrument Error and Instrument Uncertainty

An estimate of the *overall instrument error* is made by combining the estimates of all known errors into a term called the *instrument uncertainty*. The estimate is computed from the square root of the sum of the squares of all known uncertainty values. For M known errors, the overall instrument uncertainty, u_c , is estimated by

$$u_c = [u_1^2 + u_2^2 + \cdots + u_M^2]^{1/2} \quad (1.11)$$

For example, for an instrument having known hysteresis, linearity, and sensitivity errors, the instrument uncertainty is estimated by

$$u_c = [u_h^2 + u_L^2 + u_K^2]^{1/2} \quad (1.12)$$

1.5 STANDARDS

When a measurement system is calibrated, its indicated value is compared directly with a reference value. This reference value forms the basis of the comparison and is known as the *standard*. This standard may be based on the output from a piece of equipment, from an object having a well-defined physical attribute to be used as a comparison, or from a well-accepted technique known to produce a reliable value. Let us explore how certain standards come to be and how these standards are the foundation of all measurements.

Primary Standards

A *dimension* defines a physical variable that is used to describe some aspect of a physical system. A *unit* defines a quantitative measure of a dimension. For example, mass, length, and time describe base dimensions with which we associate the units of kilogram, meter, and second. A *primary standard* defines the value of a unit. It provides the means to describe the unit with a unique number that can be understood throughout the world. The primary standard, then, assigns a unique value to a unit by definition! As such it must define the unit exactly. In 1960, the General Conference on Weights and Measures (CGPM), the international agency responsible for maintaining exact uniform standards of measurements, formally adopted the International System of Units (SI) as the

international standard of units. The system has been adopted worldwide. Other unit systems are commonly used in the consumer market and so deserve mention. These other unit systems are not standards and are treated as conversions from SI. Examples of these include the inch-pound (I-P) unit system found in the United States and the gravitational mks (meter-kilogram-second or metric) unit system common to much of the world.

Primary standards are necessary because the value assigned to a unit is actually arbitrary. For example, over 4500 years ago the Egyptian cubit was used as a standard of length and based on the length from outstretched fingertips to the elbow. It was later codified with a master of marble, a stick about 52 cm in length, on which scratches were etched to define subunits of length. This standard served well for centuries!

So whether today's standard unit of length, the meter, is the length of a king's forearm or the distance light travels in a fraction of a second really only depends on how we want to define it. To avoid confusion, units are defined by international agreement through the use of primary standards. Once agreed upon, a primary standard forms the exact definition of the unit until it is changed by some later agreement. Important features sought in any standard should include global availability, continued reliability, and stability with minimal sensitivity to external environmental sources. Next we examine some basic dimensions and the primary standards that form the definition of the units that describe them (9).

Base Dimensions and Their Units

Mass

The dimension of mass is defined by the kilogram. Originally, the unit of the kilogram was defined by the mass of one liter of water at room temperature. But today an equivalent yet more consistent definition defines the kilogram exactly as the mass of a particular platinum-iridium cylindrical bar that is maintained under very specific conditions at the International Bureau of Weights and Measures located in Sevres, France. This particular bar (consisting of 90% platinum and 10% iridium by mass) forms the primary standard for the kilogram. It remains today as the only basic unit still defined in terms of a material object.

In the United States, the I-P unit system (also referred to as the U.S. customary units) remains widely used. In the I-P system, *mass* is defined by the pound-mass, lb_m , which is derived directly and exactly from the definition of the kilogram:

$$1 \text{ lb}_m = 0.4535924 \text{ kg} \quad (1.13)$$

Equivalent standards for the kilogram and other standards units are maintained by the U.S. National Institute of Standards and Technology (NIST) in Gaithersburg, Maryland, and other national labs around the globe. NIST claims that their mass standard is accurate to an uncertainty of within 1 mg in 27,200 kg.

Time and Frequency

The dimension of time is defined by the unit of a second. One second (s) is defined as the time elapsed during 9,192,631,770 periods of the radiation emitted between two excitation levels of the fundamental state of cesium-133 (10). Despite this seemingly unusual definition, this primary standard can be reliably reproduced at suitably equipped laboratories throughout the world to an uncertainty of within two parts in 10 trillion.

The Bureau International de l'Heure (BIH) in Paris maintains the primary standard for clock time. Periodically, adjustments to clocks around the world are made relative to the BIH clock so as to keep time synchronous.

The standard for cyclical frequency is derived from the time standard. The standard unit is the hertz (1 Hz = 1 cycle/s). The cyclical frequency is related to the circular frequency (radians/s) by

$$1 \text{ Hz} = \frac{2\pi \text{ rad}}{1 \text{ s}} \quad (1.14)$$

Both time and frequency standard signals are broadcast worldwide over designated radio stations for use in navigation and as a source of a standard for these dimensions.

Length

The meter is the standard unit for length. New primary standards are established when our ability to determine the new standard becomes more accurate (i.e., lower uncertainty) than the existing standard. In 1982, a new primary standard was adopted by the CGPM to define the unit of a meter. One meter (m) is now defined exactly as the length traveled by light in $1/299,792,458$ of a second, a number derived from the velocity of light in a vacuum (defined as 299,792,458 m/s).

The I-P system unit of the inch and the related unit of the foot are derived exactly from the meter.

$$\begin{aligned} 1 \text{ ft} &= 0.3048 \text{ m} \\ 1 \text{ in.} &= 0.0254 \text{ m} \end{aligned} \quad (1.15)$$

Temperature

The kelvin, K, is the SI unit of thermodynamic temperature and is the fraction 1/273.16 of the thermodynamic temperature of the triple point of water. This temperature scale was devised by William Thomson, Lord Kelvin (1824–1907), and forms the basis for the absolute practical temperature scale in common use. This scale is based on polynomial interpolation between the equilibrium phase change points of a number of common pure substances from the triple point of equilibrium hydrogen (13.81 K) to the freezing point of pure gold (1337.58 K). Above 1337.58 K, the scale is based on Planck's law of radiant emissions. The details of the standard have been modified over the years but are governed by the International Temperature Scale–1990 (11).

The I-P unit system uses the absolute scale of Rankine (°R). This and the common scales of Celsius (°C), used in the metric system, and Fahrenheit (°F) are related to the Kelvin scale by the following:

$$\begin{aligned} (\text{°C}) &= (\text{K}) - 273.15 \\ (\text{°F}) &= (\text{°R}) - 459.67 \\ (\text{°F}) &= 1.8 \times (\text{°C}) + 32.0 \end{aligned} \quad (1.16)$$

Current

The SI unit for current is the ampere. One ampere (A) is defined as that constant current which, if maintained in two straight parallel conductors of infinite length and of negligible circular cross

section and placed 1 m apart in vacuum, would produce a force equal to 2×10^{-7} newtons per meter of length between these conductors.

Measure of Substance

The unit of quantity of a substance is defined by the mole. One mole (mol) is the amount of substance of a system that contains as many elementary entities as there are atoms in 0.012 kilogram of carbon 12.

Luminous Intensity

The intensity of light is defined by the candela. One candela (cd) is the luminous intensity, in a given direction, of a source that emits monochromatic radiation of frequency 5.40×10^{14} hertz and that has a radiant intensity in that direction of 1/683 watt per steradian.

Derived Units

Other dimensions and their associated units are defined in terms of and derived from the base dimensions and units (9,12).

Force

From Newton's law, force is proportional to mass times acceleration:

$$\text{Force} = \frac{\text{Mass} \times \text{Acceleration}}{g_c}$$

where g_c is a proportionality constant used to maintain consistency in units.

Force is defined by a derived unit called the newton (N), which is derived from the base dimensions of mass, length, and time:

$$1 \text{ N} = 1 \frac{\text{kg} - \text{m}}{\text{s}^2} \quad (1.17)$$

So for this system the value of g_c must be $1.0 \text{ kg}\cdot\text{m/s}^2\text{-N}$. Note that the resulting expression for Newton's second law does not explicitly require the inclusion of g_c to make units match and so is often ignored.

However, in I-P units, the units of force and mass are related through the definition: One pound-mass (lb_m) exerts a force of 1 pound (lb) in a standard gravitational field. With this definition,

$$1 \text{ lb} = \frac{(1 \text{ lb}_m)(32.174 \text{ ft/s}^2)}{g_c} \quad (1.18)$$

and g_c must take on the value of $32.174 \text{ lb}_m\cdot\text{ft/lb}\cdot\text{s}^2$. In I-P units, the pound is a defined quantity and g_c must be derived through Newton's law.

Similarly, in the gravitational mks (metric) system, which uses the kilogram-force (kg_f),

$$1 \text{ kg}_f = \frac{(1 \text{ kg})(9.80665 \text{ m/s}^2)}{g_c} \quad (1.19)$$

and the value for g_c takes on a value of exactly $9.80665 \text{ kg}\cdot\text{m/s}^2\text{-kg}_f$.

Many engineers have some difficulty with using g_c in the non-SI systems. Actually, whenever force and mass appear in the same expression, just remember to relate them using g_c through Newton's law:

$$g_c = \frac{mg}{F} = 1 \frac{\text{kg} - \text{m/s}^2}{\text{N}} = 32.174 \frac{\text{lb}_m - \text{ft/s}^2}{\text{lb}} = 9.80665 \frac{\text{kg} - \text{m/s}^2}{\text{kg}_f} \quad (1.20)$$

Other Derived Dimensions and Units

Energy is defined as force times length and uses the unit of the joule (J), which is derived from base units as

$$1 \text{ J} = 1 \frac{\text{kg} - \text{m}^2}{\text{s}^2} = 1 \text{ N} - \text{m} \quad (1.21)$$

Power is defined as energy per unit time in terms of the unit of the watt (W), which is derived from base units as:

$$1 \text{ W} = 1 \frac{\text{kg} - \text{m}^2}{\text{s}^3} = 1 \frac{\text{J}}{\text{s}} \quad (1.22)$$

Stress and pressure are defined as force per unit area, where area is length squared, in terms of the pascal (Pa), which is derived from base units as

$$1 \text{ Pa} = 1 \frac{\text{kg}}{\text{m} - \text{s}^2} = 1 \text{ N/m}^2 \quad (1.23)$$

Electrical Dimensions

The units for the dimensions of electrical potential, and resistance, charge, and capacitance are based on the definitions of the absolute volt (V), and ohm (Ω), coulomb (C), and farad (F), respectively. Derived from the ampere, 1 ohm absolute is defined by 0.9995 times the resistance to current flow of a column of mercury that is 1.063 m in length and has a mass of 0.0144521 kg at 273.15 K. The volt is derived from the units for power and current, $1 \text{ V} = 1 \text{ N} \cdot \text{m/s} \cdot \text{A} = 1 \text{ W/A}$. The ohm is derived from the units for electrical potential and current, $1 \Omega = 1 \text{ kg} \cdot \text{m}^2 / \text{s}^3 \cdot \text{A}^2 = 1 \text{ V/A}$. The coulomb is derived from the units for current and time, $1 \text{ C} = 1 \text{ A} \cdot \text{s}$. One volt is the difference of potential between two points of an electrical conductor when a current of 1 ampere flowing between those points dissipates a power of 1 watt. The farad (F) is the standard unit for capacitance derived from the units for charge and electric potential, $1 \text{ F} = 1 \text{ C/V}$.

On a practical level, working standards for resistance and capacitance take the form of certified standard resistors and capacitors or resistance boxes and are used as standards for comparison in the calibration of resistance measuring devices. The practical potential standard makes use of a standard cell consisting of a saturated solution of cadmium sulfate. The potential difference of two conductors connected across such a solution is set at 1.0183 V and at 293 K. The standard cell maintains constant electromotive force over very long periods of time, provided that it is not subjected to a current drain exceeding 100 μA for more than a few minutes. The standard cell is typically used as a standard for comparison for voltage measurement devices.

Table 1.2 Dimensions and Units^a

Unit	Dimension	
	SI	I-P
Primary		
Length	meter (m)	inch (in.)
Mass	kilogram (kg)	pound-mass (lb_m)
Time	second (s)	second (s)
Temperature	kelvin (K)	rankine ($^{\circ}\text{R}$)
Current	ampere (A)	ampere (A)
Substance	mole (mol)	mole (mol)
Light intensity	candela (cd)	candela (cd)
Derived		
Force	newton (N)	pound-force (lb)
Voltage	volt (V)	volt (V)
Resistance	ohm (Ω)	ohm (Ω)
Capacitance	farad (F)	farad (F)
Inductance	henry (H)	henry (H)
Stress, pressure	pascal (Pa)	pound-force/inch ² (psi)
Energy	joule (J)	foot pound-force (ft-lb)
Power	watt (W)	foot pound-force/second (ft-lb/s)

^aSI dimensions and units are the international standards. I-P units are presented for convenience.

A chart for converting between units is included inside the text cover. Table 1.2 lists the basic standard and some derived units used in SI and the corresponding units used in the I-P and gravitational metric systems.

Hierarchy of Standards

The known value applied to a measurement system during calibration becomes the standard on which the calibration is based. So how do we pick this standard, and how good is it? Obviously, actual primary standards are impractical as standards for normal calibration use. But they serve as a reference for exactness. It would not be reasonable to travel to France to calibrate an ordinary laboratory scale using the primary standard for mass (nor would it likely be permitted!). So for practical reasons, there exists a hierarchy of reference and secondary standards used to duplicate the primary standards. Just below the primary standard in terms of absolute accuracy are the national reference standards maintained by designated standards laboratories throughout the world. These provide a reasonable duplication of the primary standard but allow for worldwide access to an extremely accurate standard. Next to these, we develop transfer standards. These are used to calibrate individual laboratory standards that might be used at various facilities within a country. Laboratory standards serve to calibrate working standards. Working standards are used to calibrate everyday devices used in manufacturing and research facilities. In the United States, NIST maintains primary, reference, and secondary standards and recommends standard procedures for the calibration of measurement systems.

Table 1.3 Hierarchy of Standards^a

Primary standard	Maintained as absolute unit standard
Transfer standard	Used to calibrate local standards
Local standard	Used to calibrate working standards
Working standard	Used to calibrate local instruments

^aThere may be additional intermediate standards between each hierarchy level.

Each subsequent level of the hierarchy is derived by calibration against the standard at the previous higher level. Table 1.3 lists an example of such a lineage for standards from a primary or reference standard maintained at a national standards lab down to a working standard used in a typical laboratory or production facility to calibrate everyday working instruments. If the facility does not maintain a local (laboratory or working) standard, then the instruments must be sent off and calibrated elsewhere. In such a case, a standards traceability certificate would be issued for the instrument.

As one moves down through the standards lineage, the degree of exactness by which a standard approximates the primary standard deteriorates. That is, increasing elements of error are introduced into the standard as one moves from one level of hierarchy of standard to the next. As a common example, an institution might maintain its own working standard (for some application) that is used to calibrate the measurement devices found in the individual laboratories throughout the institution. Periodic calibration of the working standard might be against the institution's well-maintained local standard. The local standard would be periodically sent off to be calibrated against the NIST (or appropriate national standards lab) transfer standard (and traceability certificate issued). NIST will periodically calibrate its own transfer standard against its reference or primary standard. This is illustrated for a temperature standard traceability hierarchy in Table 1.4. The uncertainty in the approximation of the known value increases as one moves down the hierarchy. It follows, then, that since the calibration determines the relationship between the input value and the output value, the accuracy of the calibration will depend in part on the accuracy of the standard. But if typical working standards contain errors, how is accuracy ever determined? At best, this closeness of agreement is quantified by the estimates of the known uncertainties in the calibration. And the confidence in that estimate depends on the quality of the standard and the calibration techniques used.

Table 1.4 Example of a Temperature Standard Traceability

Standard		
Level	Method	Uncertainty [°C] ^a
Primary	Fixed thermodynamic points	0
Transfer	Platinum resistance thermometer	±0.005
Working	Platinum resistance thermometer	±0.05
Local	Thermocouple	±0.5

^aTypical combined instrument systematic and random uncertainties.

Test Standards and Codes

The term “standard” is also applied in other ways in engineering. *Test standards* refer to well-defined test procedures, technical terminology, methods to construct test specimens or test devices, and/or methods for data reduction. The goal of a test standard is to provide consistency in the conduct and reporting of a certain type of measurement between test facilities. Similarly, *test codes* refer to procedures for the manufacture, installation, calibration, performance specification, and safe operation of equipment.

Diverse examples of test standards and codes are illustrated in readily available documents (13–16) from professional societies, such as the American Society of Mechanical Engineers (ASME), the American Society of Testing and Materials (ASTM), and the International Standards Organization (ISO). For example, ASME Power Test Code 19.5 provides detailed designs and operation procedures for flow meters, while ASTM Test Standard F558-88 provides detailed procedures for evaluating vacuum cleaner cleaning effectiveness and controls the language for product performance claims. Engineering standards and codes are consensus documents agreed on by knowledgeable parties interested in establishing, for example, some common basis for comparing equipment performance between manufacturers. These are not binding legal documents unless specifically adopted and implemented as such by a government agency. Still, they present a convincing argument for best practice.

1.6 PRESENTING DATA

Since we use several plotting formats throughout this text to present data, it is best to introduce these formats here. Data presentation conveys significant information about the relationship between variables. Software is readily available to assist in providing high-quality plots, or plots can be generated manually using graph paper. Several forms of plotting formats are discussed next.

Rectangular Coordinate Format

In rectangular grid format, both the ordinate and the abscissa have uniformly sized divisions providing a linear scale. This is the most common format used for constructing plots and establishing the form of the relationship between the independent and dependent variable.

Semilog Coordinate Format

In a semilog format, one coordinate has a linear scale and one coordinate has a logarithmic scale. Plotting values on a logarithmic scale performs a logarithmic operation on those values, for example, plotting $y = f(x)$ on a logarithmic x -axis is the same as plotting $y = \log f(x)$ on rectangular axes. Logarithmic scales are advantageous when one of the variables spans more than one order of magnitude. In particular, the semilog format may be convenient when the data approximately follow a relationship of the form $y = ae^x$ or $y = a10^x$ as a linear curve will result in each case. A natural logarithmic operation can also be conveyed on a logarithmic scale, as the relation $\ln y = 2.3 \log y$ is just a scaling operation.

Full-Log Coordinate Format

The full-log or log-log format has logarithmic scales for both axes and is equivalent to plotting $\log y$ vs. $\log x$ on rectangular axes. Such a format is preferred when both variables contain data values that

span more than one order of magnitude. With data that follow a trend of the form $y = ax^n$, a linear curve will be obtained in log-log format.

Significant Digits

Significant digits refer to the number of digits found before and after the decimal point in a reported number. While leading zeros are not significant, all trailing zeros are significant. For example, 42.0 has three significant digits, including one decimal digit. The number of significant digits needed depends on the problem and the close discretion of the engineer. But in the course of working a problem, there should be consistency in the number of significant digits used and reported. The number of digits reported reflects a measure of the uncertainty in the value assigned by the engineer. So to determine the number of significant digits required, just ask yourself: “What value makes sense to this problem?” For example, to maintain a relative uncertainty of within 1%, we need to report values to three significant figures. But because rounding errors tend to accumulate during calculations, we would perform all intermediate calculations to at least four significant figures, and then round the final result down to three significant figures.

1.7 SUMMARY

During a measurement the input signal is not known but is inferred from the value of the output signal from the measurement system. We discussed the process of calibration as the means to relate a measured input value to the measurement system output value and the role of standards in that process. An important step in the design of a measurement system is the inclusion of a means for a reproducible calibration that closely simulates the type of signal to be input during actual measurements. A test is the process of “asking a question.” The idea of a test plan was developed to answer that question. However, a measured output signal can be affected by many variables that will introduce variation and trends and confuse that answer. Careful test planning is required to reduce such effects. A number of test plan strategies were developed, including randomization. The popular term “accuracy” was explained in terms of the more useful concepts of random error, systematic error, random uncertainty, and systematic uncertainty and their effects on a measured value. We also explored the idea of test standards and engineering codes, legal documents that influence practically every manufactured product around us.

REFERENCES

1. Peace, G. S., *Taguchi Methods*, Addison-Wesley, Reading, MA, 1993.
2. Bridgeman, P. W., *Dimensional Analysis*, 2nd ed., Yale University Press, New Haven, CT, 1931.
3. Duncan, W. J., *Physical Similarity and Dimensional Analysis*, Arnold, London, 1953.
4. Massey, B. S., *Units, Dimensions and Physical Similarity*, Van Nostrand-Reinhold, New York, 1971.
5. Lipsen, C., and N. J. Sheth, *Statistical Design and Analysis of Engineering Experimentation*, McGraw-Hill, New York, 1973.
6. Peterson, R. G., *Design and Analysis of Experiments*, Marcel-Dekker, New York, 1985.
7. Mead, R., *The Design of Experiments: Statistical Principles for Practical Application*, Cambridge Press, New York, 1988.

8. Montgomery, D., *Design and Analysis of Experiments*, 7th ed., Wiley, New York, 2009.
9. Taylor, B., *Guide for the Use of the International System of Units*, NIST Special Publication, 330, 2001.
10. NBS Technical News Bulletin 52(1), January 1968.
11. International Temperature Scale–1990, *Metrologia* 27(3), 1990.
12. Taylor, B., NIST Guide to SI Units, NIST Special Publication 811, 1995.
13. *ASME Power Test Codes*, American Society of Mechanical Engineers, New York.
14. *ASHRAE Handbook of Fundamentals*, American Society of Heating, Refrigeration and Air Conditioning Engineers, New York, 2009.
15. *ANSI Standard*, American National Standards Institute, New York, 2009.
16. *Annual Book of ASTM Standards*, American Society for Testing and Materials, Philadelphia, PA, 2010.

NOMENCLATURE

e	absolute error	u_R	repeatability uncertainty; uncertainty assigned to repeatability error
p	pressure ($ml^{-1}t^{-2}$)	u_z	zero uncertainty; uncertainty assigned to zero error
r_i	input span	x	independent variable; input value; measured variable
r_o	output span	y	dependent variable; output value
s_x	standard deviation of x	y_L	linear polynomial
u_c	overall instrument uncertainty	A	relative error; relative accuracy
u_h	hysteresis uncertainty; uncertainty assigned to hysteresis error	K	static sensitivity
u_K	sensitivity uncertainty; uncertainty assigned to sensitivity error	T	temperature (°)
u_L	linearity uncertainty; uncertainty assigned to linearity error	\forall	volume (l^3)

PROBLEMS

- 1.1 Discuss your understanding of the hierarchy of standards beginning with the primary standard. In general, what is meant by the term “standard”? Can you cite examples of standards in everyday use?
- 1.2 What is the purpose of a calibration? Suppose an instrument is labeled as “calibrated.” What should this mean to you as an engineer?
- 1.3 Suppose you found a dial thermometer in a stockroom. Discuss several methods by which you might estimate random and systematic error in the thermometer? How would you estimate its uncertainty?
- 1.4 Consider the example described in Figure 1.6. Discuss the effect of the extraneous variable, barometric pressure, in terms of noise and interference relative to any one test and relative to several tests. Discuss how the interference effect can be broken up into noise.
- 1.5 How would the resolution of the display scale of an instrument affect its uncertainty? Suppose the scale was somehow offset by one least count of resolution. How would this affect its uncertainty? Explain in terms of random and systematic error.
- 1.6 How would the hysteresis of an instrument affect its uncertainty? Explain in terms of random and systematic error.

- 1.7** Select three different types of measurement systems with which you have experience, and identify which attributes of the system comprise the measurement system stages of Figure 1.5.
- 1.8** Identify the measurement system stages for the following systems (refer back to Figure 1.5 and use other resources, such as a library or Internet search, as needed to learn more about each system):
- Room thermostat
 - Automobile speedometer
 - Portable CD stereo system
 - Antilock braking system (automobile)
 - Automobile cruise control
 - Throttle position sensor for a Formula One race car
- 1.9** What is the range of the calibration data of Table 1.5?

Table 1.5 Calibration Data

X [cm]	Y [V]	X [cm]	Y [V]
0.5	0.4	10.0	15.8
1.0	1.0	20.0	36.4
2.0	2.3	50.0	110.1
5.0	6.9	100.0	253.2

- 1.10** For the calibration data of Table 1.5, plot the results using rectangular and log-log scales. Discuss the apparent advantages of either presentation.
- 1.11** For the calibration data of Table 1.5, determine the static sensitivity of the system at (a) $X = 5$; (b) $X = 10$; and (c) $X = 20$. For which input values is the system more sensitive? Explain what this might mean in terms of a measurement and in terms of measurement errors.
- 1.12** Consider the voltmeter calibration data in Table 1.6. Plot the data using a suitable scale. Specify the percent maximum hysteresis based on full-scale range. Input X is based on a standard known to be accurate to better than 0.05 mV.

Table 1.6 Voltmeter Calibration Data

Increasing Input [mV]		Decreasing Input [mV]	
X	Y	X	Y
0.0	0.1	5.0	5.0
1.0	1.1	4.0	4.2
2.0	2.1	3.0	3.2
3.0	3.0	2.0	2.2
4.0	4.1	1.0	1.2
5.0	5.0	0.0	0.2

- 1.13** Three clocks are compared to a time standard at three successive hours. The data are given in Table 1.7. Using Figure 1.12 as a guide, arrange these clocks in order of estimated accuracy. Discuss your choices.

Table 1.7 Clock Calibration Data

Clock	Standard Time		
	1:00:00	2:00:00	3:00:00
	Indicated Time		
A	1:02:23	2:02:24	3:02:25
B	1:00:05	2:00:05	3:00:05
C	1:00:01	1:59:58	3:00:01

- 1.14** Each of the following equations can be represented as a straight line on an x - y plot by choosing the appropriate axis scales. Plot them both in rectangular coordinate format and then in an appropriate format to yield a straight line. Explain how the plot operation yields the straight line. Variable y has units of volts. Variable x has units of meters (use a range of $0:01 < x < 10:0$). Note: This is easily done using a spreadsheet program where you can compare the use of different axis scales.

- a. $y = x^2$
- b. $y = 1.1x$
- c. $y = 2x^{0.5}$
- d. $y = 10x^4$
- e. $y = 10e^{-2x}$

- 1.15** Plot $y = 10e^{-5x}$ volts on in semilog format (use three cycles). Determine the slope of the equation at $x = 0$; $x = 2$; and $x = 20$.

- 1.16** Plot the following data on appropriate axes. Estimate the static sensitivity K at each X .

Y [V]	X [V]
2.9	0.5
3.5	1.0
4.7	2.0
9.0	5.0

- 1.17** The following data have the form $y = ax^b$. Plot the data in an appropriate format to estimate the coefficients a and b . Estimate the static sensitivity K at each value of X . How is K affected by X ?

Y [cm]	X [m]
0.14	0.5
2.51	2.0
15.30	5.0
63.71	10.0

- 1.18** For the calibration data given, plot the calibration curve using suitable axes. Estimate the static sensitivity of the system at each X . Then plot K against X . Comment on the behavior of the static sensitivity with static input magnitude for this system.

Y [cm]	X [kPa]
4.76	0.05
4.52	0.1
3.03	0.5
1.84	1.0

- 1.19** Consider the function

$$y = \frac{1}{x}$$

- a. Plot the function on rectangular coordinates.
 - b. Plot the function on semilog coordinates.
 - c. Plot the function on log-log coordinates.
 - d. Discuss the implications of each plot as it would relate to analyzing experimental data.
- 1.20** A bulb thermometer hangs outside a window and is used to measure the outside temperature. Comment on some extraneous variables that might affect the difference between the actual outside temperature and the indicated temperature from the thermometer.
- 1.21** A synchronous electric motor test stand permits either the variation of input voltage or output shaft load and the subsequent measurement of motor efficiency, winding temperature, and input current. Comment on the independent, dependent, and extraneous variables for a motor test.
- 1.22** The transducer specified in Table 1.1 is chosen to measure a nominal pressure of 500 cm H₂O. The ambient temperature is expected to vary between 18° and 25°C during tests. Estimate the magnitude of each elemental error affecting the measured pressure.
- 1.23** A force measurement system (weight scale) has the following specifications:

Range:	0 to 1000 N
Linearity error:	0.10% FSO
Hysteresis error:	0.10% FSO
Sensitivity error:	0.15% FSO
Zero drift:	0.20% FSO

Estimate the overall instrument uncertainty for this system based on available information. FSO refers to full-scale operating range.

- 1.24** An engineer ponders a test plan, thinking: “What strategy should I include to estimate any variation over time of the measured variable? What strategy should I include to estimate my control of the independent variable during the test?” What does the engineer mean?
- 1.25** If the outcome of a test was suspected to be dependent on the ability to control the test operating conditions, what strategy should be incorporated into the test plan to estimate this effect?
- 1.26** State the purpose of using randomization methods during a test. Develop an example to illustrate your point.
- 1.27** Provide an example of repetition and replication in a test plan from your own experience.
- 1.28** Develop a test plan that might be used to estimate the average temperature that could be maintained in a heated room as a function of the heater thermostat setting.

- 1.29** Develop a test plan that might be used to evaluate the fuel efficiency of a production model automobile. Explain your reasoning.
- 1.30** A race engine shop has just completed two engines of the same design. How might you determine which engine performs better: (a) on a test stand (engine dynamometer) or (b) at the race track? Describe some measurements that you feel might be useful and how you might use that information. Discuss possible differences between the two tests and how these might influence the results (e.g., you can control room conditions on a test stand but not at a track).
- 1.31** A large batch of carefully made machine shafts can be manufactured on 1 of 4 lathes by 1 of 12 quality machinists. Set up a test matrix to estimate the tolerances that can be held within a production batch. Explain your reasoning.
- 1.32** Suggest an approach(es) to estimate the linearity error and the hysteresis error of a measurement system.
- 1.33** Suggest a test matrix to evaluate the wear performance of four different brands of aftermarket passenger car tires of the same size, load, and speed ratings on a fleet of eight cars of the same make. If the cars were not of the same make, what would change?
- 1.34** The relation between the flow rate, Q , through a pipeline of area A and the pressure drop, Δp , across an orifice-type flow meter inserted in that line (Fig. 1.14) is given by

$$Q = CA \sqrt{\frac{2\Delta p}{\rho}}$$

where ρ is density and C is a coefficient. For a pipe diameter of 1 m and a flow range of 20°C water between 2 and 10 m³/min and $C = 0.75$, plot the expected form of the calibration curve for flow rate versus pressure drop over the flow range. Is the static sensitivity a constant? Incidentally, such an instrument test is described by ANSI/ASME Test Standard PTC 19.5.

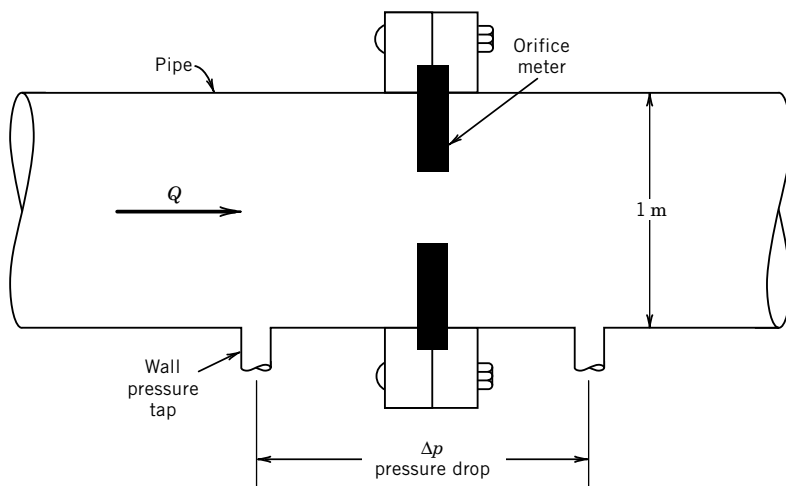


Figure 1.14 Orifice flow meter setup used for Problem 1.34.

- 1.35** The sale of motor fuel is an essential business in the global economy. Federal (US) law requires accurate measurement of the quantity of fuel delivered at a retail establishment. Determine:
- The federal standard for minimum accuracy of a gas pump.
 - The maximum allowable error in the delivery of 25 gallons of fuel (or 100 L of fuel).
 - An estimate of the cost of the maximum allowable error over the 10-year life of a vehicle that is driven 15,000 miles per year at the average fuel mileage of the American passenger car fleet.
- 1.36** For the orifice meter calibration in Problem 1.34: Would the term “linearity error” have a meaning for this system? Explain. Also, list the dependent and independent variables in the calibration.
- 1.37** A piston engine manufacturer uses four different subcontractors to plate the pistons for a make of engine. Plating thickness is important in quality control (performance and part life). Devise a test matrix to assess how well the manufacturer can control plating under its current system.
- 1.38** A simple thermocouple circuit is formed using two wires of different alloy: one end of the wires is twisted together to form the measuring junction, while the other ends are connected to a voltmeter and form the reference junction. A voltage is set up by the difference in temperature between the two junctions. For a given pair of alloy material and reference junction temperature, the temperature of the measuring junction is inferred from the measured voltage difference. For a measurement, what variables need to be controlled? What are the dependent and independent variables?
- 1.39** A linear variable displacement transducer (LVDT) senses displacement and indicates a voltage output, which is linear to the input. Figure 1.15 shows an LVDT setup used for static calibration. It uses a micrometer to apply the known displacement and a voltmeter for the output. A well-defined voltage powers the transducer. What are the independent and dependent variables in this calibration? Can you suggest any extraneous variables? What would be involved in a replication?
- 1.40** For the LVDT calibration of the previous problem, what would be involved in determining the repeatability of the instrument? The reproducibility? What effects are different in the two tests? Explain.

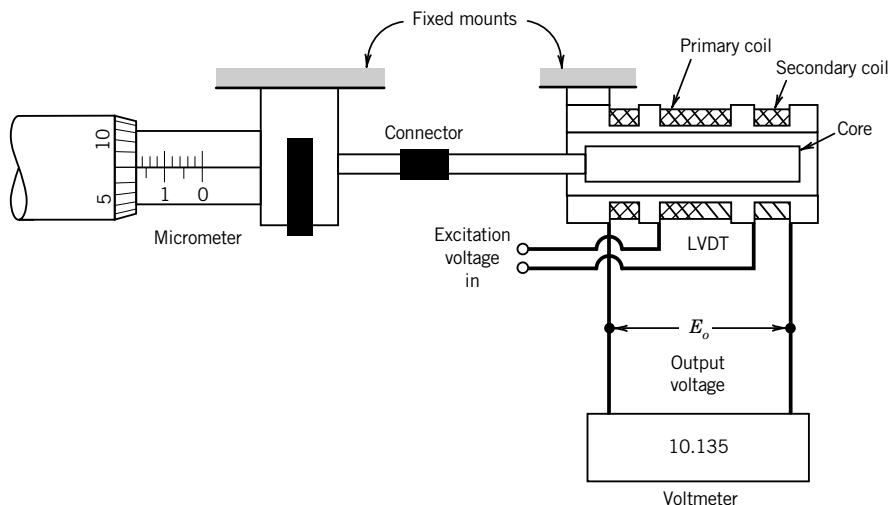


Figure 1.15 LVDT setup used for Problem 1.39.

1.41 A manufacturer wants to quantify the expected average fuel mileage of a product line of automobiles. They decide that they can put one or more cars on a chassis dynamometer and run the wheels at desired speeds and loads to assess this, or they can use drivers and drive the cars over some selected course instead. (a) Discuss the merits of either approach, considering the control of variables and identifying extraneous variables. (b) Can you recognize that somewhat different tests might provide answers to different questions? For example, discuss the difference in meanings possible from the results of operating one car on the dynamometer and comparing it to one driver on a course. Cite other examples. (c) Are these two test methods examples of concomitant methods?

1.42 We need to measure the coefficient of restitution of a volleyball by dropping the ball from a known height H and measuring the height of the bounce, h . The coefficient of restitution, C_R , is then calculated as

$$C_R = \sqrt{\frac{h}{H}}$$

a. Develop a test plan for measuring C_R that includes the range of conditions expected in college-level volleyball play.

b. Identify extraneous variables that may affect the resulting values of C_R .

1.43 Light gates may be used to measure the speed of projectiles, such as arrows shot from a bow. English long bows made of yew wood in the 1400s achieved launch speeds of 60 m/s. Determine the relationship between the distance between light gates and the accuracy required for sensing the times when the light gate senses the presence of the arrow.

1.44 You estimate your car's fuel use by comparing fuel volume used over a known distance. Your brother, who drives the same model car, disagrees with your claimed results based on his own experience. How might you justify the differences based on the concepts of control of variables, interference and noises effects, and test matrix used?

1.45 In discussing concomitant methods, we cited an example of computing the volume of a cylindrical rod based on its average dimensions versus known weight and material properties. While we should not expect too different an answer with either technique, identify where noise and interference effects will affect the result of either method.

1.46 When a strain gauge is stretched under uniaxial tension, its resistance varies with the imposed strain. A resistance bridge circuit is used to convert the resistance change into a voltage. Suppose a known tensile load were applied to the system shown in Figure 1.16 and the output measured on a voltmeter. What are the independent and dependent variables in this calibration? Can you suggest any extraneous variables? What would be involved in a replication?

1.47 For the strain gauge calibration of the previous problem, what would be involved in determining the repeatability of the instrument? The reproducibility? What effects are different in the tests? Explain.

1.48 A major tennis manufacturer is undertaking a test program for shoes, tennis balls, and tennis strings. Develop a test plan for the situations described below. In each case provide details for how the test should be conducted, and describe expected difficulties in interpreting the results. In each case the tests are to be conducted during college tennis matches. Four teams of six players each are to test the products under match (as opposed to practice) conditions. A tennis team consists of six players, and a match consists of six singles matches and three doubles matches.

a. Tennis shoes: Two different sole designs and materials are to be wear tested. The life of the soles are known to be strongly affected by court surface and playing style.

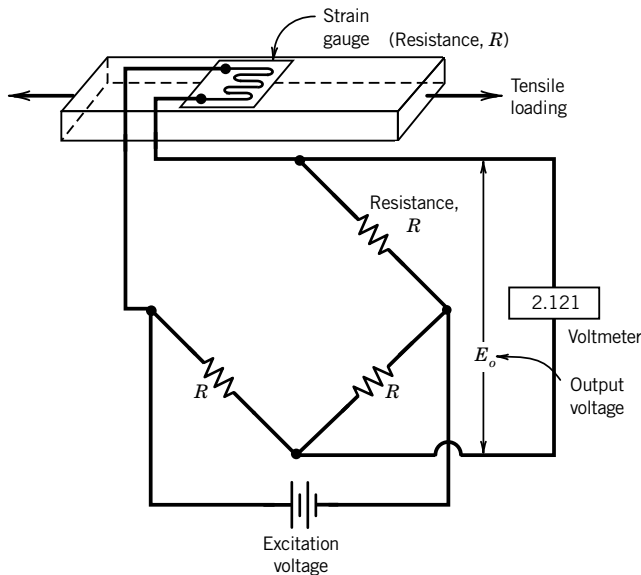


Figure 1.16 Strain gauge setup used for Problem 1.46.

- b. Tennis strings: A new tennis string material is to be tested for durability. String failure occurs due to breakage or due to loss of tension. String life is a function of the racquet, the player's style, and string tension.
 - c. Tennis balls: Two tennis balls are to be play tested for durability. The condition of a tennis ball can be described by the coefficient of restitution, and the total weight (since the cover material actually is lost during play). A player's style and the court surface are the primary determining factors on tennis ball wear.
- 1.49** The acceleration of a cart down a plane inclined at an angle α to horizontal can be determined by measuring the change in speed of the cart at two points, separated by a distance s , along the inclined plane. Suppose two photocells are fixed at the two points along the plane. Each photocell measures the time for the cart, which has a length L , to pass it. Identify the important variables in this test. List any assumptions that you feel are intrinsic to such a test. Suggest a concomitant approach. How would you interpret the data to answer the question?
- 1.50** Is it more fuel efficient to drive a car in warm, humid weather with the air conditioning on and windows closed, or with the air conditioning off and the windows open for ventilation? Develop a test plan to address this question. Include a concomitant approach (experimental or analytical) that might assess the validity of your test results.
- 1.51** Explain the potential differences in the following evaluations of an instrument's accuracy. Figure 1.12 will be useful, and you may refer to ASTM E177, if needed.
 - a. The closeness of agreement between the true value and the average of a large set of measurements.
 - b. The closeness of agreement between the true value and an individual measurement.
- 1.52** Suggest a reasonable number of significant digits for reporting the following common values and give some indication as to your reasoning:
 - a. Your body weight for a passport
 - b. A car's fuel usage (use liters per 100 km)

- c. The weight of a bar of pure (at least 99.5%) gold (consider a 1 kg_f bar and a 100 oz bar)
 - d. Distance traveled by a body in 1 second if moving at 1 m/s (use meters)
- 1.53** Research the following test codes (these are available in most libraries). Write a short (200-word) report that describes the intent and an overview of the code:
- a. ASTM F 558-88 (Air Performance of Vacuum Cleaners)
 - b. ANSI Z21.86 (Gas Fired Space Heating Appliances)
 - c. ISO 10770-1:1998 (Test Methods for Hydraulic Control Valves)
 - d. ANSI/ASME PTC19.1-2005 (Test Uncertainty)
 - e. ISO 7401:1988 (Road Vehicles: Lateral Response Test Methods)
 - f. Your local municipal building code or housing ordinance
 - g. Any other code assigned by your instructor
- 1.54** Show how the following functions can be transformed into a linear curve of the form $Y = a_1X + a_0$ where a_1 and a_0 are constants. Let m , b , and c be constants.
- a. $y = bx^m$
 - b. $y = be^{mx}$
 - c. $y = b + c \sqrt[m]{x}$

Chapter 2

Static and Dynamic Characteristics of Signals

2.1 INTRODUCTION

A measurement system takes an *input* quantity and transforms it into an *output* quantity that can be observed or recorded, such as the movement of a pointer on a dial or the magnitude of a digital display. This chapter discusses the characteristics of both the input signals to a measurement system and the resulting output signals. The shape and form of a signal are often referred to as its *waveform*. The waveform contains information about the *magnitude* and *amplitude*, which indicate the size of the input quantity, and the *frequency*, which indicates the way the signal changes in time. An understanding of waveforms is required for the selection of measurement systems and the interpretation of measured signals.

2.2 INPUT/OUTPUT SIGNAL CONCEPTS

Two important tasks that engineers face in the measurement of physical variables are (1) selecting a measurement system and (2) interpreting the output from a measurement system. A simple example of selecting a measurement system might be the selection of a tire gauge for measuring the air pressure in a bicycle tire or in a car tire, as shown in Figure 2.1. The gauge for the car tire would be required to indicate pressures up to 275 kPa (40 lb/in.²), but the bicycle tire gauge would be required to indicate higher pressures, maybe up to 700 kPa (100 lb/in.²). This idea of the *range* of an instrument, its lower to upper measurement limits, is fundamental to all measurement systems and demonstrates that some basic understanding of the nature of the input signal, in this case the magnitude, is necessary in evaluating or selecting a measurement system for a particular application.

A much more difficult task is the evaluation of the output of a measurement system when the time or spatial behavior of the input is not known. The pressure in a tire does not change while we are trying to measure it, but what if we wanted to measure pressure in a cylinder in an automobile engine? Would the tire gauge or another gauge based on its operating principle work? We know that the pressure in the cylinder varies with time. If our task was to select a measurement system to determine this time-varying pressure, information about the pressure variations in the cylinder would be necessary. From thermodynamics and the speed range of the engine, it may be possible to estimate the magnitude of pressures to be expected and the rate with which they change. From that

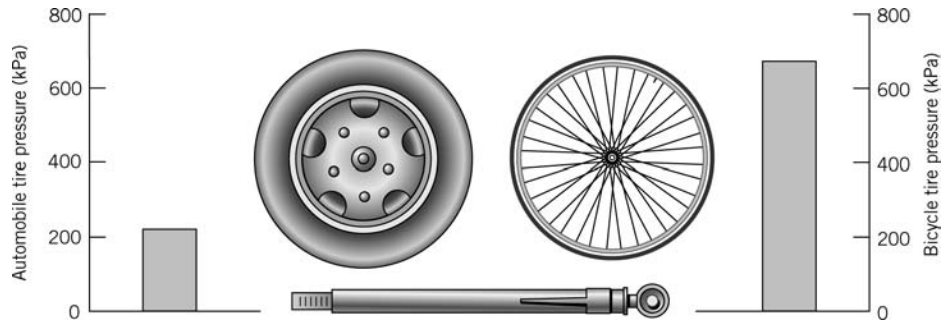


Figure 2.1 Measurement system selection based on input signal range.

we can select an appropriate measurement system. But to do this we need to develop a way to express this idea of the magnitude and rate of change of a variable.

Upon completion of this chapter, the reader will be able to

- define the range of an instrument,
- classify signals as analog, discrete time, or digital,
- compute the mean and rms values for time-varying signals, and
- characterize signals in the frequency domain.

Generalized Behavior

Many measurement systems exhibit similar responses under a variety of conditions, which suggests that the performance and capabilities of measuring systems may be described in a generalized way. To examine further the generalized behavior of measurement systems, we first examine the possible forms of the input and output signals. We will associate the term “signal” with the “transmission of information.” A *signal* is the physical information about a measured variable being transmitted between a process and the measurement system, between the stages of a measurement system, or as the output from a measurement system.

Classification of Waveforms

Signals may be classified as analog, discrete time, or digital. *Analog* describes a signal that is continuous in time. Because physical variables tend to be continuous, an analog signal provides a ready representation of their time-dependent behavior. In addition, the magnitude of the signal is continuous and thus can have any value within the operating range. An analog signal is shown in Figure 2.2a; a similar continuous signal would result from a recording of the pointer rotation with time for the output display shown in Figure 2.2b. Contrast this continuous signal with the signal shown in Figure 2.3a. This format represents a *discrete time signal*, for which information about the magnitude of the signal is available only at discrete points in time. A discrete time signal usually results from the sampling of a continuous variable at repeated finite time intervals. Because information in the signal shown in Figure 2.3a is available only at discrete times, some assumption must be made about the behavior of the measured variable during the times when it is not available. One approach is to assume the signal is constant between samples, a sample and hold method. The

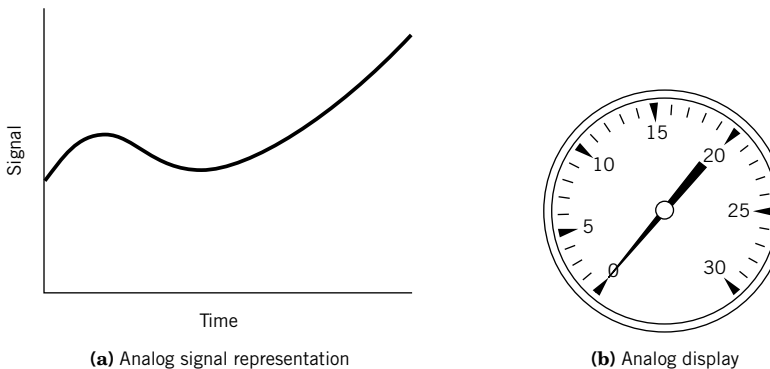


Figure 2.2 Analog signal concepts.

resulting waveform is shown in Figure 2.3b. Clearly, as the time between samples is reduced, the difference between the discrete variable and the continuous signal it represents decreases.

Digital signals are particularly useful when data acquisition and processing are performed using a digital computer. A digital signal has two important characteristics. First, a digital signal exists at discrete values in time, like a discrete time signal. Second, the magnitude of a digital signal is discrete, determined by a process known as quantization at each discrete point in time. *Quantization* assigns a single number to represent a range of magnitudes of a continuous signal.

Figure 2.4a shows digital and analog forms of the same signal where the magnitude of the digital signal can have only certain discrete values. Thus, a digital signal provides a quantized magnitude at discrete times. The waveform that would result from assuming that the signal is constant between sampled points in time is shown in Figure 2.4b.

As an example of quantization, consider a digital clock that displays time in hours and minutes. For the entire duration of 1 minute, a single numerical value is displayed until it is updated at the next discrete time step. As such, the continuous physical variable of time is quantized in its conversion to a digital display.

Sampling of an analog signal to produce a digital signal can be accomplished by using an *analog-to-digital (A/D) converter*, a solid-state device that converts an analog voltage signal to a

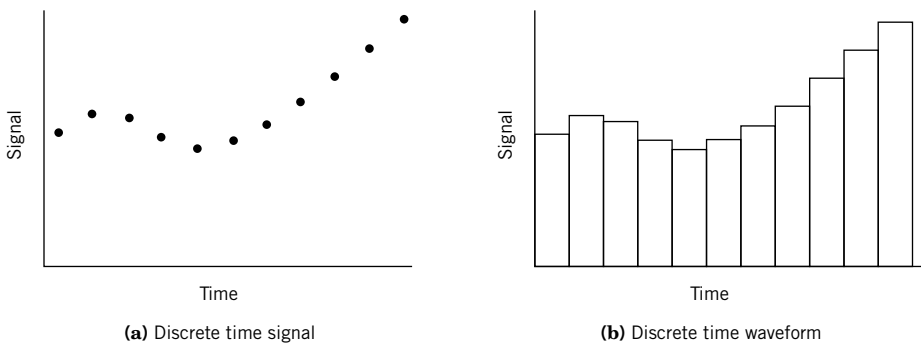


Figure 2.3 Discrete time signal concepts.

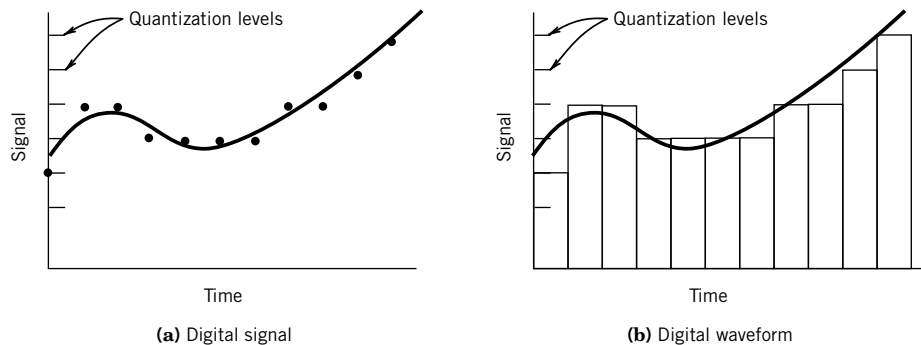


Figure 2.4 Digital signal representation and waveform.

binary number system representation. The limited resolution of the binary number that corresponds to a range of voltages creates the quantization levels and ranges.

For example, a compact disk player is built around technology that relies on the conversion of a continuously available signal, such as music from a microphone, into a digital form. The digital information is stored on a compact disk and later read in digital form by a laser playback system (1). However, to serve as input to a traditional stereo amplifier, and since speakers and the human ear are analog devices, the digital information is converted back into a continuous voltage signal for playback.

Signal Waveforms

In addition to classifying signals as analog, discrete time, or digital, some description of the waveform associated with a signal is useful. Signals may be characterized as either static or dynamic. A *static signal* does not vary with time. The diameter of a shaft is an example. Many physical variables change slowly enough in time, compared to the process with which they interact, that for all practical purposes these signals may be considered static in time. For example, the voltage across the terminals of a battery is approximately constant over its useful life. Or consider measuring temperature by using an outdoor thermometer; since the outdoor temperature does not change significantly in a matter of minutes, this input signal might be considered static when compared to our time period of interest. A mathematical representation of a static signal is given by a constant, as indicated in Table 2.1. In contrast, often we are interested in how the measured variable changes with time. This leads us to consider time-varying signals further.

A *dynamic signal* is defined as a time-dependent signal. In general, dynamic signal waveforms, $y(t)$, may be classified as shown in Table 2.1. A *deterministic signal* varies in time in a predictable manner, such as a sine wave, a step function, or a ramp function, as shown in Figure 2.5. A signal is *steady periodic* if the variation of the magnitude of the signal repeats at regular intervals in time. Examples of steady periodic behaviors are the motion of an ideal pendulum, and the temperature variations in the cylinder of an internal combustion engine under steady operating conditions. Periodic waveforms may be classified as simple or complex. A *simple periodic waveform* contains only one frequency. A *complex periodic waveform* contains multiple frequencies and is represented as a superposition of multiple simple periodic waveforms. *Aperiodic* is the term used to describe deterministic signals that do not repeat at regular intervals, such as a step function.

Table 2.1 Classification of Waveforms

I.	Static	$y(t) = A_0$
II.	Dynamic	
	Periodic waveforms	
	Simple periodic waveform	$y(t) = A_0 + C \sin(\omega t + \phi)$
	Complex periodic waveform	$y(t) = A_0 + \sum_{n=1}^{\infty} C_n \sin(n\omega t + \phi_n)$
	Aperiodic waveforms	
	Step ^a	$y(t) = A_0 U(t)$ $= A_0$ for $t > 0$
	Ramp	$y(t) = A_0 t$ for $0 < t < t_f$
	Pulse ^b	$y(t) = A_0 U(t) - A_0 U(t - t_1)$
III.	Nondeterministic waveform	$y(t) \approx A_0 + \sum_{n=1}^{\infty} C_n \sin(n\omega t + \phi_n)$

^a $U(t)$ represents the unit step function, which is zero for $t < 0$ and 1 for $t \geq 0$.

^b t_1 represents the pulse width.

Also described in Figure 2.5 is a *nondeterministic signal* that has no discernible pattern of repetition. A nondeterministic signal cannot be prescribed before it occurs, although certain characteristics of the signal may be known in advance. As an example, consider the transmission of data files from one computer to another. Signal characteristics such as the rate of data transmission and the possible range of signal magnitude are known for any signal in this system. However, it would not be possible to predict future signal characteristics based on existing information in such a signal. Such a signal is properly characterized as nondeterministic. Nondeterministic signals are generally described by their statistical characteristics or a model signal that represents the statistics of the actual signal.

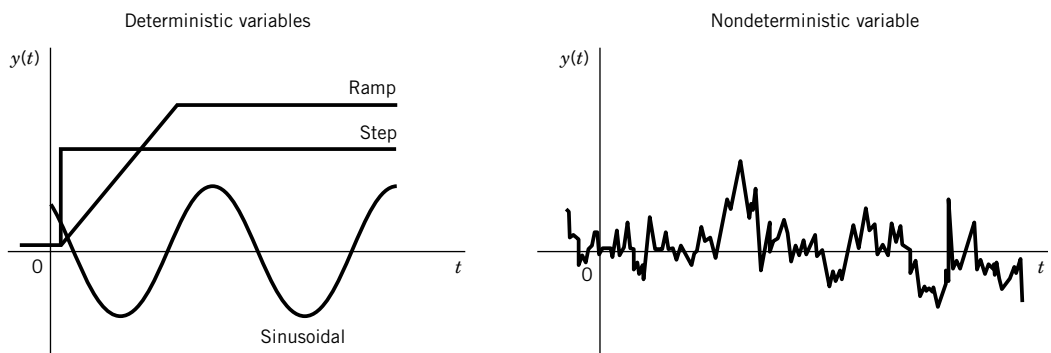


Figure 2.5 Examples of dynamic signals.

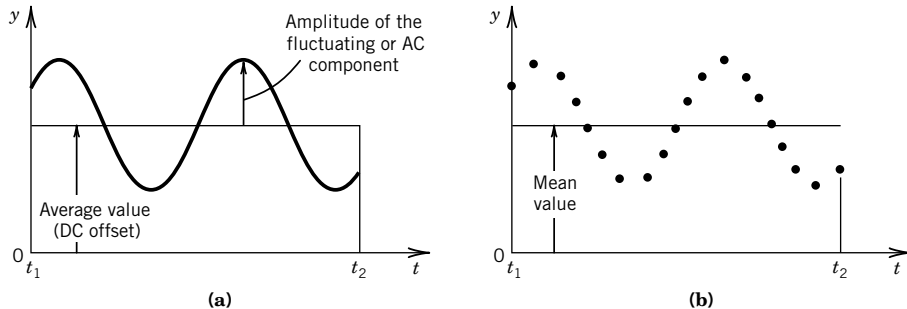


Figure 2.6 Analog and discrete representations of a dynamic signal.

2.3 SIGNAL ANALYSIS

In this section, we consider concepts related to the characterization of signals. A measurement system produces a signal that may be analog, discrete time, or digital. An analog signal is continuous with time and has a magnitude that is analogous to the magnitude of the physical variable being measured. Consider the analog signal shown in Figure 2.6a, which is continuous over the recorded time period from t_1 to t_2 . The average or mean value¹ of this signal is found by

$$\bar{y} \equiv \frac{\int_{t_1}^{t_2} y(t) dt}{\int_{t_1}^{t_2} dt} \quad (2.1)$$

The mean value, as defined in Equation 2.1, provides a measure of the static portion of a signal over the time $t_2 - t_1$. It is sometimes called the *DC component* or DC offset of the signal.

The mean value does not provide any indication of the amount of variation in the dynamic portion of the signal. The characterization of the dynamic portion, or *AC component*, of the signal may be illustrated by considering the average power dissipated in an electrical resistor through which a fluctuating current flows. The power dissipated in a resistor due to the flow of a current is

$$P = I^2 R$$

where

P = power dissipated = time rate of energy dissipated

I = current

R = resistance

If the current varies in time, the total electrical energy dissipated in the resistor over the time t_1 to t_2 would be

$$\int_{t_1}^{t_2} P dt = \int_{t_1}^{t_2} [I(t)]^2 R dt \quad (2.2)$$

The current $I(t)$ would, in general, include both a DC component and a changing AC component.

¹ Strictly speaking, for a continuous signal the mean value and the average value are the same. This is not true for discrete time signals.

Signal Root-Mean-Square Value

Consider finding the magnitude of a constant effective current, I_e , that would produce the same total energy dissipation in the resistor as the time-varying current, $I(t)$, over the time period t_1 to t_2 . Assuming that the resistance, R , is constant, this current would be determined by equating $(I_e)^2 R(t_2 - t_1)$ with Equation 2.2 to yield

$$I_e = \sqrt{\frac{1}{t_2 - t_1} \int_{t_1}^{t_2} [I(t)]^2 dt} \quad (2.3)$$

This value of the current is called the root-mean-square (rms) value of the current. Based on this reasoning, the rms value of any continuous analog variable $y(t)$ over the time, $t_2 - t_1$, is expressed as

$$y_{\text{rms}} = \sqrt{\frac{1}{t_2 - t_1} \int_{t_1}^{t_2} y^2 dt} \quad (2.4)$$

Discrete-Time or Digital Signals

A time-dependent analog signal, $y(t)$, can be represented by a discrete set of N numbers over the time period from t_1 to t_2 through the conversion

$$y(t) \rightarrow \{y(r\delta t)\} \quad r = 0, 1, \dots, (N - 1)$$

which uses the sampling convolution

$$\{y(r\delta t)\} = y(t)\delta(t - r\delta t) = \{y_i\} \quad i = 0, 1, 2, \dots, (N - 1)$$

Here, $\delta(t - r\delta t)$ is the delayed unit impulse function, δt is the sample time increment between each number, and $N\delta t = t_2 - t_1$ gives the total sample period over which the measurement of $y(t)$ takes place. The effect of discrete sampling on the original analog signal is demonstrated in Figure 2.6b in which the analog signal has been replaced by $\{y(r\delta t)\}$, which represents N values of a discrete time signal representing $y(t)$.

For either a discrete time signal or a digital signal, the mean value can be estimated by the discrete equivalent of Equation 2.1 as

$$\bar{y} = \frac{1}{N} \sum_{i=0}^{N-1} y_i \quad (2.5)$$

where each y_i is a discrete number in the data set of $\{y(r\delta t)\}$. The mean approximates the static component of the signal over the time interval t_1 to t_2 . The rms value can be estimated by the discrete equivalent of Equation 2.4 as

$$y_{\text{rms}} = \sqrt{\frac{1}{N} \sum_{i=0}^{N-1} y_i^2} \quad (2.6)$$

The rms value takes on additional physical significance when either the signal contains no DC component or the DC component has been subtracted from the signal. The rms value of a signal having a zero mean is a statistical measure of the magnitude of the fluctuations in the signal.

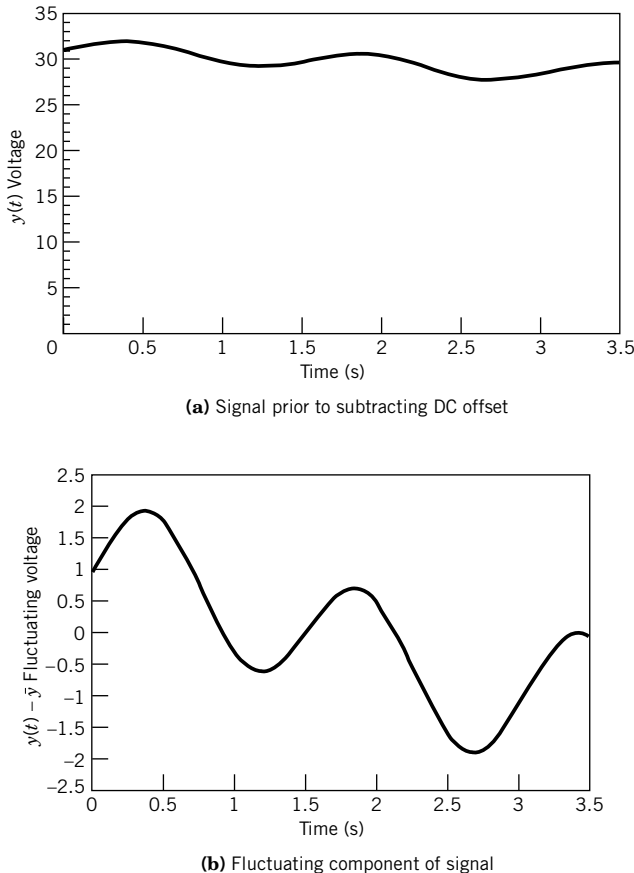


Figure 2.7 Effect of subtracting DC offset for a dynamic signal.

Direct Current Offset

When the AC component of the signal is of primary interest, the DC component can be removed. This procedure often allows a change of scale in the display or plotting of a signal such that fluctuations that were a small percentage of the DC signal can be more clearly observed without the superposition of the large DC component. The enhancement of fluctuations through the subtraction of the average value is illustrated in Figure 2.7.

Figure 2.7a contains the entire complex waveform consisting of both static (DC) and dynamic (AC) parts. When the DC component is removed, the characteristics of the fluctuating component of the signal are readily observed, as shown in Figure 2.7b. The statistics of the fluctuating component of the signal dynamic portion may contain important information for a particular application.

Example 2.1

Suppose the current passing through a resistor can be described by

$$I(t) = 10 \sin t$$

where I represents the time-dependent current in amperes. Establish the mean and rms values of current over a time from 0 to t_f , with $t_f = \pi$ and then with $t_f = 2\pi$. How do the results relate to the power dissipated in the resistor?

KNOWN $I(t) = 10 \sin t$

FIND \bar{I} and I_{rms} with $t_f = \pi$ and 2π

SOLUTION The average value for a time from 0 to t_f is found from Equation 2.1 as

$$\bar{I} = \frac{\int_0^{t_f} I(t) dt}{\int_0^{t_f} dt} = \frac{\int_0^{t_f} 10 \sin t dt}{t_f}$$

Evaluation of this integral yields

$$\bar{I} = \frac{1}{t_f} [-10 \cos t]_0^{t_f}$$

With $t_f = \pi$, the average value, \bar{I} , is $20/\pi$. For $t_f = 2\pi$, the evaluation of the integral yields an average value of zero.

The rms value for the time period 0 to t_f is given by the application of Equation 2.4, which yields

$$I_{\text{rms}} = \sqrt{\frac{1}{t_f} \int_0^{t_f} I(t)^2 dt} = \sqrt{\frac{1}{t_f} \int_0^{t_f} (10 \sin t)^2 dt}$$

This integral is evaluated as

$$I_{\text{rms}} = \sqrt{\frac{100}{t_f} \left(-\frac{1}{2} \cos t \sin t + \frac{t}{2} \right) \Big|_0^{t_f}}$$

For $t_f = \pi$, the rms value is $\sqrt{50}$. Evaluation of the integral for the rms value with $t_f = 2\pi$ also yields $\sqrt{50}$.

COMMENT Although the average value over the period 2π is zero, the power dissipated in the resistor must be the same over both the positive and negative half-cycles of the sine function. Thus, the rms value of current is the same for the time period of π and 2π and is indicative of the rate at which energy is dissipated.

2.4 SIGNAL AMPLITUDE AND FREQUENCY

A key factor in measurement system behavior is the nature of the input signal to the system. A means is needed to classify waveforms for both the input signal and the resulting output signal relative to their magnitude and frequency. It would be very helpful if the behavior of measurement systems could be defined in terms of their response to a limited number and type of input signals. This is, in fact, exactly the case. A very complex signal, even one that is nondeterministic in nature, can be approximated as an infinite series of sine and cosine functions, as suggested in Table 2.1. The method of expressing such a complex signal as a series of sines and cosines is called *Fourier analysis*.

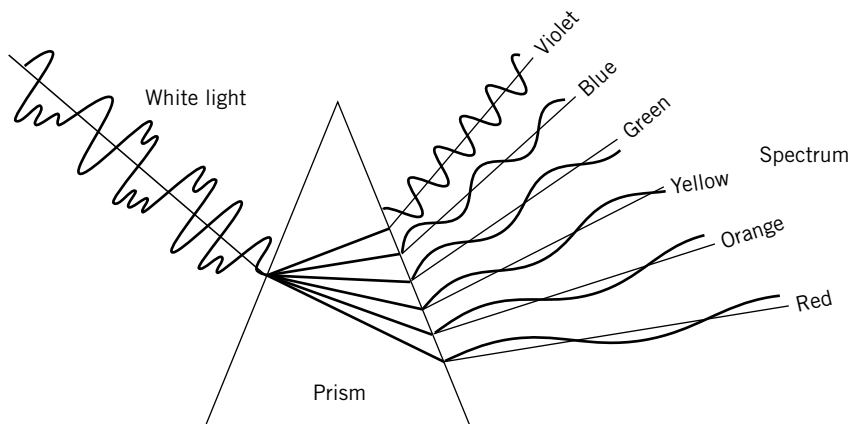


Figure 2.8 Separation of white light into its color spectrum. Color corresponds to a particular frequency or wavelength; light intensity corresponds to varying amplitudes.

Nature provides some experiences that support our contention that complex signals can be represented by the addition of a number of simpler periodic functions. For example, combining a number of different pure tones can generate rich musical sound. And an excellent physical analogy for Fourier analysis is provided by the separation of white light through a prism. Figure 2.8 illustrates the transformation of a complex waveform, represented by white light, into its simpler components, represented by the colors in the spectrum. In this example, the colors in the spectrum are represented as simple periodic functions that combine to form white light. Fourier analysis is roughly the mathematical equivalent of a prism and yields a representation of a complex signal in terms of simple periodic functions.

The representation of complex and nondeterministic waveforms by simple periodic functions allows measurement system response to be reasonably well defined by examining the output resulting from a few specific input waveforms, one of which is a simple periodic. As represented in Table 2.1, a simple periodic waveform has a single, well-defined amplitude and a single frequency. Before a generalized response of measurement systems can be determined, an understanding of the method of representing complex signals in terms of simpler functions is necessary.

Periodic Signals

The fundamental concepts of frequency and amplitude can be understood through the observation and analysis of periodic motions. Although sines and cosines are by definition geometric quantities related to the lengths of the sides of a right triangle, for our purposes sines and cosines are best thought of as mathematical functions that describe specific physical behaviors of systems. These behaviors are described by differential equations that have sines and cosines as their solutions. As an example, consider a mechanical vibration of a mass attached to a linear spring, as shown in Figure 2.9. For a linear spring, the spring force F and displacement y are related by $F = ky$, where k is the constant of proportionality, called the spring constant. Application of Newton's second law to this system yields a governing equation for the displacement y as a function of time t as

$$m \frac{d^2y}{dt^2} + ky = 0 \quad (2.7)$$

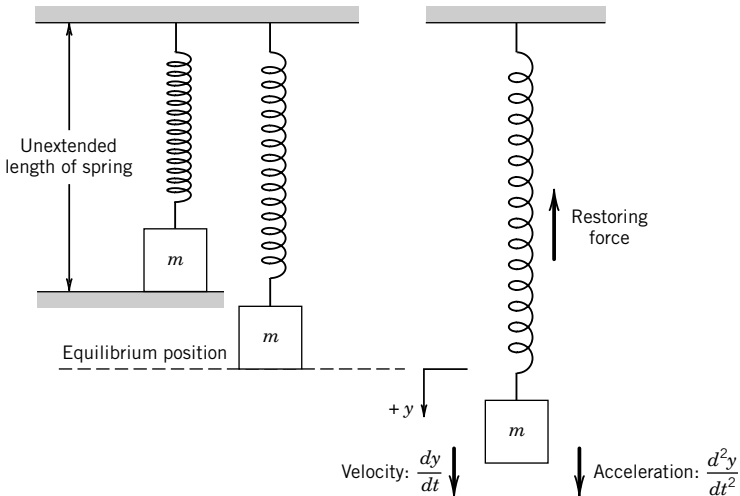


Figure 2.9 Spring-mass system.

This linear, second-order differential equation with constant coefficients describes the motion of the idealized spring mass system when there is no external force applied. The general form of the solution to this equation is

$$y = A \cos \omega t + B \sin \omega t \quad (2.8)$$

where $\omega = \sqrt{k/m}$. Physically we know that if the mass is displaced from the equilibrium point and released, it will oscillate about the equilibrium point. The time required for the mass to finish one complete cycle of the motion is called the *period*, and is generally represented by the symbol T .

Frequency is related to the period and is defined as the number of complete cycles of the motion per unit time. This *frequency*, f , is measured in cycles per second (Hz; 1 cycle/s = 1 Hz). The term ω is also a frequency, but instead of having units of cycles per second it has units of radians per second. This frequency, ω , is called the *circular frequency* since it relates directly to cycles on the unit circle, as illustrated in Figure 2.10. The relationship among ω , f , and the period, T , is

$$T = \frac{2\pi}{\omega} = \frac{1}{f} \quad (2.9)$$

In Equation 2.8, the sine and cosine terms can be combined if a phase angle is introduced such that

$$y = C \cos (\omega t - \phi) \quad (2.10a)$$

or

$$y = C \sin (\omega t + \phi^*) \quad (2.10b)$$

The values of C , ϕ , and ϕ^* are found from the following trigonometric identities:

$$\begin{aligned} A \cos \omega t + B \sin \omega t &= \sqrt{A^2 + B^2} \cos(\omega t - \phi) \\ A \cos \omega t + B \sin \omega t &= \sqrt{A^2 + B^2} \sin(\omega t + \phi^*) \\ \phi &= \tan^{-1} \frac{B}{A} \quad \phi^* = \tan^{-1} \frac{A}{B} \quad \phi^* = \frac{\pi}{2} - \phi \end{aligned} \quad (2.11)$$

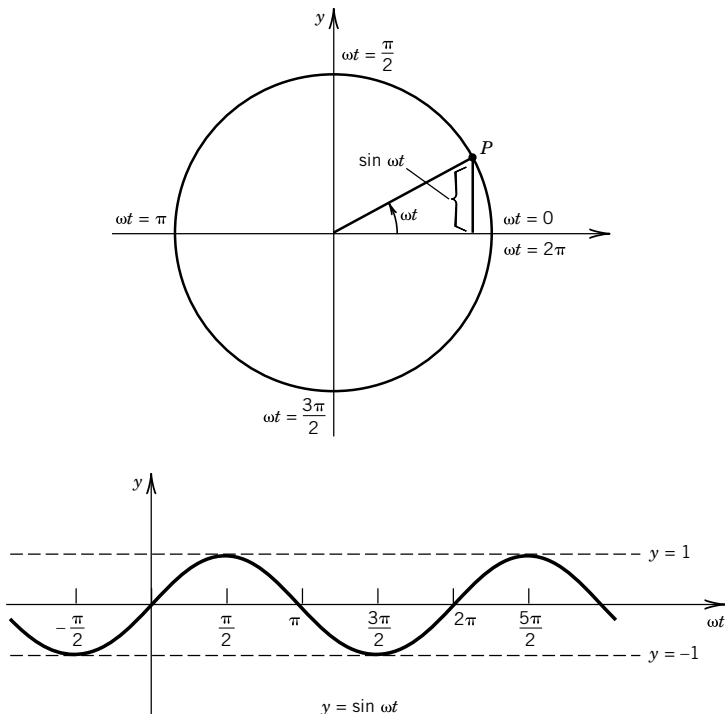


Figure 2.10 Relationship between cycles on the unit circle and circular frequency.

The size of the maximum and minimum displacements from the equilibrium position, or the value C , is the amplitude of the oscillation. The concepts of amplitude and frequency are essential for the description of time-dependent signals.

Frequency Analysis

Many signals that result from the measurement of dynamic variables are nondeterministic in nature and have a continuously varying rate of change. These signals, having *complex waveforms*, present difficulties in the selection of a measurement system and in the interpretation of an output signal. However, it is possible to separate a complex signal, or any signal for that matter, into a number of sine and cosine functions. *In other words, any complex signal can be thought of as made up of sines and cosines of differing periods and amplitudes, which are added together in an infinite trigonometric series.* This representation of a signal as a series of sines and cosines is called a *Fourier series*. Once a signal is broken down into a series of periodic functions, the importance of each frequency can be easily determined. This information about frequency content allows proper choice of a measurement system, and precise interpretation of output signals.

In theory, Fourier analysis allows essentially all mathematical functions of practical interest to be represented by an infinite series of sines and cosines.²

² A periodic function may be represented as a Fourier series if the function is piecewise continuous over the limits of integration and the function has a left- and right-hand derivative at each point in the interval. The sum of the resulting series is equal to the function at each point in the interval except points where the function is discontinuous.

The following definitions relate to Fourier analysis:

1. A function $y(t)$ is a *periodic function* if there is some positive number T such that

$$y(t + T) = y(t)$$

The *period* of $y(t)$ is T . If both $y_1(t)$ and $y_2(t)$ have period T , then

$$ay_1(t) + by_2(t)$$

also has a period of T (a and b are constants).

2. A *trigonometric series* is given by

$$A_0 + A_1 \cos t + B_1 \sin t + A_2 \cos 2t + B_2 \sin 2t + \dots$$

where A_n and B_n are the coefficients of the series.

Example 2.2

As a physical (instead of mathematical) example of frequency content of a signal, consider stringed musical instruments, such as guitars and violins. When a string is caused to vibrate by plucking or bowing, the sound is a result of the motion of the string and the resonance of the instrument. (The concept of resonance is explored in Chapter 3.) The musical pitch for such an instrument is the lowest frequency of the string vibrations. Our ability to recognize differences in musical instruments is primarily a result of the higher frequencies present in the sound, which are usually integer multiples of the fundamental frequency. These higher frequencies are called *harmonics*.

The motion of a vibrating string is best thought of as composed of several basic motions that together create a musical tone. Figure 2.11 illustrates the vibration modes associated with a string plucked at its center. The string vibrates with a fundamental frequency and odd-numbered harmonics, each having a specific phase relationship with the fundamental. The relative strength of each harmonic is graphically illustrated through its amplitude in Figure 2.11. Figure 2.12 shows the motion, which is caused by plucking a string one-fifth of the distance from a fixed end. The resulting frequencies are illustrated in Figure 2.13. Notice that the fifth harmonic is missing from the resulting sound.

Musical sound from a vibrating string is analogous to a measurement system input or output, which contains many frequency components. Fourier analysis and frequency spectra provide insightful and practical means of reducing such complex signals into a combination of simple waveforms. Next, we explore the frequency and amplitude analysis of complex signals.

Available on the companion software site, *Program Sound.vi* uses your computer's microphone and sound board to sample ambient sounds and to decompose them into harmonics (try humming a tune).

Fourier Series and Coefficients

A periodic function $y(t)$ with a period $T = 2\pi$ is to be represented by a trigonometric series, such that for any t ,

$$y(t) = A_0 + \sum_{n=1}^{\infty} (A_n \cos nt + B_n \sin nt) \quad (2.12)$$

With $y(t)$ known, the coefficients A_n and B_n are to be determined; this requires a well-established mathematical procedure, but not one that we need to reinvent. For A_0 to be determined,

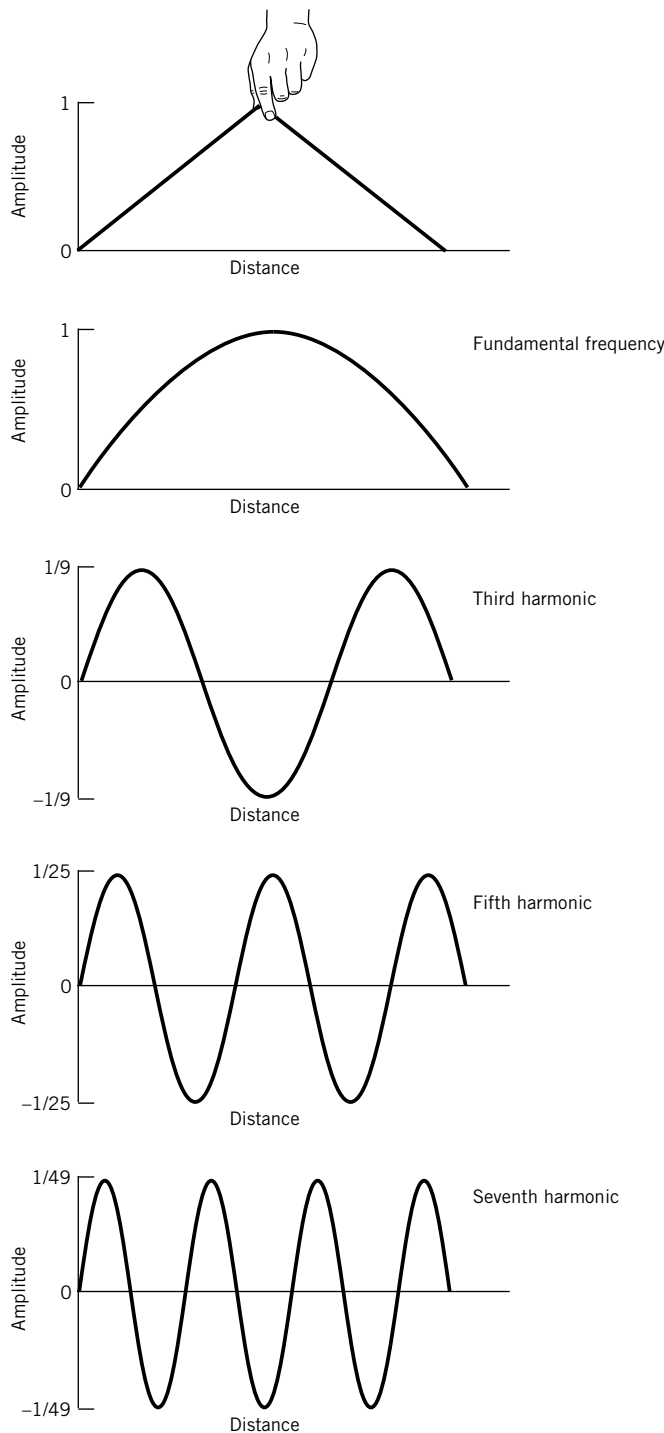


Figure 2.11 Modes of vibration for a string plucked at its center.

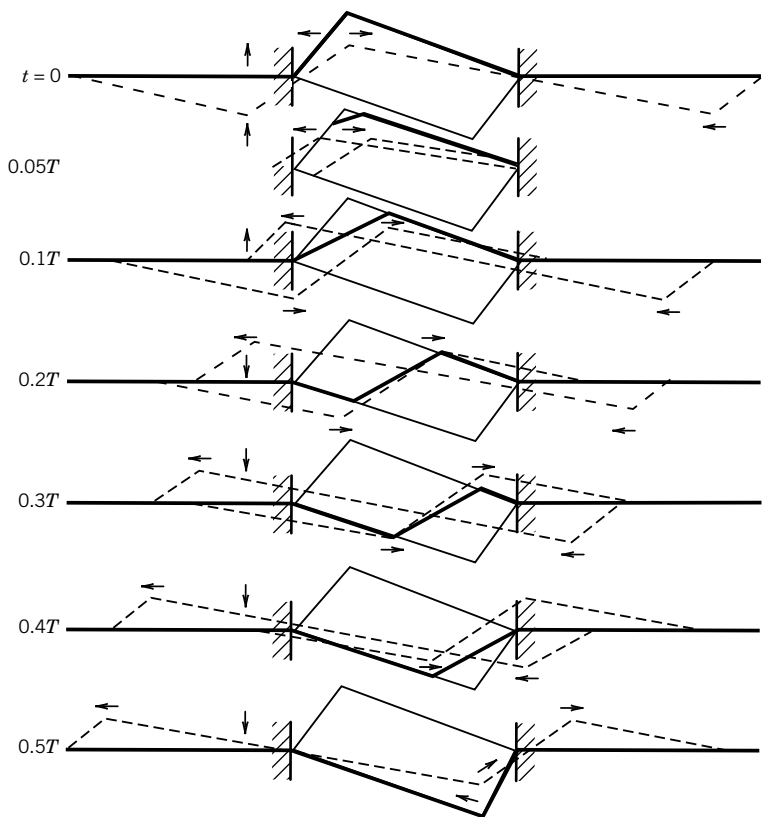


Figure 2.12 Motion of a string plucked one-fifth of the distance from a fixed end. (From N. H. Fletcher and T. D. Rossing, *The Physics of Musical Instruments*. Copyright © 1991 by Springer-Verlag, New York. Reprinted by permission.)

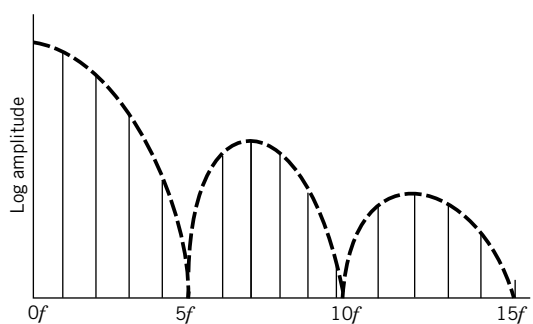


Figure 2.13 Frequency spectrum for a string plucked one-fifth of the distance from a fixed end. (From N. H. Fletcher and T. D. Rossing, *The Physics of Musical Instruments*. Copyright © 1991 by Springer-Verlag, New York. Reprinted by permission.)

Equation 2.12 is integrated from $-\pi$ to π :

$$\int_{-\pi}^{\pi} y(t)dt = A_0 \int_{-\pi}^{\pi} dt + \sum_{n=1}^{\infty} \left(A_n \int_{-\pi}^{\pi} \cos ntdt + B_n \int_{-\pi}^{\pi} \sin ntdt \right) \quad (2.13)$$

Since

$$\int_{-\pi}^{\pi} \cos ntdt = 0 \quad \text{and} \quad \int_{-\pi}^{\pi} \sin ntdt = 0$$

Equation 2.13 yields

$$A_0 = \frac{1}{2\pi} \int_{-\pi}^{\pi} y(t)dt \quad (2.14)$$

The coefficient A_m may be determined by multiplying Equation 2.12 by $\cos mt$ and integrating from $-\pi$ to π . The resulting expression for A_m is

$$A_m = \frac{1}{\pi} \int_{-\pi}^{\pi} y(t)\cos mtdt \quad (2.15)$$

Similarly, multiplying Equation 2.12 by $\sin mt$ and integrating from $-\pi$ to π yields B_m . Thus, for a function $y(t)$ with a period 2π , the coefficients of the trigonometric series representing $y(t)$ are given by the Euler formulas:

$$\begin{aligned} A_0 &= \frac{1}{2\pi} \int_{-\pi}^{\pi} y(t) \\ A_n &= \frac{1}{\pi} \int_{-\pi}^{\pi} y(t)\cos ntdt \\ B_n &= \frac{1}{\pi} \int_{-\pi}^{\pi} y(t)\sin ntdt \end{aligned} \quad (2.16)$$

The trigonometric series corresponding to $y(t)$ is called the *Fourier series for $y(t)$* , and the coefficients A_n and B_n are called the *Fourier coefficients* of $y(t)$. In the series for $y(t)$ in Equation 2.12, when $n = 1$ the corresponding terms in the Fourier series are called *fundamental* and have the lowest frequency in the series. The *fundamental frequency* for this Fourier series is $\omega = 2\pi/2\pi = 1$. Frequencies corresponding to $n = 2, 3, 4, \dots$ are known as *harmonics*, with, for example, $n = 2$ representing the second harmonic.

Functions represented by a Fourier series normally do not have a period of 2π . However, the transition to an arbitrary period can be affected by a change of scale, yielding a new set of Euler formulas described below.

Fourier Coefficients for Functions Having Arbitrary Periods

The coefficients of a trigonometric series representing a function having an arbitrary period T are given by the Euler formulas:

$$\begin{aligned}
 A_0 &= \frac{1}{T} \int_{-T/2}^{T/2} y(t) dt \\
 A_n &= \frac{2}{T} \int_{-T/2}^{T/2} y(t) \cos n\omega t dt \\
 B_n &= \frac{2}{T} \int_{-T/2}^{T/2} y(t) \sin n\omega t dt
 \end{aligned} \tag{2.17}$$

where $n = 1, 2, 3, \dots$, and $T = 2\pi/\omega$ is the period of $y(t)$. The trigonometric series that results from these coefficients is a Fourier series and may be written as

$$y(t) = A_0 + \sum_{n=1}^{\infty} (A_n \cos n\omega t + B_n \sin n\omega t) \tag{2.18}$$

A series of sines and cosines may be written as a series of either sines or cosines through the introduction of a phase angle, so that the Fourier series in Equation 2.18,

$$y(t) = A_0 + \sum_{n=1}^{\infty} (A_n \cos n\omega t + B_n \sin n\omega t)$$

may be written as

$$y(t) = A_0 + \sum_{n=1}^{\infty} C_n \cos(n\omega t - \phi_n) \tag{2.19}$$

or

$$y(t) = A_0 + \sum_{n=1}^{\infty} C_n \sin(n\omega t + \phi_n^*) \tag{2.20}$$

where

$$\begin{aligned}
 C_n &= \sqrt{A_n^2 + B_n^2} \\
 \tan \phi_n &= \frac{B_n}{A_n} \quad \text{and} \quad \tan \phi_n^* = \frac{A_n}{B_n}
 \end{aligned} \tag{2.21}$$

Even and Odd Functions

A function $g(t)$ is even if it is symmetric about the origin, which may be stated, for all t ,

$$g(-t) = g(t)$$

A function $h(t)$ is odd if, for all t ,

$$h(-t) = -h(t)$$

For example, $\cos nt$ is even, while $\sin nt$ is odd. A particular function or waveform may be even, odd, or neither even nor odd.

Fourier Cosine Series

If $y(t)$ is even, its Fourier series will contain only cosine terms:

$$y(t) = \sum_{n=1}^{\infty} A_n \cos \frac{2\pi nt}{T} = \sum_{n=1}^{\infty} A_n \cos n\omega t \quad (2.22)$$

Fourier Sine Series

If $y(t)$ is odd, its Fourier series will contain only sine terms

$$y(t) = \sum_{n=1}^{\infty} B_n \sin \frac{2\pi nt}{T} = \sum_{n=1}^{\infty} B_n \sin n\omega t \quad (2.23)$$

Note: Functions that are neither even nor odd result in Fourier series that contain both sine and cosine terms.

Example 2.3

Determine the Fourier series that represents the function shown in Figure 2.14.

KNOWN $T = 10$ (i.e., -5 to $+5$)

$$A_0 = 0$$

FIND The Fourier coefficients A_1, A_2, \dots and B_1, B_2, \dots

SOLUTION Since the function shown in Figure 2.14 is odd, the Fourier series will contain only sine terms (see Eq. 2.23):

$$y(t) = \sum_{n=1}^{\infty} B_n \sin \frac{2\pi nt}{T}$$

where

$$\begin{aligned} B_n &= \frac{2}{10} \left[\int_{-5}^0 (-1) \sin \left(\frac{2\pi nt}{10} \right) dt + \int_0^5 (1) \sin \left(\frac{2\pi nt}{10} \right) dt \right] \\ B_n &= \frac{2}{10} \left\{ \left[\frac{10}{2n\pi} \cos \left(\frac{2\pi nt}{10} \right) \right]_{-5}^0 + \left[\frac{-10}{2n\pi} \cos \left(\frac{2\pi nt}{10} \right) \right]_0^5 \right\} \\ B_n &= \frac{2}{10} \left\{ \frac{10}{2n\pi} [1 - \cos(-n\pi) - \cos(n\pi) + 1] \right\} \end{aligned}$$

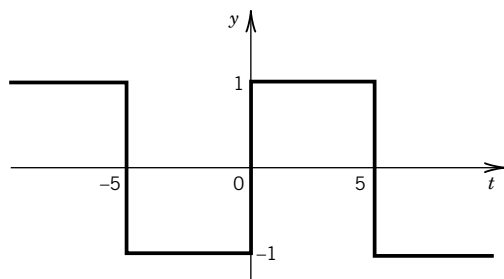


Figure 2.14 Function represented by a Fourier series in Example 2.3.

The reader can verify that all $A_n = 0$ for this function. For even values of n , B_n is identically zero and for odd values of n ,

$$B_n = \frac{4}{n\pi}$$

The resulting Fourier series is then

$$y(t) = \frac{4}{\pi} \sin \frac{2\pi}{10} t + \frac{4}{3\pi} \sin \frac{6\pi}{10} t + \frac{4}{5\pi} \sin \frac{10\pi}{10} t + \dots$$

Note that the fundamental frequency is $\omega = \frac{2\pi}{10}$ rad/s and the subsequent terms are the odd-numbered harmonics of ω .

COMMENT Consider the function given by

$$y(t) = 1 \quad 0 < t < 5$$

We may represent $y(t)$ by a Fourier series if we extend the function beyond the specified range (0 – 5) either as an even periodic extension or as an odd periodic extension. (Because we are interested only in the Fourier series representing the function over the range $0 < t < 5$, we can impose any behavior outside of that domain that helps to generate the Fourier coefficients!) Let's choose an odd periodic extension of $y(t)$; the resulting function remains identical to the function shown in Figure 2.14.

Example 2.4

Find the Fourier coefficients of the periodic function

$$y(t) = -5 \text{ when } -\pi < t < 0$$

$$y(t) = +5 \text{ when } 0 < t < \pi$$

and $y(t + 2\pi) = y(t)$. Plot the resulting first four partial sums for the Fourier series.

KNOWN Function $y(t)$ over the range $-\pi$ to π

FIND Coefficients A_n and B_n

SOLUTION The function as stated is periodic, having a period of $T = 2\pi$ (i.e., $\omega = 1$ rad/s), and is identical in form to the odd function examined in Example 2.3. Since this function is also odd, the Fourier series contains only sine terms, and

$$B_n = \frac{1}{\pi} \int_{-\pi}^{\pi} y(t) \sin n\omega t dt = \frac{1}{\pi} \left[\int_{-\pi}^0 (-5) \sin nt dt + \int_0^{\pi} (+5) \sin nt dt \right]$$

which yields upon integration

$$\frac{1}{\pi} \left\{ \left[(5) \frac{\cos nt}{n} \right]_{-\pi}^0 - \left[(5) \frac{\cos nt}{n} \right]_0^{\pi} \right\}$$

Thus,

$$B_n = \frac{10}{n\pi} (1 - \cos n\pi)$$

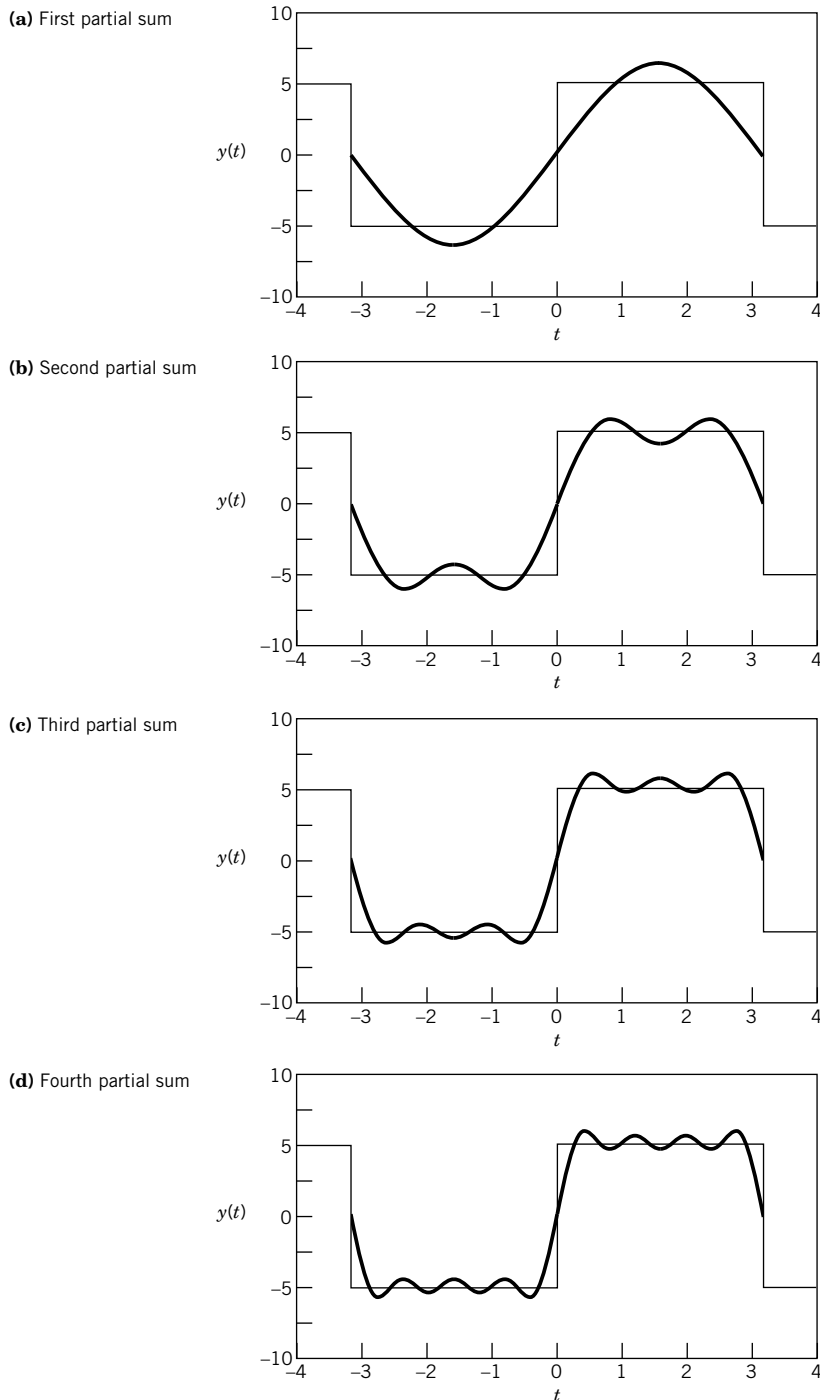


Figure 2.15 First four partial sums of the Fourier series $(20/\pi)(\sin t + 1/3 \sin 3t + 1/5 \sin 5t + \dots)$ in comparison with the exact waveform.

which is zero for even n , and $20/n\pi$ for odd values of n . The Fourier series can then be written³

$$y(t) = \frac{20}{\pi} \left(\sin t + \frac{1}{3} \sin 3t + \frac{1}{5} \sin 5t + \dots \right)$$

Figure 2.15 shows the first four partial sums of this function, as they compare with the function they represent. Note that at the points of discontinuity of the function, the Fourier series takes on the arithmetic mean of the two function values.

COMMENT As the number of terms in the partial sum increases, the Fourier series approximation of the square wave function becomes even better. For each additional term in the series, the number of “humps” in the approximate function in each half-cycle corresponds to the number of terms included in the partial sum.

The Matlab[®]⁴ program file *FourCoef* with the companion software illustrates the behavior of the partial sums for several waveforms. The LabView[®] program *Waveform-Generation.vi* creates signals from trigonometric series.

Example 2.5

As an example of interpreting the frequency content of a given signal, consider the output voltage from a rectifier. A rectifier functions to “flip” the negative half of an alternating current (AC) into the positive half plane, resulting in a signal that appears as shown in Figure 2.16. For the AC signal the voltage is given by

$$E(t) = 120 \sin 120\pi t$$

The period of the signal is $1/60$ s, and the frequency is 60 Hz.

KNOWN The rectified signal can be expressed as

$$E(t) = |120 \sin 120\pi t|$$

FIND The frequency content of this signal as determined from a Fourier series analysis.

SOLUTION The frequency content of this signal can be determined by expanding the function in a Fourier series. The coefficients may be determined using the Euler formulas, keeping in mind

³If we assume that the sum of this series most accurately represents the function y at $t = \pi/2$, then

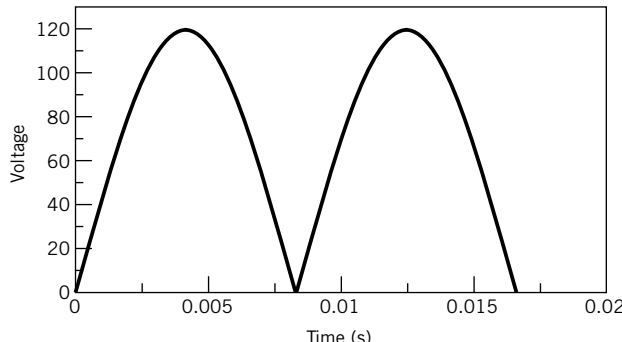
$$y\left(\frac{\pi}{2}\right) = 5 = \frac{20}{\pi} \left(1 - \frac{1}{3} + \frac{1}{5} - \dots \right)$$

or

$$\frac{\pi}{4} = 1 - \frac{1}{3} + \frac{1}{5} - \frac{1}{7} + \dots$$

This series approximation of π was first obtained by Gottfried Wilhelm Leibniz (1646–1716) in 1673 from geometrical reasoning.

⁴Matlab is a registered trademark of Mathworks, Inc.

**Figure 2.16** Rectified sine wave.

that the rectified sine wave is an even function. The coefficient A_0 is determined from

$$A_0 = 2 \left[\frac{1}{T} \int_0^{T/2} y(t) dt \right] = \frac{2}{1/60} \int_0^{1/120} 120 \sin 120\pi t dt$$

with the result that

$$A_0 = \frac{2 \times 60 \times 2}{\pi} = 76.4$$

The remaining coefficients in the Fourier series may be expressed as

$$\begin{aligned} A_n &= \frac{4}{T} \int_0^{T/2} y(t) \cos \frac{2n\pi t}{T} dt \\ &= \frac{4}{1/60} \int_0^{1/120} 120 \sin 120\pi t \cos n\pi t dt \end{aligned}$$

For values of n that are odd, the coefficient A_n is identically zero. For values of n that are even, the result is

$$A_n = \frac{120}{\pi} \left(\frac{-2}{n-1} + \frac{2}{n+1} \right) \quad (2.24)$$

The Fourier series for the function $|120 \sin 120\pi t|$ is

$$76.4 - 50.93 \cos 240\pi t - 10.10 \cos 480\pi t - 4.37 \cos 720\pi t \dots$$

Figure 2.17 shows the amplitude versus frequency content of the rectified signal, based on a Fourier series expansion.

COMMENT The frequency content of a signal is determined by examining the amplitude of the various frequency components that are present in the signal. For a periodic mathematical function, expanding the function in a Fourier series and plotting the amplitudes of the contributing sine and cosine terms can illustrate these frequency contributions.

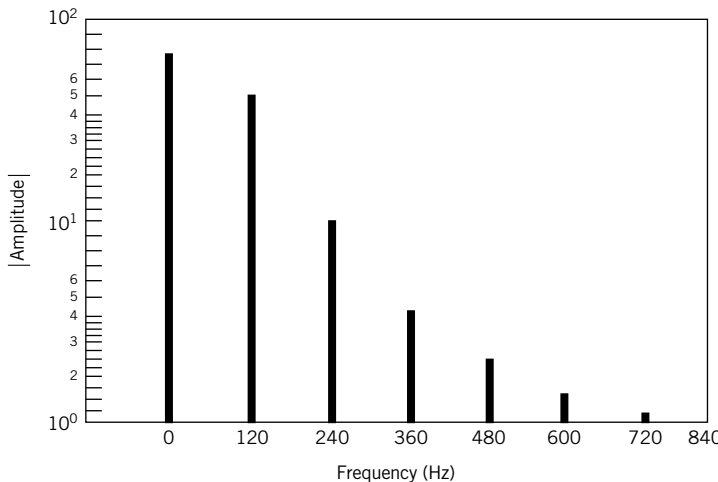


Figure 2.17 Frequency content of the function $y(t) = |120 \sin 20\pi t|$ displayed as an amplitude-frequency spectrum.

The LabView program *WaveformGeneration.vi* follows Examples 2.4 and 2.5 and provides the spectra for a number of signals. Several Matlab programs are provided also (e.g., *FourCoef*, *FunSpect*, *DataSpect*) to explore the concept of superposition of simple periodic signals to create a more complex signal. The software allows you to create your own functions and then explore their frequency and amplitude content.

2.5 FOURIER TRANSFORM AND THE FREQUENCY SPECTRUM

The previous discussion of Fourier analysis demonstrates that an arbitrary, but known, function can be expressed as a series of sines and cosines known as a Fourier series. The coefficients of the Fourier series specify the amplitudes of the sines and cosines, each having a specific frequency. Unfortunately, in most practical measurement applications the input signal may not be known in functional form. Therefore, although the theory of Fourier analysis demonstrates that any function can be expressed as a Fourier series, the analysis presented so far has not provided a specific technique for analyzing measured signals. Such a technique for the decomposition of a measured dynamic signal in terms of amplitude and frequency is now described.

Recall that the dynamic portion of a signal of arbitrary period can be described from Equation 2.17.

$$\begin{aligned} A_n &= \frac{2}{T} \int_{-T/2}^{T/2} y(t) \cos n\omega t dt \\ B_n &= \frac{2}{T} \int_{-T/2}^{T/2} y(t) \sin n\omega t dt \end{aligned} \quad (2.25)$$

where the amplitudes A_n and B_n correspond to the n th frequency of a Fourier series.

If we consider the period of the function to approach infinity, we can eliminate the constraint on Fourier analysis that the signal be a periodic waveform. In the limit as T approaches infinity the Fourier series becomes an integral. The spacing between frequency components becomes

infinitesimal. This means that the coefficients A_n and B_n become continuous functions of frequency and can be expressed as $A(\omega)$ and $B(\omega)$ where

$$\begin{aligned} A(\omega) &= \int_{-\infty}^{\infty} y(t)\cos \omega t dt \\ B(\omega) &= \int_{-\infty}^{\infty} y(t)\sin \omega t dt \end{aligned} \quad (2.26)$$

The Fourier coefficients $A(\omega)$ and $B(\omega)$ are known as the components of the Fourier transform of $y(t)$.

To develop the Fourier transform, consider the complex number defined as

$$Y(\omega) \equiv A(\omega) - iB(\omega) \quad (2.27)$$

where $i = \sqrt{-1}$. Then from Equations 2.26 it follows directly that

$$Y(\omega) \equiv \int_{-\infty}^{\infty} y(t)(\cos \omega t - i\sin \omega t) dt \quad (2.28)$$

Introducing the identity

$$e^{-i\theta} = \cos \theta - i\sin \theta$$

leads to

$$Y(\omega) \equiv \int_{-\infty}^{\infty} y(t)e^{-i\omega t} dt \quad (2.29)$$

Alternately, recalling from Equation 2.9 that the cyclical frequency f , in hertz, is related to the circular frequency and its period by

$$f = \frac{\omega}{2\pi} = \frac{1}{T}$$

Equation 2.29 is rewritten as

$$Y(f) \equiv \int_{-\infty}^{\infty} y(t)e^{-i2\pi f t} dt \quad (2.30)$$

Equation 2.29 or 2.30 provides the two-sided *Fourier transform* of $y(t)$. If $y(t)$ is known, then its Fourier transform will provide the amplitude-frequency properties of the signal, $y(t)$, which otherwise are not readily apparent in its time-based form. We can think of the Fourier transform as a decomposition of $y(t)$ into amplitude versus frequency information. This property is analogous to the optical properties displayed by the prism in Figure 2.8.

If $Y(f)$ is known or measured, we can recover the signal $y(t)$ from

$$y(t) = \int_{-\infty}^{\infty} Y(f)e^{i2\pi f t} df \quad (2.31)$$

Equation 2.31 describes the *inverse Fourier transform* of $Y(f)$. It suggests that given the amplitude-frequency properties of a signal we can reconstruct the original signal $y(t)$. The Fourier transform is a complex number having a magnitude and a phase,

$$Y(f) = |Y(f)|e^{i\phi(f)} = A(f) - iB(f) \quad (2.32)$$

The magnitude of $Y(f)$, also called the modulus, is given by

$$|Y(f)| = \sqrt{\operatorname{Re}[Y(f)]^2 + \operatorname{Im}[Y(f)]^2} \quad (2.33)$$

and the phase by

$$\phi(f) = \tan^{-1} \frac{\operatorname{Im}[Y(f)]}{\operatorname{Re}[Y(f)]} \quad (2.34)$$

As noted earlier, the Fourier coefficients are related to cosine and sine terms. Then the amplitude of $y(t)$ can be expressed by its amplitude-frequency spectrum, or simply referred to as its amplitude spectrum, by

$$C(f) = \sqrt{A(f)^2 + B(f)^2} \quad (2.35)$$

and its phase spectrum by

$$\phi(f) = \tan^{-1} \frac{B(f)}{A(f)} \quad (2.36)$$

Thus the introduction of the Fourier transform provides a method to decompose a measured signal $y(t)$ into its amplitude-frequency components. Later we will see how important this method is, particularly when digital sampling is used to measure and interpret an analog signal.

A variation of the amplitude spectrum is the power spectrum, which is given by magnitude $C(f)^2/2$. Further details concerning the properties of the Fourier transform and spectrum functions can be found in Bracewell (2) and Champeney (3). An excellent historical account and discussion of the wide-ranging applications are found in Bracewell (4).

Discrete Fourier Transform

As a practical matter, it is likely that if $y(t)$ is measured and recorded, then it will be stored in the form of a discrete time or digital signal. A computer-based data-acquisition system is the most common method for recording data. These data are acquired over a finite period of time rather than the mathematically convenient infinite period of time. A discrete data set containing N values representing a time interval from 0 to t_f will accurately represent the signal provided that the measuring period has been properly chosen and is sufficiently long. We deal with the details for such period selection in a discussion on sampling concepts in Chapter 7. The preceding analysis is now extended to accommodate a discrete series.

Consider the time-dependent portion of the signal $y(t)$, which is measured N times at equally spaced time intervals δt . In this case, the continuous signal $y(t)$ is replaced by the discrete time signal given by $y(r\delta t)$ for $r = 0, 1, \dots, (N-1)$. In effect, the relationship between $y(t)$ and $\{y(r\delta t)\}$ is described by a set of impulses of an amplitude determined by the value of $y(t)$ at each time step $r\delta t$. This transformation from a continuous to discrete time signal is described by

$$\{y(r\delta t)\} = y(t)\delta(t - r\delta t) \quad r = 0, 1, 2, \dots, N - 1 \quad (2.37)$$

where $\delta(t - r\delta t)$ is the delayed unit impulse function and $\{y(r\delta t)\}$ refers to the discrete data set given by $y(r\delta t)$ for $r = 0, 1, 2, \dots, N - 1$.

An approximation to the Fourier transform integral of Equation 2.30 for use on a discrete data set is the discrete Fourier transform (DFT). The DFT is given by

$$\begin{aligned} Y(f_k) &= \frac{2}{N} \sum_{r=0}^{N-1} y(r\delta t) e^{-i2\pi rk/N} \\ f_k &= k\delta f \quad k = 0, 1, 2, \dots, \left(\frac{N}{2} - 1\right) \\ \delta f &= 1/N\delta t \end{aligned} \tag{2.38}$$

Here, δf is the frequency resolution of the DFT with each value of $Y(f_k)$ corresponding to frequency increments of δf . In developing Equation 2.38 from Equation 2.30, t was replaced by $r\delta t$ and f replaced by $k/N\delta t$. The factor $2/N$ scales the transform when it is obtained from a data set of finite length (use $1/N$ for $k = 0$ only).

The DFT as expressed by Equation 2.38 yields $N/2$ discrete values of the Fourier transform of $\{y(r\delta t)\}$. This is the so-called one-sided or half-transform as it assumes that the data set is one-sided, extending from 0 to t_f , and it returns only positive valued frequencies.

Equation 2.38 performs the numerical integration required by the Fourier integral. Equations 2.35, 2.36, and 2.38 demonstrate that the application of the DFT on the discrete series of data, $y(r\delta t)$, permits the decomposition of the discrete data in terms of frequency and amplitude content. Hence, by using this method a measured discrete signal of unknown functional form can be reconstructed as a Fourier series through Fourier transform techniques.

Software for computing the Fourier transform of a discrete signal is included in the companion software. The time required to compute directly the DFT algorithm described in this section increases at a rate that is proportional to N^2 . This makes it inefficient for use with data sets of large N . A fast algorithm for computing the DFT, known as the *fast Fourier transform* (FFT), was developed by Cooley and Tukey (5). This method is widely available and is the basis for most Fourier analysis software packages. The FFT algorithm is discussed in most advanced texts on signal analysis (6, 7). The accuracy of discrete Fourier analysis depends on the frequency content⁵ of $y(t)$ and on the Fourier transform frequency resolution. An extensive discussion of these interrelated parameters is given in Chapter 7.

Example 2.6

Convert the continuous signal described by $y(t) = 10 \sin 2\pi t$ V into a discrete set of eight numbers using a time increment of 0.125 s.

KNOWN The signal has the form $y(t) = C_1 \sin 2\pi f_1 t$
where

$$f_1 = \omega_1 / 2\pi = 1 \text{ Hz}$$

$$C(f_1 = 1 \text{ Hz}) = 10 \text{ V}$$

$$\phi(f_1) = 0$$

$$\delta t = 0.125 \text{ s}$$

$$N = 8$$

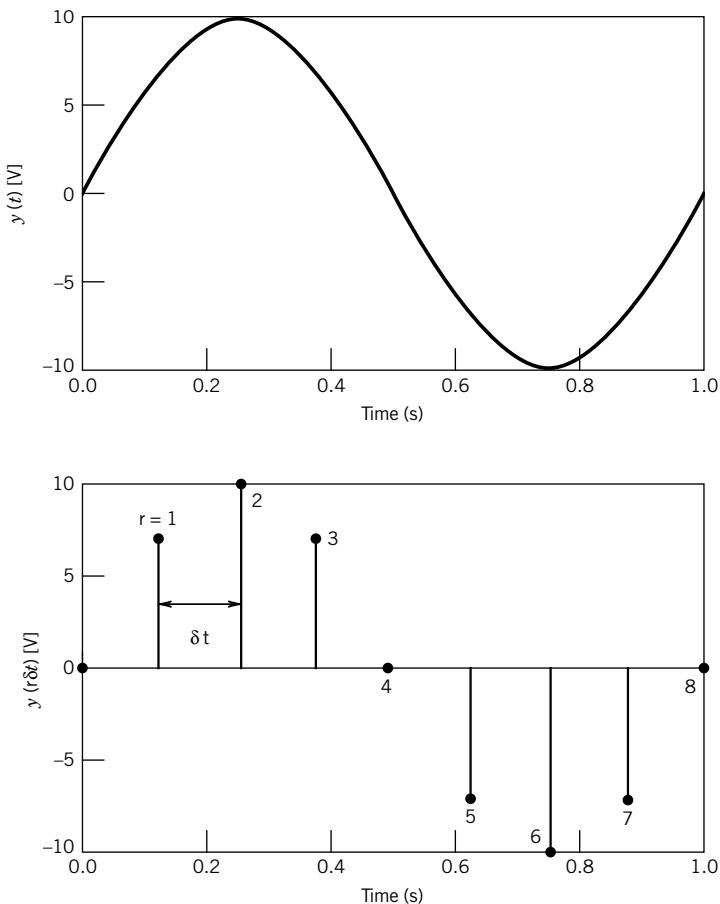
⁵The value of $1/\delta t$ must be more than twice the highest frequency contained in $y(t)$.

Table 2.2 Discrete Data Set for $y(t) = 10 \sin 2\pi t$

r	$y(r\delta t)$	r	$y(r\delta t)$
0	0.000	4	0.000
1	7.071	5	-7.071
2	10.000	6	-10.000
3	7.071	7	-7.071

FIND $\{y(r\delta t)\}$

SOLUTION Measuring $y(t)$ every 0.125 s over 1 s produces the discrete data set $\{y(r\delta t)\}$ given in Table 2.2. Note that the measurement produces four complete periods of the signal and that the signal duration is given by $N\delta t = 1$ s. The signal and its discrete representation as a series of impulses in a time domain are plotted in Figure 2.18. See Example 2.7 for more on how to create this discrete series by using common software.

**Figure 2.18** Representation of a simple periodic function as a discrete signal.

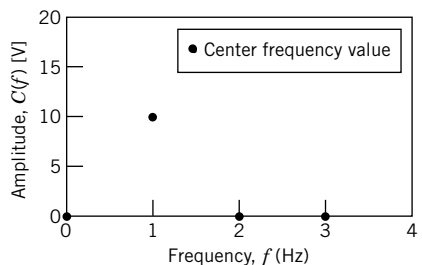


Figure 2.19 Amplitude as a function of frequency for a discrete representation of $10 \sin 2\pi t$ resulting from a discrete Fourier transform algorithm.

Example 2.7

Estimate the amplitude spectrum of the discrete data set in Example 2.6.

KNOWN Discrete data set $\{y(r\delta t)\}$ of Table 2.2

$$\delta t = 0.125 \text{ s}$$

$$N = 8$$

FIND $C(f)$

SOLUTION We can use either the Matlab Fourier transform software (file *FunSpect*), the LabView program *WaveformGeneration*, or a spreadsheet program to find $C(f)$ (see the Comment for details). For $N=8$, a one-sided Fourier transform algorithm will return $N/2$ values for $C(f)$, with each successive amplitude corresponding to a frequency spaced at intervals of $1/N\delta t = 0.125$ Hz. The amplitude spectrum is shown in Figure 2.19 and has a spike of 10 V centered at a frequency of 1 Hz.

COMMENT The discrete series and the amplitude spectrum are easily reproduced by using the Matlab program file called *FunSpect*, the LabView program *Waveform-Generation*, or spreadsheet software. The Fourier analysis capability of this software can also be used on an existing data set, such as with the Matlab program file called *DataSpect*.

The following discussion of Fourier analysis using a spreadsheet program makes specific references to procedures and commands from Microsoft® Excel;⁶ similar functions are available in other engineering analysis software. When a spreadsheet is used as shown, the $N=8$ data point sequence $\{y(r\delta t)\}$ is created as in column 3. Under Data/Data Analysis, select Fourier Analysis. At the prompt, define the N cells containing $\{y(r\delta t)\}$ and define the cell destination (column 4). The analysis executes the DFT of Equation 2.38 by using the FFT algorithm, and it returns N complex numbers, the Fourier coefficients $Y(f)$ of Equation 2.32. The analysis returns the two-sided transform. However, a finite data set is one-sided, so we are interested in only the first $N/2$ Fourier coefficients of column 4 (the second $N/2$ coefficients just mirror the first $N/2$). To find the coefficient magnitude as given in Equation 2.33, compute or use the function IMABS($=\sqrt{A^2 + B^2}$) on each of the first $N/2$ coefficients, and then scale each coefficient magnitude by dividing by $N/2$ (for $r=0$,

⁶ Microsoft® and Excel are either registered trademarks or trademarks of Microsoft Corporation in the United States and/or other countries.

divide by N). The $N/2$ scaled coefficients (column 5) now represent the discrete amplitudes corresponding to $N/2$ discrete frequencies (column 6) extending from $f=0$ to $(N/2 - 1)/N\delta t$ Hz, with each frequency separated by $1/N\delta t$.

Column					
1	2	3	4	5	6
r	$t(s)$	$y(r\delta t)$	$Y(f)=A - Bi$	$C(f)$	$f(\text{Hz})$
0	0	0	0	0	0
1	0.125	7.07	-40i	10	1
2	0.25	10	0	0	2
3	0.375	7.07	0	0	3
4	0.5	0	0		
5	0.625	-7.07	0		
6	0.75	-10	0		
7	0.875	-7.07	40i		

These same operations in Matlab are as follows:

$t = 1/8: 1/8: 1$	defines time from 0.125 s to 1 s in increments of 0.125 s
$y = 10*\sin(2*pi*t)$	creates the discrete time series with $N = 8$
$ycoef = fft(y)$	performs the Fourier analysis; returns N coefficients
$c = coef/4$	divides by $N/2$ to scale and determine the magnitudes

When signal frequency content is not known prior to conversion to a discrete signal, it is necessary to experiment with the parameters of frequency resolution, N and δt , to obtain an unambiguous representation of the signal. Techniques for this are explored in Chapter 7.

Analysis of Signals in Frequency Space

Fourier analysis is a tool for extracting details about the frequencies that are present in a signal. Frequency analysis is routinely used in vibration analysis and isolation, determining the condition of bearings, and a wide variety of acoustic applications. An example from acoustics follows.

Example 2.8

Examine the frequency spectra of representative brass and woodwind instruments to illustrate why the characteristic sound of these instruments is so easily distinguished.

KNOWN Figures 2.20 and 2.21 provide a representative frequency spectrum for a clarinet, a woodwind instrument having a reed, and brass instruments.

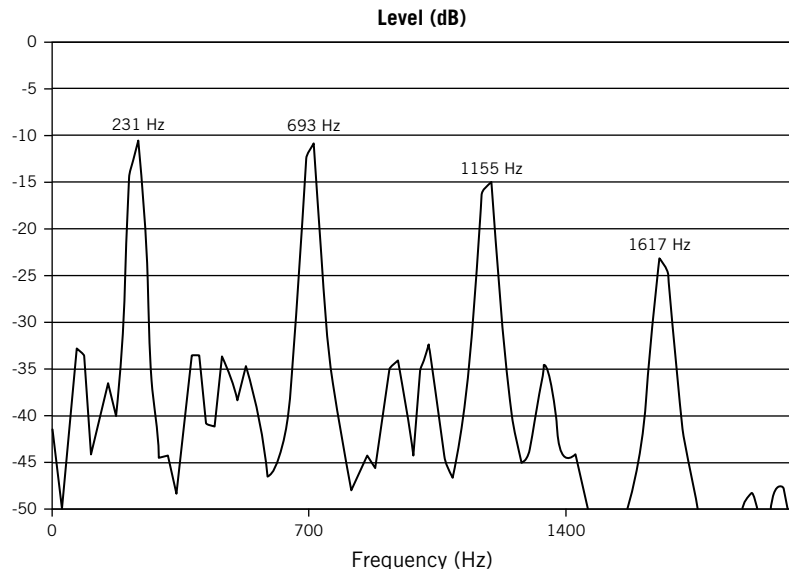


Figure 2.20 Frequency spectrum for a clarinet playing the note one whole tone below middle C. (Adapted from Campbell, D.M., Nonlinear Dynamics of Musical Reed and Brass Wind Instruments, *Contemporary Physics*, 40(6) November 1999, pages 415–431.)

DISCUSSION Figure 2.20 displays the frequency spectrum for a clarinet playing a B-flat. The base tone, f_o , is at 231 Hz, with the harmonics having frequencies of $3f_o$, $5f_o$, etc. Contrast this with the frequency spectrum, shown in Figure 2.21, of the first few seconds of Aaron Copland's "Fanfare for the Common Man," which is played by an ensemble of brass instruments, like French horns, and has a fundamental frequency of approximately 700 Hz. This spectrum contains harmonics that are $2f_o$, $3f_o$, $4f_o$, etc.

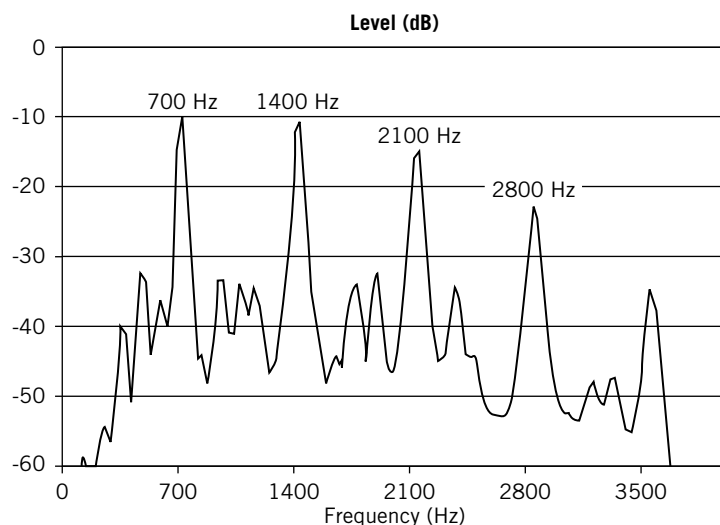


Figure 2.21 Frequency spectrum for the first three seconds of Aaron Copland's "Fanfare for the Common Man" that is played by the brass section of the orchestra.

COMMENT Fourier analysis and the examination of a signal's frequency content have myriads of applications. In this example, we demonstrated through frequency analysis a clear reason why clarinets and trumpets sound quite different. The presence of only odd harmonics, or both even and odd harmonics, is a very recognizable difference, easily perceived by the human ear.

2.6 SUMMARY

This chapter has provided a fundamental basis for the description of signals. The capabilities of a measurement system can be properly specified when the nature of the input signal is known. The descriptions of general classes of input signals will be seen in Chapter 3 to allow universal descriptions of measurement system dynamic behavior.

Any signal can be represented by a static magnitude and a series of varying frequencies and amplitudes. As such, measurement system selection and design must consider the frequency content of the input signals the system is intended to measure. Fourier analysis was introduced to allow a precise definition of the frequencies and the phase relationships among various frequency components within a particular signal. In Chapter 7, it will be shown as a tool for the accurate interpretation of discrete signals.

Signal characteristics form an important basis for the selection of measurement systems and the interpretation of measurement system output. In Chapter 3 these ideas are combined with the concept of a generalized set of measurement system behaviors. The combination of generalized measurement system behavior and generalized descriptions of input waveforms provides for an understanding of a wide range of instruments and measurement systems.

REFERENCES

1. Monforte, J., The digital reproduction of sound, *Scientific American*, 251(6): 78, 1984.
2. Bracewell, R. N., *The Fourier Transform and Its Applications*, 3d ed., rev., McGraw Hill, New York, 1999.
3. Champeney, D. C., *Fourier Transforms and Their Physical Applications*, Academic, London, 1973.
4. Bracewell, R. N., The Fourier transform, *Scientific American*, 260(6): 86, 1989.
5. Cooley, J. W., and J. W. Tukey, An Algorithm for the Machine Calculation of Complex Fourier Series, *Mathematics of Computation* 19: 207, April 1965 (see also Special Issue on the fast Fourier transform, *IEEE Transactions on Audio and Electroacoustics* AU-2, June 1967).
6. Bendat, J. S., and A. G. Piersol, *Random Data: Analysis and Measurement Procedures*, 3rd ed., Wiley, New York, 2000 (see also Bendat, J. S., and A. G. Piersol, *Engineering Applications of Correlation and Spectral Analysis*, 2nd ed., Wiley, New York, 1993).
7. Cochran, W. T., et al. What is the fast Fourier transform?, *Proceedings of the IEEE* 55(10): 1664, 1967.

SUGGESTED READING

Halliday, D., and R. Resnick, *Fundamentals of Physics*, 6th ed., Wiley, New York, 2000.
Kreyszig, E., *Advanced Engineering Mathematics*, 9th ed., Wiley, New York, 2005.

NOMENCLATURE

f	frequency, in Hz (t^{-1})	N	total number of discrete data points; integer
k	spring constant (mt^{-2})	T	period (t)
m	mass (m)	U	unit step function
t	time (t)	Y	Fourier transform of y
y	dependent variable	α	angle (rad)
y_m	discrete data points	β	angle (rad)
A	amplitude	δf	frequency resolution (t^{-1})
B	amplitude	δt	sample time increment (t)
C	amplitude	ϕ	phase angle (rad)
F	force (mlt^{-2})	ω	circular frequency in rad/s (t^{-1})

PROBLEMS

- 2.1** Define the term “signal” as it relates to measurement systems. Provide two examples of static and dynamic input signals to particular measurement systems.
- 2.2** List the important characteristics of input and output signals and define each.
- 2.3** Determine the average and rms values for the function

$$y(t) = 25 + 10 \sin 6\pi t$$

over the time periods (a) 0 to 0.1 s, (b) 0.4 to 0.5 s, (c) 0 to 1/3 s, and (d) 0 to 20 s. Comment on the nature and meaning of the results in terms of analysis of dynamic signals.

- 2.4** The following values are obtained by sampling two time-varying signals once every 0.4 s:

t	$y_1(t)$	$y_2(t)$	t	$y_1(t)$	$y_2(t)$
0	0	0			
0.4	11.76	15.29	2.4	-11.76	-15.29
0.8	19.02	24.73	2.8	-19.02	-24.73
1.2	19.02	24.73	3.2	-19.02	-24.73
1.6	11.76	15.29	3.6	-11.76	-15.29
2.0	0	0	4.0	0	0

Determine the mean and the rms values for this discrete data. Discuss the significance of the rms value in distinguishing these signals.

- 2.5** A *moving average* is an averaging technique that can be applied to an analog, discrete time, or digital signal. A moving average is based on the concept of windowing, as illustrated in Figure 2.22. That portion of the signal that lies inside the window is averaged and the average values plotted as a function of time as the window moves across the signal. A 10-point moving average of the signal in Figure 2.22 is plotted in Figure 2.23.
- Discuss the effects of employing a moving average on the signal depicted in Figure 2.22.
 - Develop a computer-based algorithm for computing a moving average, and determine the effect of the width of the averaging window on the signal described by

$$y(t) = \sin 5t + \cos 11t$$

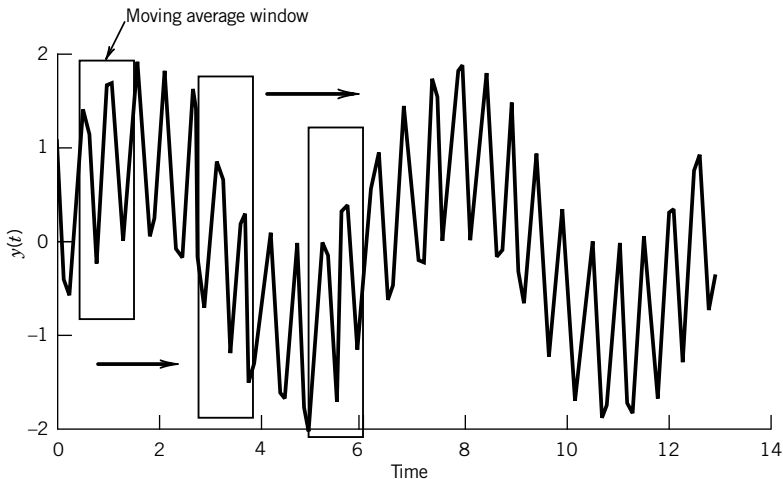


Figure 2.22 Moving average and windowing.

This signal should be represented as a discrete time signal by computing the value of the function at equally spaced time intervals. An appropriate time interval for this signal would be 0.05 s. Examine the signal with averaging windows of 4 and 30 points.

- 2.6 The data file in the companion software *noisy.txt* provides discrete time-varying signal that contains random noise. Apply a 2-, 3-, and 4-point moving average (see Problem 2.5) to these data, and plot the results. How does the moving average affect the noise in the data? Why?
- 2.7 Determine the value of the spring constant that would result in a spring-mass system that would execute one complete cycle of oscillation every 2.7 s, for a mass of 0.5 kg. What natural frequency does this system exhibit in radians/second?

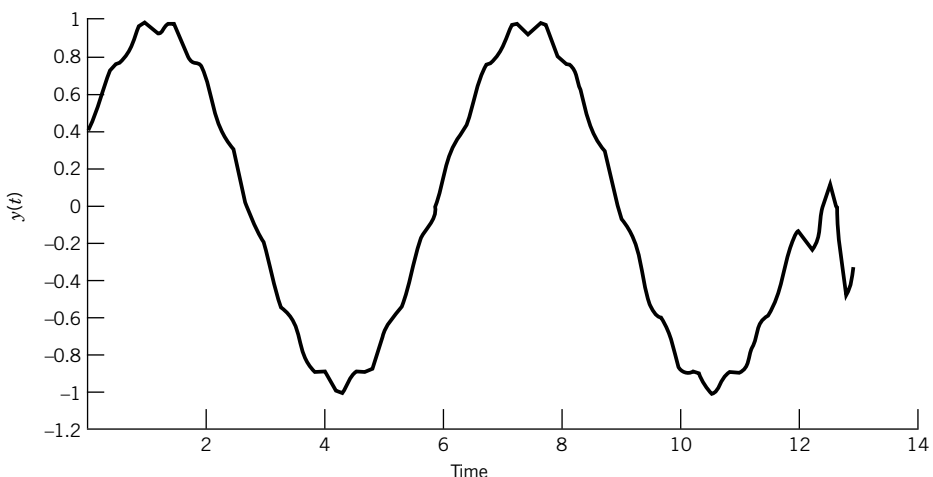


Figure 2.23 Effect of moving average on signal illustrated in Figure 2.22.

- 2.8** A spring with $k = 5000$ N/cm supports a mass of 1 kg. Determine the natural frequency of this system in radians/second and hertz.
- 2.9** For the following sine and cosine functions determine the period, the frequency in hertz, and the circular frequency in radians/second. (Note: t represents time in seconds).
- $\sin 10\pi t/5$
 - $8 \cos 8t$
 - $\sin 5n\pi t$ for $n = 1$ to ∞
- 2.10** Express the following function in terms of (a) a cosine term only and (b) a sine term only:

$$y(t) = 5 \sin 4t + 3 \cos 4t$$

- 2.11** Express the function

$$y(t) = 4 \sin 2\pi t + 15 \cos 2\pi t$$

in terms of (a) a cosine term only and (b) a sine term only.

- 2.12** Express the Fourier series given by

$$y(t) = \sum_{n=1}^{\infty} \frac{2\pi n}{6} \sin n\pi t + \frac{4\pi n}{6} \cos n\pi t$$

using only cosine terms.

- 2.13** The n th partial sum of a Fourier series is defined as

$$A_0 + A_1 \cos \omega_1 t + B_1 \sin \omega_1 t + \cdots + A_n \cos \omega_n t + B_n \sin \omega_n t$$

For the third partial sum of the Fourier series given by

$$y(t) = \sum_{n=1}^{\infty} \frac{3n}{2} \sin nt + \frac{5n}{3} \cos nt$$

a. What is the fundamental frequency and the associated period?

b. Express this partial sum as cosine terms only.

- 2.14** For the Fourier series given by

$$y(t) = 4 + \sum_{n=1}^{\infty} \frac{2\pi n}{10} \cos \frac{n\pi}{4} t + \frac{120n\pi}{30} \sin \frac{n\pi}{4} t$$

where t is time in seconds:

a. What is the fundamental frequency in hertz and radians/second?

b. What is the period T associated with the fundamental frequency?

c. Express this Fourier series as an infinite series containing sine terms only.

- 2.15** Find the Fourier series of the function shown in Figure 2.24, assuming the function has a period of 2π . Plot an accurate graph of the first three partial sums of the resulting Fourier series.

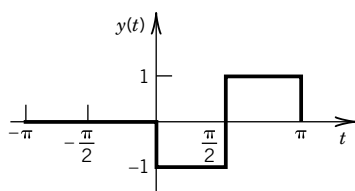


Figure 2.24 Function to be expanded in a Fourier series in Problem 2.15.

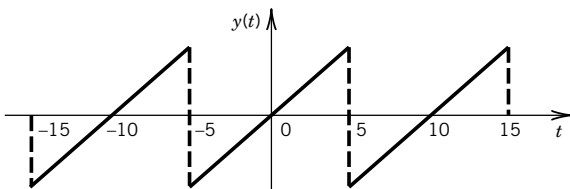


Figure 2.25 Sketch for Problem 2.16.

- 2.16** Determine the Fourier series for the function

$$y(t) = t \text{ for } -5 < t < 5$$

by expanding the function as an odd periodic function with a period of 10 units, as shown in Figure 2.25. Plot the first, second, and third partial sums of this Fourier series.

- 2.17** a. Show that $y(t) = t^2$ ($-\pi < t < \pi$), $y(t + 2\pi) = y(t)$ has the Fourier series

$$y(t) = \frac{\pi^2}{3} - 4 \left(\cos t - \frac{1}{4} \cos 2t + \frac{1}{9} \cos 3t - \dots \right)$$

- b. By setting $t = \pi$ in this series, show that a series approximation for π , first discovered by Euler, results as

$$\sum_{n=1}^{\infty} \frac{1}{n^2} = 1 + \frac{1}{4} + \frac{1}{9} + \frac{1}{16} + \dots = \frac{\pi^2}{6}$$

- 2.18** Determine the Fourier series that represents the function $y(t)$ where

$$y(t) = t \text{ for } 0 < t < 1$$

and

$$y(t) = 2 - t \text{ for } 0 < t < 1$$

Clearly explain your choice for extending the function to make it periodic.

- 2.19** Classify the following signals as static or dynamic, and identify any that may be classified as periodic:
- $\sin 10t$ V
 - $5 + 2 \cos 2t$ m
 - $5t$ s
 - 2 V
- 2.20** A particle executes linear harmonic motion around the point $x = 0$. At time zero the particle is at the point $x = 0$ and has a velocity of 5 cm/s. The frequency of the motion is 1 Hz. Determine: (a) the period, (b) the amplitude of the motion, (c) the displacement as a function of time, and (d) the maximum speed.
- 2.21** Define the following characteristics of signals: (a) frequency content, (b) amplitude, (c) magnitude, and (d) period.
- 2.22** Construct an amplitude spectrum plot for the Fourier series in Problem 2.16 for $y(t) = t$. Discuss the significance of this spectrum for measurement or interpretation of this signal. Hint: The plot can be done by inspection or by using software such as *DataSpec*.
- 2.23** Construct an amplitude spectrum plot for the Fourier series in Problem 2.17 for $y(t) = t^2$. Discuss the significance of this spectrum for selecting a measurement system. Hint: The plot can be done by inspection or by using software such as *DataSpec* or *WaveformGeneration.vi*.

- 2.24** Sketch representative waveforms of the following signals, and represent them as mathematical functions (if possible):

- The output signal from the thermostat on a refrigerator.
- The electrical signal to a spark plug in a car engine.
- The input to a cruise control from an automobile.
- A pure musical tone (e.g., 440 Hz is the note A).
- The note produced by a guitar string.
- AM and FM radio signals.

- 2.25** Represent the function

$$e(t) = 5 \sin 31.4t + 2 \sin 44t$$

as a discrete set of $N = 128$ numbers separated by a time increment of $(1/N)$. Use an appropriate algorithm to construct an amplitude spectrum from this data set. (Hint: A spreadsheet program or the program file *DataSpect* will handle this task.)

- 2.26** Repeat Problem 2.25 using a data set of 256 numbers at $\delta t = (1/N)$ and $\delta t = (1/2N)$ seconds. Compare and discuss the results.
- 2.27** A particular strain sensor is mounted to an aircraft wing that is subjected to periodic wind gusts. The strain measurement system indicates a periodic strain that ranges from 3250×10^{-6} in./in. to 4150×10^{-6} in./in. at a frequency of 1 Hz. Determine:
- The average value of this signal.
 - The amplitude and the frequency of this output signal when expressed as a simple periodic function.
 - A one-term Fourier series that represents this signal.
 - Construct an amplitude spectrum plot for the output signal.
- 2.28** For a dynamic calibration involving a force measurement system, a known force is applied to a sensor. The force varies between 100 and 170 N at a frequency of 10 rad/s. State the average (static) value of the input signal, its amplitude, and its frequency. Assuming that the signal may be represented by a simple periodic waveform, express the signal as a one-term Fourier series and create an amplitude spectrum from an equivalent discrete time series.
- 2.29** A displacement sensor is placed on a dynamic calibration rig known as a *shaker*. This device produces a known periodic displacement that serves as the input to the sensor. If the known displacement is set to vary between 2 and 5 mm at a frequency of 100 Hz, express the input signal as a one-term Fourier series. Plot the signal in the time domain, and construct an amplitude spectrum plot.
- 2.30** Consider the upward flow of water and air in a tube having a circular cross section, as shown in Figure 2.26. If the water and air flow rates are within a certain range, there are slugs of liquid and large gas bubbles flowing upward together. This type of flow is called “slug flow.” The data file *gas_liquid_data.txt* with the companion software contains measurements of pressure made at the wall of a tube in which air and water were flowing. The data were acquired at a sample frequency of 300 Hz. The average flow velocity of the air and water is 1 m/s.
- Construct an amplitude spectrum from the data, and determine the dominant frequency.
 - Using the frequency information from part a, determine the length L shown in the drawing in Figure 2.26. Assume that the dominant frequency is associated with the passage of the bubbles and slugs across the pressure sensor.

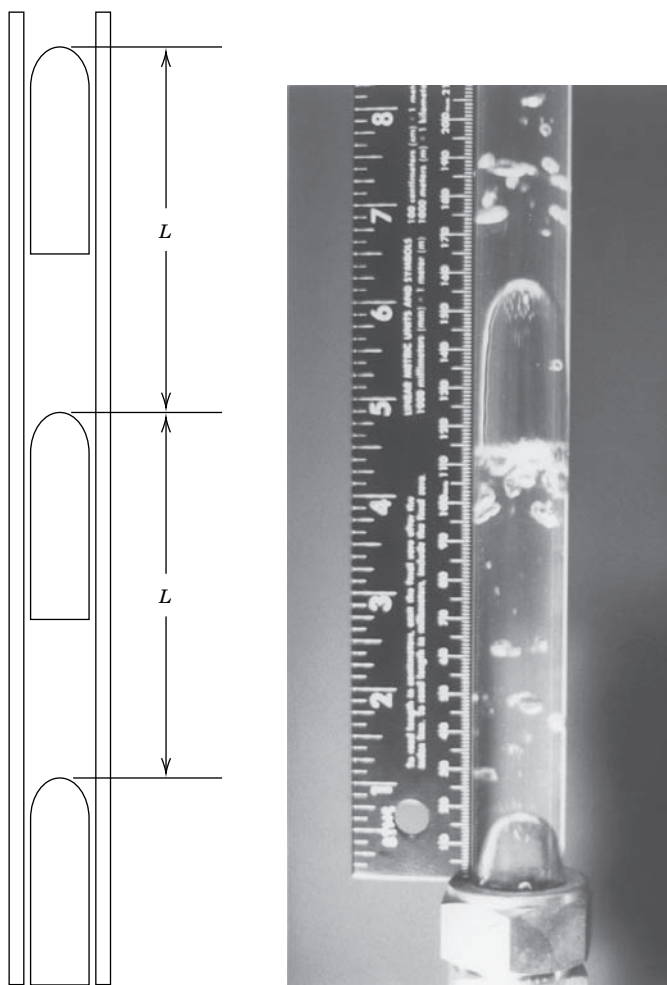
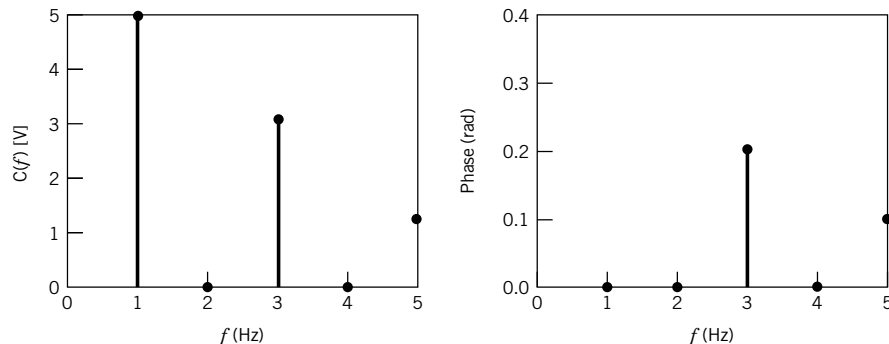


Figure 2.26 Upward gas–liquid flow: slug flow regime.

- 2.31** The file *sunspot.txt* contains data from monthly observations of sunspot activity from January 1746 to September 2005. The numbers are a relative measure of sunspot activity.
- Using the companion software program Dataspect, plot the data and create an amplitude spectrum.
 - From the spectrum, identify any cycles present in the sunspot activity and determine the period(s).
 - The Dalton minimum describes a period of low sunspot activity lasting from about 1790 to 1830; this is apparent in your plot of the data. The Dalton minimum occurred near the end of the Little Ice Age and coincided with a period of lower-than-average global temperatures. Research the “year without a summer” and its relationship to the Dalton minimum.
- 2.32** Classify the following signals as completely as possible:
- Clock face having hands.
 - Morse code.

**Figure 2.27** Spectrum for Problem 2.33.

c. Musical score, as input to a musician.

d. Flashing neon sign.

e. Telephone conversation.

f. Fax transmission.

2.33 Describe the signal defined by the amplitude spectrum and its phase shift of Figure 2.27 in terms of its Fourier series. What is the frequency resolution of these plots? What was the sample time increment used?

2.34 For the even-functioned triangle wave signal defined by

$$\begin{aligned} y(t) &= (4C/T)t + C & -T/2 \leq t \leq 0 \\ y(t) &= (-4C/T)t + C & 0 \leq t \leq T/2 \end{aligned}$$

where C is an amplitude and T is the period:

a. Show that this signal can be represented by the Fourier series

$$y(t) = \sum_{n=1}^{\infty} \frac{4C(1 - \cos n\pi)}{(\pi n)^2} \cos \frac{2\pi n t}{T}$$

b. Expand the first three nonzero terms of the series. Identify the terms containing the fundamental frequency and its harmonics.

c. Plot each of the first three terms on a separate graph. Then plot the sum of the three. For this, set $C = 1 \text{ V}$ and $T = 1 \text{ s}$. Note: The program *FourCoef* or *Waveform Generation* is useful in this problem.

d. Sketch the amplitude spectrum for the first three terms of this series, first separately for each term and then combined.

2.35 Figure 2.15 illustrates how the inclusion of higher frequency terms in a Fourier series refine the accuracy of the series representation of the original function. However, measured signals often display an amplitude spectrum for which amplitudes decrease with frequency. Using Figure 2.15 as a resource, discuss the effect of high-frequency, low-amplitude noise on a measured signal. What signal characteristics would be unaffected? Consider both periodic and random noise.

2.36 The program *Sound.vi* samples the ambient room sounds using your laptop computer microphone and sound board and returns the amplitude spectrum of the sounds. Experiment with different sounds (e.g., tapping, whistling, talking, humming) and describe your findings in a brief report.

Chapter 3

Measurement System Behavior

3.1 INTRODUCTION

This chapter introduces the concept of simulating measurement system behavior through mathematical modeling. From such a modeling study, the important aspects of measurement system response that are pertinent to system design and specification can be obtained. Each measurement system responds differently to different types of input signals and to the dynamic content within these signals. So a particular system may not be suitable for measuring certain signals or at least portions of some signals. Yet a measurement system always provides information regardless of how well (or poorly!) this reflects the actual input signal being measured. To explore this concept, this chapter discusses system response to certain types of input signals.

Throughout this chapter, we use the term “measurement system” in a generic sense. It refers either to the response of the measurement system as a whole or to the response of any component or instrument that makes up that system. Either is important, and both are interpreted in similar ways. Each individual stage of the measurement system has its own response to a given input. The overall system response is affected by the response of each stage of the complete system.

Upon completion of this chapter, the reader will be able to

- relate generalized measurement system models to dynamic response,
- describe and analyze models of zero-, first-, and second-order measurement systems and predict their general behavior,
- calculate static sensitivity, magnitude ratio, and phase shift for a range of systems and input waveforms,
- state the importance of phase linearity in reducing signal distortion,
- analyze the response of a measurement system to a complex input waveform, and
- determine the response of coupled measurement systems.

3.2 GENERAL MODEL FOR A MEASUREMENT SYSTEM

As pointed out in Chapter 2, all input and output signals can be broadly classified as being static, dynamic, or some combination of the two. For a static signal, only the signal magnitude is needed to reconstruct the input signal based on the indicated output signal. Consider measuring the length of a board using a ruler. Once the ruler is positioned, the indication (output) of the magnitude of length is immediately displayed because the board length (input) does not change over the time required to

make the measurement. Thus, the board length represents a static input signal that is interpreted through the static magnitude output indicated by the ruler. But consider measuring the vibration of a motor. Vibration signals vary in amplitude and time, and thus are a dynamic input signal to the measuring instrument. But the ruler is not very useful in determining this dynamic information, so we need an instrument that can follow the input time signal faithfully.

Dynamic Measurements

For dynamic signals, signal amplitude, frequency, and general waveform information is needed to reconstruct the input signal. Because dynamic signals vary with time, the measurement system must be able to respond fast enough to keep up with the input signal. Further, we need to understand how the input signal is applied to the sensor because that plays a role in system response. Consider the time response of a common bulb thermometer for measuring body temperature. The thermometer, initially at approximately room temperature, is placed under the tongue. But even after several seconds, the thermometer does not indicate the expected value of body temperature and its display continually changes. What has happened? Surely your body temperature is not changing. If you were to use the magnitude of the output signal after only several seconds, you would come to a false conclusion about your health! Experience shows that within a few minutes, the correct body temperature will be indicated; so we wait. Experience also tells us that if we need accurate information faster, we would need a different type of temperature sensor. In this example, body temperature itself is constant (static) during the measurement, but the input signal to the thermometer is suddenly changed from room temperature to body temperature, that is, mathematically, a step change. This is a dynamic event as the thermometer (the measurement system) sees it! The thermometer must gain energy from its new environment to reach thermal equilibrium, and this takes a finite amount of time. The ability of any measurement system to follow dynamic signals is a characteristic of the design of the measuring system components.

Now consider the task of assessing the ride quality of an automobile suspension system. A simplified view for one wheel of this system is shown in Figure 3.1. As a tire moves along the road, the road surface provides the time-dependent input signal, $F(t)$, to the suspension at the tire contact

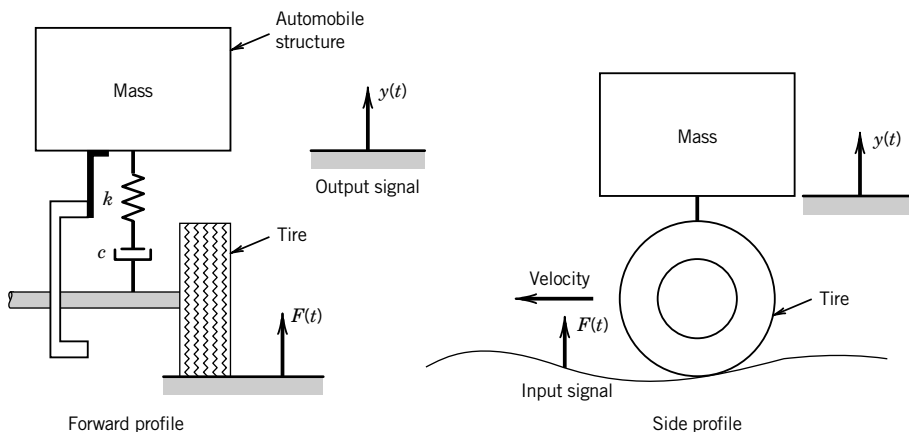


Figure 3.1 Lumped parameter model of an automobile suspension showing input and output signals.

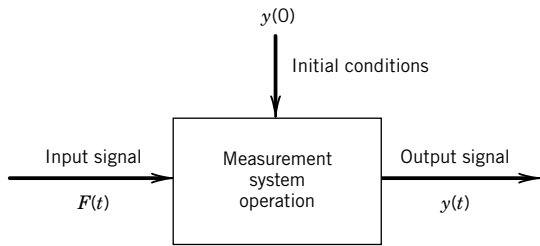


Figure 3.2 Measurement system operation on an input signal, $F(t)$, provides the output signal, $y(t)$.

point. The motion sensed by the passengers, $y(t)$, is a basis for the ride quality and can be described by a waveform that depends on the input from the road and the behavior of the suspension. An engineer must anticipate the form of the input signals so as to design the suspension to attain a desirable output signal.

Measurement systems play a key role in documenting ride quality. But just as the road and car interact to provide ride quality, the input signal and the measurement system interact in creating the output signal. In many situations, the goal of the measurement is to deduce the input signal based on the output signal. Either way, we see that it is important to understand how a measurement system responds to different forms of input signals.

The general behavior of measurement systems for a few common inputs defines, for the most part, the input–output signal relationships necessary to correctly interpret measured signals. We will show that only a few measurement system characteristics (specifications) are needed to predict the system response.

With the previous discussion in mind, consider that the primary task of a measurement system is to sense an input signal and to translate that information into a readily understandable and quantifiable output form. We can reason that a measurement system performs some mathematical operation on a sensed input. In fact, a general measurement system can be represented by a differential equation that describes the operation that a measurement system performs on the input signal. This concept is illustrated in Figure 3.2. For an input signal, $F(t)$, the system performs some operation that yields the output signal, $y(t)$. Then we must use $y(t)$ to infer $F(t)$. Therefore, at least a qualitative understanding of the operation that the measurement system performs is imperative to correctly interpret the input signal. We will propose a general mathematical model for a measurement system. Then, by representing a typical input signal as some function that acts as an input to the model, we can study just how the measurement system would behave by solving the model equation. In essence, we perform the analytical equivalent of a system calibration. This information can then be used to determine those input signals for which a particular measurement system is best suited.

Measurement System Model

In this section, we apply lumped parameter modeling to measurement systems. In lumped parameter modeling, the spatially distributed physical attributes of a system are modeled as discrete elements. The automotive suspension model discussed earlier is a lumped parameter model. As a simpler example, the mass, stiffness, and damping of a coil spring are properties spatially distributed along its length, but these can be replaced by the discrete elements of a mass, spring, and damper. An advantage is that the governing equations of the models reduce from partial to ordinary differential equations.

Consider the following general model of a measurement system, which consists of an n th-order linear ordinary differential equation in terms of a general output signal, represented by variable $y(t)$,

and subject to a general input signal, represented by the forcing function, $F(t)$:

$$a_n \frac{d^n y}{dt^n} + a_{n-1} \frac{d^{n-1} y}{dt^{n-1}} + \cdots + a_1 \frac{dy}{dt} + a_0 y = F(t) \quad (3.1)$$

where

$$F(t) = b_m \frac{d^m x}{dt^m} + b_{m-1} \frac{d^{m-1} x}{dt^{m-1}} + \cdots + b_1 \frac{dx}{dt} + b_0 x \quad m \leq n$$

The coefficients $a_0, a_1, a_2, \dots, a_n$ and b_0, b_1, \dots, b_m represent physical system parameters whose properties and values depend on the measurement system itself. Real measurement systems can be modeled this way by considering their governing system equations. These equations are generated by application of pertinent fundamental physical laws of nature to the measurement system. Our discussion is limited to measurement system concepts, but a general treatment of systems can be found in text books dedicated to that topic (1–3).

Example 3.1

As an illustration, consider the seismic accelerometer depicted in Figure 3.3a. Various configurations of this instrument are used in seismic and vibration engineering to determine the motion of large bodies to which the accelerometer is attached. Basically, as the small accelerometer mass reacts to motion, it places the piezoelectric crystal into compression or tension, causing a surface charge to develop on the crystal. The charge is proportional to the motion. As the large body moves, the mass of the accelerometer will move with an inertial response. The stiffness of the spring, k , provides a restoring force to move the accelerometer mass back to equilibrium while internal frictional damping, c , opposes any displacement away from equilibrium. A model of this

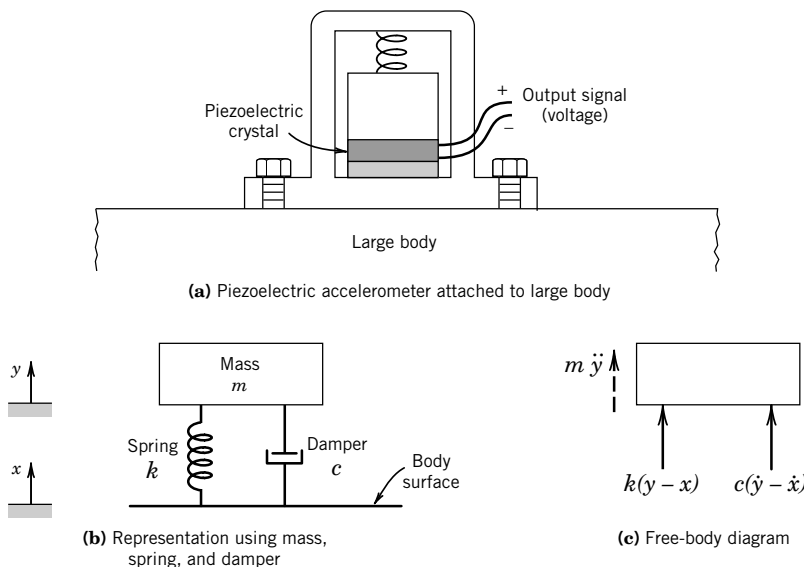


Figure 3.3 Lumped parameter model of accelerometer (Ex. 3.1).

measurement device in terms of ideal lumped elements of stiffness, mass, and damping is given in Figure 3.3b and the corresponding free-body diagram in Figure 3.3c. Let y denote the position of the small mass within the accelerometer and x denote the displacement of the body. Solving Newton's second law for the free body yields the second-order linear, ordinary differential equation

$$m \frac{d^2y}{dt^2} + c \frac{dy}{dt} + ky = c \frac{dx}{dt} + kx$$

Since the displacement y is the pertinent output from the accelerometer due to displacement x , the equation has been written such that all output terms, that is, all the y terms, are on the left side. All other terms are to be considered as input signals and are placed on the right side. Comparing this to the general form for a second-order equation ($n=2$; $m=1$) from Equation 3.1,

$$a^2 \frac{d^2y}{dt^2} + a_1 \frac{dy}{dt} + a_0 y = b_1 \frac{dx}{dt} + b_0 x$$

we can see that $a_2 = m$, $a_1 = b_1 = c$, $a_0 = b_0 = k$, and that the forces developed due to the velocity and displacement of the body become the inputs to the accelerometer. If we could anticipate the waveform of x , for example, $x(t) = x_0 \sin \omega t$, we could solve for $y(t)$, which gives the measurement system response.

Fortunately, many measurement systems can be modeled by zero-, first-, or second-order linear, ordinary differential equations. More complex systems can usually be simplified to these lower orders. Our intention here is to attempt to understand how systems behave and how such response is closely related to the design features of a measurement system; it is not to simulate the exact system behavior. The exact input-output relationship is found from calibration. But modeling guides us in choosing specific instruments and measuring methods by predicting system response to signals, and in determining the type, range, and specifics of calibration. Next, we examine several special cases of Equation 3.1 that model the most important concepts of measurement system behavior.

3.3 SPECIAL CASES OF THE GENERAL SYSTEM MODEL

Zero-Order Systems

The simplest model of a measurement systems and one used with static signals is the zero-order system model. This is represented by the zero-order differential equation:

$$a_0 y = F(t)$$

Dividing through by a_0 gives

$$y(t) = KF(t) \quad (3.2)$$

where $K = 1/a_0$. K is called the static sensitivity or steady gain of the system. This system property was introduced in Chapter 1 as the relation between the change in output associated with a change in static input. In a zero-order model, the system output is considered to respond to the input signal instantaneously. If an input signal of magnitude $F(t) = A$ were applied, the instrument would indicate KA , as modeled by Equation 3.2. The scale of the measuring device would be calibrated to indicate A directly.

For real systems, the zero-order system concept is used to model the non-time-dependent measurement system response to static inputs. In fact, the zero-order concept appropriately models any system during a static calibration. When dynamic input signals are involved, a zero-order model

is valid only at static equilibrium. This is because most real measurement systems possess inertial or storage capabilities that require higher-order differential equations to correctly model their time-dependent behavior to dynamic input signals.

Determination of K

The static sensitivity is found from the static calibration of the measurement system. It is the slope of the calibration curve, $K = dy/dx$.

Example 3.2

A pencil-type pressure gauge commonly used to measure tire pressure can be modeled at static equilibrium by considering the force balance on the gauge sensor, a piston that slides up and down a cylinder. An exploded view of an actual gauge is shown in Figure 3.4c. In Figure 3.4a, we model the piston motion¹ as being restrained by an internal spring of stiffness, k , so that at static equilibrium the absolute pressure force, F , bearing on the piston equals the force exerted on the piston by the spring, F_s , plus the atmospheric pressure force, F_{atm} . In this manner, the transduction of pressure into mechanical displacement occurs. Considering the piston free-body at static equilibrium in Figure 3.4b, the static force balance, $\Sigma F = 0$, gives

$$ky = F - F_{atm}$$

where y is measured relative to some static reference position marked as zero on the output display. Pressure is simply the force acting inward over the piston surface area, A . Dividing through by area

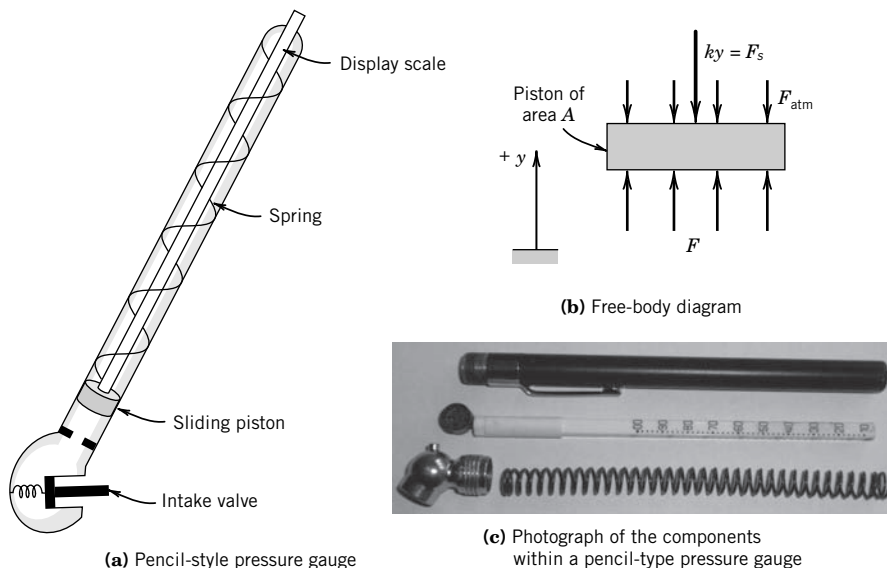


Figure 3.4 Lumped parameter model of pressure gauge (Ex. 3.2).

¹ In a common gauge there may or may not be the mechanical spring shown.

provides the zero-order response equation between output displacement and input pressure and gives

$$y = (A/k)(p - p_{\text{atm}})$$

The term $(p - p_{\text{atm}})$ represents the pressure relative to atmospheric pressure. It is the pressure indicated by this gauge. Direct comparison with Equation 3.2 shows that the input pressure magnitude equates to the piston displacement through the static sensitivity, $K = A/k$. Drawing from the concept of Figure 3.2, the system operates on pressure so as to bring about the relative displacement of the piston, the magnitude of which is used to indicate the pressure. The equivalent of spring stiffness and piston area affect the magnitude of this displacement—factors considered in its design. The exact static input–output relationship is found through calibration of the gauge. Because elements such as piston inertia and frictional dissipation were not considered, this model would not be appropriate for studying the dynamic response of the gauge.

First-Order Systems

Measurement systems that contain storage elements do not respond instantaneously to changes in input. The bulb thermometer discussed in Section 3.2 is a good example. The bulb exchanges energy with its environment until the two are at the same temperature, storing energy during the exchange. The temperature of the bulb sensor changes with time until this equilibrium is reached, which accounts physically for its lag in response. The rate at which temperature changes with time can be modeled with a first-order derivative and the thermometer behavior modeled as a first-order equation. In general, systems with a storage or dissipative capability but negligible inertial forces may be modeled using a first-order differential equation of the form

$$a_1 \dot{y} + a_0 y = F(t) \quad (3.3)$$

with $\dot{y} = dy/dt$. Dividing through by a_0 gives

$$\tau \dot{y} + y = KF(t) \quad (3.4)$$

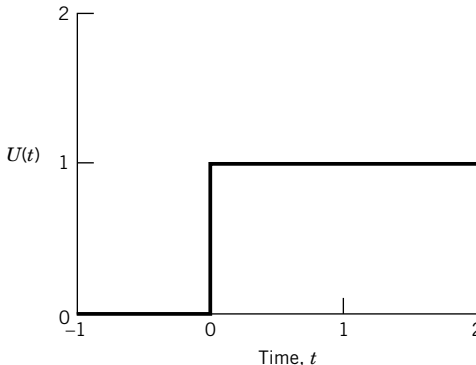
where $\tau = a_1/a_0$. The parameter τ is called the *time constant* of the system. Regardless of the physical dimensions of a_0 and a_1 , their ratio will always have the dimensions of time. The time constant provides a measure of the speed of system response, and as such is an important specification in measuring dynamic input signals. To explore this concept more fully, consider the response of the general first-order system to the following two forms of an input signal: the step function and the simple periodic function.

Step Function Input

The step function, $AU(t)$, is defined as

$$\begin{aligned} AU(t) &= 0 & t \leq 0^- \\ AU(t) &= A & t \geq 0^+ \end{aligned}$$

where A is the amplitude of the step function and $U(t)$ is defined as the unit step function as depicted in Figure 3.5. Physically, this function describes a sudden change in the input signal from a constant value of one magnitude to a constant value of some other magnitude, such as a sudden change in

Figure 3.5 The unit step function, $U(t)$.

loading, displacement, or any physical variable. When we apply a step function input to a measurement system, we obtain information about how quickly a system will respond to a change in input signal. To illustrate this, let us apply a step function as an input to the general first-order system. Setting $F(t) = AU(t)$ in Equation 3.4 gives

$$\tau \dot{y} + y = KAU(t) = KF(t)$$

with an arbitrary initial condition denoted by, $y(0) = y_0$. Solving for $t \geq 0^+$ yields

$$\underbrace{y(t)}_{\text{Time response}} = \underbrace{KA}_{\text{Steady response}} + \underbrace{(y_0 - KA)e^{-t/\tau}}_{\text{Transient response}} \quad (3.5)$$

The solution of the differential equation, $y(t)$, is the time response (or simply the response) of the system. Equation 3.5 describes the behavior of the system to a step change in input. This means that $y(t)$ is in fact the output indicated by the display stage of the system. It should represent the time variation of the output display of the measurement system if an actual step change were applied to the system. We have simply used mathematics to simulate this response.

Equation 3.5 consists of two parts. The first term is known as the steady response because, as $t \rightarrow \infty$, the response of $y(t)$ approaches this steady value. The steady response is that portion of the output signal that remains after the transient response has decayed to zero. The second term on the right side of Equation 3.5 is known as the transient response of $y(t)$ because, as $t \rightarrow \infty$, the magnitude of this term eventually reduces to zero.

For illustrative purposes, let $y_0 < A$ so that the time response becomes as shown in Figure 3.6. Over time, the indicated output value rises from its initial value, at the instant the change in input is applied, to an eventual constant value, $y_\infty = KA$, at steady response. As an example, compare this general time response to the recognized behavior of the bulb thermometer when measuring body temperature as discussed earlier. We see a qualitative similarity. In fact, in using a bulb thermometer to measure body temperature, this is a real step function input to the thermometer, itself a first-order measuring system.

Suppose we rewrite the response Equation 3.5 in the form

$$\Gamma(t) = \frac{y(t) - y_\infty}{y_0 - y_\infty} = e^{-t/\tau} \quad (3.6)$$

The term $\Gamma(t)$ is called the *error fraction* of the output signal. Equation 3.6 is plotted in Figure 3.7, where the time axis is nondimensionalized by the time constant. We see that the error fraction

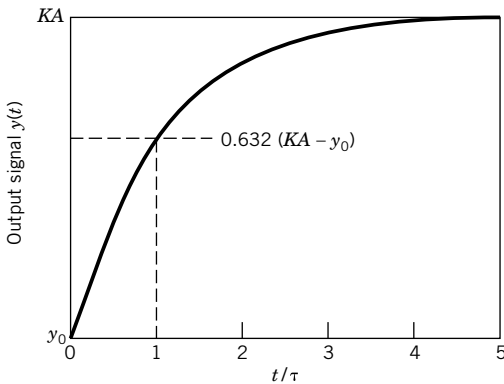


Figure 3.6 First-order system time response to a step function input: the time response, $y(t)$.

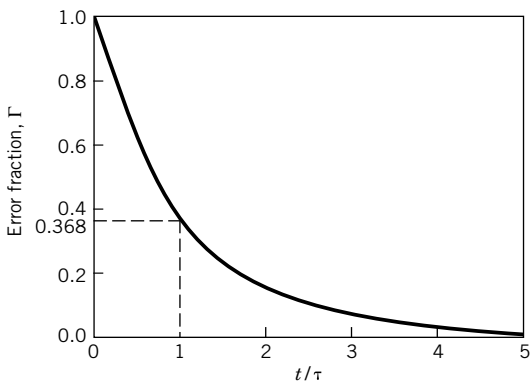


Figure 3.7 First-order system time response to a step function input: the error fraction, Γ .

decreases from a value of 1 and approaches a value of 0 with increasing t/τ . At the instant just after the step change in input is introduced, $\Gamma = 1.0$, so that the indicated output from the measurement system is 100% in error. This implies that the system has responded 0% to the input change, that is, it has not changed. From Figure 3.7, it is apparent that as time moves forward the system does respond, and with decreasing error in its indicated value. Let the percent response of the system to a step change be given as $(1 - \Gamma) \times 100$. Then by $t = \tau$, where $\Gamma = 0.368$, the system will have responded to 63.2% of the step change. Further, when $t = 2.3\tau$ the system will have responded ($\Gamma = 0.10$) to 90% of the step change; by $t = 5\tau$, we find the response to be 99.3%. Values for the percent response and the corresponding error as functions of t/τ are summarized in Table 3.1. The time required for a system to respond to a value that is 90% of the step input, $y_\infty - y_0$, is important and is called the *rise time* of the system.

Based on this behavior, we can see that the time constant is in fact a measure of how quickly a first-order measurement system will respond to a change in input value. A smaller time constant indicates a shorter time between the instant that an input is applied and when the system reaches an essentially steady output. We define the *time constant* as the time required for a first-order system to achieve 63.2% of the step change magnitude, $y_\infty - y_0$. The time constant is a system property.

Determination of τ From the development above, the time constant can be experimentally determined by recording the system's response to a step function input of a known magnitude.

Table 3.1 First-Order System Response and Error Fraction

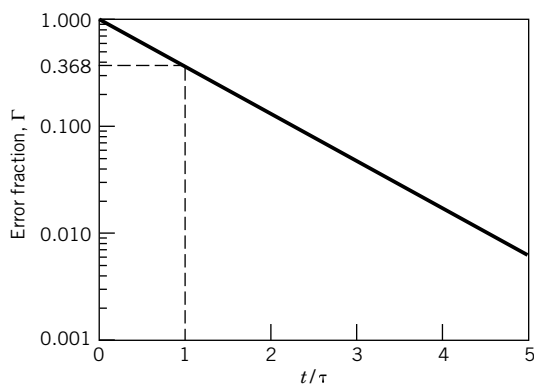
t/τ	% Response	Γ	% Error
0	0.0	1.0	100.0
1	63.2	0.368	36.8
2	86.5	0.135	13.5
2.3	90.0	0.100	10.0
3	95.0	0.050	5.0
5	99.3	0.007	0.7
∞	100.0	0.0	0.0

In practice, it is best to record that response from $t = 0$ until steady response is achieved. The data can then be plotted as error fraction versus time on a semilog plot, such as in Figure 3.8. This type of plot is equivalent to the transformation

$$\ln \Gamma = 2.3 \log \Gamma = -(1/\tau)t \quad (3.7)$$

which is of the linear form, $Y = mX + B$ (where $Y = \ln \Gamma$, $m = -(1/\tau)$, $X = t$, and $B = 0$ here). A linear curve fit through the data will provide a good estimate of the slope, m , of the resulting plot. From Equation 3.7, we see that $m = -1/\tau$, which yields the estimate for τ .

This method offers advantages over attempting to compute τ directly from the time required to achieve 63.2% of the step-change magnitude. First, real systems will deviate somewhat from perfect first-order behavior. On a semilog plot (Figure 3.8), such deviations are readily apparent as clear trends away from a straight line. Modest deviations do not pose a problem. But strong deviations indicate that the system is not behaving as expected, thus requiring a closer examination of the system operation, the step function experiment, or the assumed form of the system model. Second, acquiring data during the step function experiment is prone to some random error in each data point. The use of a data curve fit to determine τ utilizes all of the data over time so as to minimize the influence of an error in any one data point. Third, the method eliminates the need to determine the $\Gamma = 1.0$ and 0.368 points, which are difficult to establish in practice and so are prone to a systematic error.

**Figure 3.8** The error fraction plotted on semilog coordinates.

Example 3.3

Suppose a bulb thermometer originally indicating 20°C is suddenly exposed to a fluid temperature of 37°C. Develop a model that simulates the thermometer output response.

$$\text{KNOWN } T(0) = 20^\circ\text{C}$$

$$T_\infty = 37^\circ\text{C}$$

$$F(t) = [T_\infty - T(0)]U(t)$$

ASSUMPTIONS To keep things simple, assume the following: no installation effects (neglect conduction and radiation effects); sensor mass is mass of liquid in bulb only; uniform temperature within bulb (lumped mass); and thermometer scale is calibrated to indicate temperature

$$\text{FIND } T(t)$$

SOLUTION Consider the energy balance developed in Figure 3.9. According to the first law of thermodynamics, the rate at which energy is exchanged between the sensor and its environment through convection, \dot{Q} , must be balanced by the storage of energy within the thermometer, dE/dt . This conservation of energy is written as

$$\frac{dE}{dt} = \dot{Q}$$

Energy storage in the bulb is manifested by a change in bulb temperature so that for a constant mass bulb, $dE(t)/dt = mc_v dT(t)/dt$. Energy exchange by convection between the bulb at $T(t)$ and an environment at T_∞ has the form $\dot{Q} = hA_s\Delta T$. The first law can be written as

$$mc_v \frac{dT(t)}{dt} = hA_s[T_\infty - T(t)]$$

This equation can be written in the form

$$mc_v \frac{dT(t)}{dt} + hA_s[T(t) - T(0)] = hA_sF(t) = hA_s[T_\infty - T(0)]U(t)$$

with initial condition $T(0)$ and

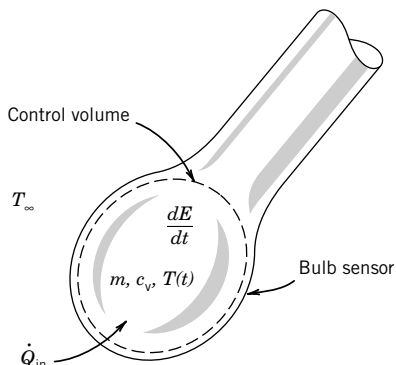


Figure 3.9 Lumped parameter model of thermometer and its energy balance (Ex. 3.3).

where

m = mass of liquid within thermometer

c_v = specific heat of liquid within thermometer

h = convection heat transfer coefficient between bulb and environment

A_s = thermometer surface area

The term hA_s controls the rate at which energy can be transferred between a fluid and a body; it is analogous to electrical conductance. By comparison with Equation 3.3, $a_0 = hA_s$, $a_1 = mc_v$, and $b_0 = hA_s$. Rewriting for $t \geq 0^+$ and simplifying yields

$$\frac{mc_v}{hA_s} \frac{dT(t)}{dt} + T(t) = T_\infty$$

From Equation 3.4, this implies that the time constant and static sensitivity are

$$\tau = \frac{mc_v}{hA_s} \quad K = \frac{hA_s}{hA_s} = 1$$

Direct comparison with Equation 3.5 yields this thermometer response:

$$\begin{aligned} T(t) &= T_\infty + [T(0) - T_\infty] e^{-t/\tau} \\ &= 37 - 17e^{-t/\tau} \text{ [} ^\circ\text{C}] \end{aligned}$$

COMMENT Two interactive examples of the thermometer problem (from Exs 3.3–3.5) are available. In the program *FirstOrd*, the user can choose input functions and study the system response. In the LabView program *Temperature_response*, the user can apply interactively a step change in temperature and study the first-order system response of a thermal sensor.

Clearly the time constant, τ , of the thermometer can be reduced by decreasing its mass-to-area ratio or by increasing h (for example, increasing the fluid velocity around the sensor). Without modeling, such information could be ascertained only by trial and error, a time-consuming and costly method with no assurance of success. Also, it is significant that we found that the response of the temperature measurement system in this case depends on the environmental conditions of the measurement that control h , because the magnitude of h affects the magnitude of τ . If h is not controlled during response tests (i.e., if it is an extraneous variable), ambiguous results are possible. For example, the curve of Figure 3.8 will become nonlinear, or replications will not yield the same values for τ .

Review of this example should make it apparent that the results of a well-executed step calibration may not be indicative of an instrument's performance during a measurement if the measurement conditions differ from those existing during the step calibration.

Example 3.4

For the thermometer in Example 3.3 subjected to a step change in input, calculate the 90% rise time in terms of t/τ .

KNOWN Same as Example 3.3

ASSUMPTIONS Same as Example 3.3

FIND 90% response time in terms of t/τ

SOLUTION The percent response of the system is given by $(1 - \Gamma) \times 100$ with the error fraction, Γ , defined by Equation 3.6. From Equation 3.5, we note that at $t = \tau$, the thermometer will indicate $T(t) = 30.75^\circ\text{C}$, which represents only 63.2% of the step change from 20° to 37°C . The 90% rise time represents the time required for Γ to drop to a value of 0.10. Then

$$\Gamma = 0.10 = e^{-t/\tau}$$

or $t/\tau = 2.3$.

COMMENT In general, a time equivalent to 2.3τ is required to achieve 90% of the applied step input for a first-order system.

Example 3.5

A particular thermometer is subjected to a step change, such as in Example 3.3, in an experimental exercise to determine its time constant. The temperature data are recorded with time and presented in Figure 3.10. Determine the time constant for this thermometer. In the experiment, the heat transfer coefficient, h , is estimated to be $6 \text{ W/m}^2\text{-}^\circ\text{C}$ from engineering handbook correlations.

KNOWN Data of Figure 3.10

$$h = 6 \text{ W/m}^2\text{-}^\circ\text{C}$$

ASSUMPTIONS First-order behavior using the model of Example 3.3, constant properties

FIND τ

SOLUTION According to Equation 3.7, the time constant should be the negative reciprocal of the slope of a line drawn through the data of Figure 3.10. Aside from the first few data points, the data appear to follow a linear trend, indicating a nearly first-order behavior and validating our model assumption. The data is fit to the first-order equation²

$$2.3 \log \Gamma = (-0.194)t + 0.00064$$

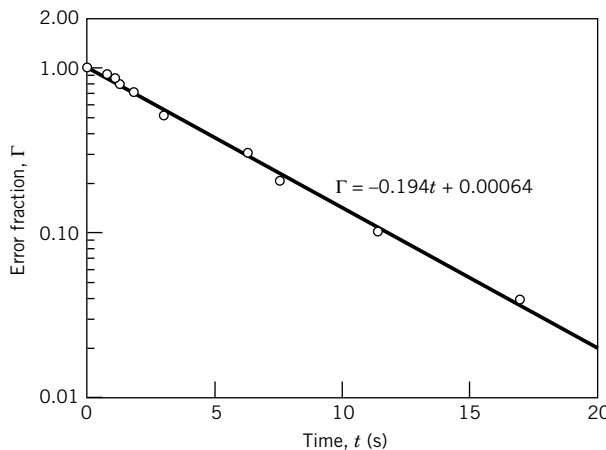


Figure 3.10 Temperature–time history of Example 3.5.

²The least-squares approach to curve fitting is discussed in detail in Chapter 4.

With $m = -0.194 = -1/\tau$, the time constant is calculated as $\tau = 5.15$ seconds.

COMMENT If the experimental data were to deviate significantly from first-order behavior, this would be a clue that either our assumptions do not fit the real-problem physics or that the test conduct has control or execution problems.

Simple Periodic Function Input

Periodic signals are commonly encountered in engineering processes. Examples include vibrating structures, vehicle suspension dynamics, biological circulations, and reciprocating pump flows. When periodic inputs are applied to a first-order system, the input signal frequency has an important influence on measuring system time response and affects the output signal. This behavior can be studied effectively by applying a simple periodic waveform to the system. Consider the first-order measuring system to which an input of the form of a simple periodic function, $F(t) = A \sin \omega t$, is applied for $t \geq 0^+$:

$$\tau \dot{y} + y = KA \sin \omega t$$

with initial conditions $y(0) = y_0$. Note that ω in [rad/s] = $2\pi f$ with f in [Hz]. The general solution to this differential equation yields the measurement system output signal, that is, the time response to the applied input, $y(t)$:

$$y(t) = Ce^{-t/\tau} + \frac{KA}{\sqrt{1 + (\omega\tau)^2}} \sin(\omega t - \tan^{-1}\omega\tau) \quad (3.8)$$

where the value for C depends on the initial conditions.

So what has happened? The output signal, $y(t)$, of Equation 3.8 consists of a transient and a steady response. The first term on the right side is the transient response. As t increases, this term decays to zero and no longer influences the output signal. Transient response is important only during the initial period following the application of the new input. We already have information about the system transient response from the step function study, so we focus our attention on the second term, the steady response. This term persists for as long as the periodic input is maintained. From Equation 3.8, we see that the frequency of the steady response term remains the same as the input signal frequency, but note that the amplitude of the steady response depends on the value of the applied frequency, ω . Also, the phase angle of the periodic function has changed.

Equation 3.8 can be rewritten in a general form:

$$\begin{aligned} y(t) &= Ce^{-t/\tau} + B(\omega)\sin[\omega t + \Phi] \\ B(\omega) &= \frac{KA}{\sqrt{1 + (\omega\tau)^2}} \\ \Phi(\omega) &= -\tan^{-1}(\omega\tau) \end{aligned} \quad (3.9)$$

where $B(\omega)$ represents the amplitude of the steady response and the angle $\Phi(\omega)$ represents the *phase shift*. A relative illustration between the input signal and the system output response is given in Figure 3.11 for an arbitrary frequency and system time constant. From Equation 3.9, both B and ϕ are frequency dependent. Hence, the exact form of the output response depends on the value of the frequency

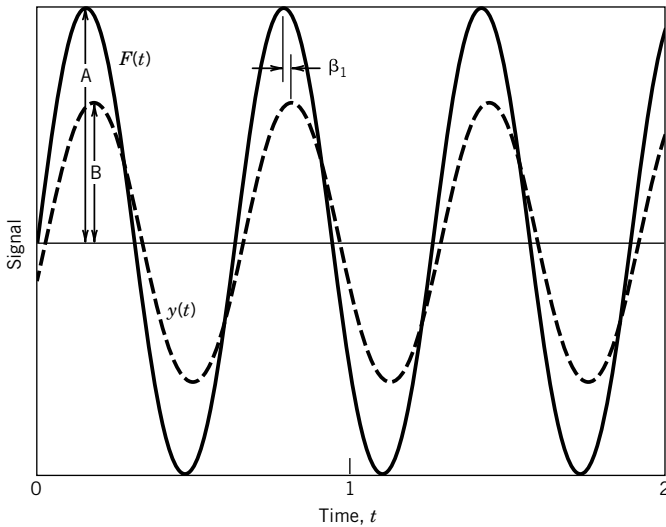


Figure 3.11 Relationship between a sinusoidal input and output: amplitude, frequency, and time delay.

of the input signal. The steady response of any system to which a periodic input of frequency, ω , is applied is known as the frequency response of the system. The frequency affects the magnitude of amplitude B and also can bring about a time delay. This time delay, β_1 , is seen in the phase shift, $\Phi(\omega)$, of the steady response. For a phase shift given in radians, the time delay in units of time is

$$\beta_1 = \frac{\Phi}{\omega}$$

that is, we can write

$$\sin(\omega t + \Phi) = \sin\left[\omega\left(t + \frac{\Phi}{\omega}\right)\right] = \sin[\omega(t + \beta_1)]$$

The value for β_1 will be negative, indicating that the time shift is a delay between the output and input signals. Since Equation 3.9 applies to all first-order measuring systems, the magnitude and phase shift by which the output signal differs from the input signal are predictable.

We define a magnitude ratio, $M(\omega)$, as the ratio of the output signal amplitude to the input signal amplitude, $M(\omega) = B/KA$. For a first-order system subjected to a simple periodic input, the magnitude ratio is

$$M(\omega) = \frac{B}{KA} = \frac{1}{\sqrt{1 + (\omega\tau)^2}} \quad (3.10)$$

The magnitude ratio for a first-order system is plotted in Figure 3.12, and the corresponding phase shift is plotted in Figure 3.13. The effects of both system time constant and input signal frequency on frequency response are apparent in both figures. This behavior can be interpreted in the following manner. For those values of ωt for which the system responds with values of $M(\omega)$ near unity, the measurement system transfers all or nearly all of the input signal amplitude to the output and with very little time delay; that is, B will be nearly equal to KA in magnitude and $\Phi(\omega)$ will be near zero degrees. At large values of $\omega\tau$ the measurement system filters out any frequency information of the

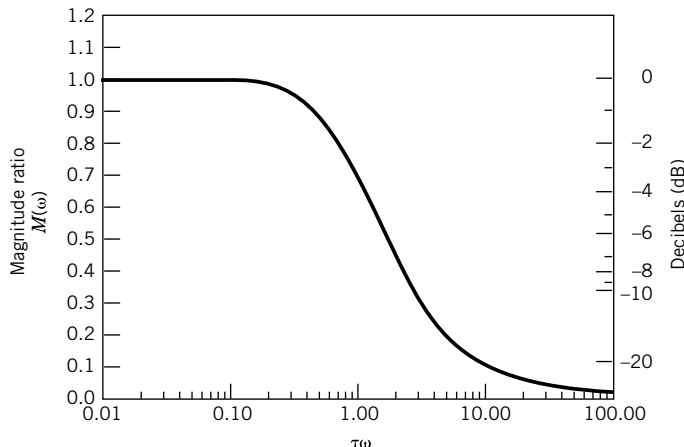


Figure 3.12 First-order system frequency response: magnitude ratio.

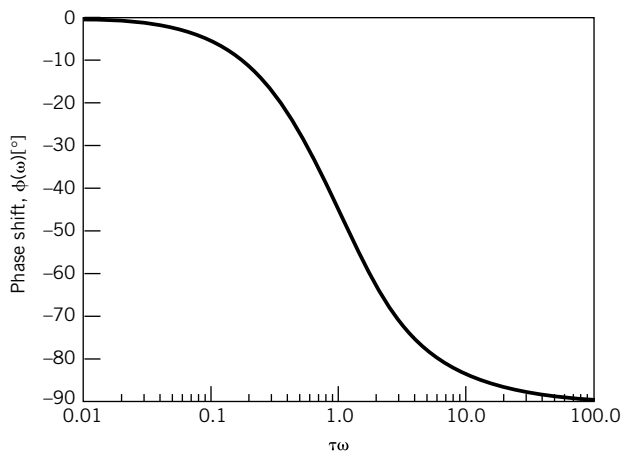


Figure 3.13 First-order system frequency response: phase shift.

input signal by responding with very small amplitudes, which is seen by the small $M(\omega)$, and by large time delays, as evidenced by increasingly nonzero β_1 .

Any combination of ω and τ produces the same results. If we wanted to measure signals with high-frequency content, then we would need a system having a small τ . On the other hand, systems of large τ may be adequate to measure signals of low-frequency content. Often the trade-offs compete available technology against cost.

The *dynamic error*, $\delta(\omega)$, of a system is defined as $\delta(\omega) = M(\omega) - 1$. It is a measure of the inability of a system to adequately reconstruct the amplitude of the input signal for a particular input frequency. We normally want measurement systems to have a magnitude ratio at or near unity over the anticipated frequency band of the input signal to minimize $\delta(\omega)$. Perfect reproduction of the input signal is not possible, so some dynamic error is inevitable. We need some way to state this. For a first-order system, we define a *frequency bandwidth* as the frequency band over which $M(\omega) \geq 0.707$; in terms of the decibel (plotted in Figure 3.12) defined as

$$\text{dB} = 20 \log M(\omega) \quad (3.11)$$

this is the band of frequencies within which $M(\omega)$ remains above -3 dB.

The functions $M(\omega)$ and $\Phi(\omega)$ represent the frequency response of the measurement system to periodic inputs. These equations and universal curves provide guidance in selecting measurement systems and system components.

Determination of Frequency Response The frequency response of a measurement system is found by a dynamic calibration. In this case, the calibration would entail applying a simple periodic waveform of known amplitude and frequency to the system sensor stage and measuring the corresponding output stage amplitude and phase shift. In practice, developing a method to produce a periodic input signal in the form of a physical variable may demand considerable ingenuity and effort. Hence, in many situations an engineer elects to rely on modeling to infer system frequency response behavior. We can predict the dynamic behavior if the time constant and static sensitivity of the system and the range of input frequencies are all known.

Example 3.6

A temperature sensor is to be selected to measure temperature within a reaction vessel. It is suspected that the temperature will behave as a simple periodic waveform with a frequency somewhere between 1 and 5 Hz. Sensors of several sizes are available, each with a known time constant. Based on time constant, select a suitable sensor, assuming that a dynamic error of $\pm 2\%$ is acceptable.

$$\begin{aligned} \text{KNOWN} \quad & 1 \leq f \leq 5 \text{ Hz} \\ & |\delta(\omega)| \leq 0.02 \end{aligned}$$

ASSUMPTIONS First-order system

$$F(t) = A \sin \omega t$$

FIND Time constant, τ

SOLUTION With $|\delta(\omega)| \leq 0.02$, we would set the magnitude ratio between $0.98 \leq M \leq 1.02$. From Figure 3.12, we see that first-order systems never exceed $M = 1$. So the constraint becomes $0.98 \leq M \leq 1$. Then,

$$0.98 \leq M(\omega) = \frac{1}{\sqrt{1 + (\omega\tau)^2}} \leq 1$$

From Figure 3.12, this constraint is maintained over the range $0 \leq \omega\tau \leq 0.2$. We can also see in this figure that for a system of fixed time constant, the smallest value of $M(\omega)$ will occur at the largest frequency. So with $\omega = 2\pi f = 2\pi(5)\text{rad/s}$ and solving for $M(\omega) = 0.98$ yields, $\tau \leq 6.4 \text{ ms}$. Accordingly, a sensor having a time constant of 6.4 ms or less will work.

Second-Order Systems

Systems possessing inertia contain a second-derivative term in their model equation (e.g., see Ex. 3.1). A system modeled by a second-order differential equation is called a second-order

system. Examples of second-order instruments include accelerometers and pressure transducers (including microphones and loudspeakers).

In general, a second-order measurement system subjected to an arbitrary input, $F(t)$, can be described by an equation of the form

$$a_2\ddot{y} + a_1\dot{y} + a_0y = F(t) \quad (3.12)$$

where a_0 , a_1 , and a_2 are physical parameters used to describe the system and $\ddot{y} = d^2y/dt^2$. This equation can be rewritten as

$$\frac{1}{\omega_n^2}\ddot{y} + \frac{2\zeta}{\omega_n}\dot{y} + y = KF(t) \quad (3.13)$$

where

$$\omega_n = \sqrt{\frac{a_0}{a_2}} = \text{natural frequency of the system}$$

$$\zeta = \frac{a_1}{2\sqrt{a_0 a_2}} = \text{damping ratio of the system}$$

Consider the homogeneous solution to Equation 3.13. Its form depends on the roots of the characteristic equation of Equation 3.13:

$$\frac{1}{\omega_n^2}\lambda^2 + \frac{2\zeta}{\omega_n}\lambda + 1 = 0$$

This quadratic equation has two roots,

$$\lambda_{1,2} = -\zeta\omega_n \pm \omega_n\sqrt{\zeta^2 - 1}$$

Depending on the value for ζ three forms of homogeneous solution are possible:

$0 \leq \zeta < 1$ (underdamped system solution)

$$y_h(t) = Ce^{-\zeta\omega_n t} \sin\left(\omega_n\sqrt{1 - \zeta^2}t + \Theta\right) \quad (3.14a)$$

$\zeta = 1$ (critically damped system solution)

$$y_h(t) = C_1e^{\lambda_1 t} + C_2te^{\lambda_2 t} \quad (3.14b)$$

$\zeta > 1$ (overdamped system solution)

$$y_h(t) = C_1e^{\lambda_1 t} + C_2e^{\lambda_2 t} \quad (3.14c)$$

The homogeneous solution determines the transient response of a system. The damping ratio, ζ , is a measure of system damping, a property of a system that enables it to dissipate energy internally. For systems with $0 \leq \zeta \leq 1$, the transient response will be oscillatory, whereas for $\zeta \geq 1$, the transient response will not oscillate. The critically damped solution, $\zeta = 1$, denotes the demarcation between oscillatory and nonoscillatory behavior in the transient response.

Step Function Input

Again, the step function input is applied to determine the general behavior and speed at which the system will respond to a change in input. The response of a second-order measurement system to a step function input is found from the solution of Equation 3.13, with $F(t) = AU(t)$, to be

$$y(t) = KA - KAE^{-\zeta\omega_n t} \left[\frac{\zeta}{\sqrt{1-\zeta^2}} \sin(\omega_n t \sqrt{1-\zeta^2}) + \cos(\omega_n t \sqrt{1-\zeta^2}) \right] \quad 0 \leq \zeta < 1 \quad (3.15a)$$

$$y(t) = KA - KA(1 + \omega_n t)e^{-\omega_n t} \quad \zeta = 1 \quad (3.15b)$$

$$y(t) = KA - KA \left[\frac{\zeta + \sqrt{\zeta^2 - 1}}{2\sqrt{\zeta^2 - 1}} e^{(-\zeta + \sqrt{\zeta^2 - 1})\omega_n t} + \frac{\zeta - \sqrt{\zeta^2 - 1}}{2\sqrt{\zeta^2 - 1}} e^{(-\zeta - \sqrt{\zeta^2 - 1})\omega_n t} \right] \quad \zeta > 1 \quad (3.15c)$$

where we set the initial conditions, $y(0) = \dot{y}(0) = 0$ for convenience.

Equations 3.15a–c are plotted in Figure 3.14 for several values of ζ . The interesting feature is the transient response. For under-damped systems, the transient response is oscillatory about the steady value and occurs with a period

$$T_d = \frac{2\pi}{\omega_d} = \frac{1}{f_d} \quad (3.16)$$

$$\omega_d = \omega_n \sqrt{1 - \zeta^2} \quad (3.17)$$

where ω_d is called the *ringing frequency*. In instruments, this oscillatory behavior is called “ringing.” The ringing phenomenon and the associated ringing frequency are properties of the measurement system and are independent of the input signal. It is the free oscillation frequency of a system displaced from its equilibrium.

The duration of the transient response is controlled by the $\zeta\omega_n$ term. In fact, its influence is similar to that of a time constant in a first-order system, such that we could define a second-order time constant as $\tau = 1/\zeta\omega_n$. The system settles to KA more quickly when it is designed with a larger

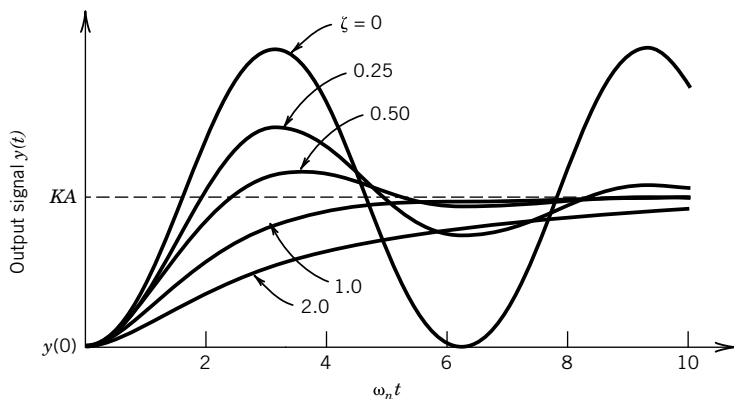


Figure 3.14 Second-order system time response to a step function input.

$\zeta\omega_n$ (i.e., smaller τ). Nevertheless, for all systems with $\zeta > 0$, the response eventually indicates the steady value of $y_\infty = KA$ as $t \rightarrow \infty$.

Recall that the *rise time* is defined as the time required to achieve a value within 90% of the step input. For a second-order system, the rise time is the time required to first achieve 90% of $(KA - y_0)$. Rise time is reduced by decreasing the damping ratio, as seen in Figure 3.14. However, the severe ringing associated with very lightly damped systems can delay the time to achieve a steady value compared to systems of higher damping. This is demonstrated by comparing the response at $\zeta = 0.25$ with the response at $\zeta = 1$ in Figure 3.14. With this in mind, the time required for a measurement system's oscillations to settle to within $\pm 10\%$ of the steady value, KA , is defined as its *settling time*. The settling time is an approximate measure of the time to achieve a steady response. A damping ratio of about 0.7 appears to offer a good compromise between ringing and settling time. If an error fraction (Γ) of a few percent is acceptable, then a system with $\zeta = 0.7$ will settle to steady response in about one-half the time of a system having $\zeta = 1$. For this reason, most measurement systems intended to measure sudden changes in input signal are typically designed such that parameters a_0 , a_1 , and a_2 provide a damping ratio of between 0.6 and 0.8.

Determination of Ringing Frequency and Rise and Settling Times The experimental determination of the ringing frequency associated with under-damped systems is performed by applying a step input to the second-order measurement system and recording the response with time. This type of calibration also yields information concerning the time to steady response of the system, which includes rise and settling times. Example 3.8 describes such a test. Typically, measurement systems suitable for dynamic signal measurements have specifications that include 90% rise time and settling time. *Adjust Second Order Parameters.vi* explores system values and response.

Determination of Natural Frequency and Damping Ratio From the under-damped system response to a step function test, values for the damping ratio and natural frequency can be extracted. From Figure 3.14, we see that with ringing the amplitude decays logarithmically with time towards a steady-state value. Let y_{\max} represent the peak amplitude occurring with each cycle. Then for the first two successive peak amplitudes, let $y_1 = (y_{\max})_1 - y_\infty$ and $y_2 = (y_{\max})_2 - y_\infty$. The damping ratio is found from

$$\zeta = \frac{1}{\sqrt{1 + \left(2\pi/\ln(y_1/y_2)\right)^2}} \quad (3.18)$$

From the calculation to find the ringing frequency using Equation 3.16, the natural frequency is found using Equation 3.17. Alternately, we could perform the step function test with $y(0) = KA$ and $y_\infty = 0$ and still use the same approach.

Example 3.7

Determine the physical parameters that affect the natural frequency and damping ratio of the accelerometer of Example 3.1.

KNOWN Accelerometer shown in Figure 3.3

ASSUMPTIONS Second-order system as modeled in Example 3.1

FIND ω_n , ζ

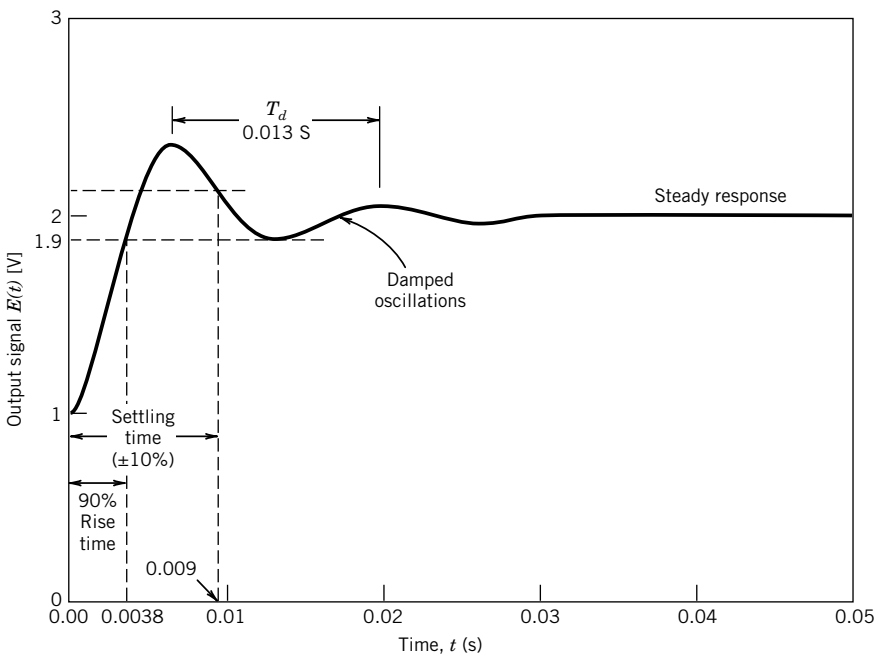


Figure 3.15 Pressure transducer time response to a step input for Example 3.8.

SOLUTION A comparison between the governing equation for the accelerometer in Example 3.1 and Equation 3.13 gives

$$\omega_n = \sqrt{\frac{k}{m}} \quad \zeta = \frac{c}{2\sqrt{km}}$$

Accordingly, the physical parameters of mass, spring stiffness, and frictional damping control the natural frequency and damping ratio of this measurement system.

Example 3.8

The curve shown in Figure 3.15 is the recorded voltage output signal of a diaphragm pressure transducer subjected to a step change in input. From a static calibration, the pressure–voltage relationship was found to be linear over the range 1 atmosphere (atm) to 4 atm with a static sensitivity of 1 V/atm. For the step test, the initial pressure was atmospheric pressure, p_a , and the final pressure was $2p_a$. Estimate the rise time, the settling time, and the ringing frequency of this measurement system.

KNOWN $p(0) = 1 \text{ atm}$

$p_\infty = 2 \text{ atm}$

$K = 1 \text{ V/atm}$

ASSUMPTIONS Second-order system behavior

FIND Rise and settling times; ω_d

SOLUTION The ringing behavior of the system noted on the trace supports the assumption that the transducer can be described as having a second-order behavior. From the given information,

$$E(0) = Kp(0) = 1 \text{ V}$$

$$E_{\infty} = Kp_{\infty} = 2 \text{ V}$$

so that the step change observed on the trace should appear as a magnitude of 1 V. The 90% rise time occurs when the output first achieves a value of 1.9 V. The 90% settling time will occur when the output settles between $1.9 < E(t) < 2.1$ V. From Figure 3.15, the rise occurs in about 4 ms and the settling time is about 9 ms. The period of the ringing behavior, T_d , is judged to be about 13 ms for an $\omega_d \approx 485 \text{ rad/s}$.

Simple Periodic Function Input

The response of a second-order system to a simple periodic function input of the form $F(t) = A \sin \omega t$ is given by

$$y(t) = y_h + \frac{KA \sin[\omega t + \Phi(\omega)]}{\left\{ \left[1 - (\omega/\omega_n)^2 \right]^2 + [2\zeta\omega/\omega_n]^2 \right\}^{1/2}} \quad (3.19)$$

with frequency-dependent phase shift

$$\Phi(\omega) = \tan^{-1} \left(-\frac{2\zeta\omega/\omega_n}{1 - (\omega/\omega_n)^2} \right) \quad (3.20)$$

The exact form for y_h is found from Equations 3.14a–c and depends on the value of ζ . The steady response, the second term on the right side, has the general form

$$y_{\text{steady}}(t) = y(t \rightarrow \infty) = B(\omega) \sin[\omega t + \Phi(\omega)] \quad (3.21)$$

with amplitude $B(\omega)$. Comparing Equations 3.19 and 3.21 shows that the amplitude of the steady response of a second-order system subjected to a sinusoidal input is also dependent on ω . So the amplitude of the output signal is frequency dependent. In general, we can define the magnitude ratio, $M(\omega)$, for a second-order system as

$$M(\omega) = \frac{B(\omega)}{KA} = \frac{1}{\left\{ \left[1 - (\omega/\omega_n)^2 \right]^2 + [2\zeta\omega/\omega_n]^2 \right\}^{1/2}} \quad (3.22)$$

The magnitude ratio-frequency dependence for a second-order system is plotted in Figure 3.16 for several values of damping ratio. A corresponding plot of the phase-shift dependency on input frequency and damping ratio is shown in Figure 3.17. For an ideal measurement system, $M(\omega)$ would equal unity and $\Phi(\omega)$ would equal zero for all values of measured frequency. Instead, $M(\omega)$ approaches zero and $\Phi(\omega)$ approaches $-\pi$ as ω/ω_n becomes large. Keep in mind that ω_n is a property of the measurement system, while ω is a property of the input signal.

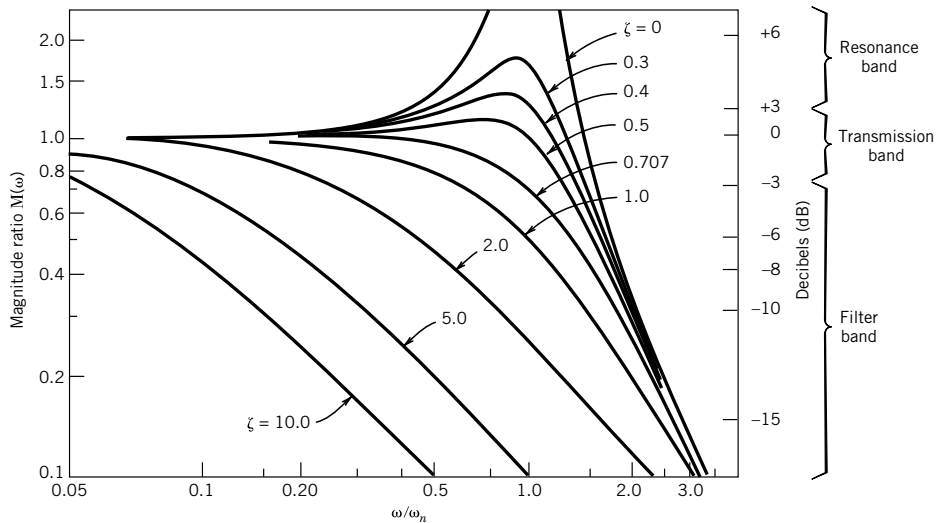


Figure 3.16 Second-order system frequency response: magnitude ratio.

System Characteristics

Several tendencies are apparent in Figures 3.16 and 3.17. For a system of zero damping, $\zeta = 0$, $M(\omega)$ will approach infinity and $\Phi(\omega)$ jumps to $-\pi$ in the vicinity of $\omega = \omega_n$. This behavior is characteristic of system resonance. Real systems possess some amount of damping, which modifies

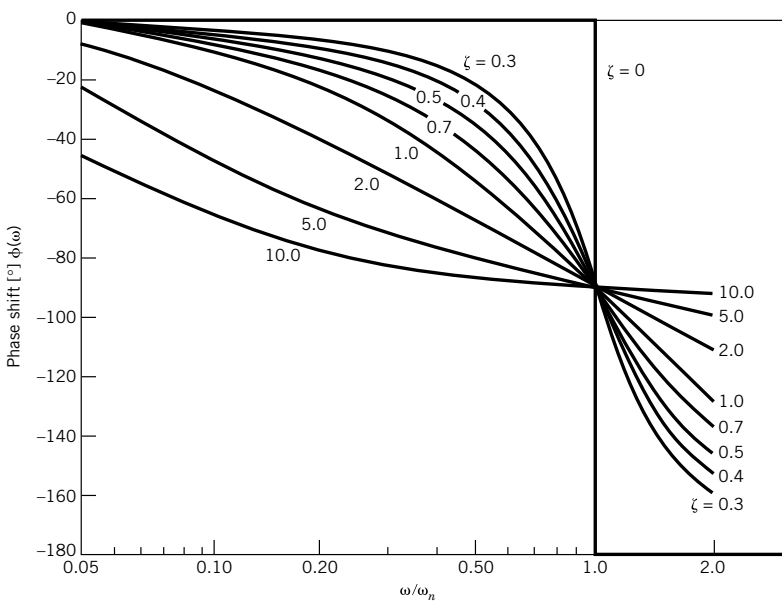


Figure 3.17 Second-order system frequency response: phase shift.

the abruptness and magnitude of resonance, but under-damped systems may still achieve resonance. This region on Figures 3.16 and 3.17 is called the *resonance band* of the system, referring to the range of frequencies over which the system is in resonance. Resonance in under-damped systems occurs at the *resonance frequency*,

$$\omega_R = \omega_n \sqrt{1 - 2\zeta^2} \quad (3.23)$$

The resonance frequency is a property of the measurement system. Resonance is excited by a periodic input signal frequency. The resonance frequency differs from the ringing frequency of free oscillation. Resonance behavior results in values of $M(\omega) > 1$ and considerable phase shift. For most applications, operating at frequencies within the resonance band is undesirable, confusing, and could even be damaging to some delicate sensors. Resonance behavior is very nonlinear and results in distortion of the signal. On the other hand, systems having $\zeta > 0.707$ do not resonate.

At small values of ω/ω_n , $M(\omega)$ remains near unity and $\Phi(\omega)$ near zero. This means that information concerning the input signal of frequency ω will be passed through to the output signal with little alteration in the amplitude or phase shift. This region on the frequency response curves is called the *transmission band*. The actual extent of the frequency range for near unity gain depends on the system damping ratio. The transmission band of a system is either specified by its frequency bandwidth, typically defined for a second-order system as $-3 \text{ dB} \leq M(\omega) \leq 3 \text{ dB}$, or otherwise specified explicitly. You need to operate within the transmission band of a measurement system to measure correctly the dynamic content of the input signal.

At large values of ω/ω_n , $M(\omega)$ approaches zero. In this region, the measurement system attenuates the amplitude information in the input signal. A large phase shift occurs. This region is known as the *filter band*, typically defined as the frequency range over which $M(\omega) \leq -3 \text{ dB}$. Most readers are familiar with the use of a filter to remove undesirable features from a desirable product. When you operate a measurement system within its filter band, the amplitudes of the portion of dynamic signal corresponding to those frequencies within the filter band will be reduced or eliminated completely. So you need to match carefully the measurement system characteristics with the signal being measured.

Example 3.9

Determine the frequency response of a pressure transducer that has a damping ratio of 0.5 and a ringing frequency (found by a step test) of 1200 Hz.

KNOWN $\zeta = 0.5$

$$\omega_d = 2\pi(1200 \text{ Hz}) = 7540 \text{ rad/s}$$

ASSUMPTIONS Second-order system behaviour

FIND $M(\omega)$ and $\Phi(\omega)$

SOLUTION The frequency response of a measurement system is determined by $M(\omega)$ and $\Phi(\omega)$ as defined in Equations 3.20 and 3.22. Since $\omega_d = \omega_n \sqrt{1 - \zeta^2}$, the natural frequency of the pressure transducer is found to be $\omega_n = 8706 \text{ rad/s}$. The frequency response at selected frequencies is computed from Equations 3.20 and 3.22:

ω (rad/s)	$M(\omega)$	$\Phi(\omega)$ [°]
500	1.00	-3.3
2,600	1.04	-18.2
3,500	1.07	-25.6
6,155	1.15	-54.7
7,540	1.11	-73.9
8,706	1.00	-90.0
50,000	0.05	-170.2

COMMENT The resonance behavior in the transducer response peaks at $\omega_R = 6155$ rad/s. As a rule, resonance effects can be minimized by operating at input frequencies of less than $\sim 30\%$ of the system's natural frequency. The response of second-order systems can be studied in more detail using the companion software. Try the Matlab program *SecondOrd* and LabView program *Second_order*.

Example 3.10

An accelerometer is to be selected to measure a time-dependent motion. In particular, input signal frequencies below 100 Hz are of prime interest. Select a set of acceptable parameter specifications for the instrument assuming a dynamic error of $\pm 5\%$.

KNOWN $f \leq 100\text{Hz}$ (i.e., $\omega \leq 628 \text{ rad/s}$)

ASSUMPTIONS Second-order system
Dynamic error of $\pm 5\%$ acceptable

FIND Select ω_n and ζ

SOLUTION To meet a $\pm 5\%$ dynamic error constraint, we want $0.95 \leq M(\omega) \leq 1.05$ over the frequency range $0 \leq \omega \leq 628 \text{ rad/s}$. This solution is open ended in that a number of instruments with different ω_n will do the task. So as one solution, let us set $\zeta = 0.7$ and then solve for the required ω_n using Equation 3.22:

$$0.95 \leq M(\omega) = \frac{1}{\left\{ \left[1 - (\omega/\omega_n)^2 \right]^2 + [2\zeta\omega/\omega_n]^2 \right\}^{1/2}} \leq 1.05$$

With $\omega = 628 \text{ rad/s}$, these equations give $\omega_n \geq 1047 \text{ rad/s}$. We could plot Equation 3.22 with $\zeta = 0.7$, as shown in Figure 3.18. In Figure 3.18, we find that $0.95 \leq M(\omega) \leq 1.05$ over the frequency range $0 \leq \omega/\omega_n \leq 0.6$. Again, this makes $\omega_n \geq 1047 \text{ rad/s}$ acceptable. So as one solution, an instrument having $\zeta = 0.7$ and $\omega_n \geq 1047 \text{ rad/s}$ meets the problem constraints.

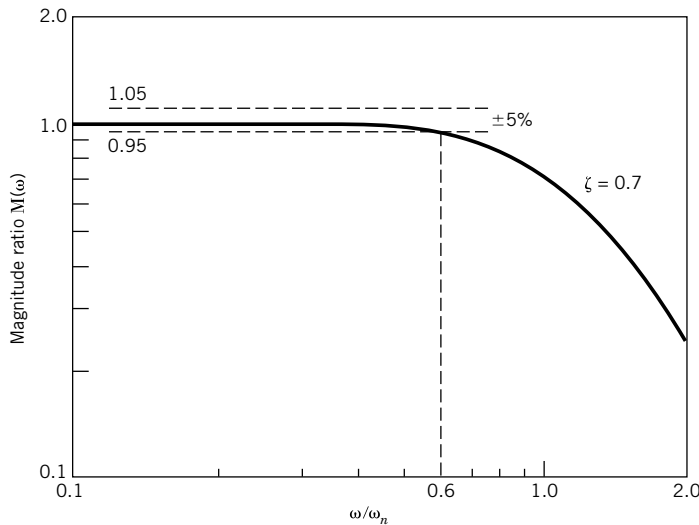


Figure 3.18 Magnitude ratio for second-order system with $\zeta = 0.7$ for Example 3.10.

3.4 TRANSFER FUNCTIONS

Consider the schematic representation in Figure 3.19. The measurement system operates on the input signal, $F(t)$, by some function, $G(s)$, so as to indicate the output signal, $y(t)$. This operation can be explored by taking the Laplace transform of both sides of Equation 3.4, which describes the general first-order measurement system. One obtains

$$Y(s) = \frac{1}{\tau s + 1} K F(s) + \frac{y_0}{\tau s + 1}$$

where $y_0 = y(0)$. This can be rewritten as

$$Y(s) = G(s) K F(s) + G(s) Q(s) \quad (3.24)$$

where $G(s)$ is the transfer function of the first-order system given by

$$G(s) = \frac{1}{\tau s + 1} \quad (3.25)$$

and $Q(s)$ is the system initial state function. Because it includes $KF(s)$, the first term on the right side of Equation 3.24 contains the information that describes the steady response of the measurement

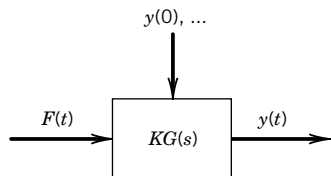


Figure 3.19 Operation of the transfer function. Compare with Figure 3.2.

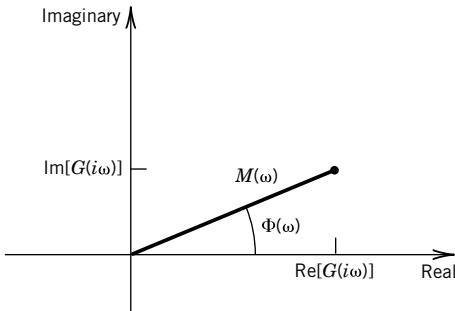


Figure 3.20 Complex plane approach to describing frequency response.

system to the input signal. The second term describes its transient response. Included in both terms, the transfer function $G(s)$ plays a role in the complete time response of the measurement system. As indicated in Figure 3.19, the *transfer function* defines the mathematical operation that the measurement system performs on the input signal $F(t)$ to yield the time response (output signal) of the system. As a review, Appendix C provides common Laplace transforms with their application to the solution of ordinary differential equations.

The system frequency response, which has been shown to be given by $M(\omega)$ and $\Phi(\omega)$, can be found by finding the value of $G(s)$ at $s = i\omega$. This yields the complex number

$$G(s = i\omega) = G(i\omega) = \frac{1}{\tau i\omega + 1} = M(\omega)e^{i\Phi(\omega)} \quad (3.26)$$

where $G(i\omega)$ is a vector on the real–imaginary plane having a magnitude, $M(\omega)$, and inclined at an angle, $\Phi(\omega)$, relative to the real axis as indicated in Figure 3.20. For the first-order system, the magnitude of $G(i\omega)$ is simply that given by $M(\omega)$ from Equation 3.10 and the phase shift angle by $\Phi(\omega)$ from Equation 3.9.

For a second-order or higher system, the approach is the same. The governing equation for a second-order system is defined by Equation 3.13, with initial conditions $y(0) = y_0$ and $\dot{y}(0) = \dot{y}_0$. The Laplace transform yields

$$Y(s) = \frac{1}{(1/\omega_n^2)s^2 + (2\zeta/\omega_n)s + 1} KF(s) + \frac{s\dot{y}_0 + y_0}{(1/\omega_n^2)s^2 + (2\zeta/\omega_n)s + 1} \quad (3.27)$$

which can again be represented by

$$Y(s) = G(s)KF(s) + G(s)Q(s) \quad (3.28)$$

By inspection, the transfer function is given by

$$G(s) = \frac{1}{(1/\omega_n^2)s^2 + (2\zeta/\omega_n)s + 1} \quad (3.29)$$

Solving for $G(s)$ at $s = i\omega$, we obtain for a second-order system

$$G(s = i\omega) = \frac{1}{(i\omega)^2/\omega_n^2 + 2\zeta i\omega/\omega_n + 1} = M(\omega)e^{i\Phi(\omega)} \quad (3.30)$$

which gives exactly the same magnitude ratio and phase shift relations as given by Equations 3.20 and 3.22.

3.5 PHASE LINEARITY

We can see from Figures 3.16 and 3.17 that systems having a damping ratio near 0.7 possess the broadest frequency range over which $M(\omega)$ will remain at or near unity and that over this same frequency range the phase shift essentially varies in a linear manner with frequency. Although it is not possible to design a measurement system without accepting some amount of phase shift, it is desirable to design a system such that the phase shift varies linearly with frequency. This is because a nonlinear phase shift is accompanied by a significant distortion in the waveform of the output signal. *Distortion* refers to a notable change in the shape of the waveform from the original, as opposed to simply an amplitude alteration or relative phase shift. To minimize distortion, many measurement systems are designed with $0.6 \leq \zeta \leq 0.8$.

Signal distortion can be illustrated by considering a particular complex waveform represented by a general function, $u(t)$:

$$u(t) = \sum_{n=1}^{\infty} \sin n\omega t = \sin \omega t + \sin 2\omega t + \dots \quad (3.31)$$

Suppose during a measurement a phase shift of this signal were to occur such that the phase shift remained linearly proportional to the frequency; that is, the measured signal, $v(t)$, could be represented by

$$v(t) = \sin(\omega t - \Phi) + \sin(2\omega t - 2\Phi) + \dots \quad (3.32)$$

Or, by setting

$$\theta = (\omega t - \Phi) \quad (3.33)$$

we write

$$v(t) = \sin \theta + \sin 2\theta + \dots \quad (3.34)$$

We see that $v(t)$ in Equation 3.22 is equivalent to the original signal, $u(t)$. If the phase shift were not linearly related to the frequency, this would not be so. This is demonstrated in Example 3.11.

Example 3.11

Consider the effect of the variations in phase shift with frequency on a measured signal by examination of the signal defined by the function

$$u(t) = \sin t + \sin 5t$$

Suppose this signal is measured in such a way that a phase shift that is linearly proportional to the frequency occurs in the form

$$v(t) = \sin(t - 0.35) + \sin[5t - 5(0.35)]$$

Both $u(t)$ and $v(t)$ are plotted in Figure 3.21. We can see that the two waveforms are identical except that $v(t)$ lags $u(t)$ by some time increment.

Now suppose this signal is measured in such a way that the relation between phase shift and frequency was nonlinear, such as in the signal output form

$$w(t) = \sin(t - 0.35) + \sin(5t - 5)$$

The $w(t)$ signal is also plotted in Figure 3.21. It behaves differently from $u(t)$, and this difference is the signal distortion. In comparison of $u(t)$, $v(t)$, and $w(t)$, it is apparent that distortion is caused by a nonlinear relation between phase shift and frequency.

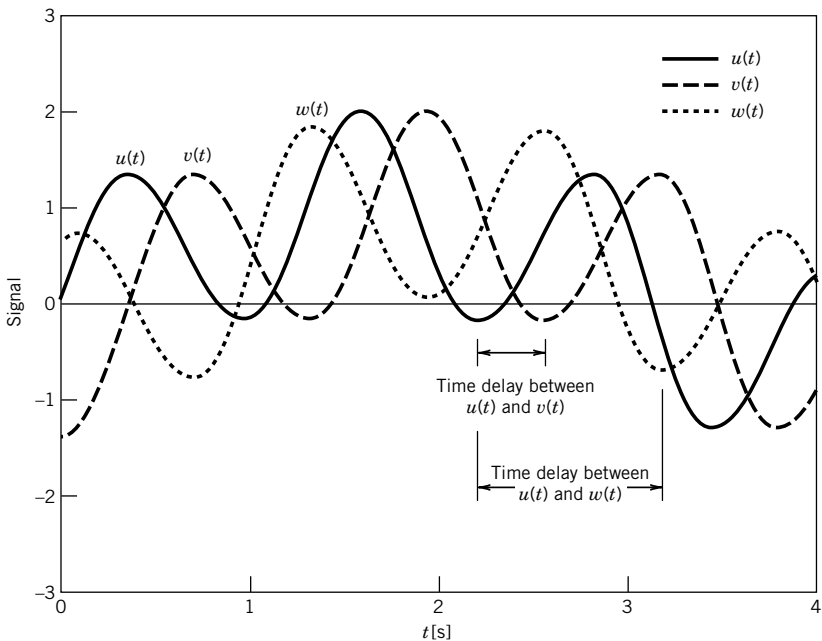


Figure 3.21 Waveforms for Example 3.11.

3.6 MULTIPLE-FUNCTION INPUTS

So far we have discussed measurement system response to a signal containing only a single frequency. What about measurement system response to multiple input frequencies? Or to an input that consists of both a static and a dynamic part, such as a periodic strain signal from an oscillating beam? When using models that are linear, such as ordinary differential equations subjected to inputs that are linear in terms of the dependent variable, the principle of superposition of linear systems applies in the solution of these equations. *The principle of superposition* states that a linear combination of input signals applied to a linear measurement system produces an output signal that is simply the linear addition of the separate output signals that would result if each input term had been applied separately. Because the form of the transient response is not affected by the input function, we can focus on the steady response. In general, we can write that if the forcing function of a form

$$F(t) = A_0 + \sum_{k=1}^{\infty} A_k \sin \omega_k t \quad (3.35)$$

is applied to a system, then the combined steady response will have the form

$$y_{\text{steady}}(t) = KA_0 + \sum_{k=1}^{\infty} B(\omega_k) \sin[\omega_k t + \Phi(\omega_k)] \quad (3.36)$$

where $B(\omega_k) = KA_k M(\omega_k)$. The development of the superposition principle can be found in basic texts on dynamic systems (4).

Example 3.12

Predict the steady output signal from a second-order instrument having $K = 1$ unit/unit, $\zeta = 2$, and $\omega_n = 628$ rad/s, which is used to measure the input signal

$$F(t) = 5 + 10 \sin 25t + 20 \sin 400t$$

KNOWN Second-order system

$$K = 1 \text{ unit/unit}; \zeta = 2.0; \omega_n = 628 \text{ rad/s}$$

$$F(t) = 5 + 10 \sin 25t + 20 \sin 400t$$

ASSUMPTIONS Linear system (superposition holds)

FIND $y(t)$

SOLUTION Since $F(t)$ has a form consisting of a linear addition of multiple input functions, the steady response signal will have the form of Equation 3.33 of $y_{\text{steady}}(t) = KF(t)$ or

$$y(t) = 5K + 10KM(25 \text{ rad/s})\sin[25t + \Phi(25 \text{ rad/s})] + 20KM(400 \text{ rad/s})\sin[400t + \Phi(400 \text{ rad/s})]$$

Using Equations 3.20 and 3.22, or, alternatively, using Figures 3.16 and 3.17, with $\omega_n = 628$ rad/s and $\zeta = 2.0$, we calculate

$$\begin{aligned} M(25 \text{ rad/s}) &= 0.99 & \Phi(25 \text{ rad/s}) &= -9.1^\circ \\ M(400 \text{ rad/s}) &= 0.39 & \Phi(400 \text{ rad/s}) &= -77^\circ \end{aligned}$$

So that the steady output signal will have the form

$$y(t) = 5 + 9.9 \sin(25t - 9.1^\circ) + 7.8 \sin(400t - 77^\circ)$$

The output signal is plotted against the input signal in Figure 3.22. The amplitude spectra for both the input signal and the output signal are shown in Figure 3.23. Spectra can also be generated by using the accompanying software programs *FunSpec* and *DataSpec*.

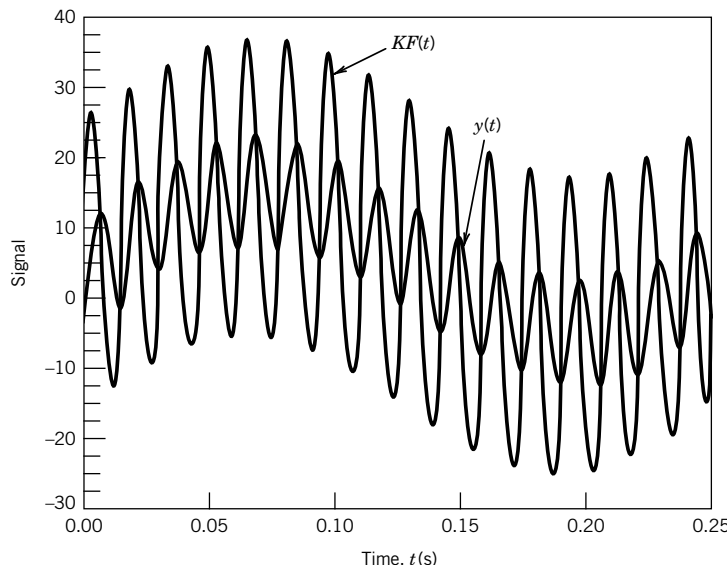


Figure 3.22 Input and output signals for Example 3.12.

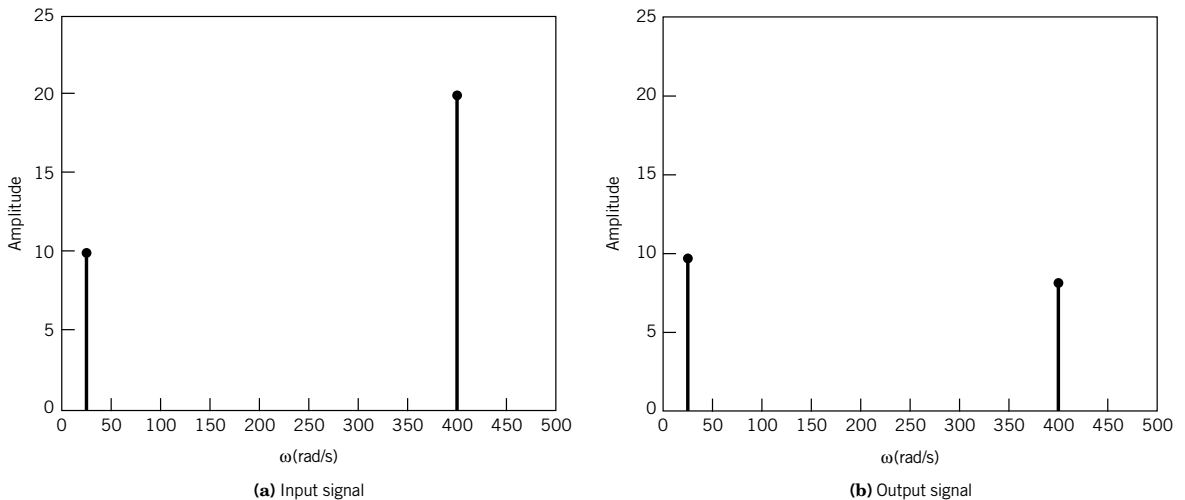


Figure 3.23 Amplitude spectrum of Example 3.12.

COMMENT The magnitude of average value and amplitude of the 25 rad/s component of the input signal are passed along to the output signal without much loss. However, the amplitude of the 400-rad/s component is severely reduced (down 61%). This is a filtering effect due to the measurement system frequency response.

3.7 COUPLED SYSTEMS

As instruments in each stage of a measurement system are connected (transducer, signal conditioner, output device, etc.), the output from one stage becomes the input to the next stage to which it is connected, and so forth. The overall measurement system will have a coupled output response to the original input signal that is a combination of each individual response to the input. However, the system concepts of zero-, first-, and second-order systems studied previously can still be used for a case-by-case study of the coupled measurement system.

This concept is easily illustrated by considering a first-order sensor that may be connected to a second-order output device (for example, a temperature sensor-transducer connected to a recorder). Suppose the input to the sensor is a simple periodic waveform, $F_1(t) = A \sin \omega t$. The transducer responds with an output signal of the form of Equation 3.8:

$$y_t(t) = Ce^{-t/\tau} + \frac{K_t A}{\sqrt{1 + (\omega\tau)^2}} \sin(\omega t + \Phi_t) \quad (3.37)$$

where the subscript t refers to the transducer. However, the transducer output signal now becomes the input signal, $F_2(t) = y_t$, to the second-order recorder device. The output from the second-order

device, $y_s(t)$, will be a second-order response appropriate for input $F_2(t)$,

$$y_s(t) = y_h(t) + \frac{K_t K_s A \sin[\omega t + \Phi_t + \Phi_s]}{\left[1 + (\omega\tau)^2\right]^{1/2} \left\{ \left[1 - (\omega/\omega_n)^2\right]^2 + [2\zeta\omega/\omega_n]^2 \right\}^{1/2}} \quad (3.38)$$

$$\Phi_s = -\tan^{-1} \frac{2\zeta\omega/\omega_n}{1 - (\omega/\omega_n)^2}$$

where subscript s refers to the chart recorder and $y_h(t)$ is the transient response. The output signal displayed on the recorder, $y_s(t)$, is the measurement system response to the original input signal to the transducer, $F_1(t) = A \sin \omega t$. The steady amplitude of the recorder output signal is the product of the static sensitivities and magnitude ratios of the first- and second-order systems. The phase shift is the sum of the phase shifts of the two systems.

Based on the concept behind Equation 3.38 we can make a general observation. Consider the schematic representation in Figure 3.24, which depicts a measurement system consisting of H interconnected devices, $j = 1, 2, \dots, H$, each device described by a linear system model. The overall transfer function of the combined system, $G(s)$, is the product of the transfer functions of each of the individual devices, $G_j(s)$, such that

$$KG(s) = K_1 G_1(s) K_2 G_2(s) \dots K_H G_H(s) \quad (3.39)$$

At $s = i\omega$, Equation 3.37 becomes

$$KG(i\omega) = (K_1 K_2 \dots K_H) \times [M_1(\omega) M_2(\omega) \dots M_H(\omega)] e^{i[\Phi_1(\omega) + \Phi_2(\omega) + \dots + \Phi_H(\omega)]} \quad (3.40)$$

According to Equation 3.40, given an input signal to device 1, the system steady output signal at device H will be described by the system frequency response $G(i\omega) = M(\omega) e^{i\Phi(\omega)}$, with an overall system static sensitivity described by

$$K = K_1 K_2 \dots K_H \quad (3.41)$$

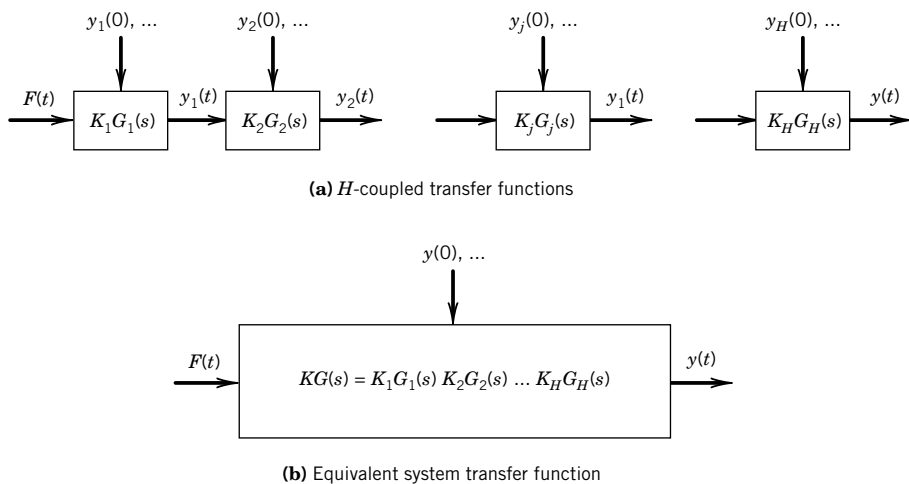


Figure 3.24 Coupled systems: describing the system transfer function.

The overall system magnitude ratio is the product

$$M(\omega) = M_1(\omega)M_2(\omega)\dots M_H(\omega) \quad (3.42)$$

and the overall system phase shift is the sum

$$\Phi(\omega) = \Phi_1(\omega) + \Phi_2(\omega) + \dots + \Phi_H(\omega) \quad (3.43)$$

This holds true provided that significant loading effects do not exist, a situation discussed in Chapter 6.

3.8 SUMMARY

Just how a measurement system responds to a time-dependent input signal depends on the properties of the signal and the frequency response of the system. Modeling has enabled us to develop and to illustrate these concepts. Those system design parameters that affect system response are exposed through modeling, which assists in instrument selection. Modeling has also suggested the methods by which measurement system specifications such as time constant, response time, frequency response, damping ratio, and resonance frequency can be determined both analytically and experimentally. Interpretation of these system properties and their effect on system performance was determined.

The rate of response of a system to a change in input is estimated by use of the step function input. The system parameters of time constant, for first-order systems, and natural frequency and damping ratio, for second-order systems, are used as indicators of system response rate. The magnitude ratio and phase shift define the frequency response of any system and are found by an input of a periodic waveform to a system. Figures 3.12, 3.13, 3.16, and 3.17 are universal frequency response curves for first- and second-order systems. These curves can be found in most engineering and mathematical handbooks and can be applied to any first- or second-order system, as appropriate.

REFERENCES

1. Close, C. M., and D. K. Frederick, *Modeling and Analysis of Dynamic Systems*, 2nd ed., Wiley, Boston, 1994.
2. Doebelin, E. O., *System Modeling and Response, Theoretical and Experimental Approaches*, Wiley, New York, 1980.
3. Ogata, K., *System Dynamics*, 4th ed., Prentice-Hall, Englewood Cliffs, NJ, 2003.
4. Palm, W. J., III, *Modeling, Analysis and Control of Dynamic Systems*, 2nd ed., Wiley, New York, 2000.
5. Burgess, J.C., A quick estimation of damping from free damped oscillograms, Wright Air Development Center, WADC TR 59-676, March 1961, pp. 457–460

NOMENCLATURE

a_0, a_1, \dots, a_n	physical coefficients	m	mass (m)
b_0, b_1, \dots, b_m	physical coefficients	$p(t)$	pressure ($m l^{-1} t^{-2}$)
c	damping coefficient ($m t^{-1}$)	t	time (t)
f	cyclical frequency ($f = \omega/2\pi$) (Hz)	$x(t)$	independent variable
k	spring constant or stiffness ($m t^{-2}$)	$y(t)$	dependent variable
		y^n	n th time derivative of $y(t)$

$y''(0)$	initial condition of y''	$U(t)$	unit step function
A	input signal amplitude	β_1	time lag (t)
$B(\omega)$	output signal amplitude	$\delta(\omega)$	dynamic error
C	constant	τ	time constant (t)
$E(t)$	voltage (V) or energy	$\Phi(\omega)$	phase shift
F	force ($m l t^{-2}$)	ω	circular frequency (t^{-1})
$F(t)$	forcing function	ω_n	natural frequency magnitude(t^{-1})
$G(s)$	transfer function	ω_d	ringing frequency (t^{-1})
K	static sensitivity	ω_R	resonance frequency (t^{-1})
$M(\omega)$	magnitude ratio, B/KA	ζ	damping ratio
$T(t)$	temperature ($^{\circ}$)	Γ	error fraction
T_d	ringing period (t)		

Subscripts

- 0 initial value
- ∞ final or steady value
- h homogeneous solution

PROBLEMS

Note: Although not required, the companion software can be used for solving many of these problems. We encourage the reader to explore the software provided.

- 3.1 A mass measurement system has a static sensitivity of 2 V/kg. An input range of 1 to 10 kg needs to be measured. A voltmeter is used to display the measurement. What range of voltmeter is needed. What would be the significance of changing the static sensitivity?
- 3.2 Determine the 75%, 90%, and 95% response time for each of the systems given (assume zero initial conditions):
 - a. $0.4\ddot{T} + T = 4U(t)$
 - b. $\ddot{y} + 2\dot{y} + 4y = U(t)$
 - c. $2\ddot{P} + 8\dot{P} + 8P = 2U(t)$
 - d. $5\ddot{y} + 5y = U(t)$
- 3.3 A special sensor is designed to sense the percent vapor present in a liquid–vapor mixture. If during a static calibration the sensor indicates 80 units when in contact with 100% liquid, 0 units with 100% vapor, and 40 units with a 50:50% mixture, determine the static sensitivity of the sensor.
- 3.4 A measurement system can be modeled by the equation

$$0.5\dot{y} + y = F(t)$$

Initially, the output signal is steady at 75 volts. The input signal is then suddenly increased to 100 volts.

- a. Determine the response equation.
- b. On the same graph, plot both the input signal and the system time response from $t = 0$ s through steady response.

- 3.5** Suppose a thermometer similar to that in Example 3.3 is known to have a time constant of 30 s in a particular application. Plot its time response to a step change from 32° to 120°F. Determine its 90% rise time.
- 3.6** Referring back to Example 3.3, a student establishes the time constant of a temperature sensor by first holding it immersed in hot water and then suddenly removing it and holding it immersed in cold water. Several other students perform the same test with similar sensors. Overall, their results are inconsistent, with estimated time constants differing by as much as a factor of 1.2. Offer suggestions as to why this might happen. Hint: Try this yourself and think about control of test conditions.
- 3.7** A thermocouple, which responds as a first-order instrument, has a time constant of 20 ms. Determine its 90% rise time.
- 3.8** During a step function calibration, a first-order instrument is exposed to a step change of 100 units. If after 1.2 s the instrument indicates 80 units, estimate the instrument time constant. Estimate the error in the indicated value after 1.5 s. $y(0) = 0$ units; $K = 1$ unit/unit.
- 3.9** Estimate any dynamic error that could result from measuring a 2-Hz periodic waveform using a first-order system having a time constant of 0.7 s.
- 3.10** A signal expected to be of the form $F(t) = 10 \sin 15.7t$ is to be measured with a first-order instrument having a time constant of 50 ms. Write the expected indicated steady response output signal. Is this instrument a good choice for this measurement? What is the expected time lag between input and output signal? Plot the output amplitude spectrum; $y(0) = 0$ and $K = 1$ V/V.
- 3.11** A first-order instrument with a time constant of 2 s is to be used to measure a periodic input. If a dynamic error of $\pm 2\%$ can be tolerated, determine the maximum frequency of periodic input that can be measured. What is the associated time lag (in seconds) at this frequency?
- 3.12** Determine the frequency response [$M(\omega)$ and $\phi(\omega)$] for an instrument having a time constant of 10 ms. Estimate the instrument's usable frequency range to keep its dynamic error within 10%.
- 3.13** A temperature measuring device with a time constant of 0.15 s outputs a voltage that is linearly proportional to temperature. The device is used to measure an input signal of the form $T(t) = 115 + 12 \sin 2t$ °C. Plot the input signal and the predicted output signal with time assuming first-order behavior and a static sensitivity of 5 mV/°C. Determine the dynamic error and time lag in the steady response. $T(0) = 115$ °C.
- 3.14** A first-order sensor is to be installed into a reactor vessel to monitor temperature. If a sudden rise in temperature greater than 100°C should occur, shutdown of the reactor will need to begin within 5 s after reaching 100°C. Determine the maximum allowable time constant for the sensor.
- 3.15** A single-loop LR circuit having a resistance of $1 \text{ M}\Omega$ is to be used as a low-pass filter between an input signal and a voltage measurement device. To attenuate undesirable frequencies above 1000 Hz by at least 50%, select a suitable inductor size. The time constant for this circuit is given by L/R .
- 3.16** A measuring system has a natural frequency of 0.5 rad/s, a damping ratio of 0.5, and a static sensitivity of 0.5 m/V. Estimate its 90% rise time and settling time if $F(t) = 2 U(t)$ and the initial condition is zero. Plot the response $y(t)$ and indicate its transient and steady responses.
- 3.17** Plot the frequency response, based on Equations 3.20 and 3.22, for an instrument having a damping ratio of 0.6. Determine the frequency range over which the dynamic error remains within 5%. Repeat for a damping ratio of 0.9 and 2.0.
- 3.18** The output from a temperature system indicates a steady, time-varying signal having an amplitude that varies between 30° and 40°C with a single frequency of 10 Hz. Express the output signal as a

waveform equation, $y(t)$. If the dynamic error is to be less than 1%, what must be the system's time constant?

- 3.19** A cantilever beam instrumented with strain gauges is used as a force scale. A step-test on the beam provides a measured damped oscillatory signal with time. If the signal behavior is second order, show how a data-reduction design plan could use the information in this signal to determine the natural frequency and damping ratio of the cantilever beam. (Hint: Consider the shape of the decay of the peak values in the oscillation.)
- 3.20** A step test of a transducer brings on a damped oscillation decaying to a steady value. If the period of oscillation is 0.577 ms, what is the transducer ringing frequency?
- 3.21** An input signal oscillates sinusoidally between 12 and 24 V with a frequency of 120 Hz. It is measured with an instrument with damping ratio of 0.7, ringing frequency of 1000 Hz, and static sensitivity of 1 V/V. Determine and plot the output signal amplitude spectrum at steady response.
- 3.22** An application demands that a sinusoidal pressure variation of 250 Hz be measured with no more than 2% dynamic error. In selecting a suitable pressure transducer from a vendor catalog, you note that a desirable line of transducers has a fixed natural frequency of 600 Hz but that you have a choice of transducer damping ratios of between 0.5 and 1.5 in increments of 0.05. Select a suitable transducer.
- 3.23** A DVD/CD player is to be isolated from room vibrations by placing it on an isolation pad. The isolation pad can be considered as a board of mass m , a foam mat of stiffness k , and with a damping coefficient c . For expected vibrations in the frequency range of between 2 and 40 Hz, select reasonable values for m , k , and c such that the room vibrations are attenuated by at least 50%. Assume that the only degree of freedom is in the vertical direction.
- 3.24** A single-loop RCL electrical circuit can be modeled as a second-order system in terms of current. Show that the differential equation for such a circuit subjected to a forcing function potential $E(t)$ is given by

$$L \frac{d^2I}{dt^2} + R \frac{dI}{dt} + \frac{I}{C} = E(t)$$

Determine the natural frequency and damping ratio for this system. For a forcing potential, $E(t) = 1 + 0.5 \sin 2000t$ V, determine the system steady response when $L = 2$ H, $C = 1$ μF , and $R = 10,000$ Ω . Plot the steady output signal and input signal versus time. $I(0) = \dot{I}(0) = 0$.

- 3.25** A transducer that behaves as a second-order instrument has a damping ratio of 0.7 and a natural frequency of 1000 Hz. It is to be used to measure a signal containing frequencies as large as 750 Hz. If a dynamic error of $\pm 10\%$ can be tolerated, show whether or not this transducer is a good choice.
- 3.26** A strain-gauge measurement system is mounted on an airplane wing to measure wing oscillation and strain during wind gusts. The strain system has a 90% rise time of 100 ms, a ringing frequency of 1200 Hz, and a damping ratio of 0.8. Estimate the dynamic error in measuring a 1-Hz oscillation. Also, estimate any time lag. Explain in words the meaning of this information.
- 3.27** An instrument having a resonance frequency of 1414 rad/s with a damping ratio of 0.5 is used to measure a signal of ~ 6000 Hz. Estimate the expected dynamic error and phase shift.
- 3.28** Select one set of appropriate values for damping ratio and natural frequency for a second-order instrument used to measure frequencies up to 100 rad/s with no more than $\pm 10\%$ dynamic error. A catalog offers models with damping ratios of 0.4, 1, and 2 and natural frequencies of 200 and 500 rad/s. Explain your reasoning.

- 3.29** A first-order measurement system with time constant of 25 ms and $K = 1 \text{ V/N}$ measures a signal of the form $F(t) = \sin 2\pi t + 0.8 \sin 6\pi t \text{ N}$. Determine the steady response (steady output signal) from the system. Plot the output signal amplitude spectrum. Discuss the transfer of information from the input to the output. Can the input signal be resolved based on the output?
- 3.30** Demonstrate for the second-order system ($\omega_n = 100 \text{ rad/s}$, $\zeta = 0.4$) subjected to step function input, $U(t)$, that the damping ratio can be found from the logarithmic amplitude decay whether $y(0) = 0$ with $F(t) = KAU(t)$ or $y(0) = KA$ with $F(t) = -KAU(t)$. Use $K = 1 \text{ mV/mV}$ and $A = 600 \text{ mV}$. Do this by solving for the expected time response and from this response determine the successive peak amplitudes to extract the values for the damping ratio and natural frequency.
- 3.31** A force transducer having a damping ratio of 0.5 and a natural frequency of 4000 Hz is available for use to measure a periodic signal of 2000 Hz. Show whether or not the transducer passes a $\pm 10\%$ dynamic error constraint. Estimate its resonance frequency.
- 3.32** An accelerometer, whose frequency response is defined by Equations 3.20 and 3.22, has a damping ratio of 0.4 and a natural frequency of 18,000 Hz. It is used to sense the relative displacement of a beam to which it is attached. If an impact to the beam imparts a vibration at 4500 Hz, estimate the dynamic error and phase shift in the accelerometer output. Estimate its resonance frequency.
- 3.33** Derive the equation form for the magnitude ratio and phase shift of the seismic accelerometer of Example 3.1. Does its frequency response differ from that predicted by Equations 3.20 and 3.22? For what type of measurement would you suppose this instrument would be best suited?
- 3.34** Suppose the pressure transducer of Example 3.9 had a damping ratio of 0.6. Plot its frequency response $M(\omega)$ and $\phi(\omega)$. At which frequency is $M(\omega)$ a maximum?
- 3.35** A pressure transducer is attached to a stiff-walled catheter. The catheter is filled with saline from a small balloon attached at its tip. The initial system pressure is 50 mm Hg. At $t = 0 \text{ s}$, the balloon is popped, forcing a step function change in pressure from 50 to 0 mm Hg. The time-based signal is recorded and the ringing period determined to be 0.03 s. Find the natural frequency and damping ratio attributed to the pressure-catheter system; $K = 1 \text{ mV/mm Hg}$.
- 3.36** The output stage of a first-order transducer is to be connected to a second-order display stage device. The transducer has a known time constant of 1.4 ms and static sensitivity of $2 \text{ V/}^{\circ}\text{C}$ while the display device has values of sensitivity, damping ratio, and natural frequency of 1 V/V , 0.9, and 5000 Hz, respectively. Determine the steady response of this measurement system to an input signal of the form, $T(t) = 10 + 50 \sin 628t \text{ }^{\circ}\text{C}$.
- 3.37** The displacement of a solid body is to be monitored by a transducer (second-order system) with signal output displayed on a recorder (second-order system). The displacement is expected to vary sinusoidally between 2 and 5 mm at a rate of 85 Hz. Select appropriate design specifications for the measurement system for no more than 5% dynamic error (i.e., specify an acceptable range for natural frequency and damping ratio for each device).
- 3.38** The input signal

$$F(t) = 2 + \sin 15.7t + \sin 160t \text{ N}$$

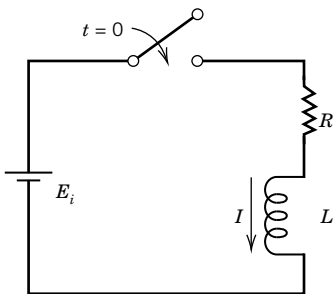
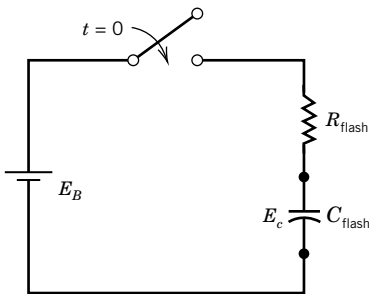
is applied to a force measurement system. The system has a known $\omega_n = 100 \text{ rad/s}$, $\zeta = 0.4$, and $K = 1 \text{ V/N}$. Write the expected form of the steady output signal in volts. Plot the resulting amplitude spectrum.

3.39 A signal suspected to be of the nominal form

$$y(t) = 5 \sin 1000t \text{ mV}$$

is input to a first-order instrument having a time constant of 100 ms and $K = 1 \text{ V/V}$. It is then to be passed through a second-order amplifier having a $K = 100 \text{ V/V}$, a natural frequency of 15,000 Hz, and a damping ratio of 0.8. What is the expected form of the output signal, $y(t)$? Estimate the dynamic error and phase lag in the output. Is this system a good choice here? If not, do you have any suggestions?

- 3.40** A typical modern DC audio amplifier has a frequency bandwidth of 0 to 20,000 Hz $\pm 1 \text{ dB}$. Explain the meaning of this specification and its relation to music reproduction.
- 3.41** The displacement of a rail vehicle chassis as it rolls down a track is measured using a transducer ($K = 10 \text{ mV/mm}$, $\omega_n = 10,000 \text{ rad/s}$, $\zeta = 0.6$) and a recorder ($K = 1 \text{ mm/mV}$, $\omega_n = 700 \text{ rad/s}$, $\zeta = 0.7$). The resulting amplitude spectrum of the output signal consists of a spike of 90 mm at 2 Hz and a spike of 50 mm at 40 Hz. Are the measurement system specifications suitable for the displacement signal? (If not, suggest changes.) Estimate the actual displacement of the chassis. State any assumptions.
- 3.42** The amplitude spectrum of the time-varying displacement signal from a vibrating U-shaped tube is expected to have a spike at 85, 147, 220, and 452 Hz. Each spike is related to an important vibrational mode of the tube. Displacement transducers available for this application have a range of natural frequencies from 500 to 1000 Hz, with a fixed damping ratio of about 0.5. The transducer output is to be monitored on a spectrum analyzer that has a frequency bandwidth extending from 0.1 Hz to 250 kHz. Within the stated range of availability, select a suitable transducer for this measurement from the given range.
- 3.43** A sensor mounted to a cantilever beam indicates beam motion with time. When the beam is deflected and released (step test), the sensor signal indicates that the beam oscillates as an underdamped second-order system with a ringing frequency of 10 rad/s. The maximum displacement amplitudes are measured at three different times corresponding to the 1st, 16th, and 32nd cycles and found to be 17, 9, and 5 mV, respectively. Estimate the damping ratio and natural frequency of the beam based on this measured signal, $K = 1 \text{ mm/mV}$.
- 3.44** Write a short essay on how system properties of static sensitivity, natural frequency, and damping ratio affect the output information from a measurement system. Be sure to discuss the relative importance of the transient and steady aspects of the resulting signal.
- 3.45** Burgess (5) reports that the damping ratio can be approximated from the system response to an impulse test by counting the number of cycles, n , required for the ringing amplitudes to fall to within 1% of steady state by $\zeta = (4.6/2\pi n)$. The estimate is further improved if n is a noninteger. Investigate the quality of this estimate for a second-order system subjected instead to a step function input. Discuss your findings.
- 3.46** The starting transient of a DC motor can be modeled as an RL circuit, with the resistor and inductor in series (Figure 3.25). Let $R = 4 \Omega$, $L = 0.1 \text{ H}$, and $E_i = 50 \text{ V}$ with $t(0) = 0$. Find the current draw with time for $t > 0^+$.
- 3.47** A camera flash light is driven by the energy stored in a capacitor. Suppose the flash operates off a 6-V battery. Determine the time required for the capacitor stored voltage to reach 90% of its maximum energy ($= \frac{1}{2} C E_B^2$). Model this as an RC circuit (Fig. 3.26). For the flash: $C = 1000 \mu\text{F}$, $R = 1 \text{ k}\Omega$, and $E_c(0) = 0$.

**Figure 3.25** Figure for Problem 3.46.**Figure 3.26** Figure for Problem 3.47.

- 3.48** Run program *Temperature Response*. The program allows the user to vary time constant τ and signal amplitude. To impose a step change move the input value up/down. Discuss the effect of time constant on the time required to achieve a steady signal following a new step change.
- 3.49** A lumped parameter model of the human systemic circulation includes the systemic vascular resistance and systemic vascular compliance. Compliance is the inverse of mechanical stiffness and is estimated by $C = \Delta V / \Delta p$, that is, the compliance is related to the pressure change required to accommodate a volume change. The typical stroke volume of each heart beat might eject 80 mL of blood into the artery during which the end-diastolic pressure of 80 mm Hg rises to a peak systolic pressure of 120 mm Hg. Similarly, the resistance to the 6 L/min of blood flow requires an average pressure over the pulse cycle of about 100 mm Hg to drive it. Estimate values for the systemic vascular compliance and resistance. Incidentally, these relations are similarly used in describing the physical properties of pressure measuring systems.

Chapter 4

Probability and Statistics

4.1 INTRODUCTION

Suppose we had a large box containing a population of thousands of similar-sized round bearings. To get an idea of the size of the bearings, we might measure two dozen from these thousands. The resulting samples of diameter values form a data set, which we then use to imply something about the entire population of the bearings in the box, such as average size and size variation. But how close are these values taken from our small data set to the actual average size and variation of all the bearings in the box? If we selected a different two dozen bearings, should we expect the size values to be exactly the same? These are questions that surround most engineering measurements. We make some measurements that we then use to try to answer questions. What is the mean value of the variable based on a finite number of measurements and how well does this value represent the entire population? Do the variations found ensure that we can meet tolerances for the population as a whole? How good are these results? These questions have answers in probability and statistics.

For a given set of measurements, we want to be able to quantify (1) a single representative value that best characterizes the average of the measured data set; (2) a representative value that provides a measure of the variation in the measured data set; and (3) how well the average of the data set represents the true average value of the entire population of the measured variable. The value of item (1) can vary with repeated data sets and so the difference between it and the true average value of the population is a type of random error. Item (3) requires establishing an interval within which the true average value of the population is expected to lie. This interval quantifies the probable range of this random error and it is called a random uncertainty.

This chapter presents an introduction to the concepts of probability and statistics at a level sufficient to provide information for a large class of engineering judgments. Such material allows for the reduction of raw data into results.

Upon completion of this chapter, the reader will be able to

- quantify the statistical characteristics of a data set as it relates to the population of the measured variable,
- explain and use probability density functions to describe the behavior of variables,
- create meaningful histograms of measured data,
- quantify a confidence interval about the measured mean value at a given probability,
- perform regression analysis on a data set and quantify the confidence intervals for the parameters of the resulting curve fit or response surface,

- identify outliers in a data set,
- specify the number of measurements required to achieve a desired confidence interval, and
- execute a Monte Carlo simulation that predicts the behavior expected in a result due to variations in the variables involved in computing that result.

4.2 STATISTICAL MEASUREMENT THEORY

Sampling refers to obtaining a set of data through repeated measurements of a variable under fixed operating conditions. This variable is known as the *measured variable* or, in statistical terms, the *measurand*. By fixed operating conditions, we mean that the external conditions that control the process are held at constant values. In actual engineering practice, truly fixed conditions are difficult to attain and the term “fixed operating conditions” is used in a nominal sense. That is, we consider the process conditions to be maintained as closely as possible and deviations from these conditions will show up in the data set variations.

This chapter considers the effects of random errors and how to quantify them. Recall that random errors are manifested through data scatter and by the statistical limitations of a finite sampling to predict the behavior of a population. For now, we will assume that any systematic errors in the measurement are negligible.¹ Recall from Chapter 1 that this is the case where the average error in a data set is zero. We begin by considering the following measurement problem: estimate the true value, x' , based on the information derived from the repeated measurement of variable x . In the absence of systematic error, the true value of x is the mean value of all possible values of x . This is the value that we want to estimate from the measurement. A sampling of the variable x under controlled, fixed operating conditions renders a finite number of data points. We use these limited data to infer x' based on the calculated sample mean value, \bar{x} . We can imagine that if the number of data points, N , is very small, then the estimation of x' from the data set could be heavily influenced by the value of any one data point. If the data set were larger, then the influence of any one data point would be offset by the larger influence of the other data. As $N \rightarrow \infty$ or towards the total number in the population, all the possible variations in x become included in the data set. From a practical view, finite-sized data sets are common, in which case the measured data can provide only an estimate of the true value.

From a statistical analysis of the data set and an analysis of sources of error that influence these data, we can estimate x' as

$$x' = \bar{x} \pm u_{\bar{x}} \quad (P\%) \quad (4.1)$$

where \bar{x} represents the most probable estimate of x' based on the available data and $\pm u_{\bar{x}}$ represents the *uncertainty interval* in that estimate at some probability level, $P\%$. *Uncertainties are numbers that quantify the possible range of the effects of errors.* The uncertainty interval is the range about \bar{x} within which we expect x' to lie. It combines the uncertainty estimates of the random error and of systematic error in the measurement of x .² This chapter discusses ways to estimate the uncertainty due to the effects of random error, called the random uncertainty. Chapter 5 discusses systematic errors and how to find the uncertainty interval by combining the uncertainties of both random and systematic errors.

¹ Systematic error does not vary with repeated measurements and so does not affect the statistics of a measurement. Systematic errors are discussed in Chapter 5.

² Statistics texts that entirely ignore systematic error refer to this uncertainty interval as a “confidence interval.”

Table 4.1 Sample of Random Variable x

i	x_i	i	x_i
1	0.98	11	1.02
2	1.07	12	1.26
3	0.86	13	1.08
4	1.16	14	1.02
5	0.96	15	0.94
6	0.68	16	1.11
7	1.34	17	0.99
8	1.04	18	0.78
9	1.21	19	1.06
10	0.86	20	0.96

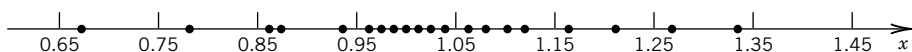
Probability Density Functions

Random scatter of the measured data occurs regardless of the care taken to obtain the set from independent measurements under identical conditions. As such, the measured variable behaves as a *random variable*. A continuous random variable is one that is continuous in time or space, such as the value of a motor's speed. A discrete random variable is one that is composed of discrete values, such as the values of the diameters of the bearings mentioned in Section 4.1. During repeated measurements of a variable, each data point may tend to assume one preferred value or lie within some interval about this value more often than not, when all the data are compared. This tendency toward one central value about which all the other values are scattered is known as a *central tendency* of a random variable.³ Probability deals with the concept that certain values of a variable may be measured more frequently relative to other values.

The central value and those values scattered about it can be determined from the probability density of the measured variable. The frequency with which the measured variable assumes a particular value or interval of values is described by its probability density. Consider a sample of x shown in Table 4.1, which consists of N individual measurements, x_i , where $i = 2, \dots, N$, each measurement taken at random but under identical test operating conditions. The measured values of this variable are plotted as data points along a single axis as shown in Figure 4.1.

In Figure 4.1, there exists a region on the axis where the data points tend to clump; this region contains the central value. Such behavior is typical of most engineering variables. We might expect that the true mean value of x is contained somewhere in this clump.

This description for variable x can be extended. Suppose we plot the data of Table 4.1 in a different way. The abscissa will be divided between the maximum and minimum measured values

**Figure 4.1** Concept of density in reference to a measured variable (from Ex. 4.1).

³ Not all random variables display a central tendency; the value in a fair roll of a die, for example, would show values from 1 through 6, each with an equal frequency of 1/6. But the fair roll of two dice will show a central tendency to the combined value of 7. Try it!

of x into K small intervals. Let the number of times, n_j , that a measured value assumes a value within an interval defined by $x - \delta x \leq x \leq x + \delta x$ be plotted on the ordinate. The resulting plot of n_j versus x is called a *histogram* of the variable (1). The histogram is just another way of viewing both the tendency and the probability density of a variable. The ordinate can be nondimensionalized as $f_j = n_j/N$, converting the histogram into a *frequency distribution*. For small N , the interval number K should be conveniently chosen with a good rule that $n_j \geq 5$ for at least one interval. A correlation for an estimate for the number of intervals K is derived from the suggestions in Bendat and Piersol (2) as

$$K = 1.87(N - 1)^{0.40} + 1 \quad (4.2)$$

As N becomes very large, a value of $K \approx N^{1/2}$ works reasonably well (1, 2). The concept of the histogram is illustrated in Example 4.1.

Example 4.1

Construct a histogram and frequency distribution for the data in Table 4.1.

KNOWN Data of Table 4.1

$$N = 20$$

ASSUMPTIONS Fixed operating conditions

FIND Histogram and frequency distribution

SOLUTION To develop the histogram, compute a reasonable number of intervals for this data set. For $N = 20$, a convenient estimate of K is found from Equation 4.2 to be

$$K = 1.87(N - 1)^{0.40} + 1 = 7$$

Next, determine the maximum and minimum values of the data set and divide this range into K intervals. For a minimum of 0.68 and a maximum of 1.34, a value of $\delta x = 0.05$ is chosen. The intervals are as follows:

j	Interval	n_j	$f_j = n_j/N$
1	$0.65 \leq x_i < 0.75$	1	0.05
2	$0.75 \leq x_i < 0.85$	1	0.05
3	$0.85 \leq x_i < 0.95$	3	0.15
4	$0.95 \leq x_i < 1.05$	7	0.35
5	$1.05 \leq x_i < 1.15$	4	0.20
6	$1.15 \leq x_i < 1.25$	2	0.10
7	$1.25 \leq x_i < 1.35$	2	0.10

The results are plotted in Figure 4.2. The plot displays a definite central tendency seen as the maximum frequency of occurrence falling within the interval 0.95 to 1.05.

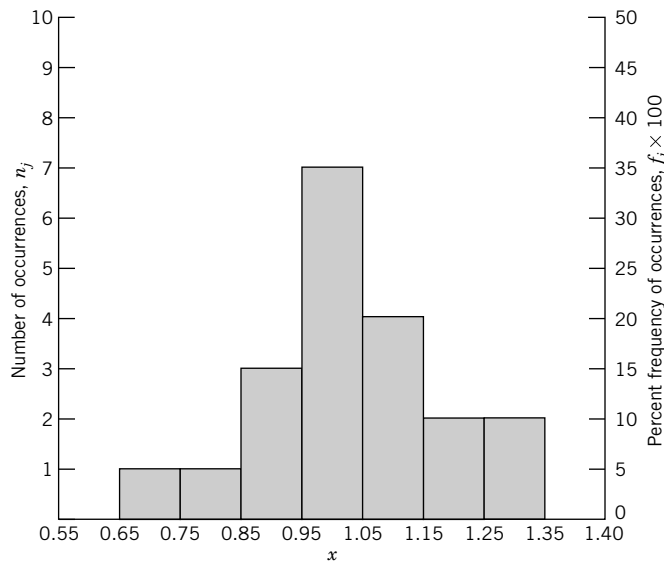


Figure 4.2 Histogram and frequency distribution for data in Table 4.1.

COMMENT The total number of measurements, N , equals the sum of the number of occurrences,

$$N = \sum_{j=1}^K n_j$$

The area under the percent frequency distribution curve equals 100%; that is,

$$100 \times \sum_{j=1}^K f_j = 100\%$$

Probability-density.vi and *Running-histogram.vi* demonstrate the influence of population size and interval numbers on the histogram.

As $N \rightarrow \infty$, the *probability density function*, $p(x)$, of the population of variable x is developed. In the limit as $\delta x \rightarrow 0$

$$p(x) = \lim_{\delta x \rightarrow 0} \frac{n_j}{N(2\delta x)} \quad (4.3)$$

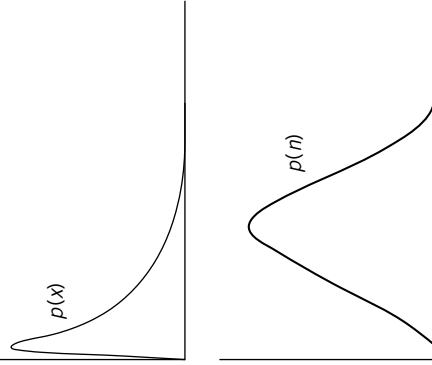
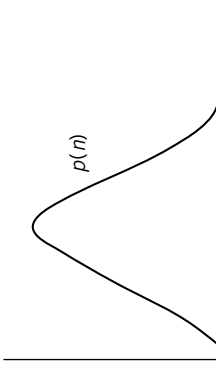
The probability density function defines the probability that a measured variable might assume a particular value upon any individual measurement. It also provides the central tendency of the variable and its variation. This central tendency is the desired representative value that gives the best estimate of the true mean value.

The actual shape that the probability density function takes depends on the nature of the variable it represents and the circumstances surrounding the process in which the variable is involved. There are a number of standard distribution shapes that suggest how a variable could be distributed on the probability density plot. The specific values of the variable and the width of the distribution depend on the actual process, but the overall shape of the plot will most likely fit some standard distribution. A number of standard distributions that engineering data are likely to follow along with specific comments regarding the types of processes from which these are likely to be found are given in Table 4.2. Often, experimentally determined histograms are used to identify which standard distribution the

Table 4.2 Standard Statistical Distributions and Relations Common to Measurements

Distribution	Applications	Density Function	Shape
Normal	Most physical properties that are continuous or regular in time or space with variations due to random error.	$p(x) = \frac{1}{\sigma(2\pi)^{1/2}} \exp\left[-\frac{1}{2} \frac{(x-x')^2}{\sigma^2}\right]$	
Log normal	Failure or durability projections; events whose outcomes tend to be skewed toward the extremity of the distribution	$p(x) = \frac{1}{\pi\sigma(2\pi)^{1/2}} \exp\left[-\frac{1}{2} \ln \frac{(x-x')^2}{\sigma^2}\right]$	
Rectangular	Processes in which a likely outcome falls in the range between minimum value a and maximum value b occurring with equal probability	$p(x) = \frac{1}{b-a}$ where $a \leq x \leq b$, otherwise $p(x) = 0$	
Triangular	Process in which the likely outcome x falls between known lower bound a and upper bound b , with a peak value or mode c ; used when population information is sparse	$p(x) = \begin{cases} \frac{2(x-a)}{(b-a)(c-a)} & \text{for } a \leq x \leq c \\ \frac{2(b-x)}{(b-a)(b-c)} & \text{for } c < x \leq b \end{cases}$	

Table 4.2 (*Continued*)

Poisson	Events randomly occurring in time; $p(x)$ refers to probability of observing x events in time t ; here λ refers to λ'	$p(x) = \frac{e^{-\lambda} \lambda^x}{x!}$	
Binomial	Situations describing the number of occurrences, n , of a particular outcome during N independent tests where the probability of any outcome, P , is the same	$p(n) = \left[\frac{N!}{(N-n)!n!} \right] P^n (1-P)^{N-n}$	

measured variable tends to follow. In turn, the standard distribution is used to interpret the data. Of course, the list in Table 4.2 is not inclusive, and the reader is referred to more complete treatments of this subject (3–5).

Regardless of its probability density form, a variable that shows a central tendency can be described and quantified through its mean value and variance. In the absence of systematic errors, the *true mean value* or central tendency of a random variable, $x(t)$, which is continuous in either time or space, and having a probability density function $p(x)$, is given by

$$x' = \lim_{T \rightarrow \infty} \frac{1}{T} \int_0^T x(t) dt \quad (4.4a)$$

which for any continuous random variable x is equivalent to

$$x' = \int_{-\infty}^{\infty} xp(x) dx \quad (4.4b)$$

If the measured variable is described by discrete data, the mean value of measured variable, x_i , where $i = 1, 2, \dots, N$, is given by

$$x' = \lim_{N \rightarrow \infty} \frac{1}{N} \sum_{i=1}^N x_i \quad (4.5)$$

Physically, the width of the density function reflects the data variation. For a continuous random variable, the *true variance* is given by

$$\sigma^2 = \lim_{T \rightarrow \infty} \frac{1}{T} \int_0^T [x(t) - x']^2 dt \quad (4.6a)$$

which is equivalent to

$$\sigma^2 = \int_{-\infty}^{\infty} (x - x')^2 p(x) dx \quad (4.6b)$$

or for discrete data, the variance is given by

$$\sigma^2 = \lim_{N \rightarrow \infty} \frac{1}{N} \sum_{i=1}^N (x_i - x')^2 \quad (4.7)$$

The *standard deviation*, σ , a commonly used statistical parameter, is defined as the square root of the variance, that is $\sigma = \sqrt{\sigma^2}$.

The fundamental difficulty in using Equations 4.3 to 4.7 is that we assume a knowledge of the values of the entire population of the variable. But what if the data-set represents only a finite portion of that population? Do these relations change? Real data-set sizes may range from a single value to a large finite number. The next section discusses the behavior of infinite data sets (entire populations) and introduces the connection between probability and statistics. After that, we will turn our attention to the practical statistical treatment of finite data sets.

4.3 DESCRIBING THE BEHAVIOR OF A POPULATION

This section discusses the relation between probability and statistics. To do this, we assume a particular distribution for $p(x)$ to characterize the behavior of the population of x . Table 4.2 lists a few of the many distributions we could use, but to develop our relations we will use the *normal*

(or *gaussian*) *distribution*.⁴ Much of the existing theory of statistics was developed using this distribution. It is particularly suited to describing the behavior of the continuous random variables common to engineering measurements. The normal distribution predicts that the scatter seen in a measured data set will be distributed symmetrically about some central tendency. Its shape is the familiar bell curve, as seen in Table 4.2.

The probability density function for a random variable, x , having a normal distribution is defined as

$$p(x) = \frac{1}{\sigma\sqrt{2\pi}} \exp\left[-\frac{1}{2}\frac{(x - x')^2}{\sigma^2}\right] \quad (4.8)$$

where x' is defined as the true mean value of x and σ^2 as the true variance of x . Hence, $p(x)$ depends on the specific values for x' and σ^2 . A maximum in $p(x)$ occurs at $x = x'$, the true mean value. This indicates that in the absence of systematic error the central tendency of a random variable having a normal distribution is toward its true mean value. The variance reflects the width or range of variation of $p(x)$.

Given $p(x)$, how can we predict the probability that any future measurement will fall within some stated interval of x values? The probability that x will assume a value within the interval $x' \pm \delta_x$ is given by the area under $p(x)$, which is found by integrating over the interval. Thus, this probability is given by

$$P(x' - \delta_x \leq x \leq x' + \delta_x) = \int_{x' - \delta_x}^{x' + \delta_x} p(x) dx \quad (4.9)$$

Integrating Equation 4.9 is easier using the following transformations. Begin by defining the terms $\beta = (x - x')/\sigma$, as the *standardized normal variate* for any value x , and $z_1 = (x_1 - x')/\sigma$, as the z variable, which, specifies an interval on $p(x)$. It follows that

$$dx = \sigma d\beta \quad (4.10)$$

so that Equation 4.9 can be written as

$$P(-z_1 \leq \beta \leq z_1) = \frac{1}{\sqrt{2\pi}} \int_{-z_1}^{z_1} e^{-\beta^2/2} d\beta \quad (4.11)$$

Since for a normal distribution, $p(x)$ is symmetrical about x' , we can write

$$\frac{1}{\sqrt{2\pi}} \int_{-z_1}^{z_1} e^{-\beta^2/2} d\beta = 2 \times \left[\frac{1}{\sqrt{2\pi}} \int_0^{z_1} e^{-\beta^2/2} d\beta \right] \quad (4.12)$$

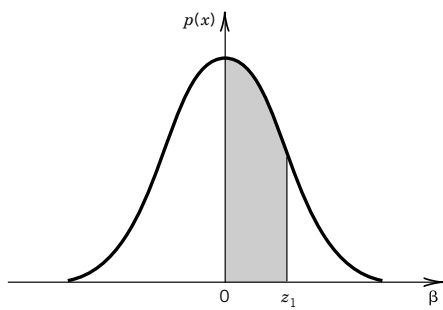
The value in brackets in Equation 4.12 is the *normal error function*. The value $P(z_1) = \frac{1}{\sqrt{2\pi}} \int_0^{z_1} e^{-\beta^2/2} d\beta$ is tabulated in Table 4.3 for the interval defined by z_1 shown in Figure 4.3. The integral is one-sided (that is, it is evaluated from 0 to z_1), so the normal error function provides one-half of the probability expressed in Equation 4.11.

It should now be clear that the statistical terms defined by Equations 4.4 to 4.7 are actually statements associated with probability. The area under the portion of the probability density function

⁴This distribution was independently suggested in the 18th century by Gauss, LaPlace, and DeMoivre. However, Gauss retains the eponymous honor.

Table 4.3 Probability Values for Normal Error Function: One-Sided Integral Solutions for $p(z_1) = \frac{1}{(2\pi)^{1/2}} \int_0^{z_1} e^{-\beta^2/2} d\beta$

$z_1 = \frac{x_1 - x'}{\sigma}$	0.00	0.01	0.02	0.03	0.04	0.05	0.06	0.07	0.08	0.09
0.0	0.0000	0.0040	0.0080	0.0120	0.0160	0.0199	0.0239	0.0279	0.0319	0.0359
0.1	0.0398	0.0438	0.0478	0.0517	0.0557	0.0596	0.0636	0.0675	0.0714	0.0753
0.2	0.0793	0.0832	0.0871	0.0910	0.0948	0.0987	0.1026	0.1064	0.1103	0.1141
0.3	0.1179	0.1217	0.1255	0.1293	0.1331	0.1368	0.1406	0.1443	0.1480	0.1517
0.4	0.1554	0.1591	0.1628	0.1664	0.1700	0.1736	0.1772	0.1809	0.1844	0.1879
0.5	0.1915	0.1950	0.1985	0.2019	0.2054	0.2088	0.2123	0.2157	0.2190	0.2224
0.6	0.2257	0.2291	0.2324	0.2357	0.2389	0.2422	0.2454	0.2486	0.2517	0.2549
0.7	0.2580	0.2611	0.2642	0.2673	0.2794	0.2734	0.2764	0.2794	0.2823	0.2852
0.8	0.2881	0.2910	0.2939	0.2967	0.2995	0.3023	0.3051	0.3078	0.3106	0.3133
0.9	0.3159	0.3186	0.3212	0.3238	0.3264	0.3289	0.3315	0.3340	0.3365	0.3389
1.0	0.3413	0.3438	0.3461	0.3485	0.3508	0.3531	0.3554	0.3577	0.3599	0.3621
1.1	0.3643	0.3665	0.3686	0.3708	0.3729	0.3749	0.3770	0.3790	0.3810	0.3830
1.2	0.3849	0.3869	0.3888	0.3907	0.3925	0.3944	0.3962	0.3980	0.3997	0.4015
1.3	0.4032	0.4049	0.4066	0.4082	0.4099	0.4115	0.4131	0.4147	0.4162	0.4177
1.4	0.4192	0.4207	0.4292	0.4236	0.4251	0.4265	0.4279	0.4292	0.4306	0.4319
1.5	0.4332	0.4345	0.4357	0.4370	0.4382	0.4394	0.4406	0.4418	0.4429	0.4441
1.6	0.4452	0.4463	0.4474	0.4484	0.4495	0.4505	0.4515	0.4525	0.4535	0.4545
1.7	0.4554	0.4564	0.4573	0.4582	0.4591	0.4599	0.4608	0.4616	0.4625	0.4633
1.8	0.4641	0.4649	0.4656	0.4664	0.4671	0.4678	0.4686	0.4693	0.4699	0.4706
1.9	0.4713	0.4719	0.4726	0.4732	0.4738	0.4744	0.4750	0.4758	0.4761	0.4767
2.0	0.4772	0.4778	0.4803	0.4788	0.4793	0.4799	0.4803	0.4808	0.4812	0.4817
2.1	0.4821	0.4826	0.4830	0.4834	0.4838	0.4842	0.4846	0.4850	0.4854	0.4857
2.2	0.4861	0.4864	0.4868	0.4871	0.4875	0.4878	0.4881	0.4884	0.4887	0.4890
2.3	0.4893	0.4896	0.4898	0.4901	0.4904	0.4906	0.4909	0.4911	0.4913	0.4916
2.4	0.4918	0.4920	0.4922	0.4925	0.4927	0.4929	0.4931	0.4932	0.4934	0.4936
2.5	0.4938	0.4940	0.4941	0.4943	0.4945	0.4946	0.4948	0.4949	0.4951	0.4952
2.6	0.4953	0.4955	0.4956	0.4957	0.4959	0.4960	0.4961	0.4962	0.4963	0.4964
2.7	0.4965	0.4966	0.4967	0.4968	0.4969	0.4970	0.4971	0.4972	0.4973	0.4974
2.8	0.4974	0.4975	0.4976	0.4977	0.4977	0.4978	0.4979	0.4979	0.4980	0.4981
2.9	0.4981	0.4982	0.4982	0.4983	0.4984	0.4984	0.4985	0.4985	0.4986	0.4986
3.0	0.49865	0.4987	0.4987	0.4988	0.4988	0.4988	0.4989	0.4989	0.4989	0.4990

**Figure 4.3** Integration terminology for the normal error function and Table 4.3.

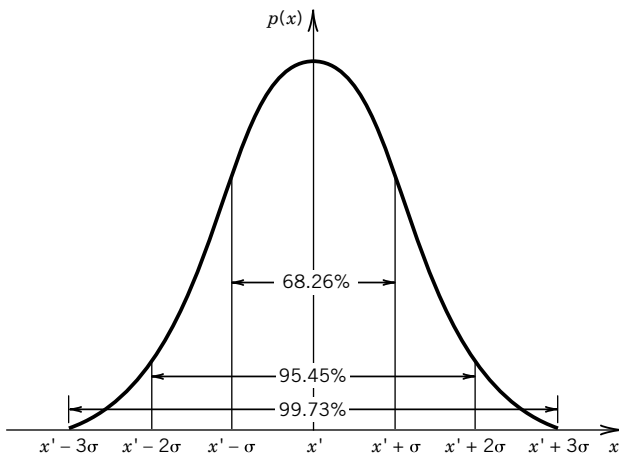


Figure 4.4 Relationship between the probability density function and its statistical parameters, x' and σ , for a normal (gaussian) distribution.

curve, $p(x)$, defined by the interval $x' - z_1\sigma \leq x \leq x' + z_1\sigma$, provides the probability that a measurement will assume a value within that interval. Direct integration of $p(x)$ for a normal distribution between the limits $x' \pm z_1\sigma$ yields that for $z_1 = 1$, 68.26% of the area under $p(x)$ lies within $\pm 1\sigma$ of x' . This means that there is a 68.26% chance that a measurement of x will have a value within the interval $x' \pm 1\sigma$. As the interval defined by z_1 is increased, the probability of occurrence increases. For

$$\begin{aligned} z_1 = 1, & \quad 68.26\% \text{ of the area under } p(x) \text{ lies within } \pm z_1\sigma \text{ of } x'. \\ z_1 = 2, & \quad 95.45\% \text{ of the area under } p(x) \text{ lies within } \pm z_1\sigma \text{ of } x'. \\ z_1 = 3, & \quad 99.73\% \text{ of the area under } p(x) \text{ lies within } \pm z_1\sigma \text{ of } x'. \end{aligned}$$

This concept is illustrated in Figure 4.4.

It follows directly that the representative value that characterizes a measure of the variation in a measured data set is the standard deviation. The probability that the i th measured value of x will have a value between $x' \pm z_1\delta$ is $2 \times P(z_1) \times 100 = P\%$.

This is written as

$$x_i = x' \pm z_1\sigma \quad (P\%) \quad (4.13)$$

Thus, simple statistical analyses provide useful quantification of a measured variable in terms of probability. This in turn can be useful in engineering situations where the probable outcome of a measured variable needs to be predicted or specified. These ideas are exercised in the Examples 4.2 and 4.3.

Example 4.2

Using the probability values in Table 4.3, show that the probability that a measurement will yield a value within $x' \pm \sigma$ is 0.6826 or 68.26%.

KNOWN Table 4.3

$$z_1 = 1$$

ASSUMPTIONS Data follow a normal distribution.

$$\mathbf{FIND} \quad P(x' - \sigma \leq x \leq x' + \sigma)$$

SOLUTION To estimate the probability that a single measurement will have a value within some interval, we need to solve the integral

$$\frac{1}{\sqrt{2\pi}} \int_0^{z_1=1} e^{-\beta^2/2} d\beta$$

over the interval defined by z_1 . Table 4.3 lists the solutions for this integral. Using Table 4.3 for $z_1 = 1$, we find $P(z_1) = 0.3413$. However, since $z_1 = (x_1 - x')/\sigma$, the probability that any measurement of x will produce a value within the interval $0 \leq x \leq x' + \sigma$ is 34.13%. Since the normal distribution is symmetric about x' , the probability that x will fall within the interval defined between $-z_1\delta$ and $+z_1\delta$ for $z_1 = 1$ is $(2)(0.3413) = 0.6826$ or 68.26%. Accordingly, if we made a single measurement of x , the probability that the value found would lie within the interval $x' - \sigma \leq x \leq x' + \sigma$ would be 68.26%.

COMMENT Similarly, for $z_1 = 1.96$, the probability would be 95.0%.

Example 4.3

The statistics of a well-defined varying voltage signal are given by $x' = 8.5$ V and $\sigma^2 = 2.25$ V². If a single measurement of the voltage signal is made, determine the probability that the measured value indicated will be between 10.0 and 11.5 V.

KNOWN $x' = 8.5$ V
 $\sigma^2 = 2.25$ V²

ASSUMPTIONS Signal has a normal distribution about x' .

FIND $P(10.0 \leq x \leq 11.5)$

SOLUTION To find the probability that x will fall into the interval $10.0 \leq x \leq 11.5$ requires finding the area under $p(x)$ bounded by this interval. The standard deviation of the variable is $\sigma = \sqrt{\sigma^2} = 1.5$ V, so our interval falls under the portion of the $p(x)$ curve bounded by $z_1 = (10.0 - 8.5)/1.5 = 1$ and $z_2 = (11.5 - 8.5)/1.5 = 2$. From Table 4.3, the probability that a value will fall between $8.5 \leq x \leq 10.0$ is $P(8.5 \leq x \leq 10.0) = P(z_1 = 1) = 0.3413$. For the interval defined by $8.5 \leq x \leq 11.5$, $P(8.5 \leq x \leq 11.5) = P(z_2 = 2) = 0.4772$. The area we need is just the overlap of these two intervals, so

$$\begin{aligned} P(10.0 \leq x \leq 11.5) &= P(8.5 \leq x \leq 11.5) - P(8.5 \leq x \leq 10.0) \\ &= 0.4772 - 0.3413 = 0.1359 \end{aligned}$$

So there is a 13.59% probability that the measurement will yield a value between 10.0 and 11.5 V.

COMMENT In general, the probability that a measured value will lie within an interval defined by any two values of z_1 , such as z_a and z_b , is found by integrating $p(x)$ between z_a and z_b . For a normal density function, this probability is identical to the operation, $P(z_b) - P(z_a)$.

4.4 STATISTICS OF FINITE-SIZED DATA SETS

We now try to predict the behavior of measured variable x based on a finite-sized sampling of x . We do this by comparing the statistics from that sampling to an assumed probability density function for the population. For example, if we recall the box of bearings discussed in Section 4.1, some two

dozen bearings were measured, each having been randomly selected from a population numbering in the thousands. So how do we use the resulting statistics from this sampling to characterize the mean size and variance of all the bearings within the box? Within the constraints imposed by probability and if we assume a probability density function for the population, it is possible to *estimate* the true mean and true variance the population of all the bearings from the statistics of the sampling. The method is now discussed.

Suppose we examine the case where we obtain N measurements of x (that is, N repetitions), each measurement represented by x_i , where $i = 1, 2, \dots, N$, and N is a finite value. In cases where N is not infinite or does not represent the total population, the statistical values calculated from such finite data sets are only estimates of the true statistics of the population of x . We will call such statistical estimates the *finite statistics*. An important point: whereas infinite statistics describe the true behavior of the population of a variable, finite statistics describe only the behavior of the sampled data set.

Finite-sized data sets provide the statistical estimates known as the *sample mean value* (\bar{x}), the *sample variance* (s_x^2), and its outcome, the *sample standard deviation* (s_x), defined by

$$\bar{x} = \frac{1}{N} \sum_{i=1}^N x_i \quad (4.14a)$$

$$s_x^2 = \frac{1}{N-1} \sum_{i=1}^N (x_i - \bar{x})^2 \quad (4.14b)$$

$$s_x = \sqrt{s_x^2} = \left(\frac{1}{N-1} \sum_{i=1}^N (x_i - \bar{x})^2 \right)^{1/2} \quad (4.14c)$$

where $(x_i - \bar{x})$ is called the *deviation* of x_i . The sample mean value provides a most probable estimate of the true mean value, x' . The sample variance represents a probable measure of the variation found in a data set. The *degrees of freedom*, v , in a statistical estimate equate to the number of data points minus the number of previously determined statistical parameters used in estimating that value. For example, the degrees of freedom in the sample variance is $v = N - 1$, as seen in denominator of Equations 4.14b and c. These equations are robust and are used regardless of the actual probability density function of the measurand.

The relation between probability and infinite statistics can be extended to data sets of finite sample size with only some modification. When data sets are finite or smaller than the population, the z variable does not provide a reliable weight estimate of the true probability. However, the sample variance can be weighted in a similar manner so as to compensate for the difference between the finite statistical estimates and the statistics based on an assumed $p(x)$. For a normal distribution of x about some sample mean value, \bar{x} , we can state that statistically

$$x_i = \bar{x} \pm t_{v,P} s_x \quad (P\%) \quad (4.15)$$

where the variable $t_{v,P}$ provides a coverage factor used for finite data sets and which replaces the z variable. This new variable is referred to as the *Student's t variable*,

$$t = \frac{\bar{x} - x'}{s_x / \sqrt{N}} \quad (4.16)$$

The interval $\pm t_{v,P} s_x$ represents a precision interval, given at probability $P\%$, within which one should expect any measured value to fall.

Table 4.4 Student's *t* Distribution

ν	t_{50}	t_{90}	t_{95}	t_{99}
1	1.000	6.314	12.706	63.657
2	0.816	2.920	4.303	9.925
3	0.765	2.353	3.182	5.841
4	0.741	2.132	2.770	4.604
5	0.727	2.015	2.571	4.032
6	0.718	1.943	2.447	3.707
7	0.711	1.895	2.365	3.499
8	0.706	1.860	2.306	3.355
9	0.703	1.833	2.262	3.250
10	0.700	1.812	2.228	3.169
11	0.697	1.796	2.201	3.106
12	0.695	1.782	2.179	3.055
13	0.694	1.771	2.160	3.012
14	0.692	1.761	2.145	2.977
15	0.691	1.753	2.131	2.947
16	0.690	1.746	2.120	2.921
17	0.689	1.740	2.110	2.898
18	0.688	1.734	2.101	2.878
19	0.688	1.729	2.093	2.861
20	0.687	1.725	2.086	2.845
21	0.686	1.721	2.080	2.831
30	0.683	1.697	2.042	2.750
40	0.681	1.684	2.021	2.704
50	0.680	1.679	2.010	2.679
60	0.679	1.671	2.000	2.660
∞	0.674	1.645	1.960	2.576

The value for the *t* estimator provides a coverage factor that is a function of the probability, P , and the degrees of freedom in the data set, $\nu = N - 1$. These *t* values can be obtained from Table 4.4, which is a tabulation from the *Student's t distribution* as developed by William S. Gosset⁵ (1876–1937). Gossett recognized that the use of the *z* variable with s_x in place of σ did not yield accurate estimates of the precision interval, particularly at small degrees of freedom. Careful inspection of Table 4.4 shows that the *t* value inflates the size of the interval required to attain a percent probability, $P\%$. That is, it has the effect of increasing the magnitude of $t_{\nu,P}s_x$ relative to $z_1\sigma$ at a desired probability. As the value of N increases, *t* approaches those values given by the *z* variable just as the value of s_x must approach σ . It should be understood that for very small sample sizes ($N \leq 10$), sample statistics can be misleading. In that situation other information regarding the measurement may be required, including additional measurements.

⁵ At the time, Gosset was employed as a brewer and statistician by a well-known Irish brewery. You might pause to reflect on his multifarious contributions.

Standard Deviation of the Means

If we were to measure another two dozen of the bearings discussed in Section 4.1, we would expect the statistics from this new sample of randomly selected bearings to differ somewhat from the previous sample. This is simply due to the combined effects of a finite sample size and random variation in bearing size from manufacturing tolerances. This difference is a random error brought on by the finite-sized data sets. So how can we quantify how good our estimate is of the true mean based on a calculated sample mean? That method is now discussed.

Suppose we were to take N measurements of x under fixed operating conditions. If we duplicated this procedure M times, we would calculate somewhat different estimates of the sample mean value and sample variance for each of the M data sets. Why? The chance occurrence of events in any finite sample affects the estimate of sample statistics; this is easily demonstrated. From the M replications of the N measurements, we could compute a set of mean values. We would find that the mean values would themselves each be normally distributed about some central value. In fact, regardless of the shape of $p(x)$ assumed, the mean values obtained from M replications will follow a normal distribution defined by $p(\bar{x})$.⁶ This process is visualized in Figure 4.5. The amount of variation possible in the sample means would depend on only two values: the sample variance, s_x^2 , and sample size, N . The discrepancy tends to increase with variance and decrease with $N^{1/2}$.

This tendency between small sample sets to have somewhat different statistics than the entire population from which they are sampled should not be surprising, for that is precisely the problem inherent to a finite data set. The variation in the sample statistics of each data set is characterized by a normal distribution of the sample mean values about the true mean. The variance of the distribution of mean values that could be expected can be estimated from a single finite data set through the *standard deviation of the means*, $s_{\bar{x}}$:

$$s_{\bar{x}} = \frac{s_x}{\sqrt{N}} \quad (4.17)$$

An illustration of the relation between the standard deviation of a data set and the standard deviation of the means is given in Figure 4.6. The standard deviation of the means is a property of a measured data set. It reflects the estimate of how the sample mean values may be distributed about a true mean value.

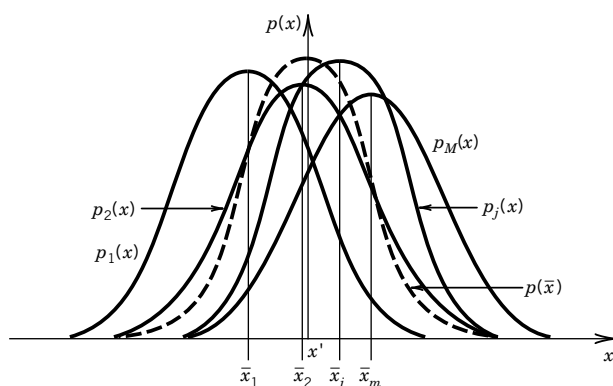


Figure 4.5 The normal distribution tendency of the sample means about a true value in the absence of systematic error.

⁶This is a consequence of what is proved in the *central limit theorem* (3, 4).

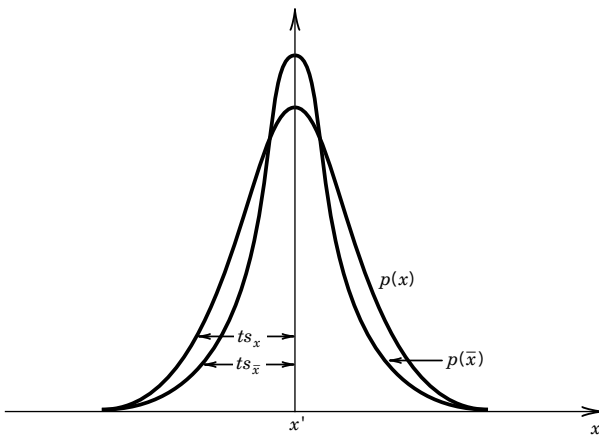


Figure 4.6 Relationships between s_x and the distribution of x and between $s_{\bar{x}}$ and the true value x' .

So how good is the estimate of the true mean of a variable based on a finite-sized sample? *The standard deviation of the means represents a measure of how well a measured mean value represents the true mean of the population.* The range over which the possible values of the true mean value might lie at some probability level P based on the information from a sample data set is given as

$$\bar{x} \pm t_{v,P}s_{\bar{x}} \quad (P\%) \quad (4.18)$$

where $\pm t_{v,P}s_{\bar{x}}$ expresses a confidence interval about the mean value, with coverage factor t at the assigned probability, $P\%$, within which one should expect the true value of x to fall. This *confidence interval* is a quantified measure of the random error in the estimate of the true value of variable x . The value $s_{\bar{x}}$ represents the random standard uncertainty in the mean value, and the value $t_{v,P}s_{\bar{x}}$ represents the *random uncertainty* in the mean value at $P\%$ confidence due to variation in the measured data set. *In the absence of systematic error in a measurement,* the confidence interval assigns the true value within a likely range about the sample mean value. The estimate of the true mean value based on a finite data set is then stated as

$$x' = \bar{x} \pm t_{v,P}s_{\bar{x}} \quad (P\%) \quad (4.19)$$

Equation 4.19 is an important and powerful equation in engineering measurements.

Example 4.4

Consider the data of Table 4.1. (a) Compute the sample statistics for this data set. (b) Estimate the interval of values over which 95% of the measurements of x should be expected to lie. (c) Estimate the true mean value of x at 95% probability based on this finite data set.

KNOWN Table 4.1

$$N = 20$$

ASSUMPTIONS Data set follows a normal distribution.

No systematic errors.

FIND $\bar{x}, \bar{x} \pm t_{v,95}s_x$, and $\bar{x} \pm t_{v,95}s_{\bar{x}}$

SOLUTION The sample mean value is computed for the $N = 20$ values by the relation

$$\bar{x} = \frac{1}{20} \sum_{i=1}^{20} x_i = 1.02$$

This, in turn, is used to compute the sample standard deviation

$$s_x = \left[\frac{1}{19} \sum_{i=1}^{20} (x_i - \bar{x})^2 \right]^{1/2} = 0.16$$

The degrees of freedom in the data set is $v = N - 1 = 19$. From Table 4.4 at 95% probability, $t_{19,95} = 2.093$. Then, the interval of values in which 95% of the measurements of x should lie is given by Equation 4.15:

$$x_i = 1.02 \pm (2.093 \times 0.16) = 1.02 \pm 0.33 \quad (95\%)$$

Accordingly, if a 21st data point were taken, there is a 95% probability that its value would lie between 0.69 and 1.35.

The true mean value is estimated by the sample mean value. However, the random uncertainty at 95% probability for this estimate is $t_{19,95}s_{\bar{x}}$, where

$$s_{\bar{x}} = \frac{s_x}{\sqrt{N}} = \frac{0.16}{\sqrt{20}} = 0.036 \approx 0.04$$

Then, in the absence of systematic errors, we write, from Equation 4.19,

$$x' = \bar{x} \pm t_{19,95}s_{\bar{x}} = 1.02 \pm 0.08 \quad (95\%)$$

So at 95% confidence, the true mean value lies between 0.94 and 1.10. Program *Finite-population.vi* demonstrates the effect of sample size on the histogram and the statistics of the data set.

Pooled Statistics

As discussed in Chapter 1, a good test plan uses duplicate tests or replication, as well as repetition. Since replications are independent estimates of the same measured value, their data represent separate data samples that can be combined to provide a better statistical estimate of a measured variable than are obtained from a single sampling. Samplings that are grouped in a manner so as to determine a common set of statistics are said to be pooled.

Consider M replicates of a measurement of variable x , each of N repeated readings so as to yield the data set x_{ij} , where $i = 1, 2, \dots, N$ and $j = 1, 2, \dots, M$. The *pooled mean* of x is defined by

$$\langle \bar{x} \rangle = \frac{1}{MN} \sum_{j=1}^M \sum_{i=1}^N x_{ij} \quad (4.20)$$

The *pooled standard deviation* of x is defined by

$$\langle s_x \rangle = \sqrt{\frac{1}{M(N-1)} \sum_{j=1}^M \sum_{i=1}^N (x_{ij} - \bar{x}_j)^2} = \sqrt{\frac{1}{M} \sum_{j=1}^M s_{x_j}^2} \quad (4.21)$$

with degrees of freedom, $v = M(N - 1)$. The *pooled standard deviation of the means of x* is defined by

$$\langle s_{\bar{x}} \rangle = \frac{\langle s_x \rangle}{\sqrt{MN}} \quad (4.22)$$

When the number of measurements of x are not the same between replications, then it is appropriate to weight each replication by its particular degrees of freedom. The pooled mean is then defined by its weighted mean

$$\langle \bar{x} \rangle = \frac{\sum_{j=1}^M N_j \bar{x}_j}{\sum_{j=1}^M N_j} \quad (4.23)$$

where subscript j refers to a particular data set. The pooled standard deviation is given by

$$\langle s_x \rangle = \sqrt{\frac{v_1 s_{x_1}^2 + v_2 s_{x_2}^2 + \cdots + v_M s_{x_M}^2}{v_1 + v_2 + \cdots + v_M}} \quad (4.24)$$

with degrees of freedom $v = \sum_{j=1}^M v_j = \sum_{j=1}^M (N_j - 1)$, and the pooled standard deviation of the means is given by

$$(s_{\bar{x}}) = \frac{\langle s_x \rangle}{\sqrt{\sum_{j=1}^M N_j}} \quad (4.25)$$

4.5 CHI-SQUARED DISTRIBUTION

We have already discussed how different finite-sized data sets of the same measured variable would have somewhat different statistics. We used this argument to develop the concept of the standard deviation of the means as a precision indicator in the mean value. Similarly, we can estimate how well s_x^2 predicts σ^2 . If we plotted the sample standard deviation for many data sets, each having N data points, we would generate the probability density function, $p(\chi^2)$. The $p(\chi^2)$ follows the so-called *chi-squared (χ^2) distribution* depicted in Figure 4.7.

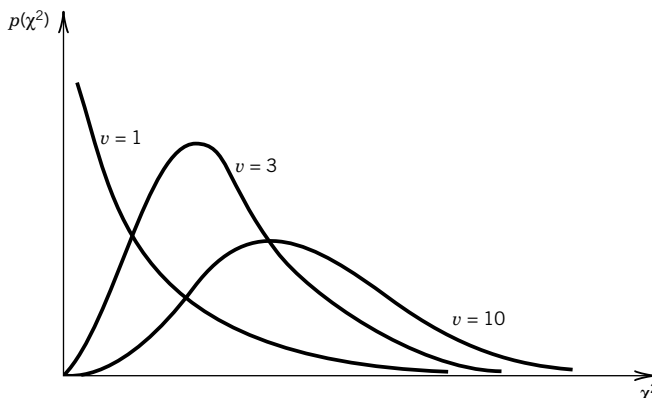


Figure 4.7 The χ^2 distribution with its dependency on degrees of freedom.

For the normal distribution, the χ^2 statistic (1, 3, 4) in Figure 4.7 is

$$\chi^2 = \nu s_x^2 / \sigma^2 \quad (4.26)$$

with degrees of freedom $\nu = N - 1$.

Precision Interval in a Sample Variance

A precision interval for the sample variance can be formulated by the probability statement

$$P(\chi_{1-\alpha/2}^2 \leq \chi^2 \leq \chi_{\alpha/2}^2) = 1 - \alpha \quad (4.27)$$

with a probability of $P(\chi^2) = 1 - \alpha$. The term α is called the *level of significance*. Combining Equations 4.26 and 4.27 gives

$$P\left(\nu s_x^2 / \chi_{\alpha/2}^2 \leq \sigma^2 \leq \nu s_x^2 / \chi_{1-\alpha/2}^2\right) = 1 - \alpha \quad (4.28)$$

For example, the 95% precision interval by which s_x^2 estimates σ^2 , is given by

$$\nu s_x^2 / \chi_{0.025}^2 \leq \sigma^2 \leq \nu s_x^2 / \chi_{0.975}^2 \quad (95\%) \quad (4.29)$$

Note that this interval is bounded by the 2.5% and 97.5% levels of significance (for 95% coverage).

The χ^2 distribution estimates the discrepancy expected due to random chance. Values for χ_{α}^2 are tabulated in Table 4.5 as a function of the degrees of freedom. The $P(\chi^2)$ value equals the area under

Table 4.5 Values for χ_{α}^2

ν	$\chi_{0.99}^2$	$\chi_{0.975}^2$	$\chi_{0.95}^2$	$\chi_{0.90}^2$	$\chi_{0.50}^2$	$\chi_{0.05}^2$	$\chi_{0.025}^2$	$\chi_{0.01}^2$
1	0.000	0.000	0.000	0.016	0.455	3.84	5.02	6.63
2	0.020	0.051	0.103	0.211	1.39	5.99	7.38	9.21
3	0.115	0.216	0.352	0.584	2.37	7.81	9.35	11.3
4	0.297	0.484	0.711	1.06	3.36	9.49	11.1	13.3
5	0.554	0.831	1.15	1.61	4.35	11.1	12.8	15.1
6	0.872	1.24	1.64	2.20	5.35	12.6	14.4	16.8
7	1.24	1.69	2.17	2.83	6.35	14.1	16.0	18.5
8	1.65	2.18	2.73	3.49	7.34	15.5	17.5	20.1
9	2.09	2.70	3.33	4.17	8.34	16.9	19.0	21.7
10	2.56	3.25	3.94	4.78	9.34	18.3	20.5	23.2
11	3.05	3.82	4.57	5.58	10.3	19.7	21.9	24.7
12	3.57	4.40	5.23	6.30	11.3	21.0	23.3	26.2
13	4.11	5.01	5.89	7.04	12.3	22.4	24.7	27.7
14	4.66	5.63	6.57	7.79	13.3	23.7	26.1	29.1
15	5.23	6.26	7.26	8.55	14.3	25.0	27.5	30.6
16	5.81	6.91	7.96	9.31	15.3	26.3	28.8	32.0
17	6.41	7.56	8.67	10.1	16.3	27.6	30.2	33.4
18	7.01	8.23	9.39	10.9	17.3	28.9	31.5	34.8
19	7.63	8.91	10.1	11.7	18.3	30.1	32.9	36.2
20	8.26	9.59	10.9	12.4	19.3	31.4	34.2	37.6
30	15.0	16.8	18.5	20.6	29.3	43.8	47.0	50.9
60	37.5	40.5	43.2	46.5	59.3	79.1	83.3	88.4

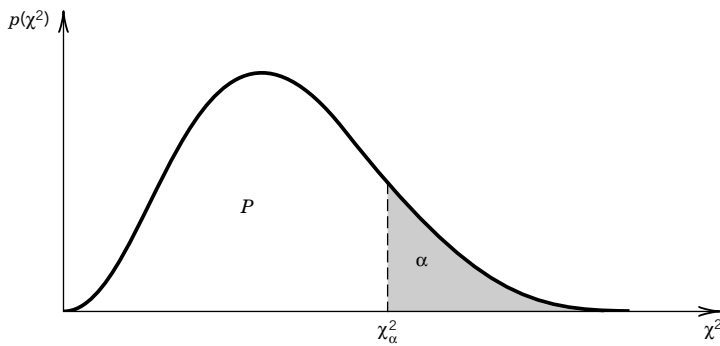


Figure 4.8 The χ^2 distribution as it relates to probability P and to the level of significance, $\alpha (=1-P)$.

$p(\chi^2)$ as measured from the left, and the α value is the area as measured from the right, as noted in Figure 4.8. The total area under $p(\chi^2)$ is equal to unity.

Example 4.5

Ten steel tension specimens are tested from a large batch, and a sample variance of $40,000 \text{ (kN/m}^2\text{)}^2$ is found. State the true variance expected at 95% confidence.

$$\begin{aligned} \text{KNOWN } s_x^2 &= 40,000 \text{ (kN/m}^2\text{)}^2 \\ N &= 10 \end{aligned}$$

FIND Precision interval for σ^2

SOLUTION With $v = N - 1 = 9$, we find from Table 4.5, $\chi^2 = 19.0$ at $\alpha = 0.025$ written $\chi^2_{0.025} = 19.0$ and $\chi^2 = 2.7$ at $\alpha = 0.975$ written $\chi^2_{0.975} = 2.7$. Thus, from Equation 4.28,

$$(9)(40,000)/19.0 \leq \sigma^2 \leq (9)(40,000)/2.7 \quad (95\%)$$

or, the precision interval for the variance is

$$18,947 \leq \sigma^2 \leq 133,333 \text{ (kN/m}^2\text{)}^2 \quad (95\%)$$

This is the precision interval about σ^2 due to random chance. As N becomes larger, the precision interval narrows as $s^2 \rightarrow \sigma^2$.

Example 4.6

A manufacturer knows from experience that the variance in the diameter of the roller bearings used in its bearings is $3.15 \mu\text{m}^2$. Rejecting bearings drives up the unit cost. However, manufacturer rejects any batch of roller bearings if the sample variance of 20 pieces selected at random exceeds $5 \mu\text{m}^2$. Assuming a normal distribution, what is the probability that any given batch will be rejected even though its true variance is actually within the tolerance limits?

$$\begin{aligned} \text{KNOWN } \sigma^2 &= 3.15 \mu\text{m}^2 \\ s_x^2 &= 5 \mu\text{m}^2 \text{ based on } N = 20 \end{aligned}$$

ASSUMPTIONS Variations between bearings fit a normal distribution.

FIND χ^2

SOLUTION This problem could be restated as follows: What is the probability that s_x^2 based on 20 measurements will not predict σ_x^2 for the entire batch?

For $\nu = N - 1 = 19$, and using Equation 4.26, the χ^2 value is

$$\chi_{\alpha}^2(\nu) = \nu s_x^2 / \sigma^2 = 30.16$$

Inspection of Table 4.5 shows $\chi_{0.05}^2(19) = 30.1$, so we can take $\alpha \approx 0.05$. Taking χ_{α}^2 as a measure of discrepancy due to random chance, we interpret this result as a 5% chance that a batch actually within tolerance will be rejected. So there is a probability, $P = 1 - \alpha$, of 95% that s_x^2 does predict the σ^2 for the batch. Rejecting a batch on this basis is a good decision.

Goodness-of-Fit Test

Just how well does a set of measurements follow an assumed distribution function? In Example 4.4, we assumed that the data of Table 4.1 followed a normal distribution based only on the rough form of its histogram (Fig. 4.2). A more rigorous approach would apply the chi-squared test using the chi-squared distribution. The chi-squared test provides a measure of the discrepancy between the measured variation of a data set and the variation predicted by the assumed density function.

To begin, construct a histogram of K intervals from a data set of N measurements. This establishes the number of measured values, n_j , that lie within the j th interval. Then calculate the degrees of freedom in the variance for the data set, $\nu = N - m$, where m is the number of restrictions imposed. From ν , estimate the predicted number of occurrences, n'_j , to be expected from the distribution function. For this test, the χ^2 value is calculated from the entire histogram by

$$\chi^2 = \frac{\sum_j (n_j - n'_j)^2}{n'_j} \quad J = 1, 2, \dots, K \quad (4.30)$$

The goodness-of-fit test evaluates the null hypotheses that the data are described by the assumed distribution against the alternative that the data are not sampled from the assumed distribution. For the given degrees of freedom, the better a data set fits the assumed distribution function, the lower its χ^2 value (left side of Table 4.5), whereas the higher the χ^2 value (right side of Table 4.5), the more dubious is the fit. For example, $P(\chi_{\alpha}^2) = 1 - \alpha \leq 0.05$ leaves only a 5% or less chance that the discrepancy is due to a systematic effect such as a different distribution, a good (unequivocal) result. As with all finite samplings of a population, statistics can be used only to suggest what is most probable. Conclusions are left to the user.

Example 4.7

Test the hypothesis that the variable x as given by the measured data of Table 4.1 is described by a normal distribution.

KNOWN Table 4.1 and histogram of Figure 4.2

From Example 4.4: $\bar{x} = 1.02$; $s_x = 0.16$; $N = 20$; $K = 7$

Table 4.6 χ^2 Test for Example 4.7

J	n_j	n'_j	$(n_j - n'_j)^2 / n'_j$
1	1	0.92	0.07
2	1	1.96	0.47
3	3	3.76	0.15
4	7	4.86	0.94
5	4	4.36	0.03
6	2	2.66	0.16
7	2	1.51	1.16
Totals	20	20	$\chi^2_\alpha = 1.98$

FIND Apply the chi-squared test to the data set to test for normal distribution.

SOLUTION Figure 4.2 (Ex. 4.1) provides a histogram for the data of Table 4.1 giving the values for n_j for $K = 7$ intervals. To evaluate the hypothesis, we must find the predicted number of occurrences, n'_j , for each of the seven intervals based on a normal distribution. To do this, substitute $x' = \bar{x}$ and $\sigma = s_x$ and compute the probabilities based on the corresponding z values.

For example, consider the second interval ($j = 2$). Using Table 4.3, the predicted probabilities are

$$\begin{aligned} P(0.75 \leq x_i \leq 0.85) &= P(0.75 \leq x_i < x') - P(0.85 \leq x_i < x') \\ &= P(z_a) - P(z_b) \\ &= P(1.6875) - P(1.0625) \\ &= 0.454 - 0.356 = 0.098 \end{aligned}$$

So for a normal distribution, we should expect the measured value to lie within the second interval for 9.8% of the measurements. With

$$n'_2 = N \times P(0.75 \leq x_i < 0.85) = 20 \times 0.098 = 1.96$$

that is, 1.96 occurrences are expected out of 20 measurements in this second interval. The actual measured data set shows $n_2 = 1$.

The results are summarized in Table 4.6 with χ^2 based on Equation 4.30. Because two calculated statistical values (\bar{x} and s_x) are used in the computations, the degrees of freedom in χ^2 are restricted by 2. So, $v = K - 2 = 7 - 2 = 5$ and from Table 4.5, for $\chi^2_\alpha(v) = 1.98$, $\alpha \approx 0.85$ or $P(\chi^2) \approx 0.15$ (note: $\alpha = 1 - P$ is found here by interpolation between columns). While there is a high probability that the discrepancy between the histogram and the normal distribution is due only to random variation of a finite data set, there is a 15% chance the discrepancy is by some other systematic tendency. We should consider this result as equivocal. The hypothesis that x is described by a normal distribution is neither proven nor disproven.

4.6 REGRESSION ANALYSIS

A measured variable is often a function of one or more independent variables that are controlled during the measurement. When the measured variable is sampled, these variables are controlled, to the extent possible, as are all the other operating conditions. Then, one of these variables is changed and a new

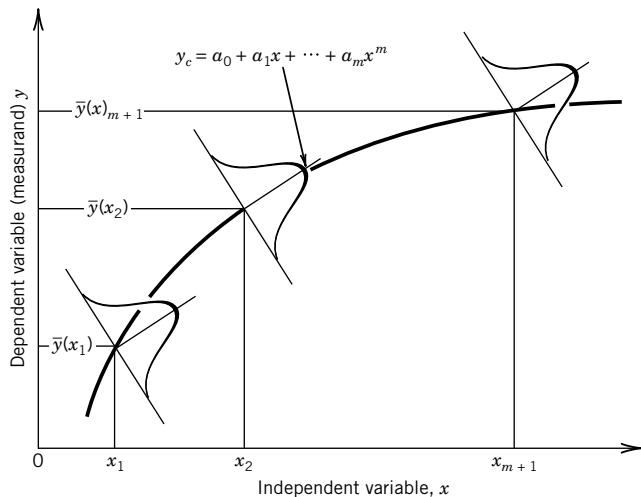


Figure 4.9 Distribution of measured value y about each fixed value of independent variable x . The curve y_c represents a possible functional relationship.

sampling is made under the new operating conditions. This is a common procedure used to document the relationship between the measured variable and an independent process variable. We can use regression analysis to establish a functional relationship between the dependent variable and the independent variable. This discussion pertains directly to polynomial curve fits. More information on regression analysis, including multiple variable regression, can be found elsewhere (4, 6).

A regression analysis assumes that the variation found in the dependent measured variable follows a normal distribution about each fixed value of the independent variable. This behavior is illustrated in Figure 4.9 by considering the dependent variable $y_{i,j}$ consisting of N measurements, $i = 1, 2, \dots, N$, of y at each of n values of independent variable, x_j , $j = 1, 2, \dots, n$. This type of behavior is common during calibrations and in many types of measurements in which the dependent variable y is measured under controlled values of x . Repeated measurements of y yield a normal distribution with variance $s_y^2(x_j)$, about some mean value, $\bar{y}(x_j)$.

Most spreadsheet and engineering software packages can perform a regression analysis on a data set. The following discussion presents the concepts of a particular type of regression analysis, its interpretation, and its limitations.

Least-Squares Regression Analysis

The regression analysis for a single variable of the form $y = f(x)$ provides an m th-order polynomial fit of the data in the form

$$y_c = a_0 + a_1x + a_2x^2 + \dots + a_mx^m \quad (4.31)$$

where y_c refers to the value of y predicted by the polynomial equation for a given value of x . For n different values of the independent variable included in the analysis, the highest order, m , of the polynomial that can be determined is restricted to $m \leq n - 1$. The values of the m coefficients a_0, a_1, \dots, a_m are determined by the analysis. A common regression analysis for engineering applications is the method of least-squares. The *method of least-squares* attempts to minimize the sum of the squares of the deviations between the actual data and the polynomial fit of a stated order by adjusting the values of the polynomial coefficients.

Consider the situation in which there are N values of x and y , referred to as x_i, y_i , where $i = 1, 2, \dots, N$. We seek an m th-order polynomial based on a set of N data points of the form (x, y) in which x and y are the independent and dependent variables, respectively. The task is to find the $m + 1$ coefficients, a_0, a_1, \dots, a_m , of the polynomial of Equation 4.31. We define the deviation between any dependent variable y_i and the polynomial as $y_i - y_{c_i}$, where y_{c_i} is the value of the polynomial evaluated at the data point (x_i, y_i) . The sum of the squares of this deviation for all values of $y_i, i = 1, 2, \dots, N$, is

$$D = \sum_{i=1}^N (y_i - y_{c_i})^2 \quad (4.32)$$

The goal of the method of least-squares is to reduce D to a minimum for a given order of polynomial.

Combining Equations 4.31 and 4.32, we write

$$D = \sum_{i=1}^N [y_i - (a_0 + a_1x + \dots + a_mx^m)]^2 \quad (4.33)$$

Now the total differential of D is dependent on the $m + 1$ coefficients through

$$dD = \frac{\partial D}{\partial a_0} da_0 + \frac{\partial D}{\partial a_1} da_1 + \dots + \frac{\partial D}{\partial a_m} da_m$$

To minimize the sum of the squares of the deviations, we want dD to be zero. This is accomplished by setting each partial derivative equal to zero:

$$\begin{aligned} \frac{\partial D}{\partial a_0} = 0 &= \frac{\partial}{\partial a_0} \left\{ \sum_{i=1}^N [y_i - (a_0 + a_1x + \dots + a_mx^m)]^2 \right\} \\ \frac{\partial D}{\partial a_1} = 0 &= \frac{\partial}{\partial a_1} \left\{ \sum_{i=1}^N [y_i - (a_0 + a_1x + \dots + a_mx^m)]^2 \right\} \\ &\vdots \\ \frac{\partial D}{\partial a_m} = 0 &= \frac{\partial}{\partial a_m} \left\{ \sum_{i=1}^N [y_i - (a_0 + a_1x + \dots + a_mx^m)]^2 \right\} \end{aligned} \quad (4.34)$$

This yields $m + 1$ equations that are solved simultaneously to yield the unknown regression coefficients, a_0, a_1, \dots, a_m .

In general, the polynomial found by regression analysis does not pass through every data point (x_i, y_i) exactly, so there is some deviation, $y_i - y_{c_i}$, between each data point and the polynomial. We compute a standard deviation based on these differences by

$$s_{yx} = \sqrt{\frac{\sum_{i=1}^N (y_i - y_{c_i})^2}{v}} \quad (4.35)$$

where v is the degrees of freedom of the fit and $v = N - (m + 1)$. The statistic s_{yx} is referred to as the *standard error of the fit* and is related to how closely a polynomial fits the data set.

The best order of polynomial fit to apply to a particular data set is that *lowest* order of fit that maintains a logical physical sense between the dependent and independent variables and reduces s_{yx} to an acceptable value. This first point is important. If the underlying physics of a problem implies that a certain order relationship should exist between dependent and independent variables, there is no sense in forcing the data to fit any other order of polynomial regardless of the value of s_{yx} . Because the method of least-squares tries to minimize the sum of the squares of the deviations, it forces inflections in the curve fit that may not be real. Consequently, while higher-order curve fits generally reduce s_{yx} , they likely do not reflect the physics behind the data set very well. In any event, it is good practice to have at least two independent data points for each order of polynomial attempted, that is, at least two data points for a first-order curve fit, four for a second-order, etc.

If we consider variability in both the independent and dependent variables, then the random uncertainty due to random data scatter about the curve fit at any value of x is estimated by (1, 4)

$$t_{v,P} s_{yx} \left[\frac{1}{N} + \frac{(x - \bar{x})^2}{\sum_{i=1}^N (x_i - \bar{x})^2} \right]^{1/2} \quad (P\%) \quad (4.36)$$

where

$$\bar{x} = \sum_{i=1}^N x_i / N$$

and x is the value used to estimate y_c in Equation 4.31. Hence, the curve fit, y_c , with confidence interval is given as

$$y_c(x) \pm t_{v,P} s_{yx} \left[\frac{1}{N} + \frac{(x - \bar{x})^2}{\sum_{i=1}^N (x_i - \bar{x})^2} \right]^{1/2} \quad (P\%) \quad (4.37)$$

The effect of the second term in the brackets of either Equations 4.36 or 4.37 is to increase the confidence interval toward the outer limits of the polynomial. Often in engineering measurements, the independent variable is a well-controlled value. In such cases, we assume that the principal source of variation in the curve fit is due to the random error in the dependent (measured) variable. A simplification to Equation 4.36 often used in a complete uncertainty analysis is to state the random uncertainty as

$$t_{v,P} \frac{s_{yx}}{\sqrt{N}} \quad (P\%) \quad (4.38)$$

We then can state that the curve fit with its confidence interval is approximated by

$$y_c \pm t_{v,P} \frac{s_{yx}}{\sqrt{N}} \quad (P\%) \quad (4.39)$$

where y_c is defined by Equation 4.31. The engineer should compare the values of Equations 4.36 and 4.38 to determine if the approximation of Equation 4.38 is acceptable. The simplification can be used when the values are not the dominant ones in an uncertainty analysis.

Multiple regression analysis involving multiple variables of the form $y = f(x_{1i}, x_{2i}, \dots)$ is also possible leading to a multidimensional response surface. The details are not discussed here, but the concepts generated for the single-variable analysis are carried through for multiple-variable analysis. The interested reader is referred elsewhere (3, 4, 6).

Example 4.8

The following data are suspected to follow a linear relationship. Find an appropriate equation of the first-order form.

x (cm)	y (V)
1.0	1.2
2.0	1.9
3.0	3.2
4.0	4.1
5.0	5.3

KNOWN Independent variable x

Dependent measured variable y

$N = 5$

ASSUMPTIONS Linear relation

FIND $y_c = a_0 + a_1x$

SOLUTION We seek a polynomial of the form $y_c = a_0 + a_1x$, that minimizes the term

$$D = \sum_{i=1}^N (y_i - y_{ci})^2$$

setting the derivatives to zero:

$$\begin{aligned}\frac{\partial D}{\partial a_0} &= 0 = -2 \left\{ \sum_{i=1}^N [y_i - (a_0 + a_1x_i)] \right\} \\ \frac{\partial D}{\partial a_1} &= 0 = -2 \left\{ \sum_{i=1}^N [y_i - (a_0 + a_1x_i)] \right\}\end{aligned}$$

Solving simultaneously for the coefficients a_0 and a_1 yields

$$\begin{aligned}a_0 &= \frac{\sum x_i \sum x_i y_i - \sum x_i^2 \sum y_i}{(\sum x_i)^2 - N \sum x_i^2} \\ a_1 &= \frac{\sum x_i \sum y_i - N \sum x_i y_i}{(\sum x_i)^2 - N \sum x_i^2}\end{aligned}\tag{4.40}$$

Substituting the data set into Equation 4.40 yields $a_0 = 0.02$ and $a_1 = 1.04$. Hence,

$$y_c = 0.02 + 1.04x \quad V$$

COMMENT Although the polynomial described by y_c is the linear curve fit for this data set, we still have no idea of how well this curve fits this data set or even if a first-order fit is appropriate. These questions are addressed below and in Example 4.9.

The LabView program *Polynomial_Fit* performs a least-squares regression analysis. It allows the user to enter data points manually or to read data from a file. Other software packages can also do this processing.

Linear Polynomials

For linear polynomials a correlation coefficient r can be found by

$$r = r_{xy} = \frac{N \sum_{i=1}^N x_i y_i - \sum_{i=1}^N x_i \sum_{i=1}^N y_i}{\sqrt{N \sum_{i=1}^N x_i^2 - \left(\sum_{i=1}^N x_i \right)^2} \sqrt{N \sum_{i=1}^N y_i^2 - \left(\sum_{i=1}^N y_i \right)^2}} \quad (4.41)$$

The correlation coefficient provides a measure of the association between x and y as predicted by the form of the curve fit equation. It is bounded by ± 1 , which represents perfect correlation; the sign indicates that y increases or decreases with x . For $\pm 0.9 < r \leq \pm 1$, a linear regression can be considered a reliable relation between y and x . Alternatively, the value r^2 is often reported, which is indicative of how well the variance in y is accounted for by the fit. However, the correlation coefficient and the r^2 value are only indicators of the hypothesis that y and x are associated; correlation does not imply cause and effect. The r and r^2 values are not effective estimators of the random error in y_c ; instead the s_{yx} value is used for that purpose.

The precision estimate in the slope of the fit can be estimated by

$$s_{a_1} = s_{yx} \sqrt{\frac{1}{\sum_{i=1}^N (x_i - \bar{x})^2}} \quad (4.42)$$

The precision estimate of the zero intercept can be estimated by

$$s_{a_0} = s_{yx} \sqrt{\frac{\sum_{i=1}^N x_i^2}{N \sum_{i=1}^N (x_i - \bar{x})^2}} \quad (4.43)$$

An error in a_0 would offset a calibration curve from its y intercept. The derivation and further discussion on Equations 4.41 to 4.43 can be found elsewhere (1, 3, 4, 6).

Example 4.9

Compute the correlation coefficient and the standard error of the fit for the data in Example 4.8. Estimate the random uncertainty associated with the fit. State the correlation with its 95% confidence interval.

KNOWN $y_c = 0.02 + 1.04x$ V

ASSUMPTIONS Errors are normally distributed. No systematic errors.

FIND r and s_{yx}

SOLUTION Direct substitution of the data set into Equation 4.41 yields the correlation coefficient of $r = 0.996$. An equivalent estimator is r^2 . Here $r^2 = 0.99$, which indicates that 99% of the variance in y is accounted for by the fit, whereas only 1% is unaccountable. These values suggest that a linear fit is a reliable relation between x and y .

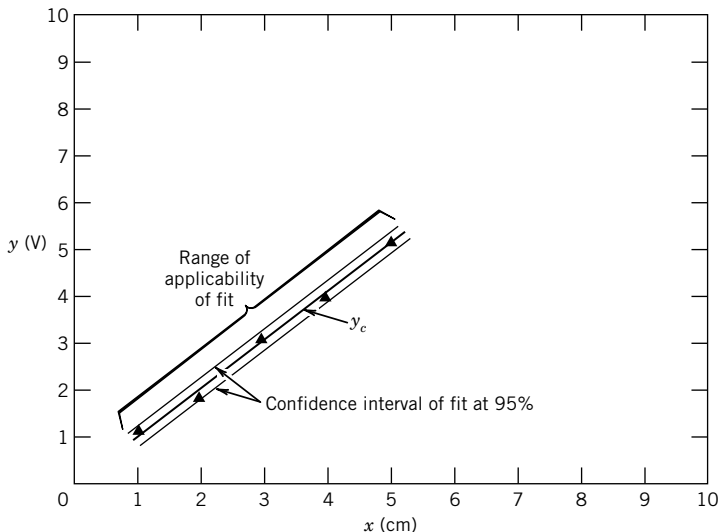


Figure 4.10 Results of the regression analysis of Example 4.9.

The random uncertainty between the data and this fit is given by the standard error of the fit, s_{yx} . Using Equation 4.35,

$$s_{yx} = \sqrt{\frac{\sum_{i=1}^N (y_i - y_{ci})^2}{v}} = 0.16$$

with degrees of freedom, $v = N - (m + 1) = 3$. The t estimator, $t_{3,95} = 3.18$, establishes a random uncertainty about the fit of $t_{3,95}s_{yx}/\sqrt{N} = 0.23$. Applying Equation 4.39, the polynomial fit can be stated at 95% confidence as

$$y_c = 1.04x + 0.02 \pm 0.23 \text{ V}(95\%)$$

This curve is plotted in Figure 4.10 with its 95% confidence interval. In comparison, Equation 4.36 varies from ± 0.23 at $x = 3$ to ± 0.39 at $x = 1$ and $x = 5$. The regression polynomial with its confidence interval is necessary when reporting a curve fit to a data set.

Example 4.10

A velocity probe provides a voltage output that is related to velocity, U , by the form $E = a + bU^m$. A calibration is performed, and the data ($N = 5$) are recorded below. Find an appropriate curve fit.

U (m/s)	E (V)
0.0	3.19
10.0	3.99
20.0	4.30
30.0	4.48
40.0	4.65

KNOWN $N = 5$

ASSUMPTIONS Data related by $E = a + bU^m$

FIND a and b

SOLUTION The suggested functional equation can be transformed into

$$\log(E - a) = \log b + m\log U$$

which has the linear form

$$Y = B + mX$$

Because at $U = 0$ m/s, $E = 3.19$ V, the value of a must be 3.19 V. The values for Y and X are computed below with the corresponding deviations from the resulting fit of 4 values:

U	$Y = \log(E-a)$	$X = \log U$	$E_i - E_{c_i}$
0.0	—	—	0.0
10.0	-0.097	1.000	-0.01
20.0	0.045	1.301	0.02
30.0	0.111	1.477	0.0
40.0	0.164	1.602	-0.01

Substituting the values for Y and X into Equation 4.40 gives $a_0 = B = -0.525$ and $a_1 = m = 0.43$. The standard error of the fit is found using Equation 4.35 to be $s_{yx} = 0.007$. From Table 4.4, $t_{2,95} = 4.30$ so that $t_{2,95}s_{yx}/\sqrt{N} = 0.015$. This gives the curve fit with confidence interval as

$$Y = -0.525 + 0.43X \pm 0.015 \quad (95\%)$$

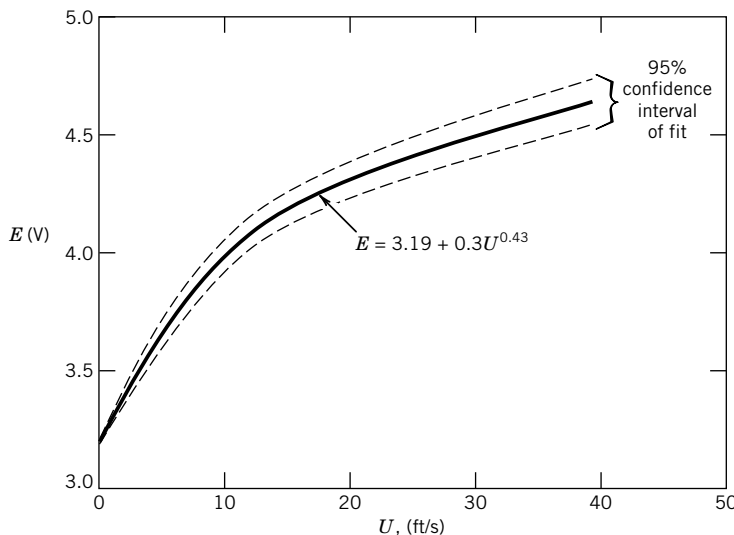


Figure 4.11 Curve fit for Example 4.10.

The polynomial is transformed back to the form $E = a + bU^m$:

$$E = 3.19 + 0.30 U^{0.43} \quad V$$

The curve fit with its 95% confidence interval is shown on Figure 4.11.

COMMENT In the present example, the intercept was chosen based on knowledge of the measurement system.

4.7 DATA OUTLIER DETECTION

It is not uncommon to find a spurious data point that does not appear to fit the tendency of the data set. Data that lie outside the probability of normal variation incorrectly offset the sample mean value estimate, inflate the random uncertainty estimates, and influence a least-squares correlation. Statistical techniques can be used to detect such data points, which are known as *outliers*. Outliers may be the result of simple measurement glitches or may reflect a more fundamental problem with test variable controls. Once detected, the decision to remove the data point from the data set must be made carefully. Once outliers are removed from a data set, the statistics are recomputed using the remaining data.

One approach to outlier detection is Chauvenet's criterion, which identifies outliers having less than a $1/2N$ probability of occurrence. To apply this criterion, let $z_0 = |x_i - \bar{x}/s_x|$ where x_i is a suspected outlier in a data set of N values. In terms of the probability values of Table 4.3, the data point is a potential outlier if

$$(1 - 2 \times P(z_0)) < 1/2N \quad (4.44)$$

For large data sets, another approach, the *three-sigma test*⁷, is to identify those data points that lie outside the range of 99.73% probability of occurrence, $\bar{x} \pm t_{v,99.7}s_x$, as potential outliers. However, either approach assumes that the sample set follows a normal distribution, which may not be true. Other methods of outlier detection are discussed elsewhere (3, 7).

Example 4.11

Consider the data given below for 10 measurements of a tire's pressure made using an inexpensive hand-held gauge (note: 14.5 psi = 1 bar). Test for outliers using the Chauvenet's criterion.

i	1	2	3	4	5	6	7	8	9	10
x_i (psi)	28	31	27	28	29	24	29	28	18	27

KNOWN Data values for $N = 10$

ASSUMPTIONS Each measurement is obtained under fixed conditions.

FIND Apply outlier detection tests.

⁷ So named since, as $v \rightarrow \infty$, $t \rightarrow 3$ for 99.7% probability.

SOLUTION Based on the 10 data points, the sample mean and sample standard deviation are found from Equations 4.14a and c to be $\bar{x} = 27$ psi with an $s_x = 3.8$. But the tire pressure should not vary much between two readings beyond the precision capabilities of the measurement system and technique, so data point 9 ($x = 18$) is a potential outlier.

Apply Chauvenet's criterion to this data point. For $N = 10$, Equation 4.44 gives $(1 - 2 \times P(z_0)) < 1/2N = 1/20 = 0.050$. So the criterion identifies the data point as an outlier if it lies outside $1 - 0.050 = 0.950$, which for 10 data points is the 95% probability spread of the data. For $x_i = 18$, $z_0 = 2.368$. Then $P(z_0) = P(2.368) = 0.4910$, so that $(1 - 2 \times 0.4910) = 0.018$. As $0.018 < 0.050$, this test identifies the data point $x = 18$ as a potential outlier.

4.8 NUMBER OF MEASUREMENTS REQUIRED

We can use the previous discussions to assist in the design and planning of a test program. For example, how many measurements, N , are required to reduce the estimated value for random error in the sample mean to an acceptable level? To answer this question, begin with Equation 4.19:

$$x' = \bar{x} \pm t_{v,P} s_{\bar{x}} \quad (P\%) \quad (4.19)$$

Let CI be the confidence interval in Equation 4.18, that is,

$$\text{CI} = \pm t_{v,P} s_{\bar{x}} = \pm t_{v,P} \frac{s_x}{\sqrt{N}} \quad (P\%) \quad (4.45)$$

This interval is two sided about the mean, defining a range from $-t_{v,P} \frac{s_x}{\sqrt{N}}$ to $+t_{v,P} \frac{s_x}{\sqrt{N}}$. We introduce the one-sided precision value d as

$$d = \frac{\text{CI}}{2} = t_{v,P} \frac{s_x}{\sqrt{N}} \quad (4.46)$$

For example, if the confidence interval is ± 1 units, an interval of width 2 units, then $d = 1$ unit. It follows that the required number of measurements is estimated by

$$N \approx \left(\frac{t_{v,P} s_x}{d} \right)^2 \quad (P\%) \quad (4.47)$$

Because the degrees of freedom in t depends on N , solving Equation 4.47 requires iteration. Equation 4.47 provides a first estimate for the number of measurements needed. How closely it reduces the range of random error to the constraint depends on how well the assumed value of s_x approximates the population σ .

A shortcoming of this method is the need to estimate s_x , which could be based on experience or other knowledge of the population. One approach is to make a preliminary number of measurements, N_1 , to obtain an estimate of the sample variance, s_1^2 , to be expected. Then use s_1 to estimate the number of measurements required. The total number of measurements, N_T , will be estimated by

$$N_T \approx \left(\frac{t_{N-1,95} s_1}{d} \right)^2 \quad (95\%) \quad (4.48)$$

This establishes that $N_T - N_1$ additional measurements are required.

Example 4.12

Determine the number of measurements required to reduce the 95% confidence interval of the mean value of a variable to within ± 1 unit, if the variance of the population is estimated to be 64 units.

$$\begin{array}{lll} \text{KNOWN} & \text{CI} = \pm 1 \text{ units} = 2 \text{ units} & P = 95\% \\ & d = 1 & \sigma^2 = 64 \text{ units} \end{array}$$

$$\text{ASSUMPTIONS } \sigma^2 \approx s_x^2$$

FIND N required

SOLUTION Equation 4.47 has two unknowns in N and t

$$N \approx \left(\frac{t_{v,95} s_x}{d} \right)^2 \quad (95\%)$$

We iterate by using a trial-and-error approach until convergence. Suppose we begin by guessing that $N = 61$ so that $t_{v,95} = 2.00$. Then, we solve Equation 4.47 with $t_{v,95} = 2.00$ and $s_x = 8$ units, to find $N = 256$. We now use $N = 256$, so that $v = 255$ and $t_{v,95} = 1.96$. This gives the new estimate of $N = 245$. Repeat again with $N = 245$, so that $v = 244$, $t_{v,95} = 1.96$. We again get $N = 245$. The analysis is converged at 245 measurements. Check the results after 245 measurements to ensure that the variance level used was representative of the actual population.

COMMENT Since the confidence interval is reduced as $N^{1/2}$, the procedure of increasing N to decrease this interval becomes one of diminishing returns.

Example 4.13

From 21 preliminary measurements of a variable, the standard deviation of the data set is 160 units. We want to reduce the 95% confidence interval in the mean value to ± 30 units. Estimate the total number of measurements required.

$$\begin{array}{lll} \text{KNOWN} & S_1 = 160 \text{ units} & N_1 = 21 \\ & d = \text{CI}/2 = 30 & t_{20,95} = 2.093 \end{array}$$

$$\text{ASSUMPTIONS } \sigma^2 \approx s_x^2$$

FIND N_T

SOLUTION At 21 measurements, the confidence interval in the mean value is $\pm (2.093)(160) / \sqrt{21} = \pm 73$ units. We need to reduce this to ± 30 units. The total number of measurements required is estimated by

$$N_T \approx \left(\frac{t_{N-1,95} s_1}{d} \right)^2 = \left(\frac{2.093 \times 160}{30} \right)^2 = 125 \quad (95\%)$$

Thus, as a first guess, a total of 125 measurements are estimated to be necessary. Take an additional 104 measurements and then reanalyze to be certain that the constraint is met.

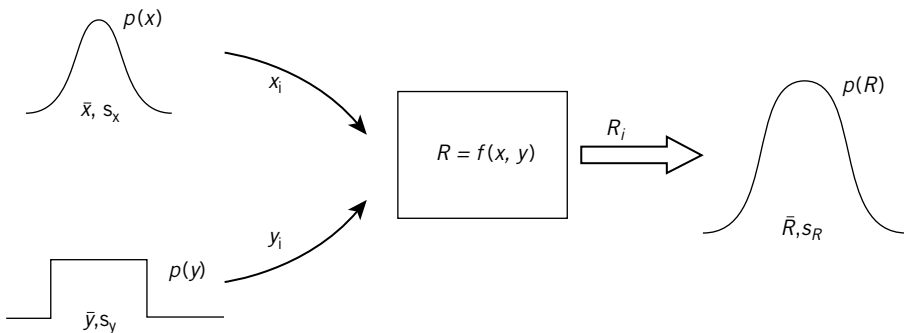


Figure 4.12 Elements of a Monte Carlo simulation of $R = f(x, y, \dots)$

4.9 MONTE CARLO SIMULATIONS

When a result is computed from the values of one or more independent random variables, the variability in the independent variables directly affects the variability in the result. *Monte Carlo simulations* provide one way to incorporate such variability into predicting the behavior of the result. The simulation outcome is the predicted probability density function of the result, $p(R)$, and its associated statistics. This outcome makes it a very useful sampling method.

To illustrate a Monte Carlo simulation, consider result R that is a known function of two variables through the parametric relationship, $R = f(x,y)$, as in Figure 4.12. Each variable is defined by its own probability density function, $p(x)$ and $p(y)$. Each iteration of a Monte Carlo simulation randomly draws one probable value for $x = x_i$ and for $y = y_i$ from their respective density functions to compute a value for $R = R_i$. This iteration process continues updating the data set for R until the predicted standard deviation for R converges to an asymptotic value (8). The quality of convergence must be traded against the cost of the simulation but values within 1% to 5% suffice for many applications.

A Monte Carlo simulation is based on assumed distributions of variables, and so it is an approximation. Yet if the assumed distributions are reasonable, then the result of the approximation will be very good. The drawback is that the typical number of iterations required can be on the order of 10^4 to 10^6 . The number of iterations can be reduced using improved sampling techniques (9).

Simulations can be run within spreadsheets, Matlab, or similar programs using built-in routines to facilitate sampling from a density function. For example, in spreadsheets, the RAND function samples from a rectangular distribution to generate a random number between 0 and 1, which can then be scaled to a population range. The NORMINV function samples from a normal distribution. In Matlab, these same operations use the RAND and NORMRND functions, respectively.

Example 4.14

A small current is passed through a resistance circuit board to achieve a prescribed voltage for a certain application. From experience with one particular board design, a manufacturer knows it can expect a mean resistance of 1000Ω with a standard deviation of 100Ω with a population best described by a normal distribution. A nominal 100 mA current is passed through the circuit, which can be set to within 5 mA , a process described by a rectangular distribution. Each circuit is tested for tolerance control. Model the expected population for this voltage test using a Monte Carlo simulation.

KNOWN	$\bar{R} = 1000 \Omega$	$s_R = 100 \Omega$	normal distribution
	$\bar{I} = 0.100 \text{ A}$	$I_{\max} = 0.105 \text{ A}$	rectangular distribution

SOLUTION The parametric model is given by Ohm's law

$$E = f(I, R) = IR$$

where E is the result. Note that here R represents the resistance. The simulation starts by generating a random value for I and R based on a sampling of their respective density functions. A value for result E is then computed. This process repeats itself throughout the simulation.

For a rectangular function, sampling is done using a random number generator set between I_{\max} and I_{\min} . The standard deviation of a rectangular distribution is $(I_{\max} - I_{\min})/\sqrt{12}$. In a spreadsheet, each i th random sample of current is given by

$$I_i = I_{\min} + \text{RAND}() * (I_{\max} - I_{\min})$$

Here $(I_{\max} - I_{\min})$ appropriately scales the RAND value to the population. Similarly, the resistance is determined by sampling from a normal distribution. In a spreadsheet, this can be done with the NORMINV function. Each i th random sample for resistance is given by

$$R_i = \text{NORMINV}(\text{RAND}(), \bar{R}, s_R)$$

As new values for I and R are created, a new voltage is computed as

$$E_i = I_i R_i$$

This creates the population for voltage that we seek. In Figure 4.13, we show the result from 100,000 iterations showing a normal distribution with the following statistics:

Variable, x	\bar{x}	s_x	$s_{\bar{x}}$
$E [V]$	100.003	10.411	0.011
$I [A]$	0.100	0.0029	9.1×10^{-6}
$R [\Omega]$	999.890	99.940	0.316

So the voltage test population is normally distributed about a mean of 100.003 V with a standard deviation of 10.411 V.

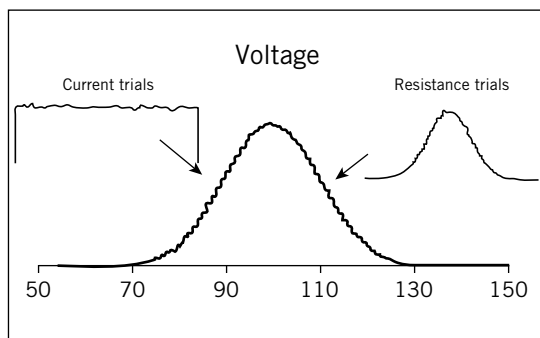


Figure 4.13 Predicted histogram for voltage (V) based on assumed distributions in current and resistance. Results of 100,000 Monte Carlo trials in Example 4.14.

Table 4.7 Summary Table for a Sample of N Data Points

Sample mean	$\bar{x} = \frac{1}{N} \sum_{i=1}^N x_i$
Sample standard deviation	$s_x = \sqrt{\frac{1}{N-1} \sum_{i=1}^N (x_i - \bar{x})^2}$
Standard deviation of the means ^a	$s_{\bar{x}} = \frac{s_x}{\sqrt{N}}$
Precision interval for a single data point, x_i	$\pm t_{v,P} s_x \quad (\text{P}\%)$
Confidence interval ^{b,c} for a mean value, \bar{x}	$\pm t_{v,P} s_{\bar{x}} \quad (\text{P}\%)$
Confidence interval ^{b,d} for curve fit, $y = f(x)$	$\pm t_{v,P} \frac{s_{yx}}{\sqrt{N}} \quad (\text{P}\%)$

^aMeasure of random standard uncertainty in x .

^bIn the absence of systematic errors.

^cMeasure of random uncertainty in \bar{x} .

^dMeasure of random uncertainty in curve fit (see conditions of Eqs. 4.37–4.39).

4.10 SUMMARY

The behavior of a random variable is defined by its unique probability density function, which provides exact information about its mean value and variability. The purpose of the measurements is to estimate this density function based on the acquired limited data set. The normal scatter of data about some central mean value is due to several contributing factors, including the process variable's own temporal unsteadiness or spatial distribution under nominally fixed operating conditions, as well as random errors in the measurement system and in the measurement procedure. Further, a finite number of measurements of a variable can only go so far in estimating the behavior of an entire population of values. We discuss how estimates based on a limited data set introduce another random error into predicting the true value of the measurement, something addressed by the sample statistics. Statistics is a powerful tool used to interpret and present data. In this chapter, we developed the most basic methods used to understand and quantify finite-sized data sets. Methods to estimate the true mean value based on a limited number of data points and the random uncertainty in such estimates were presented along with treatment of data curve fitting. A summary table of these statistical estimators is given as Table 4.7. Monte Carlo methods were presented as a tool to predict how variations in independent variables will affect the variation in a result. Throughout this chapter we have assumed negligible systematic error in the data set. In the next chapter, we expand our error considerations in our estimate of the true value of a measurement.

REFERENCES

1. Kendal, M.G., and A. Stuart, *Advanced Theory of Statistics*, Vol. 2, Griffin, London, 1961.
2. Bendat, J., and A. Piersol, *Random Data Analysis*, Wiley, New York, 1971.
3. Lipson, C., and N.J. Sheth, *Statistical Design and Analysis of Engineering Experiments*, McGraw-Hill, New York, 1973.

4. Miller, I., and J.E. Freund, *Probability and Statistics for Engineers*, 3rd ed., Prentice Hall, Englewood Cliffs, NJ, 1985.
5. Bury, K., *Statistical Distributions in Engineering*, Cambridge Press, Cambridge, UK, 1999.
6. Vardeman, S.B., *Statistics for Engineering Problem Solving*, PWS Publishing Company, Boston, 1994.
7. ASME/ANSI Power Test Codes, *Test Uncertainty PTC 19.1-2005*, American Society of Mechanical Engineers, New York, 2005.
8. Joint Committee for Guides in Metrology (JCGM), *Propagation of Distributions Using the Monte Carlo Method*, JCGM 101:2008, JCGM, Sevres Cedex, France, 2008.
9. Devroye, L., *Non-Uniform Random Variate Generation*, Springer, 1986. See also <http://cg.scs.carleton.ca/~luc/rnbookindex.html>.

NOMENCLATURE

a_0, a_1, \dots, a_m	polynomial regression coefficients	$\langle s_{\bar{x}} \rangle$	pooled standard deviation of the means of x
f_j	frequency of occurrence of a value	$\langle s_x \rangle^2$	pooled sample variance of x
x	measured variable; measurand	s_{yx}	standard error of the (curve) fit between y and x ; standard random uncertainty in a curve fit
x_i	i th measured value in a data set		
x'	true mean value of the population of x	t	Student's t variable
\bar{x}	sample mean value of x	β	normalized standard variate
$\langle \bar{x} \rangle$	pooled sample mean of x	σ	true standard deviation of the population of x
$p(x)$	probability density function of x	σ^2	true variance of the population of x
s_x	sample standard deviation x	χ^2	chi-squared value
$s_{\bar{x}}$	sample standard deviation of the means of x ; standard random uncertainty in \bar{x}	v	degrees of freedom
s_x^2	sample variance of x		
$\langle s_x \rangle$	pooled sample standard deviation of x		

PROBLEMS

- 4.1 Determine the range of values containing 50% of the population of x . From a large sampling ($N > 5000$), we find that x has a mean value of 5.2 units and a standard deviation of 1.0 units. Assume x is normally distributed.
- 4.2 Determine the range of values containing 90% of the population of x . From a very large data set ($N > 50,000$), x is found to have a mean value of 192.0 units with a standard deviation of 10 units. Assume x is normally distributed.
- 4.3 At a fixed operating setting, the pressure in a line downstream of a reciprocating compressor has a mean value of 12.0 bar with a standard deviation of 1.0 bar based on a very large data set obtained from continuous monitoring. What is the probability that the line pressure will exceed 13.0 bar during any measurement?

- 4.4** Consider the toss of four coins. There are 2^4 possible outcomes of a single toss. Develop a histogram of the number of heads (one side of the coin) that can appear on any toss. Does it look like a normal distribution? Should this be expected? What is the probability that three heads will appear on any toss?
- 4.5** As a game, slide a matchbook across a table, trying to make it stop at some predefined point on each attempt. Measure the distance from the starting point to the stopping point. Repeat this 10, 20, through 50 times. Plot the frequency distribution from each set. Would you expect them to look like a gaussian distribution? What statistical outcomes would distinguish a better player?

Problems 4.6 through 4.15 refer to the three measured data sets in Table 4.8. Assume that the data have been recorded from three replications from the same process under the same fixed operating condition.

- 4.6** Develop a histogram for the data listed in column 1. Discuss each axis and describe the overall shape of the histogram.
- 4.7** Develop a frequency distribution for the data given in column 3. Discuss each axis and describe its overall shape.
- 4.8** Develop and compare the histograms of the three data sets represented under columns 1, 2, and 3. If these are taken from the same process, why might the histograms vary? Do they appear to show a central tendency?

Table 4.8 Measured Force Data for Exercise Problems

<i>F</i> (N) Set 1	<i>F</i> (N) Set 2	<i>F</i> (N) Set 3
51.9	51.9	51.1
51.0	48.7	50.1
50.3	51.1	51.4
49.6	51.7	50.5
51.0	49.9	49.7
50.0	48.8	51.6
48.9	52.5	51.0
50.5	51.7	49.5
50.9	51.3	52.4
52.4	52.6	49.5
51.3	49.4	51.6
50.7	50.3	49.4
52.0	50.3	50.8
49.4	50.2	50.8
49.7	50.9	50.2
50.5	52.1	50.1
50.7	49.3	52.3
49.4	50.7	48.9
49.9	50.5	50.4
49.2	49.7	51.5

- 4.9** For the data in each column, determine the sample mean value, standard deviation, and standard deviation of the means. State the degrees of freedom in each.
- 4.10** Explain the concept of “central tendency” by comparing the range of the measured values and the sample mean values from each of the three data sets.
- 4.11** From the data in column 1, estimate the range of values for which you would expect 95% of all possible measured values for this operating condition to fall. Repeat for columns 2 and 3. Discuss these outcomes in terms of what you might expect from finite statistics.
- 4.12** From the data in column 1, determine the best estimate of the mean value at a 95% probability level. How does this estimate differ from the estimates made in problem 4.11? Repeat for columns 2 and 3. Why do the estimates vary for each data set? Discuss these outcomes in terms of what you might expect from finite statistics if these are measuring the same measured variable during the same process.
- 4.13** For the data in column 3, if one additional measurement were made, estimate the interval in which the value of this measurement would fall with a 95% probability.
- 4.14** Compute a pooled sample mean value for the process. State the range for the best estimate in force at 95% probability based on these data sets. Discuss whether this pooled sample mean value is reasonable given the sample mean values for the individual data sets. Write a short essay explanation in terms of the limitations of sample statistics, the number of measurements, variations in data sets, and statistical estimators.
- 4.15** Apply the χ^2 goodness-of-fit test to the data in column 1 and test the assumption of a normal distribution.
- 4.16** Consider a process in which the applied measured load has a known true mean of 100 N with variance of 400 N². An engineer takes 16 measurements at random. What is the probability that this sample will have a mean value between 90 and 110?
- 4.17** A professor grades students on a normal curve. For any grade x , based on a course mean and standard deviation developed over years of testing, the following applies:

- A: $x > \bar{x} + 1.6\sigma$
 B: $\bar{x} + 0.4\sigma < x \leq \bar{x} + 1.6\sigma$
 C: $\bar{x} - 0.4\sigma < x \leq \bar{x} + 0.4\sigma$
 D: $\bar{x} - 1.6\sigma < x \leq \bar{x} + 0.4\sigma$
 F: $x \leq \bar{x} - 1.6\sigma$

How many A, C, and D grades are given per 100 students?

- 4.18** The production of a certain polymer fiber follows a normal distribution with a true mean diameter of 20 μm and a standard deviation of 30 μm . Compute the probability of a measured value greater than 80 μm . Compute the probability of a measured value between 50 and 80 μm .
- 4.19** An automotive manufacturer removes the friction linings from the clutch plates of drag race cars following test runs. A sampling of 10 linings for wear show the following values (in μm): 204.5, 231.1, 157.5, 190.5, 261.6, 127.0, 216.6, 172.7, 243.8, and 291.0. Estimate the average wear and its variance. Based on this sample, how many clutch plates out of a large set will be expected to show wear of more than 203 μm ?
- 4.20** Determine the mean value of the life of an electric light bulb if

$$p(x) = 0.001e^{-0.001x} \quad x \geq 0$$

and $p(x) = 0$ otherwise. Here x is the life in hours.

- 4.21** Compare the reduction in the possible range of random error in estimating x' by taking a sample of 16 measurements as opposed to only four measurements. Then compare 100 measurements to 25. Explain “diminishing returns” as it applies to using larger sample sizes to reduce random error in estimating the true mean value.
- 4.22** The variance in the strength test values of 270 bricks is $6.89 \text{ (MN/m}^2\text{)}^2$ with a mean of 6.92 MN/m^2 . What is the random error in the mean value and the confidence interval at 95%?
- 4.23** During the course of a motor test, the motor rpm (revolutions per minute) is measured and recorded at regular intervals as:

990 1030 950 1050 1000 980

Calculate the mean value, standard deviation and the best estimate of the true value for this data set. Over what interval would 50% of the entire population of motor speed values fall? Test the data set for potential outliers.

- 4.24** A batch of rivets is tested for shear strength. A sample of 31 rivets shows a mean strength of 924.2 MPa with a standard deviation of 18 MPa. Estimate of the mean shear strength for the batch at 95% probability.
- 4.25** Three independent sets of data are collected from the population of a variable during similar process operating condition. The statistics are found to be

$$\begin{aligned} N_1 &= 16; \bar{x}_1 = 32; s_{x_1} = 3 \text{ units} \\ N_2 &= 21; \bar{x}_1 = 30; s_{x_2} = 2 \text{ units} \\ N_3 &= 9; \bar{x}_1 = 34; s_{x_3} = 6 \text{ units} \end{aligned}$$

Neglecting systematic errors and random errors other than the variation in the measured data set, compute an estimate of the pooled mean value of this variable and the range in which the true mean should lie with 95% confidence.

- 4.26** Eleven core samples of fresh concrete are taken by a county engineer from the loads of 11 concrete trucks used in pouring a structural footing. After curing, the engineer tests to find a mean compression strength of 3027 lb/in.^2 with a standard deviation of 53 lb/in.^2 . State codes require a minimum strength of 3000 lb/in.^2 at 95% confidence. Should the footing be repoured based on a 95% confidence interval of the test data?
- 4.27** The following data were collected by measuring the force load acting on a small area of a beam under repeated “fixed” conditions:

Reading	Output (N)	Reading Number	Output (N)
1	923	6	916
2	932	7	927
3	908	8	931
4	932	9	926
5	919	10	923

Determine if any of these data points should be considered outliers. If so, reject the data point. Estimate the true mean value from this data set assuming that the only error is from variations in the data set.

- 4.28** An engineer measures the diameter of 20 tubes selected at random from a large shipment. The sample yields: $\bar{x} = 47.5$ mm and $s_x = 8.4$ mm. The manufacturer of the tubes claims that $x' = 42.1$ mm. What can the engineer conclude about this claim?

- 4.29** In manufacturing a particular set of motor shafts, only shaft diameters of between 38.10 and 37.58 mm are usable. If the process mean is found to be 37.84 mm with a standard deviation of 0.13 mm, what percentage of the population of manufactured shafts are usable?

For Problems 4.30 through 4.33, it would be helpful to use a least-squares software package, such as Polynomial_fit, or the least-squares analytical capability of spreadsheet software.

- 4.30** Determine the static sensitivity for the following data by using a least-squares regression analysis. Plot the data and fit including the 95% confidence interval due to random scatter about the fit. Compare the uncertainty interval estimated by Equation 4.37 with that of Equation 4.39 and discuss the differences.

$Y:$	2.7	3.6	4.4	5.2	9.2
$X:$	0.4	1.1	1.9	3.0	5.0

- 4.31** Using the following data, determine a suitable least-squares fit of the data. Which order polynomial best fits this data set? Plot the data and the fit with 95% confidence interval on an appropriate graph.

$Y:$	1.4	4.7	17.3	82.9	171.6	1227.1
$X:$	0.5	1.1	2.0	2.9	5.1	10.0

- 4.32** The following data have the form $y = ax^b$. Plot the data and their best fit with 95% confidence interval. Estimate the static sensitivity at each value of X .

$Y:$	0.14	2.51	15.30	63.71
$X:$	0.5	2.0	5.0	10.0

- 4.33** A fan performance test yields the following data:

$Q:$	2000	6000	10000	14000	18000	22000
$h:$	5.56	5.87	5.73	4.95	3.52	1.08

where Q is flow rate in m^3/s and h is static head in $\text{cm-H}_2\text{O}$. Find the lowest-degree polynomial that best fits the data as $h = f(Q)$. Note: Physically, a second-order polynomial is a reasonable fit. Explain your choice.

- 4.34** A camera manufacturer purchases glass to be ground into lenses. From experience it is known that the variance in the refractive index of the glass is 1.25×10^{-4} . The company will reject any shipment of glass if the sample variance of 30 lenses measured at random exceeds 2.10×10^{-4} . What is the probability that such a batch of glass will be rejected even though it is actually within the normal variance for refractive index?

- 4.35** The setup for grinding a type of bearing is considered under control if the bearings have a mean diameter of 5.000 mm. Normal procedure is to measure 30 bearings each 10 minutes to monitor

production. Production rates are 1000 per minute. What action do you recommend if such a trial sampling of 30 bearings shows a mean of 5.060 mm with a standard deviation of 0.0025 mm?

- 4.36** Referring to the information in Problem 4.35, suppose the mean diameter of the bearings must be held to within $\pm 0.2\%$. Based on given information, how many bearings should be measured at each 10-minute interval?
- 4.37** A manufacturer of general aircraft dry vacuum pumps wishes to estimate the mean failure time of its product at 95% confidence. Initially, six pumps are tested to failure with these results (in hours of operation): 1272, 1384, 1543, 1465, 1250, and 1319. Estimate the sample mean and the 95% confidence interval of the true mean. How many more data points would be needed to improve the confidence interval to be within ± 50 hours?
- 4.38** Strength tests on a batch of cold-drawn steel yield the following:

Strength (MPa)	Occurrences
421–480	4
481–540	8
541–600	12
601–660	6

Test the hypothesis that the data are a random sample that follows a normal distribution.

- 4.39** Determine the one-sided 95th-percentile of the chi-squared distribution at 16 degrees of freedom. Refer to Figure 4.8.
- 4.40** The manufacturer of an electrical fuse claims that the fuse's link will break with a 10% electrical overload within 12.31 minutes. Independent tests on a random sampling of 20 fuses showed the mean time for link breakage was 10.59 minutes with a standard deviation of 2.61 minutes. Does the test support or refute the manufacturer's claim?
- 4.41** How many independent random measurements of a time-dependent acceleration signal obtained from a vibrating vehicle under fixed operating conditions would lead to a confidence interval about the mean of ± 0.5 g, if the standard deviation of the signal is expected to be 1 g?
- 4.42** Based on 51 measurements of a time-dependent electrical signal, the standard deviation is 1.52 V. Find the 95% confidence interval in its true mean value. How many more measurements would be required to provide a 95% confidence interval in the true mean to within ± 0.28 V?
- 4.43** Estimate the probability with which an observed $\chi^2 = 19.0$ will be exceeded if there are 10 degrees of freedom.
- 4.44** A company produces a computer battery that it claims last for 8 hours on a single charge with a standard deviation of 20 minutes. A random sampling of seven batteries are tested and found to have a sample standard deviation of 29 minutes. What is the chi-squared value and the predicted level of significance as represented by the test?
- 4.45** A conductor is insulated using an enameling process. It is known that the number of insulation breaks per meter of wire is 0.07. What is the probability of finding x breaks in a piece of wire 5 m long? Use the Poisson distribution.
- 4.46** We know that 2% of the screws made by a certain machine are defective with the defects occurring randomly. The screws are packaged 100 to a box. Estimate the probability that a box will contain x defective screws. (a) Use the Binomial distribution. (b) Use the Poisson distribution.

- 4.47** An optical velocity measuring instrument provides an updated signal on the passage of small particles through its focal point. Suppose the average number of particles passing in a given time interval is 4. Estimate the probability of observing x particle passages in a given time. Use the Poisson distribution for $x = 1$ through 10.
- 4.48** Correlation implies association but does not imply cause and effect. Provide an example in which variable y may be well associated (correlated) with variable x through some relation but in which there is little to no cause-and-effect relation between them. Discuss your reasoning.
- 4.49** A cantilever is loaded at its tip. Tip deflection is measured. The following results are obtained with 10 repetitions of loading (cm):

5.30 5.73 6.77 5.26 4.33 5.45 6.09 5.64 5.81 5.75

Determine the mean value, standard deviation and the best estimate of the true value for this data set. Over what interval would 50% of the entire population of tip deflection values fall?

- 4.50** For the data set for cantilever tip deflection in the previous problem, test for outliers using Chauvenet's criterion. Recompute as necessary: mean value, standard deviation, and the best estimate of the true value for this data set. Over what interval would 50% of the entire population of tip deflection values fall?
- 4.51** A small sample ($N = 7$) of the static coefficient of friction (μ) between two materials is measured with the following data set:

0.0043 0.0050 0.0053 0.0047 0.0031 0.0051 0.0049

Test the data for outliers. Determine the mean value and its confidence.

- 4.52** ASTM F558 describes a method to test the flow performance of vacuum cleaners. To establish performance, it requires a minimum of three units of a model be tested in a prescribed manner and repeated three times (trials) for each unit. If the spread between the maximum and minimum values in the trials exceeds 6% of the maximum trial value, that unit is to be retested (repeatability limit). The following test data are recorded. Establish the mean and standard deviation for each unit and test that repeatability limits are met. Performance is in units of air watts (flow rate times suction pressure).

Air Power (W)	Unit 1	Unit 2	Unit 3
Trial 1	293.5	274.6	301.4
Trial 2	290.7	273.6	296.8
Trial 3	276.1	281.8	296.1

- 4.53** Following the information of Problem 4.52, ASTM 558 requires calculating the 90% confidence interval for each unit tested. If that confidence interval exceeds 5% of the mean value found for that unit, then that unit and its test results must be discarded and a new unit must be taken from the population and tested. Based on the data set in the preceding problem, must another unit be tested? If not, report the pooled mean for the model.
- 4.54** To demonstrate the expected frequency of obtaining heads in a coin toss of 10 tries, you are to generate a histogram from repeated trials (1 trial = 10 tosses). In generating the histogram, continue until your expected frequency converges on a value. You might use a spreadsheet or Matlab to conduct a Monte Carlo simulation recognizing that obtaining either a heads or tails outcome in a single toss is a random event with equal probability.
- 4.55** Conduct a Monte Carlo simulation to predict the statistical outcome of a planned test to measure drag coefficient, $C_D = D/(0.5\rho U^2 A)$, on an airplane wing model. Experience shows that drag, D , and

density, ρ , follow normal distributions, while velocity, U , and area, A , follow rectangular distributions. Expected values are given below. Determine the mean, standard deviation, number of iterations for convergence, and the histogram for C_D .

$$\begin{array}{llll} \bar{D} = 5 \text{ N} & \bar{U} = 10 \text{ m/s} & \bar{\rho} = 1.225 \text{ kg/m}^3 & A = 0.50 \text{ m}^2 \\ s_D = 0.5 \text{ N} & 9 \leq U \leq 10 \text{ m/s} & s_\rho = 0.012 \text{ kg/m}^3 & 0.48 \leq A \leq 0.52 \text{ m}^2 \end{array}$$

- 4.56 Run program *Finite Population*. Describe the evolution of the measured histogram as N increases. Why do the statistical values keep changing? Is there a tendency in these values?
- 4.57 Run program *Running Histogram*. Study the influence of the number of data points and the number of intervals on the shape of the histogram and magnitude of each interval. Describe this influence. Why are some values “out of range?”
- 4.58 Run program *Probability Density*. Vary the sample size and number of intervals used to create the density function. Why does it change shape with each new data set?

Chapter 5

Uncertainty Analysis

5.1 INTRODUCTION

Whenever we plan a test or later report a test result, we need to know something about the quality of the results. Uncertainty analysis provides a methodical approach to estimating the quality of the results from an anticipated test or from a completed test. This chapter focuses on how to estimate the “ \pm what?” in a planned test or in a stated test result.

Suppose the competent dart thrower of Chapter 1 tossed several practice rounds of darts at a bull’s-eye. This would give us a good idea of the thrower’s tendencies. Then, let the thrower toss another round. Without looking, can you guess where the darts will hit? Test measurements that include systematic and random error components are much like this. We can calibrate a measurement system to get a good idea of its behavior and accuracy. However, from the calibration we can only estimate how well any measured value might estimate the actual “true” value in a subsequent measurement.

Errors are a property of the measurement. Measurement is the process of assigning a value to a physical variable based on a sampling from the population of that variable. Error causes a difference between the value assigned by measurement and the true value of the population of the variable. Measurement errors are introduced from various elements, for example, the individual instrument calibrations, the data set finite statistics, and the approach used. But because we do not know the true value and we only know the measured values, we do not know the exact values of errors. Instead, we draw from what we do know about the measurement to estimate a range of probable error. This estimate is an assigned value called the *uncertainty*. The uncertainty describes an interval about the measured value within which we suspect that the true value must fall with a stated probability. *Uncertainty analysis* is the process of identifying, quantifying, and combining the errors.

Uncertainty is a property of the result. The outcome of a measurement is a result, and the uncertainty quantifies the quality of that result. Uncertainty analysis provides a powerful design tool for evaluating different measurement systems and methods, designing a test plan, and reporting uncertainty. This chapter presents a systematic approach for identifying, quantifying, and combining the estimates of the errors in a measurement. While the chapter stresses the methodology of analyses, we emphasize the concomitant need for an equal application of critical thinking and professional judgment in applying the analyses. The quality of an uncertainty analysis depends on the engineer’s knowledge of the test, the measured variables, the equipment, and the measurement procedures (1).

Errors are effects, and uncertainties are numbers. While errors are the effects that cause a measured value to differ from the true value, the uncertainty is an assigned numerical value that quantifies the probable range of these errors.

This chapter approaches uncertainty analysis as an evolution of information from test design through final data analysis. While the structure of the analysis remains the same at each step, the number of errors identified and their uncertainty values may change as more information becomes available. In fact, the uncertainty in the result may increase. There is no exact answer to an analysis, just the result from a reasonable approach using honest numbers. This is the nature of an uncertainty analysis.

There are two accepted professional documents on uncertainty analysis. The American National Standards Institute/American Society of Mechanical Engineers (ANSI/ASME) Power Test Codes (PTC) 19.1 Test Uncertainty (2) is the United States engineering test standard, and our approach favors that method. The International Organization on Standardization’s “Guide to the Expression of Uncertainty in Measurement” (ISO GUM) (1) is an international metrology standard. The two differ in some terminology and how errors are cataloged. For example, PTC 19.1 refers to random and systematic errors, terms that classify errors by how they manifest themselves in the measurement. ISO GUM refers to type A and type B errors, terms that classify errors by how their uncertainties are estimated. These differences are real but they are not significant to the outcome. Once past the classifications, the two methods are quite similar. The important point is that the end outcome of an uncertainty analysis by either method will yield a similar result!

Upon completion of this chapter, the reader will be able to

- explain the relation between an error and an uncertainty,
- execute an appropriate uncertainty analysis regardless of the level and quantity of information available,
- explain the differences between systematic and random errors and treat their assigned uncertainties,
- analyze a test system and test approach from test design through data presentation to assign and propagate uncertainties, and
- propagate uncertainties to understand their impact on the final statement of a result.

5.2 MEASUREMENT ERRORS

In the discussion that follows, errors are grouped into two categories: systematic error and random error. We do not consider measurement blunders that result in obviously fallacious data—such data should be discarded.

Consider the repeated measurement of a variable under conditions that are expected to produce the same value of the measured variable. The relationship between the true value of the population and the measured data set, containing both systematic and random errors, can be illustrated as in Figure 5.1. The total error in a set of measurements obtained under seemingly fixed conditions can be described by the systematic errors and the random errors in those measurements. The systematic errors shift the sample mean away from the true mean by a fixed amount, and within a sample of many measurements, the random errors bring about a distribution of measured values about the sample mean. Even a so-called accurate measurement contains small amounts of systematic and random errors.

Measurement errors enter during all aspects of a test and obscure our ability to ascertain the information that we desire: the true value of the variable measured. If the result depends on more than one measured variable, these errors further propagate to the result. In Chapter 4, we stated that the best estimate of the true value sought in a measurement is provided by its sample mean value and

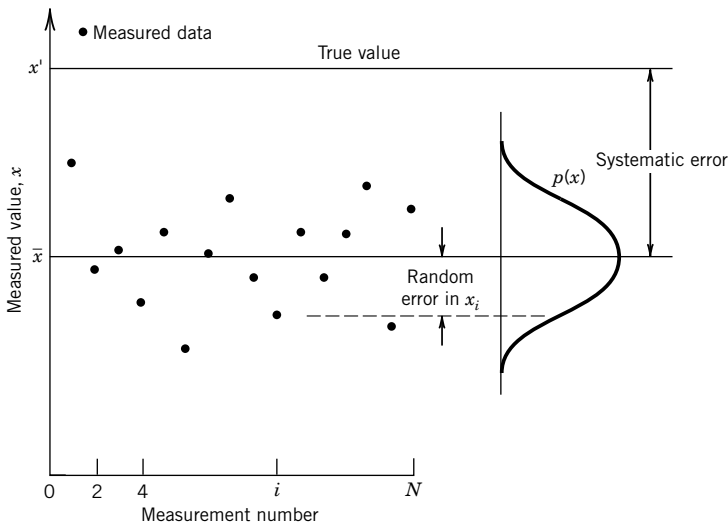


Figure 5.1 Distribution of errors on repeated measurements.

the uncertainty in that value,

$$x' = \bar{x} \pm u_x \quad (P\%) \quad (4.1)$$

But we considered only the random uncertainty due to the statistics of a measured data set. In this chapter, we extend this to uncertainty analysis so that the u_x term contains the uncertainties assigned to all known errors. Certain assumptions are implicit in an uncertainty analysis:

1. The test objectives are known and the measurement itself is a clearly defined process.
2. Any known corrections for systematic error have been applied to the data set, in which case the systematic uncertainty assigned is the uncertainty of the correction.
3. Except where stated otherwise, we assume a normal distribution of errors and reporting of uncertainties.
4. Unless stated otherwise, the errors are assumed to be independent (uncorrelated) of each other. But some errors are correlated, and we discuss how to handle these in Section 5.9.
5. The engineer has some “experience” with the system components.

In regards to item 5, by “experience” we mean that the engineer either has prior knowledge of what to expect from a system or can rely on the manufacturer’s performance specifications or on information from the technical literature.

We might begin the design of an engineering test with an idea and some catalogs, and end the project after data have been obtained and analyzed. As with any part of the design process, the uncertainty analysis evolves as the design of the measurement system and process matures. We discuss uncertainty analysis for the following measurement situations: (1) design stage, where tests are planned but information is limited; (2) advanced stage or single measurement, where additional information about process control can be used to improve a design-stage uncertainty estimate; and (3) multiple measurements, where all available test information is combined to assess the uncertainty in a test result. The methods for situation 3 follow current engineering standards.

5.3 DESIGN-STAGE UNCERTAINTY ANALYSIS

Design-stage uncertainty analysis refers to an analysis performed in the formulation stage prior to a test. It provides only an estimate of the minimum uncertainty based on the instruments and method chosen. If this uncertainty value is too large, then alternate approaches will need to be found. So, it is useful for selecting instruments and selecting measurement techniques. At the test design stage, the measurement system and associated procedures may be but a concept. Often little may be known about the instruments, which in many cases might still be just pictures in a catalog. Major facilities may need to be built and equipment ordered with a considerable lead time. Uncertainty analysis at this time is used to assist in selecting equipment and test procedures based on their relative performance. In the design stage, distinguishing between systematic and random errors might be too difficult to be of concern. So for this initial discussion, consider only sources of error and their assigned uncertainty in general. A measurement system usually consists of sensors and instruments, each with their respective contributions to system uncertainty. We first discuss individual contributions to uncertainty.

Even when all errors are otherwise zero, a measured value must be affected by our ability to resolve the information provided by the instrument. This *zero-order uncertainty* of the instrument, u_0 , assumes that the variation expected in the measured values will be only that amount due to instrument resolution and that all other aspects of the measurement are perfectly controlled. Essentially, u_0 is an estimate of the expected random uncertainty caused by the data scatter due to instrument resolution.

In lieu of any other information, assign a numerical value to u_0 of one-half of the analog instrument resolution¹ or to equal to its digital least count. This value will reasonably represent the uncertainty interval on either side of the reading with a probability of 95%. Then,

$$u_0 = \frac{1}{2} \text{resolution} = 1 \text{LSD} \quad (5.1)$$

where LSD refers to the least significant digit of the readout.

Note that because we assume that the error has a normal distribution with its uncertainty applied equally to either side of the reading, we could write this as

$$u_0 = \pm \frac{1}{2} \text{resolution} \ (95\%)$$

But unless specifically stated otherwise, the \pm sign for the uncertainty will be assumed for any computed uncertainty value and applied only when writing the final uncertainty interval of a result.

The second piece of information that is usually available is the manufacturer's statement concerning instrument error. We can assign this stated value as the *instrument uncertainty*, u_c . Essentially, u_c is an estimate of the expected systematic uncertainty due to the instrument. If no probability level is provided with such information, a 95% level can be assumed.

Sometimes the instrument errors are delineated into parts, each part due to some contributing factor (Table 1.1). A probable estimate in u_c can be made by combining the uncertainties of known errors in some reasonable manner. An accepted approach of combining uncertainties is termed the *root-sum-squares* (RSS) method.

¹ It is possible to assign a value for u_0 that differs from one-half the scale resolution. Discretion should be used. Instrument resolution is likely described by either a normal or a rectangular distribution, depending on the instrument.

Combining Elemental Errors: RSS Method

Each individual measurement error interacts with other errors to affect the uncertainty of a measurement. This is called *uncertainty propagation*. Each individual error is called an “elemental error.” For example, the sensitivity error and linearity error of a transducer are two elemental errors, and the numbers associated with these are their uncertainties. Consider a measurement of x that is subject to some K elements of error, each of uncertainty u_k , where $k = 1, 2, \dots, K$. A realistic estimate of the uncertainty in the measured variable, u_x , due to these elemental errors can be computed using the RSS *method* to propagate the elemental uncertainties:

$$\begin{aligned} u_x &= \sqrt{u_1^2 + u_2^2 + \cdots + u_K^2} \\ &= \sqrt{\sum_{k=1}^K u_k^2} \quad (P\%) \end{aligned} \quad (5.2)$$

The RSS method of combining uncertainties is based on the assumption that the square of an uncertainty is a measure of the variance (i.e., s^2) assigned to an error, and the propagation of these variances yields a probable estimate of the total uncertainty. Note that it is imperative to maintain consistency in the units of each uncertainty in Equation 5.2 and that each uncertainty term be assigned at the same probability level.

In test engineering, it is common to report final uncertainties at a 95% probability level ($P\% = 95\%$), and this is equivalent to assuming the probability covered by two standard deviations. When a probability level equivalent to a spread of one standard deviation is used, this uncertainty is called the “standard” uncertainty (1, 2). For a normal distribution, a standard uncertainty is a 68% probability level. Whatever level is used, consistency is important.

Design-Stage Uncertainty

The *design-stage uncertainty*, u_d , for an instrument or measurement method is an interval found by combining the instrument uncertainty with the zero-order uncertainty,

$$u_d = \sqrt{u_0^2 + u_c^2} \quad (P\%) \quad (5.3)$$

This procedure for estimating the design-stage uncertainty is outlined in Figure 5.2. The design-stage uncertainty for a test system is arrived at by combining each of the design-stage uncertainties for each component in the system using the RSS method while maintaining consistency of units and confidence levels.

Due to the limited information used, a design-stage uncertainty estimate is intended only as a guide for selecting equipment and procedures before a test, and is never used for reporting results. *If additional information about other measurement errors is known at the design stage, then their*

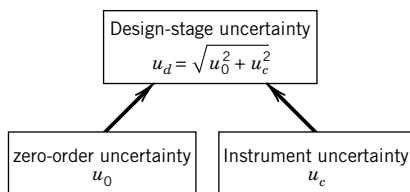


Figure 5.2 Design-stage uncertainty procedure in combining uncertainties.

uncertainties can and should be used to adjust Equation 5.3. So Equation 5.3 provides a minimum value for design stage uncertainty. In later sections of this chapter, we move towards more thorough uncertainty analyses.

Example 5.1

Consider the force measuring instrument described by the following catalog data. Provide an estimate of the uncertainty attributable to this instrument and the instrument design-stage uncertainty.

Resolution:	0.25 N
Range:	0 to 100 N
Linearity error:	within 0.20 N over range
Hysteresis error:	within 0.30 N over range

KNOWN Catalog specifications

ASSUMPTIONS Instrument uncertainty at 95% level; normal distribution

FIND u_c, u_d

SOLUTION We follow the procedure outlined in Figure 5.2. An estimate of the instrument uncertainty depends on the uncertainty assigned to each of the contributing elemental errors of linearity, e_1 , and hysteresis, e_2 , respectively assigned as

$$u_1 = 0.20 \text{ N} \quad u_2 = 0.30 \text{ N}$$

Then using Equation 5.2 with $K = 2$ yields

$$\begin{aligned} u_c &= \sqrt{(0.20)^2 + (0.30)^2} \\ &= 0.36 \text{ N} \end{aligned}$$

The instrument resolution is given as 0.25 N, from which we assume $u_0 = 0.125 \text{ N}$. From Equation 5.3, the design-stage uncertainty of this instrument would be

$$\begin{aligned} u_d &= \sqrt{u_0^2 + u_c^2} = \sqrt{(0.36)^2 + (0.125)^2} \\ &= \pm 0.38 \text{ N} \quad (95\%) \end{aligned}$$

COMMENT The design-stage uncertainty for this instrument is simply an estimate based on the “experience” on hand, in this case the manufacturer’s specifications. Additional information might justify modifying these numbers or including additional known elemental errors into the analysis.

Example 5.2

A voltmeter is used to measure the electrical output signal from a pressure transducer. The nominal pressure is expected to be about 3 psi ($3 \text{ lb/in.}^2 = 0.2 \text{ bar}$). Estimate the design-stage uncertainty in this combination. The following information is available:

Voltmeter	
Resolution:	10 μV
Accuracy:	within 0.001% of reading
Transducer	
Range:	$\pm 5 \text{ psi} (\sim \pm 0.35 \text{ bar})$
Sensitivity:	1 V/psi
Input power:	10 VDC $\pm 1\%$
Output:	$\pm 5 \text{ V}$
Linearity error:	within 2.5 mV/psi over range
Sensitivity error:	within 2 mV/psi over range
Resolution:	negligible

KNOWN Instrument specifications

ASSUMPTIONS Values at 95% probability; normal distribution of errors

FIND u_c for each device and u_d for the measurement system

SOLUTION The procedure in Figure 5.2 is used for both instruments to estimate the design-stage uncertainty in each. The resulting uncertainties are then combined using the RSS approximation to estimate the system u_d .

The uncertainty in the voltmeter at the design stage is given by Equation 5.3 as

$$(u_d)_E = \sqrt{(u_o)_E^2 + (u_c)_E^2}$$

From the information available,

$$(u_o)_E = 5 \mu\text{V}$$

For a nominal pressure of 3 psi, we expect to measure an output of 3 V. Then,

$$(u_c)_E = (3 \text{ V} \times 0.00001) = 30 \mu\text{V}$$

so that the design-stage uncertainty in the voltmeter is

$$(u_d)_E = 30.4 \mu\text{V}$$

The uncertainty in the pressure transducer output at the design stage is also found using Equation 5.2. Assuming that we operate within the input power range specified, the instrument output uncertainty can be estimated by considering the uncertainty in each of the instrument elemental errors of linearity, e_1 , and sensitivity, e_2 :

$$\begin{aligned} (u_c)_p &= \sqrt{u_1^2 + u_2^2} \\ &= \sqrt{(2.5 \text{ mV/psi} \times 3 \text{ psi})^2 + (2 \text{ mV/psi} \times 3 \text{ psi})^2} \\ &= 9.61 \text{ mV} \end{aligned}$$

Since $(u_0) \approx 0 \text{ V/psi}$, the design-stage uncertainty in the transducer in terms of indicated voltage is $(u_d)_p = 9.61 \text{ mV}$.

Finally, u_d for the combined system is found by using the RSS method for the design-stage uncertainties of the two devices. The design-stage uncertainty in pressure as indicated by this measurement system is estimated to be

$$\begin{aligned} u_d &= \sqrt{(u_d)_E^2 + (u_d)_p^2} \\ &= \sqrt{(0.030 \text{ mV})^2 + (9.61 \text{ mV})^2} \\ &= \pm 9.61 \text{ mV} \quad (95\%) \end{aligned}$$

But since the sensitivity is 1 V/psi, the uncertainty in pressure can be stated as

$$u_d = \pm 0.0096 \text{ psi} \quad (95\%)$$

COMMENT Note that essentially all of the uncertainty is due to the transducer. Design-stage uncertainty analysis shows us that a better transducer, not a better voltmeter, is needed if we must improve the uncertainty in this measurement!

5.4 IDENTIFYING ERROR SOURCES

Design-stage uncertainty provides essential information to assess instrument selection and, to a limited degree, the measurement approach. But it does not address all of the possible errors that influence a measured result. Here we provide a helpful checklist of common errors. It is not necessary to classify error sources as we do here, but it is a good bookkeeping practice.

Consider the measurement process as consisting of three distinct stages: calibration, data acquisition, and data reduction. Errors that enter during each of these steps can be grouped under their respective error source heading: (1) calibration errors, (2) data-acquisition errors, and (3) data-reduction errors. Within each of these three *error source groups*, list the types of errors encountered. Such errors are the elemental errors of the measurement. Later, we will assign uncertainty values to each error. Do not become preoccupied with these groupings. Use them as a guide. If you place an error in an “incorrect” group, it is okay. The final uncertainty is not changed!

Calibration Errors

Calibration in itself does not eliminate system errors but it can help to quantify the uncertainty in the particular pieces of equipment used. Calibration errors include those elemental errors that enter the measuring system during its calibration. *Calibration errors* tend to enter through three sources: (1) the standard or reference value used in the calibration, (2) the instrument or system under calibration, and (3) the calibration process. For example, the laboratory standard used for calibration contains some inherent uncertainty, and this is passed along with the input value on which the calibration is based. Measuring system errors, such as linearity, repeatability, hysteresis, and so forth, contribute uncertainty. Depending on how the calibration is done, there can be a difference between the value supplied by the standard and the value actually sensed by the measuring system. These effects are built into the calibration data. In Table 5.1, we list the common elemental errors contributing to this error source group.

Table 5.1 Calibration Error Source Group

Element	Error Source ^a
1	Standard or reference value errors
2	Instrument or system errors
3	Calibration process errors
4	Calibration curve fit (or see Table 5.3)
etc.	

^aSystematic error or random error in each element.

Data-Acquisition Errors

An error that arises during the act of measurement is listed as a data-acquisition error. These errors include sensor and instrument errors unaccounted for by calibration; uncontrolled variables, such as changes or unknowns in measurement system operating conditions; and sensor installation effects on the measured variable. In addition, the quality of the statistics of sampled variables is affected by sample size and assumed distributions, and any temporal and spatial variations, all contributing to uncertainty. We list some common elemental errors from this source in Table 5.2.

Data-Reduction Errors

Curve fits and correlations with their associated unknowns (Section 4.6) introduce data-reduction errors into test results. Also, truncation errors, interpolation errors, and errors from assumed models or functional relationships affect the quality of a result. We list elemental errors typical of this error source group in Table 5.3.

Table 5.2 Data-Acquisition Error Source Group

Element	Error Source ^a
1	Measurement system operating conditions
2	Sensor-transducer stage (instrument error)
3	Signal conditioning stage (instrument error)
4	Output stage (instrument error)
5	Process operating conditions
6	Sensor installation effects
7	Environmental effects
8	Spatial variation error
9	Temporal variation error
etc.	

^aSystematic error or random error in each element.

Note: A total input-to-output measurement system calibration combines elements 2, 3, 4, and possibly 1 within this error source group.

Table 5.3 Data-Reduction Error Source Group

Element	Error Source ^a
1	Curve fit error
2	Truncation error
3	Modeling error
etc.	

^aSystematic error or random error in each element.

5.5 SYSTEMATIC AND RANDOM ERRORS

Systematic Error

A systematic error² remains constant in repeated measurements under fixed operating conditions. A systematic error may cause either a high or a low offset in the estimate of the true value of the measured variable. Because its effect is constant, it can be difficult to estimate the value of a systematic error or in many cases even recognize its presence. Accordingly, an estimate of the range of systematic error is represented by an interval, defined as $\pm b$. The value b is the estimate of the *systematic standard uncertainty*. Its interval has a confidence level of one standard deviation, equivalent to a probability level of 68% for a normal distribution. The *systematic uncertainty* at any confidence level is given by $t_{v,p}b$, or simply tb . The interval defined by the systematic uncertainty at the 95% probability level is written as

$$\pm B = \pm 2b \quad (95\%) \quad (5.4)$$

which assigns a value of $t=2$. This t value assumes large degrees of freedom in an assigned systematic uncertainty for which $t=1.96$, which is rounded to 2 for convenience (2).

The reader has probably experienced systematic errors in measurements. Improperly using the floating tang at the end of a metal tape measure will offset the measurement, a systematic error. A more obvious example is reporting the barefoot height of a person based on a measurement taken while the person was wearing high-heeled shoes. In this case this systematic error, a data-acquisition error, is the height of the heels. But these errors are obvious!

Consider a home bathroom scale; does it have a systematic error? How might we assign an uncertainty to its indicated weight? Perhaps we can calibrate the scale using calibrated standard masses, account for local gravitational acceleration, and correct the output, thereby estimating the systematic error of the measurement (i.e., direct calibration against a local standard). Or perhaps we can compare it to a measurement taken in a physician's office or at the gym and compare each reading (i.e., a sort of interlaboratory comparison). Or perhaps we can carefully measure the person's volume displacement in water and compare the results to estimate differences (i.e., concomitant methodology). Or, we can use the specification provided by the manufacturer (i.e., experience). Without any of the above, what value would we assign? Would we even suspect a systematic error?

²This error was called a “bias” error in engineering documents prior to the 1990s.

But let us think about this. The insidious aspect of systematic error has been revealed. Why doubt a measurement indication and suspect a systematic error? The mean value of the data set may be offset from some true value that we do not know. Figuratively speaking, there will be no shoe heels staring at us. Experience teaches us to think through each measurement carefully because systematic error is always present at some magnitude. We see that it is difficult to estimate systematic error without comparison, so a good design should include some means to estimate it. Various methodologies can be utilized: (1) calibration, (2) concomitant methodology, (3) interlaboratory comparisons, or (4) judgment/experience. When available, calibration using a suitable standard and method can reduce instrument systematic error to predictable intervals and estimate its associated uncertainty. A quality instrument may come with a certified calibration certificate. Concomitant methodology, which is using different methods of estimating the same thing, allows for comparing the results. Concomitant methods that depend on different physical measurement principles are preferable, as are methods that rely on calibrations that are independent of each other. In this regard, analytical methods could be used for comparison³ or at least to estimate the range of systematic error due to influential sources such as environmental conditions, instrument response errors, and loading errors. Lastly, an elaborate but good approach is through interlaboratory comparisons of similar measurements, an excellent replication method. This approach introduces different instruments, facilities, and personnel into an otherwise similar measurement procedure. The variations in the results between facilities provide a statistical estimate of the systematic uncertainty (2).

In lieu of the above, a judgment value based on past experience may have to be assigned; these values are usually understood to be made at the 95% confidence level. For example, the value that first came to mind to you in the bathroom scale example above likely covered a 95% interval.

Note that calibration cannot eliminate systematic error, but it may reduce uncertainty. Consider the calibration of a temperature transducer against a National Institute of Standards and Technology (NIST) standard certified to be correct to within 0.01°C. If the calibration data show that the transducer output has a systematic offset of 0.2°C relative to the standard, then we would just correct all the data obtained with this transducer by 0.2°C. Simple enough, we correct it! But the standard itself still has an intrinsic systematic uncertainty of 0.01°C, and this uncertainty remains in the calibrated transducer. We would include any uncertainty in the correction value applied.

Random Error

When repeated measurements are made under fixed operating conditions, random errors manifest themselves as scatter of the measured data. Random error⁴ is introduced through the repeatability and resolution of the measurement system components, calibration, and measurement procedure and technique; by the measured variable's own temporal and spatial variations; and by the variations in the process operating and environmental conditions from which measurements are taken.

The estimate of the probable range of a random error is given by its random uncertainty. The *random standard uncertainty*, $s_{\bar{x}}$, is defined by the interval given by $\pm s_{\bar{x}}$, where

$$s_{\bar{x}} = s_x / \sqrt{N} \quad (5.5)$$

³ Smith and Wenhofer (3) provide examples for determining jet engine thrust, and several complementary measurements are used with an energy balance to estimate the uncertainty assigned to the systematic error.

⁴ This error was called a “precision” error in engineering documents prior to the 1990s.

with degrees of freedom $v = N - 1$ and assuming the errors are normally distributed.⁵ The interval has a confidence level of one standard deviation, equivalent to a probability of 68% for a population of x having a normal distribution. The *random uncertainty* at a desired confidence level is defined by the interval $\pm t_{v,P} s_{\bar{x}}$, where t is found from Table 4.4.

5.6 UNCERTAINTY ANALYSIS: ERROR PROPAGATION

Suppose we want to determine how long it would take to fill a swimming pool from a garden hose. One way is to measure the time required to fill a bucket of known volume to estimate the flow rate from the garden hose. Armed with a measurement of the volume of the pool, we can calculate the time to fill the pool. Clearly, small errors in estimating the flow rate from the garden hose would translate into large differences in the time required to fill the pool! Here we are using measured values, the flow rate and volume, to estimate a result, the time required to fill the pool.

Very often in engineering, results are determined through a functional relationship with measured values. For example, we just calculated a flow rate above by measuring time, t , and bucket volume, \forall , since $Q = f(t, \forall) = \forall/t$. But how do uncertainties in either measured quantity contribute to uncertainty in flow rate? Is the uncertainty in Q more sensitive to uncertainty in volume or in time? More generally, how are uncertainties in variables propagated to a calculated result? We now explore these questions.

Propagation of Error

A general relationship between some dependent variable y and a measured variable x , that is, $y = f(x)$, is illustrated in Figure 5.3. Now suppose we measure x a number of times at some operating condition so as to establish its sample mean value and the uncertainty due to random error in this mean value, $t_{v,P} s_{\bar{x}}$, which for convenience we write simply as $ts_{\bar{x}}$. This implies that, neglecting other random and systematic errors, the true value for x lies somewhere within the interval $\bar{x} \pm ts_{\bar{x}}$. It is reasonable to assume that the true value of y , which is determined from the measured values of x , falls within the interval defined by

$$\bar{y} \pm \delta y = f(\bar{x} \pm ts_{\bar{x}}) \quad (5.6)$$

Expanding this as a Taylor series yields

$$\bar{y} \pm \delta y = f(\bar{x}) \pm \left[\left(\frac{dy}{dx} \right)_{x=\bar{x}} ts_{\bar{x}} + \frac{1}{2} \left(\frac{d^2y}{dx^2} \right)_{x=\bar{x}} (ts_{\bar{x}})^2 + \dots \right] \quad (5.7)$$

By inspection, the mean value for y must be $f(\bar{x})$ so that the term in brackets estimates $\pm \delta y$. A linear approximation for δy can be made, which is valid when $ts_{\bar{x}}$ is small and neglects the higher order terms in Equation 5.7, as

$$\delta y \approx \left(\frac{dy}{dx} \right)_{x=\bar{x}} ts_{\bar{x}} \quad (5.8)$$

The derivative term, $(dy/dx)_{x=\bar{x}}$, defines the slope of a line that passes through the point specified by \bar{x} . For small deviations from the value of \bar{x} , this slope predicts an acceptable, approximate

⁵The estimate of standard uncertainty when estimated from a rectangular distribution (11) is $(b - a)/\sqrt{12}$, where b and a were defined in Table 4.2. The probability is about 58%.

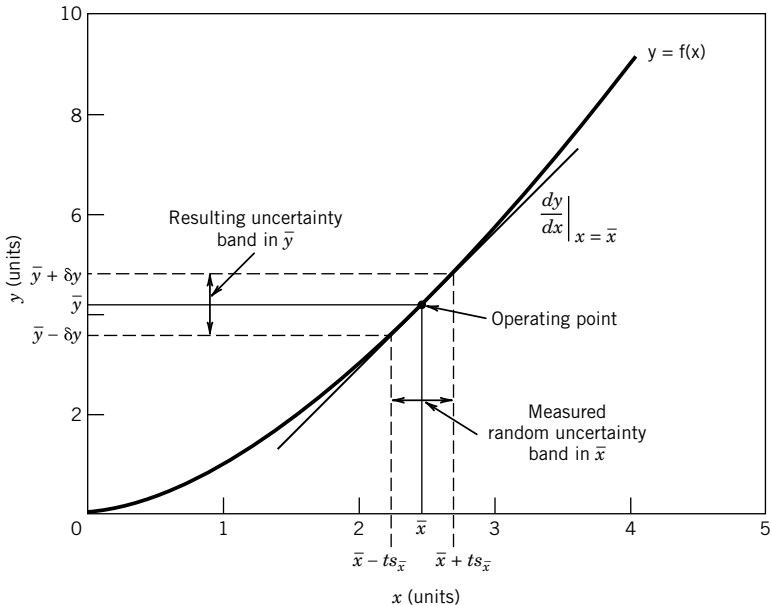


Figure 5.3 Relationship between a measured variable and a resultant calculated using the value of that variable.

relationship between $ts_{\bar{x}}$ and δy . The derivative term is a measure of the sensitivity of y to changes in x . Since the slope of the curve can be different for different values of x , it is important to evaluate the slope using a representative value of x . The width of the interval defined by $\pm ts_{\bar{x}}$ corresponds to $\pm \delta y$, within which we should expect the true value of y to lie. Figure 5.3 illustrates the concept that errors in a measured variable are propagated through to a resultant variable in a predictable way. In general, we apply this analysis to the errors that contribute to the uncertainty in x , written as u_x . The uncertainty in x is related to the uncertainty in the resultant y by

$$u_y = \left(\frac{dy}{dx} \right)_{x=\bar{x}} u_x \quad (5.9)$$

Compare the similarities between Equations 5.8 and 5.9 and in Figure 5.3.

This idea can be extended to multivariable relationships. Consider a result R , which is determined through some functional relationship between independent variables x_1, x_2, \dots, x_L defined by

$$R = f_1\{x_1, x_2, \dots, x_L\} \quad (5.10)$$

where L is the number of independent variables involved. Each variable contains some measure of uncertainty that affects the result. The best estimate of the true mean value R' would be stated as

$$R' = \bar{R} \pm u_R \quad (\text{P}\%) \quad (5.11)$$

where the sample mean of R is found from

$$\bar{R} = f_1\{\bar{x}_1, \bar{x}_2, \dots, \bar{x}_L\} \quad (5.12)$$

and the uncertainty in \bar{R} is found from

$$u_R = f_1 \{ u_{\bar{x}_1}, u_{\bar{x}_2}, \dots, u_{\bar{x}_L} \} \quad (5.13)$$

In Equation 5.13, each $u_{\bar{x}_i}$, $i = 1, 2, \dots, L$ represents the uncertainty associated with the best estimate of x_1 and so forth through x_L . The value of u_R reflects the contributions of the individual uncertainties as they are propagated through to the result.

A general sensitivity index, θ_i , results from the Taylor series expansion, Equation 5.9, and the functional relation of Equation 5.10 and is given by

$$\theta_i = \frac{\partial R}{\partial x_i}_{x=\bar{x}} \quad i = 1, 2, \dots, L \quad (5.14)$$

The sensitivity index relates how changes in each x_i affect R . Equation 5.14 can also be estimated numerically using finite differencing methods (5), which can be easily done within a spreadsheet or symbolic software package. The index is evaluated using either the mean values or, lacking these estimates, the expected nominal values of the variables.

The contribution of the uncertainty in x to the result R is estimated by the term $\theta_i u_{\bar{x}_i}$. The most probable estimate of u_R is generally accepted as that value given by the second power relation (4), which is the square root of the sum of the squares (RSS). The propagation of uncertainty in the variables to the result is by

$$u_R = \left[\sum_{i=1}^L (\theta_i u_{\bar{x}_i})^2 \right]^{1/2} \quad (5.15)$$

Sequential Perturbation

A numerical approach can also be used to estimate the propagation of uncertainty through to a result that circumvents the direct differentiation of the functional relations (6). The approach is handy to reduce data already stored in discrete form.

The method uses a finite difference method to approximate the derivatives:

1. Based on measurements for the independent variables under some fixed operating condition, calculate a result R_o where $R_o = f(x_1, x_2, \dots, x_L)$. This value fixes the operating point for the numerical approximation (e.g., see Fig. 5.3).
2. Increase the independent variables by their respective uncertainties and recalculate the result based on each of these new values. Call these values R_i^+ . That is,

$$\begin{aligned} R_1^+ &= f(x_1 + u_{x1}, x_2, \dots, x_L), \\ R_2^+ &= f(x_1, x_2 + u_{x2}, \dots, x_L), \dots \\ R_L^+ &= f(x_1, x_2, \dots, x_L + u_{xL}), \end{aligned} \quad (5.16)$$

3. In a similar manner, decrease the independent variables by their respective uncertainties and recalculate the result based on each of these new values. Call these values R_i^- .
4. Calculate the differences δR_i^+ and δR_i^- for $i = 1, 2, \dots, L$

$$\begin{aligned} \delta R_i^+ &= R_i^+ - R_o \\ \delta R_i^- &= R_i^- - R_o \end{aligned} \quad (5.17)$$

5. Evaluate the approximation of the uncertainty contribution from each variable,

$$\delta R_i = \frac{\delta R_i^+ - \delta R_i^-}{2} \approx \theta_i u_i \quad (5.18)$$

Then, the uncertainty in the result is

$$u_R = \left[\sum_{i=1}^L (\delta R_i)^2 \right]^{1/2} \quad (5.19)$$

Equations 5.15 and 5.19 provide two methods for estimating the propagation of uncertainty to a result. In most cases, each equation yields nearly the identical result and the choice of method is left to the user. The method can also be used to estimate just the sensitivity index of Equation 5.14 (2). In this case, steps 2 and 3 would apply a small deviation value, typically 1% of the nominal value of the variable, used in place of the actual uncertainty to estimate the derivative (5).

We point out that sometimes either method may calculate unreasonable estimates of u_R . When this happens the cause can be traced to a sensitivity index that changes rapidly with small changes in the independent variable x_i coupled with a large value of the uncertainty u_{x_i} . This occurs when the operating point is close to an minima or maxima inflection in the functional relationship. In these situations, the engineer should examine the cause and extent of the variation in sensitivity and use a more accurate approximation for the sensitivity, including using the higher order terms in the Taylor series of Equation 5.7.

In subsequent sections, we develop methods to estimate the uncertainty values from available information.

Example 5.3

For a displacement transducer having the calibration curve, $y = KE$, estimate the uncertainty in displacement y for $E = 5.00$ V, if $K = 10.10$ mm/V with $u_K = \pm 0.10$ mm/V and $u_E = \pm 0.01$ V at 95% confidence.

KNOWN $y = KE$
 $E = 5.00$ V $u_E = 0.01$ V
 $K = 10.10$ mm/V $u_K = 0.10$ mm/V

FIND u_y

SOLUTION Based on Equations 5.12 and 5.13, respectively,

$$\bar{y} = f(\bar{E}, \bar{K}) \quad \text{and} \quad u_y = f(u_E, u_K)$$

From Equation 5.15, the uncertainty in the displacement at $y = KE$ is

$$u_y = \left[(\theta_E u_E)^2 + (\theta_K u_K)^2 \right]^{1/2}$$

where the sensitivity indices are evaluated from Equation 5.14 as

$$\theta_E = \frac{\partial y}{\partial E} = K \quad \text{and} \quad \theta_K = \frac{\partial y}{\partial K} = E$$

or we can write Equation 5.15 as

$$u_y = \left[(K u_E)^2 + (E u_K)^2 \right]^{1/2}$$

The operating point occurs at the nominal or the mean values of $E = 5.00$ V and $y = 50.50$ mm. With $E = 5.00$ V and $K = 10.10$ mm/V and substituting for u_E and u_K , evaluate u_y at its operating point:

$$u_y|_{y=50.5} = \left[(0.10)^2 + (0.50)^2 \right]^{1/2} = 0.51 \text{ mm}$$

Alternatively, we can use sequential perturbation. The operating point for the perturbation is again $y = R_o = 50.5$ mm. Using Equations 5.16 through 5.18 gives

i	x_i	R_i^+	R_i^-	δR_i^+	δR_i^-	δR_i
1	E	50.60	50.40	0.10	-0.10	0.10
2	K	51.00	50.00	0.50	-0.50	0.50

Then, using Equation 5.19,

$$u_y|_{y=50.5} = \left[(0.10)^2 + (0.50)^2 \right]^{1/2} = 0.51 \text{ mm}$$

The two methods give the identical result. We state the calculated displacement in the form of Equation 5.11 as

$$y' = 50.50 \pm 0.51 \text{ mm} \quad (95\%)$$

Monte Carlo Method

A Monte Carlo simulation provides another effective way to estimate the propagation of the uncertainties in the independent variables to the uncertainty in a result. As presented in Chapter 4, the outcomes of a converged Monte Carlo simulation are the statistics of the predicted population in a result R (i.e., \bar{x} , s_x , $s_{\bar{x}}$) from which we calculate the random uncertainty in the result.

Generally, convergence is claimed when the computed standard deviation no longer changes by 1% to 5%. As one test for convergence, we define a numerical tolerance Δ , as being one-half of the least significant digit of the estimated standard uncertainty ($s_{\bar{x}}$),

$$\Delta = \frac{1}{2} LSD \quad (5.20)$$

For example, if the estimate of $s_{\bar{x}}$ is 2 units, then $\Delta = 0.5$ units (i.e., $1/2$ of the 10^0 digit); if $s_{\bar{x}}$ is 0.2 units, then $\Delta = 0.05$ units. The Monte Carlo simulation is converged when $2s_x < \Delta$ (7).

5.7 ADVANCED-STAGE UNCERTAINTY ANALYSIS

In designing a measurement system, a pertinent question is, How would it affect the result if this particular aspect of the technique or equipment were changed? In design-stage uncertainty analysis, we only considered the errors due to a measurement system's resolution and estimated instrument

calibration errors. But if additional information is available, we can get a better idea of the uncertainty in a measurement. So, an advanced-stage uncertainty analysis permits taking design-stage analysis further by considering procedural and test control errors that affect the measurement. We consider it as a method for a thorough uncertainty analysis when a large data set is not available. This is often the case in the early stages of a test program or for certain tests where repeating measurements may not be possible. Such an advanced-stage analysis, also known as *single-measurement uncertainty analysis* (3, 6), can be used: (1) in the advanced design stage of a test to estimate the expected uncertainty, beyond the initial design stage estimate; and (2) to report the results of a test program that involved measurements over a range of one or more parameters but with no or relatively few repeated measurements of the pertinent variables at each test condition. Essentially, the method assesses different aspects of the main test by quantifying potential errors through various well focused verification tests.

In this section, the goals are either to estimate the uncertainty in some measured value x or in some general result R through an estimation of the uncertainty in each of the factors that may affect x or R . We present a technique that uses a step-by-step approach for identifying and estimating the uncertainty associated with errors. We seek the combined value of the estimates at each step. We assume that the errors follow a normal distribution, but some errors might be better described by other distributions and these can be used. For example, calibration errors that specify only a range or operating condition errors that are related to establishing a controlled set point are well modeled by a rectangular distribution. The standard uncertainty for a rectangular distribution defined by the interval $(b - a)$ is given by

$$u_x = (b - a)/\sqrt{12} \quad (5.21)$$

which covers a 58% confidence level. Multiplying by 2 provides for two standard deviations coverage. If we assume that the errors propagate to the result with a normal distribution, then a coverage factor of 2 approximates the 95% confidence level for consistency.

Zero-Order Uncertainty

At zero-order uncertainty, all variables and parameters that affect the outcome of the measurement, including time, are assumed to be fixed except for the physical act of observation itself. Under such circumstances, any data scatter introduced upon repeated observations of the output value is the result of instrument resolution alone. The value u_0 estimates the extent of variation expected in the measured value when all influencing effects are controlled and is found using Equation 5.1. By itself, a zero-order uncertainty is inadequate for the reporting of test results.

Higher-Order Uncertainty

Higher-order uncertainty estimates consider the controllability of the test operating conditions and the variability of all measured variables. For example, at the first-order level, the effect of time as an extraneous variable in the measurement might be considered. That is, what would happen if we started the test, set the operating conditions, and sat back and watched? If a variation in the measured value is observed, then time is a factor in the test, presumably due to some extraneous influence affecting process control or simply inherent in the behavior of the variable being measured.

In practice, the uncertainty at this first level would be evaluated for each particular measured variable by operating the test facility at some single operating condition that would be within the

range of conditions to be used during the actual tests. A set of data (say, $N \geq 30$) would be obtained under some set operating condition. The first-order uncertainty of our ability to estimate the true value of a measured value could be estimated as

$$u_1 = t_{v,P} s_{\bar{x}} \quad (5.22)$$

The uncertainty at u_1 includes the effects of resolution, u_o . So only when $u_1 = u_0$ is time not a factor in the test. In itself, the first-order uncertainty is inadequate for reporting of test results.

With each successive order, another factor identified as affecting the measured value is introduced into the analysis, thus giving a higher but more realistic estimate of the uncertainty. For example, at the second level it might be appropriate to assess the limits of the ability to duplicate the exact operating conditions and the consequences on the test outcome. Or perhaps spatial variations that affect the outcome are assessed, such as when a value from a point measurement is assigned to quantify a larger volume. These are a series of verification tests conducted to assess causality.

Nth-Order Uncertainty

At the N th-order estimate, instrument calibration characteristics are entered into the scheme through the instrument uncertainty u_c . A practical estimate of the N th-order uncertainty u_N is given by

$$u_N = \left[u_c^2 + \left(\sum_{i=1}^{N-1} u_i^2 \right) \right]^{1/2} \quad (P\%) \quad (5.23)$$

Uncertainty estimates at the N th order allow for the direct comparison between results of similar tests obtained either using different instruments or at different test facilities. The procedure for a single-measurement analysis is outlined in Figure 5.4.

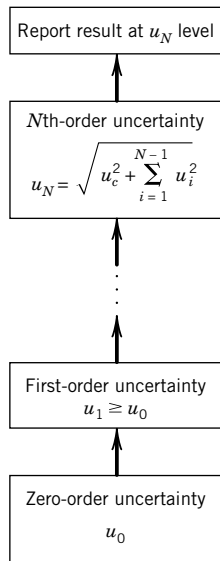


Figure 5.4 Advanced-stage and single-measurement uncertainty procedure in combining uncertainties.

Note that as a minimum, design-stage analysis includes only the effects found as a result of u_0 and u_c . It is those in-between levels that allow measurement procedure and control effects to be considered in the uncertainty analysis scheme. The N th-order uncertainty estimate provides the uncertainty value sought in advanced design stage or in single-measurement analyses. It is an appropriate value to be used to report the results from single-measurement tests.

Example 5.4

As an exercise, obtain and examine a dial oven thermometer. How would you assess the zero- and first-order uncertainty in the measurement of the temperature of a kitchen oven using the device?

KNOWN Dial thermometer

ASSUMPTION Negligible systematic error in the instrument

FIND Estimate u_0 and u_1 in oven temperature

SOLUTION The zero-order uncertainty would be that contributed by the resolution error of the measurement system only. For example, most gauges of this type have a resolution of 10°C . So from Equation 5.1 we estimate

$$u_0 = 5^\circ\text{C}$$

At the first order, the uncertainty would be affected by any time variation in the measured value (temperature) and variations in the operating conditions. If we placed the thermometer in the center of an oven, set the oven to some relevant temperature, allowed the oven to preheat to a steady condition, and then proceeded to record the temperature indicated by the thermometer at random intervals, we could estimate our ability to control the oven temperature. For J measurements, the first-order uncertainty of the measurement in this oven's mean temperature using this technique and this instrument would be, from Equation 5.22,

$$u_1 = t_{J-1,95} s_{\bar{T}}$$

COMMENT We could continue these verification tests. Let's suppose we are interested in how accurately we could set the oven mean temperature. Then the idea of setting the operating condition, the temperature, becomes important. We could estimate our ability to repeatedly set the oven to a desired mean temperature (time-averaged temperature). This could be done by changing the oven setting and then resetting the thermostat back to the original operating setting. If we were to repeat this sequence M times (reset thermostat, measure a set of data, reset thermostat, etc.), we could compute u_1 by

$$u_1 = t_{M(J-1),95} \langle s_{\bar{T}} \rangle$$

Note that now the variation in oven temperature with time at any setting is included in the pooled estimate. The effects of instrument calibration would enter at the N th order through u_c . The uncertainty in oven temperature at some setting would be well approximated by the estimate from Equation 5.23:

$$u_N = (u_1^2 + u_c^2)^{1/2}$$

By inspection of u_0 , u_c , and u_i , where $i = 1, 2, \dots, N - 1$, single-measurement analysis provides a capability to pinpoint those aspects of a test that contribute most to the overall uncertainty in the measurement, as well as a reasonable estimate of the uncertainty in a single measurement.

Example 5.5

A stopwatch is to be used to estimate the time between the start and end of an event. Event duration might range from several seconds to 10 minutes. Estimate the probable uncertainty in a time estimate using a hand-operated stopwatch that claims an accuracy of 1 min/month (95%) and a resolution of 0.01 s.

$$\text{KNOWN } u_o = 0.005 \text{ s} \quad (95\%)$$

$$u_c = 60 \text{ s/month} \quad (95\% \text{ assumed})$$

$$\text{FIND } u_d, u_N$$

SOLUTION The design-stage uncertainty gives an estimate of the suitability of an instrument for a measurement. At 60 s/month, the instrument accuracy works out to about 0.01 s/10 min of operation. This gives a design-stage uncertainty of

$$u_d = (u_o^2 + u_c^2)^{1/2} = \pm 0.01 \text{ s} \quad (95\%)$$

for an event lasting 10 minutes versus ± 0.005 s (95%) for an event lasting 10 s. Note that instrument calibration error controls the longer duration measurement, whereas instrument resolution controls the short duration measurement.

But do instrument resolution and calibration error actually control the uncertainty in this measurement? The design-stage analysis does not include the data-acquisition error involved in the act of physically turning the watch on and off. But a first-order analysis might be run to estimate the uncertainty that enters through the procedure of using the watch. Suppose a typical trial run of 20 tries of simply turning a watch on and off suggests that the uncertainty in determining the duration of an occurrence is

$$u_1 = t_{v,p} s_{\bar{x}} = 0.05 \text{ s}$$

The uncertainty in measuring the duration of an event would then be better estimated by the N th-order uncertainty of Equation 5.23,

$$u_N = (u_1^2 + u_c^2)^{1/2} = \pm 0.05 \text{ s} \quad (95\%)$$

This estimate holds for periods of up to about two hours. Clearly, procedure controls the uncertainty, not the watch. This uncertainty estimate could be further improved by considering how well the operator can synchronize the watch action with the start and finish-line action.

Example 5.6

A flow meter can be calibrated by providing a known flow rate through the meter and measuring the meter output. One method of calibration with liquid systems is the use of a catch and time technique whereby a volume of liquid, after passing through the meter, is diverted to a tank for a measured period of time from which the flow rate volume/time, is computed. There are two procedures that can be used to determine the known flow rate Q in, say, ft^3/min :

1. The volume of liquid, V , caught in known time t can be measured.

Suppose we arbitrarily set $t = 6$ s and assume that our available facilities can determine volume (at N th order) to 0.001 ft^3 . Note: The chosen time value depends on how much liquid we can accommodate in the tank.

2. The time t required to collect 1 ft^3 of liquid can be measured.

Suppose we determine an N th-order uncertainty in time of 0.15 s . In either case the same instruments are used. Determine which method is better to minimize uncertainty over a range of flow rates based on these preliminary estimates.

KNOWN $u_{\forall} = 0.001 \text{ ft}^3$

$$u_t = 0.15 \text{ s}$$

$$Q = f(\forall, t) = \forall/t$$

ASSUMPTIONS Flow diversion is instantaneous; 95% confidence levels.

FIND Preferred method

SOLUTION From the available information, the propagation of probable uncertainty to the result Q is estimated from Equation 5.15:

$$u_Q = \left[\left(\frac{\partial Q}{\partial \forall} u_{\forall} \right)^2 + \left(\frac{\partial Q}{\partial t} u_t \right)^2 \right]^{1/2}$$

By dividing through by Q , we obtain the relative (fractional percent) uncertainty in flow rate u_Q/Q

$$\frac{u_Q}{Q} = \left[\left(\frac{u_{\forall}}{\forall} \right)^2 + \left(\frac{u_t}{t} \right)^2 \right]^{1/2}$$

Representative values of Q are needed to solve this relation. Consider a range of flow rates, say, 1, 10, and $100 \text{ ft}^3/\text{min}$; the results are listed in the following table for both methods.

$Q (\text{ft}^3/\text{min})$	$t (\text{s})$	$\forall (\text{ft}^3)$	u_{\forall}/\forall	u_t/t	$\pm u_Q/Q$
Method 1					
1	6	0.1	0.01	0.025	0.027
10	6	1.0	0.001	0.025	0.025
100	6	10.0	0.0001	0.025	0.025
Method 2					
1	60.0	1.0	0.001	0.003	0.003
10	6.0	1.0	0.001	0.025	0.025
100	0.6	1.0	0.001	0.250	0.250

In method 1, it is clear the uncertainty in time contributes the most to the relative uncertainty in Q , provided that the flow diversion is instantaneous. But in method 2, uncertainty in measuring either time or volume can contribute more to the uncertainty in Q , depending on the time sample length. The results for both methods are compared in Figure 5.5. For the conditions selected and preliminary uncertainty values used, method 2 would be a better procedure for flow rates up to $10 \text{ ft}^3/\text{min}$. At higher flow rates, method 1 would be better. However, the minimum uncertainty in method 1 is limited to 2.5%. The engineer may be able to reduce this uncertainty by improvements in the time measurement procedure.

COMMENT These results are without consideration of some other elemental errors that are present in the experimental procedure. For example, the diversion of the flow may not to occur instantaneously. A first-order uncertainty estimate could be used to estimate the added uncertainty

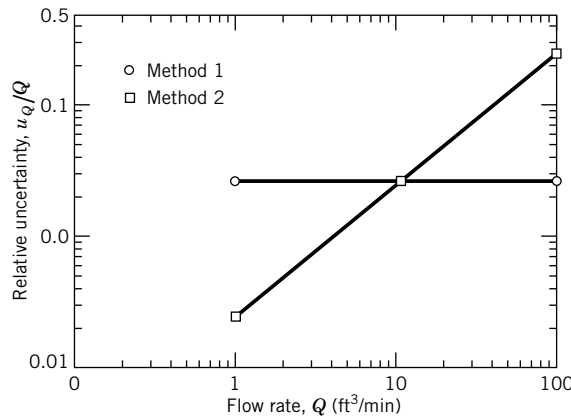


Figure 5.5 Uncertainty plot for the design analysis of Example 5.6.

to flow rate intrinsic to the time required to divert the liquid to and from the catch tank. If operator influence is a factor, it should be randomized in actual tests. Accordingly, the above calculations may be used as a guide in procedure selection.

Example 5.7

Repeat Example 5.6, using sequential perturbation for the operating conditions $\forall = 1 \text{ ft}^3$ and $t = 6 \text{ s}$.

SOLUTION The operating point is $R_o = Q = \forall/t = 0.1667 \text{ ft}^3/\text{s}$. Then, solving Equations 5.16 to 5.18 gives:

i	x_i	R_i^+	R_i^-	δR_i^+	δR_i^-	δR_i
1	\forall	0.1668	0.1665	0.000167	-0.000167	0.000167
2	t	0.1626	0.1709	-0.00407	0.00423	0.00415

Applying Equation 5.19 gives the uncertainty about this operating point

$$u_Q = [0.00415^2 + 0.000167^2]^{1/2} = \pm 4.15 \times 10^{-3} \text{ ft}^3/\text{s} \quad (95\%)$$

or

$$u_Q/Q = \pm 0.025 \quad (95\%)$$

COMMENT These last two examples give similar results for the uncertainty aside from insignificant differences due to round-off in the computations.

5.8 MULTIPLE-MEASUREMENT UNCERTAINTY ANALYSIS

This section develops a method for estimating the uncertainty in the value assigned to a variable based on a set of measurements obtained under fixed operating conditions. The method parallels the uncertainty standards approved by professional societies and by NIST in the United States (2, 7)

and is in harmony with international guidelines (1). The procedures assume that the errors follow a normal probability distribution, although the procedures are actually quite insensitive to deviations away from such behavior (4). Sufficient repetitions must be present in the measured data to assess random error; otherwise, some estimate of the magnitude of expected variation should be provided in the analysis.

Propagation of Elemental Errors

The procedures for multiple-measurement uncertainty analysis consist of the following steps:

- Identify the elemental errors in the measurement. As an aid, consider the errors in each of the three source groups (calibration, data acquisition, and data reduction).
- Estimate the magnitude of systematic and random error in each of the elemental errors.
- Calculate the uncertainty estimate for the result.

Considerable guidance can be obtained from Tables 5.1 to 5.3 for identifying the elemental errors. In multiple-measurement analysis, it is possible to divide the estimates for elemental errors into random and systematic uncertainties.

Consider the measurement of variable x , which is subject to elemental random errors each estimated by their random standard uncertainty, $(s_{\bar{x}})_k$, and systematic errors each estimated by their systematic standard uncertainty, $(b_{\bar{x}})_k$. Let subscript k , where $k = 1, 2, \dots, K$, refer to each of up to K elements of error e_k . A method to estimate the uncertainty in x based on the uncertainties in each of the elemental random and systematic errors is given below and outlined in Figure 5.6.

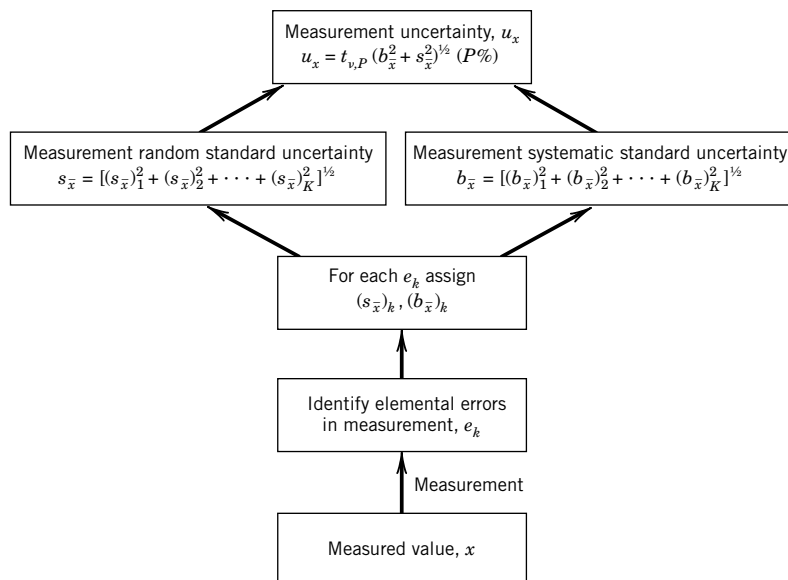


Figure 5.6 Multiple-measurement uncertainty procedure for combining uncertainties.

The *propagation of elemental random uncertainties* due to the K random errors in measuring x is given by the measurement random standard uncertainty, $s_{\bar{x}}$, as estimated by the RSS method of Equation 5.2:

$$s_{\bar{x}} = \left[(s_{\bar{x}})_1^2 + (s_{\bar{x}})_2^2 + \cdots + (s_{\bar{x}})_K^2 \right]^{1/2} \quad (5.24)$$

where each

$$(s_{\bar{x}})_k = s_{x_k} / \sqrt{N_k} \quad (5.25)$$

The *measurement random standard uncertainty* represents a basic measure of the uncertainty due to the known elemental errors affecting the variability of variable x at a one standard deviation confidence level. The degrees of freedom, v , in the standard random uncertainty, is estimated using the Welch–Satterthwaite formula (2):

$$v = \frac{\left(\sum_{k=1}^K (s_{\bar{x}}_k^2) \right)^2}{\sum_{k=1}^K (s_{\bar{x}}_k^4) / v_k} \quad (5.26)$$

where k refers to each elemental error with its own $v_k = N_k - 1$.

The *propagation of elemental systematic uncertainties* due to K systematic errors in measuring x is treated in a similar manner. The measurement systematic standard uncertainty, $b_{\bar{x}}$, is given by

$$b_{\bar{x}} = \left[(b_{\bar{x}})_1^2 + (b_{\bar{x}})_2^2 + \cdots + (b_{\bar{x}})_K^2 \right]^{1/2} \quad (5.27)$$

The *measurement systematic standard uncertainty*, $b_{\bar{x}}$, represents a basic measure of the uncertainty due to the elemental systematic errors that affect the measurement of variable x at a one standard deviation confidence level.

The *combined standard uncertainty in x* is reported as a combination of the systematic standard uncertainty and random standard uncertainty in x at a one standard deviation confidence level,

$$u_x = (b_{\bar{x}}^2 + s_{\bar{x}}^2)^{1/2} \quad (5.28)$$

For a normal distribution, this confidence interval is equivalent to a 68% probability level. A more general form of this equation extends it to include the total uncertainty at other confidence levels through the use of an appropriate t value as

$$u_x = t_{v,P} (b_{\bar{x}}^2 + s_{\bar{x}}^2)^{1/2} \quad (P\%) \quad (5.29)$$

In this form, the equation is called the *expanded uncertainty* in x at the reported confidence level (1, 2). The degrees of freedom in Equation 5.29 is found by (2)

$$v = \frac{\left(\sum_{k=1}^K (s_{\bar{x}}_k^2) + (b_{\bar{x}}_k^2) \right)^2}{\sum_{k=1}^K (s_{\bar{x}}_k^4) / v_k + \sum_{k=1}^K (b_{\bar{x}}_k^4) / v_k} \quad (5.30)$$

The degrees of freedom in an uncertainty are calculated from measurements or prior information; otherwise the degrees of freedom may be assumed to be large ($v > 30$ in Table 4.4). Reference 1

provides guidance on assigning a value for ν associated with judgment estimates of uncertainty. When the degrees of freedoms in the systematic uncertainties are large, the second term in the denominator of Equation 5.30 is small. For a 95% confidence level with large degrees of freedom, t of 1.96 is assigned in Equation 5.29. This value can be conveniently rounded off to $t = 2$ (i.e., two standard deviations) (2).

Reference 1 prefers not to assign a probability level to an uncertainty statement but rather to associate a value of the one, two, or three standard deviations, such as we do above for the standard uncertainties. This accommodates different distribution functions and their respective probability coverage in the expanded uncertainty interval. This reflects a difference between the two standards (1, 2) and either approach is acceptable.

Example 5.8

Ten repeated measurements of force F are made over time under fixed operating conditions. The data are listed below. Estimate the random standard uncertainty due to the elemental error in estimating the true mean value of the force based on the limited data set.

N	F [N]	N	F [N]
1	123.2	6	119.8
2	115.6	7	117.5
3	117.1	8	120.6
4	125.7	9	118.8
5	121.1	10	121.9

KNOWN Measured data set $N = 10$

FIND Estimate $s_{\bar{F}}$

SOLUTION The mean value of the force based on this finite data set is computed to be $\bar{F} = 120.13$ N. A random error is associated with assigning the sample mean value as the true value of force because of the small data set. This error enters the measurement during data acquisition (Table 5.2). The random standard uncertainty in this elemental error is computed through the standard deviation of the means, Equation 5.5:

$$s_{\bar{F}} = \frac{s_F}{\sqrt{N}} = \frac{3.04}{\sqrt{10}} = 0.96 \text{ N} \quad \text{with } \nu = 9$$

COMMENT (1) The uncertainty due to data scatter here could be classified as being due to a temporal variation error (i.e., variation with time under fixed conditions) as noted in Table 5.2. (2) Report the uncertainty values with the same decimal significant figures as the mean value (1).

Example 5.9

The force measuring device of Example 5.1 was used in acquiring the data set of Example 5.8. Estimate the systematic uncertainty in the measurement instrument.

KNOWN $B_1 = 0.20 \text{ N}$ (95%)
 $B_2 = 0.30 \text{ N}$

ASSUMPTIONS Manufacturer specifications reliable at 95% probability

FIND B (95%)

SOLUTION Lacking information as to the statistics used to specify the uncertainty values associated with the two element errors, e_1 and e_2 , we consider them as systematic uncertainties stated at 95% confidence level. The systematic standard uncertainties are found from Equation 5.4 as $b = B/2$,

$$b_1 = B_1/2 = 0.10 \text{ N} \quad b_2 = B_2/2 = 0.15 \text{ N}$$

The systematic standard uncertainty in the transducer is

$$b = (b_1^2 + b_2^2)^{1/2} = 0.18 \text{ N}$$

at one standard deviation confidence. The expanded systematic uncertainty with $t_{v,95} = 2$ is

$$B = 2(b_1^2 + b_2^2)^{1/2} = 0.36 \text{ N}$$

Elemental errors due to instruments are considered to be data-acquisition source errors (Table 5.2). If these uncertainties were found during a calibrations by the end-user, then we could list them as calibration source errors. In the end, as long as they are accounted for, the error source grouping assigned is not important.

COMMENT Note that the estimate for expanded systematic error due to the instrument is equal in value to the estimate of u_c in a design-stage analysis. The resolution error uncertainty u_0 used in Example 5.1 is now built into the data scatter and so included as part of the random uncertainty estimate in Example 5.8.

Example 5.10

In Examples 4.8 and 4.9, a set of measured data were used to generate a polynomial curve fit equation between variables x and y . If during a test, variable x were to be measured and y computed from x through the polynomial, estimate the random standard uncertainty due to the data-reduction error in the curve fit.

KNOWN Data set of Example 4.8
Polynomial fit of Example 4.9

ASSUMPTIONS Data fits curve $y = 1.04x + 0.02$.

FIND Random standard uncertainty in the curve fit

SOLUTION The curve fit was found to be given by $y = 1.04x + 0.02$ with a standard error of the fit, $s_{yx} = 0.16$ based on the approximation of Equation 4.38. The standard random uncertainty due to the curve fit, written as $(s_{\bar{x}})_1$ to be consistent with Table 5.3, is

$$(s_{\bar{x}})_1 = s_{yx}/\sqrt{N} = 0.072 \text{ V} \quad \text{with } v = 3$$

The expanded random uncertainty interval with $t_{3,95} = 3.18$ is $t_{3,95}(s_{\bar{x}})_1 = 0.23 \text{ V}$.

Example 5.11

The measurement of x contains three elemental random errors from data acquisition. Each elemental error is assigned a random standard uncertainty as follows:

$$(s_{\bar{x}})_1 = 0.60 \text{ units}, v_1 = 29$$

$$(s_{\bar{x}})_2 = 0.80 \text{ units}, v_2 = 9$$

$$(s_{\bar{x}})_3 = 1.10 \text{ units}, v_3 = 19$$

Assign the random standard uncertainty due to these data-acquisition errors.

KNOWN $(s_{\bar{x}})_k$ with $k = 1, 2, 3$

FIND $s_{\bar{x}}$

SOLUTION The random standard uncertainty due to data-acquisition errors is

$$s_{\bar{x}} = \left[(s_{\bar{x}})_1^2 + (s_{\bar{x}})_2^2 + (s_{\bar{x}})_3^2 \right]^{1/2} = (0.60^2 + 0.80^2 + 1.10^2)^{1/2} = 1.49 \text{ units}$$

at one standard deviation confidence and with degrees of freedom

$$v = \frac{\left(\sum_{k=1}^3 (s_{\bar{x}})_k^2 \right)^2}{\sum_{k=1}^3 (s_{\bar{x}})_k^4 / v_k} = \frac{(0.6^2 + 0.8^2 + 1.1^2)^2}{(0.6^4/29) + (0.8^4/9) + (1.1^4/19)} = 38.8 \approx 39$$

Example 5.12

In reporting the results of an experiment to measure stress in a loaded beam, an uncertainty analysis identifies three elemental errors in the stress measurement having the following values of uncertainty:

$$(b_{\bar{\sigma}})_1 = 0.5 \text{ N/cm}^2 \quad (b_{\bar{\sigma}})_2 = 1.05 \text{ N/cm}^2 \quad (b_{\bar{\sigma}})_3 = 0 \text{ N/cm}^2$$

$$(s_{\bar{\sigma}})_1 = 4.6 \text{ N/cm}^2, v_1 = 14 \quad (s_{\bar{\sigma}})_2 = 10.3 \text{ N/cm}^2, v_2 = 37 \quad (s_{\bar{\sigma}})_3 = 1.2 \text{ N/cm}^2, v_3 = 8$$

where the degrees of freedom in the systematic uncertainties are very large. If the mean value of the stress in the measurement is $\bar{\sigma} = 223.4 \text{ N/cm}^2$, determine the best estimate of the stress at a 95% confidence level, assuming all errors are accounted for.

KNOWN Experimental errors with assigned uncertainties

ASSUMPTIONS All elemental errors ($K = 3$) have been included.

FIND $\bar{\sigma} \pm u_{\sigma} (95\%)$

SOLUTION We seek values for the statement, $\sigma' = \bar{\sigma} \pm u_{\sigma}(95\%)$, given that $\bar{\sigma} = 223.4 \text{ N/cm}^2$. The measurement random standard uncertainty is

$$s_{\bar{\sigma}} = \left[(s_{\bar{\sigma}})_1^2 + (s_{\bar{\sigma}})_2^2 + (s_{\bar{\sigma}})_3^2 \right]^{1/2} = 11.3 \text{ N/cm}^2$$

The measurement systematic standard uncertainty is

$$b_{\bar{\sigma}} = \left[(b_{\bar{\sigma}})_1^2 + (b_{\bar{\sigma}})_2^2 + (b_{\bar{\sigma}})_3^2 \right]^{1/2} = 1.16 \text{ N/cm}^2$$

The combined standard uncertainty is

$$u_{\sigma} = (b_{\bar{\sigma}}^2 + s_{\bar{x}}^2)^{1/2} = 11.4 \text{ N/cm}^2$$

The expanded uncertainty requires the combined degrees of freedom. The degrees of freedom is calculated to be

$$v = \frac{\left(\sum_{k=1}^K (s_{\bar{x}}^2)_k + (b_{\bar{x}}^2)_k \right)^2}{\sum_{k=1}^K (s_{\bar{x}}^4)_k / v_k + \sum_{k=1}^K (b_{\bar{x}}^4)_k / v_k} = 49$$

where the degrees of freedoms in the systematic uncertainties are assumed to be very large so that the second term in the denominator is essentially zero. Therefore, $t_{49,95} \sim 2$ and the expanded uncertainty is

$$\begin{aligned} u_{\sigma} &= 2[b_{\bar{\sigma}}^2 + s_{\bar{x}}^2]^{1/2} = 2[(1.2 \text{ N/cm}^2)^2 + (11.3 \text{ N/cm}^2)^2]^{1/2} \\ &= 22.7 \text{ N/cm}^2 \quad (95\%) \end{aligned}$$

The best estimate of the stress measurement is

$$\sigma' = 223.4 \pm 22.7 \text{ N/cm}^2 \quad (95\%)$$

Propagation of Uncertainty to a Result

Now consider the result R , which is determined through the functional relationship between the measured independent variables x_i , $i = 1, 2, \dots, L$ as defined by Equation 5.10. Again, L is the number of independent variables involved and each x_i has an associated systematic standard uncertainty $b_{\bar{x}}$, given by the measurement systematic standard uncertainty determined for that variable by Equation 5.27, and a measurement random standard uncertainty $s_{\bar{x}}$, determined using Equation 5.24. The best estimate of the true value R' is given as

$$R' = \bar{R} \pm u_R \quad (P\%) \tag{5.31}$$

where the mean value of the result is determined by

$$\bar{R} = f(\bar{x}_1, \bar{x}_2, \dots, \bar{x}_L) \tag{5.32}$$

and where the uncertainty in the result u_R is given by

$$u_R = f(b_{\bar{x}_1}, b_{\bar{x}_2}, \dots, b_{\bar{x}_L}; s_{\bar{x}_1}, s_{\bar{x}_2}, \dots, s_{\bar{x}_L}) \tag{5.33}$$

where subscripts x_1 through x_L refer to the measurement systematic uncertainties and measurement random uncertainties in each of these L variables.

The propagation of random uncertainty through the variables to the result gives the random standard uncertainty in the result

$$s_R = \left(\sum_{i=1}^L [\theta_i s_{\bar{x}_i}]^2 \right)^{1/2} \quad (5.34)$$

where θ_i is the sensitivity index as defined by Equation 5.14.

The degrees of freedom in the random uncertainty is estimated by the Welch–Satterthwaite formula

$$\nu_s = \frac{\left\{ \sum_{i=1}^L (\theta_i s_{\bar{x}_i})^2 \right\}^2}{\sum_{i=1}^L \left\{ (\theta_i s_{\bar{x}_i})^4 / \nu_{x_i} \right\}} \quad (5.35)$$

By propagation of the systematic standard uncertainties of the variables, the systematic standard uncertainty in the result is

$$b_R = \left(\sum_{i=1}^L [\theta_i b_{x_i}]^2 \right)^{1/2} \quad (5.36)$$

The terms $\theta_i s_{\bar{x}_i}$ and $\theta_i b_{x_i}$ represent the individual contributions of the i th variable to the uncertainty in R . Comparing the magnitudes of each individual contribution identifies the relative importance of the uncertainty terms on the result.

The *combined standard uncertainty in the result*, written as u_R , is

$$u_R = [b_R^2 + s_R^2]^{1/2} \quad (5.37)$$

with a confidence level of one standard deviation. The expanded uncertainty in the result is given as

$$u_R = t_{v,P} [b_R^2 + s_R^2]^{1/2} \quad (P\%) \quad (5.38)$$

The t value is used to provide a reasonable weight to the interval defined by the random uncertainty to achieve the desired confidence. If the degrees of freedom in each variable is large ($N \geq 30$), then a reasonable approximation is to take $t_{v,95} = 2$. When the degrees of freedom in each of the variables, x_i , is not the same, the Welch–Satterthwaite formula is used to estimate the degrees of freedom in the result expressed as

$$\nu_R = \frac{\left(\sum_{i=1}^L (\theta_i s_{\bar{x}_i})^2 + (\theta_i b_{\bar{x}_i})^2 \right)^2}{\sum_{i=1}^L \left(\theta_i s_{\bar{x}_i} \right)^4 / \nu_{s_i} + \sum_{i=1}^L \left(\theta_i b_{\bar{x}_i} \right)^4 / \nu_{b_i}} \quad (5.39)$$

When the individual degrees of freedom in each of the systematic uncertainties are very large, as is often the case, the second term in the denominator is essentially zero.

Example 5.13

The density of a gas, ρ , which follows the ideal gas equation of state, $\rho = p/RT$, is estimated through separate measurements of pressure p and temperature T . The gas is housed within a rigid impermeable vessel. The literature accompanying the pressure measurement system states an instrument uncertainty to within $\pm 1\%$ of the reading (95%), and that accompanying the temperature measuring system indicates $\pm 0.6^\circ\text{R}$ (95%) uncertainty. Twenty measurements of pressure, $N_p = 20$, and 10 measurements of temperature, $N_T = 10$, are made with the following statistical outcome:

$$\bar{p} = 2253.91 \text{ psfa} \quad s_p = 167.21 \text{ psfa}$$

$$\bar{T} = 560.4^\circ\text{R} \quad s_T = 3.0^\circ\text{R}$$

where psfa refers to lb/ft^2 absolute. Determine a best estimate of the density. The gas constant is $R = 54.7 \text{ ft-lb/lb}_m \cdot ^\circ\text{R}$.

KNOWN $\bar{p}, s_p, \bar{T}, s_T$

$$\rho = p/RT; R = 54.7 \text{ ft-lb/lb}_m \cdot ^\circ\text{R}$$

ASSUMPTIONS Gas behaves as an ideal gas.

FIND $\rho' = \bar{\rho} \pm u_\rho$ (95%)

SOLUTION The measurement objective is to determine the density of an ideal gas through temperature and pressure measurements. The independent and dependent variables are related through the ideal gas law, $\rho = p/RT$. The mean value of density is

$$\bar{\rho} = \frac{\bar{p}}{R\bar{T}} = 0.0735 \text{ lb}_m/\text{ft}^3$$

The next step must be to identify and estimate the errors and determine how they contribute to the uncertainty in the mean value of density. Since no calibrations are performed and the gas is considered to behave as an ideal gas in an exact manner, the measured values of pressure and temperature are subject only to elemental errors within the data-acquisition error source group (Table 5.2): instrument errors and temporal variation errors.

The tabulated value of the gas constant is not without error. However, estimating the possible error in a tabulated value is sometimes difficult. According to Kestin (8), the systematic uncertainty in the gas constant is on the order of $\pm(0.33 \text{ J/kg-K})/(\text{gas molecular weight})$ or $\pm 0.06 (\text{ft-lb/lb}_m \cdot ^\circ\text{R})/(\text{gas molecular weight})$. Since this yields a small value for a reasonable gas molecular weight, here we assume a zero (negligible) systematic error in the gas constant.

Consider the pressure measurement. The uncertainty assigned to the temporal variation (data scatter) error is based on the variation in the measured data obtained during presumably fixed operating conditions. The instrument error is assigned a systematic uncertainty based on the manufacturer's statement, which is assumed to be stated at 95% confidence:

$$(b_{\bar{p}})_1 = (B_{\bar{p}}/2)_1 = (0.01 \times 2253.51/2) = 11.28 \text{ psfa} \quad (s_{\bar{p}})_1 = 0$$

where the subscript keeps track of the error identity. The temporal variation causes a random uncertainty in establishing the mean value of pressure and is calculated as

$$(s_{\bar{p}})_2 = s_{\bar{p}} = \frac{s_p}{\sqrt{N}} = \frac{167.21 \text{ psfa}}{\sqrt{20}} = 37.39 \text{ psfa} \quad v_{s_p} = 19$$

and assigning no systematic uncertainty to this error gives

$$(b_{\bar{p}})_2 = 0$$

In a similar manner, we assign the uncertainty in the data-acquisition source error in temperature. The instrument errors are considered as systematic only and assigned a systematic uncertainty based on the manufacturer's statement as

$$(b_{\bar{T}})_1 = (b_{\bar{T}})_1 / 2 = 0.3^{\circ}\text{R} \quad (s_{\bar{T}})_1 = 0$$

The temporal variation causes a random uncertainty in establishing the mean value of temperature and this is calculated as

$$(s_{\bar{T}})_2 = s_{\bar{T}} = \frac{s_T}{\sqrt{N}} = \frac{3.0^{\circ}\text{R}}{\sqrt{10}} = 0.9^{\circ}\text{R} \quad v_{s_T} = 9$$

$$(b_{\bar{T}})_2 = 0$$

The uncertainties in pressure and temperature due to the data-acquisition source errors are combined using the RSS method,

$$b_{\bar{p}} = \left[(11.28)^2 + (0)^2 \right]^{1/2} = 11.28 \text{ psfa}$$

$$s_{\bar{p}} = \left[(0)^2 + (37.39)^2 \right]^{1/2} = 37.39 \text{ psfa}$$

similarly,

$$b_{\bar{T}} = 0.3^{\circ}\text{R}$$

$$s_{\bar{T}} = 0.9^{\circ}\text{R}$$

with degrees of freedom in the random standard uncertainties to be

$$(v)_{s_p} = N_p - 1 = 19$$

$$(v)_{s_T} = 9$$

The degrees of freedom in the systematic standard uncertainties, v_{b_T} and v_{b_p} , are assumed large.

The systematic and random standard uncertainties propagate through to the result, calculated about the operating point as established by the mean values for temperature and pressure. That is,

$$s_{\bar{p}} = \left[\left(\frac{\partial p}{\partial T} s_{\bar{T}} \right)^2 + \left(\frac{\partial p}{\partial p} s_{\bar{p}} \right)^2 \right]^{1/2}$$

$$= \left[(1.3 \times 10^{-4} \times 0.9)^2 + (3.26 \times 10^{-5} \times 37.39)^2 \right]^{1/2}$$

$$= 0.0012 \text{ lb}_m/\text{ft}^3$$

and

$$b_{\bar{p}} = \left[\left(\frac{\partial p}{\partial T} b_{\bar{T}} \right)^2 + \left(\frac{\partial p}{\partial p} b_{\bar{p}} \right)^2 \right]^{1/2}$$

$$= \left[(1.3 \times 10^{-4} \times 0.3)^2 + (3.26 \times 10^{-5} \times 11.28)^2 \right]^{1/2}$$

$$= 0.0004 \text{ lb}_m/\text{ft}^3$$

The degrees of freedom in the density calculation is determined to be

$$\nu = \frac{\left[\left(\frac{\partial \rho}{\partial T} s_T \right)^2 + \left(\frac{\partial \rho}{\partial p} s_p \right)^2 + \left(\frac{\partial \rho}{\partial b} b_T \right)^2 + \left(\frac{\partial \rho}{\partial b} b_p \right)^2 \right]^2}{\left[\left(\frac{\partial \rho}{\partial p} s_p \right)^4 / v_{s_p} + \left(\frac{\partial \rho}{\partial T} s_T \right)^4 / v_{s_T} \right] + \left[\left(\frac{\partial \rho}{\partial b} b_T \right)^4 / v_{b_T} + \left(\frac{\partial \rho}{\partial b} b_p \right)^4 / v_{b_p} \right]} = 23$$

The expanded uncertainty in the mean value of density, using $t_{23,95} = 2.06$, is

$$\begin{aligned} u_\rho &= t_{23,95} \left[b_p^2 + s_p^2 \right]^{1/2} = 2.06 \times [0.0004^2 + 0.0012^2]^{1/2} \\ &= 0.0026 \text{ lb}_m/\text{ft}^3 \quad (95\%) \end{aligned}$$

The best estimate of the density is reported as

$$\rho' = 0.0735 \pm 0.0026 \text{ lb}_m/\text{ft}^3 \quad (95\%)$$

This measurement of density has an uncertainty of about 3.4%.

COMMENT (1) We did not consider the uncertainty associated with our assumption of exact ideal gas behavior, a potential modeling error (see Table 5.3). (2) Note how pressure contributes more to either standard uncertainty than does temperature and that the systematic uncertainty is small compared to the random uncertainty. The uncertainty in density is best reduced by actions to reduce the effects of the random errors on the pressure measurements.

Example 5.14

Consider determining the mean diameter of a shaft using a hand-held micrometer. The shaft was manufactured on a lathe presumably to a constant diameter. Identify possible elements of error that can contribute to the uncertainty in the estimated mean diameter.

SOLUTION In the machining of the shaft, possible run-out during shaft rotation can bring about an eccentricity in the shaft cross-sectional diameter. Further, as the shaft is machined to size along its length, possible run-out along the shaft axis can bring about a difference in the machined diameter. To account for such deviations, the usual measurement procedure is to repeatedly measure the diameter at one location of the shaft, rotate the shaft, and repeatedly measure again. Then the micrometer is moved to a different location along the axis of the shaft and the above procedure repeated.

It is unusual to calibrate a micrometer within a working machine shop, although an occasional offset error check against accurate gauge blocks is normal procedure. Let us assume that the micrometer is used as is without calibration. Data-acquisition errors are introduced from at least several elements:

1. Since the micrometer is not calibrated, the reading during any measurement could be affected by a possible systematic error in the micrometer markings. This can be labeled as an uncertainty due to instrument error, b_1 (see Table 5.2). Experience shows that $2b_1$ is on the order of the resolution of the micrometer at 95% confidence.
2. The random uncertainty on repeated readings is affected by the resolution of the readout, eccentricity of the shaft, and the exact placement of the micrometer on any cross section along the shaft. It is not possible to separate these errors, so they are grouped as variation errors, with random standard uncertainty, s_2 . This value can be discerned from the statistics of the measurements made at any cross section (replication).

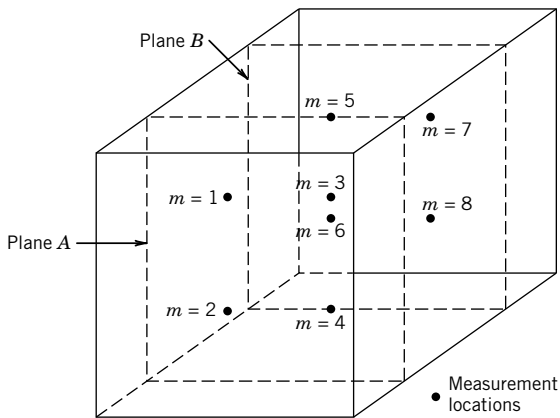


Figure 5.7 Measurement locations for Example 5.15.

- Similarly, spatial variations in the diameter along its length introduce scatter between the statistical values for each cross section. Since this affects the overall mean diameter, its effect must be accounted for. Label this error as a spatial error with random standard uncertainty, s_3 . It can be estimated by the pooled statistical standard deviation of the mean values at each measurement location (replication).

Example 5.15

The mean temperature in an oven is to be estimated by using the information obtained from a temperature probe. The manufacturer states an uncertainty of $\pm 0.6^\circ\text{C}$ (95%) for this probe. Determine the oven temperature.

The measurement process is defined such that the probe is to be positioned at several strategic locations within the oven. The measurement strategy is to make four measurements within each of two equally spaced cross-sectional planes of the oven. The positions are chosen so that each measurement location corresponds to the centroid of an area of value equal for all locations so that spatial variations in temperature throughout the oven are accounted for. The measurement locations within the cubical oven are shown in Figure 5.7. In this example, 10 measurements are made at each position, with the results given in Table 5.4. Assume that a temperature readout device with a resolution of 0.1°C is used.

KNOWN Data of Table 5.4

FIND $T' = \bar{T} \pm u_T$ (95%)

Table 5.4 Example 5.15: Oven Temperature Data, $N = 10$

Location	\bar{T}_m	s_{T_m}	Location	\bar{T}_m	s_{T_m}
1	342.1	1.1	5	345.2	0.9
2	344.2	0.8	6	344.8	1.2
3	343.5	1.3	7	345.6	1.2
4	343.7	1.0	8	345.9	1.1

$$\text{Note: } \bar{T}_m = \frac{1}{N} \sum_{n=1}^N T_{mn}; \quad s_{T_m} = \left[\frac{1}{N-1} \sum_{n=1}^N (T_{mn} - \bar{T}_m)^2 \right]^{1/2}$$

SOLUTION The mean values at each of the locations are averaged to yield a mean oven temperature using pooled averaging:

$$\langle \bar{T} \rangle = \frac{1}{8} \sum_{m=1}^8 \bar{T}_m = 344.4^\circ\text{C}$$

Elemental errors in this test are found in the data-acquisition group (Table 5.2) and due to (1) the temperature probe system (instrument error), (2) spatial variation errors, and (3) temporal variation errors. First, consider the elemental error in the probe system. The manufacturer statement of $\pm 0.6^\circ\text{C}$ is considered a systematic uncertainty at 95% confidence level. The standard uncertainties are assigned as

$$(b_{\bar{T}})_1 = 0.6/2 = 0.3^\circ\text{C} \quad (s_{\bar{T}})_1 = 0$$

Consider next the spatial error contribution to the estimate of the mean temperature \bar{T} . This error arises from the spatial nonuniformity in the oven temperature. An estimate of spatial temperature distribution within the oven can be made by examining the mean temperatures at each measured location. These temperatures show that the oven is not uniform in temperature. The mean temperatures within the oven show a standard deviation of

$$s_T = \sqrt{\frac{\sum_{m=1}^8 (\bar{T}_m - \langle \bar{T} \rangle)^2}{7}} = 1.26^\circ\text{C}$$

Thus, the random standard uncertainty of the oven mean temperature is found from $s_{\bar{T}}$ or

$$(s_{\bar{T}})_2 = \frac{s_T}{\sqrt{8}} = 0.45^\circ\text{C}$$

with degrees of freedom, $v = 7$. We do not assign a systematic uncertainty to this error, so $(b_{\bar{T}})_2 = 0$. One could reasonably argue that $(s_{\bar{T}})_2$ represents a systematic error because it is an effect that would offset the final value of the result. It does not affect the final uncertainty, but the awareness of its effect is part of the usefulness of an uncertainty analysis! This is a case where it becomes the test engineer's decision.

Time variations in probe output during each of the 10 measurements at each location cause data scatter, as evidenced by the respective s_{T_m} values. Such time variations are caused by random local temperature variations as measured by the probe, probe resolution, and oven temperature control variations during fixed operating conditions. We have insufficient information to separate these, so they are estimated together as a single error. The pooled standard deviation is

$$\langle s_T \rangle = \sqrt{\frac{\sum_{m=1}^8 \sum_{n=1}^{10} (\bar{T}_{mn} - \langle \bar{T} \rangle)^2}{M(N-1)}} = \sqrt{\frac{1}{M} \sum_{m=1}^M s_{T_m}^2} = 1.09^\circ\text{C}$$

to give a random standard uncertainty of

$$(s_{\bar{T}})_3 = \frac{\langle s_T \rangle}{\sqrt{80}} = 0.12^\circ\text{C}$$

with degrees of freedom, $v = 72$. We assign $(b_{\bar{T}})_3 = 0$.

The measurement systematic standard uncertainty is

$$b_{\bar{T}} = \left[(b_{\bar{T}})_1^2 + (b_{\bar{T}})_2^2 + (b_{\bar{T}})_3^2 \right]^{1/2} = 0.3^\circ\text{C}$$

and the measurement random standard uncertainty is

$$s_{\bar{T}} = \left[(s_{\bar{T}})_1^2 + (s_{\bar{T}})_2^2 + (s_{\bar{T}})_3^2 \right]^{1/2} = 0.46^\circ\text{C}$$

The degrees of freedom are found using Equation 5.30 giving $v = 17$, which assumes a large value for v_{b_T} .

The combined standard uncertainty in the mean oven temperature is

$$u_T = \left[b_{\bar{T}}^2 + s_{\bar{T}}^2 \right]^{1/2} = 0.55 \approx 0.6^\circ\text{C}$$

with a confidence level of one standard deviation. Assigning $t_{17,95} = 2.11$, the best estimate of the mean oven temperature is

$$T' = \bar{T} \pm t_{v,P} \left(b_{\bar{T}}^2 + s_{\bar{T}}^2 \right)^{1/2} = 344.4 \pm 1.2^\circ\text{C} \quad (95\%)$$

5.9 CORRECTION FOR CORRELATED ERRORS

So far, we have assumed that all of the different elements of error in a test are independent from the others. If two errors are not independent, they are “correlated.”

For example, when the same instrument is used to measure different variables, the instrument systematic errors between those variables are correlated. If multiple instruments are calibrated against the same standard, then the systematic uncertainty in the standard is passed to each instrument. Hence, these errors are correlated. The numerical effect of correlated errors on the uncertainty depends on the functional relationship between the variables and the magnitudes of the elemental systematic errors that are correlated. We now introduce a correction for treating the correlated systematic errors.

Consider the result R , which is determined through the functional relationship between the measured independent variables x_i , $i = 1, 2, \dots, L$ where L is the number of independent variables involved. Each x_i is subject to elemental systematic errors with standard uncertainties, b_k , where $k = 1, 2, \dots, K$, refer to each of up to any of K elements of error. Now allow that H of these K elemental errors are correlated between variables while the rest ($K - H$) are uncorrelated. When correlated errors are included, the systematic standard uncertainty in a result is estimated by

$$b_R = \left[\sum_{i=1}^L (\theta_i b_{\bar{x}_i})^2 + 2 \sum_{i=1}^{L-1} \sum_{j=i+1}^L \theta_i \theta_j b_{\bar{x}_i \bar{x}_j} \right]^{1/2} \quad (5.40)$$

where index j is a counter equal to $i + 1$ and with

$$\theta_i = \frac{\partial R}{\partial x_{i,x=\bar{x}}} \quad (5.14)$$

Equation 5.40 introduces the covariance, $b_{\bar{x}_i \bar{x}_j}$, to account for correlated errors and this is found from

$$b_{\bar{x}_i \bar{x}_j} = \sum_{h=1}^H (b_{\bar{x}_i})_h (b_{\bar{x}_j})_h \quad (5.41)$$

where H is the number of elemental errors that are correlated between variables x_i and x_j , and h is a counter for each correlated error. Note that Equation 5.40 reduces to Equation 5.36 when no errors are correlated (i.e., when $H=0$, $b_{\bar{x}_i \bar{x}_j} = 0$). References 2 and 9 discuss treatment of correlated systematic errors in extended detail.

Example 5.16

Suppose a result is a function of three variables, x_1 , x_2 , x_3 . There are four systematic errors associated with both x_1 and x_2 and five associated with x_3 . Only the first and second systematic elemental errors associated with the second and third variable (x_2 and x_3) are determined to be correlated because these errors arise from common sources. Express the systematic standard uncertainty in the result and find the covariance term.

SOLUTION Equation 5.40 is expanded to the form

$$b_R = \left[(\theta_1 b_{\bar{x}_1})^2 + (\theta_2 b_{\bar{x}_2})^2 + (\theta_3 b_{\bar{x}_3})^2 + 2\theta_1\theta_2 b_{\bar{x}_1 \bar{x}_2} + 2\theta_1\theta_3 b_{\bar{x}_1 \bar{x}_3} + 2\theta_2\theta_3 b_{\bar{x}_2 \bar{x}_3} \right]^{1/2}$$

For the two correlated errors ($H=2$) associated with variables 2 and 3 ($i=2, j=3$), the systematic uncertainty in the result reduces to

$$b_R = \left[(\theta_1 b_{\bar{x}_1})^2 + (\theta_2 b_{\bar{x}_2})^2 + (\theta_3 b_{\bar{x}_3})^2 + 2\theta_2\theta_3 b_{\bar{x}_2 \bar{x}_3} \right]^{1/2}$$

where the covariance term is

$$b_{\bar{x}_2 \bar{x}_3} = \sum_{h=1}^2 (b_{\bar{x}_2})_h (b_{\bar{x}_3})_h = (b_{\bar{x}_2})_1 (b_{\bar{x}_3})_1 + (b_{\bar{x}_2})_2 (b_{\bar{x}_3})_2$$

Example 5.17

Suppose a result R is a function of two variables, X and Y , such that $R=X+Y$, and each variable having one elemental error. If $\bar{X}=10.1$ V with $b_{\bar{X}}=1.1$ V and $\bar{Y}=12.2$ V with $b_{\bar{Y}}=0.8$ V, estimate the systematic standard uncertainty in the result if the systematic errors are (1) uncorrelated and (2) correlated.

SOLUTION From the stated information, $\bar{R}=10.1+12.2=22.3$ V. For the uncorrelated case, the systematic standard uncertainty is estimated as

$$b_{R_{\text{unc}}} = \left[(\theta_X b_{\bar{X}})^2 + (\theta_Y b_{\bar{Y}})^2 \right]^{1/2} = \left[(1 \times 1.1)^2 + ((1 \times 0.8)^2) \right]^{1/2} = 1.36 \text{ V}$$

For the correlated case, with $H=1$ and $L=2$, the uncertainty is estimated as

$$\begin{aligned} b_{R_{\text{cor}}} &= \left[(\theta_X b_{\bar{X}})^2 + (\theta_Y b_{\bar{Y}})^2 + 2\theta_X\theta_Y b_{\bar{X}\bar{Y}} \right]^{1/2} \\ &= \left[(1 \times 1.1)^2 + (1 \times 0.8)^2 + 2(1)(1)(1.1)(0.8) \right]^{1/2} = 3.12 \text{ V} \end{aligned}$$

which is stated at the one-standard deviation confidence level and where

$$b_{\bar{X}\bar{Y}} = \sum_{h=1}^1 (b_{\bar{X}})_1 (b_{\bar{Y}})_1 = b_{\bar{X}} b_{\bar{Y}}$$

COMMENT In this case, the correlated systematic errors have a large impact on the systematic uncertainty. This is not always the case as it depends on the functional relationship itself. We leave it to the reader to show that if $R = X/Y$, then the covariance term in this problem would have little impact on the systematic standard uncertainty in the result.

There are situations where random errors can be correlated (10). In those cases, the random standard uncertainty in a result is estimated by

$$s_R = \left[\sum_{i=1}^L (\theta_i s_{\bar{x}_i})^2 + 2 \sum_{i=1}^{L-1} \sum_{j=i+1}^L \theta_i \theta_j r_{\bar{x}_i \bar{x}_j} s_{\bar{x}_i} s_{\bar{x}_j} \right]^{1/2} \quad (5.42)$$

where $r_{x_i x_j}$ is the correlation coefficient between x_i and x_j as given by equation 4.41.

5.10 NONSYMMETRICAL SYSTEMATIC UNCERTAINTY INTERVAL

There are situations where the error must be bounded on one side or skewed about the measured mean value such that the systematic uncertainty is better described by a nonsymmetrical interval. To develop this case, we assume that the limits of possible systematic error are known, as is the mean of the measured data set \bar{x} . Let $\bar{x} + B_x^+$ and $\bar{x} - B_x^-$ be the upper and lower limits of the systematic uncertainty relative to the measured mean value (Fig. 5.8), with $B_x^- = 2b_x^-$ and $B_x^+ = 2b_x^+$ where b_x^- and b_x^+ are the lower and upper systematic standard uncertainty values. The modeling approach assumes that the errors are symmetric about some mean value of the error distribution but asymmetric about the measured mean value.

If we model the error distribution as a normal distribution, then we assume that the limits defined using B_x^- to B_x^+ cover 95% of the error distribution. Define the offset between the mean of the

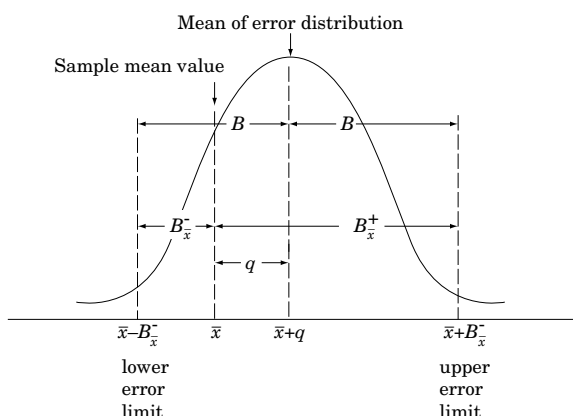


Figure 5.8 Relation between the measured mean value, the mean value of the distribution of errors, and the systematic uncertainties for treating nonsymmetrical uncertainties.

error distribution and the mean value of the measurement as

$$q = \frac{(\bar{x} + B_x^+) + (\bar{x} - B_x^-)}{2} - \bar{x} = \frac{B_x^+ - B_x^-}{2} = b_x^+ - b_x^- \quad (5.43)$$

The systematic standard uncertainty has an average width,

$$b_{\bar{x}} = \frac{(\bar{x} + B_x^+) - (\bar{x} - B_x^-)}{4} = \frac{(\bar{x} + b_x^+) - (\bar{x} - b_x^-)}{2} \quad (5.44)$$

For stating the true value, we use the combined standard uncertainty

$$u_x = \sqrt{b_x^2 + s_x^2} \quad (5.45)$$

to achieve the approximate confidence interval, $q \pm t_{v,P} u_x$. For large degrees of freedom, we can state

$$x' = \bar{x} + q - t_{v,P} u_x, \quad \bar{x} + q + t_{v,P} u_x \quad (5.46)$$

for which we choose an appropriate value for t , such as $t = 2$ for 95% confidence.

If we model the error distribution as a rectangular distribution, then we assume that the limits defined using B_x^- to B_x^+ specify the limits of that distribution. The systematic standard uncertainty is then (see footnote 5)

$$b_{\bar{x}} = \frac{(\bar{x} + B_x^+) - (\bar{x} - B_x^-)}{\sqrt{12}} \quad (5.47)$$

for use in Equations 5.45 and 5.46. Regardless of the assumed systematic error distribution, we assume that the uncertainties propagate normally.

A normal or rectangular distribution is not always the appropriate model for treating asymmetric systematic uncertainty. References 1 and 2 provide a number of scenarios to treat nonsymmetrical uncertainties including use of other error distributions. As an example, Monsch et al. (11) apply the above approach to estimating the nonsymmetrical systematic uncertainty in the induced drag on an aircraft wing in which the induced drag cannot be less than zero.

5.11 SUMMARY

Uncertainty analysis provides the “ \pm what” to a test result or the anticipated result from a proposed test plan. This chapter discussed the manner in which various errors can enter into a measurement with emphasis on their influences on the test result. Both random errors and systematic errors are considered. Random errors differ on repeated measurements, lead to data scatter, and can be quantified by statistical methods. Systematic errors remain constant in repeated measurements. Errors are quantified by uncertainties. Procedures for uncertainty analysis were introduced both as a means of estimating uncertainty propagation within a measurement and for the propagation of uncertainty among the independent measured variables that are used to determine a result through some functional relationship. We have discussed the role and use of uncertainty analysis in both the design of measurement systems, through selection of equipment and procedures, as well as in the interpretation of measured data. We have presented procedures for estimating uncertainty at various stages of a test. The procedures provide reasonable estimates of the uncertainty to be expected in measurements.

We advise the reader that test uncertainty by its very nature evades exact values. But the methodology presented gives reasonable estimates provided that the engineer has used sound, impartial judgment in its implementation. The important thing is that the uncertainty analysis be performed during the design and development stages of a test, as well as at its completion to assess the stated results. Only then can the engineer use the results with appropriate confidence and professional and ethical responsibility.

REFERENCES

1. International Organization for Standardization (ISO), *Guide to the Expression of Uncertainty in Measurement*, Geneva, Switzerland, 1993.
2. ANSI/ASME Power Test Codes-PTC 19.1, *Test Uncertainty*, American Society of Mechanical Engineers, New York, 2005.
3. Smith, R. E., and S. Wenkofer, From measurement uncertainty to measurement communications, credibility and cost control in propulsion ground test facilities, *Journal of Fluids Engineering* 107: 165–172, 1985.
4. Kline, S. J., and F. A. McClintock, Describing uncertainties in single sample experiments, *Mechanical Engineering* 75: 3–8, 1953.
5. Epperson, J.F., *An Introduction to Numerical Methods and Analysis*, Wiley-Interscience, New York, 2007.
6. Moffat, R. J., Uncertainty analysis in the planning of an experiment, *Journal of Fluids Engineering* 107: 173–181, 1985.
7. Taylor, B.N., and C. Kuyatt, *Guidelines for Evaluating and Expressing the Uncertainty of NIST Measurement Results*, NIST Technical Note 1297, Gaithersburg, MD, 1994.
8. Kestin, J., *A Course in Thermodynamics*, revised printing, Hemisphere, New York, 1979.
9. Coleman, H., and W.G. Steele, *Experimentation and Uncertainty Analysis for Engineers*, 2nd ed., Wiley-Interscience, New York, 1999.
10. Dieck, R., *Measurement Uncertainty: Methods and Applications*, 3rd ed., Instrumentation, Systems and Automation Society (ISA), Research Triangle Park, NC, 2002.
11. Monsch, S., Figliola, R.S., Thompson, E., Camberos, J., Induced Drag for 3D Wing with Volume Integral (Treffitz Plane) Technique, AIAA Paper 2007-1079, AIAA, New York, 2007.

NOMENCLATURE

a	lower bound	s_{yx}	standard deviation of a fit
b	upper bound; generic systematic standard uncertainty	$t_{v,95}$	t variable (at 95% probability)
$b_{\bar{x}}$	systematic standard uncertainty in x	t	time (t); t-variable
e_k	k th elemental error	u_x	uncertainty of a measured variable
$f()$	general functional relation	u_d	design-stage uncertainty
p	pressure ($ml^{-1}t^{-2}$)	u_c	instrument calibration uncertainty
q	offset factor	u_0	zero-order uncertainty
s_x	sample standard deviation of x	u_i	i th-order uncertainty
$s_{\bar{x}}$	random standard uncertainty in x ; sample standard deviation of the means	u_N	N th-order uncertainty
		x	measured variable
		x'	true value of the population of x

\bar{x}	sample mean value of x	\forall	volume (l^{-3})
R	result or resultant value	θ_i	sensitivity index
P	probability	ρ	gas density (ml^{-3})
B	systematic uncertainty (at 95% or 2σ probability)	σ	stress ($ml^{-1}t^{-2}$); population standard deviation
(P%)	confidence level	v	degrees of freedom
Q	flow rate ($l^3 t^{-1}$)	$\langle \rangle$	pooled statistic
T	temperature ($^\circ$)		

PROBLEMS

- 5.1** In Chapter 1, the development of a test plan is discussed. Discuss how a test plan should account for the presence of systematic and random errors. Include calibration, randomization, and repetition in your discussion.
- 5.2** Discuss how systematic uncertainty can be estimated for a measured value. How is random uncertainty estimated? What is the difference between error and uncertainty?
- 5.3** Explain what is meant by the terms “true value,” “best estimate,” “mean value,” “uncertainty,” and “confidence interval.”
- 5.4** Consider a common tire pressure gauge. How would you estimate the uncertainty in a measured pressure at the design stage and then at the N th order? Should the estimates differ? Explain.
- 5.5** A micrometer has graduations inscribed at 0.001-in. (0.025-mm) intervals. Estimate the uncertainty due to resolution. Compare the results assuming a normal distribution to results assuming a rectangular distribution.
- 5.6** A tachometer has an analog display dial graduated in 5-revolutions-per-minute (rpm) increments. The user manual states an accuracy of 1% of reading. Estimate the design-stage uncertainty in the reading at 50, 500, and 5000 rpm.
- 5.7** An automobile speedometer is graduated in 5-mph (8-kph) increments and has an accuracy rated to be within $\pm 4\%$. Estimate the uncertainty in indicated speed at 60 mph (90 kph).
- 5.8** A temperature measurement system is composed of a sensor and a readout device. The readout device has a claimed accuracy of 0.8°C with a resolution of 0.1°C . The sensor has an off-the-shelf accuracy of 0.5°C . Estimate a design-stage uncertainty in the temperature indicated by this combination.
- 5.9** Two resistors are to be combined to form an equivalent resistance of $1000\ \Omega$. The resistors are taken from available stock on hand as acquired over the years. Readily available are two common resistors rated at $500 \pm 50\ \Omega$ and two common resistors rated at $2000\ \Omega \pm 5\%$. What combination of resistors (series or parallel) would provide the smaller uncertainty in an equivalent $1000\ \Omega$ resistance?
- 5.10** An equipment catalog boasts that a pressure transducer system comes in 3½-digit (e.g., 19.99) or 4½-digit (e.g., 19.999) displays. The 4½-digit model costs substantially more. Both units are otherwise identical. The specifications list the uncertainties for three elemental errors:

Linearity error:	0.15% FSO
Hysteresis error:	0.20% FSO
Sensitivity error:	0.25% FSO

For a full-scale output (FSO) of 20 kPa, select a readout based on appropriate uncertainty calculations. Explain.

- 5.11** The shear modulus, G , of an alloy can be determined by measuring the angular twist, θ , resulting from a torque applied to a cylindrical rod made from the alloy. For a rod of radius R and a torque applied at a length L from a fixed end, the modulus is found by $G = 2LT/\pi R^4\theta$. Examine the effect of the relative uncertainty of each measured variable on the shear modulus. If during test planning all of the uncertainties are set at 1%, what is the uncertainty in G ?
- 5.12** An ideal heat engine operates in a cycle and produces work as a result of heat transfer from a thermal reservoir at an elevated temperature T_h and by rejecting energy to a thermal sink at T_c . The efficiency for such an ideal cycle, termed a “Carnot cycle,” is

$$\eta = 1 - (T_c/T_h).$$

Determine the required uncertainty in the measurement of temperature to yield an uncertainty in efficiency of 1%. Assume errors are uncorrelated. Use $T_h = 1000$ K and $T_c = 300$ K.

- 5.13** Heat transfer from a rod of diameter D immersed in a fluid can be described by the Nusselt number, $Nu = hD/k$, where h is the heat-transfer coefficient and k is the thermal conductivity of the fluid. If h can be measured to within $\pm 7\%$ (95%), estimate the uncertainty in Nu for the nominal value of $h = 150$ W/m²-K. Let $D = 20 \pm 0.5$ mm and $k = 0.6 \pm 2\%$ W/m-K.
- 5.14** Estimate the design-stage uncertainty in determining the voltage drop across an electric heating element. The device has a nominal resistance of 30 Ω and power rating of 500 W. Available is an ohmmeter (accuracy: within 0.5%; resolution: 1 Ω) and ammeter (accuracy: within 0.1%; resolution: 100 mA). Recall $E = IR$.
- 5.15** Explain the critical difference(s) between a design-stage uncertainty analysis and an advanced-stage uncertainty analysis.
- 5.16** From an uncertainty analysis perspective, what important information does replication provide that is not found by repetition alone? How is this information included in an uncertainty analysis?
- 5.17** A displacement transducer has the following specifications:

Linearity error:	$\pm 0.25\%$ reading
Drift:	$\pm 0.05\%/{^\circ}\text{C}$ reading
Sensitivity error:	$\pm 0.25\%$ reading
Excitation:	10–25 V dc
Output:	0–5 V dc
Range:	0–5 cm

The transducer output is to be indicated on a voltmeter having a stated accuracy of $\pm 0.1\%$ reading with a resolution of 10 μV. The system is to be used at room temperature, which can vary by $\pm 10^\circ\text{C}$. Estimate an uncertainty in a nominal displacement of 2 cm at the design stage. Assume 95% confidence.

- 5.18** The displacement transducer of Problem 5.17 is used in measuring the displacement of a body impacted by a mass. Twenty measurements are made, which yield

$$\bar{x} = 17.20 \text{ mm} \quad s_x = 1.70 \text{ mm}$$

Determine a best estimate for the mass displacement at 95% probability based on all available information.

- 5.19** A pressure transducer outputs a voltage to a readout device that converts the signal back to pressure. The device specifications are:

Resolution:	0.1 psi
Sensitivity error:	0.1 psi
Linearity error:	within 0.1% of reading
Drift:	less than 0.1 psi/6 months (32–90°F)

The transducer has a claimed accuracy of within 0.5% of reading. For a nominal pressure of 100 psi at 70°F, estimate the design-stage uncertainty in a measured pressure.

- 5.20** For a thin-walled pressure vessel of diameter D and wall thickness t subjected to an internal pressure p , the tangential stress is given by $\sigma = pD/2t$. During one test, 10 measurements of pressure yielded a mean of 8610 lb/ft² with a standard deviation of 273.1 lb/ft². Cylinder dimensions are to be based on a set of 10 measurements which yielded: $\bar{D} = 6.2$ in. with $s_D = 0.18$ in. and $\bar{t} = 0.22$ in. with $s_t = 0.04$ in. Estimate the degrees of freedom in the standard uncertainty for stress. Determine the best estimate of stress at 95% confidence. Pressure measurements and dimensions have a systematic uncertainty of 1% of the reading assumed at 95% confidence.
- 5.21** Suppose a measured normal stress contains three elemental random errors in its calibration with the following values:

$$(s_{\bar{x}})_1 = 0.90 \text{ N/m}^2 \quad (s_{\bar{x}})_2 = 1.10 \text{ N/m}^2 \quad (s_{\bar{x}})_3 = 0.09 \text{ N/m}^2 \\ v_1 = 21 \quad v_2 = 10 \quad v_3 = 15$$

Estimate the random standard uncertainty due to calibration errors with its degrees of freedom.

- 5.22** An experiment to determine force acting at a point on a member contains three elemental errors with resulting uncertainties:

$$(b_{\bar{x}})_1 = 1.0 \text{ N} \quad (b_{\bar{x}})_2 = 2.25 \text{ N} \quad (b_{\bar{x}})_3 = 1.8 \text{ N} \\ (s_{\bar{x}})_1 = 0 \quad (s_{\bar{x}})_2 = 6.1 \text{ N} \quad (s_{\bar{x}})_3 = 4.2 \text{ N} \\ v_2 = 17 \quad v_3 = 19$$

If the mean value for force is estimated to be 200 N, determine the uncertainty in the mean value at 95% confidence. Assume large degrees of freedom in the systematic uncertainties.

- 5.23** The area of a flat, rectangular parcel of land is computed from the measurement of the length of two adjacent sides, X and Y . Measurements are made using a scaled chain accurate to within 0.5% (95%) over its indicated length. The two sides are measured several times with the following results:

$$\bar{X} = 556 \text{ m} \quad \bar{Y} = 222 \text{ m} \\ s_x = 5.3 \text{ m} \quad s_y = 2.1 \text{ m} \\ v = 8 \quad v = 7$$

Estimate the area of the land and state the confidence interval of that measurement at 95%.

- 5.24** Estimate the random standard uncertainty in the measured value of stress for a data set of 23 measurements if $\bar{\sigma} = 1061$ kPa and $s_{\sigma} = 22$ kPa. Report the best estimate for stress at 68% confidence. Assume a normal distribution and neglect systematic errors.

- 5.25** Estimate the uncertainty at 95% confidence in the strength of a metal alloy. Six separate specimens are tested with a mean of 448.1 MPa and standard deviation of 1.23 MPa in the results. A systematic standard uncertainty of 1.48 MPa with $v_b = 19$ is estimated by the operator.
- 5.26** A pressure measuring system outputs a voltage that is proportional to pressure. It is calibrated against a transducer standard (certified error: within ± 0.5 psi) over its 0–100-psi range with the results given below. The voltage is measured with a voltmeter (instrument error: within $\pm 10 \mu\text{V}$; resolution: 1 μV). The engineer intending to use this system estimates that installation effects can cause the indicated pressure to be off by another ± 0.5 psi. Estimate the expanded uncertainty at 95% confidence in using the system based on the known information.

$E[\text{mV}]:$	0.004	0.399	0.771	1.624	2.147	4.121
$p[\text{psi}]:$	0.1	10.2	19.5	40.5	51.2	99.6

- 5.27** The density of a metal composite is to be determined from the mass of a cylindrical ingot. The volume of the ingot is determined from diameter and length measurements. It is estimated that mass m can be determined to within 0.1 lb_m using an available balance scale; length L can be determined to within 0.05 in. and diameter D to within 0.0005 in. Instrumentation for each variable has a known calibration systematic uncertainty of 1% of its reading. Estimate the design-stage uncertainty in the determination of the density. Which measurement contributes most to the uncertainty in the density? Which measurement method should be improved first if the uncertainty in density is unacceptable? Use the nominal values of $m = 4.5 \text{ lb}_m$, $L = 6$ in., and $D = 4$ in. (Note: $1 \text{ lb}_m = 0.4535 \text{ kg}$; 1 inch = 0.0254 m.)
- 5.28** For the ingot of Problem 5.27, the diameter of the ingot is measured 10 independent times at each of three cross sections. For the results below, give a best estimate in the diameter with its uncertainty (95%). (Note: 1 inch = 0.0254 m.)

$$\bar{d}_1 = 3.9900 \text{ in.} \quad \bar{d}_2 = 3.9892 \text{ in.} \quad \bar{d}_3 = 3.9961 \text{ in.}$$

$$s_{d_1} = 0.0050 \text{ in.} \quad s_{d_2} = 0.0010 \text{ in.} \quad s_{d_3} = 0.0009 \text{ in.}$$

- 5.29** For the ingot of Problem 5.27, the following measurements are obtained from the ingot:

$$\bar{m} = 4.4 \text{ lb}_m \quad \bar{L} = 5.85 \text{ in.}$$

$$s_m = 0.1 \text{ lb}_m \quad s_L = 0.10 \text{ in.}$$

$$N = 21 \quad N = 11$$

Based on the results of Problem 5.28, estimate the density and the uncertainty in this value. Compare your answer with that of Problem 5.27. Explain why the estimate changes. (Note: $1 \text{ lb}_m = 0.4535 \text{ kg}$; 1 inch = 0.0254 m.)

- 5.30** A temperature measurement system is calibrated against a standard system certified to an uncertainty of $\pm 0.05^\circ\text{C}$ at 95%. The system sensor is immersed alongside the standard within a temperature bath so that the two are separated by about 10 mm. The temperature uniformity of the bath is estimated at about $5^\circ\text{C}/\text{m}$. The temperature system sensor is connected to a readout that indicates the temperature in terms of voltage. The following are measured values between the temperature indicated by the standard and the indicated voltage:

T [°C]	E [mV]	T [°C]	E [mV]
0.1	0.004	40.5	1.624
10.2	0.399	51.2	2.147
19.5	0.771	99.6	4.121

- a. Compute the curve fit for $T=f(E)$ and its standard random uncertainty.
- b. Estimate the uncertainty in using the output from the temperature measurement system for temperature measurements.

- 5.31 The power usage of a strip heater is to be determined by measuring heater resistance and heater voltage drop simultaneously. The resistance is to be measured using an ohmmeter having a resolution of $1\ \Omega$ and uncertainty of 1% of reading, and voltage is to be measured using a voltmeter having a resolution of $1\ V$ and uncertainty of 1% of reading. It is expected that the heater will have a resistance of $100\ \Omega$ and use $100\ W$ of power. Determine the uncertainty in power determination to be expected with this equipment at the design stage.
- 5.32 The power usage of a DC strip heater can be determined in either of two ways: (1) heater resistance and voltage drop can be measured simultaneously and power computed, or (2) heater voltage drop and current can be measured simultaneously and power computed. Instrument manufacturer specifications are listed (assume 95% level):

Instrument	Resolution	Uncertainty (% reading)
Ohmmeter	$1\ \Omega$	0.5%
Ammeter	$0.5\ A$	1%
Voltmeter	$1\ V$	0.5%

For loads of $10\ W$, $1\ kW$, and $10\ kW$, determine the best method based on an appropriate uncertainty analysis. Assume nominal values as necessary for resistance, current, and voltage.

- 5.33 The density of a gas inside a tank is determined from pressure and temperature measurements. Assuming ideal gas behavior, what is the relative (percent) uncertainty expected in density if the pressure measurement has a relative uncertainty of 1%. Tank temperature is held at 25°C with an uncertainty of 2°C . Assume values are at 95% confidence.
- 5.34 Time variations in a signal require that the signal be measured often to determine its mean value. A preliminary sample is obtained by measuring the signal 50 times. The statistics from this sample show a mean value of $2.112\ V$ with a standard deviation of $0.387\ V$. Systematic errors are negligible. If it is desired to hold the random uncertainty in the mean value due to data variation to within $0.100\ V$ at 95% confidence, how many measurements of the signal will be required?
- 5.35 The diameter of a shaft is estimated in a manner consistent with Example 5.14. A hand-held micrometer (resolution: $0.001\ \text{in.}$; $B < .001\ \text{in.}$ with $v = 14$) is used to make measurements about four selected cross-sectional locations. Ten measurements of diameter are made around each location, with the results noted below. Provide a reasonable statement as to the diameter of the shaft and the uncertainty in that estimate.

Location:	1	2	3	4
\bar{d} (in.):	4.494	4.499	4.511	4.522
s_d :	0.006	0.009	0.010	0.003

- 5.36** The pressure in a large vessel is to be maintained at some set pressure for a series of tests. A compressor is to supply air through a regulating valve that is set to open and close at the set pressure. A dial gauge (resolution: 1 psi; uncertainty: 0.5 psi) is used to monitor pressure in the vessel. Thirty trial replications of pressurizing the vessel to a set pressure of 50 psi are attempted to estimate pressure controllability and a standard deviation in set pressure of 2 psi is found. Estimate the uncertainty to be expected in the vessel set pressure. Compare to the uncertainty in estimating the average set pressure.
- 5.37** A handbook value for the thermal expansion coefficient of a particular pure metal is $\alpha = 16.52 \times 10^{-6}^{\circ}\text{C}^{-1}$ and states that the possible error in this value should not exceed $0.4 \times 10^{-6}^{\circ}\text{C}^{-1}$. Assuming that the population for α follows a rectangular distribution, estimate the standard uncertainty to be assigned.
- 5.38** The cooling of a thermometer (e.g., Exs. 3.3 and 3.4) can be modeled as a first-order system with $\Gamma = e^{-t/\tau}$. If Γ can be measured to within 2% and time within 1%, determine the uncertainty in τ over the range $0 \leq \Gamma \leq 1$.
- 5.39** A J-type thermocouple monitors the temperature of air flowing through a duct. Its signal is measured by a thermostat. The air temperature is maintained constant by an electric heater whose power is controlled by the thermostat. To test the control system, 20 measurements of temperature were taken over a reasonable time period during steady operation. This was repeated three times with the results as:

Run	N	$\bar{T}[^{\circ}\text{C}]$	$s_T[^{\circ}\text{C}]$
1	20	181.0	3.01
2	20	183.1	2.84
3	20	182.1	3.08

The thermocouple itself has an instrument error with uncertainty $\pm 1^{\circ}\text{C}$ (95%) with $v = 30$. It has a 90% rise time of 20 ms. Thermocouple insertion errors are estimated to be $\pm 1.2^{\circ}\text{C}$ (95%). What information is found by performing replications? Identify the elemental errors that affect the system's control of the air temperature. What is the uncertainty in the set temperature?

- 5.40** Based on everyday experience, give an estimate of the systematic uncertainty you might expect in the following measuring instruments: bathroom scale, metal tape ruler, micrometer, kitchen window bulb thermometer, and automobile speedometer.
- 5.41** A tank is pressurized with air at $25 \pm 2^{\circ}\text{C}$ (95%). Determine the relative uncertainty in the tank's air density if tank pressure is known to within $\pm 1\%$ (95%). Assume ideal gas behavior.
- 5.42** The density of air must be known to within $\pm 0.5\%$. If the air temperature at 25°C can be determined to within $\pm 1^{\circ}\text{C}$ (95%), what uncertainty can be tolerated in the pressure measurement if air behaves as an ideal gas?
- 5.43** In pneumatic conveying, solid particles such as flour or coal are carried through a duct by a moving air stream. Solids density at any duct location can be measured by passing a laser beam of known

intensity I_o through the duct and measuring the light intensity transmitted to the other side, I . A transmission factor is found by

$$T = I/I_o = e^{-KEW} \quad 0 \leq T \leq 1$$

Here W is the width of the duct, K is the solids density, and E is a factor taken as 2.0 ± 0.04 (95%) for spheroid particles. Determine how u_K/K is related to the relative uncertainties of the other variables. If the transmission factor and duct width can be measured to within $\pm 1\%$, can solids density be measured to within 5%? 10%? Discuss your answer, remembering that the transmission factor varies from 0 to 1.

- 5.44** A step test is run to determine the time constant of a first-order instrument (see Chapter 3). If the error fraction $\Gamma(t)$ can be estimated to within $\pm 2\%$ (95%) and time t can be estimated in seconds to within $\pm 0.5\%$ (95%), plot u_τ/τ versus $\Gamma(t)$ over its range, $0 \leq \Gamma(t) \leq 1$.
- 5.45** The acceleration of a cart down a plane inclined at an angle α to horizontal can be determined by measuring the change in speed of the cart at two points, separated by a distance s , along the inclined plane. Suppose two photocells are fixed at the two points along the plane. Each photocell measures the time for the cart, which has a length L , to pass it. If $L = 5 \pm 0.5$ cm, $s = 100 \pm 0.2$ cm, $t_1 = 0.054 \pm 0.001$ s, and $t_2 = 0.031 \pm 0.001$ s, all (95%), estimate the uncertainty in acceleration:

$$a = \frac{L^2}{2s} \left(\frac{1}{t_2^2} - \frac{1}{t_1^2} \right)$$

Compare as a concomitant check $a = g \sin \alpha$ using values for $\alpha = 30^\circ$ and 90° . What uncertainty in α is needed to make this the better method?

- 5.46** Golf balls are often tested using a mechanical player called an “Iron Byron” because the robotic golfer’s swing was patterned after that of Byron Nelson, a famous golf professional. It is proposed to use initial velocity and launch angle from such testing to predict carry distance (how far the ball travels after impact). The following data represent test results for a particular golf ball when struck with a particular driver (golf club):

Initial Velocity (mph)	Launch Angle (degrees)	Carry Distance (yd)
165.5	8	254.6
167.8	8	258.0
170.0	8	261.4
172.2	8	264.8
165.5	10	258.2
167.8	10	261.6
170.0	10	264.7
172.2	10	267.9
165.5	12	260.6
167.8	12	263.7
170.0	12	266.8
172.2	12	269.8

If the initial velocity can be measured to within a systematic uncertainty of 1 mph, and the launch angle to within 0.1 degrees estimate the resulting uncertainty in the carry distance as a function of initial velocity and launch angle. Over this range of initial velocity and launch angle, can a single value of uncertainty be assigned?

- 5.47** A particular flow meter allows the volumetric flow rate Q to be calculated from a measured pressure drop Δp . Theory predicts $Q \propto \sqrt{\Delta p}$, and a calibration provides the following data:

Q (m^3/min)	Δp (Pa)
10	1,000
20	4,271
30	8,900
40	16,023

What uncertainty in the measurement of Δp is required to yield an uncertainty of 0.25% in Q over the range of flow rates from 10 to 40 m^3/min ?

- 5.48** Devise a simple experiment to estimate the true value of a variable through measurements. List the errors that enter into your measurement. Execute the experiment and estimate the uncertainty in the result. Discuss how you assigned values to each uncertainty at the design stage and after the experiment.
- 5.49** Devise a simple experiment to estimate the true value of a result that is a function of at least two variables that must be measured. List the errors that enter into your measurements. Execute the experiment and estimate the uncertainty in the result. Discuss how you assigned values to each uncertainty at the design stage and after the experiment.
- 5.50** A steel cantilever beam is fixed at one end and free to move at the other. A load (F) of 980 N with a systematic error (95%) of 10 N is applied at the free end. The beam geometry, as determined by a metric ruler having 1-mm increments, is 100 mm long (L), 30 mm wide (w), and 10 mm thick (t). Estimate the maximum stress at the fixed end and its uncertainty. The maximum stress is given by

$$\sigma = \frac{Mc}{I} = \frac{FL(t/2)}{wt^3/12}.$$

- 5.51** The heat flux in a reaction is estimated by $Q = 5(T_1 - T_2)$ kJ/s. Two thermocouples are used to measure T_1 and T_2 . Each thermocouple has a systematic uncertainty of 0.2°C (95%). Based on a large sample of measurements, $\bar{T}_1 = 180^\circ\text{C}$, $\bar{T}_2 = 90^\circ\text{C}$, and the random standard uncertainty in each temperature measurement is 0.1 °C. Assume large degrees of freedom. Compare the uncertainty in heat flux if the thermocouple systematic errors are (a) uncorrelated and (b) correlated. Explain.
- 5.52** A comparative test uses the relationship $R = p_2/p_1$, where pressure p_2 is measured to be 54.7 MPa and pressure p_1 is measured to be 42.0 MPa. Each pressure measurement has a single systematic error of 0.5 MPa. Compare the systematic uncertainty in R if these errors are (a) correlated and (b) uncorrelated. Explain.
- 5.53** A sensitive material is to be contained within a glovebox. Codes require that the transparent panels, which make up the walls of the glovebox, withstand the impact of a 22-kg mass falling at 8 m/s. An impact test is performed where the 22 kg mass is dropped a known variable height onto a panel. The mass motion is sensed by photocells from which an impact velocity is estimated. The mean kinetic energy for failure was 717 N·m, with a standard deviation of 60.7 N·m based on 61 failures. The systematic uncertainty in mass is 0.001 kg (95%). The velocity at impact is 8 m/s, with a systematic uncertainty in velocity estimated as 0.27 m/s (95%). Estimate the combined standard uncertainty and the expanded uncertainty at 95% in the kinetic energy for failure. Assume a normal distribution of errors.

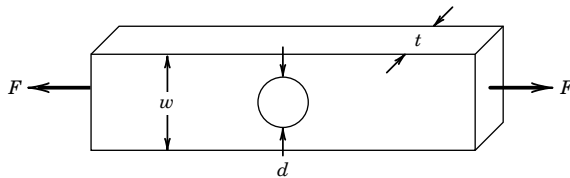


Figure 5.9 Structural member discussed in Problem 5.54.

- 5.54** A geometric stress concentration factor, K_t , is used to relate the actual maximum stress to a well-defined nominal stress in a structural member. The maximum stress is given by $\sigma_{\max} = K_t \sigma_o$, where σ_{\max} represents the maximum stress and σ_o represents the nominal stress. The nominal stress is most often stated at the minimum cross section.
- Consider the axial loading shown in Figure 5.9, where the structural member is in axial tension and experiences a stress concentration as a result of a transverse hole. In this geometry, $\sigma_o = F/A$, where area $A = (w - d)t$. If $d = 0.5 w$, then $K_t = 2.2$. Suppose $F = 10,000 \pm 500$ N, $w = 1.5 \pm 0.02$ cm, $t = 0.5 \pm 0.02$ cm, and the uncertainty in the value for d is 3%. Neglecting the uncertainty in stress concentration factor, determine the uncertainty in the maximum stress experienced by this part.
- 5.55** The result of more than 60 temperature measurements over time during fixed conditions in a furnace determines $\bar{T} = 624.7$ °C with $s_{\bar{T}} = 2.4$ °C. The engineer suspects that, due to a radiation systematic error, the measured temperature may be higher by up to 10°C at a 95% confidence level but not lower, so the lower bound of error is 0°C relative to the measured mean value. Determine the statement for the true mean temperature with its confidence interval assuming a normal distribution for the systematic error. Then repeat, assuming the systematic errors follow a rectangular distribution with upper bound 10°C and lower bound 0°C relative to the measured mean value.
- 5.56** Estimate the uncertainty at 95% confidence in drag coefficient as predicted by the Monte Carlo simulation using the information from Problem 4.55. Consider only the random uncertainties in the simulation.
- 5.57** The calibration certificate for a laboratory standard resistor lists its resistance as $10.000742 \Omega \pm 130 \mu\Omega$ (95%). The certificate lists a systematic standard uncertainty of $10 \mu\Omega$. Estimate the random standard uncertainty in the resistor.
- 5.58** The calibration certificate for a standard mass of stainless steel lists its mass as 1000.000325 g. It states that this value should not exceed $324 \mu\text{g}$ at three standard deviations. Assign a value to the standard uncertainty in the mass.
- 5.59** In a mechanical loading test, the operator is to load a specimen to a value of 100 N. The control is such that this value can be achieved with a possible error of no more than 0.5 N. Estimate a value for the uncertainty in loading at the 95% level using (1) a zero-order estimate based on instrument resolution and (2) an estimate based on the information provided assuming a rectangular distribution. Comment on the results.
- 5.60** In Problem 5.9, we assumed the errors in the known resistor values were uncorrelated. Suppose the resistors are certified by the manufacturer to have specifications based on a common calibration. Repeat Problem 5.9 by assuming the errors are correlated systematic errors.

Chapter 6

Analog Electrical Devices and Measurements

6.1 INTRODUCTION

This chapter provides an introduction to basic electrical analog devices used with analog signals or to display signals in an analog form. We include analog output meters and the more common solid-state devices used in signal conditioning. Information is often transferred between stages of a measurement system as an analog electrical signal. This signal typically originates from the measurement of a physical variable using a fundamental electromagnetic or electrical phenomenon and then propagates from stage to stage of the measurement system (see Fig. 1.1). Accordingly, we discuss some signal conditioning and output methods.

While analog devices have been supplanted by their digital equivalents in many applications, they are still widely used and remain engrained in engineered devices. An analog output format is often ergonomically superior in monitoring, as evidenced by modern car speedometer dials and dial wristwatches. Too often we qualify a digital device by its digital readout, but internal analog circuits form the foundation for both analog and many digital indicating systems. In fact, many of the systems that we interface with are analog and digital hybrids. Within a signal chain, it is common to find digital and analog electrical devices being used together and so requiring special signal conditioning. An understanding of analog device function provides insight, as well as a historical reference point, into the advantages and disadvantages of digital counterparts; such issues are discussed in this chapter.

Upon completion of this chapter, the reader will be able to

- understand the principles behind common analog voltage and current measuring devices,
- understand the operation of balanced and unbalanced resistance bridge circuits,
- define, identify, and minimize loading errors,
- understand the basic principles involved in signal conditioning, especially filtering and amplification, and
- apply proper grounding and shielding techniques in measuring system hookups.

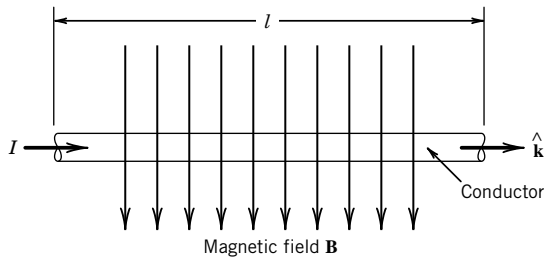


Figure 6.1 Current-carrying conductor in a magnetic field.

6.2 ANALOG DEVICES: CURRENT MEASUREMENTS

Direct Current

One way to measure a DC electrical current is to use an analog device that responds to the force exerted on a current-carrying conductor in a magnetic field. Because an electric current is a series of moving charges, a magnetic field exerts a force on a current-carrying conductor. This force can be used as a measure of the flow of current in a conductor by moving a pointer on a display.

Consider a straight length l of a conductor through which a current I flows, as shown in Figure 6.1. The magnitude of force on this conductor due to a magnetic field strength B is

$$F = IIB \quad (6.1)$$

This relation is valid only when the direction of the current flow and the magnetic field are at right angles. In the general case

$$\mathbf{F} = Il\hat{\mathbf{k}} \times \mathbf{B} \quad (6.2)$$

where $\hat{\mathbf{k}}$ is a unit vector along the direction of the current flow, and the force \mathbf{F} and the magnetic field \mathbf{B} are also vector quantities. Equation 6.2 provides both the magnitude of the developed force \mathbf{F} , and, by the right-hand rule, the direction in which the force on the conductor acts.

Similarly, a current loop in a magnetic field experiences a torque if the loop is not aligned with the magnetic field, as illustrated in Figure 6.2. The torque¹ on a loop composed of N turns is given by

$$T_{\mu} = NIAB \sin \alpha \quad (6.3)$$

where

A = cross-sectional area defined by the perimeter of the current loop

B = magnetic field strength (magnitude)

I = current

α = angle between the normal cross-sectional area of the current loop and the magnetic field

One approach to implementing Equation 6.3 to measure current is in the very common D'Arsonval movement shown in Figure 6.3. In this arrangement, the uniform radial magnetic field and torsional spring result in a steady angular deflection of the coil that corresponds to the existing current through the coil. The coil and fixed permanent magnet are arranged in the normal direction to the current loop, that is, $\alpha = 90$ degrees. If an analog dial indicates current, voltage, or resistance, then it is likely to employ this mechanism.

¹ In vector form, the torque on a current loop can be written $\mathbf{T}_{\mu} = \mu \times \mathbf{B}$ where μ is the magnetic dipole moment.

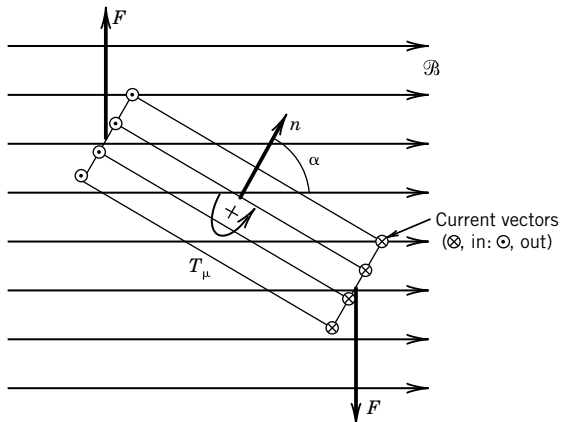


Figure 6.2 Forces and resulting torque on a current loop in a magnetic field.

Most devices that use the D'Arsonval movement employ a pointer whose deflection increases with the magnitude of current applied. This mode of operation is called the *deflection mode*. A typical circuit for an analog current measuring device, an ammeter, is shown in Figure 6.4. Here the deflection of the pointer indicates the magnitude of the current flow. The range of current that can be measured is determined by selection of the combination of shunt resistor and the internal resistance of the meter movement. The shunt resistor provides a bypass for current flow, reducing the current that flows through the movement. A make-before-break switch prevents current overload through the meter coil.

A *galvanometer* is a measuring device used to detect a current flow in a circuit. It is a highly sensitive D'Arsonval movement calibrated about zero current; the indicator normally indicates zero but can deflect to the plus or minus direction. The pointer is used to adjust a circuit to a zero current state. This mode of operation is called the *null mode*. The highest sensitivity of commercial galvanometers is approximately $0.1 \mu\text{A}/\text{division}$ for a galvanometer with a mechanical pointer. That's quite sensitive.

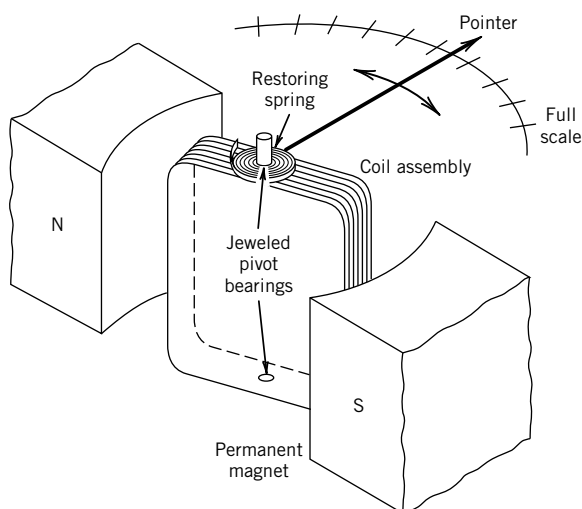


Figure 6.3 Basic D'Arsonval meter movement.

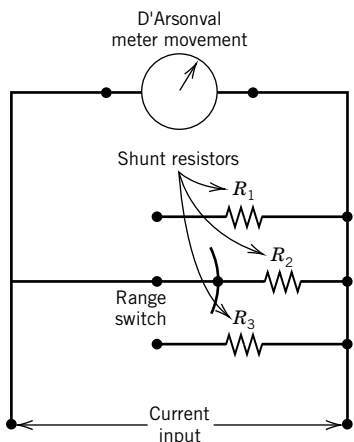


Figure 6.4 Simple multirange ammeter (with make-before-break selector switch). Shunt resistors determine meter range.

Errors inherent to the D'Arsonval movement include hysteresis and repeatability errors due to mechanical friction in the pointer-bearing movement, and linearity errors in the spring that provides the restoring force for equilibrium. Also, in developing a torque, the D'Arsonval movement must extract energy from the current flowing through it. This draining of energy from the signal being measured changes the measured signal, and such an effect is called a *loading error*. This is a consequence of all instruments that operate in deflection mode. A quantitative analysis of loading errors is provided later.

Alternating Current

An AC current can be measured in any number of ways. One technique, found in common deflection meters, uses diodes to form a rectifier that converts the time-dependent AC current into a DC current. This current then can be measured with a calibrated D'Arsonval movement meter as previously described. This is the same technique used in those ubiquitous small transformers used to convert AC wall current into a DC current at a set voltage to power or to charge electronic devices. An *electrodynamometer* is basically a D'Arsonval movement modified for use with AC current by replacing the permanent magnet with an electromagnet in series with the current coil. These AC meters have upper limits on the frequency of the alternating current that they can effectively measure; most common instruments are calibrated for use with standard line frequency.

An accurate measuring solution for large AC current is the Hall effect probe. This is a probe clamped over the current-carrying wire (conductor) to measure its unknown current flow. To understand its use, let us mention two phenomena. The first is the *Hall effect*, which is a voltage that is developed from any current-carrying conductor placed perpendicular to a magnetic field. For a known current, the magnitude of this voltage directly depends on the magnitude of the magnetic field. The second is that a current passing through a wire generates a magnetic field. So in practice, a Hall-effect probe is realized by coupling these two processes concurrently: use the unknown current within a wire to generate a magnetic field that develops a measurable voltage across a Hall-effect sensor.

The Hall-effect sensor is a thin conducting semiconductor wafer driven by a known current; this current is unrelated to the unknown current being measured and is provided by a separate source, such as a battery. The Hall-effect probe is an iron-core ring that is placed around the wire of an

unknown current and used to concentrate the magnetic field, and a Hall-effect sensor that is attached to the iron core so as to be aligned parallel to the wire of an unknown current being measured.

Example 6.1

A galvanometer consists of N turns of a conductor wound about a core of length l and radius r that is situated perpendicular to a magnetic field of uniform flux density \mathbf{B} . A DC current passes through the conductor due to an applied potential, $E_i(t)$. The output of the device is the rotation of the core and pointer, θ , as shown in Figure 6.5. Develop a lumped parameter model relating pointer rotation and current.

FIND A dynamic model relating θ and I

SOLUTION The galvanometer is a rotational system consisting of a torsional spring, a pointer, and core that are free to deflect; the rotation is subject to frictional damping. The mechanical portion of the device consists of a coil having moment of inertia J , bearings that provide damping from friction, with a damping coefficient c , and a torsional spring of stiffness k . The electrical portion of the device consists of a coil with a total inductance L_g and a resistance R_g .

We apply Newton's second law with the mechanical free-body diagram shown in Figure 6.5a.

$$J \frac{d^2\theta}{dt^2} + c \frac{d\theta}{dt} + k\theta = T_\mu \quad (6.4)$$

As a current passes through the coil, a force is developed that produces a torque on the coil:

$$T_\mu = 2NBrlrI \quad (6.5)$$

This torque, which tends to rotate the coil, is opposed by an electromotive force E_m , due to the Hall effect:

$$E_m = \left(r \frac{d\theta}{dt} \times \mathbf{B} \right) i \hat{\mathbf{k}} = 2NBr \frac{d\theta}{dt} \quad (6.6)$$

which produces a current in the direction opposite to that produced by E_i . Applying Kirchhoff's law to the electrical free body of Figure 6.5b gives

$$L_g \frac{dI}{dt} + R_g I = E_i - E_m \quad (6.7)$$

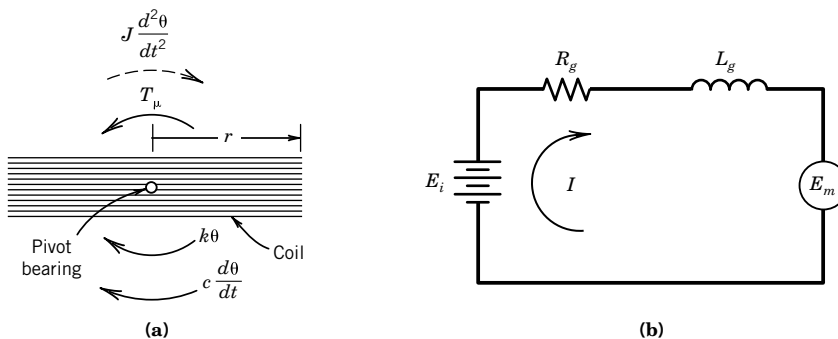


Figure 6.5 Circuit and free-body diagram for Example 6.1.

Equations 6.5 and 6.6 define the coupling relations between the mechanical Equation 6.4 and the electrical Equation 6.7. From these, we see that the current due to potential E brings about developed torque T_μ that moves the galvanometer pointer, and that this motion is opposed by the mechanical restoring force of the spring and by the development of an opposing electrical potential E_m . The system damping allows the pointer to settle to an equilibrium position.

COMMENT The system output, which is the pointer movement here, is governed by the second-order system response described in Chapter 3. However, the torque input to the mechanical system is a function of the electrical response of the system. In this measurement system, the input signal, which is the applied voltage here, is transformed into a mechanical torque to provide the measurable output deflection.

6.3 ANALOG DEVICES: VOLTAGE MEASUREMENTS

Often we are interested in measuring either static or dynamic voltage signals. Depending on the source, the magnitude of these signals may range over several orders of magnitude throughout the measured signal chain. The frequency content of dynamic voltage signals is often of interest as well. As such, a wide variety of measurement systems have been developed for voltage measurement of static and dynamic signals. This section discusses several convenient and common methods to indicate voltage in measurement systems.

Analog Voltage Meters

A DC voltage can be measured in through the analog circuit shown in Figure 6.6, where a D'Arsonval movement is used in series with a resistor. Although fundamentally sensitive to current flow, the D'Arsonval movement can be calibrated in terms of voltage by using an appropriate known fixed resistor and through Ohm's law relating it to the measured current. This basic circuit is employed in the construction of analog voltage dials and volt-ohmmeters (VOMs), which for many years served as the common measurement device for current, voltage, and resistance.

An AC voltage can be measured through rectification or through the use of an electromagnet, either in an electrodynamicmeter or with a movable iron vane. These instruments are sensitive to the *rms* (root-mean-square) value of a simple periodic AC current, and can be calibrated in terms of voltage; shunt resistors can be used to establish the appropriate scale. The circuit shown in Figure 6.6 can also be used to measure an AC voltage if the input voltage is rectified prior to

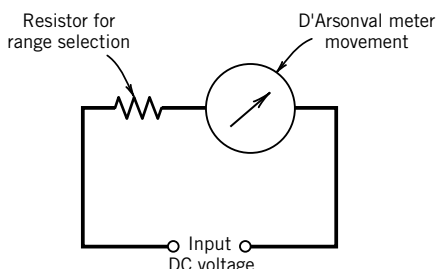


Figure 6.6 A DC voltmeter circuit.

input to this circuit. The waveform output of the rectifier must be considered if a steady meter reading is to be obtained. An AC meter indicates a true rms value for a simple periodic signal only, but a *true* rms AC voltmeter performs the signal integration (e.g., Eq. 2.4) required to accurately determine the rms value in a signal-conditioning stage and indicates true signal rms regardless of waveform.

Oscilloscope

The *oscilloscope* is a practical graphical display device providing an analog representation of a measured signal. It is used to measure and to visually display voltage magnitude versus time for dynamic signals over a wide range of frequencies with a signal bandwidth extending commonly into the megahertz range and, with some units, into the gigahertz range (1, 2). A useful diagnostic tool, the oscilloscope provides a visual output of signal magnitude, frequency, distortion, and a delineation of the DC and AC components. The visual image provides a direct means to detect the superposition of noise and interference on a measured signal, something nonvisual metering devices cannot do. In addition to signal versus time, a typical unit can also display two or more signals [$X(t)$ and $Y(t)$], perform addition and subtraction of signals ($X + Y$, $X - Y$), and display amplitude versus amplitude (XY) plots and other features. Some digital oscilloscopes have significant internal storage so as to mimic a data-logging signal recorder. Others have internal fast Fourier transform (FFT) circuitry to provide for direct spectral analysis of a signal (see Chapter 2).

Although seen less often today, the cathode ray oscilloscope is interesting in that the cathode tube operates as a time-based voltage transducer. Its schematic is shown in Figure 6.7. A beam of electrons is emitted by the cathode ray tube. The output of the oscilloscope is a signal trace on the screen of the instrument, created by the impact of the electrons on a phosphorescent coating on the screen. Because an electron beam is composed of charged particles, it can be guided by an electrical field. In the case of the oscilloscope, pairs of plates are oriented horizontally and vertically to control the location of the impact of the electron beam on the screen. The beam sweeps horizontally across the screen at a known speed or frequency. Input voltages to the oscilloscope result in vertical deflections of the beam, and produce a trace of the voltage variations (vertical or y axis) versus time (horizontal or x axis) on the screen. The horizontal sweep frequency can be varied over a wide range, and the operation of the oscilloscope is such that high-frequency waveforms can be resolved.

A digital oscilloscope, such as shown in Figure 6.8a, also provides an analog representation of the measured signal. But it does so by first sampling the signal to convert it into a digital form and then reconstructing the signal on a phosphorous or liquid-crystal display (LCD) screen as an analog

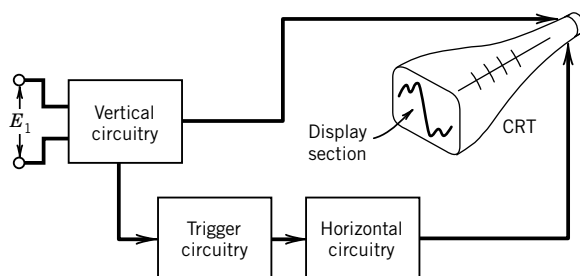


Figure 6.7 Schematic of basic cathode-ray tube oscilloscope.

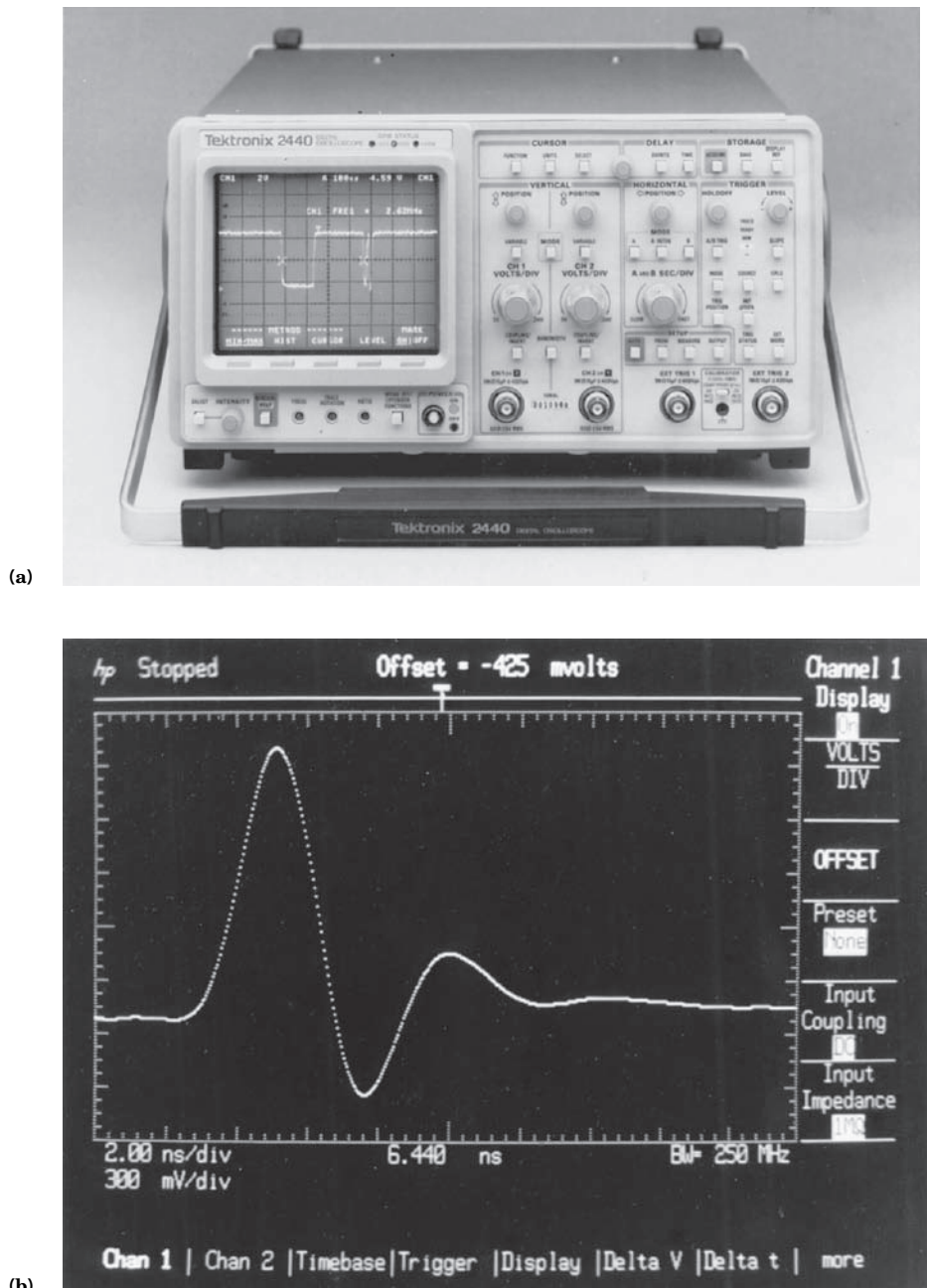


Figure 6.8 (a) Digital oscilloscope. (Photograph courtesy of Tektronix, Inc.) (b) Oscilloscope output. (Photograph courtesy of Hewlett-Packard Company.)

output, just as does a common LCD computer monitor. In this way, the digital oscilloscope measures and stores voltage in a digital manner but then displays it in an analog format as a sequence of measured points, as shown in Figure 6.8b. The amplifier and time base controls are interpreted as with the analog oscilloscope. These common lab devices can be found as small and very portable packages and are often a virtual software component of a 12- to 18-bit analog-to-digital converter data acquisition system. Analog-to-digital sampling techniques used to measure voltages are discussed in Chapter 7.

The LabView interactive program (virtual instrument) called *Oscilloscope* is available with the companion software. It features a basic two-channel oscilloscope. The user can vary channel displayed and the time sweep and gain using two built-in signals (sine wave and square wave) and an active signal trigger.

Example 6.2

We can pick the requirements for an oscilloscope based on the intended signal to be measured. For example, in the USB 1.1 protocol for data transmission, a single frame of data lasts for 1 ms with data transmitted serially at 12 Mbps (million bits per second). We can simplify this as trying to capture a 12 MHz square wave for 1 ms on the oscilloscope screen to base our requirements.

From the discussions of Chapter 2, we know that we need at least five harmonics to reconstruct a square wave with any reasonable fidelity, so that the sampling rate required to reconstruct a 12 MHz square wave is at least five times the fundamental frequency or at least 60 MHz (i.e., 60×10^6 samples/s). So that sets the lowest value on oscilloscope response. The storage capacity of the digital oscilloscope required to capture one frame of the USB data signal is 60×10^6 samples/s $\times 0.001$ s or 60,000 samples at 60 MHz. For comparison of potential oscilloscope needs, the more common USB 2.0 transmits at a nominal 480 Mbps and the new USB 3.0 transmits at 4.8 Gbps (i.e., 4.8×10^9 samples/sec).

Potentiometer

The *potentiometer*² is a device used to measure DC voltages that are in the microvolt to millivolt range. Equivalent to a balance scale, a potentiometer balances an unknown input voltage against a known internal voltage until both sides are equal. A potentiometer is a null balance instrument in that it drives the loading error to essentially zero. Potentiometers have been supplanted by digital voltmeters, which are deflection mode devices but have very high input impedances so as to keep loading errors small, even at low-level voltages.

Voltage Divider Circuit

A general purpose component found in the potentiometer circuit is the *voltage divider circuit* shown in Figure 6.9. The point labeled *A* in Figure 6.9 represents a sliding contact, which makes an

²The term “potentiometer” is used in several different ways: a sliding contact precision variable resistor, the divider circuit in Figure 6.9, and a high-precision circuit used as a voltage measuring instrument.

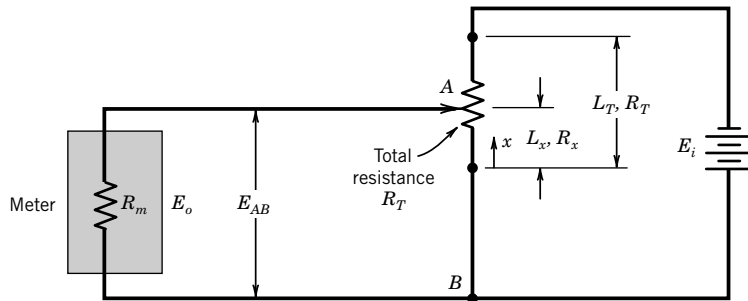


Figure 6.9 Voltage divider circuit.

electrical connection with the resistor R . The resistance between points A and B in the circuit is a linear function of the distance from A to B . So the output voltage sensed by the meter is given by

$$E_o = \frac{L_x}{L_T} E_i = \frac{R_x}{R_T} E_i \quad (6.8)$$

which holds so long as the internal resistance of the meter, R_m , is very large relative to R_T .

Potentiometer Instruments

A simple potentiometer measuring instrument can be derived from the voltage divider circuit as shown in Figure 6.10. In this arrangement a current-sensing device, such as a galvanometer, is used to detect current flow; any current flow through the galvanometer, G , would be a result of an imbalance between the measured voltage, E_m , and the voltage imposed across points A to B , E_{AB} . The voltage E_{AB} is adjusted by moving the sliding contact A ; if this sliding contact is calibrated in terms of a known supply voltage, E_i , the circuit may be used to measure voltage by creating a balanced condition, indicated by a zero current flow through the galvanometer. A null balance, corresponding to zero current flow through G , occurs only when $E_m = E_{AB}$. With a known and constant supply voltage E_i , the position of A can be calibrated to indicate E_m directly, as suggested by Equation 6.8.

A practical potentiometer includes a means for setting the supply voltage E_i . One way uses a separate divider circuit to adjust the output from a cheap, replaceable battery to equal the fixed, known output from a standard voltage cell. This way, the replaceable battery is used for subsequent measurements. Potentiometer instruments can have systematic uncertainties of $<1\text{ }\mu\text{V}$ and random uncertainties $<0.2\text{ }\mu\text{V}$.

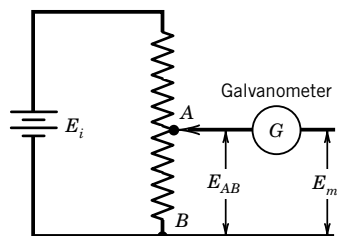


Figure 6.10 Basic potentiometer circuit.

6.4 ANALOG DEVICES: RESISTANCE MEASUREMENTS

Resistance measurements may range from simple continuity checks, to determining changes in resistance on the order of $10^{-6} \Omega$, to determining absolute resistance ranging from 10^{-5} to $10^{15} \Omega$. As a result of the tremendous range of resistance values that have practical application, numerous measurement techniques that are appropriate for specific ranges of resistance or resistance changes have been developed. Some of these measurement systems and circuits provide necessary protection for delicate instruments, allow compensation for changes in ambient conditions, or accommodate changes in transducer reference points. In addition, the working principle of many transducers is a change in resistance relative to a change in the measured variable. We will discuss the measurement of resistance using basic techniques of voltage and current measurement in conjunction with Ohm's law.

Ohmmeter Circuits

A simple way to measure resistance is by imposing a voltage across the unknown resistance and measuring the resulting current flow where $R = E/I$. Clearly, from Ohm's law the value of resistance can be determined in a circuit such as in Figure 6.11, which is the basis of a common analog ohmmeter. Practical analog ohmmeters use circuits similar to those shown in Figure 6.12, which use shunt resistors and a D'Arsonval mechanism for measuring a wide range of resistance while limiting the flow of current through the meter movement. In this technique, the lower limit on the measured resistance R_1 is determined by the upper limit of current flow through it, that is, I_1 . A practical limit to the maximum current flow through a resistance is imposed by the ability of the resistance element to dissipate the power generated by the flow of current (I^2R heating). For example, the limiting ability of a thin metallic conductor to dissipate heat is the principle on which fuses are based. At too large a value of I_1 , they melt. The same is true for delicate, small resistance sensors!

Bridge Circuits

A variety of bridge circuits have been devised for measuring capacitance, inductance, and, most often, resistance. A purely resistive bridge, called a *Wheatstone bridge*, provides a means for

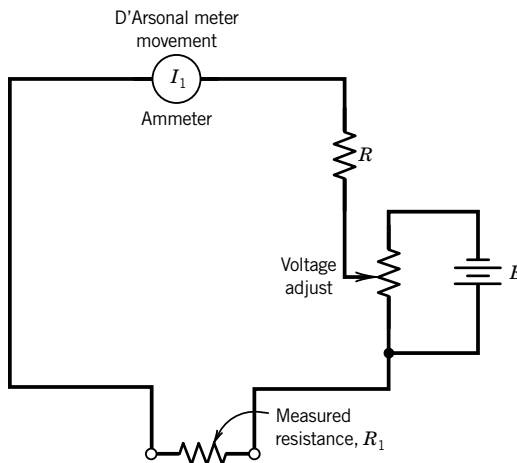


Figure 6.11 Basic analog ohmmeter (voltage is adjusted to yield full-scale deflection with terminals shorted).

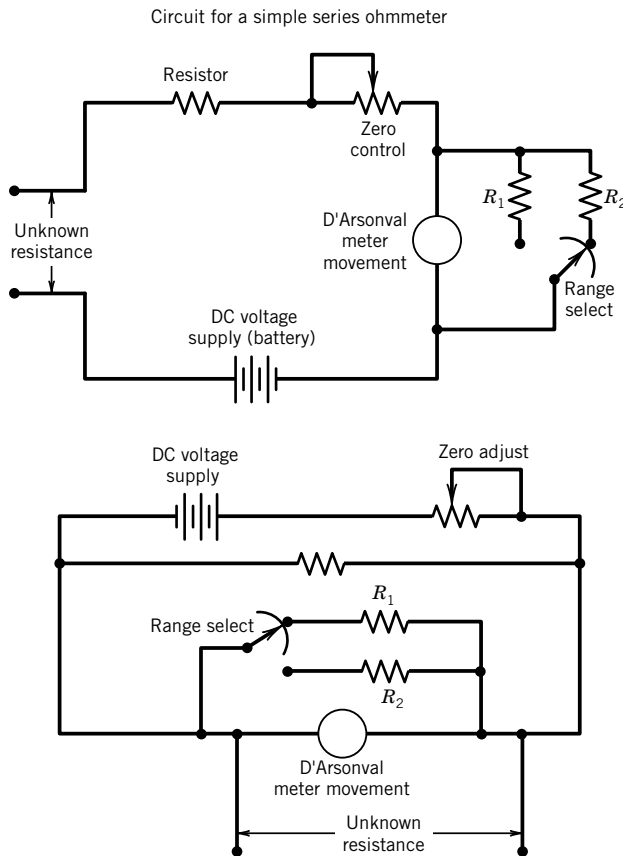


Figure 6.12 Multirange ohmmeter circuits.

accurately measuring resistance, and for detecting very small changes in resistance. Figure 6.13 shows the basic arrangement for a bridge circuit, where R_1 is a sensor that experiences a change in resistance associated with a change in some physical variable. A DC voltage is applied as an input across nodes A to D, and the bridge forms a parallel circuit arrangement between these two nodes. The currents flowing through the resistors R_1 to R_4 are I_1 to I_4 , respectively. Under the condition that the current flow through the galvanometer, I_g , is zero, the bridge is in a balanced condition (alternatively, a current-sensing digital voltmeter might be used in place of the galvanometer). A specific relationship exists between the resistances that form the bridge at balanced conditions. To find this relationship, let $I_g = 0$. Under this balanced condition, there is no voltage drop from B to C and

$$\begin{aligned} I_1R_1 - I_3R_3 &= 0 \\ I_2R_2 - I_4R_4 &= 0 \end{aligned} \tag{6.9}$$

Under balanced conditions, the current through the galvanometer is zero, and the currents through the arms of the bridge are equal:

$$I_1 = I_2 \quad \text{and} \quad I_3 = I_4 \tag{6.10}$$

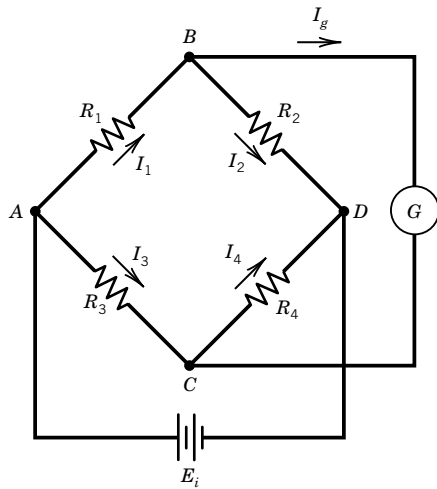


Figure 6.13 Basic current-sensitive Wheatstone bridge circuit (G , galvanometer).

Solving Equations 6.9 simultaneously, with the condition stated in Equation 6.10, yields the necessary relationship among the resistances for a balanced bridge:

$$\frac{R_2}{R_1} = \frac{R_4}{R_3} \quad (6.11)$$

Resistance and resistance change can be measured in one of two ways with this bridge circuit. If the resistor R_1 varies with changes in the measured physical variable, one of the other arms of the bridge can be adjusted to null the circuit and determine resistance. Another method uses a voltage measuring device to measure the voltage unbalance in the bridge as an indication of the change in resistance. Both of these methods will be analyzed further.

Null Method

Consider the circuit shown in Figure 6.13, where R_2 is an adjustable variable resistance. If the resistance R_1 changes due to a change in the measured variable, the resistance R_2 can be adjusted to compensate so that the bridge is once again balanced. In this null method of operation, the resistance R_2 must be a calibrated variable resistor, such that adjustments to R_2 directly indicate the value of R_1 . The balancing operation may be accomplished either manually or automatically through a closed-loop controller circuit. An advantage of the null method is that the applied input voltage need not be known, and changes in the input voltage do not affect the accuracy of the measurement. In addition, the current detector or controller need only detect if there is a flow of current, not measure its value.

However, even null methods are limited. Earlier in this section, we assumed that the galvanometer current was exactly zero when the bridge was balanced. In fact, because the resolution of the galvanometer is limited, the current cannot be set exactly to zero. Consider a bridge that has been balanced within the sensitivity of the meter, such that I_g is smaller than the smallest current detectable. This current flow due to the meter resolution is a loading error with an associated (systematic) uncertainty in the measured resistance, u_R . A basic analysis of the circuit with a current

flow through the galvanometer yields

$$\frac{u_R}{R_1} = \frac{I_g(R_1 + R_g)}{E_i} \quad (6.12)$$

where R_g is the internal resistance of the galvanometer. Alternatively, if a current-sensing digital voltmeter is used, then the input bias current from this meter remains and a small offset voltage is present as a loading error.

Equation 6.12 can serve to guide the choice in a galvanometer or digital meter and a battery voltage for a particular application. Clearly, the range of error is reduced by increased input voltages. However, the input voltage is limited by the power-dissipating capability of the resistance device, R_1 . The power that must be dissipated by this resistance is $I_1^2 R_1$.

Deflection Method

In an unbalanced condition, the magnitude of the current or voltage drop for the meter portion of the bridge circuit is a direct indication of the change in resistance of one or more of the arms of the bridge. Consider first the case where the voltage drop from node B to node C in the basic bridge is measured by a meter with infinite internal impedance, so that there is no current flow through the meter, as shown in Figure 6.14. Knowing the conditions for a balanced bridge given in Equation 6.10, the voltage drop from B to C can be determined, since the current I_1 must equal the current I_2 , as

$$E_o = I_1 R_1 - I_3 R_3 \quad (6.13)$$

Under these conditions, substituting Equations 6.9 to 6.11 into Equation 6.13 yields

$$E_o = E_i \left(\frac{R_1}{R_1 + R_2} - \frac{R_3}{R_3 + R_4} \right) \quad (6.14)$$

The bridge is usually initially balanced at some reference condition. Any transducer resistance change, as a result of a change in the measured variable, would then cause a deflection in the bridge voltage away from the balanced condition. Assume that from an initially balanced condition where $E_o = 0$, a change in R_1 occurs to some new value, $R'_1 = R_1 + \delta R$. The output from

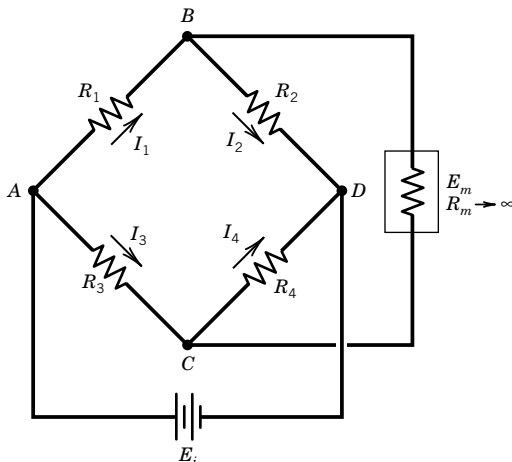


Figure 6.14 Voltage-sensitive Wheatstone bridge.

the bridge becomes

$$E_o + \delta E_o = E_i \left(\frac{R'_1}{R'_1 + R_2} - \frac{R_3}{R_3 + R_4} \right) = E_i \frac{R'_1 R_4 - R_3 R_2}{(R'_1 + R_2)(R_3 + R_4)} \quad (6.15)$$

In many designs the bridge resistances are initially equal. Setting $R_1 = R_2 = R_3 = R_4 = R$ allows Equation 6.15 to be reduced to

$$\frac{\delta E_o}{E_i} = \frac{\delta R/R}{4 + 2(\delta R/R)} \quad (6.16)$$

In contrast to the null method of operation of a Wheatstone bridge, the deflection bridge requires a meter capable of accurately indicating the output voltage, as well as a stable and known input voltage. But the bridge output should follow any resistance changes over any frequency input, up to the frequency limit of the detection device! So a deflection mode is often used to measure time-varying signals.

If the high-impedance voltage measuring device in Figure 6.14 is replaced with a relatively low-impedance current measuring device and the bridge is operated in an unbalanced condition, a current-sensitive bridge circuit results. Consider Kirchhoff's laws applied to the Wheatstone bridge circuit for a current-sensing device with resistance R_g . The input voltage is equal to the voltage drop in each arm of the bridge,

$$E_i = I_1 R_1 + I_2 R_2 \quad (6.17)$$

but $I_2 = I_1 - I_g$, which gives

$$E_i = I_1(R_1 + R_2) - I_g R_2 \quad (6.18)$$

If we consider the voltage drops in the path through R_1 , R_g , and R_3 , the total voltage drop must be zero:

$$I_1 R_1 + I_g R_g - I_3 R_3 = 0 \quad (6.19)$$

For the circuit formed by R_g , R_4 , and R_2 ,

$$I_g R_g + I_4 R_4 - I_2 R_2 = 0 \quad (6.20)$$

or with $I_2 = I_1 - I_g$ and $I_4 = I_3 + I_g$,

$$I_g R_g + (I_3 + I_g) R_4 - (I_1 - I_g) R_2 = 0 \quad (6.21)$$

Equations 6.18 to 6.21 form a set of three simultaneous equations in the three unknowns I_1 , I_g , and I_3 . Solving these three equations for I_g yields

$$I_g = \frac{E_i(R_1 R_4 - R_2 R_3)}{R_1 R_4(R_2 + R_3) + R_2 R_3(R_1 + R_4) + R_g(R_1 + R_2)(R_3 + R_4)} \quad (6.22)$$

and $E_o = I_g R_g$. Then, the change in resistance of R_1 can be found in terms of the bridge deflection voltage, E_o , by

$$\frac{\delta R}{R_1} = \frac{(R_3/R_1)[E_o/E_i + R_2/(R_2 + R_4)]}{1 - E_o/E_i - R_2/(R_2 + R_4)} - 1 \quad (6.23)$$

Consider the case when all of the resistances in the bridge are initially equal to R , and subsequently R_1 changes by an amount δR . The current through the meter is given by

$$I_g = E_i \frac{\delta R/R}{4(R + R_g)} \quad (6.24)$$

and the output voltage is given by $E_o = I_g R_g$

$$E_o = E_i \frac{\delta R/R}{4(1 + R/R_g)} \quad (6.25)$$

The bridge impedance can affect the output from a constant voltage source having an internal resistance R_s . The effective bridge resistance, based on a Thévenin equivalent circuit analysis, is given by

$$R_B = \frac{R_1 R_3}{R_1 + R_3} + \frac{R_2 R_4}{R_2 + R_4} \quad (6.26)$$

such that for a power supply of voltage E_s

$$E_i = \frac{E_s R_B}{R_s + R_B} \quad (6.27)$$

In a similar manner, the bridge impedance can affect the voltage indicated by the voltage-measuring device. For a voltage-measuring device of internal impedance R_g , the actual bridge deflection voltage, relative to the indicated voltage, E_m , is

$$E_o = \frac{E_m}{R_g} \left(\frac{R_1 R_2}{R_1 + R_2} + \frac{R_3 R_4}{R_3 + R_4} + R_g \right) \quad (6.28)$$

The difference between the measured voltage E_m and the actual voltage E_o is a loading error, in this case due to the bridge impedance load. Loading errors are discussed next.

Example 6.3

A certain temperature sensor experiences a change in electrical resistance with temperature according to the equation

$$R = R_o [1 + \alpha(T - T_o)] \quad (6.29)$$

where

R = sensor resistance (Ω)

R_o = sensor resistance at the reference temperature, T_o (Ω)

T = temperature ($^{\circ}\text{C}$)

T_o = reference temperature (0°C)

α = the constant $0.00395^{\circ}\text{C}^{-1}$

This temperature sensor is connected in a Wheatstone bridge like the one shown in Figure 6.13, where the sensor occupies the R_1 location, and R_2 is a calibrated variable resistance. The bridge is operated using the null method. The fixed resistances R_3 and R_4 are each equal to $500\ \Omega$. If the

temperature sensor has a resistance of 100Ω at 0°C , determine the value of R_2 that would balance the bridge at 0°C .

KNOWN $R_1 = 100 \Omega$
 $R_3 = R_4 = 500 \Omega$

FIND R_2 for null balance condition

SOLUTION From Equation 6.11, a balanced condition for this bridge would be achieved when $R_2 = R_1R_4/R_3$ or $R_2 = 100 \Omega$. Notice that to be a useful circuit, R_2 must be adjustable and provide an indication of its resistance value at any setting.

Example 6.4

Consider a deflection bridge, which initially has all four arms of the bridge equal to 100Ω , with the temperature sensor described in Example 6.3 again as R_1 . The input or supply voltage to the bridge is 10 V. If the temperature of R_1 is changed such that the bridge output is 0.569 V, what is the temperature of the sensor? How much current flows through the sensor and how much power must it dissipate?

KNOWN $E_i = 10 \text{ V}$

Initial (reference) state: $R_1 = R_2 = R_3 = R_4 = 100 \Omega$

$$E_o = 0 \text{ V}$$

Deflection state: $E_o = 0.569 \text{ V}$

ASSUMPTION Voltmeter has infinite input impedance but source has negligible impedance ($E_s = E_i$).

FIND T_1, I_1, P_1

SOLUTION The change in the sensor resistance can be found from Equation 6.16 as

$$\frac{\delta E_o}{E_i} = \frac{\delta R/R}{4 + 2(\delta R/R)} \Rightarrow \frac{0.569}{10} = \frac{\delta R}{400 + 2\delta R}$$

$$\delta R = 25.67 \Omega$$

This gives a total sensor resistance of $R_1 + \delta R = 125.7 \Omega$, which equates to a sensor temperature of $T_1 = 65^\circ\text{C}$.

To determine the current flow through the sensor, consider first the balanced case where all the resistances are equal to 100Ω . The equivalent bridge resistance R_B is simply 100Ω and the total current flow from the supply, $E_i/R_B = 100 \text{ mA}$. Thus, at the initially balanced condition, the current flow through each arm of the bridge and through the sensor is 50 mA. If the sensor resistance changes to 125.67Ω , the current will be reduced. If the output voltage is measured by a high-impedance device, such that the current flow to the meter is negligible, the current flow through the sensor is given by

$$I_1 = E_i \frac{1}{(R_1 + \delta R) + R_2} \quad (6.30)$$

This current flow is then 44.3 mA.

The power, $P_1 = I_1^2(R_1 + \delta R)$, that must be dissipated from the sensor is 0.25 W, which, depending on the surface area and local heat transfer conditions, may cause a change in the temperature of the sensor.

COMMENT The current flow through the sensor results in a sensor temperature higher than would occur with zero current flow due to I^2R heating. This is a loading error that offsets the indicated temperature, a systematic error. There is a trade-off between the increased sensitivity, dE_o/dR_1 , and the correspondingly increased current associated with E_1 . The input voltage must be chosen appropriately for a given application.

6.5 LOADING ERRORS AND IMPEDANCE MATCHING

In an ideal sense, an instrument or measurement system should not in itself affect the variable being measured. Any such effect will alter the variable and be considered as a “loading” that the measurement system exerts on the measured variable. A *loading error* is the difference between the value of the measurand and the indicated value brought on by the act of measurement. Loading effects can be of any form: mechanical, electrical, or optical. When the insertion of a sensor into a process somehow changes the physical variable being measured, that is a loading error. A loading error can occur anywhere along the signal path of a measurement system. If the output from one system stage is in any way affected by the subsequent stage, then the signal is affected by *interstage loading error*. Good measurement system design minimizes all loading errors.

To illustrate this idea, consider measuring the temperature of a volume of a high-temperature liquid using a mercury-in-glass thermometer. Some finite quantity of energy must flow from the liquid to the thermometer to achieve thermal equilibrium between the thermometer and the liquid (i.e., the thermometer may cool down or heat up the liquid). As a result of this energy flow, the liquid temperature is changed, and the measured value does not correspond to the initial liquid temperature sought. This measurement has introduced a loading error.

Or consider the current flow that drives the galvanometer in the Wheatstone bridge of Figure 6.13. Under deflection conditions, some energy must be removed from the circuit to deflect the pointer. This reduces the current in the circuit, bringing about a loading error in the measured resistance. On the other hand, under null balance conditions, there is no perceptible pointer deflection, and so a negligible amount of current is removed from the circuit. There is then negligible loading error.

In general, null balance techniques minimize the magnitude of loading error to negligible levels. Deflection methods derive energy from the process being measured. Therefore, deflection methods need careful consideration to make sure the resulting loading errors are kept to an acceptable level.

Loading Errors for Voltage-Dividing Circuit

Consider the voltage-divider circuit shown in Figure 6.9 for the case where R_m is finite. Under these conditions, the circuit can be represented by the equivalent circuit shown in Figure 6.15. As the sliding contact at point A moves, it divides the full-scale deflection resistance R into R_1 and R_2 , such

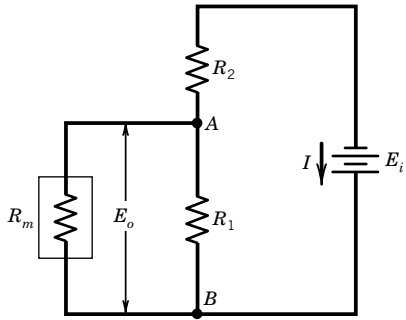


Figure 6.15 Instruments in parallel to signal path form an equivalent voltage-dividing circuit.

that $R_1 + R_2 = R_T$. The resistances R_m and R_1 form a parallel loop, yielding an equivalent resistance, R_L , given by

$$R_L = \frac{R_1 R_m}{R_1 + R_m} \quad (6.31)$$

The equivalent resistance for the entire circuit, as seen from the voltage source, is R_{eq} :

$$R_{\text{eq}} = R_2 + R_L = R_2 + \frac{R_1 R_m}{R_1 + R_m} \quad (6.32)$$

The current flow from the voltage source is then

$$I = \frac{E_i}{R_{\text{eq}}} = \frac{E_i}{R_2 + R_1 R_m / (R_1 + R_m)} \quad (6.33)$$

and the output voltage is given by

$$E_o = E_i - IR_2 \quad (6.34)$$

This result can be expressed as

$$\frac{E_o}{E_i} = \frac{1}{1 + (R_2/R_1)(R_1/R_m + 1)} \quad (6.35)$$

The limit of this expression as R_m tends to infinity is

$$\frac{E_o}{E_i} = \frac{R_1}{R_1 + R_2} \quad (6.36)$$

which is just Equation 6.8. Also, as R_2 approaches zero, the output voltage approaches the supply voltage, as expected. Expressing the value found from Equation 6.8 as the true value (E_o/E_i), the loading error e_I may be given by

$$e_I = E_i \left[\left(\frac{E_o}{E_i} \right) - \left(\frac{E_o}{E_i} \right)' \right] \quad (6.37)$$

Here the loading error goes to zero as $R_m \rightarrow \infty$. Hence, a high meter resistance reduces loading error in voltage measurements.

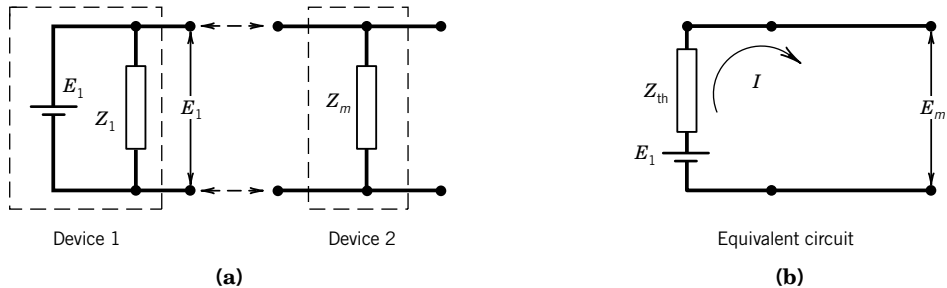


Figure 6.16 Equivalent circuit formed by interstage (parallel) connections.

Interstage Loading Errors

Consider the common situation of Figure 6.16, in which the output voltage signal from one measurement system device provides the input to the following device. The open circuit potential E_1 is present at the output terminal of device 1 with output impedance Z_1 . However, the output signal from device 1 provides the input to a second device, which, at its input terminals, has an input impedance Z_m . As shown, the Thévenin equivalent circuit of device 1 consists of a voltage generator, of open circuit voltage E_1 , with internal series impedance Z_1 . Connecting device 2 to the output terminals of device 1 is equivalent to placing Z_m across the Thévenin equivalent circuit. The finite impedance of the second device causes a current, I , to flow in the loop formed by the two terminals, and Z_m acts as a load on the first device. The potential sensed by device 2 is

$$E_m = IZ_m = E_1 \frac{1}{1 + Z_1/Z_m} \quad (6.38)$$

The original potential has been changed due to the interstage connection that has caused a loading error, $e_I = E_m - E_1$,

$$e_I = E_1 \left(\frac{1}{1 + Z_1/Z_m} - 1 \right) \quad (6.39)$$

For a maximum in the voltage potential between stages, it is required that $Z_m \gg Z_1$ such that $e_I \rightarrow 0$. As a practical matter, this can be a challenge to achieve at reasonable cost and some design compromise is inevitable.

When the signal is current driven, the maximum current transfer between devices 1 and 2 is desirable. Consider the circuit shown in Figure 6.17 in which device 2 is current sensitive, such as with a current-sensing galvanometer. The current through the loop indicated by the device 2 is given by

$$I_m = \frac{E_1}{Z_1 + Z_m} \quad (6.40)$$

However, if the measurement device is removed from the circuit, the current is given by the short-circuit value

$$I' = \frac{E_1}{Z_1} \quad (6.41)$$

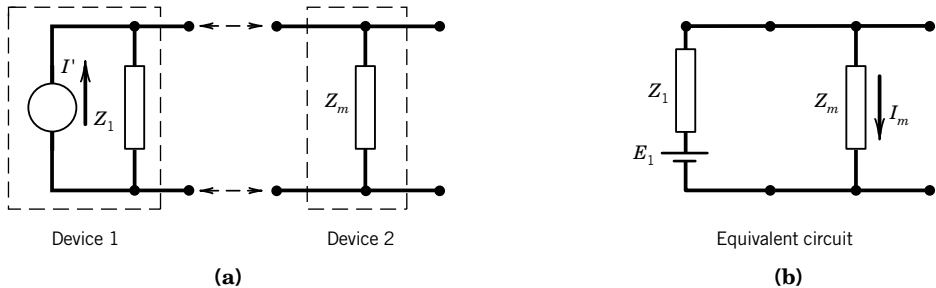


Figure 6.17 Instruments in series with signal path.

The loading error, $e_I = I_m - I'$, is

$$e_I = E_1 \frac{-Z_m}{Z_1^2 + Z_1 Z_m} \quad (6.42)$$

From Equation 6.42 or Equations 6.40 and 6.41, it is clear that to reduce current-driven loading error, then $Z_m \ll Z_1$, such that $e_I \rightarrow 0$.

Example 6.5

For the Wheatstone bridge shown in Figure 6.18, find the open circuit output voltage (when $R_m \rightarrow \infty$) if the four resistances change by

$$\delta R_1 = +40 \Omega \quad \delta R_2 = -40 \Omega \quad \delta R_3 = +40 \Omega \quad \delta R_4 = -40 \Omega$$

KNOWN Measurement device resistance given by R_m

ASSUMPTIONS $R_m \rightarrow \infty$
Negligible source impedance

FIND E_o

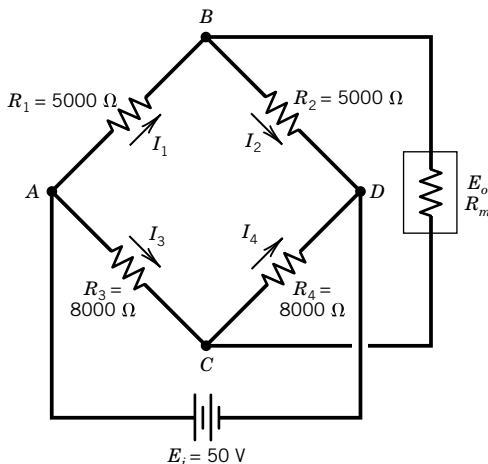


Figure 6.18 Bridge circuit for Example 6.5.

SOLUTION From Equation 6.14

$$\begin{aligned} E_o &= E_i \left(\frac{R_1}{R_1 + R_2} - \frac{R_3}{R_3 + R_4} \right) \\ &= 50 \text{ V} \left(\frac{5040 \Omega}{5040 \Omega + 4960 \Omega} - \frac{8040 \Omega}{8040 \Omega + 7960 \Omega} \right) = +0.0750 \text{ V} \end{aligned}$$

Example 6.6

Now consider the case where a meter with internal impedance $R_m = 200 \text{ k}\Omega$ is used in Example 6.5. What is the output voltage with this particular meter in the circuit? Estimate the loading error.

KNOWN $R_m = 200,000 \Omega$

FIND E_o, e_l

SOLUTION Because the output voltage E_o is equal to $I_m R_m$, where I_m is found from Equation 6.22,

$$E_o = R_g I_m = \frac{E_i R_m (R_1 R_4 - R_2 R_3)}{R_1 R_4 (R_2 + R_3) + R_2 R_3 (R_1 + R_4) + R_m (R_1 + R_2)(R_3 + R_4)}$$

which for $R_m = 200,000 \Omega$, gives $E_o = 0.0726 \text{ V}$.

The loading error e_l is the difference in the two output voltages between infinite meter impedance (Ex. 6.5) and finite meter impedance. This gives $e_l = 0.0726 - 0.0750 = -2.4 \text{ mV}$ with the negative sign reflecting a lower measured value under load.

The bridge output may also be expressed as a ratio of the output voltage with $R_m \rightarrow \infty, E'_o$, and the output voltage with a finite meter resistance E_o :

$$\frac{E_o}{E'_o} = \frac{1}{1 + R_e/R_g}$$

where $R_e = \frac{R_1 R_2}{R_1 + R_2} + \frac{R_3 R_4}{R_3 + R_4}$, which yields for the present example

$$\frac{E_o}{E'_o} = \frac{1}{1 + 6500/200,000} = 0.969$$

The percent loading error, $100 \times \left(\frac{E_o}{E'_o} - 1 \right)$, is -3.15% .

6.6 ANALOG SIGNAL CONDITIONING: AMPLIFIERS

An amplifier is a device that scales the magnitude of an analog input signal according to the relation

$$E_o(t) = h\{E_i(t)\}$$

where $h\{E_i(t)\}$ defines a mathematical function. The simplest amplifier is the linear scaling amplifier in which

$$h\{E_i(t)\} = GE_i(t) \quad (6.43)$$

where the gain G is a constant that may be any positive or negative value. Many other types of operation are possible, including the “base x ” logarithmic amplifier in which

$$h\{E_i(t)\} = G \log_x(E_i(t)) \quad (6.44)$$

Amplifiers have a finite frequency response and limited input voltage range.

The most widely used type of amplifier is the solid-state operational amplifier. This device is characterized by a high input impedance ($Z_i > 10^7 \Omega$), a low output impedance ($Z_o < 100 \Omega$), and a high internal gain ($A_o \approx 10^5$ to 10^6). As shown in the general diagram of Figure 6.19a, an operational amplifier has two input ports, a noninverting and an inverting input, and one output port. The signal at the output port is in phase with a signal passed through the noninverting input port but is 180 degrees out of phase with a signal passed through the inverting input port. The amplifier requires dual-polarity DC excitation power ranging from ± 5 V to ± 15 V. In addition, two DC voltage offset null (bias) input ports provide a means to zero out any output offset signal at zero input; usually a variable $10 \text{ k}\Omega$ resistor is placed across these inputs to adjust offset null.

As an example, the pin connection layout of a common operational amplifier circuit, the type 741, is shown in Figure 6.19b in its eight-pin, dual-in-line ceramic package form. This is the familiar rectangular black integrated circuit package seen on circuit boards. Each pin port is numbered and labeled as to function. An internal schematic diagram is shown in Figure 6.19c with the corresponding pin connections labeled. As shown, each input port (i.e., 2 and 3) is attached to the base of an npn transistor.

The high internal open loop gain, A_o , of an operational amplifier is given as

$$E_o = A_o(E_{i_2}(t) - E_{i_1}(t)) \quad (6.45)$$

The magnitude of A_o , flat at low frequencies, falls off rapidly at high frequencies, but this intrinsic gain curve is overcome by using external input and feedback resistors that set the circuit gain G and circuit response. Some possible amplifier configurations using an operational amplifier are shown in Figure 6.20.

Because the amplifier has a very high internal gain and negligible current draw, resistors R_1 and R_2 are used to form a feedback loop and control the overall amplifier circuit gain, called the *closed loop gain*, G . The noninverting linear scaling amplifier circuit of Figure 6.20a has a closed loop gain of

$$G = \frac{E_o(t)}{E_i(t)} = \frac{R_1 + R_2}{R_2} \quad (6.46)$$

Resistor R_s does not affect the gain but is used to balance out potential variation problems at small currents. Its value is selected such that $R_s \approx R_1 R_2 / (R_1 + R_2)$. The inverting linear scaling amplifier circuit of Figure 6.20b provides a gain of

$$G = \frac{E_o(t)}{E_i(t)} = \frac{R_2}{R_1} \quad (6.47)$$

By utilizing both inputs, the arrangement forms a differential amplifier, Figure 6.20c, in which

$$E_o(t) = (E_{i_2}(t) - E_{i_1}(t))(R_2/R_1) \quad (6.48)$$

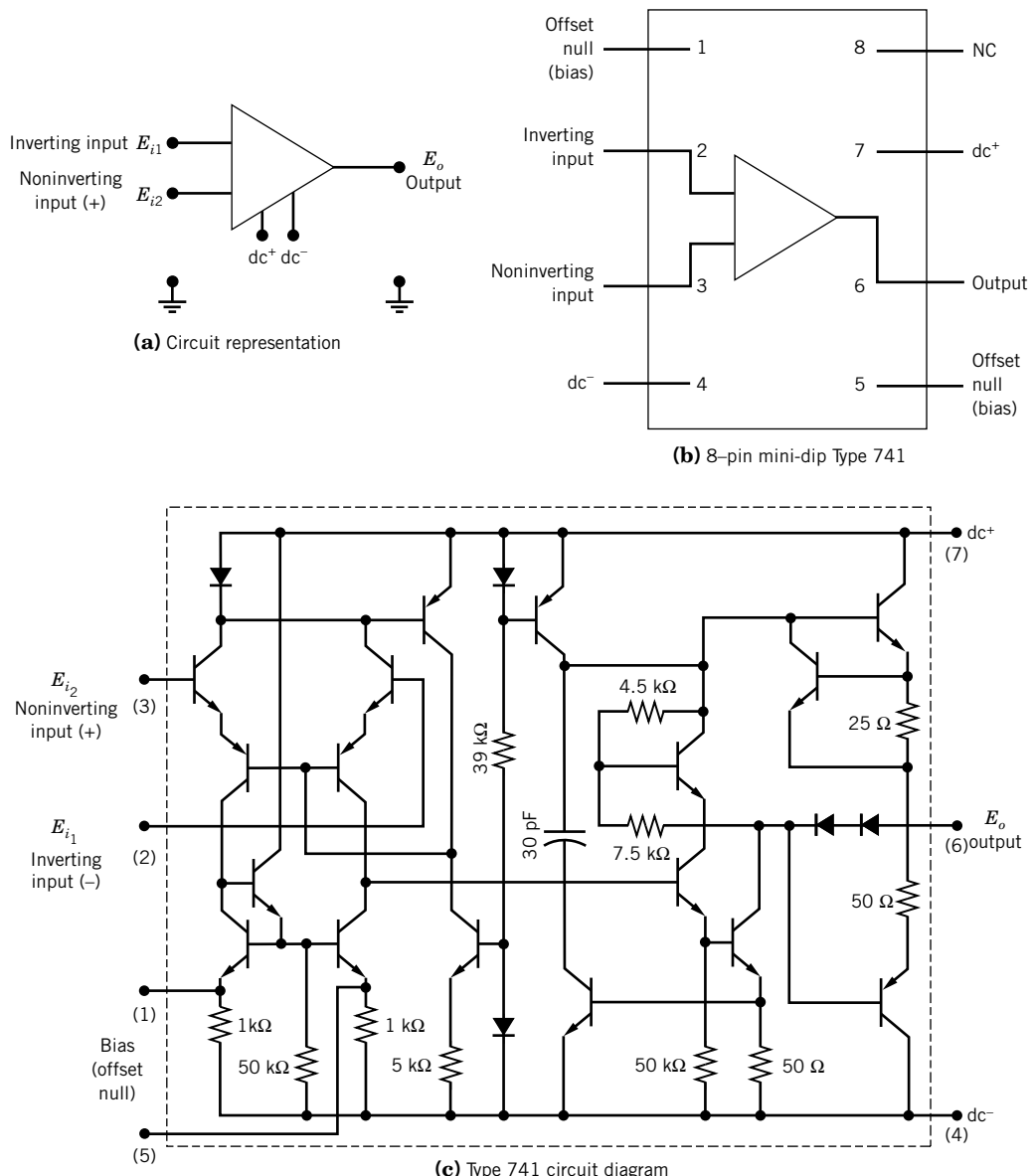


Figure 6.19 Operational amplifier.

The differential amplifier circuit is effective as a voltage comparator for many instrument applications (see Section 6.7).

A voltage follower circuit is commonly used to isolate an impedance load from other stages of a measurement system, such as might be needed with a high-output impedance transducer. A schematic diagram of a voltage follower circuit is shown in Figure 6.20d. Note that the feedback

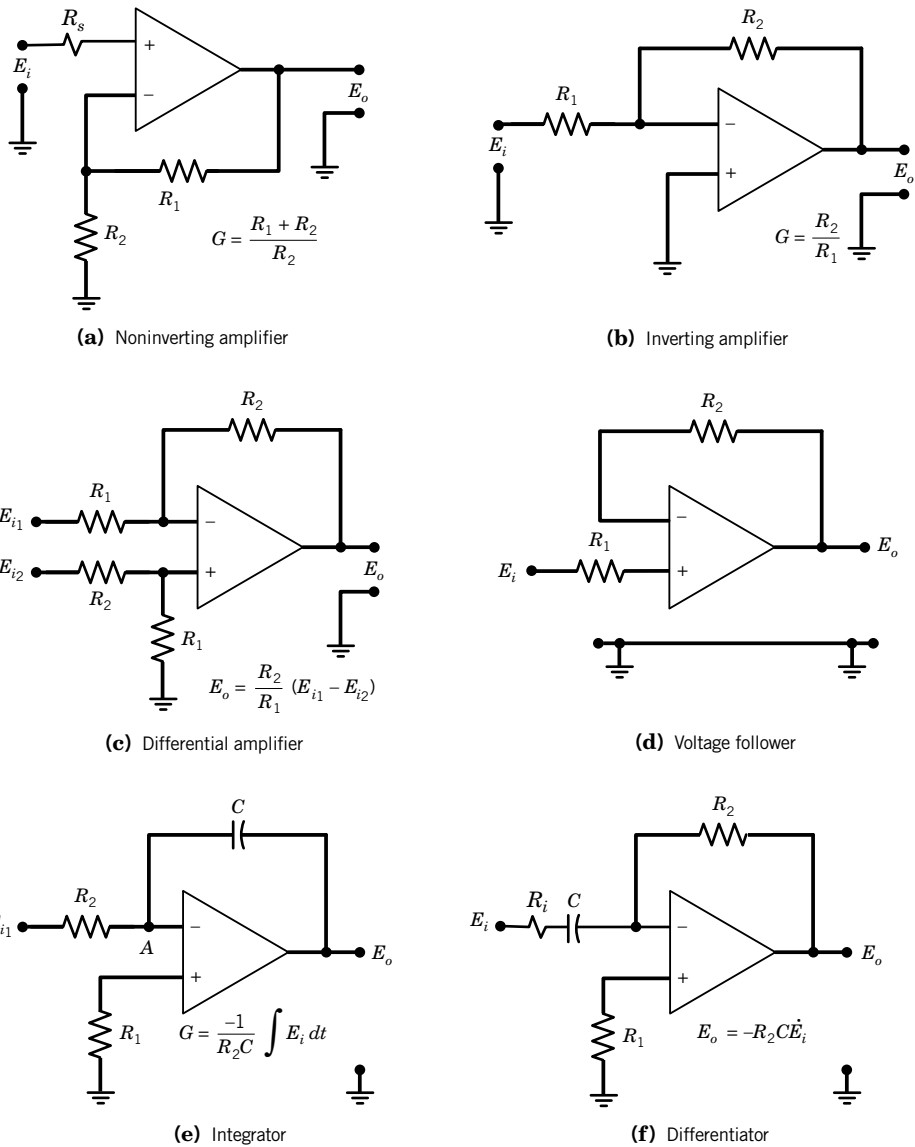


Figure 6.20 Some common amplifier circuits using operational amplifiers.

signal is sent directly to the inverting port. The output for such a circuit, using Equation 6.45, is

$$E_o(t) = A_o(E_i(t) - E_o(t))$$

or writing in terms of the circuit gain, $G = E_o(t)/E_i(t)$,

$$G = \frac{A_o}{1 + A_o} \approx 1 \quad (6.49)$$

Using Kirchhoff's law about the noninverting input loop yields

$$I_i(t)R_1 + E_o(t) = E_i(t)$$

Then the circuit input resistance R_i is

$$R_i = \frac{E_i(t)}{I_i(t)} = \frac{E_i(t)R_1}{E_i(t) - E_o(t)} \quad (6.50)$$

Likewise the output resistance is found to be

$$R_o = \frac{R_2}{1 + A_o} \quad (6.51)$$

Because A_o is large, Equations 6.49 to 6.51 show that the input impedance, developed as a resistance, of the voltage follower can be large, its output impedance can be small, and the circuit will have near unity gain. Acceptable values for R_1 and R_2 range from 10 to 100 kΩ to maintain stable operation.

Input signal integration and differentiation can be performed with the operational amplifier circuits. For the integration circuit in Figure 6.20e, the currents through R_2 and C are given by

$$\begin{aligned} I_{R_2}(t) &= \frac{E_i(t) - E_A(t)}{R_2} \\ I_C(t) &= C \frac{d}{dt}(E_o(t) - E_A(t)) \end{aligned}$$

Summing currents at node A yields the integrator circuit operation:

$$E_o(t) = -\frac{1}{R_2 C} \int E_i(t) dt \quad (6.52)$$

As a special note, if the input voltage is a constant positive DC voltage, then the output signal will be a negative linear ramp, $E_0 = -E_i t / RC$, with t in seconds, a feature used in ramp converters and integrating digital voltmeters (see Section 7.5 in Chapter 7). Integrator circuits are relatively unaffected by high-frequency noise as integration averages out noise.

Following a similar analysis, the differentiator circuit shown in Figure 6.20f performs the operation

$$E_o(t) = -R_2 C \frac{dE_i(t)}{dt} \quad (6.53)$$

Differentiator circuits amplify high-frequency noise in signals to the point of masking the true signal. Adding resistor R_i limits high-frequency gain to a -3 dB cutoff frequency of $f_c = 1/2\pi R_i C$. In noisy environments, a passive RC differentiator may simply perform better.

6.7 ANALOG SIGNAL CONDITIONING: SPECIAL-PURPOSE CIRCUITS

Analog Voltage Comparator

A voltage comparator provides an output that is proportional to the difference between two input voltages. As shown in Figure 6.21a, a basic comparator consists of an operational amplifier operating in a high-gain differential mode. In this case, any difference between inputs E_{i_1} and E_{i_2} is amplified at the large open-loop gain A_o . Accordingly, the output from the comparator saturates

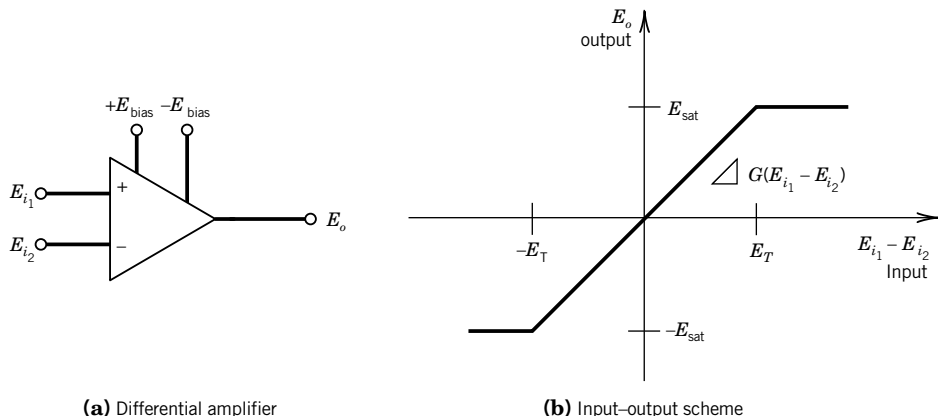


Figure 6.21 Analog voltage comparator.

when $E_{i_1} - E_{i_2}$ is either slightly positive or negative, the actual value set by the threshold voltage E_T . The saturation output value E_{sat} is nearly the supply voltage E_s . For example, a 741 op-amp driven at ± 15 V might saturate at ± 13.5 V. The value for E_T can be adjusted by the amplifier bias (offset null) voltage E_{bias} . The comparator output is given by

$$\begin{aligned} E_o &= A_o(E_{i_1} - E_{i_2}) \quad \text{for} \quad |E_{i_1} - E_{i_2}| \leq E_T \\ &= +E_{\text{sat}} \quad \text{for} \quad E_{i_1} - E_{i_2} > E_T \\ &= -E_{\text{sat}} \quad \text{for} \quad E_{i_1} - E_{i_2} < -E_T \end{aligned} \quad (6.54)$$

This input-output relation is shown in Figure 6.21b. For a ± 15 V supply and a gain of about 200,000, the comparator might saturate with a voltage difference of only $\sim 68 \mu\text{V}$.

Often E_{i_2} is a known reference voltage. This allows the comparator output to be used for control circuits to decide if E_{i_1} is less than or greater than E_{i_2} ; a positive difference gives a positive output. One frequent use of the comparator is in an analog-to-digital converter (see Chapter 7). A zener-diode connected between the + input and the output provides a TTL(transistor-transistor logic) compatible output signal for digital system use.

Sample-and-Hold Circuit

The sample-and-hold circuit (SHC) is used to take a narrow-band measurement of a time-changing signal and to hold that measured value until reset. It is widely used in data acquisition systems using analog-to-digital converters. The circuit tracks the signal until it is triggered to hold it at a fixed value while measuring it. This is illustrated in Figure 6.22a, in which the track-and-hold logic provides the appropriate trigger.

The basic circuit for sample and hold is shown in Figure 6.22b. The switch S_1 is a fast analog device. When the switch is closed, the “hold” capacitor C is charged through the source resistor R_s . When the capacitor is charged, the switch is opened. The amplifier presents a very high input impedance and very low current, which, together with a very low leakage capacitor, allows for a sufficiently long hold time. The typical SHC is noninverting with a unit gain ($G = 1$).

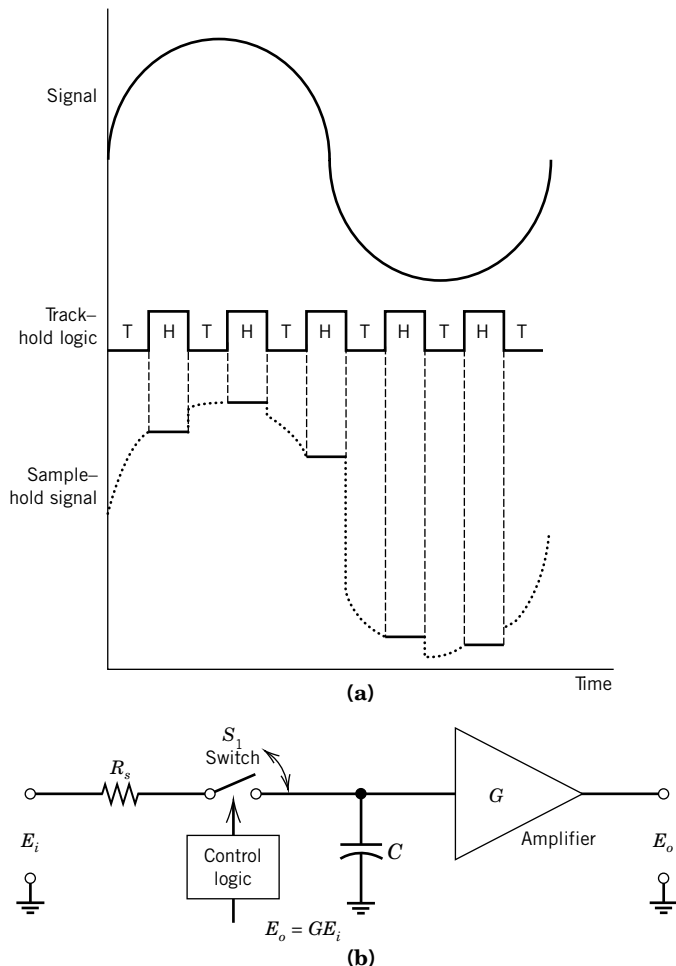


Figure 6.22 Sample and hold technique. (a) Original signal and the sample and hold signal (time intervals exaggerated for illustrative purposes), (b) Circuit.

Charge Amplifier

A *charge amplifier* is used to convert a high-impedance charge q into an output voltage E_o . The circuit consists of a high-gain, inverting voltage operational amplifier such as shown in Figure 6.23. These circuits are commonly used with transducers that utilize piezoelectric crystals or capacitance sensors. A piezoelectric crystal develops a time-dependent surface charge under varying mechanical load.

The circuit output voltage is determined by

$$E_o = -q[C_r + (C_T/A_o)] \quad (6.55)$$

with $C_T = C_t + C_c + C_r$ where C_t , C_c , and C_r represent the transducer, cable, and feedback capacitances, respectively, R_c is the cable and transducer resistances, and A_o is the amplifier

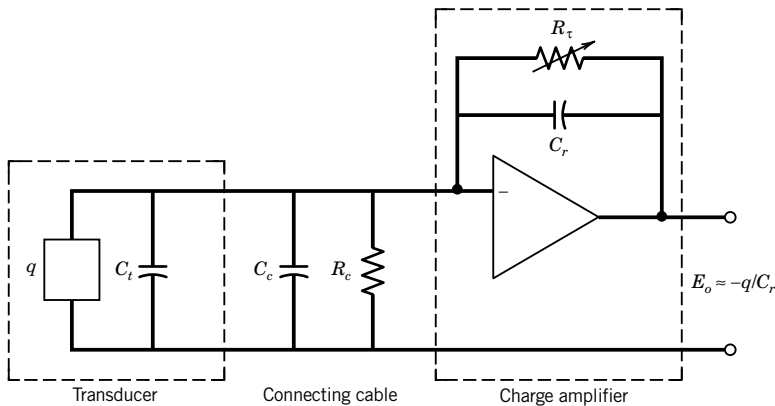


Figure 6.23 Charge amplifier circuit shown connected to a transducer.

open-loop gain. Because the open-loop gain of operational amplifiers is very large, Equation 6.55 can often be simplified to

$$E_o \approx -q/C_r \quad (6.56)$$

A variable resistance R_f and fixed feedback capacitor are used to average out low-frequency fluctuations in the signal.

4–20 mA Current Loop

Low-level voltage signals below about 100 mV are quite vulnerable to noise. Examples of transducers having low-level signals include strain gauges, pressure gauges, and thermocouples. One means of transmitting such signals over long distances is by signal boosting through amplification. But amplification also boosts noise. A practical alternative method that is well suited to an industrial environment is a *4–20 mA current loop* (read as “4 to 20”). In this approach, the low-level voltage is converted into a standard current loop signal of between 4 and 20 mA, the lower value for the minimum voltage and the higher value for the maximum voltage in the range. The 4–20 mA current loop can be transmitted over several hundred meters without degradation. The 4–20 mA output is a common option for transducers.

At the output display end, a receiver converts the current back to a low-level voltage. This can be as simple as a single resistor in parallel with the loop. For example, a 4–20 mA signal can be converted back to a 1–5 V signal by terminating the loop with a $250\ \Omega$ resistor.

Multivibrator and Flip-Flop Circuits

Multivibrator and *flip-flop* circuits are analog circuits that also form the basis of digital signals. They are useful for system control and triggering of events. The *astable multivibrator* is a switching circuit that toggles on and off continuously between a high- and low-voltage state in response to an applied time-dependent input voltage. It is used to generate a square waveform on a prompt, where typically amplitudes vary between 0 V (low) and 5 V (high) in a manner known as a *TTL signal*. Because the circuit continuously switches between high and low state, it is astable. The heart of this

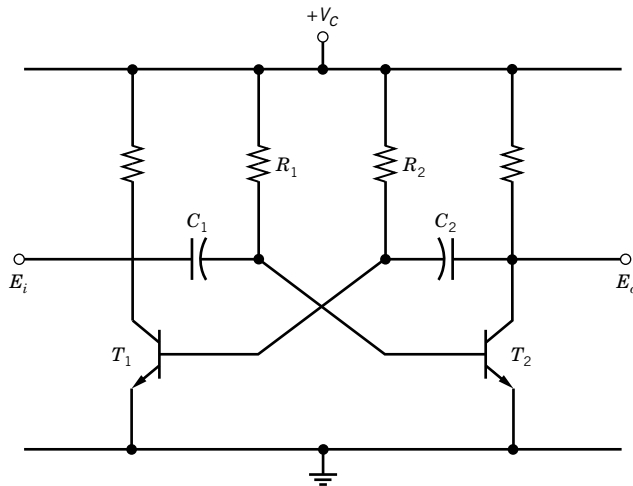
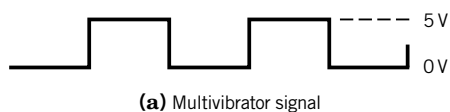


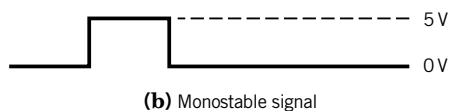
Figure 6.24 Basic multivibrator circuit.

circuit, as shown in Figure 6.24, is the two transistors T_1 and T_2 , which conduct alternately; the circuit is symmetric around the transistors. This generates a square wave signal of fixed period and amplitude at the output as shown in Figure 6.25a. The working mechanism is straightforward. The two transistors change state as the currents through capacitors C_1 and C_2 increase and decrease due to the applied input. For example, when T_2 turns on and its collector switches from V_c toward 0, the base of T_1 is driven negative, which turns T_1 off. While C_2 discharges, C_1 charges. As the voltage across C_1 increases, the current across it decreases. But so long as the current through C_1 is large enough, T_2 remains on. It eventually falls to a value that turns T_2 off. This causes C_2 to charge, which turns T_1 on. The period of the resulting square wave is proportional to R_1C_1 .

A useful variation of the multivibrator circuit is the *monostable*. In this arrangement T_2 stays on until a positive external pulse or change in voltage is applied to the input. At that moment, T_2 turns off for a brief period of time, providing a jump in the output voltage. The monostable circuit cycles



(a) Multivibrator signal



(b) Monostable signal



Figure 6.25 Circuit output response to an applied input signal.

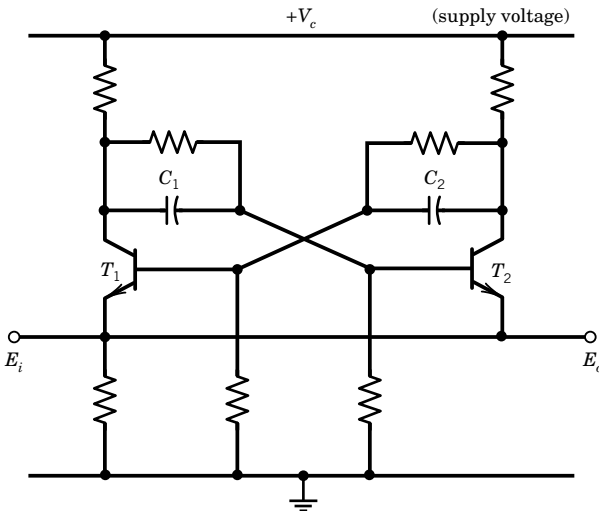


Figure 6.26 Basic flip-flop circuit.

just once, awaiting another pulse as shown in Figure 6.25b. Hence, it is often referred to as a *one-shot*. Because it fires just once and resets itself, the monostable is an effective trigger.

Another variation of this circuit is the *flip-flop* or *bistable multivibrator* in Figure 6.26. This circuit is an effective electronic switch. Its operation is analogous to that of a light switch; it is either in an “on” (high) or an “off” (low) state. In practice, transistors T_1 and T_2 change state every time a pulse is applied. If T_1 is on with T_2 off, a pulse turns T_2 off, turning T_1 on, producing the output shown in Figure 6.25c. So the flip-flop output level changes from low to high voltage or high to low voltage on command. The flip-flop is also the basic circuit of computer memory chips as it is capable of holding a single bit of information (represented by either a high or low state) at any instant.

6.8 ANALOG SIGNAL CONDITIONING: FILTERS

A *filter* is used to remove undesirable frequency information from a dynamic signal. A filter permits signal information associated with a defined band (range) of frequencies to pass, known as the *passband*, while blocking the signal information associated with a band of frequencies, known as the *stopband*. The filter is designed around its cutoff frequency f_c , which fixes the boundary between the *passband* and the *stopband*. Filters can be broadly classified as being low pass, high pass, bandpass, and notch. The ideal gain characteristics of such filters can be described by the magnitude ratio plots shown in Figure 6.27, which are described as follows. A *low-pass filter* permits frequencies below the prescribed cutoff frequency f_c to pass while blocking the passage of frequency information above the cutoff frequency. Similarly, a *high-pass filter* permits only frequency information above the cutoff frequency to pass. A *bandpass filter* combines features of both the low- and high-pass filters. It is described by a low cutoff frequency f_{c1} and a high cutoff frequency f_{c2} to define a band of frequency information that is permitted to pass through the filter. A *notch filter* permits the passage of all frequency information except that within a narrow frequency band. An intensive treatment of filters for analog and digital signals can be found in many specialized texts (3–8).

Filters work by performing a well-defined mathematical operation on the input signal as specified by their transfer function. The transfer function is defined by the position and values of

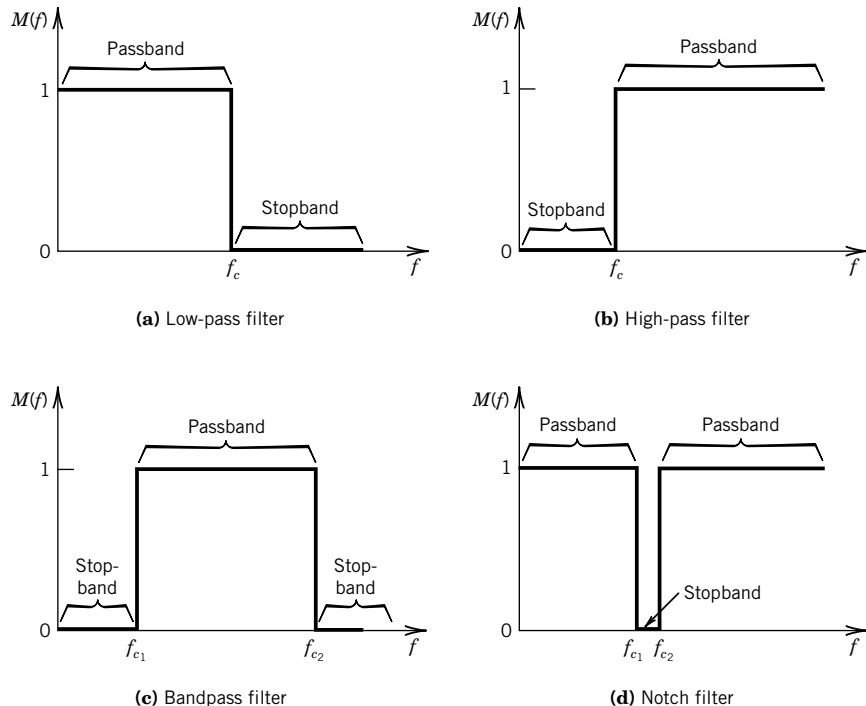


Figure 6.27 Ideal filter characteristics.

elements in the filter design. Passive analog filter circuits consist of combinations of resistors, capacitors, and inductors. Active filters incorporate operational amplifiers into the circuit, as well.

The sharp cutoff of the ideal filter cannot be realized in a practical filter. As an example, a plot of the magnitude ratio for a real low-pass filter is shown in Figure 6.28. All filter response curves contain a transition band over which the magnitude ratio decreases relative to the frequency from the

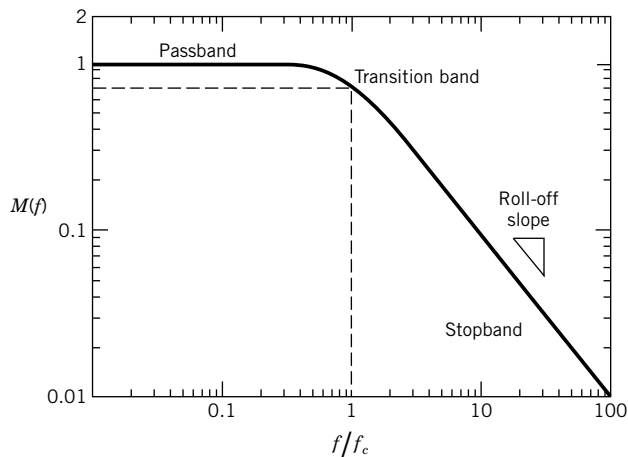


Figure 6.28 Magnitude ratio for a low-pass Butterworth filter.

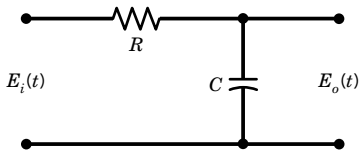


Figure 6.29 Simple first-order low-pass resistor-and-capacitor (RC) Butterworth filter circuit.

passband to the stopband. This rate of transition is known as the filter *roll-off*, usually specified in units of dB/decade. In addition, the filter introduces a phase shift between its input and output signal. The design of real filters is focused on certain desirable response features. The magnitude and phase characteristics of a real filter can be optimized to meet one of the following: (1) maximum magnitude flatness over the passband, (2) a linear phase response over the passband, or (3) a sharp transition from the passband to stopband with steep roll-off. No one filter can meet all three, characteristics but we can design for any one of them. For example, a relatively flat magnitude ratio over its passband with a moderately steep initial roll-off and acceptable phase response is a characteristic of a *Butterworth* filter response. On the other hand, a very linear phase shift over its passband but with a relatively gradual initial roll-off is a characteristic of a *Bessel* filter response. The frequency-dependent behavior of low-pass, bandpass, and high-pass filters can be explored in the LabView programs *Butterworth filters* and *Bessel filters*.

Butterworth Filter Design

A Butterworth filter is optimized to achieve maximum flatness in magnitude ratio over the passband. A simple passive low-pass Butterworth filter can be constructed using the resistor-and-capacitor (RC) circuit of Figure 6.29. By applying Kirchhoff's law about the input loop, we derive the model relating the input voltage E_i to the output voltage E_o :

$$RC\dot{E}_o(t) + E_o(t) = E_i(t) \quad (6.57)$$

This real filter model is a first-order system with one reactive (capacitor) component. Its magnitude and phase response has already been given by Equations 3.9 and 3.10 with $\tau = RC$ and $\omega = 2\pi f$ and its magnitude response is shown in Figure 6.28. The roll-off slope is 20 dB/decade.

A filter is designed around its cutoff frequency f_c , defined as the frequency at which the signal power is reduced by one-half. This is equivalent to the magnitude ratio being reduced to 0.707. In terms of the decibel (dB),

$$\text{dB} = 20 \log M(f) \quad (3.11)$$

f_c occurs at -3 dB, that is, the frequency where the signal is attenuated by 3 dB. For the filter of Figure 6.29, this requires that $\tau = RC = 1/(2\pi f_c)$.

Improved Butterworth Filter Designs

With its simplicity, the RC filter begins to roll off well before the cutoff frequency; the roll-off is not very sharp, and the phase shift response (recall Fig. 3.13) is not linear, leading to potential signal distortion. But the flatness in the passband can be extended and the roll-off slope of a filter improved by staging multiple filters in series, called cascading filters. This is done by adding reactive elements, such as by alternating inductors (L) and capacitors (C), to the circuit as shown in the

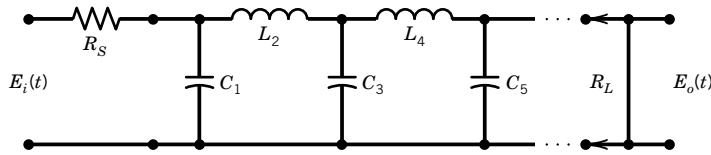


Figure 6.30 Ladder circuit for multistage (cascading) low-pass LC filter to achieve a higher-order response.

resulting LC ladder circuit of Figure 6.30. The resistances R_s and R_L refer to the circuit source and load impedances, respectively. A k th-order or k -stage filter contains k reactive elements in stages. The magnitude ratio and phase shift for a k -stage low-pass Butterworth filter are given by

$$M(f) = \frac{1}{\left[1 + (f/f_c)^{2k}\right]^{1/2}} \quad (6.58a)$$

$$\Phi(f) = \sum_{i=1}^k \Phi_i(k) \quad (6.58b)$$

where f/f_c is the normalized frequency. The general normalized magnitude response curves for k -stage Butterworth filters are shown in Figure 6.31. The roll-off slope is $20 \times k$ (dB/decade) or $6 \times k$ (dB/octave). Frequency-dependent signal attenuation is found from the dynamic error, $\delta(f)$, or directly in decibels by

$$A(f/f_c) = \text{Attenuation(dB)} = 10 \log \left[1 + (f/f_c)^{2k} \right] \quad (6.59)$$

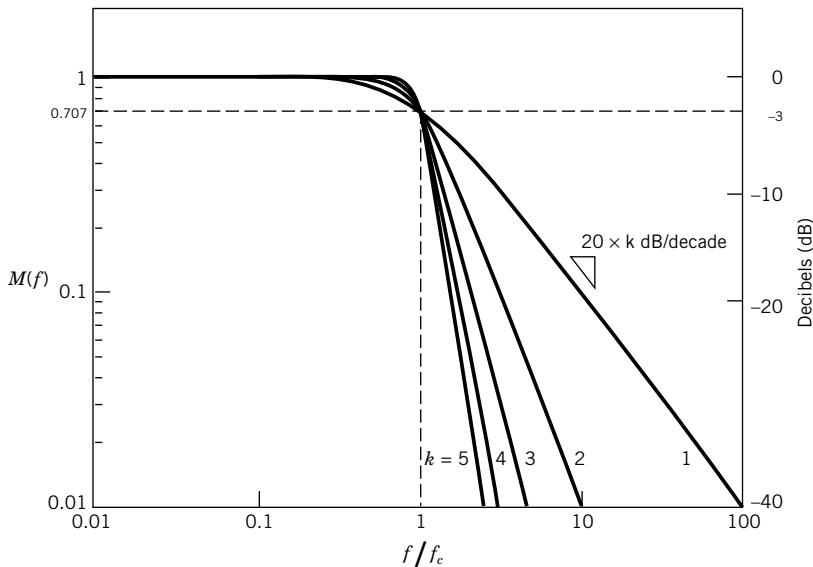


Figure 6.31 Magnitude characteristics for Butterworth low-pass filters of various stages.

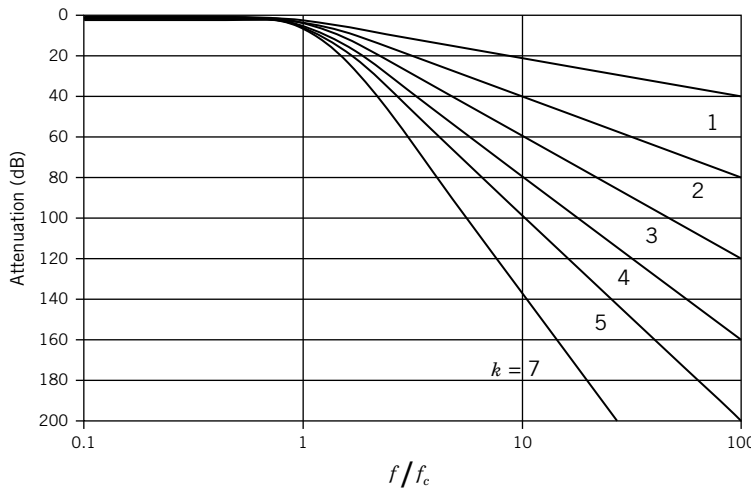


Figure 6.32 Attenuation with various stages of Butterworth filters.

Equation 6.59 is useful for specifying the required order of a filter based on desired response needs. This is emphasized in Figure 6.32, showing how the stages affect attenuation versus normalized frequency.

The specific elements values used in filter design are normalized to accommodate any specific application. To achieve a Butterworth response in the case where $R_L = R_S$, the ladder circuit of Figure 6.30 uses circuit element values based on the scheme

$$C_i = 2 \sin \left[\frac{(2i-1)\pi}{2k} \right] \quad \text{where } i \text{ is odd} \quad (6.60a)$$

$$L_i = 2 \sin \left[\frac{(2i-1)\pi}{2k} \right] \quad \text{where } i \text{ is even} \quad (6.60b)$$

where $i = 1, 2, \dots, k$. Specific values are provided in Table 6.1 for elements C_i and L_i for a two-through five-stage Butterworth filter associated with Figure 6.30 (3, 8). The lead reactive element is assumed to be a capacitor; if the lead reactive element is switched to an inductor (such that L_i is odd),

Table 6.1 Normalized Element Values for Low-Pass LC Butterworth Filter^a (8)

k	C_1	L_2	C_3	L_4	C_5
2	1.414	1.414			
3	1.000	2.000	1.000		
4	0.765	1.848	1.848	0.765	
5	0.618	1.618	2.000	1.618	0.618

^aValues for C_i in farads L_i in henrys are referenced to $R_s = R_L = 1 \Omega$ and $\omega_c = 1 \text{ rad/s}$. See discussion for proper scaling. For $k = 1$, use $C_1 = 1 \text{ F}$ or $L_1 = 1 \text{ H}$.

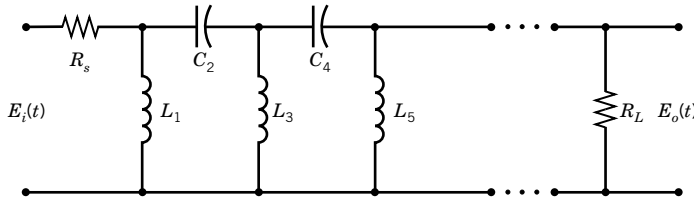


Figure 6.33 Ladder circuit for multistage high-pass LC filter.

then the table values assigned to C and L switch. The values in Table 6.1 are normalized with $R_s = R_L = 1 \Omega$ and $\omega_c = 2\pi f_c = 1 \text{ rad/s}$. For other values, L_i and C_i are scaled by

$$L = L_i R / 2\pi f_c \quad (6.61a)$$

$$C = C_i / (R 2\pi f_c) \quad (6.61b)$$

When $R_L \neq R_s$ the impedances can be properly scaled but the reader is referred to published scaling tables, such as given in reference 8. Butterworth filters are quite common and are found in consumer products such as audio equipment. With their flat passband, they are commonly chosen as anti-aliasing filters for data acquisition systems.

A Butterworth high-pass filter is shown in Figure 6.33. In comparing with Figure 6.30, we see that the capacitors and inductors have been swapped. To estimate the high-pass filter values for Figure 6.33, let $(L_i)_{\text{HP}} = (1/C_i)_{\text{LP}}$ and $(C_i)_{\text{HP}} = (1/L_i)_{\text{LP}}$ where subscript LP refers to the low-pass values from Table 6.1 and HP refers to the high-pass filter values to be used with Figure 6.33. Reflecting this, the scaling values for a high-pass filter are

$$L = R / 2\pi f_c C_i \quad (6.62a)$$

$$C = 1 / 2\pi f_c R L_i \quad (6.62b)$$

The magnitude ratio for a high-pass filter is given by

$$M(f) = \frac{1}{\left[1 + (f_c/f)^{2k}\right]^{1/2}} \quad (6.63)$$

The phase shift properties described by Equation 6.58b apply.

Example 6.7

Design a one-stage Butterworth RC low-pass filter with a cutoff frequency of 100 Hz at -3 dB if the source and load impedances are 50Ω . Calculate the expected dynamic error and attenuation at 192 Hz in the realized filter.

KNOWN $f_c = 100 \text{ Hz}$
 $k = 1$

FIND C and δ

SOLUTION A single-stage low-pass Butterworth RC filter circuit would be similar to that of Figure 6.28, which is just a first-order system with time constant $\tau = RC$. With the relation $\omega = 2\pi f$,

the magnitude ratio for this circuit is given by

$$M(f) = \frac{1}{\left[1 + (\omega\tau)^2\right]^{1/2}} = \frac{1}{\left[1 + (2\pi f\tau)^2\right]^{1/2}} = \frac{1}{\left[1 + (f/f_c)^2\right]^{1/2}}$$

Setting $M(f) = 0.707 = -3$ dB with $f = f_c = 100$ Hz gives

$$\tau = 1/2\pi f_c = RC = 0.0016 \text{ s}$$

With $R = 50 \Omega$, we need a capacitor of $C = 32 \mu\text{F}$.

Alternately, we could use Figure 6.30 and Table 6.1 with $k = 1$ for which the normalized value is $C = 1 \text{ F}$. This value is scaled to $R = 50 \Omega$ and $f_c = 100 \text{ Hz}$ by

$$C = C_1/(R2\pi f_c) = (1\text{F})/(50 \Omega)(2\pi)(100\text{Hz}) = 32 \mu\text{F}$$

A commercially available capacitor size is $33 \mu\text{F}$. Using this size in our realized circuit, the cutoff frequency shifts to 96 Hz. We use $f_c = 96 \text{ Hz}$ below.

At $f = 192 \text{ Hz}$, the dynamic error, $\delta(f) = M(f) - 1$ is

$$\delta(192 \text{ Hz}) = M(192 \text{ Hz}) - 1 = -0.55$$

meaning that the input signal frequency content at 192 Hz is reduced by 55%. The attenuation at the normalized frequency of $f/f_c = 2$ is given by equation 6.59 as

$$A(2) = 10 \log \left[1 + (2)^2 \right] = 46 \text{ dB}$$

Example 6.8

How many filter stages are required to design a low-pass Butterworth filter with a cutoff frequency of 3 kHz if the filter must provide attenuation of at least 60 dB at 30 kHz? If $R_s = R_L = 50 \Omega$, find the filter element values.

KNOWN $f_c = 3 \text{ kHz}; f = 30 \text{ kHz}$

FIND k to achieve $A \geq 60 \text{ dB}$ at 30 kHz

SOLUTION The normalized frequency is $f/f_c = 30,000/3000 = 10$.

$$A(f/f_c = 10) = A(10) = 10 \log \left[1 + (f/f_c)^{2k} \right]$$

We can solve directly for k with $A(10) = 60 \text{ dB}$ to get $k = 3$. Or, using Figure 6.32, we find that $A(10) \geq 60 \text{ dB}$ for $k \geq 3$.

Using the ladder circuit of Figure 6.30 with $R_s = R_L = 1 \Omega$ and $\omega_c = 2\pi f_c = 1 \text{ rad/s}$, Table 6.1 gives $C_1 = C_3 = 1 \text{ F}$ and $L_2 = 2 \text{ H}$. Scaling these to $f_c = 3 \text{ kHz}$ and $R_s = R_L = 50 \Omega$, the element values are

$$L = L_2 R / 2\pi f_c = 5.3 \text{ mH}$$

$$C = C_1 / (R2\pi f_c) = C_3 / (R2\pi f_c) = 106 \mu\text{F}$$

Example 6.9

In a two-speaker (two-way) system, the low-pass circuit passes only low-frequency signal content to the woofer, while the high-pass circuit passes high-frequency content to the wide-frequency speaker.

The Linkwitz–Riley high-pass or low-pass filter demonstrates a practical use of Butterworth filters for loudspeaker designs. The 4th order ($k = 4$) design is a cult standard achieving a 24 dB/octave slope. As shown in Figure 6.34 with component design values listed below, the fourth-order design uses two each of inductors and capacitors in conjunction with the natural impedance of the loudspeaker driver to achieve a high-pass or low-pass design, or the two can be coupled as a band-pass filter.

High-Pass Circuit ^a		Low-Pass Circuit ^a	
C_1 (farad)	$= 0.0844/(R_{L_H} \times f_c)$	C_2 (farad)	$= 0.2533/(R_{L_L} \times f_c)$
C_3 (farad)	$= 0.1688/(R_{L_H} \times f_c)$	C_4 (farad)	$= 0.0563/(R_{L_L} \times f_c)$
L_2 (henry)	$= 0.1000 \times R_{L_H}/f_c$	L_1 (henry)	$= 0.3000 \times R_{L_L}/f_c$
L_4 (henry)	$= 0.04501 \times R_{L_H}/f_c$	L_3 (henry)	$= 0.1500 \times R_{L_L}/f_c$

^a f_c refers to the cutoff frequency for that particular circuit; R_{L_H} and R_{L_L} refer to the impedances of the high and low frequency speakers, respectively.

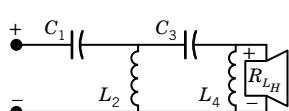
Design a filter for a 120-Hz cut off frequency to be used with a speaker system composed of a woofer and a wide frequency speaker. Assume 8Ω drivers.

KNOWN $f_c = 120 \text{ Hz}$; $R_{L_H} = 8 \Omega$; $R_{L_L} = 8 \Omega$

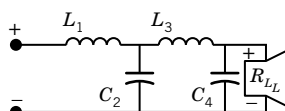
FIND C and L for the circuit

SOLUTION Because the filter circuits have identical qualities when using the same f_c , the output power to each driver is halved at f_c , so the total output sum to each of the two drivers remains at near 0 dB at the crossover frequency. This provides for a desirable nearly flat filter response across the listening frequency range. Applying the information with $f_c = 120 \text{ Hz}$, we get

High-Pass Circuit		Low-Pass Circuit	
C_1 (μf)	$= 87.9$	C_2 (μf)	$= 263.9$
C_3 (μf)	$= 175.8$	C_4 (μf)	$= 58.7$
L_2 (mh)	$= 6.7$	L_1 (mh)	$= 20.0$
L_4 (mh)	$= 30.0$	L_3 (mh)	$= 10.0$



Fourth-order high-pass filter



Fourth-order low-pass filter

Figure 6.34 Linkwitz–Riley fourth-order Butterworth filters.

Commercial values for each element that are close to these calculated would be used in the circuit of Figure 6.34 to achieve a cutoff as close to 120 Hz as possible.

Bessel Filter Design

A Bessel filter will sacrifice a flat gain over its passband with a gradual initial roll-off in order to maximize a linear phase response over portions of the passband. A linear phase response closely resembles a time delay, reducing distortion. Thus, the attractiveness of a Bessel filter is the ability to pass wideband signals with a minimum of distortion. The filter is widely used for different applications, including audio design where crossover phase shift can have an effect on sound quality.

A k -stage low-pass Bessel filter has the transfer function

$$KG(s) = \frac{a_0}{a_0 + a_1 s + \cdots + a_k s^k} \quad (6.64)$$

For design purposes, this can be rewritten as

$$KG(s) = \frac{a_0}{D_k(s)} \quad (6.65)$$

where $D_k(s) = (2k - 1)D_{k-1}(s) + s^2 D_{k-2}(s)$, $D_0(s) = 1$ and $D_1(s) = s + 1$.

A k -stage LC low-pass Bessel filter can be designed based on the filter circuit shown in Figure 6.30. Table 6.2 lists the normalized corresponding values for elements L_i and C_i to achieve a two-through five-stage Bessel filter corresponding to $\omega_c = 1$ rad with $R_s = R_L = 1 \Omega$ (6, 7). For other values, L_i and C_i are found from Equations 6.61a and 6.61b. Similarly, a high-pass filter with Bessel characteristics and topology similar to Figure 6.33 could be scaled using Table 6.2 and values found from Equations 6.62a and 6.62b.

Active Filters

An active filter capitalizes on the high-frequency gain characteristics of the operational amplifier to form an effective analog filter. A low-pass active filter is shown in Figure 6.35a using the type 741 operational amplifier. This is a first-order, inverting single-stage, low-pass Butterworth filter. It has a low-pass cutoff frequency given by

$$f_c = \frac{1}{2\pi R_2 C_2} \quad (6.66)$$

Table 6.2 Normalized Element Values for Low-Pass LC Bessel Filters^a (8)

k	C_1	L_2	C_3	L_4	C_5
2	0.576	2.148			
3	0.337	0.971	2.203		
4	0.233	0.673	1.082	2.240	
5	0.174	0.507	0.804	1.111	2.258

^aValues for C_i in farads and L_i in henrys are referenced to $R_s = R_L = 1 \Omega$ and $\omega_c = 1$ rad/s. See discussion for proper scaling. For $k = 1$, use $C_1 = 2$ F or $L_1 = 2$ H.

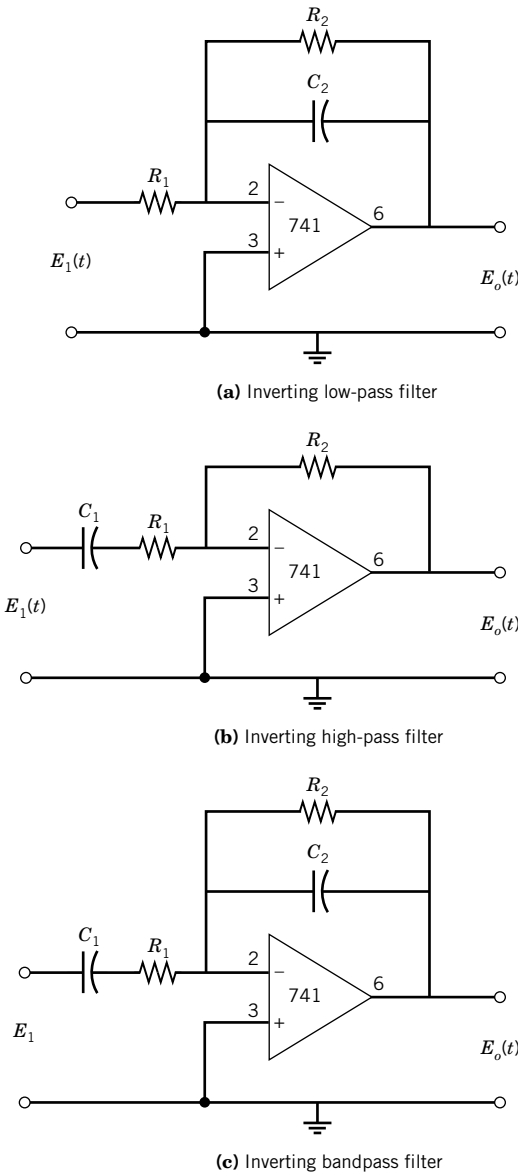
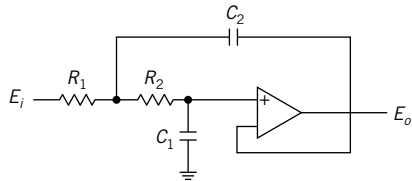


Figure 6.35 Common basic active filters. **(a)** Inverting low pass. **(b)** Inverting high pass. **(c)** Inverting bandpass.

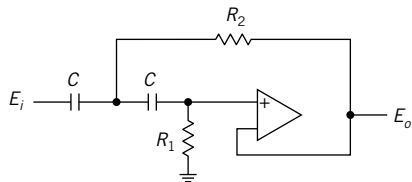
The static sensitivity (or gain) of the filter is given by $K = R_2/R_1$. The filter retains the Butterworth characteristics described by Equation 6.58a.

A first-order, inverting single-stage, high-pass Butterworth active filter is shown in Figure 6.35b, using the 741 operational amplifier. The filter has a high-pass cutoff frequency of

$$f_c = \frac{1}{2\pi R_1 C_1} \quad (6.67)$$



(a) Low-Pass Filter



(b) High-Pass Filter

Figure 6.36 Sallen–Key unit-gain filter. (a) Low pass.
(b) High pass.

with static sensitivity (or gain) of $K = R_2/R_1$. The magnitude ratio is given by

$$M(f) = \frac{1}{\left[1 + (f_c/f)^2\right]^{1/2}} \quad (6.68)$$

An active inverting bandpass filter can be formed by combining the high- and low-pass filters above and is shown in Figure 6.35c. The low cutoff frequency f_{c_1} is given by Equation 6.66 and the high cutoff frequency f_{c_2} by Equation 6.67. This simple circuit is limited in the width of its bandpass. A narrow bandpass requires a higher order filter than the one shown. The design of active filters can be studied with the accompanying LabView program *Lowpass Butterworth Active Filter*.

A commonly used second-order low-pass filter is the unit-gain Sallen–Key topology shown in Figure 6.36a. The generic transfer function is

$$G(s) = \frac{1}{1 + as + bs^2} \quad (6.69)$$

with $a = \omega_c C_1 (R_1 - R_2)$ and $b = \omega_c^2 C_1 C_2 R_1 R_2$ where $\omega_c = 2\pi f_c$. The values for a and b enabling Butterworth or Bessel filter characteristics are listed in Table 6.3. As capacitors come in fewer stock sizes than resistors, usually the capacitor sizes are first selected with $C_2 = nC_1$, where n is a multiple

Table 6.3 Parameters for second-order Sallen–Key filter design

Parameter	Bessel	Butterworth
a	1.3617	1.4142
b	0.618	1
Q	$1/\sqrt{3}$	$1/\sqrt{2}$

number, such that $C_2 \geq 4bC_1/a^2$, and the resistors are then found by

$$R_{1,2} = \frac{aC_2 \mp \sqrt{(aC_2)^2 - 4bC_1C_2}}{4\pi f_c C_1 C_2} \quad (6.70)$$

The filter cutoff frequency is set by

$$f_c = \frac{1}{2\pi\sqrt{R_1 R_2 C_1 C_2}} \quad (6.71)$$

The unit-gain Sallen–Key high-pass filter is shown in Figure 6.36b. The design switches the resistors and capacitors from the low-pass filter. For high-pass filters, we can simplify the design and set $C_1 = C_2 = C$. The high-pass filter transfer function is

$$G(s) = \frac{1}{1 + a/s + b/s^2} \quad (6.72)$$

where $a = 2/\omega_c CR_1$ and $b = 1/\omega_c^2 C^2 R_1 R_2$. Values for a and b to meet Butterworth or Bessel filter characteristics are given in Table 6.3 with the resistor values set by $R_1 = 1/\pi f_c aC$ and $R_2 = a/4\pi f_c bC$.

At some frequency, the reactive elements in a filter circuit resonate, leading to a peak in the response behavior. This is behavior predicted by its Q -factor, an inverse damping ratio-like parameter. For $Q = 1/2$ response is critically damped, for $Q < 1/2$ response is overdamped, and for $Q > 1/2$ response is underdamped. A higher Q-factor generally allows for sharper roll-off and is used in place of using a higher number of stages in a design. Like its mechanical system analog ($Q = \sqrt{mk}/\zeta$), an underdamped filter shows ringing and has a resonance behavior. The Q -factors for Butterworth and Bessel filters are shown in Table 6.3, where

$$Q = \sqrt{b}/a \quad (6.73)$$

6.9 GROUNDS, SHIELDING, AND CONNECTING WIRES

The type of connecting wires used between electrical devices can have a significant impact on the noise level of the signal. Low-level signals of <100 mV are particularly susceptible to errors induced by noise. Some simple rules help to keep noise levels low: (1) keep the connecting wires as short as possible, (2) keep signal wires away from noise sources, (3) use a wire shield and proper ground, and (4) twist wire pairs along their lengths.

Ground and Ground Loops

The voltage at the end of a wire that is connected to a rod driven far into the soil would likely be at the same voltage level as the earth—a reference datum called zero or *earth ground*. A *ground* is simply a return path to earth. Now suppose that wire is connected from the rod through an electrical box and then through various building routings to the ground plug of an outlet. Would the ground potential at the outlet still be at zero? The answer is probably not. The network of wires that form the return path to earth would likely act as antennae and pick up some voltage potential relative to earth ground. Any instrument grounded at the outlet would be referenced back to this voltage potential, not to earth ground. The point is that an electrical ground does not represent an absolute value. Ground values vary between ground points because the ground returns pass through different

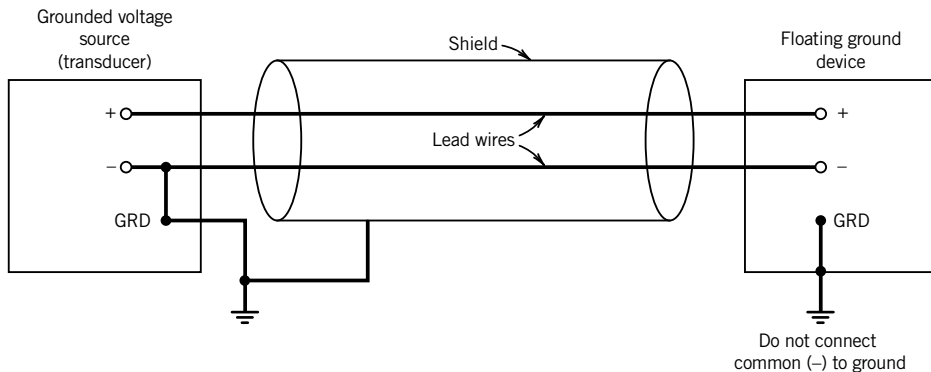


Figure 6.37 Signal grounding arrangements: grounded source with shield and floating signal at the measuring device. It is important to ground the shield at one end only.

equipment or building wiring on their return path to earth. Thus, if a signal is grounded at two points, say at a power source ground and then at an earth ground, the two grounds could be at different voltage levels. The difference between the two ground point voltages is called the *common-mode voltage* (cmv). This can lead to problems, as discussed next.

Ground loops are caused by connecting a signal circuit to two or more grounds that are at different potentials. A ground wire of finite resistance usually carries some current, and so it develops a potential. Thus two separate and different grounds, even two in close proximity, can be at different potential levels. So when these ground points are connected into a circuit the potential difference itself drives a small unwanted current. The result is a ground loop—an electrical interference superimposed onto the signal. A ground loop can manifest itself in various forms, such as a sinusoidal signal or simply a voltage offset.

Ensure that a system, including its sensors and all electrical components, has only one ground point. Figure 6.37 shows one proper connection between a grounded source, such as a transducer, and a measuring device. In this case, the ground is at the transducer. Note that the common (−) line at the measuring device is not grounded because it is grounded at the source. As such, it is referred to as being isolated or as a floating ground device. Alternately, the ground can be at the measuring device rather than at the source. The key point is to ground the circuit and all equipment back to only one point, the common ground point. For stationary devices, an excellent ground is created by driving a conducting rod well into the earth for use as the common ground point. Incidentally, many devices are grounded through their AC power lines by means of a third prong. Unless the device power supply is isolated from the circuit, this can set up a ground loop relative to other circuit grounds. To create a floating ground, it is necessary to break this ground connection at this point.

Shields

Long wires act as antennas and pick up stray signals from nearby electrical fields. The most common problem is AC line noise. Electrical shields are effective against such noise. A *shield* is a piece of metal foil or wire braid wrapped around the signal wires and connected to ground. The shield intercepts external electrical fields, returning them to ground. A shield ground loop is prevented by grounding the shield to only one point, usually the signal ground at the transducer.

Figure 6.37 shows such a shield-to-ground arrangement for a grounded voltage source connected to a floating ground measuring device.

A common source of electrical fields is an AC power supply transformer. A capacitance coupling between the 60- or 50-Hz power supply wires and the signal wires is set up. For example, a 1-pF capacitance superimposes a 40-mV interference on a 1-mV signal.

A different source of noise is from a magnetic field. When a lead wire moves within a magnetic field, a voltage is induced in the signal path. The same effect occurs with a lead wire in proximity to an operating motor. The best prevention is to separate the signal lead wires from such sources. Also, twisting the lead wires together tends to cancel any induced voltage, as the currents through the two wires are in opposite directions; the more twists per meter, the better. A final recourse is a magnetic shield made from a material having a high ferromagnetic permeability.

Connecting Wires

There are several types of wire available. *Single cable* refers to a single length of common wire or wire strand. The conductor is coated for electrical insulation. The wire is readily available and cheap, but should not be used for low-level signal (millivolt level) connections or for connections of more than a few wires. Flat cable is similar but consists of multiple conductors arranged in parallel strips, usually in groups of 4, 9, or 25. Flat cable is commonly used for short connections between adjacent electrical boards, but in such applications the signals are on the order of 1 V or more or are TTL signals. Neither of these two types of wire offer any shielding.

Twisted pairs of wires consist of two electrically insulated conductors twisted about each other along their lengths. Twisted pairs are widely used to interconnect transducers and equipment. The intertwining of the wires offers some immunity to noise with that effectiveness increasing with the number of twists per meter. Cables containing several twisted pairs are available; for example, CAT5 network cable (such as Internet cable) consists of four twisted pairs of wires. Shielded twisted pairs wrap the twisted pairs within a metallic foil shield. CAT6 network cable consists of four twisted pairs with a shield separating its wire pairs. Shielded twisted pairs are one of the best choices for applications requiring low-level signals or high data transfer rates.

Coaxial cable consists of an electrically insulated inner single conductor surrounded within an outer conductor made of stranded wire and a metal foil shield. In general, current flows in one direction along the inner wire and the opposite direction along the outer wire. Any electromagnetic fields generated will cancel. Coaxial cable is often the wire of choice for low-level, high-frequency signals. Signals can be sent over very long distances with little loss. A variation of coaxial cable is *triaxial cable*, which contains two inner conductors. It is used in applications as with twisted pairs but offers superior noise immunity.

Optical cable is widely used to transmit low-level signals over long distances. This cable may contain one or more fiber-optic ribbons within a polystyrene shell. A transmitter converts the low-level voltage signal into infrared light. The light is transmitted through the cable to a receiver, which converts it back to a low-level voltage signal. The cable is virtually noise-free from magnetic fields and harsh environments and is incredibly light and compact compared to its metal wire counterpart.

6.10 SUMMARY

This chapter has focused on classic but basic analog electrical measurement and signal conditioning devices. Devices that are sensitive to current, resistance, and voltage were presented. Signal

conditioning devices that can modify or condition a signal include amplifiers, current loops, and filters, and these were also presented. Because all of these devices are widely used, often in combination and often masked within more complicated circuits, the reader should strive to become familiar with the workings of each.

The important issue of loading error was presented. Loading errors, which are due to the act of measurement or to the presence of a sensor, can only be minimized by proper choice of sensor and technique. Loading errors that occur between the connecting stages of a measurement system can be minimized by proper impedance matching. Such impedance matching was discussed, including using the versatile voltage follower circuit for this purpose.

REFERENCES

1. Hickman, I., *Oscilloscopes*, 5th ed., Newnes, Oxford, UK, 2000.
2. Bleuler, E., and R. O. Haxby, *Methods of Experimental Physics*, 2nd ed., Vol. 2, Academic, New York, NY, 1975.
3. Lacanette, K., *A Basic Introduction to Filters: Active, Passive, and Switched-Capacitor Application Note 779*, National Semiconductor, Santa Clara, CA, 1991.
4. Stanley, W. D., G. R. Dougherty, and R. Dougherty, *Digital Signal Processing*, 2nd ed., Reston (a Prentice Hall company), Reston, VA, 1984.
5. DeFatta, D. J., J. Lucas, and W. Hodgkiss, *Digital Signal Processing*, Wiley, New York, 1988.
6. Lam, H. Y., *Analog and Digital Filters: Design and Realization*, Prentice-Hall, Englewood Cliffs, NJ, 1979.
7. Niewizdomski, S., *Filter Handbook—A Practical Design Guide*, CRC Press, Boca Raton, FL, 1989.
8. Bowick, C., C. Ajluni, and J. Blyler, *RF Circuit Design*, 2nd ed., Newnes, Oxford, UK, 2007.

NOMENCLATURE

c	damping coefficient	E_1	open circuit potential (V)
e	error	E_i	input voltage (V)
f	frequency (t^{-1})	E_m	indicated output voltage (V)
f_c	filter cutoff frequency (t^{-1})	E_o	output voltage (V)
f_m	maximum analog signal frequency (t^{-1})	F	force (mlt^{-2})
$h\{E_i(t)\}$	function	G	amplifier closed-loop gain
k	cascaded filter stage order	$G(s)$	transfer function
\hat{k}	unit vector aligned with current flow	I	electric current ($C \cdot t^{-1}$)
l	length (l)	I_e	effective current ($C \cdot t^{-1}$)
\hat{n}	unit vector normal to current loop	I_g	galvanometer or current device current ($C \cdot t^{-1}$)
q	charge (C)	K	static sensitivity
r	radius, vector (l)	L	inductance (H)
t	time (t)	$M(f)$	magnitude ratio at frequency f
u_R	uncertainty in resistance R	N	number of turns in a current-carrying loop
A	cross-sectional area of a current-carrying loop; attenuation	R	resistance (Ω)
A_o	operational amplifier open-loop gain	R_B	effective bridge resistance (Ω)
E	voltage (V)	R_g	galvanometer or detector resistance (Ω)

R_{eq}	equivalent resistance (Ω)	α	angle
R_m	meter resistance (Ω)	τ	time constant (t)
δR	change in resistance (Ω)	$\Phi(f)$	phase shift at frequency f
T_μ	torque on a current carrying loop in a magnetic field ($m^2 t^{-2}$)	θ	angle

PROBLEMS

- 6.1** Determine the maximum torque on a current loop having 20 turns, a cross-sectional area of 1 in.², and experiencing a current of 20 mA. The magnetic field strength is 0.4 Wb/m².
- 6.2** A 10-V voltage is applied across a Wheatstone bridge of Figure 6.13 to measure the value of a variable resistance sensor R_1 . Arms are fixed at $R_2 = R_4 = 250 \Omega$. Variable resistance arm 3 is adjusted to $R_3 = 300 \Omega$ to achieve a condition of zero current through the galvanometer. What is the value of R_1 ? Should we be concerned about loading error? Explain or estimate.
- 6.3** Determine the loading error as a percentage of the output for the voltage dividing circuit of Figure 6.15, if $R_T = R_1 + R_2$ and $R_1 = kR_T$. The parameters of the circuit are

$$R_T = 500 \Omega; \quad E_i = 10 \text{ V}; \quad R_m = 10,000 \Omega; \quad k = 0.5$$

What would be the loading error if expressed as a percentage of the full-scale output? Show that the two answers for the loading error are equal when expressed in volts.

- 6.4** Consider the Wheatstone bridge shown in Figure 6.13. Suppose

$$\begin{aligned} R_3 &= R_4 = 200 \Omega \\ R_2 &= \text{variable calibrated resistor} \\ R_1 &= \text{transducer resistance} = 40x + 100 \end{aligned}$$

- a. When $x = 0$, what is the value of R_2 required to balance the bridge?
- b. If the bridge is operated in a balanced condition in order to measure x , determine the relationship between R_2 and x .
- 6.5** For the voltage-dividing circuit of Figure 6.15, develop and plot the family of solutions for loading error versus $r = R_1/(R_1 + R_2)$ as a function of $(R_1 + R_2)/R_m$. Under what conditions will the loading error in measuring the open circuit potential E_o be less than 7% of the input voltage?
- 6.6** For the Wheatstone bridge shown in Figure 6.13, R_1 is a sensor whose resistance is related to a measured variable x by the equation $R_1 = 20x^2$. If $R_3 = R_4 = 100 \Omega$ and the bridge is balanced when $R_2 = 46 \Omega$, determine x .
- 6.7** A force sensor has as its output a change in resistance. The sensor forms one leg (R_1) of a basic Wheatstone bridge. The sensor resistance with no force load is 500 Ω , and its static sensitivity is 0.5 Ω/N . Each arm of the bridge is initially 500 Ω .
- a. Determine the bridge output for applied loads of 100, 200, and 350 N. The bridge is operated as a deflection bridge, with an input voltage of 10 V.
- b. Determine the current flow through the sensor.
- c. Repeat parts **a** and **b** with $R_m = 10 \text{ k}\Omega$ and $R_s = 600 \Omega$.

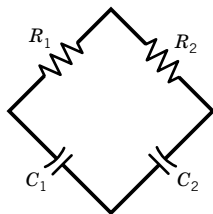


Figure 6.38 Bridge circuit for Problem 6.8.

- 6.8** A reactance bridge arrangement replaces the resistor in a Wheatstone bridge with a capacitor or inductor. Such a reactance bridge is then excited by an AC voltage. Consider the bridge arrangement shown in Figure 6.38. Show that the balance equations for this bridge are given by $C_2 = C_1 R_1 / R_2$.
- 6.9** Circuits containing inductance- and capacitance-type elements exhibit varying impedance depending on the frequency of the input voltage. Consider the bridge circuit of Figure 6.39. For a capacitor and an inductor connected in a series arrangement, the impedance is a function of frequency, such that a minimum impedance occurs at the resonance frequency $f = 1/2\pi\sqrt{LC}$ where f is the frequency (Hz), L is the inductance (H), and C is the capacitance (F). Design a bridge circuit that could be used to calibrate a frequency source at 500 Hz.
- 6.10** A Wheatstone bridge initially has resistances equal to $R_1 = 200 \Omega$, $R_2 = 400 \Omega$, $R_3 = 500 \Omega$, and $R_4 = 600 \Omega$. For an input voltage of 5 V, determine the output voltage at this condition. If R_1 changes to 250Ω , what is the bridge output?
- 6.11** Construct a plot of the voltage output of a Wheatstone bridge having all resistances initially equal to 500Ω , with a voltage input of 10 V for the following cases:
- R_1 changes over the range $500 - 1000 \Omega$.
 - R_1 and R_2 change equally, but in opposite directions, over the range $500 - 600 \Omega$.
 - R_1 and R_3 change equally over the range $500 - 600 \Omega$.
- Discuss the possible implications of these plots for using bridge circuits for measurements with single and multiple transducers connected as arms of the bridge.
- 6.12** Consider the simple potentiometer circuit shown in Figure 6.10 with reference to Figure 6.9. Perform a design-stage uncertainty analysis to determine the minimum uncertainty in measuring a voltage. The following information is available concerning the circuit (assume 95% confidence):

$$E_i = 10 \pm 0.1 \text{ V} \quad R_T = 100 \pm 1 \Omega \quad R_g = 100 \Omega \quad R_x = \text{reading} \pm 2\%$$

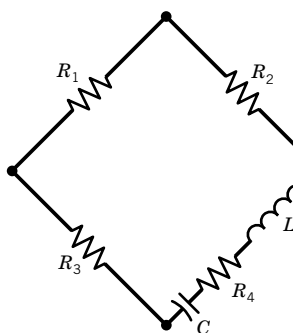


Figure 6.39 Bridge circuit for Problem 6.9.

where R_g is the internal resistance of a galvanometer. The null condition of the galvanometer may be assumed to have negligible error. The uncertainty associated with R_x is associated with the reading obtained from the location of the sliding contact. Estimate the uncertainty in the measured value of voltage at nominal values of 2 and 8 V.

- 6.13** The temperature sensor of Example 6.2 is connected to a Wheatstone bridge using $R_3 = R_4 = 100 \Omega$. The sensor is immersed into boiling water at 1 atm abs. pressure. What is the resistance of balancing resistor R_2 to balance the bridge? $R_{\text{sensor}}(0^\circ C) = 100 \Omega$

Problems 6.14 through 6.17 relate to the comparison of two sinusoidal input signals using a dual-trace oscilloscope. A schematic diagram of the measurement system is shown in Figure 6.40, where one of the signals is assumed to be a reference standard signal, having a known frequency and amplitude. The oscilloscope trace for these inputs is called a Lissajous diagram. The problems can also be worked in the laboratory.

- 6.14** Develop the characteristic shape of the Lissajous diagrams for two sinusoidal inputs having the same amplitude, but with the following phase relationships:
- in phase
 - ± 90 degrees out of phase
 - 180 degrees out of phase
- 6.15** Show that the phase angle for two sinusoidal signals can be determined from the relationship

$$\sin \Phi = y_i/y_a$$

where the values of y_i and y_a are illustrated in Figure 6.40, and represent the vertical distance to the y intercept and the maximum y value, respectively.

- 6.16** Draw a schematic diagram of a measurement system to determine the phase lag resulting from an electronic circuit. Your schematic diagram should include a reference signal, the electronic circuit, and the dual-trace oscilloscope. Discuss the expected result and how a quantitative estimate of the phase lag can be determined.
- 6.17** Construct Lissajous diagrams for sinusoidal inputs to a dual trace oscilloscope having the following horizontal signal to vertical signal frequency ratios: (a) 1:1, (b) 1:2, (c) 2:1, (d) 1:3, (e) 2:3, (f) 5:2.

These plots can be easily developed using spreadsheet software and plotting a sufficient number of cycles of each of the input signals.

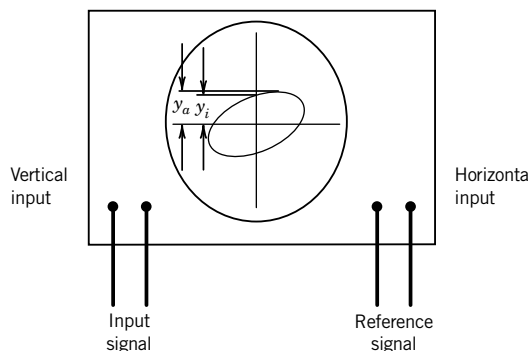


Figure 6.40 Dual-trace oscilloscope for measuring signal characteristics by using Lissajous diagrams.

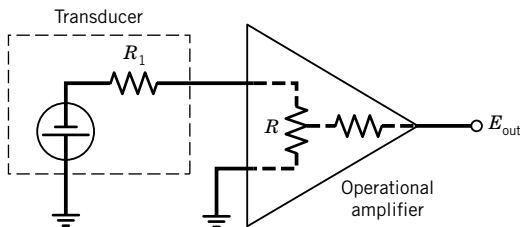


Figure 6.41 pH transducer circuit for Problem 6.23.

- 6.18** As a data acquisition anti-alias filter, an RC Butterworth filter is designed with a cutoff frequency of 100 Hz using a single-stage topology. Determine the attenuation of the filtered analog signal at 10, 50, 75, and 200 Hz.
- 6.19** A three-stage LC Bessel filter with $f_c = 100$ Hz is used to filter an analog signal. Determine the attenuation of the filtered analog signal at 10, 50, 75, and 200 Hz.
- 6.20** Design a cascading LC low-pass filter with maximally flat magnitude response. Use a passband of 0 to 5 kHz with 5 kHz cutoff frequency and filter to attenuate all frequencies at and above 10 kHz by at least 30 dB. Use $R_s = R_L = 50 \Omega$.
- 6.21** An electrical displacement transducer has an output impedance of $Z = 500 \Omega$. Its voltage is input to a voltage measuring device that has an input impedance of $Z = 100 \text{ k}\Omega$. Estimate the ratio of true voltage to the voltage measured by the measuring device.
- 6.22** Consider a transducer connected to a voltage measuring device. Plot the ratio E_m/E_1 as the ratio of output impedance of the transducer to input impedance of the measuring device varies from 1:1 to 1:10,000 (just look at each order of magnitude). Comment on the effect that input impedance has on measuring a voltage. What value of input impedance would be acceptable in a quality instrument?
- 6.23** The pH meter of Figure 6.41 consists of a transducer of glass containing paired electrodes. This transducer can produce voltage potentials up to 1 V with an internal output impedance of up to $10^9 \Omega$. If the signal is to be conditioned, estimate the minimum input impedance required to keep loading error below 0.1% for the op-amp shown.
- 6.24** Consider the circuit of Figure 6.42, which consists of an amplifier providing 32-dB gain, followed by a filter, which causes an attenuation of 12 dB at the frequency of interest, followed by a voltage divider. Find E_o/E_i across the $60\text{-}\Omega$ resistor.

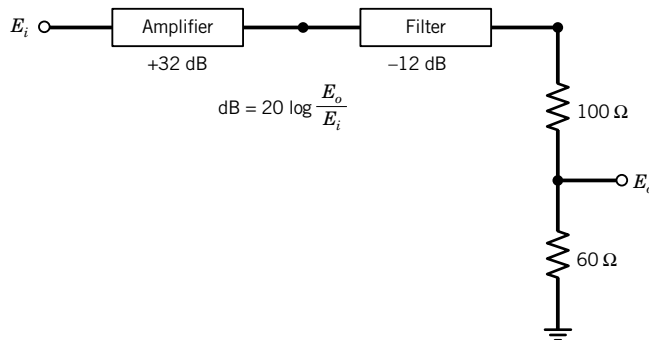


Figure 6.42 Multistage signal path for Problem 6.24.

- 6.25** What internal impedance is needed for the bridge circuit of Figure 6.18 for the loading error to be under 1% if the bridge resistances change by

$$\delta R_1 = +40 \Omega \quad \delta R_2 = -40 \Omega \quad \delta R_3 = +40 \Omega \quad \delta R_4 = -40 \Omega$$

- 6.26** The input to a subwoofer loudspeaker is to pass through a passive low-pass Butterworth filter having a cutoff frequency of 100 Hz. Specify a filter that meets the following specifications: At 50 Hz, the signal magnitude ratio should be at least at 0.95 and at 200 Hz, the magnitude ratio should be no more than 0.01. The sensor and load resistances are 10 Ω . You will need to specify the number of even stages and the values for the components.
- 6.27** For the application in Problem 6.26, repeat using a Linkwitz-Riley topology to specify the reactive element values in both a 4th-order low-pass filter and high-pass filter for 10 Ω speakers.
- 6.28** A high-pass Butterworth filter with cutoff frequency of 5000 Hz is used as a crossover to a high-frequency loudspeaker. Specify a filter such that at 2500 Hz, the attenuation should be at least -20 dB. The source and load resistances are 10 Ω . You need to specify the number of stages and the values for the components.
- 6.29** Design an active-RC low-pass first-order Butterworth filter for a cutoff frequency of 10 kHz, and a passband gain of 20. Use a 741 op-amp and 0.1- μ F capacitors for your design. Program *Lowpass Butterworth Active Filter* can be used.
- 6.30** Design an active-RC first-order high-pass filter for a cutoff frequency of 10 kHz and passband gain of 10. Use a 741 op-amp.
- 6.31** Use the LabView program *Oscilloscope* to explore the workings of an actual oscilloscope. Vary between channel A and B.
- a.** Characterize each signal by its waveform (i.e., triangle, square, sine). Determine the amplitude and the period of both signals.
 - b.** Vary the signal gain (volts/division). Explain the effect on the displayed signals.
 - c.** Vary the time base (ms/div). Explain the effect on the displayed signals.
 - d.** Make sure channel B is active. With the trigger source set to channel B, vary the trigger level dial. Explain the function of the trigger level. Why do the waveforms disappear at some settings of the trigger?
 - e.** Repeat **c**, but now vary the trigger slope. Explain the effect on the signals.
- 6.32** Use the LabView program *Butterworth_Filters* to explore the behavior of low-pass, bandpass, and high-pass Butterworth filters chosen for their flat amplitude passband. In this program, the signal $y(t) = 2 \sin 2\pi ft$ is passed through the filter and it is the filtered signal $y^*(t) = B \sin[2\pi ft + \phi(f)]$ that is displayed. The single-tone results show the effect at the input frequency f . The amplitude spectrum results show the effect over the full-frequency band of interest. Describe the amplitude behavior of the filtered signal as the single input frequency is increased. Pay particular attention near the filter cutoff frequencies, which are set at 300 and 500 Hz.
- 6.33** Use the LabView program *Bessel_Filters* to explore the behavior of low-pass, bandpass, and high-pass Bessel filters. Using the information from Problem 6.32, describe the amplitude behavior of the filtered signal as a single-input frequency is increased from 1 to 1000 Hz.
- 6.34** The program *Filtering_Noise* demonstrates the effect of using a low-pass Butterworth filter to treat a signal containing high-frequency noise. Set the signal frequency at 5 Hz. Set the cutoff frequency at 10 Hz. Discuss the behavior of the filter as the number of stages is increased. Then incrementally

decrease the cutoff frequency and discuss the behavior. Tie your discussion back to filter roll-off. What happens when the cutoff frequency is less than the signal frequency? Why?

- 6.35** Program *Monostable Circuit* provides a simulation of a monostable integrated circuit based on the type 555 op-amp. The trigger controls the simulation. The user can vary the “on” time and values for R and C . Discuss the output vs. time results for a simulation. Vary R and C to create a 1-s square wave.
- 6.36** Program *741 Op amp* simulates op-amp gain characteristics. Determine if it is noninverting or inverting and explain. For an input voltage of 1 V, find a resistor combination for a gain of 5. What is this op-amp’s maximum output? Repeat for a gain of 0.5.

Chapter 7

Sampling, Digital Devices, and Data Acquisition

7.1 INTRODUCTION

Integrating analog electrical transducers with digital devices is cost-effective and commonplace. Digital microprocessors are central to most controllers and data-acquisition systems today. There are many advantages to digital data acquisition and control, including the efficient handling and rapid processing of large amounts of data and varying degrees of artificial intelligence. But there are fundamental differences between analog and digital systems that impose some limitations and liabilities upon the engineer. As pointed out in Chapter 2, the most important difference is that analog signals are continuous in both amplitude and time, whereas digital signals are discrete (noncontinuous) in both amplitude and time. It is not immediately obvious how a digital signal can be used to represent the continuous behavior of a process variable.

This chapter begins with an introduction to the fundamentals of *sampling*, the process by which continuous signals are made discrete. The major pitfalls are explored. Criteria are presented that circumvent the loss or the misinterpretation of signal information while undergoing the sampling process. We show how a discrete series of data can actually contain all of the information available in a continuous signal, or at least provide a very good approximation.

The discussion moves on to the devices most often involved in analog and digital systems. Analog devices interface with digital devices through an analog-to-digital (A/D) converter. The reverse process of a digital device interfacing with an analog device occurs through a digital-to-analog (D/A) converter. A digital device interfaces with another digital device through a digital input–output (I/O) port. These interfaces are the major components of computer-based data-acquisition systems. Necessary components and the basic layout of these systems are introduced, and standard methods for communication between digital devices are presented. Digital image acquisition and processing are introduced because of their increasing importance in a wide variety of applications ranging from quality assurance inspection to high-speed imaging.

Upon completion of this chapter, the reader will be able to

- describe analog, discrete time, and digital signals,
- properly choose a sample rate for data acquisition to eliminate aliasing,
- clearly describe the functioning of A/D and D/A converters,
- define and calculate quantization errors,

- understand how instruments interface with data-acquisition systems, and
- perform basic image processing on digital images.

7.2 SAMPLING CONCEPTS

Consider an analog signal and its discrete time series representation in Figure 7.1. The information contained in the analog and discrete representations may appear to be quite different. However, the important analog signal information concerning amplitude and frequency can be well represented by such a discrete series—just how well represented depends on

1. the frequency content of the analog signal,
2. the size of the time increment between each discrete number, and
3. the total sample period of the measurement.

Chapter 2 discussed how a continuous dynamic signal could be represented by a Fourier series. The discrete Fourier transform (DFT) was also introduced as a method for reconstructing a dynamic signal from a discrete set of data. The DFT conveys all the information needed to reconstruct the Fourier series of a continuous dynamic signal from a representative discrete time series. Hence, Fourier analysis provides certain guidelines for sampling continuous data. This section discusses the concept of converting a continuous analog signal into an equivalent discrete time series. Extended discussions on this subject of signal analysis can be found in many texts (1–3).

Sample Rate

Just how frequently must a time-dependent signal be measured to determine its frequency content? Consider Figure 7.2a, in which the magnitude variation of a 10-Hz sine wave is plotted versus time over time period t_f . Suppose this sine wave is measured repeatedly at successive sample time increments δt . This corresponds to measuring the signal with a sample frequency (in samples/

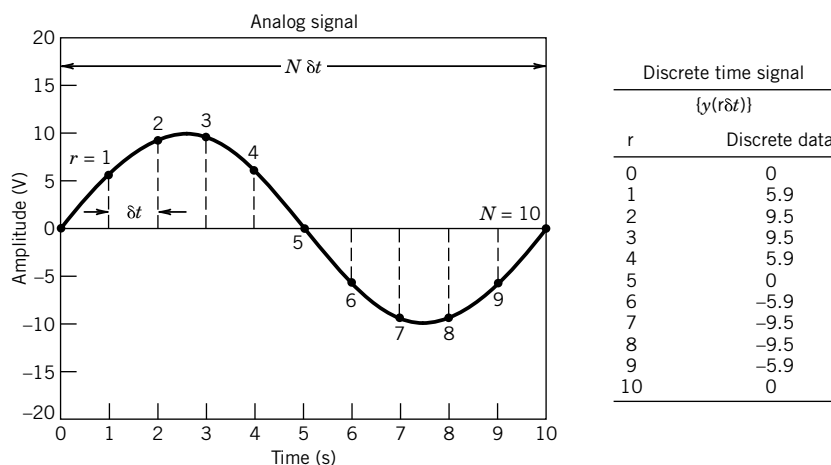


Figure 7.1 Analog and discrete representations of a time-varying signal.

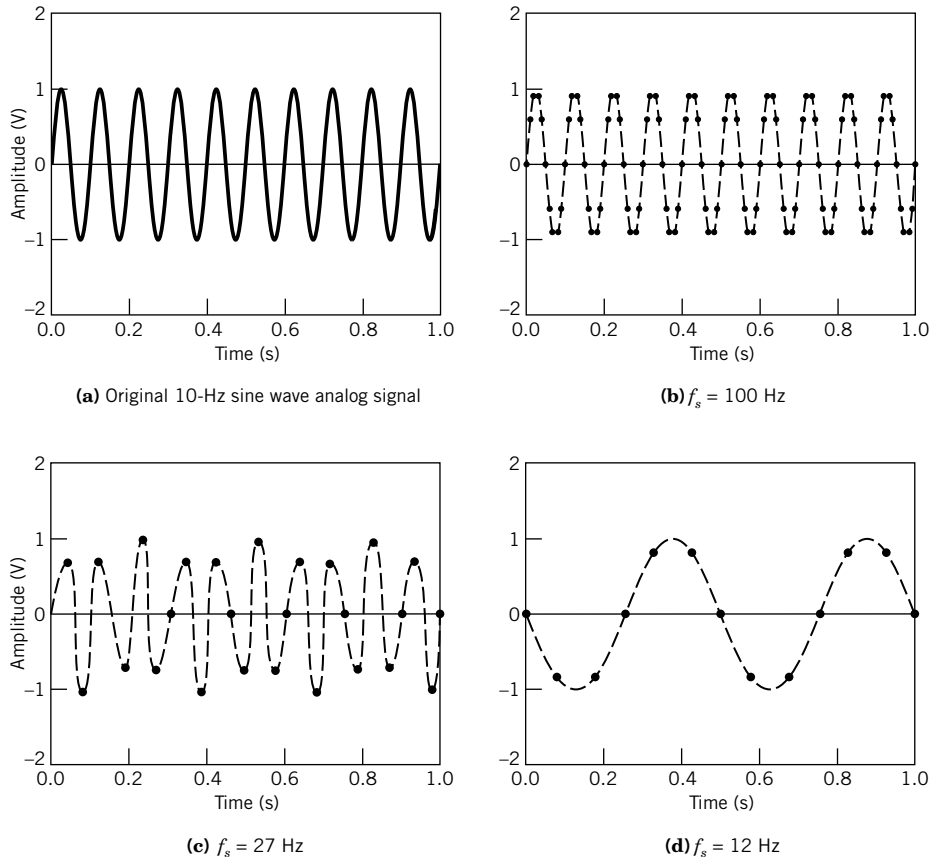


Figure 7.2 The effect of sample rate on signal frequency and amplitude interpretation.

second) or sample rate (in Hz) of

$$f_s = 1/\delta t \quad (7.1)$$

For this discussion, we assume that the signal measurement occurs at a constant sample rate. For each measurement, the amplitude of the sine wave is converted into a number. For comparison, in Figures 7.2b–d the resulting series versus time plots are given when the signal is measured using sample time increments (or the equivalent sample rates) of (b) 0.010 second ($f_s = 100 \text{ Hz}$), (c) 0.037 second ($f_s = 27 \text{ Hz}$), and (d) 0.083 second ($f_s = 12 \text{ Hz}$). We can see that the sample rate has a significant effect on our perception and reconstruction of a continuous analog signal in the time domain. As sample rate decreases, the amount of information per unit time describing the signal decreases. In Figures 7.2b,c we can still discern the 10-Hz frequency content of the original signal. But we see in Figure 7.2d that an interesting phenomenon occurs if the sample rate becomes too slow: the sine wave appears to be of a lower frequency.

We can conclude that the sample time increment or the corresponding sample rate plays a significant role in signal frequency representation. The *sampling theorem* states that to reconstruct

the frequency content of a measured signal accurately, the sample rate must be more than twice the highest frequency contained in the measured signal.

Denoting the maximum frequency in the analog signal as f_m , the sampling theorem requires

$$f_s > 2f_m \quad (7.2)$$

or, equivalently, in terms of sample time increment,

$$\delta t < \frac{1}{2f_m} \quad (7.3)$$

When signal frequency content is important, Equations 7.2 and 7.3 provide a criterion for the minimum sample rate or maximum sample time increment, respectively, to be used in converting data from a continuous to a discrete form. The frequencies that are extracted from the DFT of the resulting discrete series provide an accurate representation of the original signal frequencies regardless of the sample rate used, provided that the requirements of the sampling theorem are satisfied.

Alias Frequencies

When a signal is sampled at a sample rate that is less than $2f_m$, the higher frequency content of the analog signal takes on the false identity of a lower frequency in the resulting discrete series. This is seen to occur in Figure 7.2d, where, because $f_s < 2f_m$, the 10-Hz analog signal is observed to take on the false identity of a 2-Hz signal. As a result, we misinterpret the frequency content of the original signal! Such a false frequency is called an *alias frequency*.

The alias phenomenon is an inherent consequence of a discrete sampling process. To illustrate this, consider a simple periodic signal:

$$y(t) = C \sin [2\pi f t + \phi(f)] \quad (7.4)$$

Suppose $y(t)$ is measured with a sample time increment of δt , so that its discrete time signal is given by

$$\{y(r\delta t)\} = C \sin [2\pi f r \delta t + \phi(f)] \quad r = 0, 1, \dots, N - 1 \quad (7.5)$$

Now using the identity $\sin x = \sin(x + 2\pi q)$, where q is any integer, we rewrite $\{y(r\delta t)\}$ as

$$\begin{aligned} C \sin [2\pi f r \delta t + \phi(f)] &= C \sin [2\pi f r \delta t + 2\pi q + \phi(f)] \\ &= C \sin \left[2\pi \left(f + \frac{m}{\delta t} \right) r \delta t + \phi(f) \right] \end{aligned} \quad (7.6)$$

where $m = 0, 1, 2, \dots$ (and hence, $mr = q$ is an integer). This shows that for any value of δt , the frequencies of f and $f + m/\delta t$ are indistinguishable in a sampled discrete series. Hence, all frequencies given by $f + m/\delta t$ are the alias frequencies of f . However, by adherence to the sampling theorem criterion of either Equation 7.2 or 7.3, all $m \geq 1$ are eliminated from the sampled signal, and thus this ambiguity between frequencies is avoided.

This same discussion applies equally to complex periodic, aperiodic, and nondeterministic waveforms. This is shown by examining the general Fourier series used to represent such signals. A discrete series such as

$$\{y(r\delta t)\} = \sum_{n=1}^{\infty} C_n \sin [2\pi n f r \delta t + \phi_n(f)] \quad (7.7)$$

for $r = 0, 1, \dots, N-1$ can be rewritten as

$$\{y(r\delta t)\} = \sum_{n=1}^{\infty} C_n \sin \left[2\pi \left(nf + \frac{nm}{\delta t} \right) r\delta t + \phi_n(f) \right] \quad (7.8)$$

and so it displays the same aliasing phenomenon shown in Equation 7.6. In general, the Nyquist frequency defined by

$$f_N = \frac{f_s}{2} = \frac{1}{2\delta t} \quad (7.9)$$

represents a folding point for the aliasing phenomenon. All frequency content in the analog signal that is at frequencies above f_N appears as alias frequencies of less than f_N in the sampled signal. That is, such frequencies are folded back and superimposed on the signal as lower frequencies. The aliasing phenomenon occurs in spatial sampling [i.e., $y(x)$ at sampling intervals δx] as well, and the above discussion applies equally.

The alias frequency f_a , can be predicted from the folding diagram of Figure 7.3. Here the original input frequency axis is folded back over itself at the folding point of f_N and again for each of its harmonics mf_N , where $m = 1, 2, \dots$. For example and as noted by the solid arrows in Figure 7.3, the frequencies $f = 0.5 f_N, 1.5 f_N, 2.5 f_N, \dots$ that may be present in the original input signal all appear as the frequency $0.5 f_N$ in the discrete series $y(r\delta t)$. Use of the folding diagram is illustrated further in Example 7.1.

How does one avoid this alias phenomenon when sampling a signal of unknown frequency content? The preferred option is to choose a sample rate based on the maximum frequency of interest while adhering to the criterion of Equation 7.2 and to pass the signal through a low-pass filter prior to sampling. Based on Equation 7.9, the filter is set to remove signal content at and above f_N . This type of filter is called an *anti-aliasing filter*. Another option is to assign a sample rate so large that the measured signal does not have significant amplitude content above f_N . In this way, you choose f_s high enough such that the amplitudes of any frequency content above f_N are small compared to those below f_N . With this option, the resulting effects of aliasing can be minimized but not eliminated.

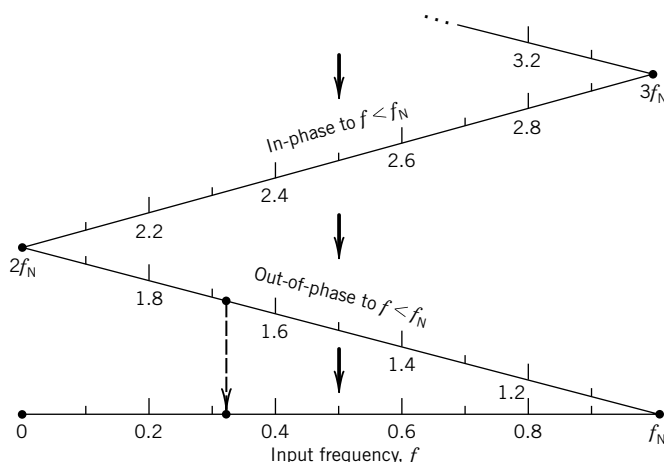


Figure 7.3 The folding diagram for alias frequencies.

Example 7.1

A 10-Hz sine wave is sampled at 12 Hz. Compute the maximum frequency that can be represented in the resulting discrete signal. Compute the alias frequency.

KNOWN $f = 10 \text{ Hz}$
 $f_s = 12 \text{ Hz}$

ASSUMPTION Constant sample rate

FIND f_N and f_a

SOLUTION The Nyquist frequency f_N sets the maximum frequency that can be represented in a resulting data set. Using Equation 7.9 with $f_s = 12 \text{ Hz}$ gives the Nyquist frequency $f_N = 6 \text{ Hz}$. This is the maximum frequency that can be sampled correctly. So the measured frequency is in error.

All frequency content in the analog signal above f_N appears as an alias frequency f_a between 0 and f_N . Because $f/f_N \approx 1.67$, f is folded back and appears in the sampled signal as a frequency between 0 and f_N . Reading Figure 7.3, $f = 1.67f_N$ is located directly above $0.33f_N$. So f is folded back to appear as $f_a = 0.33f_N$ or 2 Hz. This folding is indicated by the dashed arrow in Figure 7.3. As a consequence, the 10-Hz sine wave sampled at 12 Hz is completely indistinguishable from a 2-Hz sine wave sampled at 12 Hz in the discrete time series. The 10-Hz signal takes on the identity of a 2-Hz signal—that's aliasing.

COMMENT The programs *Sampling.m* and *Aliasing.vi* can be used to explore the effects of sample rate on the resulting signal. *Aliasing.vi* exercises the folding diagram concept.

Example 7.2

A complex periodic signal has the form

$$y(t) = A_1 \sin 2\pi(25)t + A_2 \sin 2\pi(75)t + A_3 \sin 2\pi(125)t$$

If the signal is sampled at 100 Hz, determine the frequency content of the resulting discrete series.

KNOWN $f_s = 100 \text{ Hz}$
 $f_1 = 25 \text{ Hz}$ $f_2 = 75 \text{ Hz}$ $f_3 = 125 \text{ Hz}$

ASSUMPTION Constant sample rate

FIND The alias frequencies f_{a1} , f_{a2} , and f_{a3} and discrete set $\{y(r\delta t)\}$

SOLUTION From Equation 7.9 for a sample rate of 100 Hz, the Nyquist frequency is 50 Hz. All frequency content in the analog signal above f_N takes on an alias frequency between 0 and f_N in the sampled data series. With $f_1 = 0.5 f_N$, $f_2 = 1.5 f_N$, and $f_3 = 2.5 f_N$, we can use Figure 7.3 to determine the respective alias frequencies.

i	f_i	f_{a_i}
1	25 Hz	25 Hz
2	75 Hz	25 Hz
3	125 Hz	25 Hz

In the resulting series, $f_{a_1} = f_{a_2} = f_{a_3} = 25$ Hz. Because of the aliasing phenomenon, the 75- and 125-Hz components would be completely indistinguishable from the 25-Hz component. The discrete series would be described by

$$y(r\delta t) = (B_1 + B_2 + B_3)\sin 2\pi(25)r\delta f \quad r = 0, 1, 2, \dots$$

where $B_1 = A_1$, $B_2 = -A_2$, and $B_3 = A_3$. Note from Figure 7.3 that when the original frequency component is out of phase with the alias frequency, the corresponding amplitude is negative. Clearly, this series misinterprets the original analog signal in both its frequency and amplitude content.

COMMENT Example 7.2 illustrates the potential for misrepresenting a signal with improper sampling. With signals for which the frequency content is not known prior to their measurement, sample frequencies should be increased according to the following scheme:

- Sample the input signal at increasing sample rates using a fixed total sample time, and examine the time plots for each signal. Look for changes in the shape of the waveform (Fig. 7.2).
 - Compute the amplitude spectrum for each signal at increasing sample rates and compare the resulting frequency content.
 - Always use (anti-aliasing) analog filters set at the Nyquist frequency.
-

Amplitude Ambiguity

For simple and complex periodic waveforms, the DFT of the sampled discrete time signal remains unaltered by a change in the total sample period $N\delta t$ provided that (1) the total sample period remains an integer multiple of the fundamental period T_1 of the measured continuous waveform, that is $mT_1 = N\delta t$ where m is an integer; and (2) the sample frequency meets the sampling theorem criterion. If both criteria are met, the amplitudes associated with each frequency in the periodic signal, the spectral amplitudes, are accurately represented by the DFT. This means that an original periodic waveform can be completely reconstructed from a discrete time series regardless of the sample time increment used. The total sample period defines the frequency resolution of the DFT:

$$\delta f = \frac{1}{N\delta t} = \frac{f_s}{N} \quad (7.10)$$

The frequency resolution plays a crucial role in the reconstruction of the signal amplitudes, as noted below.

An important difficulty arises when $N\delta t$ is not coincident with an integer multiple of the fundamental period of $y(t)$: The resulting DFT cannot *exactly* represent the spectral amplitudes of the sampled continuous waveform. This is exaggerated when $N\delta t$ represents only a relatively few fundamental periods of the signal. The problem is brought on by the truncation of one complete cycle of the signal (Fig. 7.4) and from spectral resolution, because the associated fundamental frequency and its harmonics are not coincident with a center frequency of the DFT. However, this error decreases either as the value of $N\delta t$ more closely approximates an exact integer multiple of T_1 or as f_s becomes very large relative to f_m .

This situation is illustrated in Figure 7.4, which compares the amplitude spectrum resulting from sampling the signal $y(t) = 10 \cos 628t$ over different sample periods. Two sample periods of

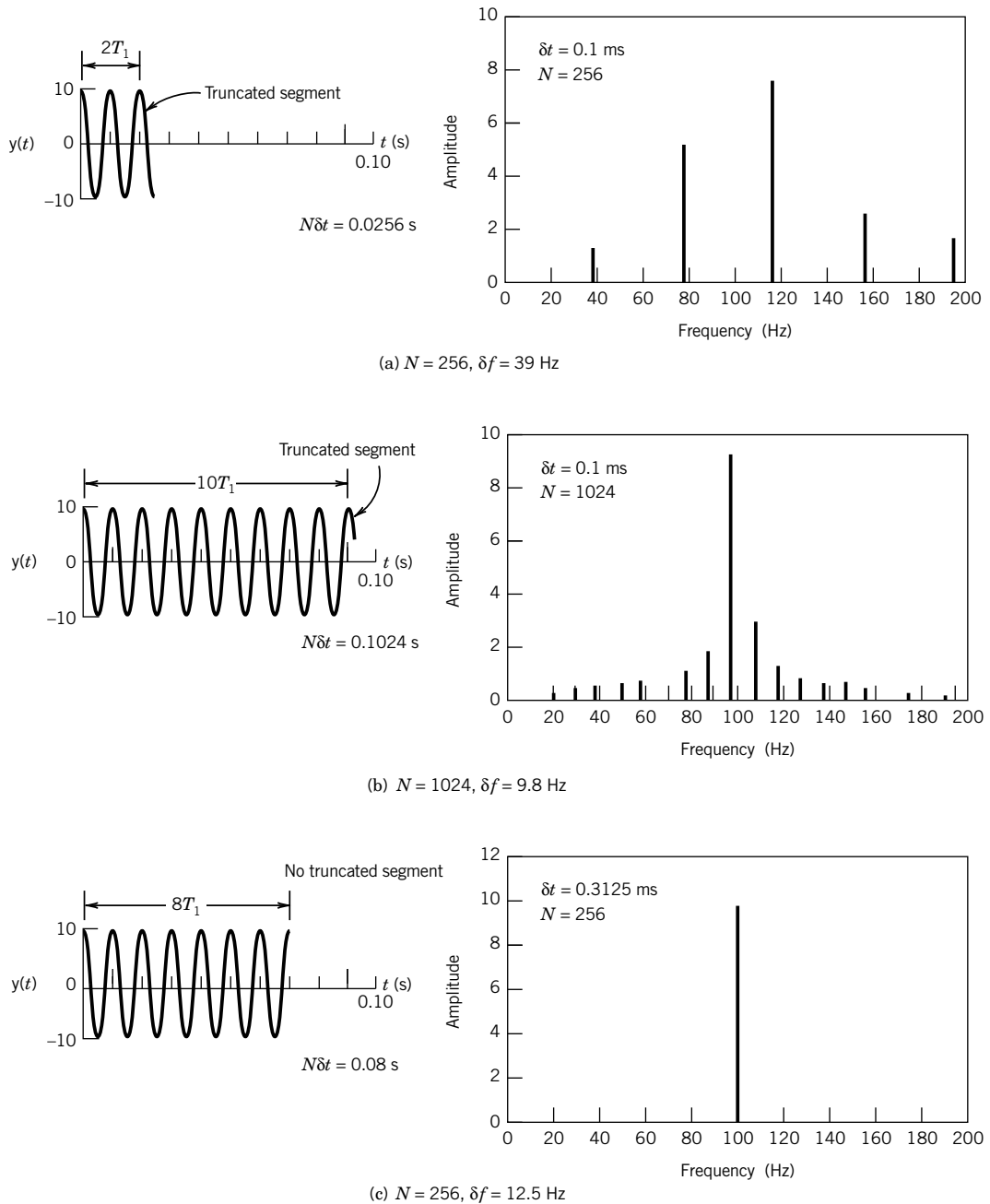


Figure 7.4 Amplitude spectra for $y(t)$. (a) $\delta f = 39$ Hz. (b) $\delta f = 9.8$ Hz. (c) $\delta f = 12.5$ Hz.

0.0256 and 0.1024 second were used with $\delta t = 0.1$ ms, and a third sample period of 0.08 second with $\delta t = 0.3125$ ms.¹ These sample periods provide for a DFT frequency resolution δf of about 39, 9.8, and 12.5 Hz, respectively.

Leakage

The two spectra shown in Figures 7.4a,b display a spike near the correct 100 Hz with surrounding noise spikes, known as *leakage*, at adjacent frequencies. Note that the original signal $y(t)$ cannot be exactly reconstructed from either of these spectra. The spectrum in Figure 7.4c has been constructed using a longer sample time increment (i.e., lower sample rate) than that of the spectra in Figures 7.4a,b and with fewer data points than the spectrum of Figure 7.4b. Yet the spectrum of Figure 7.4c provides an exact representation of $y(t)$. The N and δt combination used has reduced leakage to zero, which maximizes the amplitude at 100 Hz. Its sample period corresponds to exactly eight periods of $y(t)$, and the frequency of 100 Hz corresponds to the center frequency of the eighth frequency interval of the DFT. As seen in Figure 7.4, the loss of accuracy in a DFT representation occurs in the form of amplitude “leakage” to adjacent frequencies. To the DFT, the truncated segment of the sampled signal appears as an aperiodic signal. The DFT returns the correct spectral amplitudes for both the periodic and aperiodic signal portions. But as a result, the spectral amplitudes for any truncated segment are superimposed onto portions of the spectrum adjacent to the correct frequency. Recall how the amplitude varied in Figure 7.2c. This is how leakage affects the time domain reconstruction. By varying the sample period or its equivalent, the DFT resolution, one can minimize leakage and control the accuracy of the spectral amplitudes.

If $y(t)$ is an aperiodic or nondeterministic waveform, there may not be a fundamental period. In such situations, one controls the accuracy of the spectral amplitudes by varying the DFT resolution δf to minimize leakage. As δf tends toward zero, leakage decreases.

In summary, the reconstruction of a measured waveform from a discrete signal is controlled by the sampling rate and the DFT resolution. By adherence to the sampling theorem, one controls the frequency content of both the measured signal and the resulting spectrum. By variation of δf , one can control the accuracy of the spectral amplitude representation.

Programs *Sampling.m*, *Aliasing.vi*, and *Aliasing frequency domain.vi* explore the concept of sample rate and amplitude ambiguity. Program *Leakage.2.vi* allows the user to vary sample rate and number of points; it follows the discussion of Figure 7.4. Program *DataSpec.m* explores sampling concepts on user-generated data series. *Signal generation.vi* explores sample rate effects on different wave forms.

For an exact discrete representation in both frequency and amplitude of any periodic analog waveform, both the number of data points and the sample rate should be chosen based on the preceding discussion using the criteria of Equations 7.2 and 7.10. Equation 7.2 sets the maximum value for δt , or equivalently, the minimum sample rate f_s , and Equation 7.10 sets the total sampling time $N\delta t$ from which the data number N is estimated.

Waveform Fidelity

While choosing the sampling frequency in accordance with the sampling theorem ensures that there will be no aliasing associated with frequency content, it does not address the “shape” of the

¹ Many DFT (including fast Fourier transform [FFT]) algorithms require that $N = 2^M$, where M is an integer. This affects the selection of δt .

waveform. If sampling cannot be exact, then what is good enough? As an example, consider the original compact disk for musical recording. The sampling rate was limited by existing technology at the time (circa 1980), and the sampling rate was chosen so that frequencies up to the ~ 20 kHz limits of human hearing would not be aliased; thus, a sampling rate of 44.1 kHz was chosen.

What does $f_s = 44.1$ kHz imply for the musical tones at 22 kHz? Essentially it means that at the highest frequencies we are representing a sine wave with two discrete points. Thus, there was much criticism and speculation that the higher frequencies present in the music were distorted. Technology has advanced since 1980, and we now have Super Audio CD (SACD) format recordings, first introduced in 1999. The sampling rate for SACD recordings is 2822.4 kHz. Now a 20-kHz frequency in the recorded music is represented by ~ 140 data points and any distortion is inaudible.

As a general rule waveform fidelity is acceptable for $f_s \geq 5f_m$ to $10f_m$ depending on the application.

7.3 DIGITAL DEVICES: BITS AND WORDS

The history of computing hardware begins around World War II with mechanical and vacuum-tube-based hardware (4). Some types of recording devices used holes punched in paper cards or tape; one example is the historically significant player piano rolls. In the 1970s punch cards were used to communicate computer programs to mainframe computers; each letter or number was represented by appropriately punched holes in a single column of the card. The most important concept in digital computing is that all of the required information can be represented as an appropriately structured series of binary representations, either a 0 or a 1. For holes in a paper tape, there are only two possibilities—a hole is there or it is not! All of these representations correspond to a binary numbering system.

Digital systems use some variation of a binary numbering system both to represent and transmit signal information. Binary systems use the binary digit or *bit* as the smallest unit of information. A bit is a single digit, either a 1 or a 0. Bits are like electrical switches and are used to convey both logical and numerical information. From a logic standpoint, the 1 and 0 are represented by the on and off switch settings. By appropriate action a bit can be reset to either on or off, thereby permitting control and logic actions. By combining bits it is possible to define integer numbers greater than 1 or 0. A numerical *word* is an ordered sequence of bits, with a *byte* being a specific sequence of 8 bits. Computer memory is usually byte addressed. The memory location where numerical information is stored is known as a *register*, with each register assigned its own *address*.

A combination of M bits can be arranged to represent 2^M different words. For example, a combination of 2 bits can represent 2^2 or four possible combinations of bit arrangements: 00, 01, 10, or 11. We can alternatively reset this 2-bit word to produce these four different arrangements that represent the decimal, that is, base 10, integer numbers 0, 1, 2, or 3, respectively. So an 8-bit word can represent the numbers 0 through 255; a 16-bit word can represent 0 through 65,535.

The numerical value for a word is computed by moving by bit from right to left. From the right side, each successive bit increases the value of the word by a unit, a 2, a 4, an 8, and so forth through the progression of 2^M , provided that the bit is in its on (value of 1) position; otherwise, the particular bit increases the value of the word by zero. A weighting scheme of an M -bit word is given as follows:

Bit $M-1$...	Bit 3	Bit 2	Bit 1	Bit 0
2^{M-1}	...	2^3	2^2	2^1	2^0
2^{M-1}	...	8	4	2	1

Table 7.1 Binary Codes (Example: 4-Bit Words)

Bits	(Hex)	Straight	Offset	Twos Complement	Ones Complement	AVPS ¹
0000	0		-7	+0	+0	-0
0001	1		-6	+1	+1	-1
0010	2		-5	+2	+2	-2
0011	3		-4	+3	+3	-3
0100	4		-3	+4	+4	-4
0101	5		-2	+5	+5	-5
0110	6		-1	+6	+6	-6
0111	7		-0	+7	+7	-7
1000	8		+0	-8	-7	+0
1001	9		+1	-7	-6	+1
1010	A		+2	-6	-5	+2
1011	B		+3	-5	-4	+3
1100	C		+4	-4	-3	+4
1101	D		+5	-3	-2	+5
1110	E		+6	-2	-1	+6
1111	F		+7	-1	-0	+7

¹AVPS, absolute-value plus-sign code.

Using this scheme, bit $M - 1$ is known as the most significant bit (MSB) because its contribution to the numerical level of the word is the largest relative to the other bits. Bit 0 is known as the least significant bit (LSB). In hexadecimal (base 16), a sequence of 4 bits is used to represent a single digit, so that the 2^4 different digits (0 through 9 plus A through F) form the alphabet for creating a word.

Several binary codes are in common use. In 4-bit straight binary, 0000 is equivalent to analog zero and 1111 is equivalent to decimal 15 or hexadecimal F. Straight binary is considered to be a unipolar code because all numbers are of like sign. Bipolar codes allow for sign changes. *Offset binary* is a bipolar code with 0000 equal to -7 and 1111 equal to +7. The comparison between these two codes and several others is shown in Table 7.1. In offset binary there are two zero levels, with true zero being centered between them. Note how the MSB is used as a sign bit in a bipolar code.

The *ones-* and *twos-complement binary codes* shown in Table 7.1 are both bipolar. They differ in the positioning of the zero, with the twos-complement code containing one more negative level (-8) than positive (+7). Twos-complement code is widely used in digital computers. The bipolar AVPS code uses the MSB as the sign bit but uses the lower bits in a straight binary representation; for example, 1100 and 0100 represent -4 and +4, respectively.

A code often used for digital decimal readouts and for communication between digital instruments is binary coded decimal (BCD). In this code, each individual digit of a decimal number is represented separately by its equivalent value coded in straight binary. For example, the three digits of the base 10 number 532_{10} are represented by the BCD number 0101 0011 0010 (i.e., binary 5, binary 3, binary 2). In this code each binary number need span but a single decade, that is, have values from 0 to 9. Hence, in digital readouts, when the limits of the lowest decade are exceeded, that is, 9 goes to 10, the code just carries into the next higher decade.

Example 7.3

A 4-bit register contains the binary word 0101. Convert this to its decimal equivalent assuming a straight binary code.

KNOWN 4-bit register

FIND Convert to base 10

ASSUMPTION Straight binary code

SOLUTION The content of the 4-bit register is the binary word 0101. This represents

$$0 \times 2^3 + 1 \times 2^2 + 0 \times 2^1 + 1 \times 2^0 = 5$$

The equivalent of 0101 in decimal is 5.

7.4 TRANSMITTING DIGITAL NUMBERS: HIGH AND LOW SIGNALS

Electrical devices transmit binary code by using differing voltage levels. Because a bit can have a value of 1 or 0, the presence of a particular voltage (call it HIGH) at a junction could be used to represent a 1-bit value, whereas a different voltage (LOW) could represent a 0. Most simply, this voltage can be affected by use of an open or closed switch using a flip-flop (see Chapter 6), such as depicted in Figure 7.5a.

For example, a signal method common with many digital devices is a +5 V form of TTL (true transistor logic), which uses a nominal +5 V HIGH/0 V LOW scheme for representing the value of a bit. To avoid any ambiguity due to voltage fluctuations and provide for more precision, a voltage level between +2 and +5.5 V is taken as HIGH and therefore a bit value of 1, whereas a voltage between -0.6 and +0.8 V is taken as LOW or a 0-bit value. But this scheme is not unique.

Binary numbers can be formed through a combination of HIGH and LOW voltages. Several switches can be grouped in parallel to form a register. Such an M -bit register forms a number based on the value of the voltages at its M output lines. This is illustrated in Figure 7.5b for a 4-bit register forming the number 1010. So the bit values can be changed simply by changing the opened or closed state of the switches that connect to the output lines. This defines a parallel form in which all of the bits needed to form a word are available simultaneously. But another form is serial, where the bits are separated in a time sequence of HIGH/LOW pulses, each pulse lasting for only one predefined time duration, δt . This is illustrated in the pulse sequence of Figure 7.5c, which also forms the number 1010.

7.5 VOLTAGE MEASUREMENTS

Digital measurement devices consist of several components that interface the digital device with the analog world. In particular, the digital-to-analog converter and the analog-to-digital converter are discussed next. They form the major components of a digital voltmeter and an analog-to-digital/digital-to-analog data acquisition system.

Digital-to-Analog Converter

A digital-to-analog converter is an M -bit digital device that converts a digital binary word into an analog voltage (5–8). One possible scheme uses an M -bit register with a weighted resistor ladder

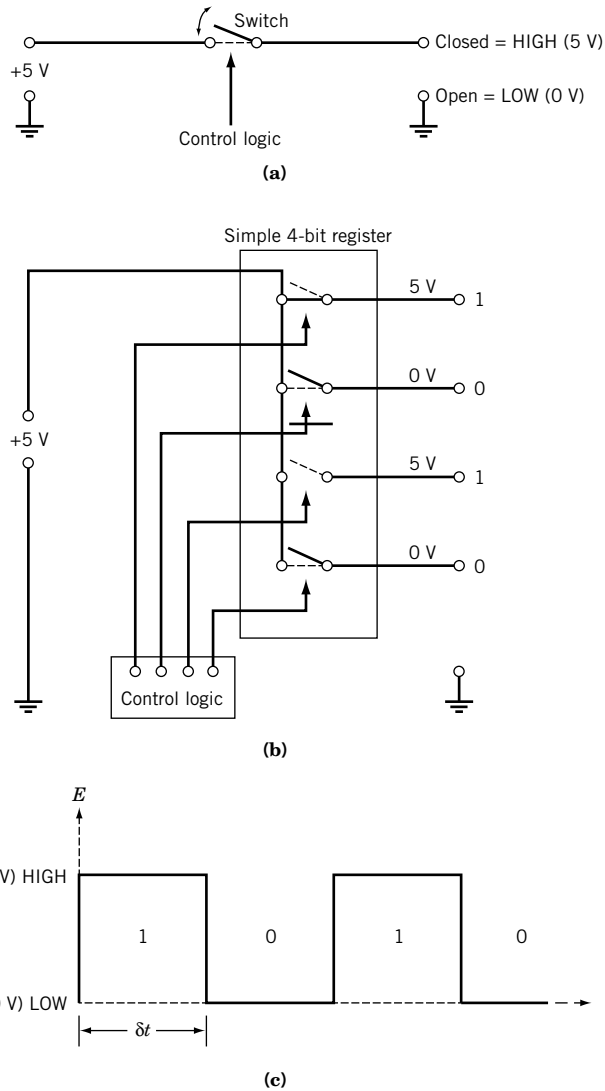


Figure 7.5 Methods for transmitting digital information. (a) Simple on/off (1 or 0) switch. (b) Four-bit register transmitting 1010 in parallel. (c) Serial transmission of 1010.

circuit and operational amplifier, as depicted in Figure 7.6. The circuit consists of M binary weighted resistors having a common summing point. The resistor associated with the register MSB has a value of R . At each successive bit the resistor value is doubled, so that the resistor associated with the LSB has a value of $(2^{M-1}R)$. The circuit output is a current, I , given by

$$I = E_{\text{ref}} \sum_{m=1}^M \frac{c_m}{2^{m-1}R} \quad (7.11)$$

The values for c_m are either 0 or 1 depending on the associated m th bit value of the register that controls the switch setting. The output voltage from the amplifier is

$$E_o = IR_r \quad (7.12)$$

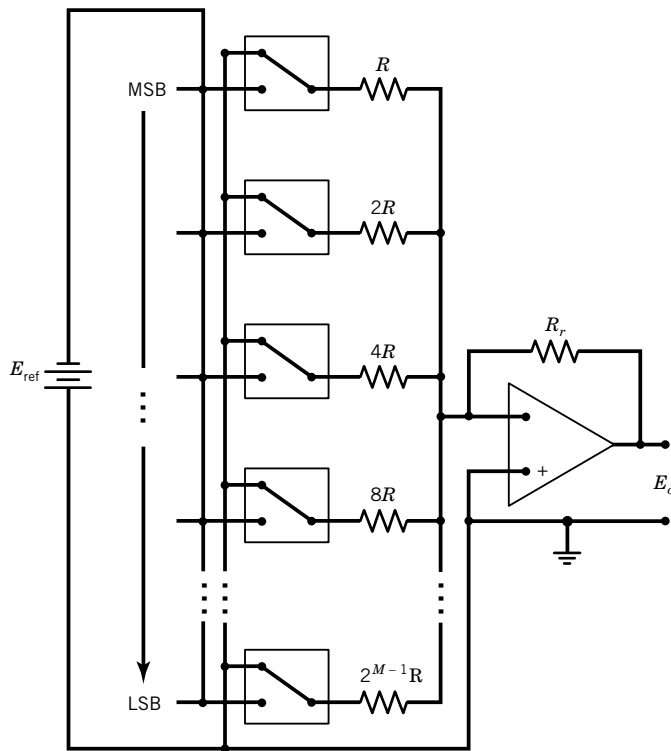


Figure 7.6 Digital-to-analog converter.

Note that this is equivalent to an operation in which an M -bit D/A converter would compare the magnitude of the actual input binary number, X , contained within its register to the largest possible number 2^M . This ratio determines E_o from

$$E_o = \frac{X}{2^M} \quad (7.13)$$

The D/A converter will have both digital and analog specifications, the latter expressed in terms of its full-scale analog voltage range output (E_{FSR}). Typical values for E_{FSR} are 0 to 10 V (unipolar) and ± 5 V (bipolar) and for M are 8, 12, 16, and 18 bits.

Analog-to-Digital Converter

An analog-to-digital converter converts an analog voltage value into a binary number through a process called *quantization*. The conversion is discrete, taking place one number at a time.

The A/D converter is a hybrid device having both an analog side and a digital side. The analog side is specified in terms of a full-scale voltage range, E_{FSR} . The E_{FSR} defines the voltage range over which the device operates. The digital side is specified in terms of the number of bits of its register. An M -bit A/D converter outputs an M -bit binary number. It can represent 2^M different binary numbers. For example, a typical 8-bit A/D converter with an $E_{FSR} = 10$ V would be able to represent analog voltages in the range between 0 and 10 V (unipolar) or the range between ± 5 V (bipolar) with

$2^8 = 256$ different binary values. Principal considerations in selecting a type of A/D converter include resolution, voltage range, and conversion speed.

Resolution

The A/D converter resolution is defined in terms of the smallest voltage increment that causes a bit change. Resolution is specified in volts and is determined by

$$Q = E_{\text{FSR}}/2^M \quad (7.14)$$

Primary sources of error intrinsic to any A/D converter are the resolution and associated quantization error, saturation error, and conversion error.

Quantization Error

An A/D converter has a finite resolution, and any input voltage that falls between two adjacent output codes results in an error. This error is referred to as the *quantization error* e_Q . It behaves as noise imposed on the digital signal.

The analog input to digital output relationship for a 0- to 4-V, 2-bit A/D converter is represented in Figure 7.7. From Equation 7.14, the resolution of this device is $Q = 1 \text{ V}$. For such a converter, an input voltage of 0.0 V would result in the same binary output of 00 as would an input of 0.9 V. Yet an input of 1.1 V results in an output of 01. Clearly, the output error is directly related to the resolution. In this encoding scheme, e_Q is bounded between 0 and 1 LSB above E_i , so we estimate $e_Q = Q$. This scheme is common in digital readout devices.

A second common scheme makes the quantization error symmetric about the input voltage. For this, the analog voltage is shifted internally within the A/D converter by a bias voltage, E_{bias} , of an amount equivalent to $\frac{1}{2}$ LSB. This shift is transparent to the user. The effect of such a shift is shown on the second lower axis in Figure 7.7. This now makes e_Q bounded by $\pm\frac{1}{2}$ LSB about E_i .

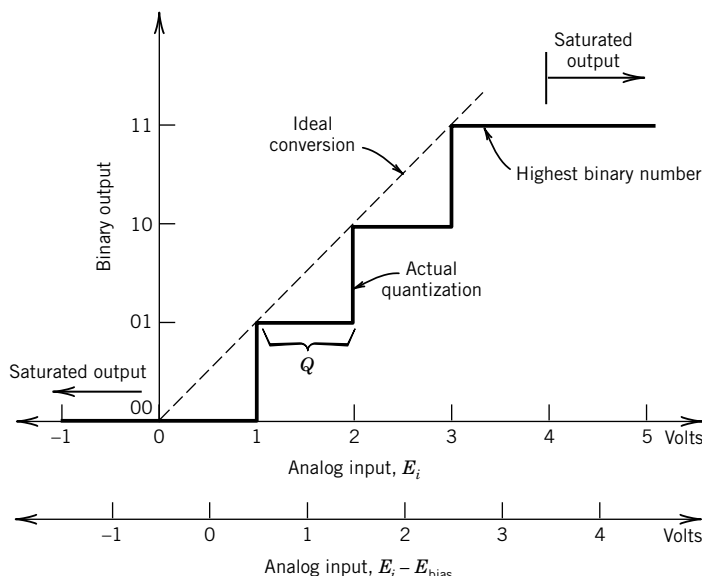


Figure 7.7 Binary quantization and saturation.

Table 7.2 Conversion Resolution

Bits <i>M</i>	Q^a (V)	SNR (dB)
2	2.5	12
4	0.625	24
8	0.039	48
12	0.0024	72
16	$0.15 (10^{-3})$	96
18	$0.0381 (10^{-3})$	108

^aAssumes $E_{FSR} = 10$ V.

that is, $e_Q = \pm 1/2Q$. This scheme is also common in data-acquisition systems. Regardless of the scheme used, the span of the quantization error remains 1 LSB, and its effect is significant only at small voltages. In an uncertainty analysis we would set the resolution uncertainty to $u_Q = e_Q$.

The resolution of an A/D converter is sometimes specified in terms of signal-to-noise ratio (SNR). The SNR relates the power of the signal, given by Ohm's law as E^2/R , to the power that can be resolved by quantization, given by $E^2/(R \times 2^M)$. The SNR is just the ratio of these values. Defined in terms of the decibel (dB), this gives

$$SNR \text{ (dB)} = 20 \log 2^M \quad (7.15)$$

The effect of bit number on resolution and SNR is detailed in Table 7.2. Program *Bits of Resolution.vi* explores the influence of a combination of *M*, E_{FSR} , and Q on a measured signal.

Saturation Error

The analog range of an A/D converter limits the minimum and maximum analog voltage. If either limit is exceeded, the A/D converter output saturates and does not change with a subsequent increase in input level. As noted in Figure 7.7, an input to the 0- to 4-V, 2-bit A/D converter above 4 V results in an output of binary 11 and below 0 V of binary 00. A saturation error is defined by the difference between the input analog signal level and the equivalent digital value assigned by the A/D converter. Saturation error can be avoided by conditioning signals to remain within the limits of the A/D converter.

Conversion Error

An A/D converter is not immune to elemental errors arising during the conversion process that lead to misrepresenting the input value. As with any device, the A/D errors can be delineated into hysteresis, linearity, sensitivity, zero, and repeatability errors. The extent of such errors depends on the particular method of A/D conversion. Factors that contribute to conversion error include A/D converter settling time, signal noise during the analog sampling, temperature effects, and excitation power fluctuations (5–7).

Linearity errors result from the ideal assumption that an *M*-bit A/D converter resolves the analog input range into $2^M - 1$ equal steps of width Q . In practice, the steps may not be exactly equal, which causes a nonlinearity in the ideal conversion line drawn in Figure 7.7. This error is specified in terms of bits.

Example 7.4

Compute the relative effect of quantization error (e_Q/E_i) in the quantization of a 100-mV and a 1-V analog signal using an 8-bit and a 12-bit A/D converter, both having a full-scale range of 0 to 10 V.

KNOWN $E_i = 100 \text{ mV}$ and 1V

$M = 8$ and 12

$E_{\text{FSR}} = 0\text{-}10 \text{ V}$

FIND e_Q/E_i , where e_Q is the quantization error

SOLUTION The resolutions for the 8-bit and 12-bit converters can be estimated from Equation 7.14 as

$$Q_8 = \frac{E_{\text{FSR}}}{2^8} = \frac{10}{256} = 39 \text{ mV}$$

$$Q_{12} = \frac{E_{\text{FSR}}}{2^{12}} = \frac{10}{4096} = 2.4 \text{ mV}$$

Assume the A/D converter is designed so that the absolute quantization error is given by $\pm \frac{1}{2}Q$. The relative effect of the quantization error can be computed by e_Q/E_i . The results are tabulated as follows:

E_i	M	e_Q	$100 \times e_Q/E_i$
100 mV	8	$\pm 19.5 \text{ mV}$	19.5%
100 mV	12	$\pm 1.2 \text{ mV}$	1.2%
1 V	8	$\pm 19.5 \text{ mV}$	1.95%
1 V	12	$\pm 1.2 \text{ mV}$	0.12%

From a relative point of view, the quantization error is much greater at lower voltage levels.

Example 7.5

The A/D converter with the specifications listed below is to be used in an environment in which the A/D converter temperature may change by $\pm 10^\circ\text{C}$. Estimate the contributions of conversion and quantization errors to the uncertainty in the digital representation of an analog voltage by the converter.

Analog-to-Digital Converter

E_{FSR}	0–10 V
M	12 bits
Linearity error	$\pm 3 \text{ bits}$
Temperature drift error	1 bit/ 5°C

KNOWN 12-bit resolution (see Ex. 7.4)

FIND $(u_c)_E$ measured

SOLUTION We can estimate a design-stage uncertainty as a combination of uncertainty due to quantization errors u_Q and due to conversion errors u_c :

$$(u_d)_E = \sqrt{u_o^2 + u_c^2}$$

The resolution of a 12-bit A/D converter with full-scale range of 0 to 10 V is (see Ex. 7.3) $u_Q = 2.4 \text{ mV}$, so that the quantization error is estimated by the zero-order uncertainty:

$$u_o = \frac{1}{2}Q = 1.2 \text{ mV}$$

Now the conversion error is affected by two elements:

$$\begin{aligned} \text{Linearity uncertainty} &= u_2 = 3 \text{ bits} \times 2.4 \text{ mV} \\ &= 7.2 \text{ mV} \end{aligned}$$

$$\begin{aligned} \text{Temperature uncertainty} &= u_3 = \frac{1 \text{ bit}}{5^\circ\text{C}} \times 10^\circ\text{C} \times 2.4 \text{ mV} \\ &= 4.8 \text{ mV} \end{aligned}$$

An estimate of the uncertainty due to conversion errors is found using the RSS method:

$$u_c = \sqrt{u_2^2 + u_3^2} = \sqrt{(7.2 \text{ mV})^2 + (4.8 \text{ mV})^2} = 8.6 \text{ mV}$$

The combined uncertainty in the digital representation of an analog value due to these uncertainties is an interval described as

$$\begin{aligned} (u_d)_E &= \sqrt{(1.2 \text{ mV})^2 + (8.6 \text{ mV})^2} \\ &= \pm 8.7 \text{ mV} \text{ (95% assumed)} \end{aligned}$$

The effects of the conversion errors dominate the uncertainty.

Successive Approximation Converters

We next discuss several common methods for converting voltage signals into binary words. Additional methods for A/D conversion are discussed in specialized texts (5,7).

The most common type of A/D converter uses the *successive approximation* technique. This technique uses a trial-and-error approach for converting the input voltage. Basically, the successive approximation A/D converter guesses successive binary values as it narrows in on the appropriate binary representation for the input voltage. As depicted in Figure 7.8, this A/D converter uses an M -bit register to generate a trial binary number, a D/A converter to convert the register contents into an analog voltage, and a voltage comparator (see Section 6.7 in Chapter 6) to compare the input voltage to the internally generated voltage. The conversion sequence is as follows:

1. The MSB is set to 1. All other bits are set to 0. This produces a value of E^* at the D/A converter output equivalent to the register setting. If $E^* > E_i$, the comparator goes LOW, causing the MSB to be reset to 0. If $E^* < E_i$, the MSB is kept HIGH at 1.

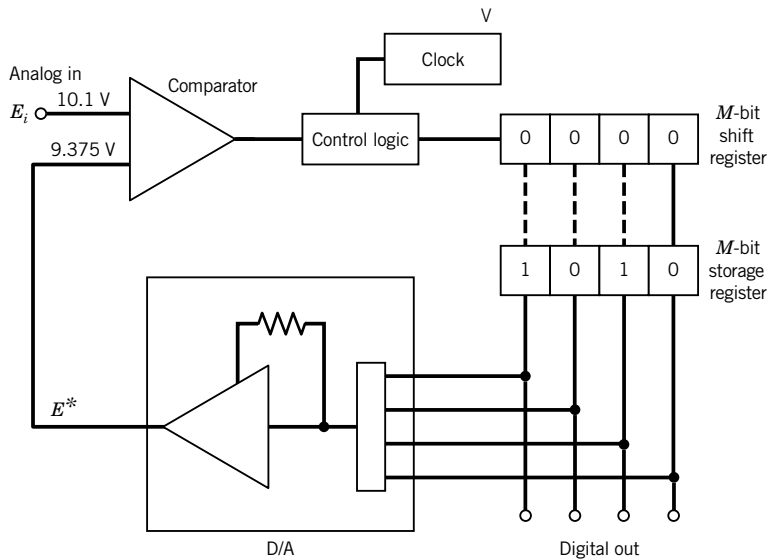


Figure 7.8 Successive approximation A/D converter. Four-bit scheme is shown with register = 1010 with $E_i = 10.1$ V.

2. The next highest bit (MSB-1) is set to 1. Again, if $E^* > E_i$, it is reset to 0; otherwise its value remains 1.
3. The process continues through to the LSB. The final register value gives the quantization of E_i .

The process requires a time of one clock tick per bit.

An example of this sequence is shown in Table 7.3 for an input voltage of $E_i = 10.1$ V and using the 0 to 15 V, 4-bit successive approximation A/D converter of Figure 7.8. For this case, the converter has a resolution of 0.9375 V. The final register count of 1010 or its equivalent of 9.375 V is the output from the A/D converter. Its value differs from the input voltage of 10.1 V as a result of the quantization error. This error can be reduced by increasing the bit size of the register.

The successive approximation converter is typically used when conversion speed at a reasonable cost is important. The number of steps required to perform a conversion equals the number of bits in the A/D converter register. With one clock tick per step, a 12-bit A/D converter operating with

Table 7.3 Example of Successive Approximation Conversion Sequence for a 4-Bit Converter

Sequence	Register	E^*	E_i	Comparator
Initial status	0000	0	10.1	
MSB set to 1	1000	7.5	10.1	High
Leave at 1	1000	7.5		
Next highest bit set to 1	1100	11.25		Low
Reset to 0	1000	7.5	10.1	
Next highest bit set to 1	1010	9.375		High
Leave at 1	1010	9.375		
LSB set to 1	1011	10.3125	10.1	Low
Reset to 0	1010	9.375		

a 1-MHz clock would require a maximum time of 12 μs per conversion. But this also reveals the trade-off between increasing the number of bits to lower quantization error and the resulting increase in conversion time. Faster clocks enable higher sample rates. Common maximum sample rates are on the order of 100 kHz to 1 MHz using 12, 16, or 24 bits.

Sources of conversion error originate in the accuracies of the D/A converter and the comparator. Noise is the principal weakness of this type of converter, particularly at the decision points for the higher-order bits. The successive approximation process requires that the voltage remain constant during the conversion process. Because of this, a sample-and-hold circuit (SHC), as introduced in Chapter 6, is used ahead of the converter input to measure and to hold the input voltage value constant throughout the duration of the conversion. The SHC also minimizes noise during the conversion.

Ramp (Integrating) Converters

Low-level (<1-mV) measurements often rely on ramp converters for their low-noise features. These integrating analog-to-digital converters use the voltage level of a linear reference ramp signal to discern the voltage level of the analog input signal and convert it to its binary equivalent. Principal components, as shown in Figure 7.9, consist of an analog comparator, ramp function generator, and counter and M -bit register. The reference signal, initially at zero, is increased at set time steps, within which the ramp level is compared to the input voltage level. This comparison is continued until the two are equal.

The usual method for generating the ramp signal is to use a capacitor of known fixed capacitance C , which is charged from a constant current source of amperage, I . Because the charge is related to current and time by

$$q = \int_0^t Idt \quad (7.16)$$

the reference ramp voltage is linearly related to the elapsed time by

$$E_{\text{ref}} = \frac{q}{C} = \text{constant} \times t \quad (7.17)$$

Time is integrated by a counter that increases the register value by 1 bit at each time step. Time step size depends on the value of 2^M . When the input voltage and ramp voltage magnitudes cross during a time step, the comparator output goes to zero, which flips a flip-flop halting the process. The register count value then indicates the digital binary equivalent of the input voltage.

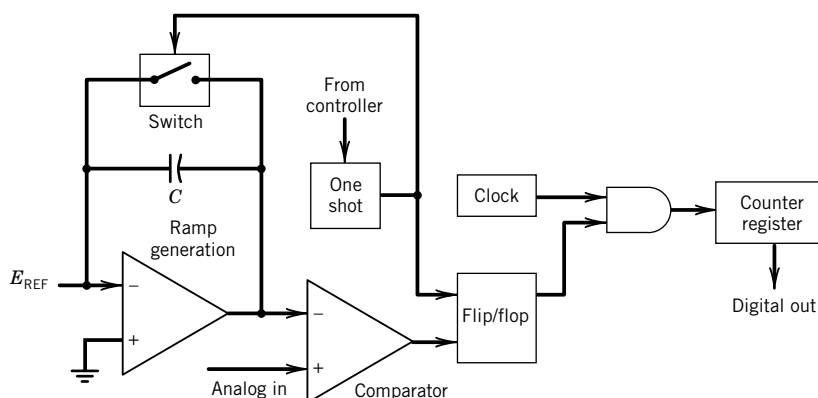


Figure 7.9 Ramp A/D converter.

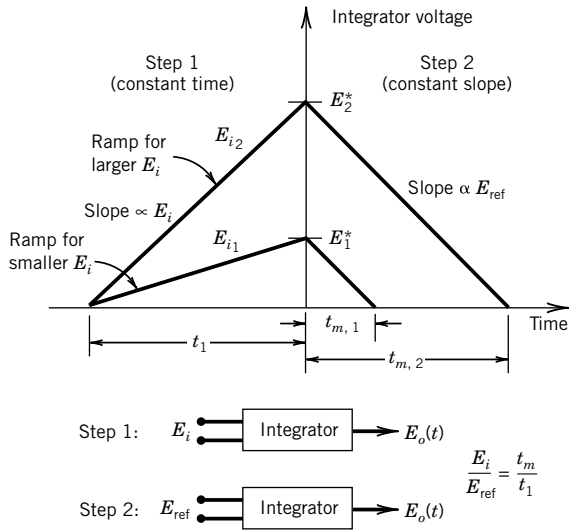


Figure 7.10 Dual-ramp analog voltage to digital conversion.

The accuracy of this single ramp operation is limited by the accuracy of the timing clock and the known values and constancy of the capacitor and the charging current. Increased accuracy can be achieved using a dual ramp converter, sometimes referred to as a dual-slope integrator, in which the measurement is accomplished in two steps, as illustrated in Figure 7.10. In the first step, the input voltage E_i is applied to an integrator for a fixed time period t_1 . The integrator output voltage increases in time with a slope proportional to the input voltage. At the end of the time interval, the output of the integrator has reached the level E^* . The second step in the process involves the application of a fixed reference voltage E_{ref} to the integrator. This step occurs immediately at the end of the fixed time interval in the first step, with the integrator voltage at exactly the same level established by the input. The reference voltage has the opposite polarity to the input voltage, and thus reduces the output of the integrator at a known rate. The time required for the output to return to zero is a direct measure of the input voltage. The time intervals are measured using a digital counter, which accumulates pulses from a stable oscillator. The input voltage is given by the relationship

$$E_i/E_{\text{ref}} = t_m/t_1 \quad (7.18)$$

where t_m is the time required for step two. Dual-ramp converter accuracy depends on the stability of the counter during conversion and requires a very accurate reference voltage.

Ramp converters are inexpensive but relatively slow devices. However, their integration process tends to average out any noise in the input signal. This is the feature that makes them so attractive for measuring low-level signals. The maximum conversion time using a ramp converter is estimated as

$$\text{Maximum conversion time} = 2^M / \text{Clock speed} \quad (7.19)$$

For a dual-ramp converter, this time is doubled. If one assumes that a normal distribution of input values are applied over the full range, the average conversion time can be taken to be one-half of the maximum value. For a 12-bit register with a 1-MHz clock and required to count the full 2^{12} pulses, a dual-ramp converter would require ~ 8 ms for a single conversion, corresponding to a sample rate of 125 Hz.

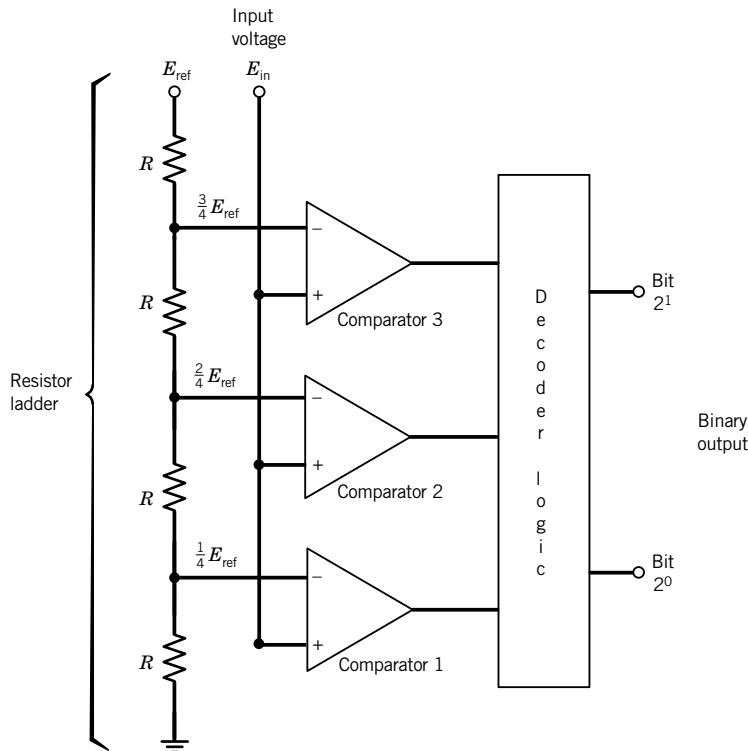


Figure 7.11 Parallel or flash A/D converter.
Two-bit scheme is shown.

Parallel Converters

A very fast A/D converter is the parallel or flash converter depicted in Figure 7.11. These converters are common to high-end stand-alone digital oscilloscopes and spectral analyzers. An M -bit parallel converter uses $2^M - 1$ separate voltage comparators to compare a reference voltage to the applied input voltage. As indicated in Figure 7.11, the reference voltage applied to each successive comparator is increased by the equivalent of 1 LSB by using a voltage-dividing resistor ladder. If the input voltage is less than its reference voltage, a comparator will go LOW; otherwise it will go HIGH.

Consider the 2-bit converter shown in Figure 7.11. If $E_{in} \geq \frac{1}{2}E_{ref}$ but $E_{in} < \frac{3}{4}E_{ref}$, then comparators 1 and 2 will be HIGH but comparator 3 will be LOW. In this manner, there can only be $2^M = 2^2 = 4$ different HIGH/LOW combinations from $2^2 - 1$ comparators, as noted in Table 7.4.

Table 7.4 Logic Scheme of a 2-Bit Parallel A/D Converter

Comparator			Binary Output
1	2	3	
HIGH	HIGH	HIGH	11
LOW	HIGH	HIGH	10
LOW	LOW	HIGH	01
LOW	LOW	LOW	00

which shows how these combinations correspond to the 2^2 possible values of a 2-bit binary output. Logic circuits transfer this information to a register.

Because all the comparators act simultaneously, the conversion occurs in a single clock count. Thus an attraction of this converter is its speed, with typical sample rates on the order of 150 MHz at 8 bits. Its disadvantage lies in the cost associated with its $2^M - 1$ comparators and the associated logic circuitry. For example, an 8-bit converter requires 255 comparators.

Digital Voltmeters

The digital voltmeter must convert an analog input signal to a digital output. This conversion can be done through several basic techniques (7). The most common method used in digital meters is with dual-ramp converters. The limits of performance for digital voltmeters can be significantly higher than for analog meters. Because of their very high input impedance, loading errors are very small at low-voltage levels, nearly as low as null balance instruments such as the potentiometer. The resolution (1 LSB) of these meters may be significantly better than their accuracy, so care must be taken in estimating uncertainty in their output. These devices are able to perform integration in both DC and true root-mean-square (rms) AC architecture.

Example 7.6

A 0- to 10-V, three-digit digital voltmeter (DVM) is built around a 10-bit, single-ramp A/D converter. A 100-kHz clock is used. For an applied input voltage of 6.372 V, what is the DVM output value? How long will the conversion process take?

KNOWN	$E_{\text{FSR}} = 10 \text{ V}$; $M = 10$
	Clock speed = 100 kHz
	Three significant digit readout (x.xx)
	Input voltage, $E_i = 6.372 \text{ V}$
FIND	Digital output display value
	Conversion time

SOLUTION The resolution of the A/D converter is

$$Q = E_{\text{FSR}} / 2^M = 10 \text{ V} / 1024 = 9.77 \text{ mV}$$

Because each ramp step increases the counter value by one bit, the ramp converter has a slope

$$\text{slope} = Q \times 1 \text{ bit/step} = 9.77 \text{ mV/step}$$

The number of steps required for conversion is

$$\text{steps required} = \frac{E_i}{\text{slope}} = \frac{6.372 \text{ V}}{0.00977 \text{ V/step}} = 652.29 \text{ or } 653 \text{ steps}$$

so the indicated output voltage is

$$\begin{aligned} E_0 &= \text{slope} \times \text{number of steps} \\ &= 9.77 \text{ mV/step} \times 653 \text{ steps} = 6.3769 \text{ V} \approx 6.38 \text{ V} \end{aligned}$$

A three-digit display rounds E_0 to 6.38 V. The difference between the input and output values is attributed to quantization error. With a clock speed of 100 kHz, each ramp step requires 10 $\mu\text{s}/\text{step}$, and conversion time = 653 steps \times 10 $\mu\text{s}/\text{step}$ = 6530 μs .

COMMENT A similar dual-ramp converter would require twice as many steps and twice the conversion time.

7.6 DATA-ACQUISITION SYSTEMS

A *data-acquisition system* is the portion of a measurement system that quantifies and stores data. There are many ways to do this. The engineer who reads a transducer dial, associates a number with the dial position, and records the number in a log book, performs all of the tasks germane to a data-acquisition system. This section focuses on microprocessor-based data-acquisition systems, which are used to perform automated data quantification and storage.

Figure 7.12 shows how a data-acquisition system (DAS) might fit into the general measurement scheme between the actual measurement and the subsequent data reduction. A typical signal flow scheme is shown in Figure 7.13 for multiple input signals to a single microprocessor-based/controller DAS.

Dedicated microprocessor systems can continuously perform their programming instructions to measure, store, interpret and provide process control without any intervention. Such microprocessors

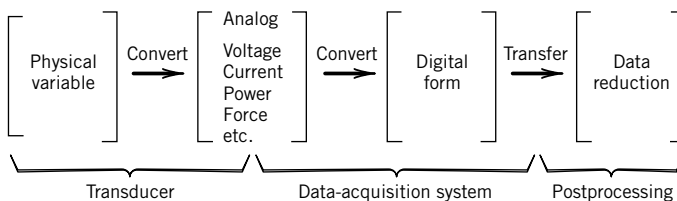


Figure 7.12 Typical signal and measurement scheme.

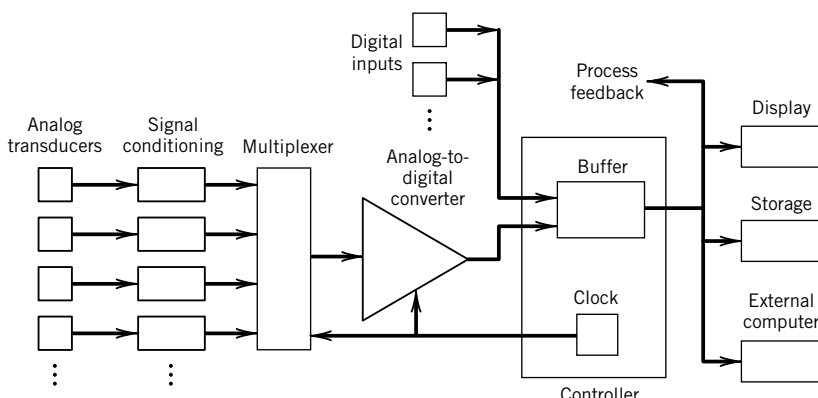


Figure 7.13 Signal flow scheme for an automated data-acquisition system.

have I/O ports to interface with other devices to measure and to output instructions. Programming allows for such operations as which sensors to measure and when and how often, and data reduction. Programming can allow for decision-making and feedback to control process variables. A cost-effective microprocessor system may be derived from a programmable logic controller (PLC).

Computer-based data-acquisition systems are hybrid systems combining a data-acquisition package with both the microprocessor and human interface capability of a personal computer (PC). The interface between external instruments and the PC is done either through the use of an I/O board, an external serial or parallel communication port, an external serial bus, or a wireless port. They all provide direct access to memory storage and connection to the Internet, an increasingly useful method to transmit data between locations.

7.7 DATA-ACQUISITION SYSTEM COMPONENTS

Signal Conditioning: Filters and Amplification

Analog signals usually require some type of signal conditioning to properly interface with a digital system. Filters and amplifiers are the most common components used.

Filters

Analog filters are used to control the frequency content of the signal being sampled. Anti-alias analog filters remove signal information above the Nyquist frequency prior to sampling. Not all data-acquisition boards contain analog filters, so these necessary components are often overlooked and may need to be added.

Digital filters are effective for signal analysis. They cannot be used to prevent aliasing. One digital filtering scheme involves taking the Fourier transform of the sampled signal, multiplying the signal amplitude in the targeted frequency domain to attain the desired frequency response (i.e., type of filter and desired filter settings), and transforming the signal back into time domain using the inverse Fourier transform (1,2).

A simpler digital filter is the moving average or smoothing filter, which is used for removing noise or showing trends. Essentially, this filter replaces a current data point value with an average based on a series of successive data point values. A center-weighted moving averaging scheme takes the form

$$y_i^* = (y_{i-n} + \dots + y_{i-1} + y_i + y_{i+1} + \dots + y_{i+n}) / (2n + 1) \quad (7.20)$$

where y_i^* is the averaged value that is calculated and used in place of y_i , and $(2n + 1)$ equals the number of successive values used for the averaging. For example, if $y_4 = 3$, $y_5 = 4$, $y_6 = 2$, then a three-term average of y_5 produces $y_5^* = 3$.

In a similar manner, a forward-moving averaging smoothing scheme takes the form

$$y_i^* = (y_i + y_{i+1} + \dots + y_{i+n}) / (n + 1) \quad (7.21)$$

and a backward moving averaging smoothing scheme takes the form

$$y_i^* = (y_{i-n} + \dots + y_{i-1} + y_i) / (n + 1) \quad (7.22)$$

Lighter filtering might use three terms, while heavier filtering might use 10 or more terms. This filtering scheme is easily accomplished within a spreadsheet program.

Amplifiers

All data-acquisition systems are input range limited; that is, there is a minimum value of a signal that they can resolve, and a maximum value that initiates the onset of saturation. Thus, some transducer signals need amplification or attenuation prior to conversion. Most data-acquisition systems contain on-board instrumentation amplifiers as part of the signal conditioning stage, as depicted in Figure 7.13, with selectable gains ranging from less than to greater than unity. Gain is varied either by a resistor jumper or by logic switches set by software, which effectively reset resistor ratios across op-amp amplifiers. Section 6.6 in Chapter 6 discusses amplifiers.

Although instrument amplifiers offer good output impedance characteristics, voltages can also be attenuated using a voltage divider. The output voltage from the divider circuit of Figure 7.14 is determined by

$$E_o = E_i \frac{R_2}{R_1 + R_2} \quad (7.23)$$

For example, a 0- to 50-V signal can be measured by a 0- to 10-V A/D converter using $R_1 = 40\text{ k}\Omega$ and $R_2 = 10\text{ k}\Omega$.

When only the dynamic content of time-dependent signals is important, amplification may require a strategy. For example, suppose the mean value of a voltage signal is large but the dynamic content is small, such as with the 5-Hz signal

$$y(t) = 2 + 0.1 \sin 10 \pi t \text{ (V)} \quad (7.24)$$

Setting the amplifier gain at or more than $G = 2.5$ to improve the resolution of the dynamic content would saturate a $\pm 5\text{-V}$ A/D converter. In such situations, you can remove the mean component from the signal prior to amplification by (1) adding a mean voltage of equal but opposite sign, such as -2 V here, or (2) passing the signal through a very low frequency high-pass filter (also known as *AC coupling*).

Shunt Resistor Circuits

An A/D converter requires a voltage signal at its input. It is straightforward to convert current signals into voltage signals using a shunt resistor. The circuit in Figure 7.15 provides a voltage

$$E_o = IR_{\text{shunt}} \quad (7.25)$$

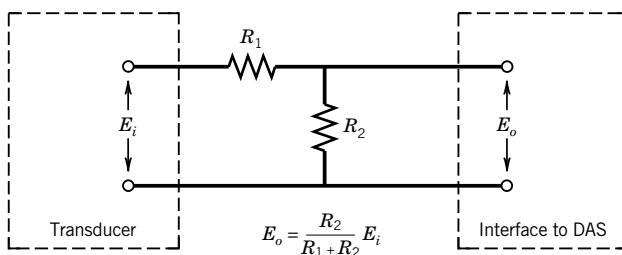


Figure 7.14 Voltage divider circuit for signal amplitude attenuation.

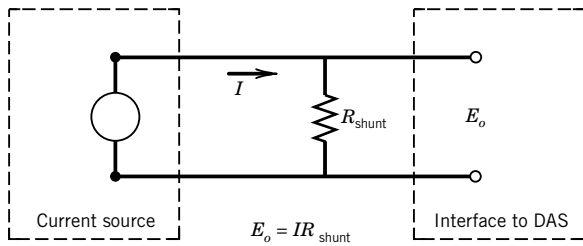


Figure 7.15 Simple shunt resistor circuit.

for signal current I . For a transducer using a standard 4- to 20-mA current loop, a 250- Ω shunt would convert this current output to a 1- to 5-V signal.

Offset Nulling Circuit

Offset nulling is used to subtract out a small voltage from a signal, such as to zero out a transducer output signal. The technique uses a trim potentiometer (R_{null}) in conjunction with a bridge circuit, such as shown in Figure 7.16, to produce the null voltage, E_{null} . The available null voltage is

$$E_{\text{null}} = \pm \left[\frac{E_i}{2} - \frac{E_i R_3 (R_{\text{null}} + R_{\text{sensor}})}{R_{\text{null}} R_{\text{sensor}} + R_3 (R_{\text{null}} + R_{\text{sensor}})} \right] \quad (7.26)$$

The corrected signal voltage is $E_0 = E_i - E_{\text{null}}$.

Components for Acquiring Data

Multiplexer

When multiple input signal lines are connected by a common throughput line to a single A/D converter, a multiplexer is used to switch between connections, one at a time. This is illustrated by the multiplexer depicted in Figure 7.17, which uses parallel flip-flops (see Chapter 6) to open and close the connection paths sequentially. The switching rate is determined by the conversion timing control logic. Advanced applications may employ the transmission of the signals from several transducers over a single line in a time-sharing scheme; the transmission line may be fiber optic and the signal digital.

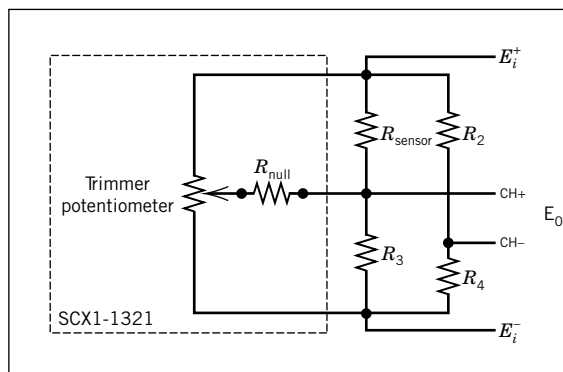


Figure 7.16 Circuit for applying a null offset voltage. (Courtesy of National Instruments, Inc.)

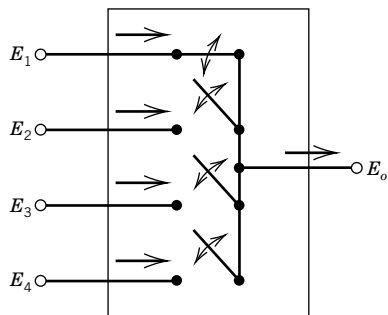


Figure 7.17 Multiplexer (four-channel shown).

A/D Converters

High-speed data-acquisition boards employ successive approximation converters with conversion rates typically up to the 100-kHz to 10-MHz range or parallel converters for rates up to and over 150 MHz. Low-level voltage measurements require the high noise rejection of the dual-ramp converter. Here the trade-off is in speed, with maximum conversion rates of 1 to 100 Hz more common.

D/A Converters

A digital-to-analog converter permits a DAS to convert digital numbers into analog voltages, which might be used for process control, such as to change a process variable, activate a device, or to drive a sensor positioning motor. The digital-to-analog signal is initiated by software or a controller.

Digital Input/Output

Digital signals are composed of discrete states, either high or low. Digital input/output lines may be used to communicate between instruments (see Section 7.9), control relays (to power equipment on or off), or indicate the state or status of a device. A common way to transmit digital information is the use of a 5-V TTL signal (e.g., see Fig. 7.5).

Digital I/O signals may be as a single state (HIGH or LOW; 5 V or 0 V) or as a series of pulses of HIGH/LOW states. The single-state signal might be used to operate a switch or relay, or to signal an alarm. A series of pulses transmits a data series. Gate-pulse counting entails counting pulses that occur over a specified period of time. This enables frequency determination (number of pulses/unit time) and counting/timing applications. Pulse stepping, sending a predetermined number of pulses in a series, is used to drive stepper motors and servos. Several I/O ports can be grouped to send parallel information.

Closed-Loop Controller

In closed-loop control, the controller is used to compare the state of a process, as determined through the value of a measured variable, with the value of a set condition and to take appropriate action to reduce the difference in value of the two. This difference in value is called the error signal. This error can change as part of the dynamics of the process, which causes the measured variable to change value, or because the set condition itself is changed. The controller action is to adjust the process so as to keep the error within a desired range.

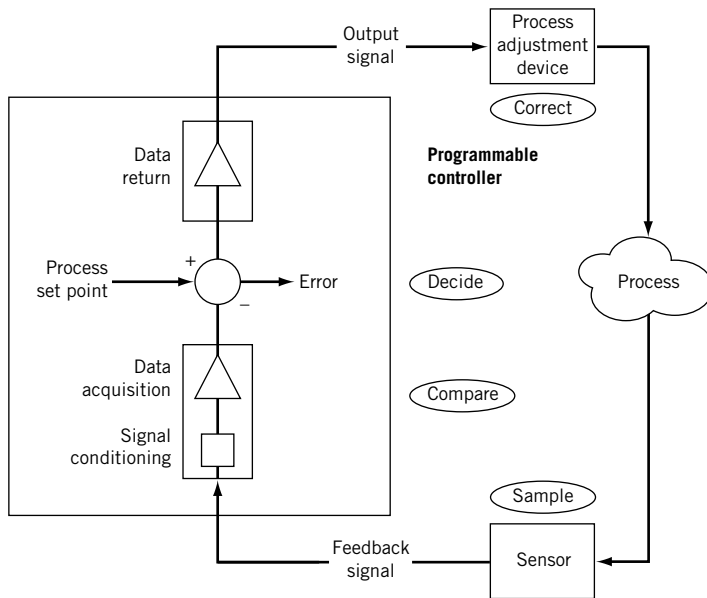


Figure 7.18 Closed-loop control concept built around a data-acquisition-based programmable controller.

The control process consists of this sequence: sample, compare, decide, and correct. An example of a digital control loop is depicted in Figure 7.18. Here the controller receives input about the process through a sensor that monitors the measured variable. The controller measures the sensor signal by sampling through an A/D converter or some digital input. The controller compares the measured value to the set value, computes the error signal, executes calculations through its control algorithm to decide on the correction needed, and acts to correct the process. In this example, we anticipate that the corrective elements are analog based, and so the controller sends the necessary signal for appropriate corrective action at the output of a D/A converter. The controller repeats this procedure at each cycle. A more extensive treatment of feedback control is provided in Chapter 12.

7.8 ANALOG INPUT-OUTPUT COMMUNICATION

Data-Acquisition Boards

Analog interfacing with a computer is most often affected using a general purpose DAS I/O board or DAS module (board, connection terminals, and interface package). Commonly available units are in the form of an expansion plug-in board, an external module with USB (universal serial bus) interface, or modules using wireless communication to transmit/receive data. So the discussion narrows on these devices. To illustrate a full feature board, we discuss the generic layout shown in Figure 7.19. Field wiring from/to transducers or other analog equipment is usually made through a mechanical screw terminal with subsequent connection directly to the board, which connects to a computer through a communications interface.

A multipurpose, multichannel high-speed data-acquisition plug-in board is shown in Figure 7.20. The representative board uses a 16-channel multiplexer and instrument amplifier. With its 12-bit successive approximation A/D converter with an 8- to 9- μ s conversion rate and its 800-ns

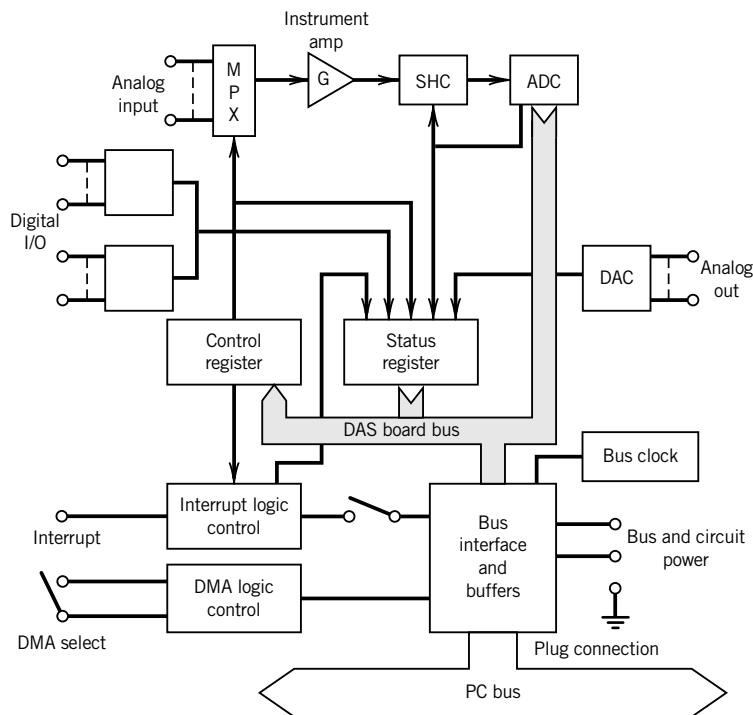


Figure 7.19 Typical layout for a data-acquisition plug-in board.
(Courtesy of National Instruments, Inc.)



Figure 7.20 Photograph of a data-acquisition plug-in board. (Courtesy of National Instruments, Inc.)

sample-hold time, sample rates of up to 333,000 Hz are possible. Input signals may be unipolar (e.g., 0–10 V) or bipolar (e.g., ± 5 V). For the board shown, this allows input resolution for the 12-bit converter with an $E_{\text{FSR}} = 10$ V range of approximately

$$Q = \frac{E_{\text{FSR}}}{2^M} = \frac{10 \text{ V}}{2^{12}} = 2.44 \text{ mV}$$

The amplifier permits signal conditioning with gains from $G = 0.5$ to 1000. This improves the minimum detectable voltage when set at maximum gain to

$$Q = \frac{E_{\text{FSR}}}{(G)(2^M)} = \frac{10 \text{ V}}{(1000)(2^{12})} = 2.44 \mu\text{V}$$

Digital I/O can usually be accomplished through these boards for instrument control applications and external triggering. For the board shown, 16-TTL compatible lines are available.

Single- and Differential-Ended Connections

Analog signal input connections to a DAS board may be single or differential ended. *Single-ended connections* use only one signal line (+ or HIGH) that is measured relative to ground (GRD), as shown in Figure 7.21. The return line (− or LOW) and ground are connected together. There is a common external ground point, usually through the DAS board. Multiple single-ended connections to a DAS board are shown in Figure 7.22.

Single-ended connecting wires should never be long, as they are susceptible to EMI (electromagnetic interference) noise. Because of noise, the signal should be large compared to the DAS resolution. Single-ended connections are suitable only when all of the analog signals can be made relative to the common ground point.

Why the concern over ground points? Electrical grounds are not all at the same voltage value (see Ground and Ground Loops, in Chapter 6). So if a signal is grounded at two different points, such as at its source and at the DAS board, the grounds could be at different voltage levels. When a grounded source is wired as a single-ended connection, the difference between the source ground voltage and the board ground voltage gives rise to a *common-mode voltage* (CMV). The CMV combines with the input signal superimposing interference and noise on the signal. This effect is referred to as a ground loop. The measured signal is unreliable.

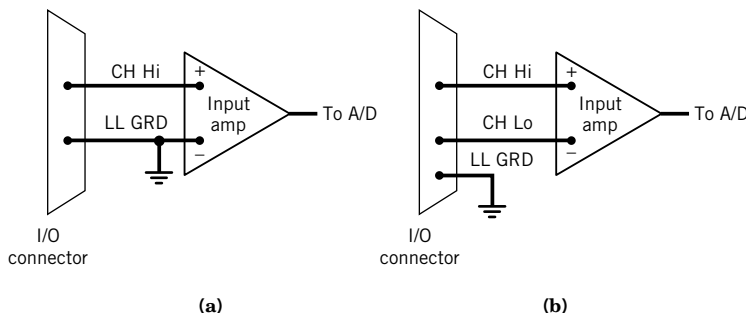


Figure 7.21 (a) Single-ended connection. (b) Differential-ended connection.

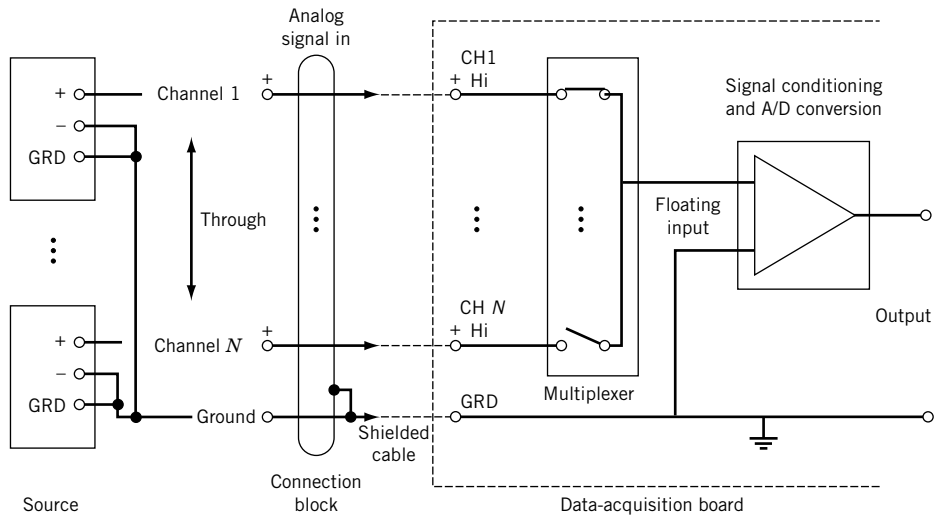


Figure 7.22 Multiple single-ended analog connections to a data-acquisition board.

Differential-ended connections allow the voltage difference between two distinct input signals to be measured. Here the signal input (+ or HIGH) line is paired with a signal return (– or LOW) line, which is isolated from ground (GRD), as shown in Figure 7.21. By using twisted pairs, the effects of noise are greatly reduced. A differential-ended connection to a DAS board is shown in Figure 7.23. The measured voltage is the voltage difference between these two (+ and –) lines for each channel.

Differential-ended connections are the preferred way to measure low-level signals. However, for low-level measurements, a 10-k Ω to 100-k Ω resistor should be connected between the signal

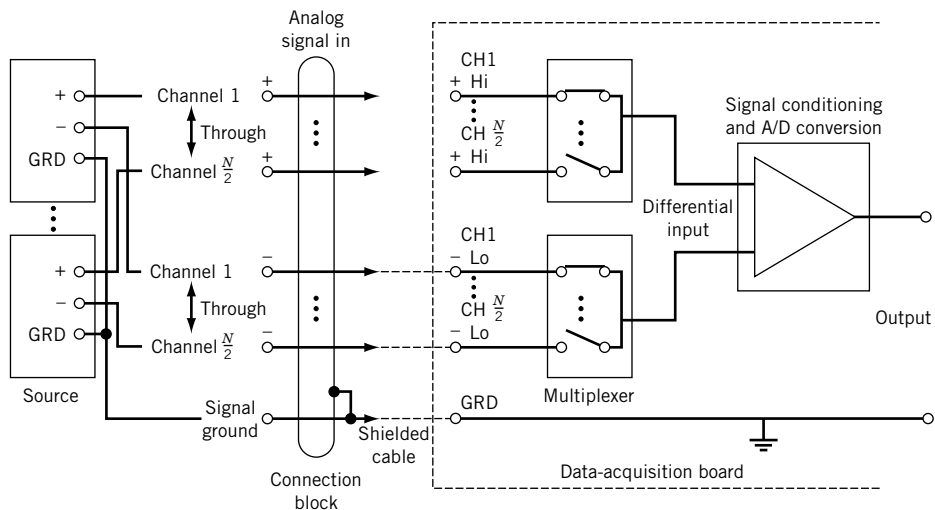


Figure 7.23 Multiple differential-ended analog connections to a data-acquisition board.

return (– or LOW) line and ground (GRD) at the DAS board. The differential-ended connection is less prone to common-mode voltage errors. But if the measured voltage exceeds the board's CMV range limit specification, it can be damaged.

Special Signal Conditioning Modules

Signal conditioning modules exist for different transducer applications. They connect between the transducer and the data-acquisition module. For example, resistance bridge modules allow the direct interfacing of strain gauges or other resistance sensors through an on-board Wheatstone bridge, such as depicted in Figure 7.24. There are temperature modules to allow for electronic thermocouple cold junction compensation that can provide for signal linearization for reasonably accurate (down to 0.5°C) temperature measurements.

Data-Acquisition Triggering

With DAS boards, data acquisition or equipment control can be triggered by software command, external pulse, or on-board clock. Software-controlled triggers can send TTL-level pulses to external devices for synchronization, activation, and control.

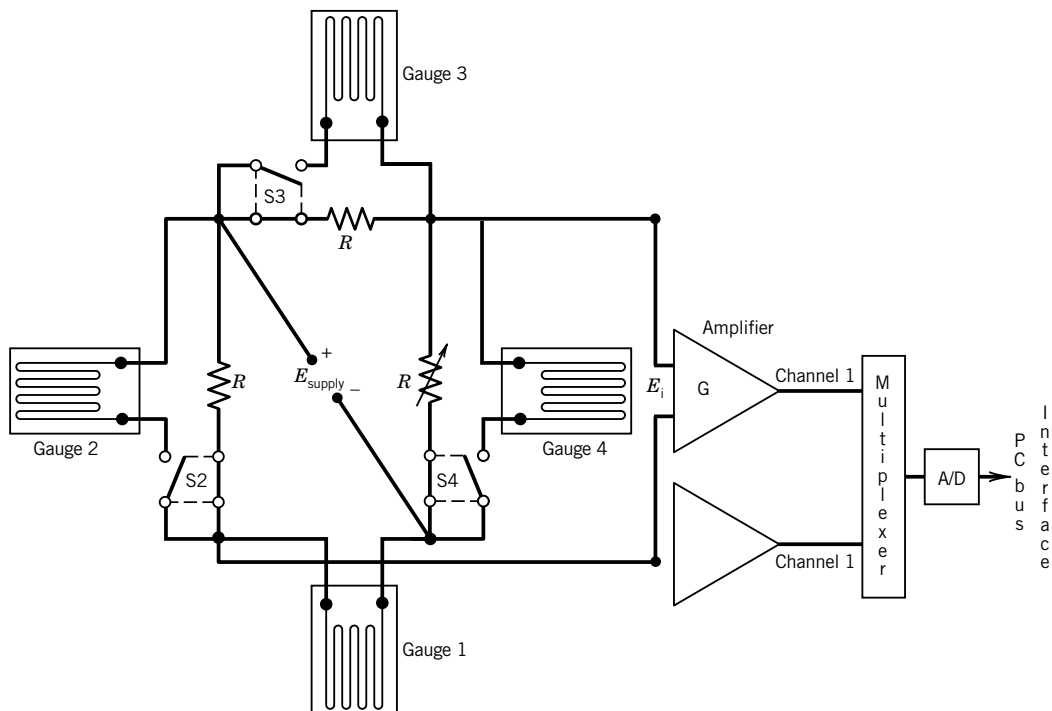


Figure 7.24 A strain-gauge interface. Gauges are connected by wires to the interface.

7.9 DIGITAL INPUT–OUTPUT COMMUNICATION

Certain standards exist for the manner in which digital information is communicated between digital devices (6,7). Serial communication methods transmit data bit by bit. Parallel communication methods transmit data in simultaneous groups of bits, for example, byte by byte. Both methods use a *handshake*, an interface protocol that initiates, allows, and terminates the data transfer between devices and TTL-level signals. Most lab equipment can be equipped to communicate by at least one of these means, and standards have been defined to codify communications between devices of different manufacturers. Standards continuously evolve, so the present discussion focuses on concepts and application of representative standards.

Serial Communications: RS-232C

The RS-232C protocol, which was initially set up to translate signals between telephone lines and computers via a modem (modulator-demodulator), remains a well-used interface for communication between a computer and any serial device. Basically, this protocol allows two-way communication using two single-ended signal (+) wires, noted as TRANSMIT and RECEIVE, between data communications equipment (DCE), such as an instrument, and data terminal equipment (DTE), such as the data acquisition system or computer. These two signals are analogous to a telephone's mouthpiece and earpiece signals. A signal GROUND wire allows signal return (−) paths.

Most lab computers have an RS-232C-compatible I/O port. The popularity of this interface is due to the wide range of equipment that can utilize it. Either a 9-pin or 25-pin connector can be used. The full connection protocol is shown in Figure 7.25. Communications can be half-duplex or full-duplex. Half-duplex allows one device to transmit while the other receives. Full-duplex allows both devices to transmit simultaneously.

The minimum number of wires required between DTE and DCE equipment is the three-wire connection shown in Figure 7.26. This connects only the TRANSMIT, RECEIVE, and GROUND lines while bypassing the handshaking lines. The handshaking lines can be jumpered to fool either device into handshaking with itself, thereby allowing the communication. This is a popular wiring scheme when using a 9-pin connector. Communication between similar equipment, DTE to DTE or DCE to DCE, needs only nine lines. The full 9-pin connector wiring scheme is shown in Figure 7.27.

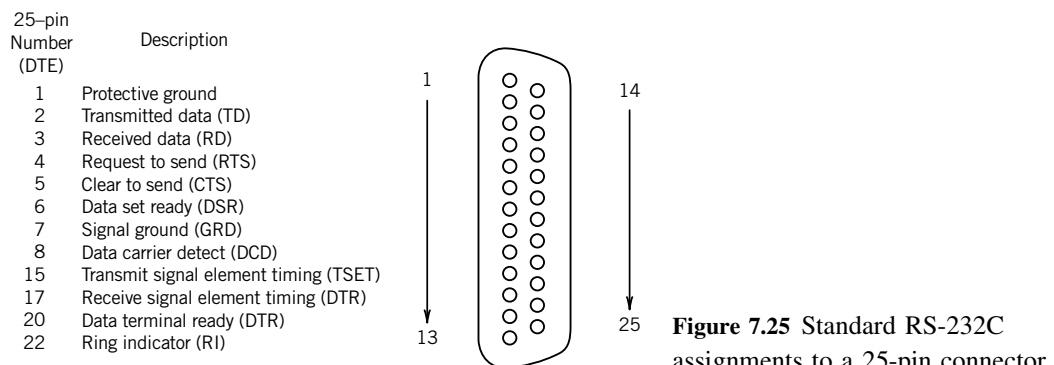


Figure 7.25 Standard RS-232C assignments to a 25-pin connector.

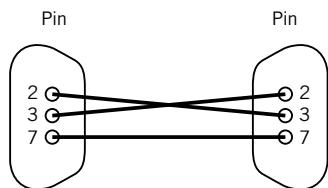


Figure 7.26 Minimum serial connections between DTE to DCE or DTE to DTE equipment (RS-232C).

9-pin Number	Description
1	Data carrier detect (DCD)
2	Transmitted data (TD)
3	Received data (RD)
4	Data terminal ready (DTR)
5	Signal ground (GRD)
6	Data set ready (DSR)
7	Request to send (RTS)
8	Clear to send (CTS)
9	Ring Indicator (RI)
Shell	Chassis ground

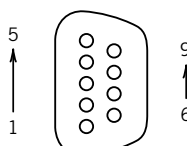


Figure 7.27 Nine-wire serial connection between DTE to DTE or DCE to DCE equipment (RS-232C).

Data Transmission

Serial communication implies that data are sent in successive streams of information, one bit at a time. The value of each bit is represented by an analog voltage pulse with a 1 and 0 distinguished by two equal voltages of opposite polarity in the 3- to 25-V range. Communication rates are measured in baud, which refers to the number of signal pulses per second.

A typical asynchronous transmission is 10 serial bits composed of a start bit followed by a 7- or 8-bit data stream, either one or no parity bit, and terminated by 1 or 2 stop bits. The start and stop bits form the serial “handshake”. *Asynchronous transmission* means that information may be sent at random intervals. So the start and stop bits are signals used to initiate and to end the transmission of each byte of data transmitted, hence the analogy of a handshake. The start bit allows for synchronization of the clocks of the two communicating devices. The parity bit allows for limited error checking. *Parity* involves counting the number of 1's in a byte. In 1 byte of data, there will be an even or odd number of bits with a value of 1. An additional bit added to each byte to make the number of 1 bits a predetermined even or odd number is called a parity bit. The receiving device counts the number of transmitted bits, checking for the predetermined even (even parity) or odd (odd parity) number. In *synchronous transmission*, the two devices initialize and synchronize communication with each other. Even when there are no data to send, the devices transmit characters just to maintain synchronization. Stop and start bits are then unnecessary, allowing for higher data transfer rates.

Devices that employ data buffers, a region of RAM that serves as a data holding area, use a software handshaking protocol such as XON/XOFF. With this, the receiving device transmits an XOFF signal to halt transmission as the buffer nears full and an XON signal when it has emptied and is again ready to receive.

Bluetooth Communications

Bluetooth is a standardized specification permitting wireless communication between devices. The specification is based on the use of radio waves to transmit information, allowing signals to pass

through enclosures, walls, and clothes. Devices are independent of aiming position. As such, the specification overcomes problems inherent with popular infrared port communication devices, for example those used on common electronic remote controls, which require line-of-sight interaction. However, Bluetooth is not intended or written to be a wireless LAN network protocol, such as is IEEE 802.11. Instead, it does permit communication between peripheral devices that use their own protocol by setting up a personal area network (PAN). Up to eight devices can communicate simultaneously over distances of up to about 10 m of separation within the 2.402- and 2.480-GHz radio spectrum on a PAN. Bluetooth 2.0 can manage data transfer rates up to 3 Mbps.

Universal Serial Bus and Firewire

The USB permits peripheral expansion for up to 128 devices at low- to high-speed data transfer rates. The original USB (USB 1.0/1.1) supports transfer rates from 1.5 Mbs up to 12Mbs, and the high-speed USB (USB 2.0) supports rates up to 480 Mbs. In January 2010 the first certified USB 3.0 consumer products were announced; the USB 3.0 achievable data rate is 3.2 Gbit/sec. Notably the maximum current that a USB 3.0 device can draw is 900 mA, an 80% increase over USB 2.0. The USB supports a “hot swap” feature that allows the user to plug in a USB-compatible device and to use it without reboot. This bus connects USB devices to a single computer host through a USB root hub. The USB physical interconnect is a tiered star topology, as illustrated in Figure 7.28a. In this setup, the root hub permits one to four attachments, which can be a combination of USB peripheral devices and additional USB hubs. Each successive hub can in turn support up to four devices or hubs. Cable length between a device and hub or between two hubs is limited to 5 m for USB. The connecting cable (Fig. 7.28b) is a four-line wire consisting of a hub power line, two signal lines (+ and –), and a ground (GRD) line.

Firewire is a trademark for the IEEE 1394 High Speed Serial Bus, currently governed by IEEE standard 1394-2008 (9). It was developed largely to support digital audio and video equipment. The IEEE 1394 communication standard uses six wires consisting of two pairs of signal lines and two power lines, with cable length limited to 4.5 m. Firewire connections can provide power to an external device.

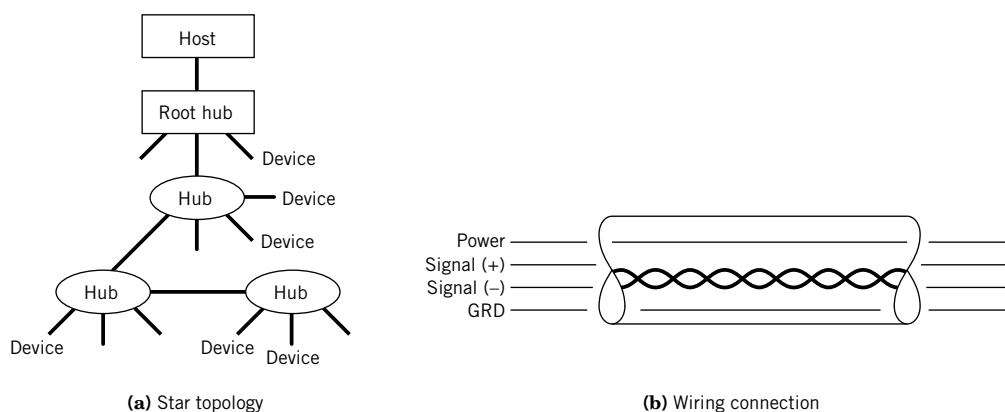


Figure 7.28 General purpose interface bus (GPIB) assignments to a 25-pin connector.

Parallel Communications GPIB (IEEE-488)

The *general purpose interface bus (GPIB)* is a high-speed parallel interface. Originally developed by Hewlett-Packard, it is sometimes referred to as the HP-IB. The GPIB is usually operated under the IEEE-488 communication standard. In 2004 the international and IEEE standards were combined and the current standard is designated IEC-60488-1. The bus allows for the control of other devices through a central controller, and it allows devices to receive/transmit information from/to the controller. This standard is well defined and widely used to interface communication between computers and printers and scientific instrumentation.

The standard for the GPIB operates from a 16-wire bus with a 24-wire connector (Table 7.5). A 25-pin connector is standard. The bus is formed by eight data lines plus eight lines for bus management and handshaking (two-way control communication). The additional eight lines are used for grounds and shield. Bit-parallel, byte-serial communication at data rates up to 8 Mbytes/s are possible. Connector lines are limited to a length of roughly 4 m.

The standard requires a controller, a function usually served by the laboratory computer, and permits multidrop operation, allowing up to 15 devices to be attached to the bus at any time. Each device has its own bus address (addresses 1–14). The bus controller (address 0) controls all the bus

Table 7.5 General Purpose Interface Bus (GPIB) Assignments to a 25-Pin Connector

Pin number	Description
Data lines	
1	Digital I/O data line 1
2	Digital I/O data line 2
3	Digital I/O data line 3
4	Digital I/O data line 4
13	Digital I/O data line 5
14	Digital I/O data line 6
15	Digital I/O data line 7
16	Digital I/O data line 8
Handshake lines	
6	Data valid (DAV)
7	Not ready for data (NRFD)
8	Not data accepted (NDAC)
Bus management lines	
5	End or identify (EOI)
9	Interface clear (IFC)
10	Service request (SRQ)
11	Attention (ATN)
17	Remote enable (REN)
Ground lines	
12	Shield
18–24	Ground

activities and sequences all communications to and between devices, such as which bus device transmits or receives and when. This is done along the bus management and handshaking lines. The communication along the bus is bidirectional. Normally, ground true TTL logic (i.e., ≤ 0.8 V HIGH, ≥ 2 V LOW) is used. The interplay between the controller and the devices on the bus is controlled by software programs.

Example 7.7

A strain transducer has a static sensitivity of 2.5 V/unit strain ($2.5 \mu\text{V}/\mu\epsilon$) and requires a supply voltage of 5 VDC. It is to be connected to a DAS having a ± 5 V, 12-bit A/D converter and its signal measured at 1000 Hz. The transducer signal is to be amplified and filtered. For an expected measurement range of 1 to $500 \mu\epsilon$, specify appropriate values for amplifier gain, filter type, and cutoff frequency, and show a signal flow diagram for the connections.

SOLUTION The signal flow diagram is shown in Figure 7.29. Power is drawn off the data-acquisition board and routed to the transducer. Transducer signal wires are shielded and routed through the amplifier, filter, and connected to the data-acquisition board connector block using twisted pairs to channel 0, as shown. The differential-ended connection at the board reduces noise.

The amplifier gain is determined by considering the minimum and maximum signal magnitudes expected, and the quantization error of the DAS. The nominal signal magnitude ranges from $2.5 \mu\text{V}$ to 1.25 mV. An amplifier gain of $G = 1000$ boosts this from 2.5 mV to 1.25 V. This lower value is on the order of the quantization error of the 12-bit converter. A gain of $G = 3000$ raises the low end of the signal out of quantization noise while keeping the high end out of saturation.

With a sample rate of $f_s = 1000$ Hz, an anti-alias, low-pass Butterworth filter with 12 dB/octave roll-off and a cutoff frequency set at $f_c = f_N = 500$ Hz would meet the task.

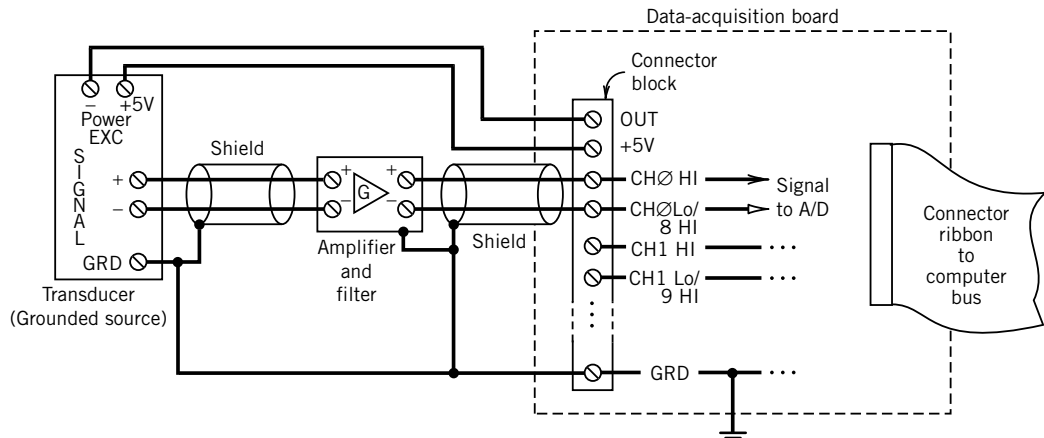


Figure 7.29 Line connections for Example 7.7.

Example 7.8

The output from an analog device (nominal output impedance of $600\ \Omega$) is the input to the 12-bit A/D converter (nominal input impedance of $1\ M\Omega$) of a data-acquisition system. For a 2-V signal, will interstage loading be a problem?

KNOWN $Z_1 = 600\ \Omega$

$Z_m = 1\ M\Omega$

$E_1 = 2\ V$

FIND e_1

SOLUTION The loading error is given by $e_1 = E_m - E_I$, where E_1 is the true voltage and E_m is the measured voltage. From Equation 6.39,

$$e_1 = E_1 \left(\frac{1}{1 + Z_1/Z_m} - 1 \right) = -1.2\ mV$$

The interstage loading error at 2-V input actually is less than the $\pm 2.4\text{-mV}$ quantization error of the 12-bit device.

Example 7.9

An analog signal is to be sampled at a rate of 200 Hz with a 12-bit A/D converter that has an input range of -10 to $10\ V$. The signal contains a 200-Hz component, f_1 , with an amplitude of $100\ mV$. Specify a suitable LC filter that attenuates the 200-Hz component down to the A/D converter quantization resolution level and acts as an anti-alias filter for quantization.

KNOWN $f_s = 200\ Hz$

$f_1 = 200\ Hz$

$A_1 = 100\ mV$

$E_{FSR} = 10V$

$M = 12$

FIND Specify a suitable filter

SOLUTION For $f_s = 200\ Hz$, the Nyquist frequency f_N is $100\ Hz$. So an appropriate design for an anti-alias filter might have the properties of $f_c = 100\ Hz$ and $M(100\ Hz) = -3\ dB$ and a maximally flat passband (Butterworth). The A/D converter quantization resolution level is

$$Q = \frac{E_{FSR}}{2^M} = \frac{20\ V}{4096} = 4.88\ mV$$

For a 100-mV signal at $200\ Hz$, this requires a k -stage, low-pass Butterworth filter with an attenuation of

$$\begin{aligned} M(200Hz) &= \frac{4.88\ mV}{100\ mV} = 0.0488 \ (\text{or } -26\ dB) \\ &= \left[1 + (f/f_c)^{2k} \right]^{-1/2} = \left[1 + (200/100)^{2k} \right]^{-1/2} \end{aligned}$$

so, $k = 4.3 \approx 5$. Appropriate values for L and C can be set from Table 6.1 and Figure 6.30 and scaled.

7.10 DIGITAL IMAGE ACQUISITION AND PROCESSING

Digital images are widely used in applications as varied as inspection, medical imaging, quality assurance, and sorting. This section serves as a brief introduction to acquiring and processing digital images.

Image Acquisition

Consider the characteristics of a digital grayscale image, such as the one in Figure 7.30. A digital image is composed of an $m \times n$ array of pixels, as illustrated in Figure 7.31. Here we have zoomed in on the edge of one of the coins in Figure 7.30, and we see that the image is composed of pixels having

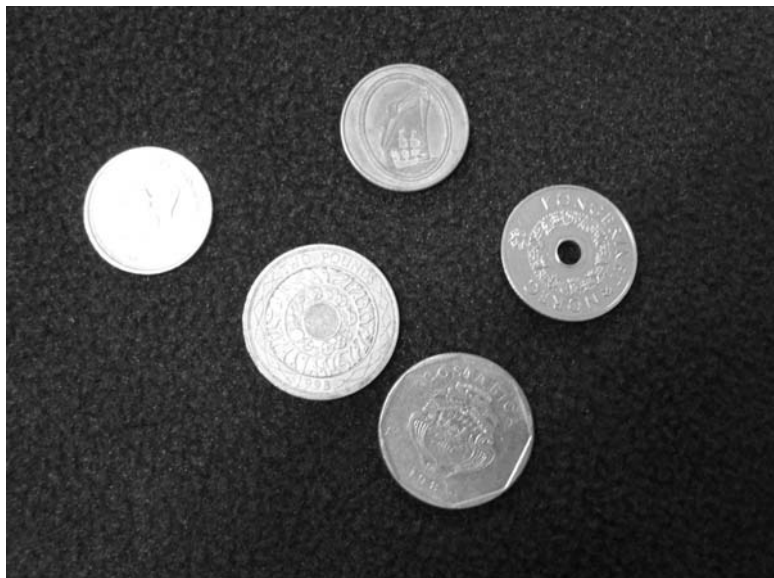


Figure 7.30 Characteristics of a digital grayscale image.

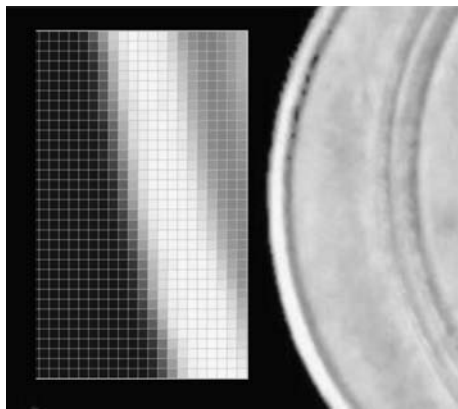


Figure 7.31 Digital image of an $m \times n$ pixel array.

various levels of gray shading. The grayscale images in Figures 7.30 and 7.31 are 8-bit digital images; each pixel is assigned a number between 0 and 256, with zero corresponding to pure black.

The device that enables digital imaging is termed a charge-coupled device (CCD).² A CCD image sensor is essentially an array of capacitors that gain charge when exposed to light. Each capacitor represents one pixel in the resulting digital image. A digital camera may have a physical or an electronic shutter, but in either case the CCD array is active for an exposure time exactly as film cameras function. Once the exposure is over, the CCD accumulated charge is converted to a digital representation of the image. The resolution of the image is determined by the number of pixels. Common cameras may have resolutions that range from 0.3 million pixels (MP) to 21 MP, but higher resolutions are available.

In many applications for digital imaging, the images are transferred directly from the camera to a computer, with image acquisition rates as fast as 200,000 frames per second. The term framegrabber is used to describe the computer hardware that acquires the images from a CCD camera. Most framegrabber hardware is in the form of a plug-in board or an external module for a PC. As with any photography, very short exposure times require high-intensity lighting.

Image Processing

A basic treatment of the fundamentals and applications of digital image processing would easily require an entire book. So our purpose here is to describe one basic issue as illustrative of the impact of digital image processing. Let's consider again Figure 7.30, which shows five coins. Two tasks that might be reasonable to ask an imaging system to accomplish are to locate the coins and determine their diameter.

Both of these tasks can be accomplished if we can locate the outer edges of the coins. Edge detection methods are a widely researched and documented area of image processing. In principle, an edge occurs where the gradient of the pixel intensity is a maximum. So, some numerical scheme for finding the gradient is required. In a two-dimensional image, the gradient has both magnitude and direction. For the two-dimensional array that comprises a grayscale image, two gradients are calculated, one in the x -direction and one in the y -direction (horizontal and vertical in the image). Using these two numerical estimates of the gradient, a magnitude and direction can be determined. We will explore two gradient-based methods, *Sobel* and *Canny* as they are implemented in Matlab. The basic differences in these two methods are the degree of smoothing and the criteria for defining an edge. The *Canny* method smoothes the image to suppress noise and uses two threshold values in determining the location of an edge. Gradient values that are below the low threshold result in a pixel being assigned as a non-edge. Pixels where gradient values are above the high threshold are set as edges pixels. Gradient values between the two thresholds are examined to see if adjacent pixels are an edge, and if there is a direct path to an edge pixel that pixel is included as an edge.

The implementation of edge detection in Matlab is a very straightforward process for grayscale images. The function *imread* creates the $m \times n$ matrix of grayscale values. The function *edge* identifies the edges with the method selected. The function *imshow* views the image.

Figure 7.32 shows the results of the two edge detection methods for our image of coins. Clearly the grayscale image contains information that causes the edge detection methods to find many edges that have nothing to do with our coins. One method to improve the chances of finding the edges of

²The CCD was invented in 1969 at AT&T Bell Labs by Willard Boyle and George Smith (*Bell Sys Tech J.* 49(4), 1970). In 2009 they shared the Nobel Prize in physics for their invention of the CCD.

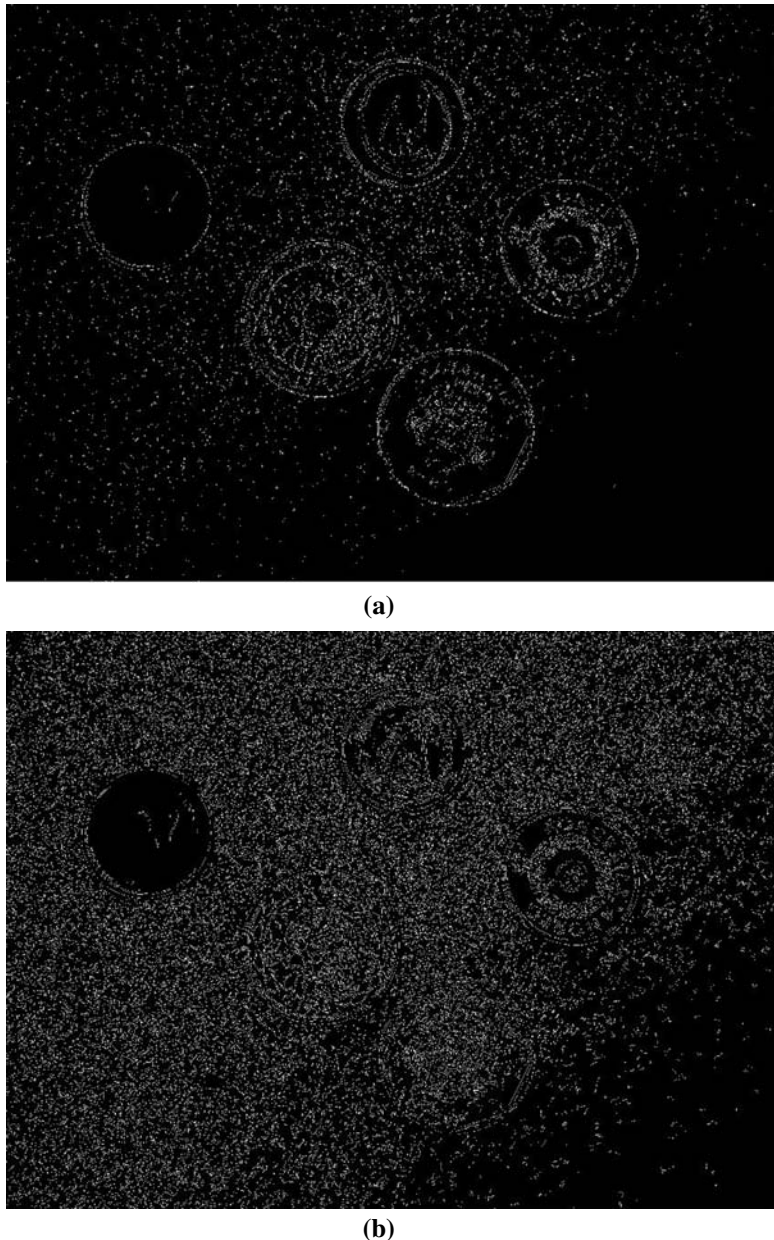


Figure 7.32 Edge detection methods. (a) Sobel method of edge detection.
(b) Canny method of edge detection.

the coins is to subject the image to a process called *thresholding*. In this process all pixel values above a certain level are set to pure white, and all below are set to pure black. Let's threshold our image at a level of 127. The resulting image is shown in Figure 7.33. When we apply the same edge detection methods used on the grayscale image, the image shown in Figure 7.34 results. Clearly this is a step closer to finding the edges of the coins.

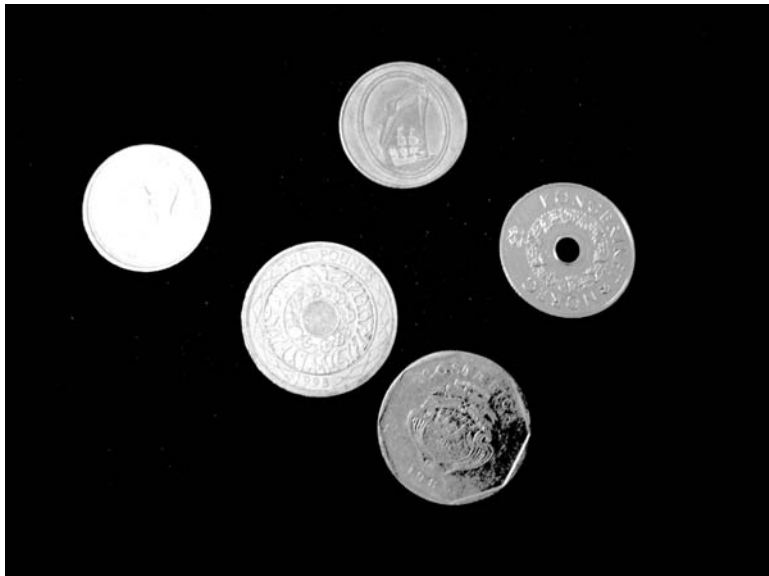
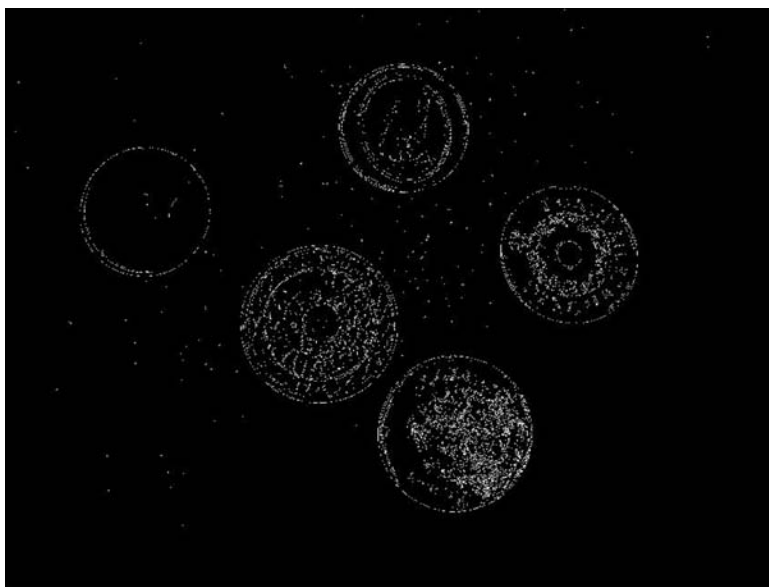


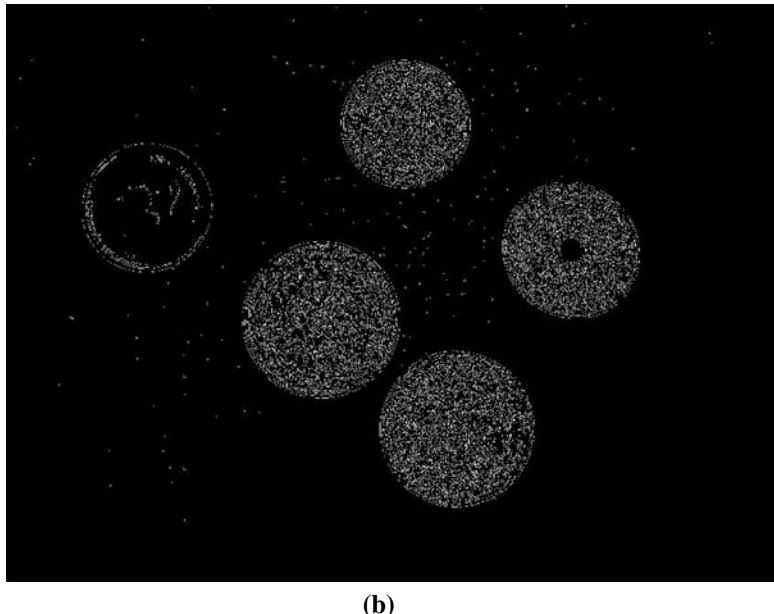
Figure 7.33 Improved effect of using threshold values to eliminate noise.



(a)

Figure 7.34 Effects of using threshold values on a grayscale image.

(a) Sobel method of edge detection.



(b)

Figure 7.34 (b) Canny method of edge detection. (*Continued*)

7.11 SUMMARY

This chapter has focused on sampling concepts, the interfacing of analog and digital devices, and data-acquisition systems. Despite the advantages of digital systems, they must interact with an analog world and the back-and-forth exchange between an analog and digital signal has limitations. With this in mind, a thorough discussion has been provided on the selection of sample rate and the number of measurements required to reconstruct a continuous process variable from a discrete representation. Equations 7.2 and 7.10 explain the criteria by which a periodic waveform can be accurately represented by such a discrete time series. The limitations resulting from improper sampling and the discrete representation include frequency alias and leakage, and amplitude ambiguity.

The fact that practically any electrical instrument can be interfaced with a microcontroller or a data-acquisition system is significant. The working mechanics of A/D and D/A converters is basic to interfacing such analog and digital devices with data-acquisition systems. The limitations imposed by the resolution and range of these devices mandate certain signal conditioning requirements in terms of signal gain and filtering prior to acquisition. These require analog amplifiers and filters, devices discussed previously. Communication between digital devices surrounds us. But their proliferation means that standards for communication must be set. These standards are evaluated and replaced as newer devices demand faster data transfer.

REFERENCES

1. Bendat, J., and A. Piersol, *Random Data: Analysis and Measurement Procedures*, Wiley-Interscience, New York, 1971.

2. Stanley, W. D., G. R. Dougherty, and R. Dougherty, *Digital Signal Processing*, 2nd ed., Reston (a Prentice Hall company), Reston, VA, 1984.
3. Lyons, R., *Understanding Digital Signal Processing*, 3rd ed., Pearson Education, Upper Saddle River, NJ, 2010.
4. Swedlin, E.G. and D.L. Ferro, *Computers: The Life Story of a Technology*, Johns Hopkins University Press, Baltimore, MD, 2007.
5. Vandoren, A., *Data-Acquisition Systems*, Reston (a Prentice Hall company), Reston, VA, 1982.
6. Krutz, R., *Interfacing Techniques in Digital Design: Emphasis on Microprocessors*, Wiley, New York, 1988.
7. Hnatek, E., *A User's Handbook of D/A and A/D Converters*, Wiley-Interscience, New York, 1976.
8. Money, S. A., *Microprocessors in Instrumentation and Control*, McGraw-Hill, New York, 1985.
9. IEEE Standard for a High-Performance Serial Bus, IEEE Standard 1394-2008, 2008.

SUGGESTED READING

- Ahmed, H., and P. J. Spreadbury, *Analogue and Digital Electronics for Engineers*, 2nd ed., Cambridge University Press, Cambridge, UK, 1984.
- Beauchamp, K.G., and C.K. Yuen, *Data Acquisition for Signal Analysis*, Allen & Unwin, London, 1980.
- Evans, Alvis J., J. D. Mullen, and D. H. Smith, *Basic Electronics Technology*, Texas Instruments Inc., Dallas, TX, 1985.
- Seitzer, D., G. Pretzel, and N. Hamdy, *Electronic Analog-to-Digital Converters: Principles, Circuits, Devices, Testing*, Wiley, New York, 1983.
- Wobschall, D., *Circuit Design for Electronic Instrumentation: Analog and Digital Devices from Sensor to Display*, McGraw Hill, New York, 1979.

NOMENCLATURE

e	error	E_o	output voltage (V)
e_Q	quantization error	E_{FSR}	full-scale analog voltage range
f	frequency (t^{-1})	G	amplifier gain
f_a	alias frequency (t^{-1})	I	electric current (A)
f_c	filter cutoff frequency (t^{-1})	M	number of bits
f_m	maximum analog signal frequency (t^{-1})	$M(f)$	magnitude ratio at frequency f
f_N	Nyquist frequency (t^{-1})	N	data set size
f_s	sample rate frequency (t^{-1})	$N\delta t$	total digital sample period (t)
k	cascaded filter stage number	R	resistance (Ω)
t	time (t)	Q	A/D converter resolution (V)
$y(t)$	analog signal	δf	frequency resolution of DFT (t^{-1})
$y_i, y(r\delta t)$	discrete values of a signal, $y(t)$	δR	change in resistance (Ω)
$\{y(r\delta t)\}$	complete discrete time signal of $y(t)$	δt	sample time increment (t)
A	amplifier open loop gain; also, constant	t	time constant (t)
E	voltage (V)	$\phi (f)$	phase shift at frequency f
E_i	input voltage (V)		

PROBLEMS

For many of these problems, using spreadsheet software or the accompanying software will facilitate solution.

- 7.1 Convert the analog voltage $E(t) = 2 \sin 4\pi t$ mV into a discrete time signal. Specifically, use sample time increments of (a) 1/8 second, (b) 1/5 second, (c) 1/3 second, and (d) 1/21 second, and use a data set of 128 points. Plot 4 seconds of each series as a function of time. Discuss apparent differences between the discrete representations of the analog signal.
- 7.2 For the analog voltage $E(t) = 2 \sin 4\pi t$ mV sampled at time increments of (a) 1/8 second, (b) 1/5 second, (c) 1/3 second, and (d) 1/21 second, you are to compute the DFT for each. Use a data set of 128 points. Discuss apparent differences.
- 7.3 An analog signal has the form $E(t) = 4 \sin 8\pi t$ (V). Compute the DFT at sample rates of 4 Hz and 16 Hz. Use a data set of 256 points. Discuss and compare your results.
- 7.4 Determine the alias frequency that results from sampling f_1 at sample rate f_s :
 - a. $f_1 = 60$ Hz; $f_s = 90$ Hz
 - b. $f_1 = 1.2$ kHz; $f_s = 2$ kHz
 - c. $f_1 = 10$ Hz; $f_s = 6$ Hz
 - d. $f_1 = 16$ Hz; $f_s = 8$ Hz
- 7.5 A particular data-acquisition system is used to convert the analog signal $E(t) = (\sin 2\pi t + 2 \sin 8\pi t)$ V into a discrete time signal using a sample rate of 16 Hz. Build the discrete time signal and from that use the Fourier transform to reconstruct the Fourier series.
- 7.6 Consider the continuous signal found in Example 2.3. What would be an appropriate sample rate and sample period to use in sampling this signal if the resulting discrete series must have a size of 2^M , where M is an integer and the signal is to be filtered at and above 2 Hz?
- 7.7 Convert the analog signal $E(t) = (4 + 2 \sin 4\pi t + 3 \sin 16\pi t)$ V into a discrete time signal using a sample rate of 32 Hz. Build the discrete time signal and its amplitude and phase spectra. Then try at $f_s = 16$ Hz and at $f_s = 40$ Hz. Discuss results.
- 7.8 Convert the following straight binary numbers to positive integer base 10 numbers:
 - a. 1010
 - b. 11111
 - c. 10111011
 - d. 1100001
- 7.9 Convert: (a) 1100111.1101 (binary) into a base 10 number; (b) 4B2F into straight binary; (c) 278.632 (base 10) into straight binary.
- 7.10 Convert the following decimal (base 10) numbers into bipolar binary numbers using a two's complement code:
 - a. 10
 - b. -10
 - c. -247
 - d. 1013
- 7.11 A computer does integer arithmetic in two's complement binary code. How is the largest positive binary number represented in this code for an 8-bit byte? Add one to this number. What base 10 decimal numbers do these represent?
- 7.12 How is the largest negative binary number represented in two's complement code for an 8-bit byte. Subtract one from this number. What base 10 decimal numbers do these represent?
- 7.13 List some possible sources of uncertainty in the dual-slope procedure for A/D conversion. Derive a relationship between the uncertainty in the digital result and the slope of the integration process.
- 7.14 Compute the resolution and SNR for an M -bit A/D converter having a full-scale range of ± 5 V. Let M be 4, 8, 12, and 16.

- 7.15** A 12-bit A/D converter having an $E_{FSR} = 5$ V has a relative accuracy of 0.03% FS (full-scale). Estimate its quantization error in volts. What is the total possible error expected in volts? What value of relative uncertainty might be used for this device?
- 7.16** A 16-bit A/D converter has a full-scale range of +10 V. What is the resolution of this A/D in volts? If this A/D were used to measure temperature using a sensor having a sensitivity of 0.1 mV/°C, what is the resolution in °C?
- 7.17** An 8-bit single-ramp A/D converter with $E_{FSR} = 10$ V uses a 2.5-MHz clock and a comparator having a threshold voltage of 1 mV. Estimate:
- The binary output when the input voltage is $E = 6.000$ V; when $E = 6.035$ V.
 - The actual conversion time for the 6.000-V input and average conversion times.
 - The resolution of the converter.
- 7.18** Compare the maximum conversion times of a 10-bit successive approximation A/D converter to a dual-slope ramp converter if both use a 1-MHz clock and $E_{FSR} = 10$ V.
- 7.19** An 8-bit D/A converter shows an output of 3.58 V when straight binary 10110011 is applied. What is the output voltage when 01100100 is applied?
- 7.20** A 0- to 10-V, 4-bit successive approximation A/D converter is used to measure an input voltage of 4.9 V.
 - Determine the binary representation and its analog approximation of the input signal. Explain your answer in terms of the quantization error of the A/D converter.
 - If we wanted to ensure that the analog approximation be within 2.5 mV of the actual input voltage, estimate the number of bits required of an A/D converter.
- 7.21** Discuss the trade-offs between resolution and conversion rate for successive approximation, ramp, and parallel converters.
- 7.22** A 0- to 10-V, 10-bit A/D converter displays an output in straight binary code of 1010110111. Estimate the input voltage to within 1 LSB.
- 7.23** A ±5-V, 8-bit A/D converter displays an output in twos-complement code of 10101011. Estimate the input voltage to within 1 LSB.
- 7.24** A dual-slope A/D converter has 12-bit resolution and uses a 10-kHz internal clock. Estimate the conversion time required for an output code equivalent to 2011_{10} .
- 7.25** How long does it take an 8-bit single ramp A/D converter using a 1-MHz clock to convert the number 173_{10} ?
- 7.26** A successive approximation A/D converter has a full-scale output of 0 to 10 V and uses an 8-bit register. An input of 6.2 V is applied. Estimate the final register value.
- 7.27** A 12-bit A/D converter has a full-scale output of 0 to 10 V. A voltage measurement is performed, and the register value is 010101001000. What is the value of the measured voltage?
- 7.28** The voltage from a 0- to 5-kg strain gauge balance scale is expected to vary from 0 to 3.50 mV. The signal is to be recorded using a 12-bit A/D converter having a ±5-V range with the weight displayed on a computer monitor. Suggest an appropriate amplifier gain for this situation.
- 7.29** An aircraft wing oscillates under wind gusts. The oscillations are expected to be at about 2 Hz. Wing-mounted strain-gauge sensors are connected to a ±5-V, 12-bit A/D converter and data-acquisition system to measure this. For each test block, 10 seconds of data are sampled.
 - Suggest an appropriate sample rate. Explain.
 - If the signal oscillates with an amplitude of 2 V, express the signal as a Fourier series,

- c. Based on (a) and (b), sketch a plot of the expected amplitude spectrum. What is the frequency spacing on the abscissa? What is its Nyquist frequency?
- 7.30** An electrical signal from a transducer is sampled at 20,000 Hz using a 12-bit successive approximation A/D converter. A total of 5 seconds of data are acquired and passed to computer memory. How much 16-bit computer memory (in kbytes) is required?
- 7.31** How many data points can be sampled by passing a signal through a 12-bit parallel A/D converter and stored in computer memory, if 8 MB of 32-bit computer memory is available? If the A/D converter uses a 100-MHz clock and acquisition is by DMA, estimate the duration of signal that can be measured.
- 7.32** Select an appropriate sample rate and data number to acquire with minimal leakage the first five terms of a square wave signal having a fundamental period of 1 second. Select an appropriate cutoff frequency for an anti-alias filter. Hint: Approximate the square wave as a Fourier series.
- 7.33** A triangle wave with a period of 2 seconds can be expressed by the Fourier series

$$y(t) = \sum [2D_1(1 - \cos n\pi)/n\pi] \cos \pi nt \quad n = 1, 2, \dots$$

Specify an appropriate sample rate and data number to acquire the first seven terms with minimal leakage. Select an appropriate cutoff frequency for an anti-alias filter.

- 7.34** Using Fourier transform software (or equivalent software), generate the amplitude spectrum for the square wave of Problem 7.32.
- 7.35** Using Fourier transform software (or equivalent software), generate the amplitude spectrum for the triangle wave of Problem 7.33. Use $D_1 = 1$ V.
- 7.36** A single-stage low-pass RC Butterworth filter with $f_c = 100$ Hz is used to filter an analog signal. Determine the attenuation of the filtered analog signal at 10, 50, 75, and 200 Hz.
- 7.37** A three-stage LC Bessel filter with $f_c = 100$ Hz is used to filter an analog signal. Determine the attenuation of the filtered analog signal at 10, 50, 75, and 200 Hz.
- 7.38** Design a cascading LC Butterworth low-pass filter that has a magnitude ratio flat to within 3 dB from 0 to 5 kHz but with an attenuation of at least 30 dB for all frequencies at and above 10 kHz.
- 7.39** Choose an appropriate cascading low-pass filter to remove a 500-Hz component contained within an analog signal that is to be passed through an 8-bit A/D converter having 10-V range and 200-Hz sample rate. Attenuate the component to within the A/D converter quantization error.
- 7.40** The voltage output from a J-type thermocouple referenced to 0°C is to be used to measure temperatures from 50 to 70°C. The output voltages vary linearly over this range from 2.585 to 3.649 mV.
 - If the thermocouple voltage is input to a 12-bit A/D converter having a ± 5 -V range, estimate the percent quantization error in the digital value.
 - If the analog signal can be first passed through an amplifier circuit, compute the amplifier gain required to reduce the quantization error to 5% or less.
 - If the ratio of signal-to-noise level (SNR) in the analog signal is 40 dB, compute the magnitude of the noise after amplification. Discuss the results of 7.40b in light of this.
- 7.41** Specify an appropriate ± 5 -V M-bit A/D converter (8- or 12-bit), sample rate (up to 100 Hz) and signal conditioning to convert these analog signals into digital series. Estimate the quantization error and dynamic error resulting from the system specified:
 - $E(t) = 2 \sin 20\pi t$ V
 - $E(t) = 1.5 \sin \pi t + 20 \sin 32\pi t - 3 \sin (60\pi t + \pi/4)$ V
 - $P(t) = -10 \sin 4\pi t + 5 \sin 8\pi t$ psi; $K = 0.4$ V/psi

- 7.42** The following signal is to be sampled using a 12-bit, ± 5 -V data-acquisition board

$$y(t) = 4\sin 8\pi t + 2\sin 20\pi t + 3\sin 42\pi t$$

Select an appropriate sample rate and sample size that provide minimal spectral leakage.

- 7.43** A strain-gauge sensor is used with a bridge circuit and connected to a DAS as indicated in Figure 7.16. Estimate the range of offset nulling voltage available if the bridge excitation is 3.333 V, sensor and bridge resistors are each at a nominal value of 120Ω , and the adjustable trim potentiometer is rated at $39 \text{ k}\Omega$.
- 7.44** Design a low-pass Butterworth filter around a 10 Hz cutoff (-3 dB) frequency. The filter is to pass 95% of signal magnitude at 5 Hz but no more than 10% at 20 Hz. Source and load impedances are 10Ω .
- 7.45** A two-stage LC Butterworth filter with $f_c = 100 \text{ Hz}$ is used as an anti-alias filter for an analog signal. Determine the signal attenuation experienced at 10, 50, 75, and 200 Hz.

The following problems make use of the accompanying software.

- 7.46** In the discussion of Figure 7.4, we point out the effects of sample rate and total sample period on the reconstructed time signal and its amplitude spectrum. Use program *Leakage.2* to duplicate Figure 7.4. Then develop a similar example (signal frequency, sample rate, and sample period) in which fewer points and a slower sample rate lead to a better reconstruction in both time and frequency domains. Incidentally, for a fixed sample rate, you can increment N and watch the acquired waveform develop such that the leakage decreases to zero as the acquired signal reaches an exact integer period of the waveform. For a fixed N , the same can be shown for changes in sample rate.
- 7.47** Using program *Aliasing*, solve Example 7.1 to find the alias frequency. Observe the plot of the original and the acquired signal, as well as the amplitude spectrum. Decrement the signal frequency 1 Hz at a time until it is within the region where there no longer is aliasing. Based on these observations, discuss how the acquired time signal changes and how this is related to aliasing.
- 7.48** Use program *Aliasing* to understand the folding diagram of Figure 7.3. For a sample rate of 20 Hz, vary the signal frequency over its full range. Determine the frequencies corresponding to f_N , $2f_N$, $3f_N$, and $4f_N$ on Figure 7.3. Determine the alias frequencies corresponding to $1.6f_N$, $2.1f_N$, $2.6f_N$, and $3.2f_N$.
- 7.49** Using program *Signal generation*, examine the rule that when exact discrete representations are not possible, a sample rate of at least five to ten times the maximum signal frequency gives adequate approximation. Select a sine wave of 2 Hz and discuss the acquired waveform as the sample rate is increased incrementally from a low to a high value. At what sample rate does the signal look like a sine wave? Compare with the corresponding frequency and amplitude content from the amplitude spectrum. Write up a short discussion of your observations and conclusions.
- 7.50** Program *Leakage.2* samples a single frequency signal at a user-defined sample rate and period. Describe how sample period corresponds to the length of the signal measured and how this affects leakage in the amplitude spectrum. Does frequency resolution matter?
- 7.51** The image file with the companion software coins.jpg is the original color photograph of the coins used in Figures 7.30 through 7.34. The image file graycoins.jpg is the corresponding grayscale image. Using the Matlab commands IMREAD, IMSHOW, IM2BW, and EDGE reproduce the results in Figures 7.30 through 7.34.
- 7.52** Using an image you download from the Internet or acquire with your own camera, create a grayscale image and employ edge detection to process the image. Explore the effects of the gradient threshold value on the quality of the edge detection. Create a binary image and repeat the process.

Chapter 8

Temperature Measurements

8.1 INTRODUCTION

Temperature is one of the most commonly used and measured engineering variables. Much of our lives is affected by the diurnal and seasonal variations in ambient temperature, but the fundamental scientific definition of temperature and a scale for the measurement of temperature are not commonly understood. This chapter explores the establishment of a practical temperature scale and common methods of temperature measurement. In addition, errors associated with the design and installation of a temperature sensor are discussed.

Upon completion of this chapter, the reader will be able to

- describe the primary standards for temperature,
- state the role of fixed point calibration and the necessity for an interpolation method in establishing a temperature standard,
- describe and analyze thermal expansion thermometry,
- state the physical principle underlying electrical resistance thermometry,
- employ standard relationships to determine temperature from resistance devices,
- analyze thermoelectric circuits designed to measure temperature,
- describe experiments to determine thermoelectric potential for material pairs,
- state the principles employed in radiation temperature measurements, and
- estimate the impact of loading errors in temperature measurement.

Historical Background

Guillaume Amontons (1663–1705), a French scientist, was one of the first to explore the thermodynamic nature of temperature. His efforts examined the behavior of a constant volume of air that was subject to temperature changes. The modern liquid-in-glass bulb thermometer traces its origin to Galileo (1565–1642), who attempted to use the volumetric expansion of liquids in tubes as a relative measure of temperature. Unfortunately, this open tube device was actually sensitive to both barometric pressure and temperature changes. A major advance in temperature measurement occurred in 1630 as a result of a seemingly unrelated event: the

development of the technology to manufacture capillary glass tubes. These tubes were then used with water and alcohol in a thermometric device resembling the bulb thermometer, and these devices eventually led to the development of a practical temperature-measuring instrument.

A temperature scale proposed by Gabriel D. Fahrenheit, a German physicist (1686–1736), in 1715 attempted to incorporate body temperature as the median point on a scale having 180 divisions between the freezing point and the boiling point of water. Fahrenheit also successfully used mercury as the liquid in a bulb thermometer, making significant improvements over the attempts of Ismael Boulliau in 1659. In 1742, the Swedish astronomer Anders Celsius¹ (1701–1744) described a temperature scale that divided the interval between the boiling and freezing points of water at 1 atm pressure into 100 equal parts. The boiling point of water was fixed as 0, and the freezing point of water as 100. Shortly after Celsius's death, Carolus Linnaeus (1707–1778) reversed the scale so that the 0 point corresponded to the freezing point of water at 1 atm. Even though this scale may not have been originated by Celsius (1), in 1948 the change from degrees centigrade to degrees Celsius was officially adopted.

As stated by H. A. Klein in *The Science of Measurement: A Historical Survey* (2),

From the original thermoscopes of Galileo and some of his contemporaries, the measurement of temperature has pursued paths of increasing ingenuity, sophistication and complexity. Yet temperature remains in its innermost essence the average molecular or atomic energy of the least bits making up matter, in their endless dance. Matter without motion is unthinkable. Temperature is the most meaningful physical variable for dealing with the effects of those infinitesimal, incessant internal motions of matter.

8.2 TEMPERATURE STANDARDS AND DEFINITION

Temperature can be loosely described as the property of an object that describes its hotness or coldness, concepts that are clearly relative. Our experiences indicate that heat transfer tends to equalize temperature, or more precisely, systems that are in thermal communication eventually have equal temperatures. The zeroth law of thermodynamics states that two systems in thermal equilibrium with a third system are in thermal equilibrium with each other. Thermal equilibrium implies that no heat transfer occurs between the systems, defining the equality of temperature. Although the zeroth law of thermodynamics essentially provides the definition of the equality of temperature, it provides no means for defining a temperature scale.

A temperature scale provides for three essential aspects of temperature measurement: (1) the definition of the size of the degree, (2) fixed reference points for establishing known temperatures, and (3) a means for interpolating between these fixed temperature points. These provisions are consistent with the requirements for any standard, as described in Chapter 1.

¹ It is interesting to note that in addition to his work in thermometry, Celsius published significant papers on the aurora borealis and the falling level of the Baltic Sea.

Fixed Point Temperatures and Interpolation

To begin, consider the definition of the triple point of water as having a value of 0.01 for our temperature scale, as is done for the Celsius scale (0.01°C). This provides for an arbitrary starting point for a temperature scale; in fact, the number value assigned to this temperature could be anything. On the Fahrenheit temperature scale it has a value very close to 32. Consider another fixed point on our temperature scale. Fixed points are typically defined by phase-transition temperatures or the triple point of a pure substance. The point at which pure water boils at one standard atmosphere pressure is an easily reproducible fixed temperature. For our purposes let's assign this fixed point a numerical value of 100.

The next problem is to define the size of the degree. Since we have two fixed points on our temperature scale, we can see that the degree is 1/100th of the temperature difference between the ice point and the boiling point of water at atmospheric pressure.

Conceptually, this defines a workable scale for the measurement of temperature; however, as yet we have made no provision for interpolating between the two fixed-point temperatures.

Interpolation

The calibration of a temperature measurement device entails not only the establishment of fixed temperature points but also the indication of any temperature between fixed points. The operation of a mercury-in-glass thermometer is based on the thermal expansion of mercury contained in a glass capillary where the level of the mercury is read as an indication of the temperature. Imagine that we submerged the thermometer in water at the ice point, made a mark on the glass at the height of the column of mercury, and labeled it 0°C , as illustrated in Figure 8.1. Next we submerged the thermometer in boiling water, and again marked the level of the mercury, this time labeling it 100°C .

Using reproducible fixed temperature points we have calibrated our thermometer at two points; however, we want to be able to measure temperatures other than these two fixed points. How can we determine the appropriate place on the thermometer to mark, say, 50°C ?

The process of establishing 50°C without a fixed-point calibration is called interpolation. The simplest option would be to divide the distance on the thermometer between the marks representing

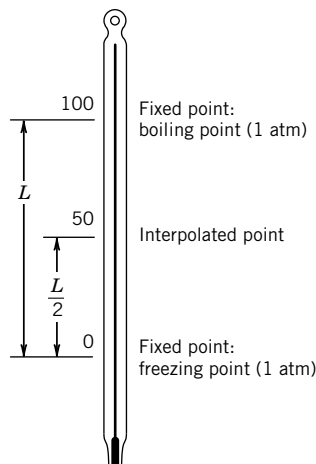


Figure 8.1 Calibration and interpolation for a liquid-in-glass thermometer.

0 and 100 into equally spaced degree divisions. This places 50°C as shown in Figure 8.1. What assumption is implicit in this method of interpolation? It is obvious that we do not have enough information to appropriately divide the interval between 0 and 100 on the thermometer into degrees. A theory of the behavior of the mercury in the thermometer or many fixed points for calibration are necessary to resolve our dilemma.

Even by the late eighteenth century, there was no standard for interpolating between fixed points on the temperature scale; the result was that different thermometers indicated different temperatures away from fixed points, sometimes with surprisingly large errors.

Temperature Scales and Standards

At this point, it is necessary to reconcile this arbitrary temperature scale with the idea of absolute temperature. Thermodynamics defines a temperature scale that has an absolute reference, and defines an absolute zero for temperature. For example, this absolute temperature governs the energy behavior of an ideal gas, and is used in the ideal gas equation of state. The behavior of real gases at very low pressure may be used as a temperature standard to define a practical measure of temperature that approximates the thermodynamic temperature. The unit of degrees Celsius (°C) is a practical scale related to the Kelvin as °C = K – 273.15.

The modern engineering definition of the temperature scale is provided by a standard called the International Temperature Scale of 1990 (ITS-90) (3). This standard establishes fixed points for temperature, and provides standard procedures and devices for interpolating between fixed points. It establishes the Kelvin (K) as the unit for the fundamental increment in temperature. Temperatures established according to ITS-90 do not deviate from the thermodynamic temperature scale by more than the uncertainty in the thermodynamic temperature at the time of adoption of ITS-90. The primary fixed points from ITS-90 are shown in Table 8.1. In addition to these fixed points, other fixed points of secondary importance are available in ITS-90.

Table 8.1 Temperature Fixed Points as Defined by ITS-90

Defining Suite	Temperature ^a	
	K	°C
Triple point of hydrogen	13.8033	-259.3467
Liquid-vapor equilibrium for hydrogen at 25/76 atm	≈17	≈-256.15
Liquid-vapor equilibrium for hydrogen at 1 atm	≈20.3	≈-252.87
Triple point of neon	24.5561	-248.5939
Triple point of oxygen	54.3584	-218.7916
Triple point of argon	83.8058	-189.3442
Triple point of water	273.16	0.01
Solid-liquid equilibrium for gallium at 1 atm	302.9146	29.7646
Solid-liquid equilibrium for tin at 1 atm	505.078	231.928
Solid-liquid equilibrium for zinc at 1 atm	692.677	419.527
Solid-liquid equilibrium for silver at 1 atm	1234.93	961.78
Solid-liquid equilibrium for gold at 1 atm	1337.33	1064.18
Solid-liquid equilibrium for copper at 1 atm	1357.77	1084.62

^asignificant digits shown are as provided in ITS-90.

Standards for Interpolation

Along with the fixed temperature points established by ITS-90, a standard for interpolation between these fixed points is necessary. Standards for acceptable thermometers and interpolating equations are provided in ITS-90. For temperatures ranging from 13.8033 to 1234.93 K, ITS-90 establishes a platinum resistance thermometer as the standard interpolating instrument, and establishes interpolating equations that relate temperature to resistance. Above 1234.93 K, temperature is defined in terms of blackbody radiation, without specifying an instrument for interpolation (3).

In summary, temperature measurement, a practical temperature scale, and standards for fixed points and interpolation have evolved over a period of about two centuries. Present standards for fixed-point temperatures and interpolation allow for practical and accurate measurements of temperature. In the United States, the National Institute of Standards and Technology (NIST) provides for a means to obtain accurately calibrated platinum wire thermometers for use as secondary standards in the calibration of a temperature measuring system to any practical level of uncertainty.

8.3 THERMOMETRY BASED ON THERMAL EXPANSION

Most materials exhibit a change in size with changes in temperature. Since this physical phenomenon is well defined and repeatable, it is useful for temperature measurement. The liquid-in-glass thermometer and the bimetallic thermometer are based on this phenomenon.

Liquid-in-Glass Thermometers

A liquid-in-glass thermometer measures temperature by virtue of the thermal expansion of a liquid. The construction of a liquid-in-glass thermometer is shown in Figure 8.2. The liquid is contained in a glass structure that consists of a bulb and a stem. The bulb serves as a reservoir and provides sufficient fluid for the total volume change of the fluid to cause a detectable rise of the liquid in the

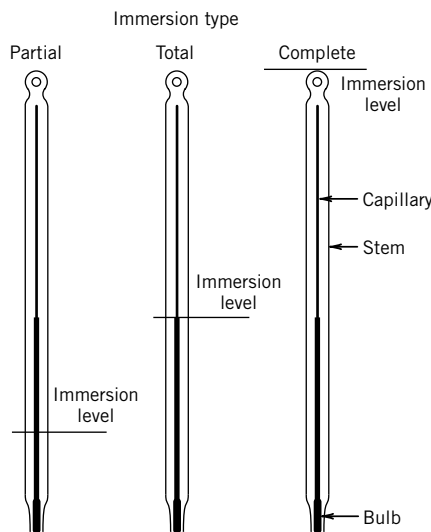


Figure 8.2 Liquid-in-glass thermometers.

stem of the thermometer. The stem contains a capillary tube, and the difference in thermal expansion between the liquid and the glass produces a detectable change in the level of the liquid in the glass capillary. Principles and practices of temperature measurement using liquid-in-glass thermometers are described elsewhere (4).

During calibration, such a thermometer is subject to one of three measuring environments:

1. For a *complete immersion thermometer*, the entire thermometer is immersed in the calibrating temperature environment or fluid.
2. For a *total immersion thermometer*, the thermometer is immersed in the calibrating temperature environment up to the liquid level in the capillary.
3. For a *partial immersion thermometer*, the thermometer is immersed to a predetermined level in the calibrating environment.

For the most accurate temperature measurements, the thermometer should be immersed in the same manner in use as it was during calibration.²

Temperature measurements using liquid-in-glass thermometers can provide uncertainties as low as 0.01°C under very carefully controlled conditions; however, extraneous variables such as pressure and changes in bulb volume over time can introduce significant errors in scale calibration. For example, pressure changes increase the indicated temperature by approximately 0.1°C per atmosphere (6). Practical measurements using liquid-in-glass thermometers typically result in total uncertainties that range from 0.2 to 2°C, depending on the specific instrument.

Mercury-in-glass thermometers have limited engineering applications, but do provide reliable, accurate temperature measurement. As such, they are often used as a local standard for calibration of other temperature sensors.

Bimetallic Thermometers

The physical phenomenon employed in a bimetallic temperature sensor is the differential thermal expansion of two metals. Figure 8.3 shows the construction and response of a bimetallic sensor to an input signal. The sensor is constructed by bonding two strips of different metals, A and B. The resulting bimetallic strip may be in a variety of shapes, depending on the particular application. Consider the simple linear construction shown in Figure 8.3. At the assembly temperature, T_1 , the bimetallic strip is straight; however, for temperatures other than T_1 the strip has a curvature. The physical basis for the relationship between the radius of curvature and temperature is given as

$$r_c \propto \frac{d}{[(C_\alpha)_A - (C_\alpha)_B](T_2 - T_1)} \quad (8.1)$$

where

r_c = radius of curvature

C_α = material thermal expansion coefficient

T = temperature

d = thickness

² In practice, it may not be possible to employ the thermometer in exactly the same way as when it was calibrated. In this case, stem corrections can be applied to the temperature reading (5).

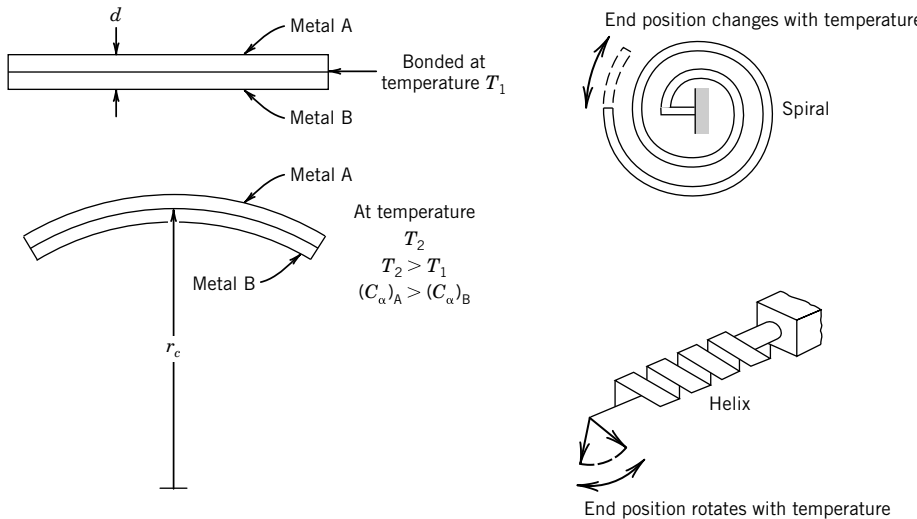


Figure 8.3 Expansion thermometry using bimetallic materials: strip, spiral, and helix forms.

Bimetallic strips employ one metal having a high coefficient of thermal expansion with another having a low coefficient, providing increased sensitivity. Invar is often used as one of the metals, since for this material $C_\alpha = 1.7 \times 10^{-8} \text{ m/m}^\circ\text{C}$, as compared to typical values for other metals, such as steels, which range from approximately 2×10^{-5} to $20 \times 10^{-5} \text{ m/m}^\circ\text{C}$.

The bimetallic sensor is used in temperature control systems, and is the primary element in most dial thermometers and many thermostats. The geometries shown in Figure 8.3 serve to provide the desired deflection in the bimetallic strip for a given application. Dial thermometers using a bimetallic strip as their sensing element typically provide temperature measurements with uncertainties of $\pm 1^\circ\text{C}$.

8.4 ELECTRICAL RESISTANCE THERMOMETRY

As a result of the physical nature of the conduction of electricity, electrical resistance of a conductor or semiconductor varies with temperature. Using this behavior as the basis for temperature measurement is extremely simple in principle, and leads to two basic classes of resistance thermometers: resistance temperature detectors (conductors) and thermistors (semiconductors). Resistance temperature detectors (RTDs) may be formed from a solid metal wire that exhibits an increase in electrical resistance with temperature. Depending on the materials selected, the resistance may increase or decrease with temperature. As a first-order approximation, the resistance change of a thermistor may be expressed as

$$R - R_0 = k(T - T_0) \quad (8.2)$$

where k is termed the temperature coefficient. A thermistor may have a positive temperature coefficient (PTC) or a negative temperature coefficient (NTC). Figure 8.4 shows resistance as a function of temperature for a variety of conductor and semiconductor materials used to measure temperature. The PTC materials are metals or alloys and the NTC materials are semiconductors. Cryogenic temperatures are included in this figure, and germanium is clearly an excellent choice for low temperature measurement because of its large sensitivity.

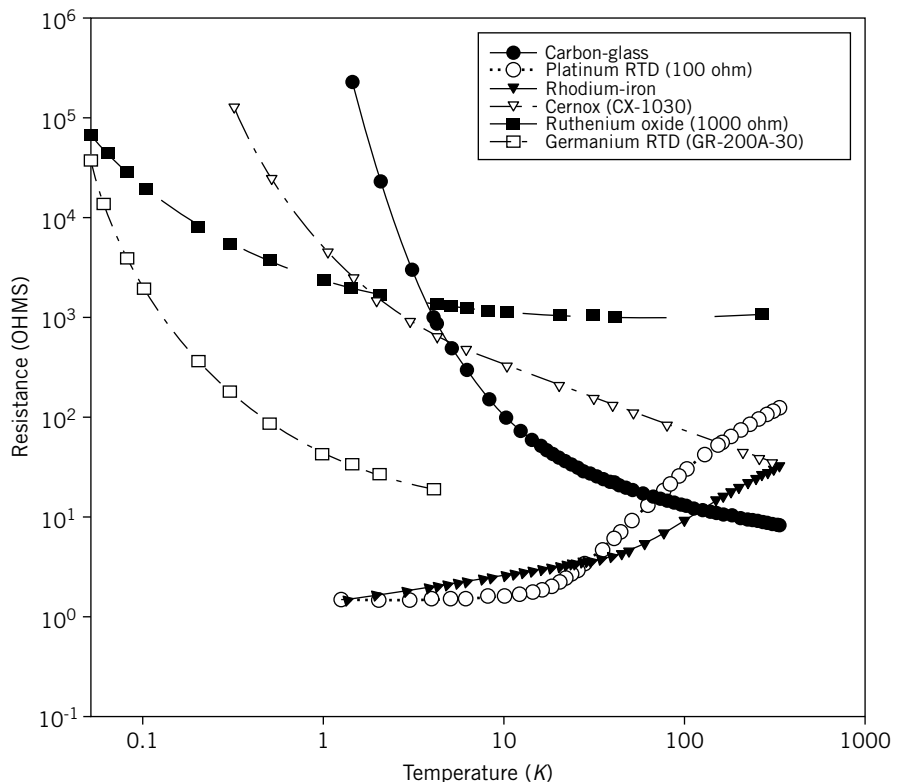


Figure 8.4 Resistance as a function of temperature for selected materials used as temperature sensors.
(Adapted from Yeager, C. J. and S. S. Courts, A Review of Cryogenic Thermometry and Common Temperature Sensors, *IEEE Sensors Journal*, 1 (4), 2001.)

Resistance Temperature Detectors

In the case of a resistance temperature detector (RTD),³ the sensor is generally constructed by mounting a metal wire on an insulating support structure to eliminate mechanical strains, and by encasing the wire to prevent changes in resistance due to influences from the sensor's environment, such as corrosion. Figure 8.5 shows such a typical RTD construction.

Mechanical strain changes a conductor's resistance and must be eliminated if accurate temperature measurements are to be made. This factor is essential because the resistance changes with mechanical strain are significant, as evidenced by the use of metal wire as sensors for the direct measurement of strain. Such mechanical stresses and resulting strains can be created by thermal expansion. Thus, provision for strain-free expansion of the conductor as its temperature changes is essential in the construction of an RTD. The support structure also expands as the temperature of the RTD increases, and the construction allows for strain-free differential expansion.

³The term RTD in this context refers to metallic PTC resistance sensors.

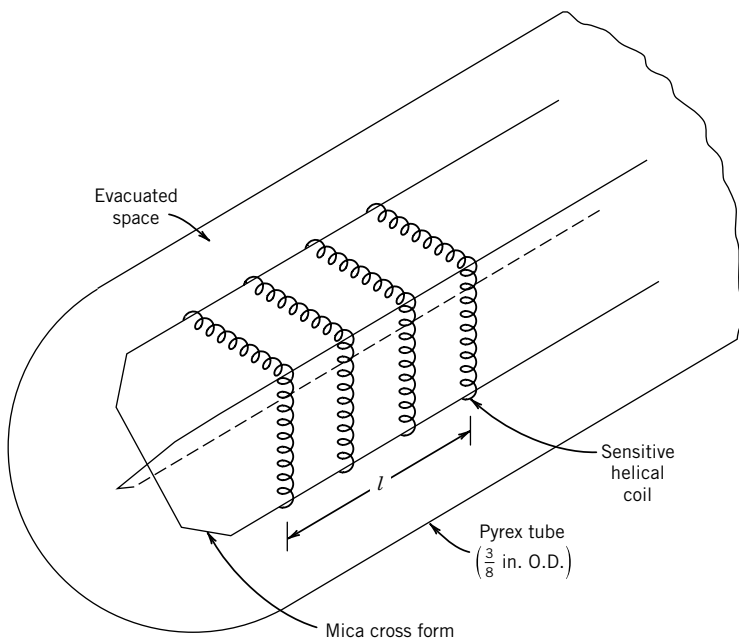


Figure 8.5 Construction of a platinum RTD. (From Benedict, R. P., *Fundamentals of Temperature, Pressure, and Flow Measurements*, 3rd ed. Copyright © 1984 by John Wiley and Sons, New York.)

The physical basis for the relationship between resistance and temperature is the temperature dependence of the resistivity ρ_e of a material. The resistance of a conductor of length l and cross-sectional area A_c may be expressed in terms of the resistivity ρ_e as

$$R = \frac{\rho_e l}{A_c} \quad (8.3)$$

The relationship between the resistance of a metal conductor and its temperature may also be expressed as the polynomial expansion:

$$R = R_0 [1 + \alpha(T - T_0) + \beta(T - T_0)^2 + \dots] \quad (8.4)$$

where R_0 is a reference resistance measured at temperature T_0 . The coefficients α, β, \dots are material constants. Figure 8.6 shows the relative relation between resistance and temperature for three common metals. This figure provides evidence that the relationship between temperature and resistance over specific small temperature ranges is linear. This approximation can be expressed as

$$R = R_0[1 + \alpha(T - T_0)] \quad (8.5)$$

where α is the temperature coefficient of resistivity. For example, for platinum conductors the linear approximation is accurate to within an uncertainty of $\pm 0.3\%$ over the range 0 – 200°C and $\pm 1.2\%$ over the range 200 – 800°C . Table 8.2 lists a number of temperature coefficients of resistivity α for materials at 20°C .

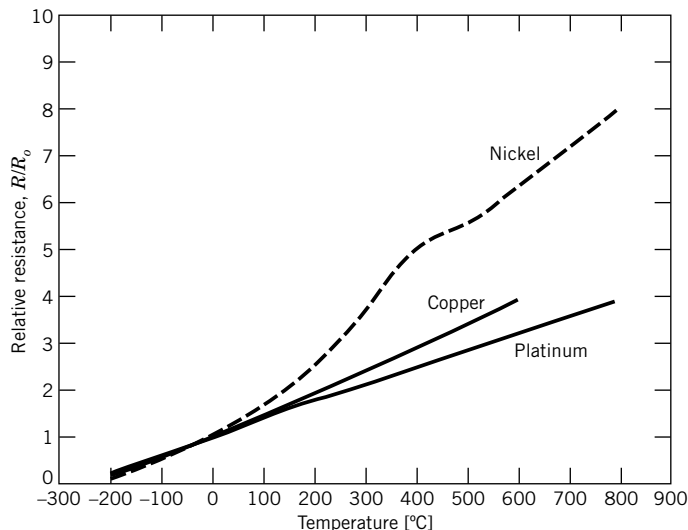


Figure 8.6 Relative resistance of three pure metals (R_0 at 0°C).

Platinum Resistance Temperature Device (RTD)

Platinum is the most common material chosen for the construction of RTDs. The principle of operation is quite simple: platinum exhibits a predictable and reproducible change in electrical resistance with temperature, which can be calibrated and interpolated to a high degree of accuracy. The linear approximation for the relationship between temperature and resistance is valid over a wide temperature range, and platinum is highly stable. To be suitable for use as a secondary temperature standard, a platinum resistance thermometer should have a value of α not less than $0.003925^\circ\text{C}^{-1}$. This minimum value is an indication of the purity of the platinum. In general, RTDs may be used for the measurement of temperatures ranging from cryogenic to approximately 650°C .

Table 8.2 Temperature Coefficient of Resistivity for Selected Materials at 20°C

Substance	$\alpha [\text{ }^\circ\text{C}^{-1}]$
Aluminum (Al)	0.00429
Carbon (C)	-0.0007
Copper (Cu)	0.0043
Gold (Au)	0.004
Iron (Fe)	0.00651
Lead (Pb)	0.0042
Nickel (Ni)	0.0067
Nichrome	0.00017
Platinum (Pt)	0.003927
Tungsten (W)	0.0048

By properly constructing an RTD, and correctly measuring its resistance, an uncertainty in temperature measurement as low as $\pm 0.005^\circ\text{C}$ is possible. Because of this potential for low uncertainties and the predictable and stable behavior of platinum, the platinum RTD is widely used as a local standard. For an NIST-certified RTD, a table and interpolating equation would be provided.

Resistance Temperature Device Resistance Measurement

The resistance of an RTD may be measured by a number of means, and the choice of an appropriate resistance measuring device must be made based on the required level of uncertainty in the final temperature measurement. Conventional ohmmeters cause a small current to flow during resistance measurements, creating self-heating in the RTD. An appreciable temperature change of the sensor may be caused by this current, in effect causing a loading error. This is an important consideration for RTDs.

Bridge circuits, as described in Chapter 6, are used to measure the resistance of RTDs to minimize loading errors and provide low uncertainties in measured resistance values. Wheatstone bridge circuits are commonly used for these measurements. However, the basic Wheatstone bridge circuit does not compensate for the resistance of the leads in measuring the resistance of an RTD, which is a major source of error in electrical resistance thermometers. When greater accuracies are required, three-wire and four-wire bridge circuits are used. Figure 8.7a shows a three-wire Callendar-Griffiths bridge circuit. The lead wires numbered 1, 2, and 3 have resistances r_1 , r_2 , and r_3 , respectively. At balanced conditions neglecting lead wire effects,

$$\frac{R_1}{R_2} = \frac{R_3}{R_{\text{RTD}}} \quad (8.6)$$

but with the lead wire resistances included in the circuit analysis,

$$\frac{R_1}{R_2} = \frac{R_3 + r_1}{R_{\text{RTD}} + r_3} \quad (8.7)$$

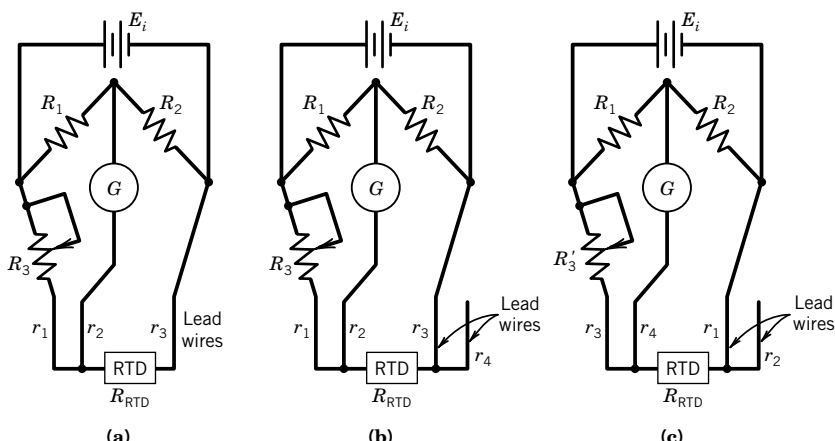


Figure 8.7 Bridge circuits. (a) Callendar-Griffiths 3-wire bridge; (b) and (c) Mueller 4-wire bridge. An average of the readings in (b) and (c) eliminates the effect of lead wire resistances.

and with $R_1 = R_2$, the resistance of the RTD, R_{RTD} , can be found as

$$R_{\text{RTD}} = R_3 + r_1 - r_3 \quad (8.8)$$

If $r_1 = r_3$, the effect of these lead wires is eliminated from the determination of the RTD resistance by this bridge circuit. Note that the resistance of lead wire 2 does not contribute to any error in the measurement at balanced conditions, since no current flows through the galvanometer G .

The four-wire Mueller bridge, as shown in Figure 8.7b,c, provides increased compensation for lead-wire resistances compared to the Callendar-Griffiths bridge and is used with four-wire RTDs. The four-wire Mueller bridge is typically used when low uncertainties are desired, as in cases where the RTD is used as a laboratory standard. A circuit analysis of the bridge circuit in the first measurement configuration, Figure 8.7b, yields

$$R_{\text{RTD}} + r_3 = R_3 + r_1 \quad (8.9)$$

and in the second measurement configuration, Figure 8.7c, yields

$$R_{\text{RTD}} + r_1 = R'_3 + r_3 \quad (8.10)$$

where R_3 and R'_3 represent the indicated values of resistance in the first and second configurations, respectively. Adding Equations 8.8 and 8.9 results in an expression for the resistance of the RTD in terms of the indicated values for the two measurements:

$$R_{\text{RTD}} = \frac{R_3 + R'_3}{2} \quad (8.11)$$

With this approach, the effect of variations in lead wire resistances is essentially eliminated.

Example 8.1

An RTD forms one arm of an equal-arm Wheatstone bridge, as shown in Figure 8.8. The fixed resistances, R_2 and R_3 are equal to 25Ω . The RTD has a resistance of 25Ω at a temperature of 0°C and is used to measure a temperature that is steady in time.

The resistance of the RTD over a small temperature range may be expressed, as in Equation 8.5:

$$R_{\text{RTD}} = R_0[1 + \alpha(T - T_0)]$$

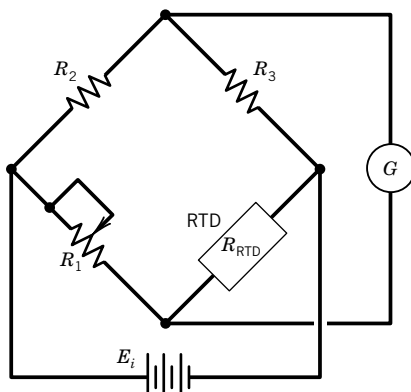


Figure 8.8 RTD Wheatstone bridge arrangement.

Suppose the coefficient of resistance for this RTD is $0.003925^{\circ}\text{C}^{-1}$. A temperature measurement is made by placing the RTD in the measuring environment and balancing the bridge by adjusting R_1 . The value of R_1 required to balance the bridge is 37.36Ω . Determine the temperature of the RTD.

KNOWN $R(0^{\circ}\text{C}) = 25 \Omega$

$$\alpha = 0.003925^{\circ}\text{C}^{-1}$$

$$R_1 = 37.36 \Omega \text{ (when bridge is balanced)}$$

FIND The temperature of the RTD.

SOLUTION The resistance of the RTD is measured by balancing the bridge; recall that in a balanced condition

$$R_{\text{RTD}} = R_1 \frac{R_3}{R_2}$$

The resistance of the RTD is measured to be 37.36Ω . With $R_0 = 25 \Omega$ at $T = 0^{\circ}\text{C}$ and $\alpha = 0.003925^{\circ}\text{C}^{-1}$, Equation 8.5 becomes

$$37.36 \Omega = 25(1 + \alpha T)\Omega$$

The temperature of the RTD is 126°C .

Example 8.2

Consider the bridge circuit and RTD of Example 8.1. To select or design a bridge circuit for measuring the resistance of the RTD in this example, the required uncertainty in temperature would be specified. If the required uncertainty in the measured temperature is $\leq 0.5^{\circ}\text{C}$, would a 1% total uncertainty in each of the resistors that make up the bridge be acceptable? Neglect the effects of lead wire resistances for this example.

KNOWN A required uncertainty in temperature of $\pm 0.5^{\circ}\text{C}$, measured with the RTD and bridge circuit of Example 8.1.

FIND The uncertainty in the measured temperature for a 1% total uncertainty in each of the resistors that make up the bridge circuit.

ASSUMPTION All uncertainties are provided and evaluated at the 95% confidence level.

SOLUTION Perform a design-stage uncertainty analysis. Assuming at the design stage that the total uncertainty in the resistances is 1%, then with initial values of the resistances in the bridge equal to 25Ω , the design-stage uncertainties are set at

$$u_{R_1} = u_{R_2} = u_{R_3} = (0.01)(25) = 0.25 \Omega$$

The root-sum-squares (RSS) method is used to estimate the propagation of uncertainty in each resistor to the uncertainty in determining the RTD resistance by

$$u_{\text{RTD}} = \sqrt{\left[\frac{\partial R}{\partial R_1} u_{R_1} \right]^2 + \left[\frac{\partial R}{\partial R_2} u_{R_2} \right]^2 + \left[\frac{\partial R}{\partial R_3} u_{R_3} \right]^2}$$

where

$$R = R_{\text{RTD}} = \frac{R_1 R_3}{R_2}$$

and we assume that the uncertainties are not correlated. Then, the design-stage uncertainty in the resistance of the RTD is

$$u_{\text{RTD}} = \sqrt{\left[\frac{R_3}{R_2} u_{R_1} \right]^2 + \left[\frac{-R_1 R_3}{R_2^2} u_{R_2} \right]^2 + \left[\frac{R_1}{R_2} u_{R_3} \right]^2}$$

$$u_{\text{RTD}} = \sqrt{(1 \times 0.25)^2 + (1 \times -0.25)^2 + (1 \times 0.25)^2} = 0.433 \Omega$$

To determine the uncertainty in temperature, we know

$$R = R_{\text{RTD}} = R_0 [1 + \alpha(T - T_0)]$$

and

$$u_T = \sqrt{\left(\frac{\partial T}{\partial R} u_{\text{RTD}} \right)^2}$$

Setting $T_0 = 0^\circ\text{C}$ with $R_0 = 25 \Omega$, and neglecting uncertainties in T_0 , α , and R_0 , we have

$$\frac{\partial T}{\partial R} = \frac{1}{\alpha R_0}$$

$$\frac{1}{\alpha R_0} = \frac{1}{(0.003925^\circ\text{C}^{-1})(25 \Omega)}$$

Then the design-stage uncertainty in temperature is

$$u_T = u_{\text{RTD}} \left(\frac{\partial T}{\partial R} \right) = \frac{0.433 \Omega}{0.098 \Omega/\text{ }^\circ\text{C}} = 4.4^\circ\text{C}$$

The desired uncertainty in temperature is not achieved with the specified levels of uncertainty in the pertinent variables.

COMMENT Uncertainty analysis, in this case, would have prevented performing a measurement that would not provide acceptable results.

Example 8.3

Suppose the total uncertainty in the bridge resistances of Example 8.1 was reduced to 0.1%. Would the required level of uncertainty in temperature be achieved?

KNOWN The uncertainty in each of the resistors in the bridge circuit for temperature measurement from Example 8.1 is $\pm 0.1\%$.

FIND The resulting uncertainty in temperature.

SOLUTION The uncertainty analysis from the previous example may be directly applied, with the uncertainty values for the resistances appropriately reduced. The uncertainties for the resistances

are reduced from 0.25 to 0.025, yielding

$$u_{\text{RTD}} = \sqrt{(1 \times 0.025)^2 + (1 \times -0.025)^2 + (1 \times 0.025)^2} = 0.0433 \Omega$$

and the resulting 95% uncertainty interval in temperature is $\pm 0.44^\circ\text{C}$, which satisfies the design constraint.

COMMENT This result provides confidence that the effect of the resistors' uncertainties will not cause the uncertainty in temperature to exceed the target value. However, the uncertainty in temperature also depends on other aspects of the measurement system. The design-stage uncertainty analysis performed in this example may be viewed as ensuring that the factors considered do not produce a higher than acceptable uncertainty level.

Practical Considerations

The transient thermal response of typical commercial RTDs is generally quite slow compared with other temperature sensors, and for transient measurements bridge circuits must be operated in a deflection mode or use expensive auto-balancing circuits. For these reasons, RTDs are not generally chosen for transient temperature measurements. A notable exception is the use of very small platinum wires and films for temperature measurements in noncorrosive flowing gases. In this application, wires having diameters on the order of 10 μm can have frequency responses higher than any other temperature sensor, because of their extremely low thermal capacitance. Obviously, the smallest impact would destroy this sensor. Other resistance sensors in the form of thin metallic films provide fast transient response temperature measurements, often in conjunction with anemometry or heat flux measurements. Such metallic films are constructed by depositing a film, commonly of platinum, onto a substrate and coating the film with a ceramic glass for mechanical protection (7). Typical film thickness ranges from 1 to 2 μm , with a 10- μm protective coating. Continuous exposure at temperatures of 600°C is possible with this construction. Some practical uses for film sensors include temperature control circuits for heating systems and cooking devices and surface temperature monitoring on electronic components subject to overheating. Uncertainty levels range from about ± 0.1 to 2°C .

Thermistors

Thermistors (from *thermally sensitive resistors*) are ceramic-like semiconductor devices. The most common thermistors are NTC, and the resistance of these thermistors decreases rapidly with temperature, which is in contrast to the small increases of resistance with temperature for RTDs.

Equation 8.2 is too simple to accurately describe resistance changes over practical temperature ranges; a more accurate functional relationship between resistance and temperature for a thermistor is generally assumed to be of the form

$$R = R_0 e^{\beta(1/T - 1/T_0)} \quad (8.12)$$

The parameter β ranges from 3500 to 4600 K, depending on the material, temperature, and individual construction for each sensor, and therefore must be determined for each thermistor. Figure 8.9 shows the variation of resistance with temperature for two common thermistor materials;

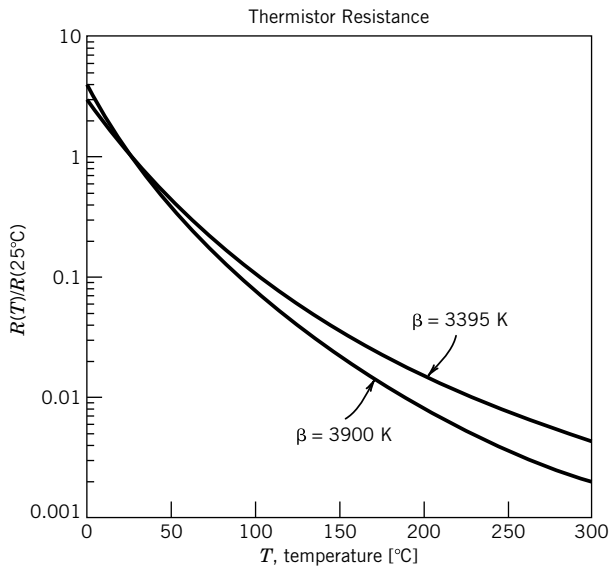


Figure 8.9 Representative thermistor resistance variations with temperature.

the ordinate is the ratio of the resistance to the resistance at 25°C . Thermistors exhibit large resistance changes with temperature in comparison to typical RTD as indicated by comparison of Figures 8.6 and 8.9. Equation 8.12 is not accurate over a wide range of temperature, unless β is taken to be a function of temperature; typically the value of β specified by a manufacturer for a sensor is assumed to be constant over a limited temperature range. A simple calibration is possible for determining β as a function of temperature, as illustrated in the circuits shown in Figure 8.10. Other circuits and a more complete discussion of measuring β may be found in the Electronic Industries Association standard Thermistor Definitions and Test Methods (8).

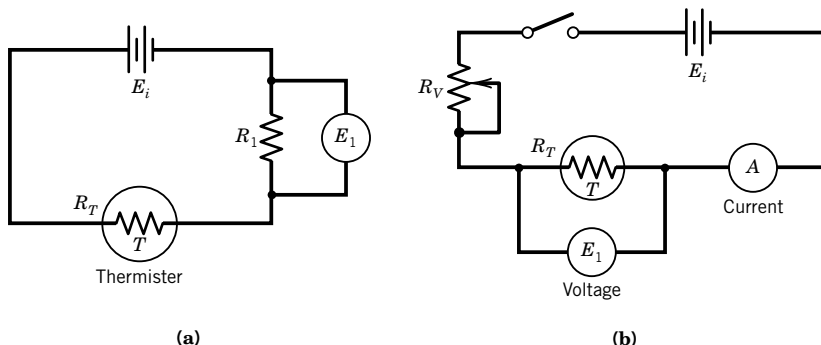


Figure 8.10 Circuits for determining β for thermistors. (a) Voltage divider method: $R_T = R_1(E_i/E_1 - 1)$. Note: Both R_1 and E_i must be known values. The value of R_1 may be varied to achieve appropriate values of thermistor current. (b) Volt-ammeter method. Note: Both current and voltage are measured.

Thermistors are generally used when high sensitivity, ruggedness, or fast response times are required (9). Thermistors are often encapsulated in glass, and thus can be used in corrosive or abrasive environments. The resistance characteristics of the semiconductor material may change at elevated temperatures, and some aging of a thermistor occurs at temperatures above 200° C. The high resistance of a thermistor, compared to that of an RTD, eliminates the problems of lead wire resistance compensation.

A commonly reported specification of a thermistor is the zero-power resistance and dissipation constant. The zero-power resistance of a thermistor is the resistance value of the thermistor with no flow of electric current. The zero power resistance should be measured such that a decrease in the current flow to the thermistor results in not more than a 0.1% change in resistance. The dissipation constant for a thermistor is defined at a given ambient temperature as

$$\delta = \frac{P}{T - T_{\infty}} \quad (8.13)$$

where

δ = dissipation constant

P = power supplied to the thermistor

T, T_{∞} = thermistor and ambient temperatures, respectively

Example 8.4

The output of a thermistor is highly nonlinear with temperature, and there is often a benefit to linearizing the output through appropriate circuit, whether active or passive. In this example we examine the output of an initially balanced bridge circuit where one of the arms contains a thermistor. Consider a Wheatstone bridge as shown in Figure 8.8, but replace the RTD with a thermistor having a value of $R_0 = 10,000 \Omega$ with $\beta = 3680 \text{ K}$. Here we examine the output of the circuit over two temperature ranges: (a) 25–325°C, and (b) 25–75°C.

KNOWN A Wheatstone bridge where $R_2 = R_3 = R_4 = 10,000 \Omega$ and where R_1 is a thermistor.

FIND The output of the bridge circuit as a function of temperature.

SOLUTION The fundamental relationship between resistances in a Wheatstone bridge and the normalized output voltage is provided in Equation 6.14:

$$\frac{E_o}{E_i} = \left(\frac{R_1}{R_1 + R_2} - \frac{R_3}{R_3 + R_4} \right) \quad (6.14)$$

And the resistance of the thermistor is

$$R = R_o e^{\beta(1/T - 1/T_o)}$$

Substituting in Equation 6.14 for R_1 yields

$$\frac{E_o}{E_i} = \left(\frac{R_o e^{\beta(1/T - 1/T_o)}}{R_o e^{\beta(1/T - 1/T_o)} + R_2} - \frac{R_3}{R_3 + R_4} \right)$$

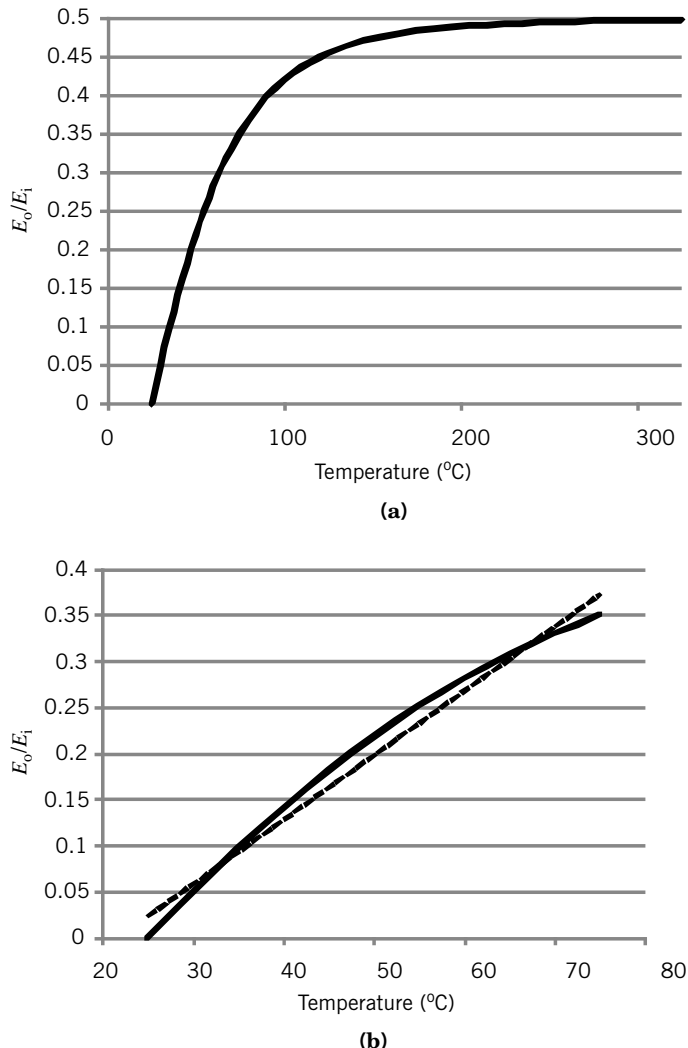


Figure 8.11 Normalized bridge output voltage as a function of temperature with a thermistor as the temperature sensor: (a) 25° to 325°C, (b) 25° to 75°C.

Figure 8.11a is a plot of this function over the range 25° to 325°C. Clearly the sensitivity of the circuit to changes in temperature greatly diminishes as the temperature increases above 100°C, with an asymptotic value of 0.5. Figure 8.11b shows the behavior over the restricted range 25° to 75°C; a linear curve fit is also shown for comparison. Over this range of temperature, assuming a linear relationship between normalized output and temperature would be suitable for many applications provided that the accompanying linearity error is acceptable.

Example 8.5

The material constant β is to be determined for a particular thermistor using the circuit shown in Figure 8.10a. The thermistor has a resistance of $60 \text{ k}\Omega$ at 25°C . The reference resistor in the circuit, R_1 , has a resistance of $130.5 \text{ k}\Omega$. The dissipation constant δ is $0.09 \text{ mW}/^\circ\text{C}$. The voltage source used for the measurement is constant at 1.564 V . The thermistor is to be used at temperatures ranging from 100 to 150°C . Determine the value of β .

KNOWN The temperature range of interest is from 100° to 150°C .

$$R_0 = 60,000 \Omega, \quad T_0 = 25^\circ\text{C}$$

$$E_i = 1.564 \text{ V}, \quad \delta = 0.09 \text{ mW}/^\circ\text{C}, \quad R_1 = 130.5 \text{ k}\Omega$$

FIND The value of β over the temperature range from 100° to 150°C .

SOLUTION The voltage drop across the fixed resistor is measured for three known values of thermistor temperature. The thermistor temperature is controlled and determined by placing the thermistor in a laboratory oven and measuring the temperature of the oven. For each measured voltage across the reference resistor, the thermistor resistance R_T is determined from

$$R_T = R_1 \left(\frac{E_i}{E_1} - 1 \right)$$

The results of these measurements are as follows:

Temperature ($^\circ\text{C}$)	R_1 Voltage (V)	R_T (Ω)
100	1.501	5477.4
125	1.531	2812.9
150	1.545	1604.9

Equation 8.12 can be expressed in the form of a linear equation as

$$\ln \frac{R_T}{R_0} = \beta \left(\frac{1}{T} - \frac{1}{T_0} \right) \quad (8.14)$$

Applying this equation to the measured data, with $R_0 = 60,000 \Omega$, the three data points above yield the following:

$\ln(R_T/R_0)$	$(1/T - 1/T_0)[\text{K}^{-1}]$	$\beta(\text{K})$
-2.394	-6.75×10^{-4}	3546.7
-3.060	-8.43×10^{-4}	3629.9
-3.621	-9.92×10^{-4}	3650.2

COMMENT These results are for constant β and are based on the behavior described by Equation 8.12, over the temperature range from T_0 to the temperature T . The significance of the measured differences in β is examined further.

The measured values of β in Example 8.5 are different at each value of temperature. If β were truly a temperature-independent constant, and these measurements had negligible uncertainty, all three measurements would yield the same value of β . The variation in β may be due to a physical effect of temperature, or may be attributable to the uncertainty in the measured values.

Are the measured differences significant, and if so, what value of β best represents the behavior of the thermistor over this temperature range? To perform the necessary uncertainty analysis, additional information must be provided concerning the instruments and procedures used in the measurement.

Example 8.6

Perform an uncertainty analysis to determine the uncertainty in each measured value of β in Example 8.5, and evaluate a single best estimate of β for this temperature range. The measurement of β involves the measurement of voltages, temperatures, and resistances. For temperature there is a random error associated with spatial and temporal variations in the oven temperature with a random standard uncertainty of $s_T = 0.19^\circ\text{C}$ for 20 measurements. In addition, based on a manufacturer's specification, there is a known measurement systematic uncertainty for temperature of 0.36°C (95%) in the thermocouple.

The systematic errors in measuring resistance and voltage are negligible, and estimates of the instrument repeatability, which are based on the manufacturer's specifications in the measured values and assumed to be at a 95% confidence level, are assigned systematic uncertainties of 1.5% for resistance and 0.002 V for the voltage.

KNOWN Standard deviation of the means for oven temperature, $s_T = 0.19^\circ\text{C}$, $N = 20$. The remaining errors are assigned systematic uncertainties at 95% confidence assuming large degrees of freedom, such that $B_x = 2b_x$:

$$\begin{aligned}B_T &= 2b_T = 0.36^\circ\text{C} \\B_R/R &= (2b_R)/R = 1.5\% \\B_E &= 2b_E = 0.002 \text{ V}\end{aligned}$$

FIND The uncertainty in β at each measured temperature, and a best estimate for β over the measured temperature range.

SOLUTION Consider the problem of providing a single best estimate of β . One method of estimation might be to average the three measured values. This results in a value of 3609 K. However, since the relationship between (R_T/R_0) and $(1/T - 1/T_0)$ is expected to be linear, a least-squares fit can be performed on the three data points, and include the point $(0, 0)$. The resulting value of β is 3638 K. Is this difference significant, and which value best represents the behavior of the thermistor? To answer these questions, an uncertainty analysis is performed for β .

For each measured value,

$$\beta = \frac{\ln(R_T/R_0)}{1/T - 1/T_0}$$

Uncertainties in voltage, temperature, and resistance are propagated into the resulting value of β for each measurement.

Consider first the sensitivity indices θ_i for each of the variables R_T , R_0 , T , and T_0 . These may be tabulated by computing the appropriate partial derivatives of β , evaluated at each of the three temperatures, as follows:

T (°C)	θ_{R_T} (K/Ω)	θ_{R_0} (K/Ω)	θ_T	θ_{T_0}
100	-0.270	0.0247	-37.77	59.17
125	-0.422	0.0198	-27.18	48.48
150	-0.628	0.0168	-20.57	41.45

The determination of the uncertainty in β , u_β , requires the uncertainty in the measured value of resistance for the thermistor, u_{R_T} . But R_T is determined from the expression

$$R_T = R_1[(E_i/E_1) - 1]$$

and thus requires an analysis of the uncertainty in the resulting value of R_T , from measured values of R_1 , E_i , and E_1 . All errors in R_T are treated as uncorrelated systematic errors, yielding

$$b_{R_T} = \sqrt{\left[\frac{\partial R_T}{\partial R_1} b_{R_1}\right]^2 + \left[\frac{\partial R_T}{\partial E_i} b_{E_i}\right]^2 + \left[\frac{\partial R_T}{\partial E_1} b_{E_1}\right]^2} = \sqrt{[\theta_{R_1} b_{R_1}]^2 + [\theta_{E_i} b_{E_i}]^2 + [\theta_{E_1} b_{E_1}]^2}$$

To arrive at a representative value, we compute b_{R_T} at 125°C. The systematic standard uncertainty in R_1 is 0.75% of 130.5 kΩ, or 978 Ω, and in R_0 is 450 Ω. The systematic standard uncertainties in E_i and E_1 are each 0.001 V, and $\theta_{R_1} = 0.022$, $\theta_{E_i} = 85238$, and $\theta_{E_1} = 87076$. This gives $b_{R_T} = 123.7$ Ω.

An uncertainty for β is determined for each of the measured temperatures. The propagation of the measurement systematic errors for temperature and resistance is found as

$$b_\beta = \sqrt{[b_T]^2 + [b_{T_0}]^2 + [b_{R_T}]^2 + [b_{R_0}]^2}$$

where

$$\begin{aligned} b_T &= 0.18^\circ\text{C} & b_{R_T} &= 123.7 \Omega \\ b_{T_0} &= 0.18^\circ\text{C} & b_{R_0} &= 450 \Omega \end{aligned}$$

The random standard uncertainty for β contains contributions only from the statistically determined oven temperature characteristics and is found from

$$s_{\bar{\beta}} = \sqrt{(\theta_T s_{\bar{T}})^2 + (\theta_{T_0} s_{\bar{T}_0})^2}$$

where both $s_{\bar{T}}$ and $s_{\bar{T}_0}$ are 0.19, as determined with $v = 19$.

The resulting values of uncertainty in β are found from

$$u_\beta = t_{v,95} \sqrt{b_\beta^2 + s_{\bar{\beta}}^2}$$

where v_β is sufficiently large (see Eq. 5.39) so that $t_{v,95} \approx 2$. At each temperature the uncertainty in β is determined as shown in Table 8.3. The effect of increases in the sensitivity indices θ_i on the total uncertainty is to cause increased uncertainty in β as the temperature increases.

Table 8.3 Uncertainties in β

T [°C]	Uncertainty		
	Random	Systematic	Total
	$s_{\bar{\beta}}$ [K]	$b_{\bar{\beta}}$ [K]	$\pm u_{\bar{\beta}} \text{ 95\%}$ [K]
100	13.3	37.4	79.4
125	10.6	53.9	109.9
150	8.8	78.4	157.8

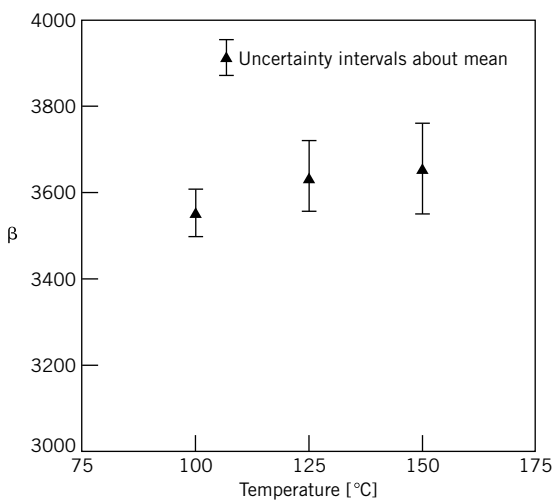
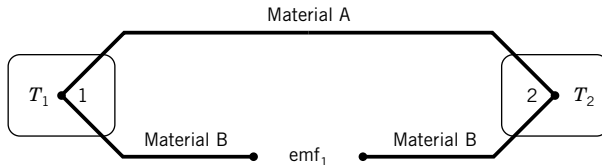


Figure 8.12 Measured values of β and associated uncertainties for three temperatures. Each data point represents $\bar{\beta} \pm u_{\bar{\beta}}$.

The original results of the measured values of β must now be reexamined. The results from Table 8.3 are plotted as a function of temperature in Figure 8.12, with 95% uncertainty limits on each data point. Clearly, there is no justification for assuming that the measured values indicate a trend of changes with temperature, and it would be appropriate to use either the average value of β or the value determined from the linear least-squares curve fit.

8.5 THERMOELECTRIC TEMPERATURE MEASUREMENT

The most common method of measuring and controlling temperature uses an electrical circuit called a thermocouple. A *thermocouple* consists of two electrical conductors that are made of dissimilar metals and have at least one electrical connection. This electrical connection is referred to as a *junction*. A thermocouple junction may be created by welding, soldering, or by any method that provides good electrical contact between the two conductors, such as twisting the wires around one another. The output of a thermocouple circuit is a voltage, and there is a definite relationship between this voltage and the temperatures of the junctions that make up the thermocouple circuit. We will examine the causes of this voltage, and develop the basis for using thermocouples to make engineering measurements of temperature.

**Figure 8.13** Basic thermocouple circuit.

Consider the thermocouple circuit shown in Figure 8.13. The junction labeled 1 is at a temperature T_1 and the junction labeled 2 is at a temperature T_2 . This thermocouple circuit measures the difference between T_1 and T_2 . If T_1 and T_2 are not equal, a finite open-circuit electric potential, emf_1 , is measured. The magnitude of the potential depends on the difference in the temperatures and the particular metals used in the thermocouple circuit.

A thermocouple junction is the source of an *electromotive force* (emf), which gives rise to the potential difference in a thermocouple circuit. It is the basis for temperature measurement using thermocouples. The circuit shown in Figure 8.13 is the most common form of a thermocouple circuit used for measuring temperature.

It is our goal to understand the origin of thermoelectric phenomena and the requirements for providing accurate temperature measurements using thermocouples. In an electrical conductor that is subject to a temperature gradient, there will be both a flow of thermal energy and a flow of electricity. These phenomena are closely tied to the behavior of the free electrons in a metal; it is no coincidence that good electrical conductors are, in general, good thermal conductors. The characteristic behavior of these free electrons in an electrical circuit composed of dissimilar metals results in a useful relationship between temperature and emf. There are three basic phenomena that can occur in a thermocouple circuit: (1) the *Seebeck effect*, (2) the *Peltier effect*, and (3) the *Thomson effect*.

Under measurement conditions with no loading errors, the emf generated by a thermocouple circuit would be the result of the Seebeck effect only.

Seebeck Effect

The Seebeck effect, named for Thomas Johann Seebeck (1770–1831), refers to the generation of a voltage potential, or emf, in an open thermocouple circuit due to a difference in temperature between junctions in the circuit. The Seebeck effect refers to the case when there is no current flow in the circuit, as for an open circuit. There is a fixed, reproducible relationship between the emf and the junction temperatures T_1 and T_2 (Fig. 8.13). This relationship is expressed by the Seebeck coefficient, α_{AB} , defined as

$$\alpha_{AB} = \left[\frac{\partial(\text{emf})}{\partial T} \right]_{\text{open circuit}} \quad (8.15)$$

where A and B refer to the two materials that comprise the thermocouple. Since the Seebeck coefficient specifies the rate of change of voltage with temperature for the materials A and B , it is equal to the static sensitivity of the open-circuit thermocouple.

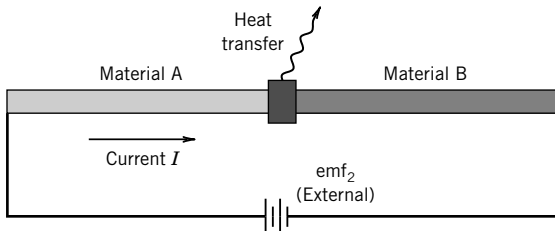


Figure 8.14 Peltier effect due to current flow across a junction of dissimilar metals.

Peltier Effect

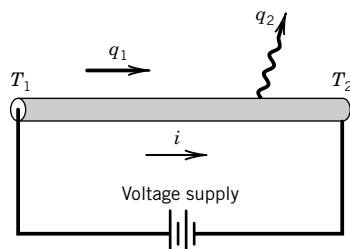
A familiar concept is that of I^2R or joule heating in a conductor through which an electrical current flows. Consider the two conductors having a common junction, shown in Figure 8.14, through which an electrical current I flows due to an externally applied emf. For any portion of either of the conductors, the energy removal rate required to maintain a constant temperature is I^2R , where R is the resistance to a current flow and is determined by the resistivity and size of the conductor. However, at the junction of the two dissimilar metals the removal of a quantity of energy different than I^2R is required to maintain a constant temperature. The difference in I^2R and the amount of energy generated by the current flowing through the junction is due to the Peltier effect. The Peltier effect is due to the thermodynamically reversible conversion of energy as a current flows across the junction, in contrast to the irreversible dissipation of energy associated with I^2R losses. The Peltier heat is the quantity of heat in addition to the quantity I^2R that must be removed from the junction to maintain the junction at a constant temperature. This amount of energy is proportional to the current flowing through the junction; the proportionality constant is the Peltier coefficient π_{AB} , and the heat transfer required to maintain a constant temperature is

$$Q_\pi = \pi_{AB}I \quad (8.16)$$

caused by the Peltier effect alone. This behavior was discovered by Jean Charles Athanase Peltier (1785–1845) during experiments with Seebeck's thermocouple. He observed that passing a current through a thermocouple circuit having two junctions, as in Figure 8.13, raised the temperature at one junction, while lowering the temperature at the other junction. This effect forms the basis of a device known as a Peltier refrigerator, which provides cooling without moving parts.

Thomson Effect

In addition to the Seebeck effect and the Peltier effect, there is a third phenomenon that occurs in thermoelectric circuits. Consider the conductor shown in Figure 8.15, which is subject to a



q_1 Energy flow as a result of a temperature gradient
 q_2 Heat transfer to maintain constant temperature

Figure 8.15 Thomson effect due to simultaneous flows of current and heat.

longitudinal temperature gradient and also to a potential difference, such that there is a flow of current and heat in the conductor. Again, to maintain a constant temperature in the conductor it is found that a quantity of energy different than the joule heat, I^2R , must be removed from the conductor. First noted by William Thomson (1824–1907, Lord Kelvin from 1892) in 1851, this energy is expressed in terms of the Thomson coefficient, σ , as

$$Q_\sigma = \sigma I(T_1 - T_2) \quad (8.17)$$

For a thermocouple circuit, all three of these effects may be present and may contribute to the overall emf of the circuit.

Fundamental Thermocouple Laws

The basic thermocouple circuit shown in Figure 8.16 can be used to measure the difference between the two temperatures T_1 and T_2 . For practical temperature measurements, one of these junctions becomes a reference junction, and is maintained at some known, constant reference temperature, say T_2 . The other junction then becomes the measuring junction, and the emf existing in the circuit provides a direct indication of the temperature of the measuring junction T_1 .

The use of thermocouple circuits to measure temperature is based on observed behaviors of carefully controlled thermocouple materials and circuits. The following laws provide the basis necessary for temperature measurement with thermocouples:

- 1. Law of homogeneous materials:** *A thermoelectric current cannot be sustained in a circuit of a single homogeneous material by the application of heat alone, regardless of how it might vary in cross section.* Simply stated, this law requires that at least two materials be used to construct a thermocouple circuit for the purpose of measuring temperature. It is interesting to note that a current may occur in an inhomogeneous wire that is nonuniformly heated; however, this is neither useful nor desirable in a thermocouple.
- 2. Law of intermediate materials:** *The algebraic sum of the thermoelectric forces in a circuit composed of any number of dissimilar materials is zero if all of the circuit is at a uniform temperature.* This law allows a material other than the thermocouple materials to be inserted into a thermocouple circuit without changing the output emf of the circuit. As an example, consider the thermocouple circuit shown in Figure 8.16, where the junctions of the measuring device are made of copper and material B is an alloy (not pure copper). The electrical connection between the measuring device and the thermocouple circuit forms yet another thermocouple junction. The law of intermediate materials, in this case, provides that

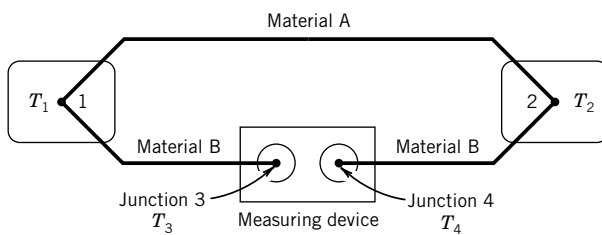


Figure 8.16 Typical thermocouple measuring circuit.

the measured emf will be unchanged from the open-circuit emf, which corresponds to the temperature difference between T_1 and T_2 , if $T_3 = T_4$. Another practical consequence of this law is that copper extension wires may be used to transmit thermocouple emfs to a measuring device.

- 3. Law of successive or intermediate temperatures:** *If two dissimilar homogeneous materials that form a thermocouple circuit produce emf₁ when the junctions are at T₁ and T₂ and produce emf₂ when the junctions are at T₂ and T₃, the emf generated when the junctions are at T₁ and T₃ will be emf₁ + emf₂.* This law allows a thermocouple calibrated for one reference temperature, say T₂, to be used at another reference temperature, such as T₃, to determine temperature T₁.

Basic Temperature Measurement with Thermocouples

Let's first examine a historically significant method of using a thermocouple circuit to measure temperature. Figure 8.17 shows two basic thermocouple circuits, using a chromel–constantan thermocouple and an ice bath to create a reference temperature. In Figure 8.17a, the thermocouple wires are connected directly to a potentiometer to measure the emf. In Figure 8.17b, copper extension wires are employed, creating two reference junctions. The law of intermediate materials ensures that neither the potentiometer nor the extension wires will change the emf of the circuit, as long as the two connecting junctions at the potentiometer and the two in the ice bath experience no temperature difference. All that is required to be able to measure temperature with this circuit is to know the relationship between the output emf and the temperature of the measuring junction, for the particular reference temperature. One method of determining this relationship is to calibrate the thermocouple. However, we shall see that for reasonable levels of uncertainty for temperature measurement, standard materials and procedures allow thermocouples to be accurate temperature measuring devices without the necessity of calibration.

Reference Junction

The provisions for a reference junction should provide a temperature that is accurately known, stable, and reproducible. A very common reference junction temperature is provided by the ice point, 0°C, because of the ease with which it can be obtained.

The creation of a reference junction temperature of 0°C is accomplished in either of two basic ways. Prior to the development of an electronic means of creating a reference point in the electric circuit, an ice bath served to provide the reference junction temperature. An ice bath is typically made by filling a vacuum flask, or Dewar, with finely crushed ice, and adding just enough water to create a transparent slush. When done correctly, the method is surprisingly accurate and reproducible. A few ice cubes floating in water do not create a 0°C environment! Ice baths can be constructed to provide a reference junction temperature to an uncertainty within $\pm 0.01^\circ\text{C}$.

Electronic reference junctions provide a convenient means of the measurement of temperature without the necessity to construct an ice bath. Numerous manufacturers produce commercial

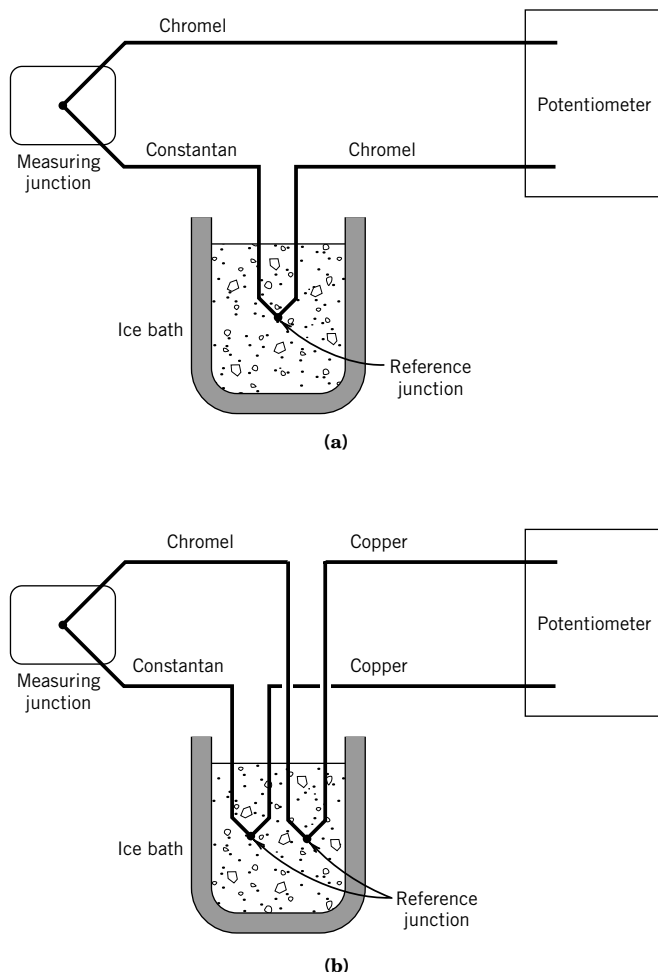


Figure 8.17 Thermocouple temperature measurement circuits.

temperature measuring devices with built-in reference junction compensation, and many digital data acquisition cards for personal computers include built-in reference junction compensation. The electronics generally rely on a thermistor, a temperature-sensitive integrated circuit, or an RTD to determine the reference junction temperature, as shown for a thermistor in Figure 8.18.

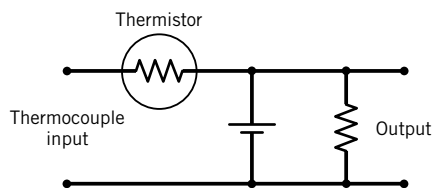


Figure 8.18 Basic thermistor circuit for thermocouple reference junction compensation.

Table 8.4 Thermocouple Designations

Type	Material Combination		Applications
	Positive	Negative	
E	Chromel(+)	Constantan(-)	Highest sensitivity (<1000°C)
J	Iron(+)	Constantan(-)	Nonoxidizing environment (<760°C)
K	Chromel(+)	Alumel(-)	High temperature (<1372°C)
S	Platinum/ 10% rhodium	Platinum(-)	Long-term stability high temperature (<1768°C)
T	Copper(+)	Constantan(-)	Reducing or vacuum environments (<400°C)

Uncertainties for the reference junction temperature in this case are on the order of $\pm 0.1^\circ\text{C}$, with $\pm 0.5^\circ\text{C}$ as typical.

Thermocouple Standards

The National Institute of Standards and Technology (NIST) provides specifications for the materials and construction of standard thermocouple circuits for temperature measurement (10). Many material combinations exist for thermocouples; these material combinations are identified by a thermocouple type and denoted by a letter. Table 8.4 shows the letter designations and the polarity of common thermocouples, along with some basic application information for each type. The choice of a type of thermocouple depends on the temperature range to be measured, the particular application, and the desired uncertainty level.

To determine the emf output of a particular material combination, a thermocouple is formed from a candidate material and a standard platinum alloy to form a thermocouple circuit having a 0°C reference temperature. Figure 8.19 shows the output of various materials in combination with platinum-67. The notation indicates the thermocouple type. The law of intermediate temperatures then allows the emf of any two materials, whose emf relative to platinum is known, to be determined. Figure 8.20 shows a plot of the emf as a function of temperature for some common thermocouple material combinations. The slope of the curves in this figure corresponds to the static sensitivity of the thermocouple measuring circuit.

Standard Thermocouple Voltage

Table 8.5 provides the standard composition of thermocouple materials, along with standard limits of error for the various material combinations. These limits specify the expected maximum errors resulting from the thermocouple materials. The NIST uses high-purity materials to establish the standard value of voltage output for a thermocouple composed of two specific materials. This results in standard tables or equations used to determine a measured temperature from a measured value of

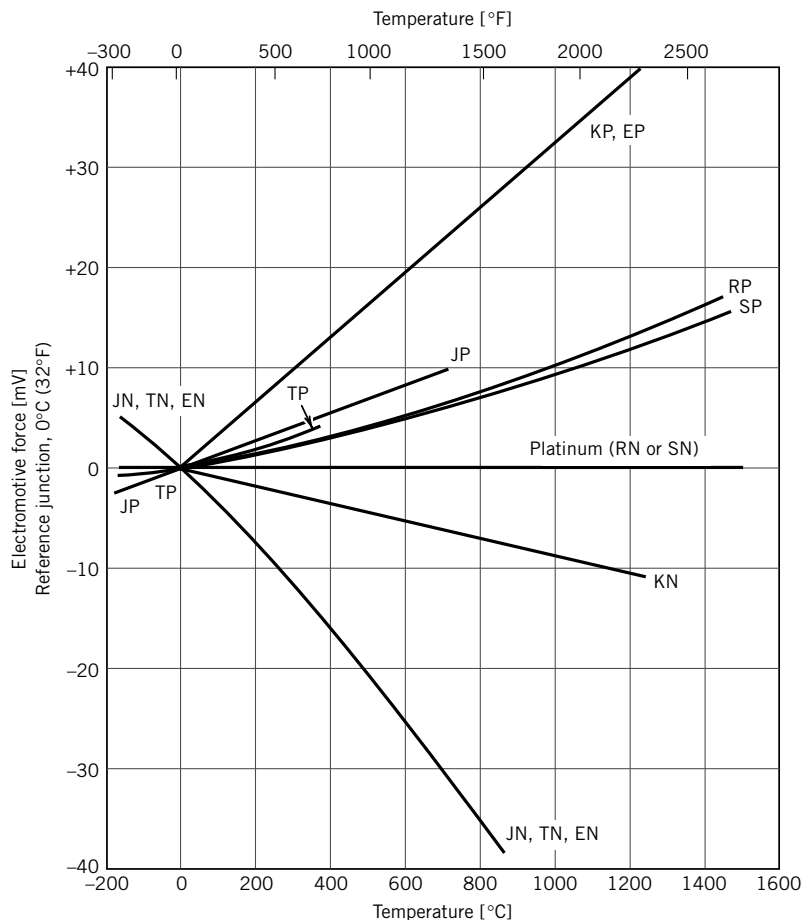


Figure 8.19 Thermal emf of thermocouple materials relative to platinum-67. Note: For example, JP indicates the positive leg of a J thermocouple, or iron. JN indicates the negative leg of a J thermocouple, or constantan. All other notations are similar for each type of thermocouple. (From Benedict, R. P., *Fundamentals of Temperature, Pressure, and Flow Measurements*, 3rd ed. Copyright © 1984 by John Wiley and Sons, New York. Reprinted by permission.)

emf (10). An example of such a table is provided in Table 8.6 for an iron/constantan thermocouple, usually referred to as a J-type thermocouple. Table 8.7 provides the corresponding polynomial equations that relate emf and temperature for standard thermocouples. Because of the widespread need to measure temperature, an industry has grown up to supply high-grade thermocouple wire. Manufacturers can also provide thermocouples having special tolerance limits relative to the NIST standard voltages with uncertainties in temperature ranging from $\pm 1.0^{\circ}\text{C}$ to perhaps $\pm 0.1^{\circ}\text{C}$. Thermocouples constructed of standard thermocouple wire do not require calibration to provide measurement of temperature within the tolerance limits given in Table 8.5.

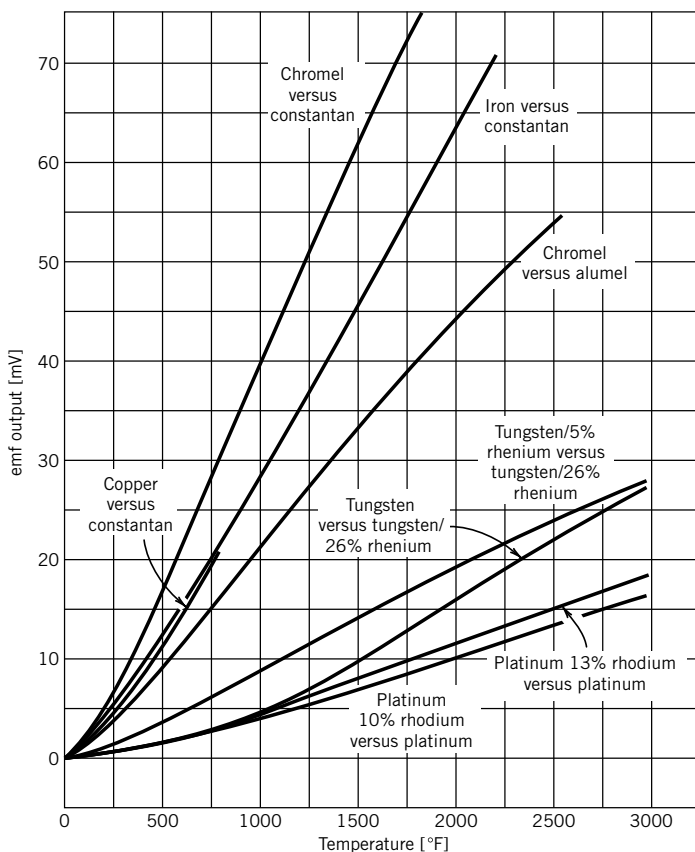


Figure 8.20 Thermocouple voltage output as a function of temperature for some common thermocouple materials. Reference junction is at 32°F (0°C). (From Benedict, R. P., *Fundamentals of Temperature, Pressure and Flow Measurements*, 3rd ed. Copyright © 1984 by John Wiley and Sons, New York. Reprinted by permission.)

Thermocouple Voltage Measurement

The Seebeck voltage for a thermocouple circuit is measured with no current flow in the circuit. From our discussion of the Thomson and Peltier effects, it is clear that the emf is different from the open-circuit value when there is a current flow in the thermocouple circuit. As such, the best method for the measurement of thermocouple voltages is a device that minimizes current flow. For many years, the potentiometer was the laboratory standard for voltage measurement in thermocouple circuits. A potentiometer, as described in Chapter 6, has nearly zero loading error at a balanced condition. However, modern voltage-measuring devices, such as digital voltmeters or data-acquisition cards, have sufficiently large values of input impedance that they can be used with minimal loading error. These devices can also be used in either static or dynamic measuring situations where the loading error created by the measurement device is acceptable for the particular application. For such needs,

Table 8.5 Standard Thermocouple Compositions^a

Type	Wire		Expected Systematic Uncertainty ^b
	Positive	Negative	
S	Platinum	Platinum/10% rhodium	±1.5°C or 0.25%
R	Platinum	Platinum/13% rhodium	±1.5°C
B	Platinum/30% rhodium	Platinum/6% rhodium	±0.5%
T	Copper	Constantan	±1.0°C or 0.75%
J	Iron	Constantan	±2.2°C or 0.75%
K	Chromel	Alumel	±2.2°C or 0.75%
E	Chromel	Constantan	±1.7°C or 0.5%
<i>Alloy Designations</i>			
Constantan: 55% copper with 45% nickel			
Chromel: 90% nickel with 10% chromium			
Alumel: 94% nickel with 3% manganese, 2% aluminum, and 1% silicon			

^aFrom Temperature Measurements ANSI PTC 19.3-1974.^bUse greater value; these limits of error do not include installation errors.**Table 8.6** Thermocouple Reference Table for Type-J Thermocouple^a

Temperature (°C)	Thermocouple emf (mV)									
	0	-1	-2	-3	-4	-5	-6	-7	-8	-9
-210	-8.095									
-200	-7.890	-7.912	-7.934	-7.955	-7.976	-7.996	-8.017	-8.037	-8.057	-8.076
-190	-7.659	-7.683	-7.707	-7.731	-7.755	-7.778	-7.801	-7.824	-7.846	-7.868
-180	-7.403	-7.429	-7.456	-7.482	-7.508	-7.534	-7.559	-7.585	-7.610	-7.634
-170	-7.123	-7.152	-7.181	-7.209	-7.237	-7.265	-7.293	-7.321	-7.348	-7.376
-160	-6.821	-6.853	-6.883	-6.914	-6.944	-6.975	-7.005	-7.035	-7.064	-7.094
-150	-6.500	-6.533	-6.566	-6.598	-6.631	-6.663	-6.695	-6.727	-6.759	-6.790
-140	-6.159	-6.194	-6.229	-6.263	-6.298	-6.332	-6.366	-6.400	-6.433	-6.467
-130	-5.801	-5.838	-5.874	-5.910	-5.946	-5.982	-6.018	-6.054	-6.089	-6.124
-120	-5.426	-5.465	-5.503	-5.541	-5.578	-5.616	-5.653	-5.690	-5.727	-5.764
-110	-5.037	-5.076	-5.116	-5.155	-5.194	-5.233	-5.272	-5.311	-5.350	-5.388
-100	-4.633	-4.674	-4.714	-4.755	-4.796	-4.836	-4.877	-4.917	-4.957	-4.997
-90	-4.215	-4.257	-4.300	-4.342	-4.384	-4.425	-4.467	-4.509	-4.550	-4.591
-80	-3.786	-3.829	-3.872	-3.916	-3.959	-4.002	-4.045	-4.088	-4.130	-4.173
-70	-3.344	-3.389	-3.434	-3.478	-3.522	-3.566	-3.610	-3.654	-3.698	-3.742
-60	-2.893	-2.938	-2.984	-3.029	-3.075	-3.120	-3.165	-3.210	-3.255	-3.300
-50	-2.431	-2.478	-2.524	-2.571	-2.617	-2.663	-2.709	-2.755	-2.801	-2.847
-40	-1.961	-2.008	-2.055	-2.103	-2.150	-2.197	-2.244	-2.291	-2.338	-2.385
-30	-1.482	-1.530	-1.578	-1.626	-1.674	-1.722	-1.770	-1.818	-1.865	-1.913
-20	-0.995	-1.044	-1.093	-1.142	-1.190	-1.239	-1.288	-1.336	-1.385	-1.433
-10	-0.501	-0.550	-0.600	-0.650	-0.699	-0.749	-0.798	-0.847	-0.896	-0.946
0	0.000	-0.050	-0.101	-0.151	-0.201	-0.251	-0.301	-0.351	-0.401	-0.451

(continued)

Table 8.6 (Continued)

Thermocouple emf (mV)										
Temperature (°C)										
	0	+1	+2	+3	+4	+5	+6	+7	+8	+9
0	0.000	0.050	0.101	0.151	0.202	0.253	0.303	0.354	0.405	0.451
10	0.507	0.558	0.609	0.660	0.711	0.762	0.814	0.865	0.916	0.968
20	1.019	1.071	1.122	1.174	1.226	1.277	1.329	1.381	1.433	1.485
30	1.537	1.589	1.641	1.693	1.745	1.797	1.849	1.902	1.954	2.006
40	2.059	2.111	2.164	2.216	2.269	2.322	2.374	2.427	2.480	2.532
50	2.585	2.638	2.691	2.744	2.797	2.850	2.903	2.956	3.009	3.062
60	3.116	3.169	3.222	3.275	3.329	3.382	3.436	3.489	3.543	3.596
70	3.650	3.703	3.757	3.810	3.864	3.918	3.971	4.025	4.079	4.133
80	4.187	4.240	4.294	4.348	4.402	4.456	4.510	4.564	4.618	4.672
90	4.726	4.781	4.835	4.889	4.943	4.997	5.052	5.106	5.160	5.215
100	5.269	5.323	5.378	5.432	5.487	5.541	5.595	5.650	5.705	5.759
110	5.814	5.868	5.923	5.977	6.032	6.087	6.141	6.196	6.251	6.306
120	6.360	6.415	6.470	6.525	6.579	6.634	6.689	6.744	6.799	6.854
130	6.909	6.964	7.019	7.074	7.129	7.184	7.239	7.294	7.349	7.404
140	7.459	7.514	7.569	7.624	7.679	7.734	7.789	7.844	7.900	7.955
150	8.010	8.065	8.120	8.175	8.231	8.286	8.341	8.396	8.452	8.507
160	8.562	8.618	8.673	8.728	8.783	8.839	8.894	8.949	9.005	9.060
170	9.115	9.171	9.226	9.282	9.337	9.392	9.448	9.503	9.559	9.614
180	9.669	9.725	9.780	9.836	9.891	9.947	10.002	10.057	10.113	10.168
190	10.224	10.279	10.335	10.390	10.446	10.501	10.557	10.612	10.668	10.723
200	10.779	10.834	10.890	10.945	11.001	11.056	11.112	11.167	11.223	11.278
210	11.334	11.389	11.445	11.501	11.556	11.612	11.667	11.723	11.778	11.834
220	11.889	11.945	12.000	12.056	12.111	12.167	12.222	12.278	12.334	12.389
230	12.445	12.500	12.556	12.611	12.667	12.722	12.778	12.833	12.889	12.944
240	13.000	13.056	13.111	13.167	13.222	13.278	13.333	13.389	13.444	13.500
250	13.555	13.611	13.666	13.722	13.777	13.833	13.888	13.944	13.999	14.055
260	14.110	14.166	14.221	14.277	14.332	14.388	14.443	14.499	14.554	14.609
270	14.665	14.720	14.776	14.831	14.887	14.942	14.998	15.053	15.109	15.164
280	15.219	15.275	15.330	15.386	15.441	15.496	15.552	15.607	15.663	15.718
290	15.773	15.829	15.884	15.940	15.995	16.050	16.106	16.161	16.216	16.272
300	16.327	16.383	16.438	16.493	16.549	16.604	16.659	16.715	16.770	16.825
310	16.881	16.936	16.991	17.046	17.102	17.157	17.212	17.268	17.323	17.378
320	17.434	17.489	17.544	17.599	17.655	17.710	17.765	17.820	17.876	17.931
330	17.986	18.041	18.097	18.152	18.207	18.262	18.318	18.373	18.428	18.483
340	18.538	18.594	18.649	18.704	18.759	18.814	18.870	18.925	18.980	19.035
350	19.090	19.146	19.201	19.256	19.311	19.366	19.422	19.477	19.532	19.587
360	19.642	19.697	19.753	19.808	19.863	19.918	19.973	20.028	20.083	20.139
370	20.194	20.249	20.304	20.359	20.414	20.469	20.525	20.580	20.635	20.690
380	20.745	20.800	20.855	20.911	20.966	21.021	21.076	21.131	21.186	21.241
390	21.297	21.352	21.407	21.462	21.517	21.572	21.627	21.683	21.738	21.793

Table 8.6 (Continued)

Temperature ($^{\circ}\text{C}$)										Thermocouple emf (mV)	
400	21.848	21.903	21.958	22.014	22.069	22.124	22.179	22.234	22.289	22.345	
410	22.400	22.455	22.510	22.565	22.620	22.676	22.731	22.786	22.841	22.896	
420	22.952	23.007	23.062	23.117	23.172	23.228	23.283	23.338	23.393	23.449	
430	23.504	23.559	23.614	23.670	23.725	23.780	23.835	23.891	23.946	24.001	
440	24.057	24.112	24.167	24.223	24.278	24.333	24.389	24.444	24.499	24.555	
450	24.610	24.665	24.721	24.776	24.832	24.887	24.943	24.998	25.053	25.109	
460	25.164	25.220	25.275	25.331	25.386	25.442	25.497	25.553	25.608	25.664	
470	25.720	25.775	25.831	25.886	25.942	25.998	26.053	26.109	26.165	26.220	
480	26.276	26.332	26.387	26.443	26.499	26.555	26.610	26.666	26.722	26.778	
490	26.834	26.889	26.945	27.001	27.057	27.113	27.169	27.225	27.281	27.337	
500	27.393	27.449	27.505	27.561	27.617	27.673	27.729	27.785	27.841	27.897	
510	27.953	28.010	28.066	28.122	28.178	28.234	28.291	28.347	28.403	28.460	
520	28.516	28.572	28.629	28.685	28.741	28.798	28.854	28.911	28.967	29.024	
530	29.080	29.137	29.194	29.250	29.307	29.363	29.420	29.477	29.534	29.590	
540	29.647	29.704	29.761	29.818	29.874	29.931	29.988	30.045	30.102	30.159	
550	30.216	30.273	30.330	30.387	30.444	30.502	30.559	30.616	30.673	30.730	
560	30.788	30.845	30.902	30.960	31.017	31.074	31.132	31.189	31.247	31.304	
570	31.362	31.419	31.477	31.535	31.592	31.650	31.708	31.766	31.823	31.881	
580	31.939	31.997	32.055	32.113	32.171	32.229	32.287	32.345	32.403	32.461	
590	32.519	32.577	32.636	32.694	32.752	32.810	32.869	32.927	32.985	33.044	
600	33.102	33.161	33.219	33.278	33.337	33.395	33.454	33.513	33.571	33.630	
610	33.689	33.748	33.807	33.866	33.925	33.984	34.043	34.102	34.161	34.220	
620	34.279	34.338	34.397	34.457	34.516	34.575	34.635	34.694	34.754	34.813	
630	34.873	34.932	34.992	35.051	35.111	35.171	35.230	35.290	35.350	35.410	
640	35.470	35.530	35.590	35.650	35.710	35.770	35.830	35.890	35.950	36.010	
650	36.071	36.131	36.191	36.191	36.252	36.373	36.433	36.494	36.554	36.615	
660	36.675	36.736	36.797	36.858	36.918	36.979	37.040	37.101	37.162	37.22.3	
670	37.284	37.345	37.406	37.467	37.528	37.590	37.651	37.712	37.773	37.835	
680	37.896	37.958	38.019	38.081	38.142	38.204	38.265	38.327	38.389	38.450	
690	38.512	38.574	38.636	38.698	38.760	38.822	38.884	38.946	39.008	39.070	
700	39.132	39.194	39.256	39.318	39.381	39.443	39.505	39.568	39.630	39.693	
710	39.755	39.818	39.880	39.943	40.005	40.068	40.131	40.193	40.256	40.319	
720	40.382	40.445	40.508	40.570	40.633	40.696	40.759	40.822	40.886	40.949	
730	41.012	41.075	41.138	41.201	41.265	41.328	41.391	41.455	41.518	41.581	
740	41.645	41.708	41.772	41.835	41.899	41.962	42.026	42.090	42.153	42.217	
750	42.281	42.344	42.408	42.472	42.536	42.599	42.663	42.727	42.791	42.855	
760	42.919	42.983	43.047	43.110	43.174	43.238	43.303	43.367	43.431	43.495	

^aReference junction at 0°C.

Table 8.7 Reference Functions for Selected Letter Designated Thermocouples

The relationship between emf and temperature is provided in the form of a polynomial in temperature [10]

$$E = \sum_{i=0}^n c_i T^i$$

where E is in μV and T is in $^\circ\text{C}$. Constants are provided below.

Thermocouple Type	Temperature Range	Constants
J-type	-210 to 760°C	$c_0 = 0.000\ 000\ 000\ 0$ $c_1 = 5.038\ 118\ 7815 \times 10^1$ $c_2 = 3.047\ 583\ 693\ 0 \times 10^{-2}$ $c_3 = -8.568\ 106\ 572\ 0 \times 10^{-5}$ $c_4 = 1.322\ 819\ 529\ 5 \times 10^{-7}$ $c_5 = -1.705\ 295\ 833\ 7 \times 10^{-10}$ $c_6 = 2.094\ 809\ 069\ 7 \times 10^{-13}$ $c_7 = -1.253\ 839\ 533\ 6 \times 10^{-16}$ $c_8 = 1.563\ 172\ 569\ 7 \times 10^{-20}$
T-type	-270 to 0°C	$c_0 = 0.000\ 000\ 000\ 0$ $c_1 = 3.874\ 810\ 6364 \times 10^1$ $c_2 = 4.419\ 443\ 434\ 7 \times 10^{-2}$ $c_3 = 1.184\ 432\ 310\ 5 \times 10^{-4}$ $c_4 = 2.003\ 297\ 355\ 4 \times 10^{-5}$ $c_5 = 9.013\ 801\ 955\ 9 \times 10^{-7}$ $c_6 = 2.265\ 115\ 659\ 3 \times 10^{-8}$ $c_7 = 3.607\ 115\ 420\ 5 \times 10^{-10}$ $c_8 = 3.849\ 393\ 988\ 3 \times 10^{-12}$ $c_9 = 2.821\ 352\ 192\ 5 \times 10^{-14}$ $c_{10} = 1.425\ 159\ 477\ 9 \times 10^{-16}$ $c_{11} = 4.876\ 866\ 228\ 6 \times 10^{-19}$ $c_{12} = 1.079\ 553\ 927\ 0 \times 10^{-21}$ $c_{13} = 1.394\ 502\ 706\ 2 \times 10^{-24}$ $c_{14} = 7.979\ 515\ 392\ 7 \times 10^{-28}$
T-type	0 to 400°C	$c_0 = 0.000\ 000\ 000\ 0$ $c_1 = 3.874\ 810\ 636\ 4 \times 10^1$ $c_2 = 3.329\ 222\ 788\ 0 \times 10^{-2}$ $c_3 = 2.061\ 824\ 340\ 4 \times 10^{-4}$ $c_4 = -2.188\ 225\ 684\ 6 \times 10^{-6}$ $c_5 = 1.099\ 688\ 092\ 8 \times 10^{-8}$ $c_6 = -3.081\ 575\ 877\ 2 \times 10^{-11}$ $c_7 = 4.547\ 913\ 529\ 0 \times 10^{-14}$ $c_8 = -2.751\ 290\ 167\ 3 \times 10^{-17}$

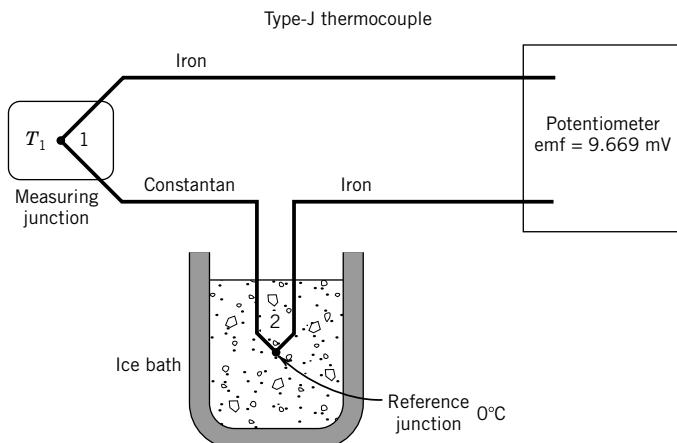


Figure 8.21 Thermocouple circuit for Example 8.7.

high-impedance voltmeters have been incorporated into commercially available temperature indicators, temperature controllers, and digital data-acquisition systems (DAS).

Example 8.7

The thermocouple circuit shown in Figure 8.21 is used to measure the temperature T_1 . The thermocouple reference junction labeled 2 is at a temperature of 0°C , maintained by an ice-point bath. The voltage output is measured using a potentiometer and found to be 9.669 mV. What is T_1 ?

KNOWN A thermocouple circuit having one junction at 0°C and a second junction at an unknown temperature. The circuit produces an emf of 9.669 mV.

FIND The temperature T_1 .

ASSUMPTION Thermocouple follows NIST standard.

SOLUTION Standard thermocouple tables such as Table 8.6 are referenced to 0°C . The temperature of the reference junction for this case is 0°C . Therefore, the temperature corresponding to the output voltage may simply be determined from Table 8.6, in this case as 180.0°C .

COMMENT Because of the law of intermediate metals, the junctions formed at the potentiometer do not affect the voltage measured for the thermocouple circuit, and the voltage output reflects accurately the temperature difference between junctions 1 and 2.

Example 8.8

Suppose the thermocouple circuit in the previous example (Ex. 8.7) now has junction 2 maintained at a temperature of 30°C , and produces an output voltage of 8.132 mV. What temperature is sensed by the measuring junction?

KNOWN The value of T_2 is 30°C , and the output emf is 8.132 mV.

ASSUMPTION Thermocouple follows NIST standard emf behavior.

FIND The temperature of the measuring junction.

SOLUTION By the law of intermediate temperatures the output emf for a thermocouple circuit having two junctions, one at 0°C and the other at T_1 , would be the sum of the emfs for a thermocouple circuit between 0° and 30°C and between 30°C and T_1 . Thus,

$$\text{emf}_{0-30} + \text{emf}_{30-T_1} = \text{emf}_{0-T_1}$$

This relationship allows the voltage reading from the nonstandard reference temperature to be converted to a 0°C reference temperature by adding $\text{emf}_{0-30} = 1.537$ to the existing reading. This results in an equivalent output voltage, referenced to 0°C as

$$1.537 + 8.132 = 9.669 \text{ mV}$$

Clearly, this thermocouple is sensing the same temperature as in the previous example, 180.0°C. This value is determined from Table 8.6.

COMMENT Note that the effect of raising the reference junction temperature is to lower the output voltage of the thermocouple circuit. Negative values of voltage, as compared with the polarity listed in Table 8.4, indicate that the measured temperature is less than the reference junction temperature.

Example 8.9

A J-type thermocouple measures a temperature of 100°C and is referenced to 0°C. The thermocouple is AWG 30 (American wire gauge [AWG]; AWG 30 is 0.010-in. wire diameter) and is arranged in a circuit as shown in Figure 8.17a. The length of the thermocouple wire is 10 ft in order to run from the measurement point to the ice bath and to a potentiometer. The resolution of the potentiometer is 0.005 mV. If the thermocouple wire has a resistance per unit length, as specified by the manufacturer, of 5.6 Ω/ft, estimate the residual current in the thermocouple when the circuit is balanced within the resolution of the potentiometer.

KNOWN A potentiometer having a resolution of 0.005 mV is used to measure the emf of a J-type thermocouple that is 10 ft long.

FIND The residual current in the thermocouple circuit.

SOLUTION The total resistance of the thermocouple circuit is 56 Ω for 10 ft of thermocouple wire. The residual current is then found from Ohm's law as

$$I = \frac{E}{R} = \frac{0.005 \text{ mV}}{56 \Omega} = 8.9 \times 10^{-8} \text{ A}$$

COMMENT The loading error due to this current flow is $\sim 0.005 \text{ mV}/54.3 \mu\text{V}/^\circ\text{C} \approx 0.09^\circ\text{C}$.

Example 8.10

Suppose a high-impedance voltmeter is used in place of the potentiometer in Example 8.9. Determine the minimum input impedance required for the voltmeter that will limit the loading error to the same level as the potentiometer.

KNOWN Loading error should be less than 8.9×10^{-8} A.

FIND Input impedance for a voltmeter that would produce the same current flow or loading error.

SOLUTION At 100°C a J-type thermocouple referenced to 0°C has a Seebeck voltage of $E_s = 5.269$ mV. At this temperature, the required voltmeter impedance to limit the current flow to 8.9×10^{-8} A is found from Ohm's law:

$$\frac{E_s}{I} = 5.269 \times 10^{-3} \text{ V} / 8.9 \times 10^{-8} \text{ A} = 59.2 \text{ k}\Omega$$

COMMENT This input impedance is not at all high for a modern microvoltmeter and such a voltmeter would be a reasonable choice in this situation. As always, the allowable loading error should be determined based on the required uncertainty in the measured temperature.

Multiple-Junction Thermocouple Circuits

A thermocouple circuit composed of two junctions of dissimilar metals produces an open-circuit emf that is related to the temperature difference between the two junctions. More than two junctions can be employed in a thermocouple circuit, and thermocouple circuits can be devised to measure temperature differences, or average temperature, or to amplify the output voltage of a thermocouple circuit.

Thermopiles

Thermopile is the term used to describe a multiple-junction thermocouple circuit that is designed to amplify the output of the circuit. Because thermocouple voltage outputs are typically in the millivolt range, increasing the voltage output may be a key element in reducing the uncertainty in the temperature measurement, or may be necessary to allow transmission of the thermocouple signal to the recording device. Figure 8.22 shows a thermopile for providing an amplified output signal; in this case the output voltage would be N times the single thermocouple output, where N is the number of measuring junctions in the circuit. The average output voltage corresponds to the average

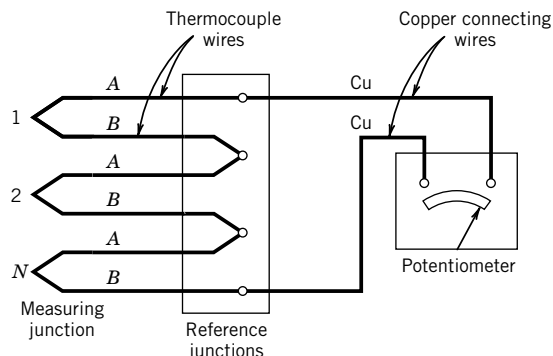


Figure 8.22 Thermopile arrangement.
(From Benedict, R. P. *Fundamentals of Temperature, Pressure and Flow Measurements*, 3rd ed. Copyright © 1984 by John Wiley and Sons, New York.
Reprinted by permission.)

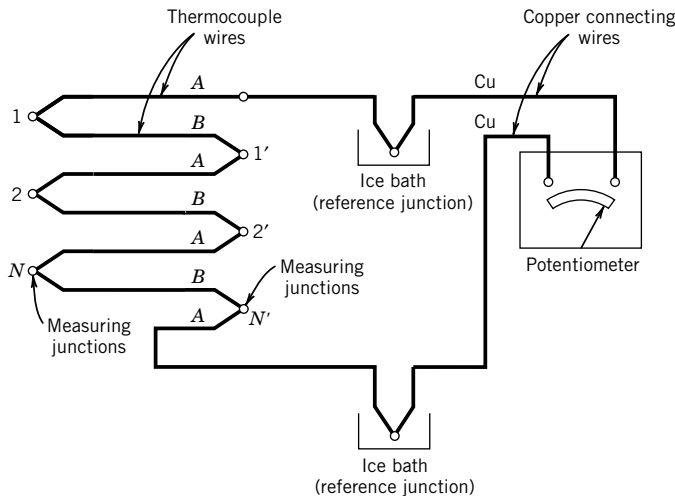


Figure 8.23 Thermocouples arranged to sense temperature differences. (From Benedict, R. P. *Fundamentals of Temperature, Pressure and Flow Measurements*, 3rd ed. Copyright © 1984 by John Wiley and Sons, New York. Reprinted by permission.)

temperature level sensed by the N junctions. Thus, local point measurements entail consideration of the physical size of a thermopile, as compared to a single thermocouple. In transient measurements, a thermopile may have a more limited frequency range than a single thermocouple, due to its increased thermal capacitance. Thermopiles are particularly useful for reducing the uncertainty in measuring small temperature differences between the measuring and reference junctions. The principle has also been used to generate small amounts of power in spacecraft and to provide thermoelectric cooling using the Peltier effect.

Figure 8.23 shows a series arrangement of thermocouple junctions designed to measure the average temperature difference between junctions. This thermocouple circuit could also be used to measure deviations from a uniform temperature. In that case, any voltage output would indicate that a temperature difference existed between two of the thermocouple junctions. Alternatively, junctions $1, 2, \dots, N$ could be located at one physical location, while junctions $1', 2', \dots, N'$ could be located at another physical location. Such a circuit might be used to measure the heat flux through a solid.

Thermocouples in Parallel

When a spatially averaged temperature is desired, multiple thermocouple junctions can be arranged, as shown in Figure 8.24. In such an arrangement of N junctions, a mean emf is produced, given by

$$\overline{\text{emf}} = \frac{1}{N} \sum_{i=1}^N (\text{emf})_i \quad (8.18)$$

The mean emf is indicative of a mean temperature,

$$\overline{T} = \frac{1}{N} \sum_{i=1}^N T_i \quad (8.19)$$

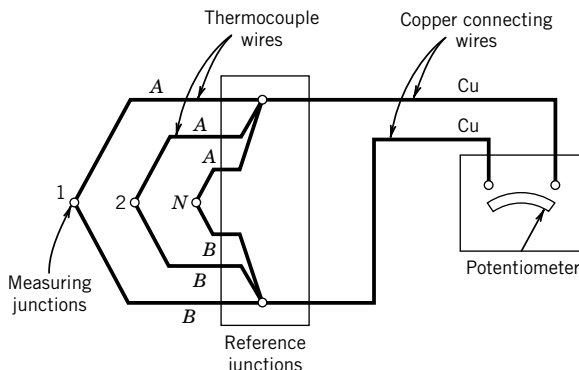


Figure 8.24 Parallel arrangement of thermocouples for sensing the average temperature of the measuring junctions. (From Benedict, R. P. *Fundamentals of Temperature, Pressure and Flow Measurements*, 3rd ed. Copyright © 1984 by John Wiley and Sons, New York. Reprinted by permission.)

Data-Acquisition Considerations

Measuring temperatures by using thermocouples connected to a data acquisition systems is common practice. However, the characteristics of the thermocouple, including the need for a reference or cold junction and the low signal voltages produced, complicate its use. Nevertheless, with a little attention and realistic expectation of achievable accuracy, the systems are quite acceptable for most monitoring and moderate accuracy measurements.

Once the appropriate thermocouple type is selected, attention must be given to the cold junction compensation method. The two connection points of the thermocouple to the data acquisition system (DAS) board form two new thermocouple connections. Use of external cold junction methods between the thermocouple and the board eliminates this problem, but more frequently the thermocouple is connected directly to the board and uses built-in electronic cold junction compensation. This is usually accomplished by using a separate thermistor sensor, which measures the temperature at the system connection point to determine the cold junction error, and providing an appropriate bias voltage correction either directly or through software. An important consideration is that the internal correction method has a typical uncertainty of the order of 0.5° to 1.5°C and, as a systematic error, this error is directly passed on to the measurement as an offset.

These boards also may use internal polynomial interpolation for converting measured voltage into temperature. If not, this can be programmed into the data-reduction scheme by using, for example, the information of Table 8.7. Nonetheless, this introduces a “linearization” error, which is a function of thermocouple material and temperature range and typically specified with the DAS board.

Thermocouples are often used in harsh, industrial environments with significant electro-magnetic interference (EMI) and radiofrequency (rf) noise sources. Thermocouple wire pairs should be twisted to reduce noise. Also, a differential-ended connection is preferred between the thermocouple and the DAS board. In this arrangement, though, the thermocouple becomes an isolated voltage source, meaning there is no longer a direct ground path keeping the input within its common mode range. As a consequence, a common complaint is that the measured signal may drift or suddenly jump in the level of its output. Usually, this interference behavior is eliminated by placing a 10- to 100-k Ω resistor between the low terminal of the input and low-level ground.

Because most DAS boards use analog-to-digital (A/D) converters having a ± 5 V full scale, the signal must be conditioned using an amplifier. Usually a gain of 100 to 500 is sufficient. High gain, very low noise amplifiers are important for accurate measurements. Consider a J-type thermocouple using a 12-bit A/D converter with a signal conditioning gain of 100. This allows for a full-scale input range of 100 mV, which is a suitable range for most measurements. Then, the A/D conversion resolution is

$$\frac{E_{\text{FSR}}}{(G)(2^M)} = \frac{10 \text{ V}}{(100)(1^{12})} = 24.4 \mu\text{V}/\text{bit}$$

A J-type thermocouple has a sensitivity of $\sim 55 \mu\text{V}/^\circ\text{C}$. Thus, the measurement resolution becomes

$$(24.4 \mu\text{V}/\text{bit}) / (55 \mu\text{V}/^\circ\text{C}) = 0.44^\circ\text{C}/\text{bit}.$$

Thermocouples tend to have long time constants relative to the typical sample rate capabilities of general-purpose DAS boards. If temperature measurements show greater than expected fluctuations, high-frequency sampling noise is a likely cause. Reducing the sample rate or using a smoothing filter are simple solutions. The period of averaging should be on the scale of the time constant of the thermocouple.

Example 8.11

It is desired to create an off-the-shelf temperature measuring system for a personal computer (PC)-based control application. The proposed temperature measuring system is illustrated schematically in Figure 8.25. The temperature measurement system consists of the following:

- A PC-based DAS composed of a data-acquisition board, a computer, and appropriate software to allow measurement of analog input voltage signals.
- A J-type thermocouple and reference junction compensator. The reference junction compensator serves to provide an output emf from the thermocouple equivalent to the value that would exist between the measuring junction and a reference temperature of 0°C .
- A J-type thermocouple, which is uncalibrated but meets NIST standard limits of error.

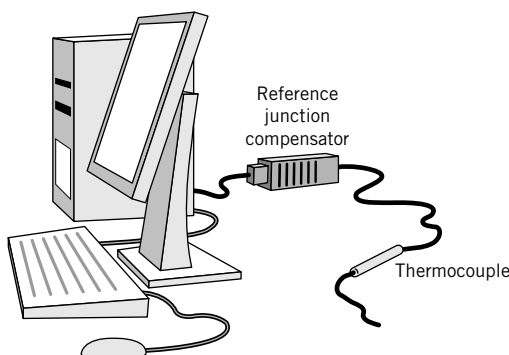


Figure 8.25 Personal computer (PC)-based temperature measurement system.

The system is designed to measure and control a process temperature that varies slowly in time compared to sampling rate of the DAS. The process nominally operates at 185°C.

The following specifications are applicable to the measurement system components:

Component	Characteristics	Accuracy Specifications
Data-acquisition board	Analog voltage input range: 0 to 0.1 V	12-bit A/D converter accuracy: $\pm 0.01\%$ of reading
Reference junction compensator	J-type compensation range from 0° to 50°C	$\pm 0.5^\circ\text{C}$ over the range 20° to 36°C
Thermocouple (J-type)	Stainless steel sheathed ungrounded junction	Accuracy: $\pm 1.0^\circ\text{C}$ based on NIST standard limits of error

The purpose of the measurement system requires that the temperature measurement have a total uncertainty of less than 1.5°C . Based on a design stage uncertainty analysis, does this measurement system meet the overall accuracy requirement?

SOLUTION The design stage uncertainty for this measurement system is determined by expressing the uncertainty of each system component as an equivalent uncertainty in temperature, and then combining these design stage uncertainties.

The 12-bit A/D converter divides the full-scale voltage range into 2^{12} or 4096 equal-sized intervals. Thus, the resolution (quantization error) of the A/D in measuring voltage is

$$\frac{0.1 \text{ V}}{4096 \text{ intervals}} = 0.0244 \text{ mV}$$

The uncertainty of the DAS is specified as 0.01% of the reading. A nominal value for the thermocouple voltage must be known or established. In the present case, the nominal process temperature is 185°C, which corresponds to a thermocouple voltage of approximately 10 mV. Thus the calibration uncertainty of the DAS is 0.001 mV.

The contribution to the total uncertainty of the temperature measurement system from the DAS can now be determined. First combine the resolution and calibration uncertainties as

$$u_{\text{DAS}} = \sqrt{(0.0244)^2 + (0.001)^2} = 0.0244 \text{ mV}$$

The relationship between uncertainty in voltage and temperature is provided by the static sensitivity, which can be estimated from Table 8.6 at 185°C as 0.055 mV/°C. Thus an uncertainty of 0.0244 mV corresponds to an uncertainty in temperature of

$$\frac{0.0244 \text{ mV}}{0.055 \text{ mV/}^\circ\text{C}} = 0.444^\circ\text{C}$$

This uncertainty can now be combined directly with the ice point uncertainty and the uncertainty interval associated with the standard limits of error for the thermocouple, as

$$u_T = \sqrt{(0.444)^2 + (1.0)^2 + (0.5)^2} = \pm 1.2^\circ\text{C} \quad (95\%)$$

COMMENT It might be appropriate in certain cases to calibrate the thermocouple against a laboratory standard, such as an RTD, which has a calibration traceable to NIST standards. With

reasonable expense and care, an uncertainty level in the thermocouple of $\pm 0.1^\circ\text{C}$ can be achieved, compared to the uncalibrated value of $\pm 1^\circ\text{C}$. If the thermocouple were so calibrated, the resulting uncertainty in the overall measurement of temperature is reduced to $\pm 0.68^\circ\text{C}$, so that by reducing the uncertainty contribution of the thermocouple by a factor of 10, the system uncertainty would be reduced by a factor of 2.

Example 8.12

An effective method of evaluating data acquisition and reduction errors associated with the use of multiple temperature sensors within a test facility is to provide a known temperature point at which the sensor outputs can be compared. Suppose the outputs from M similar thermocouple sensors (e.g., all T-type) are to be measured and stored on an M -channel data acquisition system. Each sensor is referenced to the same reference junction temperature (e.g., ice point) and operated in the normal manner. The sensors are exposed to a known and uniform temperature. N (say 30) readings for each of the M thermocouples are recorded. What information can be obtained from the data?

KNOWN $M(j = 1, 2, \dots, M)$ thermocouples
 $N(i = 1, 2, \dots, N)$ readings measured for each thermocouple

SOLUTION The mean value for all readings of the i th thermocouple is given as

$$\bar{T}_j = \frac{1}{N} \sum_{i=1}^N T_{ij}$$

The pooled mean for all the thermocouples is given as

$$\langle \bar{T} \rangle = \frac{1}{M} \sum_{j=1}^M \bar{T}_j$$

The difference between the pooled mean temperature and the known temperature would provide an estimate of the systematic uncertainty that can be expected from any channel during data acquisition. On the other hand, the differences between each \bar{T}_j and $\langle \bar{T} \rangle$ must reflect random uncertainty among the M channels. The standard random uncertainty for the data acquisition and reduction instrumentation system is then

$$s_{\bar{T}} = \frac{\langle s_T \rangle}{\sqrt{M}} \quad \text{where} \quad \langle s_T \rangle = \sqrt{\frac{\sum_{j=1}^M \sum_{i=1}^N (T_{ij} - \bar{T}_j)^2}{M(N-1)}}$$

with degrees of freedom, $v = M(N-1)$.

COMMENT Elemental errors accounted for in these estimates include

- reference junction random errors,
- random errors in the known temperature,
- data acquisition system random errors,
- extension cable and connecting plug systematic errors, and
- thermocouple emf- T correlation systematic errors.

These estimates would not include instrument calibration errors or probe insertion errors.

8.6 RADIATIVE TEMPERATURE MEASUREMENTS

There is a distinct advantage to measuring temperature by detecting thermal radiation. The sensor for thermal radiation need not be in contact with the surface to be measured, making this method attractive for a wide variety of applications. The basic operation of a radiation thermometer is predicated upon some knowledge of the radiation characteristics of the surface whose temperature is being measured, relative to the calibration of the thermometer. The spectral characteristics of radiative measurements of temperature is beyond the scope of the present discussion; an excellent source for further information is Dewitt and Nutter (11).

Radiation Fundamentals

Radiation refers to the emission of electromagnetic waves from the surface of an object. This radiation has characteristics of both waves and particles, which leads to a description of the radiation as being composed of photons. The photons generally travel in straight lines from points of emission to another surface, where they are absorbed, reflected, or transmitted. This electromagnetic radiation exists over a large range of wavelengths that includes x-rays, ultraviolet radiation, visible light, and infrared or thermal radiation, as shown in Figure 8.26. The thermal radiation emitted from an object is related to its temperature and has wavelengths ranging from approximately 10^{-7} to 10^{-3} m. It is necessary to understand two key aspects of radiative heat transfer in relation to temperature measurements. First, the radiation emitted by an object is proportional to the fourth power of its temperature. In the ideal case, this may be expressed as

$$E_b = \sigma T^4 \quad (8.20)$$

where E_b is the flux of energy radiating from an ideal surface, or the blackbody emissive power. The emissive power of a body is the energy emitted per unit area and per unit time. The term “blackbody” implies a surface that absorbs all incident radiation, and as a result emits radiation in an “ideal” manner.

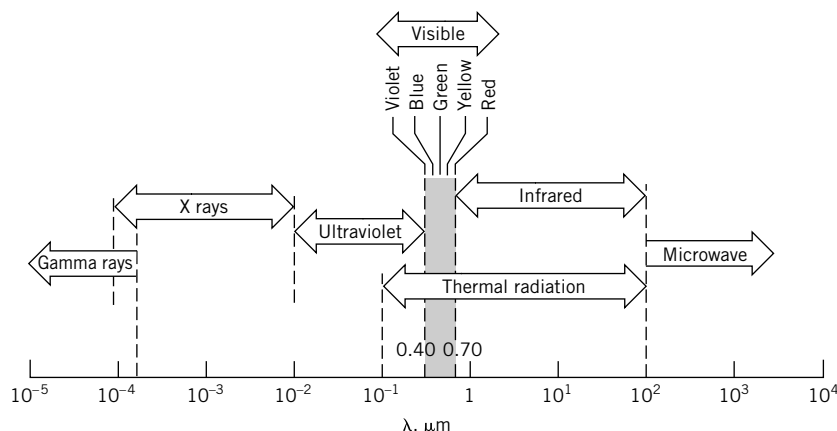


Figure 8.26 The electromagnetic spectrum. (From Incropera F. P., and D. P. DeWitt, *Fundamentals of Heat and Mass Transfer*, 2nd ed. Copyright © 1985 by John Wiley & Sons, New York. Reprinted by permission.)

Second, the emissive power is a direct measure of the total radiation emitted by an object. However, energy is emitted by an ideal radiator over a range of wavelengths, and at any given temperature the distribution of the energy emitted as a function of wavelength is unique. Max Planck (1858–1947) developed the basis for the theory of quantum mechanics in 1900 as a result of examining the wavelength distribution of radiation. He proposed the following equation to describe the wavelength distribution of thermal radiation for an ideal or blackbody radiator:

$$E_{b\lambda} = \frac{2\pi h_p c^2}{\lambda^5 [\exp(h_p c/k_B \lambda T) - 1]} \quad (8.21)$$

where

$E_{b\lambda}$ = total emissive power at the wavelength λ

λ = wavelength

c = speed of light in a vacuum = 2.998×10^8 m/s

h_p = Planck's constant = 6.6256×10^{-34} J s

k_B = Boltzmann's constant = 1.3805×10^{-23} J/K

Figure 8.27 is a plot of this wavelength distribution for various temperatures. For the purposes of radiative temperature measurements, it is crucial to note that the maximum energy emission shifts to shorter wavelengths at higher temperatures. Our experiences confirm this behavior through observation of color changes as a surface is heated.

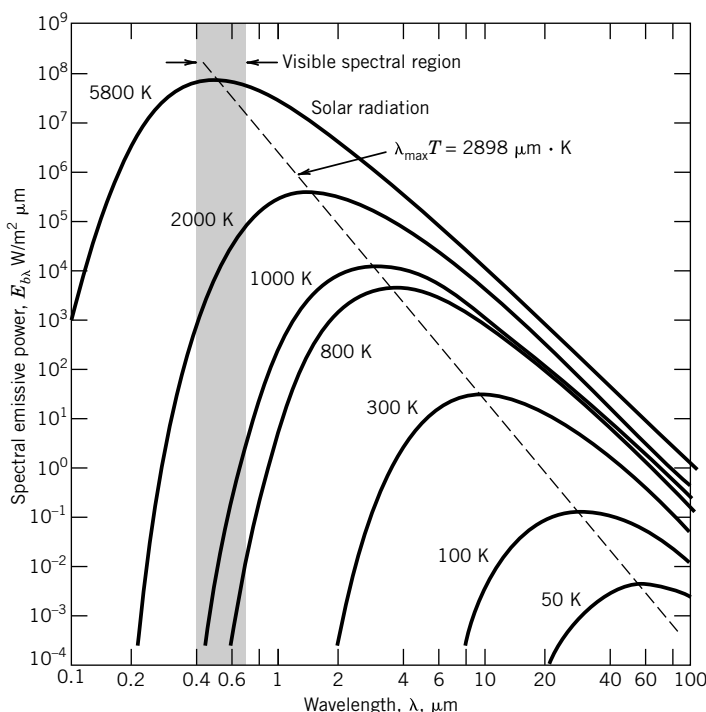


Figure 8.27 Planck distribution of blackbody emissive power as a function of wavelength. (From Incropera F. P., and D. P. DeWitt, *Fundamentals of Heat and Mass Transfer*, 2nd ed. Copyright © 1985 by John Wiley & Sons, New York. Reprinted by permission.)

Consider an electrical heating element, as can be found in an electric oven. With no electric current flow through the element, it appears almost black, its room temperature color. With a current flow, the element temperature rises and it appears to change color to a dull red, and perhaps to a reddish orange. If its temperature continued to increase, eventually it would appear white. This change in color signifies a shift in the maximum intensity of the emitted radiation to shorter wavelengths, out of the infrared and into the visible. There is also an increase in total emitted energy. The Planck distribution provides a basis for the measurement of temperature through color comparison.

Radiation Detectors

Radiative energy flux can be detected in a sensor by two basic techniques. The detector is subject to radiant energy from the source whose temperature is to be measured. The first technique involves a thermal detector in which absorbed radiative energy elevates the detector temperature, as shown in Figure 8.28. These thermal detectors are certainly the oldest sensors for radiation, and the first such detector can probably be credited to Sir William Herschel, who verified the presence of infrared radiation using a thermometer and a prism. The equilibrium temperature of the detector is a direct measure of the amount of radiation absorbed. The resulting rise in temperature must then be measured. Thermopile detectors provide a thermoelectric power resulting from a change in temperature. A thermistor can also be used as the detector, and results in a change in resistance with temperature.

A second basic type of detector relies on the interaction of a photon with an electron, resulting in an electric current. In a photomultiplier tube, the emitted electrons are accelerated and used to create an amplified current, which is measured. Photovoltaic cells may be employed as radiation detectors. The photovoltaic effect results from the generation of a potential across a positive-negative junction in a semiconductor when it is subject to a flux of photons. Electron-hole pairs are formed if the incident photon has an energy level of sufficient magnitude. This process results in the direct conversion of radiation into electrical energy, in high sensitivity, and in a fast response time when used as a detector. In general, the photon detectors tend to be spectrally selective, so that the relative sensitivity of the detector tends to change with the wavelength of the measured radiation.

Many considerations enter into the choice of a detector for radiative measurements. If time response is important, photon detectors are significantly faster than thermopile or thermistor detectors, and therefore have a much wider frequency response. Photodetectors saturate, while thermopile sensors may slowly change their characteristics over time. Some instruments have variations of sensitivity with the incident angle of the incoming radiation; this factor may be important for solar insolation measurements. Other considerations include wavelength sensitivity, cost, and allowable operating temperatures.

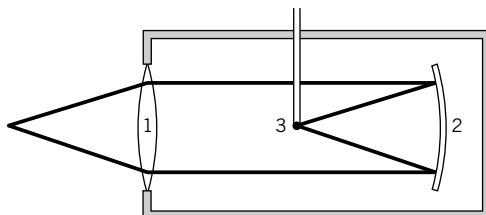


Figure 8.28 Schematic of a basic radiometer: (1) lens; (2) focusing mirror; (3) detector (thermopile or thermistor).

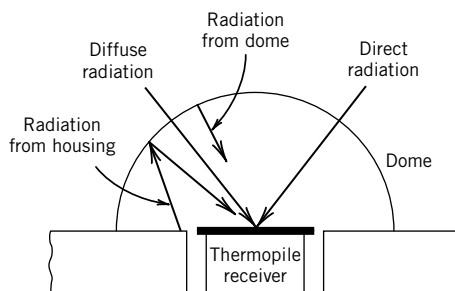


Figure 8.29 Pyranometer construction.

Radiative Temperature Measurements

Commercially applicable radiation thermometers vary widely in their complexity and the accuracy of the resultant measurements. We will consider only the basic techniques that allow measurement of temperature.

Radiometer

Perhaps the simplest form, a radiometer, measures a source temperature by measuring the voltage output from a thermopile detector. A schematic of such a device is shown in Figure 8.28. The increase in temperature of the thermopile is a direct indication of the temperature of the radiation source. One application of this principle is in the measurement of total solar radiation incident upon a surface. Figure 8.29 shows a schematic of a pyranometer, used to measure global solar irradiance. It would have a hemispherical field of view, and measures both the direct or beam radiation, and diffuse radiation. The diffuse and beam components of radiation can be separated by shading the pyranometer from the direct solar radiation, thereby measuring the diffuse component.

Figure 8.30 shows infrared (IR) thermopile sensors that are manufactured using micromachining and advanced semiconductor processing methods. The hot junction of the thermopile is placed under the IR filter and the cold junctions under the IR mask. Manufacturing methods allow hundreds

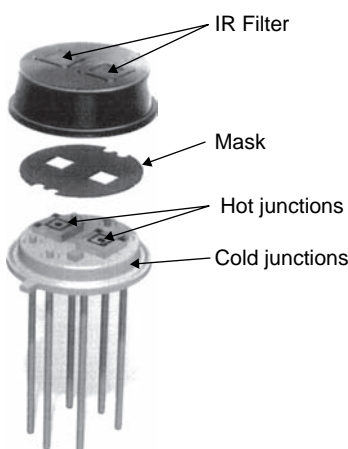


Figure 8.30 Industrial infrared (IR) thermopile sensor.

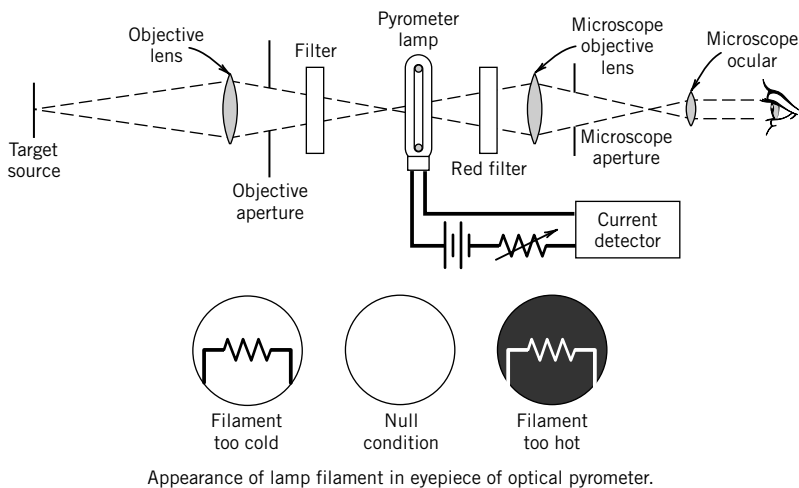


Figure 8.31 Schematic diagram of a disappearing filament optical pyrometer.

of junctions to be created in a micro-device. These sensors form the basis for many practical applications, ranging from tympanic thermometers to automatic climate control systems for automotive applications.

Pyrometry

Optical pyrometry identifies the temperature of a surface by its color, or more precisely the color of the radiation it emits. A schematic of an optical pyrometer is shown in Figure 8.31. A standard lamp is calibrated so that the current flow through its filament is controlled and calibrated in terms of the filament temperature. Comparison is made optically between the color of this filament and the surface of the object whose temperature is being measured. The comparator can be the human eye. Uncertainties in the measurement may be reduced by appropriately filtering the incoming light. Corrections must be applied for surface emissivity associated with the measured radiation; uncertainties vary with the skill of the user, and generally are on the order of 5°C. Replacing the human eye with a different detector extends the range of useful temperature measurement and reduces the random uncertainty.

The major advantage of an optical pyrometer lies in its ability to measure high temperatures remotely. For example, it could be used to measure the temperature of a furnace without having any sensor in the furnace itself. For many applications this provides a safe and economical means of measuring high temperatures.

Optical Fiber Thermometers

The optical fiber thermometer is based on the creation of an ideal radiator that is optically coupled to a fiber-optic transmission system (12, 13), as shown in Figure 8.32. The temperature sensor in this system is a thin, single-crystal aluminum oxide (sapphire) fiber; a metallic coating on the tip of the fiber forms a blackbody radiating cavity, which radiates directly along the sapphire crystal fiber. The single-crystal sapphire fiber is necessary because of the high-temperature operation of the

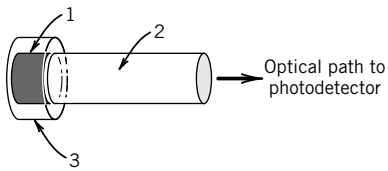


Figure 8.32 Optical fiber thermometer: (1) blackbody cavity (iridium film); (2) sapphire fiber (single crystal); (3) protective coating (Al_2O_3).

thermometer. The operating range of this thermometer is 300° to 1900°C. Signal transmission is accomplished using standard, low-temperature fiber optics. A specific wavelength band of the transmitted radiation is detected and measured, and these raw data are reduced to yield the temperature of the blackbody sensor.

The absence of electrical signals associated with the sensor signal provides excellent immunity from electromagnetic and radiofrequency interference. The measurement system has superior frequency response and sensitivity. The system has been employed for measurement in combustion applications. Temperature resolution of 0.1 mK is possible.

8.7 PHYSICAL ERRORS IN TEMPERATURE MEASUREMENT

In general, errors in temperature measurement derive from two fundamental sources. The first source of errors derives from uncertain information about the temperature of the sensor itself. Such uncertainties can result from random interpolation errors, calibration systematic errors, or a host of other error sources. Instrument and procedural uncertainty in the sensor temperature can be reduced by improved calibration or by changes in the measuring and recording instruments. However, errors in temperature measurement can still occur even if the temperature of the sensor was measured exactly. In such cases, the probe does not sense accurately the temperature it was intended to measure.

A list of typical errors associated with the use of temperature sensors is provided in Table 8.8. Random errors in temperature measurements are a result of resolution limits of measuring and recording equipment, time variations in extraneous variables, and other sources of variation. Thermocouples have some characteristics that can lead to both systematic and random errors, such as the effect of extension wires and connectors. Another major source of error for thermocouples involves the accuracy of the reference junction. Ground loops can lead to spurious readings, especially when thermocouple outputs are amplified for control or data-acquisition purposes. As with any measurement system, calibration of the entire measurement system, in place if possible, is the best means of identifying error sources and reducing the resulting measurement uncertainty to acceptable limits.

Insertion Errors

This discussion focuses on ensuring that a sensor output accurately represents the temperature it is intended to measure. For example, suppose it is desired to measure the outdoor temperature. This measurement could employ a large dial thermometer, which might be placed on a football field or a tennis court in the direct sunlight, and assumed to represent “the temperature,” perhaps as high as 50°C (120°F). But what temperature is being indicated by this thermometer? Certainly the thermometer is not measuring the air temperature, nor is it measuring the temperature of the field or the court. The thermometer is subject to the very sources of error we wish to describe and analyze. *The thermometer, very simply, indicates its own temperature!*

Table 8.8 Measuring Errors Associated with Temperature Sensors*Random Errors*

1. Imprecision of readings
2. Time and spatial variations

Systematic Errors

1. Insertion errors, heating or cooling of junctions
 - a. Conduction errors
 - b. Radiation errors
 - c. Recovery errors
2. Effects of plugs and extension wires
 - a. Nonisothermal connections
 - b. Loading errors
3. Ignorance of materials or material changes during measurements
 - a. Aging following calibration
 - b. Annealing effects
 - c. Cold work hardening
4. Ground loops
5. Magnetic field effects
6. Galvanic error
7. Reference junction inaccuracies

In our example, the temperature of the thermometer is the thermodynamic equilibrium temperature that results from the radiant energy gained from the sun, convective exchange with the air, and conduction heat transfer with the surface on which it is resting. Considering the fact that these thermometers typically have a glass cover that ensures a greenhouse effect, it is very likely that the thermometer temperature is significantly higher than the air temperature.

The physical mechanisms that may cause a temperature probe to indicate a temperature different from that intended include conduction, radiation, and velocity recovery errors. In any real measurement system, their effects could be coupled, and therefore should not be considered independently. However, for simplicity, we will consider each separately because our purpose is to provide only estimates of the errors, and not to provide predictive techniques for correcting measured temperatures. The goal of the measurement engineer should be to minimize these errors, as far as possible, through the careful installation and design of temperature probes.

Conduction Errors

Errors that result from conduction heat transfer between the measuring environment and the ambient are often called immersion errors. Consider the temperature probe shown in Figure 8.33. In many circumstances, a temperature probe extends from the measuring environment through a wall into the ambient environment, where indicating or recording systems are located. The probe and the electrical leads form a path for the conduction of energy from the measuring environment to the ambient. The fundamental nature of the error created by conduction in measured temperatures can be illustrated by the model of a temperature probe shown in Figure 8.34. The essential physics of

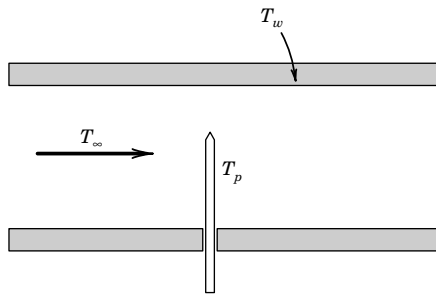


Figure 8.33 Temperature probe inserted into a measuring environment.

immersion errors associated with conduction can be discerned by modeling the temperature probe as a fin. Suppose we assume that the measured temperature is higher than the ambient temperature. If we consider a differential element of the fin, as shown in Figure 8.34b, at steady state there is energy conducted along the fin, and transferred by convection from its surface. The surface area for convection is Pdx , where P is the perimeter or circumference. Applying the first law of thermodynamics to this differential element yields

$$q_{x+dx} - q_x = hP dx [T(x) - T_\infty] \quad (8.22)$$

where h is the convection coefficient. If q is expanded in a Taylor series about the point x , and the substitutions

$$\theta = T - T_\infty \quad q = -kA \frac{dT}{dx} \quad m = \sqrt{\frac{hP}{kA}} \quad (8.23)$$

are made, then the governing differential equation becomes

$$\frac{d^2\theta}{dx^2} - m^2\theta = 0 \quad (8.24)$$

Here k is the effective thermal conductivity of the temperature probe. The solution to this differential equation for the boundary conditions that the wall has a temperature T_w , or a normalized value $\theta_w = T_w - T_\infty$, and the end of the fin is small in surface area, is

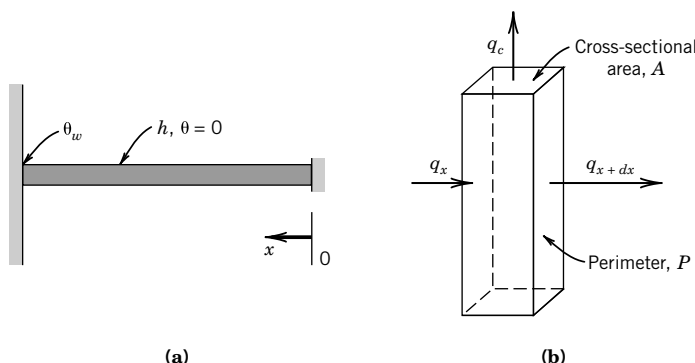


Figure 8.34 Model of a temperature probe as a one-dimensional fin.

$$\frac{\theta(x)}{\theta_w} = \frac{\cosh mx}{\cosh mL} \quad (8.25)$$

The point $x = 0$ is the location where the temperature is assumed to be measured, and therefore the solution is evaluated at $x = 0$ as

$$\frac{\theta(0)}{\theta_w} = \frac{T(0) - T_\infty}{T_w - T_\infty} = \frac{1}{\cosh mL} \quad (8.26)$$

From this analysis, the error due to conduction, e_c , can be estimated. An ideal sensor would indicate the fluid temperature T_∞ ; therefore, if the sensor temperature is $T_p = T(0)$, then the conduction error is

$$e_c = T_p - T_\infty = \frac{T_w - T_\infty}{\cosh mL} \quad (8.27)$$

Normally, the uncertainty due to conduction error is set at $u = e_c$. The uncertainty interval may not be symmetric.

Probe Design

The purpose of the preceding analysis is to gain some physical understanding of ways to minimize conduction errors (not to correct inaccurate measurements). The behavior of this solution is such that the ideal temperature probe would have $T_p = T_\infty$, or $\theta(0) = 0$, implying that $e_c = 0$. Equation 8.26 shows that a value of $\theta(0) \neq 0$ results from a nonzero value of θ_w , and a finite value of $\cosh mL$. The difference between the fluid temperature being measured and the wall temperature should be as small as possible; clearly, this implies that the wall should be insulated to minimize this temperature difference, and the resulting conduction error.

The term “ $\cosh mL$ ” should be as large as possible. The behavior of the \cosh function is shown in Figure 8.35. Since the hyperbolic cosine monotonically increases for increasing values of the argument, the goal of a probe design should be to maximize the value of the product mL , or $(hP/kA)^{1/2}L$. In general, the thermal conductivity of a temperature probe and the convection coefficient are not design parameters. Thus, two important conclusions are that the probe should be as small in diameter as possible, and should be inserted as far as possible into the measuring environment away from the bounding surface to make L large. A small diameter increases the ratio of the perimeter P to the cross-sectional area A . For a circular cross section, this ratio is $4/D$, where D is the diameter. A good rule of thumb based on Equation 8.27 is to have an $L/D > 50$ for negligible conduction error.

Although this analysis clearly indicates the fundamental aspects of conduction errors in temperature measurements, it does not provide the capability to correct measured temperatures

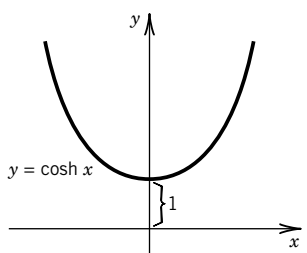


Figure 8.35 Behavior of the hyperbolic cosine.

for conduction errors. Conduction errors should be minimized through appropriate design and installation of temperature probes. Usually, the physical situation is sufficiently complex to preclude accurate mathematical description of the measurement errors. Additional information on modeling conduction errors may be found in Sparrow (14).

Radiation Errors

Consider a temperature probe used to measure a gas temperature. In the presence of significant radiation heat transfer, the equilibrium temperature of a temperature probe may be different from the fluid temperature being measured. Because radiation heat transfer is proportional to the fourth power of temperature, the importance of radiation effects increases as the absolute temperature of the measuring environment increases. The error due to radiation can be estimated by considering steady-state thermodynamic equilibrium conditions for a temperature sensor. Consider the case where energy is transferred to/from a sensor by convection from the environment and from/to the sensor by radiation to a body at a different temperature, such as a pipe or furnace wall. For this analysis conduction is neglected. A first law analysis of a system containing the probe, at steady-state conditions, yields

$$q_c + q_r = 0 \quad (8.28)$$

where

q_c = convective heat transfer

q_r = radiative heat transfer

The heat-transfer components can then be expressed in terms of the appropriate fundamental relations as

$$q_c = hA_s(T_\infty - T) \quad q_r = FA_s\epsilon\sigma(T_w^4 - T^4) \quad (8.29)$$

Assuming that the surroundings may be treated as a blackbody, the first law for a system consisting of the temperature probe is

$$hA_s(T_\infty - T_p) = FA_s\epsilon\sigma(T_p^4 - T_w^4) \quad (8.30)$$

A temperature probe is generally small compared to its surroundings, which justifies the assumption that the surroundings may be treated as black. The radiation error e_r is estimated by

$$e_r = (T_p - T_\infty) = \frac{F\epsilon\sigma}{h} (T_w^4 - T_p^4) \quad (8.31)$$

where

σ = the Stefan-Boltzmann constant ($\sigma = 5.669 \times 10^{-8} \text{ W/m}^2\text{K}^4$)

ϵ = emissivity of the sensor

F = radiation view factor

T_p = probe temperature

T_w = temperature of the surrounding walls

T_∞ = fluid temperature being measured

Again, if the sensor is small compared to the scale of the surroundings, the view factor from the sensor to the surroundings may be taken as 1. Normally, the uncertainty due to radiation error is set as $u = e_r$. The uncertainty interval is not symmetrical and might be modeled as a uniform (rectangular) distribution with bounds of 0 and e_r .

Example 8.13

A typical situation where radiation would be important occurs in measuring the temperature of a furnace. Figure 8.36 shows a small temperature probe for which conduction errors are negligible, which is placed in a high-temperature enclosure, where the fluid temperature is T_∞ and the walls of the enclosure are at T_w .

Convection and radiation are assumed to be the only contributing heat transfer modes at steady state. Develop an expression for the equilibrium temperature of the probe. Also determine the equilibrium temperature of the probe and the radiation error in the case where $T_\infty = 800^\circ\text{C}$, $T_w = 500^\circ\text{C}$, and the emissivity of the probe is 0.8. The convective heat transfer coefficient is $100 \text{ W/m}^2\text{C}$.

KNOWN Temperatures $T_\infty = 800^\circ\text{C}$ and $T_w = 500^\circ\text{C}$, with $h = 100 \text{ W/m}^2\text{C}$. The emissivity of the probe is 0.8.

FIND An expression for the equilibrium temperature of the probe, and the resulting probe temperature for the stated conditions.

ASSUMPTIONS The surroundings may be treated as black, and conduction heat transfer is neglected.

SOLUTION The probe is modeled as a small, spherical body within the enclosed furnace; the view factor from the probe to the furnace is 1. At steady state, an equilibrium temperature may be found from an energy balance. The first law for a system consisting of the temperature probe from Equation 8.30 is

$$h(T_\infty - T_p) + \sigma\epsilon(T_w^4 - T_p^4) = 0 \quad (8.32)$$

The probe is attempting to measure T_∞ . Equation 8.32 yields an equilibrium temperature for the probe of $T_p = 642.5^\circ\text{C}$. The predicted radiation error in this case can be as large as (from Equation 8.31) -157.5°C . This result indicates that radiative heat transfer can create significant measurement errors at elevated temperatures.

COMMENT Because the radiation error in this case can only lower the indicated temperature, it is an example of a nonsymmetrical error (see Section 5.10). We can use

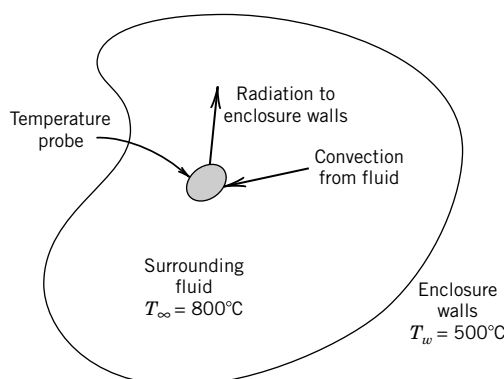


Figure 8.36 Analysis of a temperature probe in a radiative and convective environment.

this predicted value as an estimate of the uncertainty resulting from this effect, or we can use the predicted value to correct the indicated value and assign a smaller uncertainty based on the uncertainty in the correction.

Equation 8.31 and Equation 8.32, above, do not allow direct solution for the radiation error because it contains the probe temperature raised to the fourth power. Any calculator or computer-based method for the solution of nonlinear equations may be employed to affect the solution, although a trial-and-error approach converges rapidly to the correct temperature.

Radiation Shielding

Radiation shielding is a key concept in controlling radiative heat transfer; shielding for radiation is analogous to insulation to reduce conduction heat transfer. A radiation shield is an opaque surface interposed between a temperature sensor and its radiative surroundings so as to reduce electromagnetic wave interchange. In principle, the shield attains an equilibrium temperature closer to the fluid temperature than the surroundings. Because the probe can no longer “see” the surroundings, with the radiation shield in place, the probe temperature is closer to the fluid temperature. Additional information on radiation error in temperature measurements may be found in Sparrow (14). The following example serves to demonstrate radiation errors and the effect of shielding.

Example 8.14

Consider again Example 8.13, where the oven is maintained at a temperature of 800°C . Because of energy losses, the walls of the oven are cooler, having a temperature of 500°C . For the present case, consider the temperature probe as a small, spherical object located in the oven, having no thermal conduction path to the ambient. (All energy exchange is through convection and radiation.) Under these conditions, the probe temperature is 642.5°C , as found in Example 8.13.

Suppose a radiation shield is placed between the temperature probe and the walls of the furnace, which blocks the path for radiative energy transfer. Examine the effect of adding a radiation shield on the probe temperature.

KNOWN A radiation shield is added to a temperature probe in an environment with $T_{\infty} = 800^{\circ}\text{C}$ and $T_w = 500^{\circ}\text{C}$.

FIND The radiation error in the presence of the shield.

ASSUMPTIONS The radiation shield completely surrounds the probe, and the surroundings may be treated as a blackbody.

SOLUTION The shield equilibrium temperature is higher than the wall temperature by virtue of convection with the fluid. As a result, the probe “sees” a higher temperature surface, and the probe temperature is closer to the fluid temperature, resulting in less measurement error.

For a single radiation shield placed so that it completely surrounds the probe, which is small compared to the size of the enclosure and has an emissivity of 1, the equilibrium temperature of the shield can be determined from Equation 8.30. The temperature of the shield is found to be 628°C . Because the sensor now “sees” the shield, rather than the wall, the temperature measured by the probe is 697°C , which is also determined from Equation 8.30.

One shield with an emissivity of 1 provides for an improvement over the case of no shields, but a better choice of the surface characteristics of the shield material can result in much better performance. If the shield has an emissivity of 0.1, the shield temperature rises to 756°C and the probe temperature to 771°C.

COMMENT Shielding provides improved temperature measurements by reducing radiative heat transfer. Another area for improvement in this temperature measurement could be the elevation of the wall temperature through insulation. This discussion of radiation shielding serves to demonstrate the usefulness of shielding as a means of improving temperature measurements in radiative environments. As with conduction errors, the development should be used to guide the design and installation of temperature sensors rather than to correct measured temperatures. Further information on radiation errors may be found in Benedict (5).

Recovery Errors in Temperature Measurement

The kinetic energy of a gas moving at high velocity can be converted to sensible energy by reversibly and adiabatically bringing the flow to rest at a point. The temperature resulting from this process is called the stagnation or total temperature T_t . On the other hand, the static temperature of the gas, T_∞ , is the temperature that would be measured by an instrument moving at the local fluid velocity. From a molecular point of view, the static temperature measures the magnitude of the random kinetic energy of the molecules that comprise the gas, while the stagnation temperature includes both the directed and random components of kinetic energy. Generally, the engineer would be content with knowledge of either temperature, but in high-speed gas flows the sensor indicates neither temperature.

For negligible changes in potential energy, and in the absence of heat transfer or work, the energy equation for a flow may be written in terms of enthalpy and kinetic energy as

$$h_1 + \frac{U^2}{2} = h_2 \quad (8.33)$$

where state 2 refers to the stagnation condition, and state 1 to a condition where the gas is flowing with the velocity U . Assuming ideal gas behavior, the enthalpy difference $h_2 - h_1$ may be expressed as $c_p(T_2 - T_1)$, or in terms of static and stagnation temperatures

$$\frac{U^2}{2c_p} = T_t - T_\infty \quad (8.34)$$

The term $U^2/2c_p$ is called the *dynamic temperature*.

What implication does this have for the measurement of temperature in a flowing gas stream? The physical nature of gases at normal pressures and temperatures is such that the velocity of the gas on a solid surface is zero, because of the effects of viscosity. Thus, when a temperature probe is placed in a moving fluid, the fluid is brought to rest on the surface of the probe. Deceleration of the flow by the probe converts some portion of the directed kinetic energy of the flow to thermal energy, and elevates the temperature of the probe above the static temperature of the gas. The fraction of the kinetic energy recovered as thermal energy is called the recovery factor, r , defined as

$$r \equiv \frac{T_p - T_\infty}{U^2/2c_p} \quad (8.35)$$

where T_p represents the equilibrium temperature of the stationary (with respect to the flow) real temperature probe. In general, r may be a function of the velocity of the flow, or more precisely, the Mach number and Reynolds number of the flow, and the shape and orientation of the temperature probe. For thermocouple junctions of round wire, Moffat (15) reports values of

$$r = 0.68 \pm 0.07 \quad (95\%) \quad \text{for wires normal to the flow}$$

$$r = 0.86 \pm 0.09 \quad (95\%) \quad \text{for wires parallel to the flow}$$

These recovery factor values tend to be constant at velocities for which temperature errors are significant, usually flows where the Mach number is greater than 0.1. For thermocouples having a welded junction, a spherical weld bead significantly larger than the wire diameter tends to a value of the recovery factor of 0.75, for the wires parallel or normal to the flow. The relationships between temperature and velocity for temperature probes with known recovery factors are

$$T_p = T_\infty + \frac{rU^2}{2c_p} \quad (8.36)$$

or in terms of the recovery error, e_U ,

$$e_U = T_p - T_\infty = \frac{rU^2}{2c_p} \quad (8.37)$$

The probe temperature is related to the stagnation temperature by

$$T_p = T_t - \frac{(1-r)U^2}{2c_p} \quad (8.38)$$

Fundamentally, in liquids the stagnation and static temperatures are essentially equal (5), and the recovery error may generally be taken as zero for liquid flows. In any case, high-velocity flows are rarely encountered in liquids.

Normally, the uncertainty assigned to the recovery error is set at $u = e_U$. The uncertainty interval is often not symmetrical.

Example 8.15

A temperature probe having a recovery factor of 0.86 is to be used to measure a flow of air at velocities up to the sonic velocity, at a pressure of 1 atm and a static temperature of 30°C. Calculate the value of the recovery error in the temperature measurement as the velocity of the air flow increases, from 0 to the speed of sound, using Equation 8.37.

KNOWN $r = 0.86$ $p_\infty = 1 \text{ atm abs} = 101 \text{ kPa abs}$

$M \leq 1$ $T_\infty = 30^\circ\text{C} = 303 \text{ K}$

FIND The recovery error as a function of air velocity.

ASSUMPTION Air behaves as an ideal gas.

SOLUTION Assuming that air behaves as an ideal gas, the speed of sound is expressed as

$$a = \sqrt{kRT} \quad (8.39)$$

For air at 101 kPa and 303 K, with $R = 0.287 \text{ kJ/kg K}$, the speed of sound is approximately 349 m/s.

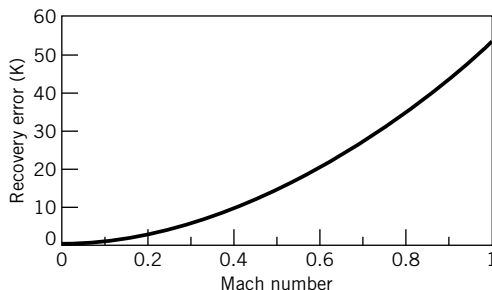


Figure 8.37 Behavior of recovery error as a function of Mach number.

Figure 8.37 shows the error in temperature measurement as a function of Mach number for this temperature probe. The *Mach number* is defined as the ratio of the flow velocity to the speed of sound.

COMMENT Typically, the static and total temperatures of the flowing fluid stream are to be determined from the measured probe temperature. In this case a second independent measurement of the velocity is necessary.

8.8 SUMMARY

Temperature is a fundamentally important quantity in science and engineering, both in concept and practice. As such, temperature is one of the most widely measured engineering variables, providing the basis for a variety of control and safety systems. This chapter provides the basis for the selection and installation of temperature sensors.

Temperature is defined for practical purposes through the establishment of a temperature scale, such as the Kelvin scale, that encompasses fixed reference points and interpolation standards. The International Temperature Scale 1990 is the accepted standard for temperature measurement.

The two most common methods of temperature measurement employ thermocouples and resistance temperature detectors. Standards for the construction and use of these temperature measuring devices have been established and provide the basis for selection and installation of commercially available sensors and measuring systems.

Installation effects on the accuracy of temperature measurements are a direct result of the influence of radiation, conduction, and convection heat transfer on the equilibrium temperature of a temperature sensor. The installation of a temperature probe into a measuring environment can be accomplished in such a way as to minimize the uncertainty in the resulting temperature measurement.

REFERENCES

1. Patterson, E. C., Eponyms: Why Celsius? *American Scientist* 77(4):413, 1989.
2. Klein, H. A., *The Science of Measurement: A Historical Survey*, Dover, Mineola, N.Y., 1988.
3. Committee Report, the International Temperature Scale of 1990, *Metrologia* 27(3), 1990. (The text of the superseded International Practical Temperature Scale of 1968 appears as an appendix in the National Bureau of Standards monograph 124. An amended version was adopted in 1975, and the English text published: *Metrologia* 12:7–17, 1976.)

4. *Temperature Measurement*, Supplement to American Society of Mechanical Engineers PTC 19.3, 1974.
5. Benedict, R. P., *Fundamentals of Temperature, Pressure, and Flow Measurements*, 3rd ed., Wiley, New York, 1984.
6. McGee, T. D., *Principles and Methods of Temperature Measurement*, Wiley-Interscience, New York, 1988.
7. Diehl, W., Thin-film PRTD, *Measurements and Control*, 155–159, December 1982.
8. Thermistor Definitions and Test Methods, Electronic Industries Association Standard RS-275-A (ANSI Standard C83.68–1972), June 1971.
9. Thermometrics, Inc., Vol. 1. NTC Thermistors, 1993.
10. Burns, G. W., Scroger, M. G., and G. F. Strouse, Temperature-Electromotive Force Reference Functions and Tables for the Letter-Designated Thermocouple Types Based on the ITS-90, *NIST Monograph 175*, April 1993 (supersedes NBS Monograph 125).
11. Dewitt, D. P. and G. D. Nutter, *Theory and Practice of Radiation Thermometry*, Wiley-Interscience, New York, 1988.
12. Dils, R. R., High-temperature optical fiber thermometer, *Journal of Applied Physics*, 54(3): 1198–1201, 1983.
13. Optical fiber thermometer, *Measurements and Control*, April 1987.
14. Sparrow, E. M., Error estimates in temperature measurement. In: E. R. G. Eckert and R. J. Goldstein (Eds.), *Measurements in Heat Transfer*, 2nd ed., Hemisphere, Washington, DC, 1976.
15. Moffat, R. J., Gas temperature measurements. In: *Temperature—Its Measurement and Control in Science and Industry*, Vol. 3, Part 2, Reinhold, New York, 1962.

NOMENCLATURE

a	speed of sound (lt^{-1})	u_d	design-stage uncertainty
$b_{\bar{x}}$	systematic standard uncertainty in x	A_c	cross-sectional area (l^2)
c	speed of light in a vacuum (lt^{-1})	A_s	surface area (l^2)
c_p	specific heat ($l^2t^{-2}/^\circ$)	B	systematic uncertainty
d	thickness; diameter (l)	C_α	coefficient of thermal expansion ($ll^{-1}/^\circ$)
e_c	conduction temperature error ($^\circ$)	D	diameter (l)
e_U	recovery temperature error ($^\circ$)	E_b	blackbody emissive power (mt^{-3})
e_r	radiation temperature error ($^\circ$)	$E_{b\lambda}$	spectral emissive power (mt^{-3})
emf	electromotive force	E_i	input voltage (V)
h	convective heat transfer coefficient ($mt^{-3}/^\circ$); enthalpy (l^2t^{-2})	E_1	voltage drop across R_1 (V)
k	thermal conductivity ($mlt^{-3}/^\circ$)	E_o	output voltage (V)
k	ratio of specific heats	F	radiation view factor
l	length (l)	I	current (A)
m	$\sqrt{hP/kA}$ (eq. 8.23) (l^{-2})	L	length of temperature probe (l)
q	heat flux (mt^3)	P	standard random uncertainty; perimeter (l)
r	recovery factor	Q	heat transfer (ml^2t^{-3})
r_c	radius of curvature (l)	R	resistance (Ω); gas constant ($l^2t^{-2}/^\circ$)
$s_{\bar{x}}$	random standard uncertainty in x	R_0	reference resistance (Ω)
u	uncertainty	R_T	thermistor resistance (Ω)

T	temperature ($^{\circ}$)	AB	Peltier coefficient ($m \text{ } l^2 t^{-3} \text{ A}^{-1}$)
T_0	reference temperature ($^{\circ}$)	σ	Thomson coefficient ($ml^2 t^{-3} \text{ A}^{-1}$); Stefan-Boltzmann constant for radiation ($mt^{-3}/(^{\circ})^4$)
T_p	probe temperature ($^{\circ}$)	θ	nondimensional temperature
T_w	wall or boundary temperature ($^{\circ}$)	θ_x	sensitivity index for variable x (uncertainty analysis)
T_{∞}	fluid temperature ($^{\circ}$)	ρ_e	resistivity (Ω, l)
U	fluid velocity (lt^{-1})	δ	thermistor dissipation constant ($ml^2 t^{-3}/^{\circ}$)
α	temperature coefficient of resistivity ($\Omega/^{\circ}$)	ε	emissivity
α_{AB}	Seebeck coefficient		
β	material constant for thermistor resistance ($^{\circ}$); constant in polynomial expansion		

PROBLEMS

- 8.1** Define and discuss the significance of the following terms, as they apply to temperature and temperature measurements:
- temperature scale
 - temperature standards
 - fixed points
 - interpolation
- 8.2** Fixed temperature points in the International Temperature Scale are phase equilibrium states for a variety of pure substances. Discuss the conditions necessary within an experimental apparatus to accurately reproduce these fixed temperature points. How would elevation, weather, and material purity affect the uncertainty in these fixed points?
- 8.3** Calculate the resistance of a platinum wire that is 2 m in length and has a diameter of 0.1 cm. The resistivity of platinum at 25°C is $9.83 \times 10^{-6} \Omega\text{-cm}$. What implications does this result have for the construction of a resistance thermometer using platinum?
- 8.4** Plot the resistance of a platinum wire that is 5 m long as a function of wire diameter ranging from 0.1 mm to 2 mm. Estimate the allowable tensile load for the 0.1 mm wire. (Hint: The modulus of elasticity of platinum is 145 GPa.)
- 8.5** An RTD forms one arm of a Wheatstone bridge, as shown in Figure 8.38. The RTD is used to measure a constant temperature, with the bridge operated in a balanced mode. The RTD has a resistance of 25Ω at a temperature of 0°C , and a thermal coefficient of resistance, $\alpha = 0.003925^{\circ}\text{C}^{-1}$. The value of the variable resistance R_1 must be set to 37Ω to balance the bridge circuit.
- Determine the temperature of the RTD.
 - Compare this circuit to the equal-arm bridge in Example 8.2. Which circuit provides the greater static sensitivity?
- 8.6** An RTD forms one arm (R_4) of a Wheatstone bridge, as shown in Figure 8.8. The RTD is used to measure a constant temperature, with the bridge operated in deflection mode. The RTD has a resistance of 25Ω at a temperature of 0°C , and a thermal coefficient of resistance, $\alpha = 0.003925^{\circ}\text{C}^{-1}$. If the RTD is subjected to a temperature of 100°C and the input voltage to the bridge is 5V, what is the output voltage?

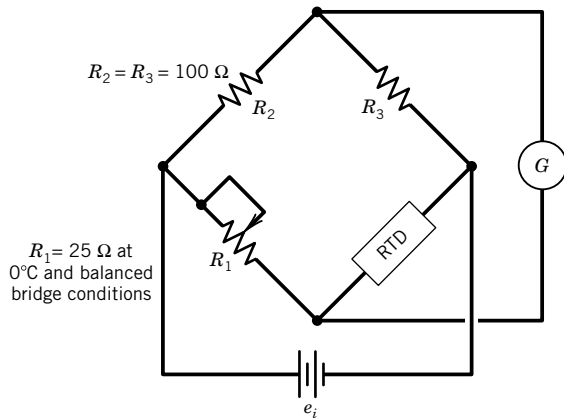


Figure 8.38 Wheatstone bridge circuit for Problem 8.5.

- 8.7 Research and describe current state-of-the-art electronic modules to measure temperature using an RTD sensor. List typical specifications that could be used in a design stage uncertainty analysis.
- 8.8 Estimate the required level of uncertainty in the measurement of resistance for a platinum RTD if it is to serve as a local standard for the calibration of a temperature measurement system for an uncertainty of $\pm 0.005^\circ\text{C}$. Assume $R(0^\circ\text{C}) = 100 \Omega$.
- 8.9 A thermistor is placed in a 100°C environment, and its resistance measured as $20,000 \Omega$. The material constant, β , for this thermistor is 3650°C . If the thermistor is then used to measure a particular temperature, and its resistance is measured as 500Ω , determine the thermistor temperature.
- 8.10 Using a spreadsheet or similar software, reproduce Figure 8.11.
- 8.11 Define and discuss the following terms related to thermocouple circuits:
 - a. thermocouple junction
 - b. thermocouple laws
 - c. reference junction
 - d. Peltier effect
 - e. Seebeck coefficient
- 8.12 The thermocouple circuit in Figure 8.39 represents a J-type thermocouple with the reference junction having $T_2 = 0^\circ\text{C}$. The output emf is 13.777 mV. What is the temperature of the measuring junction, T_1 ?
- 8.13 The thermocouple circuit in Figure 8.39 represents a J-type thermocouple. The circuit produces an emf of 15 mV for $T_1 = 750^\circ\text{C}$. What is T_2 ?

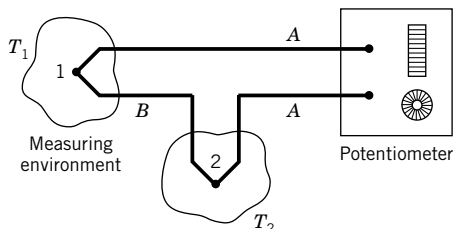
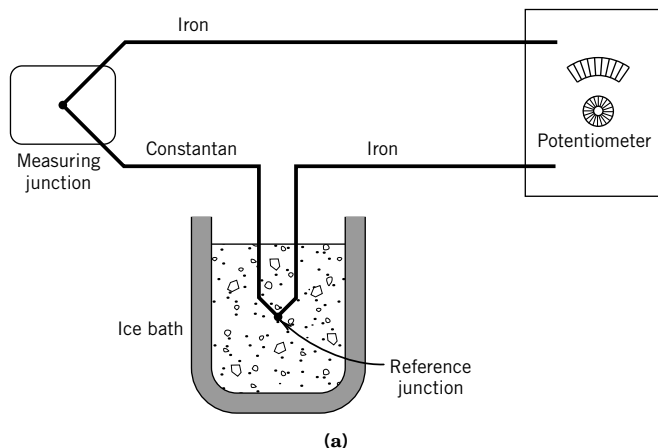


Figure 8.39 Thermocouple circuit for Problems 8.12 through 8.14; (1) measuring junction; (2) reference junction.



(a)

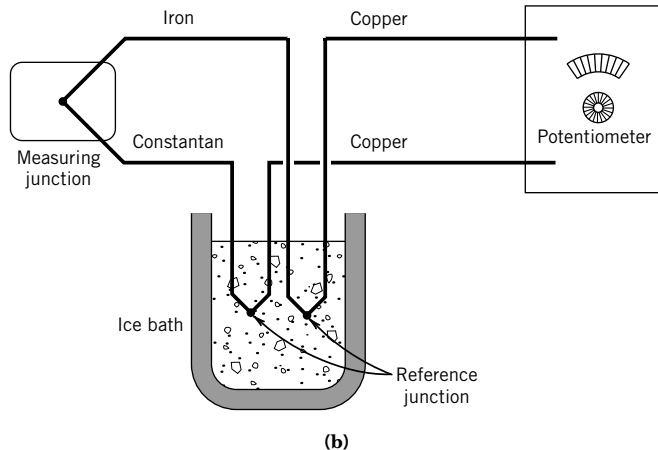


Figure 8.40 Schematic diagram for Problem 8.15.

- 8.14** The thermocouple circuit in Figure 8.39 is composed of copper and constantan and has an output voltage of 6 mV for $T_1 = 200^\circ\text{C}$. What is T_2 ?
- 8.15** a. The thermocouple shown in Figure 8.40a yields an output voltage of 7.947 mV. What is the temperature of the measuring junction?
- b. The ice bath that maintains the reference junction temperature melts, allowing the reference junction to reach a temperature of 25°C . If the measuring junction of (a) remains at the same temperature, what voltage would be measured by the potentiometer?
- c. Copper extension leads are installed as shown in Figure 8.40b. For an output voltage of 7.947 mV, what is the temperature of the measuring junction?
- 8.16** A J-type thermocouple referenced to 70°F has a measured output emf of 2.878 mV. What is the temperature of the measuring junction?

- 8.17** A J-type thermocouple referenced to 0°C indicates 4.115 mV. What is the temperature of the measuring junction?
- 8.18** A temperature measurement requires an uncertainty of $\pm 2^\circ\text{C}$ (5%) at a temperature of 200°C . A standard T-type thermocouple is to be used with a readout device that provides electronic ice-point reference junction compensation, and has a stated instrument uncertainty of 0.5°C (95%) with 0.1°C resolution. Determine whether the uncertainty constraint is met at the design stage.
- 8.19** A temperature difference of 3.0°C is measured using a thermopile having three pairs of measuring junctions, arranged as shown in Figure 8.23.
- Determine the output of the thermopile for J-type thermocouple wire, if all pairs of junctions sense the 3.0°C temperature difference. The average temperature of the junctions is 80°C .
 - If the thermopile is constructed of wire that has a maximum emf variation from the NIST standard values of $\pm 0.8\%$ (95%), and the voltage measuring capabilities in the system are such that the uncertainty is $\pm 0.0005 \text{ V}$ (95%), perform an uncertainty analysis to estimate the uncertainty in the measured temperature difference at the design stage.
- 8.20** Complete the following table for a J-type thermocouple:

Temperature ($^\circ\text{C}$)		
Measured	Reference	emf (mV)
100	0	-0.5
	0	
100	50	2.5
	50	

- 8.21** A J-type thermopile is constructed as shown in Figure 8.22, to measure a single temperature. For a four-junction thermopile referenced to 0°C, what would be the emf produced at a temperature of 125°C ? If a voltage measuring device was available that had a total uncertainty of $\pm 0.0001 \text{ V}$ (95%), how many junctions would be required in the thermopile to reduce the uncertainty in the measured temperature to $\pm 0.1^\circ\text{C}$ (95%)?
- 8.22** You are employed as a heating, ventilating, and air conditioning engineer. Your task is to decide where in a residence to place a thermostat, and how it is to be mounted on the wall. A thermostat contains a bimetallic temperature measuring device that serves as the sensor for the control logic of the heating and air conditioning system for the house. Consider the heating season. When the temperature of the sensor falls 1°C below the set-point temperature of the thermostat, the furnace is activated; when the temperature rises 1°C above the set point, the furnace is turned off. Discuss where the thermostat should be placed in the house, what factors could cause the temperature of the sensor in the thermostat to be different from the air temperature, and possible causes of discomfort for the occupants of the house. How does the thermal capacitance of the temperature sensor affect the operation of the thermostat? Why are thermostats typically set 5°C higher in the air conditioning season?
- 8.23** A J-type thermocouple for use at temperatures between 0° and 100°C was calibrated at the steam point in a device called a hygrometer. A hygrometer creates a constant temperature environment at the saturation temperature of water, at the local barometric pressure. The steam-point temperature is strongly affected by barometric pressure variations. Atmospheric pressure on the day of this

calibration was 30.1 in. Hg. The steam-point temperature as a function of barometric pressure may be expressed as

$$T_{st} = 212 + 50.422 \left(\frac{p}{p_0} - 1 \right) - 20.95 \left(\frac{p}{p_0} - 1 \right)^2 [^{\circ}\text{F}]$$

where $p_0 = 29.921$ in. Hg. At the steam point, the emf produced by the thermocouple, referenced to 0°C , is measured as 5.310 mV. Construct a calibration curve for this thermocouple by plotting the difference between the thermocouple reference table value and the measured value ($\text{emf}_{\text{ref}} - \text{emf}_{\text{meas}}$) versus temperature. What is this difference at 0°C ? Suggest a means for measuring temperatures between 0° and 100°C using this calibration, and estimate the contribution to the total uncertainty.

- 8.24** A J-type thermocouple is calibrated against an RTD standard within $\pm 0.01^{\circ}\text{C}$ (95%) between 0° and 200°C . The emf is measured with a potentiometer having 0.001 mV resolution and less than 0.015 mV (95%) systematic uncertainty. The reference junction temperature is provided by an ice bath. The calibration procedure yields the following results:

$T_{\text{RTD}} (^{\circ}\text{C})$	0.00	20.50	40.00	60.43	80.25	100.65
emf (mV)	0.010	1.038	2.096	3.207	4.231	5.336

- a. Determine a polynomial to describe the relation between the temperature and thermocouple emf.
 - b. Estimate the uncertainty in temperature using this thermocouple and potentiometer.
 - c. Suppose the thermocouple is connected to a digital temperature indicator having a resolution of 0.1°C with 0.3°C (95%) systematic uncertainty. Estimate the uncertainty in indicated temperature.
- 8.25** A beaded thermocouple is placed in a duct in a moving gas stream having a velocity of 200 ft/s. The thermocouple indicates a temperature of 1400 R.
- a. Determine the true static temperature of the fluid based on an estimate for velocity errors. Take the specific heat of the fluid to be 0.6 Btu/lbm $^{\circ}\text{R}$, and the recovery factor to be 0.22.
 - b. Estimate the possible error (uncertainty) in the thermocouple reading due to radiation if the walls of the duct are at 1200 R. The view factor from the probe to the duct walls is 1, the convective heat-transfer coefficient, h , is 30 Btu/hr-ft $^{-2}$ $^{\circ}\text{R}$, and the emissivity of the temperature probe is 1.
- 8.26** Consider a welded thermocouple bead that experiences an air flow at 90 m/s. The thermocouple indicates a temperature of 600°C . Determine the true static temperature of the air by correcting for recovery errors assuming a recovery factor of 0.25.
- 8.27** It is desired to measure the static temperature of the air outside of an aircraft flying at 20,000 ft with a speed of 300 miles per hour, or 438.3 ft/s. A temperature probe is used that has a recovery factor, r , of 0.75. If the static temperature of the air is 413 R, and the specific heat is 0.24 Btu/lbm R, what is the temperature indicated by the probe? Local atmospheric pressure at 20,000 ft is approximately 970 lb/ft 2 , which results in an air density of 0.0442 lbm/ft 3 . Discuss additional factors that might affect the accuracy of the static temperature reading.
- 8.28** The static temperature of the air outside of an aircraft flying at 7000 m with a speed of 150 m/s is to be measured. A temperature probe is used that has a recovery factor, r , of 0.75. If the static temperature of the air is -35°C , and the specific heat is 1000 J/kg-K, what is the temperature

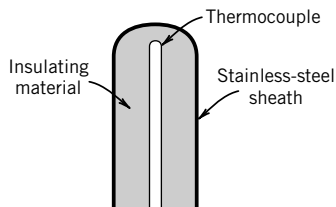


Figure 8.41 Typical construction of a sheathed thermocouple.

indicated by the probe? Local atmospheric pressure at 7000 m is approximately 45 kPa, which results in an air density of 0.66 kg/m^3 . Discuss additional factors that might affect the accuracy of the static temperature reading.

- 8.29** Consider the typical construction of a sheathed thermocouple, as shown in Figure 8.41. Analysis of this geometry to determine conduction errors in temperature measurement is difficult. Suggest a method for placing a realistic upper limit on the conduction error for such a probe, for a specified immersion depth into a convective environment.
- 8.30** An iron-constantan thermocouple is placed in a moving air stream in a duct, as shown in Figure 8.42. The thermocouple reference junction is maintained at 212°F . The wall temperature, T_w , is 500°F , and the air velocity is 200 ft/s. The emf output from the thermocouple is 14.143 mV.
- Determine the thermocouple junction temperature.
 - By considering recovery and radiation errors, estimate the possible value for total error in the indicated temperature. Discuss whether this estimate of the measurement error is conservative, and why or why not. The heat-transfer coefficient may be taken as $70 \text{ Btu/hr-ft}^{-2}\text{-}^\circ\text{F}$.

Air Properties	Thermocouple Properties
$c_p = 0.24 \text{ Btu/lbm}^\circ\text{F}$	$r = 0.7$
$U = 200 \text{ ft/s}$	$\varepsilon = 0.25$

- 8.31** An iron-constantan thermocouple is placed in a moving air stream in a duct, as shown in Figure 8.42. The air flows at 70 m/s. The emissivity of the thermocouple is 0.5 and the recovery factor is 0.6. The wall temperature, T_w , is 300°C . The thermocouple reference junction is maintained at 100°C . The emf output from the thermocouple is 16 mV.

- Determine the thermocouple junction temperature.

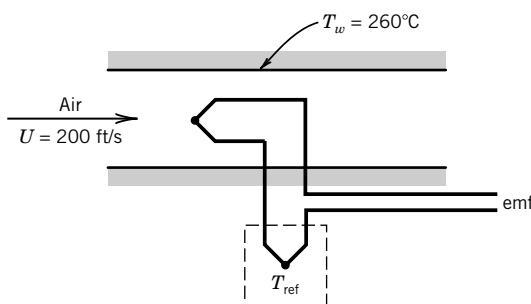


Figure 8.42 Schematic diagram for Problems 8.30 and 8.31.

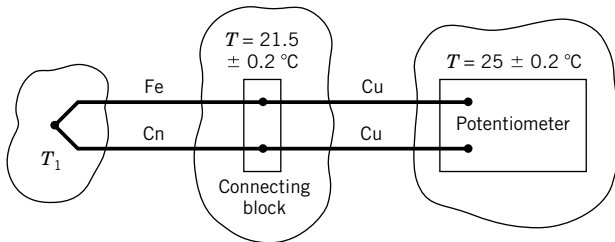


Figure 8.43 Thermocouple circuit for Problem 8.33.

- b. By considering recovery and radiation errors, estimate the possible value for total error in the indicated temperature. Discuss whether this estimate of the measurement error is conservative, and why or why not. The heat-transfer coefficient may be taken as $100 \text{ W/m}^2\text{K}$.
- 8.32 In Example 8.5, an uncertainty value for R_T was determined at 125°C as $B_{R_T} = 247 \Omega$ (95%). Show that this value is correct by performing an uncertainty analysis on R_T . In addition, determine the value of B_{R_T} at the temperatures 150°C and 100°C . What error is introduced into the uncertainty analysis for β by using the value of B_{R_T} at 125°C ?
- 8.33 The thermocouple circuit shown in Figure 8.43 measures the temperature T_1 . The potentiometer limits of error are given as:

Limits of error: $\pm 0.05\%$ (95%) of reading $+15 \mu\text{V}$ at 25°C

Resolution: $5 \mu\text{V}$

Give a best estimate for the temperature T_1 , if the output emf is 9 mV .

- 8.34 A concentration of salt of 600 ppm in tap water causes a 0.05°C change in the freezing point of water. For an ice bath prepared using tap water and ice cubes from tap water at a local laboratory and having 1500 ppm of salts, determine the error in the ice-point reference. Upon repeated measurements, is this error manifested as a systematic or random error? Explain.
- 8.35 A platinum RTD ($\alpha = 0.00392^\circ\text{C}^{-1}$) is to be calibrated in a fixed-point environment. The probe is used in a balanced mode with a Wheatstone bridge, as shown in Figure 8.44. The bridge resistances are known to an uncertainty of $\pm 0.001 \Omega$ (95%). At 0°C the bridge balances when $R_c = 100.000 \Omega$. At 100°C the bridge balances when $R_c = 139.200 \Omega$.
 - a. Find the RTD resistance corresponding to 0°C and 100°C , and the uncertainty in each value.
 - b. Calculate the uncertainty in determining a temperature using this RTD–bridge system for a measured temperature that results in $R_c = 300 \Omega$. Assume $u_\alpha = \pm 1 \times 10^{-5}/^\circ\text{C}$ (95%).

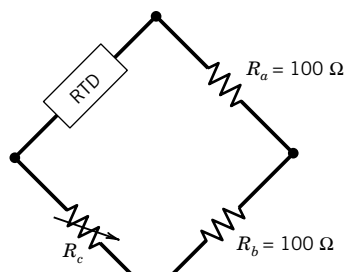


Figure 8.44 Bridge circuit for Problem 8.35.

- 8.36** A T-type thermopile is used to measure temperature difference across insulation in the ceiling of a residence in an energy monitoring program. The temperature difference across the insulation is used to calculate energy loss through the ceiling from the relationship

$$Q = kA_c(\Delta T/L)$$

where

$$A_c = \text{ceiling area} = 15 \text{ m}^2$$

$$k = \text{insulation thermal conductivity } -0.4 \text{ W/m°C}$$

$$L = \text{insulation thickness} = 0.25 \text{ m}$$

$$\Delta T = \text{temperature difference} = 5^\circ\text{C}$$

$$Q = \text{heat loss(W)}$$

The value of the temperature difference is expected to be 5°C , and the thermocouple emf is measured with an uncertainty of $\pm 0.04 \text{ mV}$. Determine the required number of thermopile junctions to yield an uncertainty in Q of $\pm 5\%$ (95%), assuming the uncertainty in all variables other than ΔT may be neglected.

- 8.37** A T-type thermocouple referenced to 0°C is used to measure the temperature of boiling water. What is the emf of this circuit at 100°C ?
- 8.38** A T-type thermocouple referenced to 0°C develops an output emf of 1.2 mV . What is the temperature sensed by the thermocouple?
- 8.39** A temperature measurement system consists of a digital voltmeter and a T-type thermocouple. The thermocouple leads are connected directly to the voltmeter, which is placed in an air conditioned space at 25°C . The output emf from the thermocouple is 10 mV . What is the measuring junction temperature?
- 8.40** The result of more than 60 temperature measurements over time during fixed conditions in a furnace determines $\bar{T} = 624.7^\circ\text{C}$ with $s_{\bar{T}} = 2.4^\circ\text{C}$. The engineer suspects a radiation systematic error. The walls of the furnace are at 400°C , so that the actual temperature in the furnace may be larger than 624.7 , but not less. As such, the lower bound of error is 0°C relative to the measured mean value. Estimate the radiation error in the measurement; assume reasonable values for the heat transfer parameters. Develop a statement for the true mean temperature with its confidence interval assuming the systematic errors follow a rectangular distribution with upper bound from your estimate and lower bound 0°C relative to the measured mean value.
- 8.41** Flexibility, k , is a property of bimetallic strips that if known allows the radius of curvature to be calculated directly as

$$r_c = \frac{d}{2k(T_2 - T_1)}$$

where T_2 is the temperature of interest, T_1 is the assembly temperature of the bimetallic strip, and r_c is infinite. If a 3-cm strip is assembled at 25°C , plot the shape of the strip at temperatures of 50°C , 75°C , and 100°C for a k value of $7.3 \times 10^{-5} \text{ K}^{-1}$.

Chapter 9

Pressure and Velocity Measurements

9.1 INTRODUCTION

This chapter introduces methods to measure the pressure and the velocity within fluids. Instruments and procedures for establishing known values of pressure for calibration purposes, as well as various types of transducers for pressure measurement, are discussed. Pressure is measured in static systems and in moving fluid systems. We also discuss well-established methods measuring the local and full-field velocity within a moving fluid. Finally, we present practical considerations, including common error sources, for pressure and velocity measurements. Although there are various practical test standards for pressure, many of which are applied to a specific application or measuring device, the American Society of Mechanical Engineers' Performance Test Code (ASME PTC) 19.2 provides an overview of basic pressure concepts and measuring instruments that has become the accepted standard (1).

Upon completion of this chapter, the reader will be able to

- explain absolute and gauge pressure concepts and describe the working standards that measure pressure directly,
- explain the physical principles underlying mechanical pressure measurements and the various types of transducers used to measure pressure,
- explain pressure concepts related to static systems or with moving fluids,
- analyze the dynamic behavior of pressure system response due to transmission line effects, and
- explain the physical principles underlying various velocity measurement methods and their practical use.

9.2 PRESSURE CONCEPTS

Pressure represents a contact force per unit area. It acts inwardly, and normally to a surface. To better understand the origin and nature of pressure, consider the measurement of pressure at the wall of a vessel containing an ideal gas. As a gas molecule with some amount of momentum collides with this solid boundary, it rebounds off in a different direction. From Newton's second law, we know that this change in linear momentum of the molecule produces an equal but opposite (normal, inward) force on the boundary. It is the net effect of these collisions averaged over brief instants in time that yields the pressure sensed at the boundary surface. Because there are so many molecules per unit volume

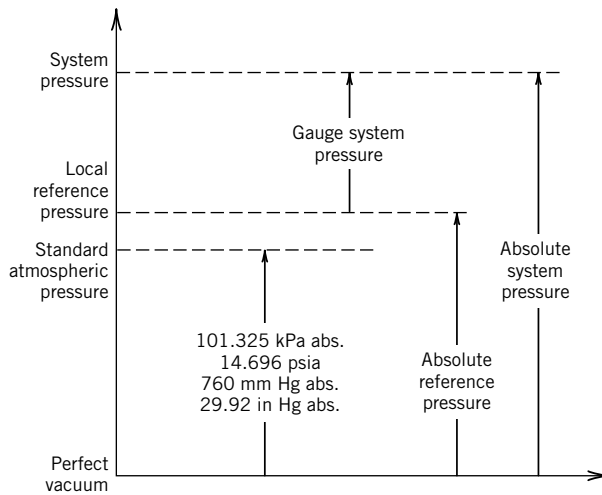


Figure 9.1 Relative pressure scales.

involved (e.g., in a gas there are roughly 10^{16} molecules per mm^3), pressure is usually considered to be continuous. Factors that affect the frequency or the number of the collisions, such as temperature and fluid density, affect the pressure. In fact, this reasoning is the basis of the kinetic theory from which the ideal gas equation of state is derived.

A pressure scale must be related to molecular activity, since a lack of any molecular activity must form the limit of absolute zero pressure. A pure vacuum, which contains no molecules, provides the limit for a primary standard for absolute zero pressure. As shown in Figure 9.1, the absolute pressure scale is quantified relative to this absolute zero pressure. The pressure under standard atmospheric conditions is defined as $1.01320 \times 10^5 \text{ Pa}$ absolute (where $1 \text{ Pa} = 1 \text{ N/m}^2$) (2). This is equivalent to

- 101.32 kPa absolute
- 1 atm absolute
- 14.696 lb/in.² absolute (written as psia)
- 1.013 bar absolute (where 1 bar = 100 kPa)

The term “absolute” might be abbreviated as “a” or “abs.”

Also indicated in Figure 9.1 is a gauge pressure scale. The gauge pressure scale is measured relative to some absolute reference pressure, which is defined in a manner convenient to the measurement. The relation between an absolute pressure, p_{abs} , and its corresponding gauge pressure, p_{gauge} , is given by

$$p_{\text{gauge}} = p_{\text{abs}} - p_0 \quad (9.1)$$

where p_0 is a reference pressure. A commonly used reference pressure is the local absolute atmospheric pressure. Absolute pressure is a positive number. Gauge pressure can be positive or negative depending on the value of measured pressure relative to the reference pressure. A differential pressure, such as $p_1 - p_2$, is a relative measure of pressure.

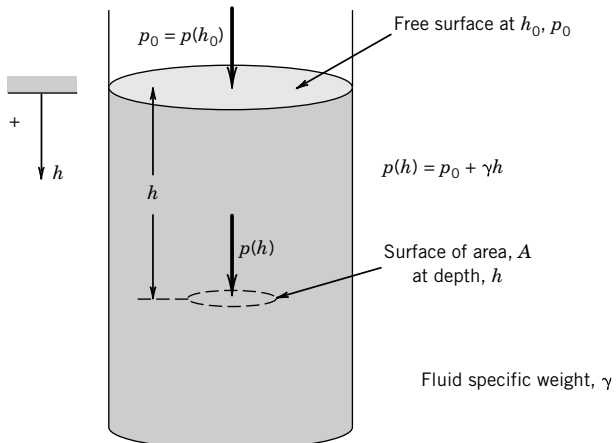


Figure 9.2 Hydrostatic-equivalent pressure head and pressure.

Pressure can also be described in terms of the pressure exerted on a surface that is submerged in a column of fluid at depth h , as depicted in Figure 9.2. From hydrostatics, the pressure at any depth within a fluid of specific weight γ can be written as

$$p_{\text{abs}}(h) = p(h_0) + \gamma h = p_0 + \gamma h \quad (9.2)$$

where p_0 is the pressure at an arbitrary datum line at h_0 , and h is measured relative to h_0 . The fluid specific weight is given by $\gamma = \rho g$ where ρ is the density. When Equation 9.2 is rearranged, the equivalent head of fluid at depth h becomes

$$h = [p_{\text{abs}}(h) - p(h)]/\gamma = (p_{\text{abs}} - p_0)/\gamma \quad (9.3)$$

The equivalent pressure head at one standard atmosphere ($p_0 = 0$ absolute) is

$$\begin{aligned} 760 \text{ mm Hg abs} &= 760 \text{ torr abs} = 1 \text{ atm abs} \\ &= 10,350.8 \text{ mm H}_2\text{O abs} = 29.92 \text{ in Hg abs} \\ &= 407.513 \text{ in H}_2\text{O abs} \end{aligned}$$

The standard is based on mercury (Hg) with a density of $0.0135951 \text{ kg/cm}^3$ at 0°C and water at $0.000998207 \text{ kg/cm}^3$ at 20°C (2).

Example 9.1

Determine the absolute and gauge pressures and the equivalent pressure head at a depth of 10 m below the free surface of a pool of water at 20°C .

KNOWN $h = 10 \text{ m}$; where $h_0 = 0$ is the free surface
T = 20°C
 $\rho_{\text{H}_2\text{O}} = 998.207 \text{ kg/m}^3$
 Specific gravity of mercury, $S_{\text{Hg}} = 13.57$

ASSUMPTION $p(h_0) = 1.0132 \times 10^5 \text{ Pa abs}$

FIND p_{abs} , p_{gauge} , and h

SOLUTION The absolute pressure is found directly from Equation 9.2. Using the pressure at the free surface as the reference pressure and the datum line for h_0 , the absolute pressure must be

$$p_{\text{abs}}(h) = 1.0132 \times 10^5 \text{ N/m}^2 + \frac{(997.4 \text{ kg/m}^3)(9.8 \text{ m/s}^2)(10 \text{ m})}{1 \text{ kg-m/N-s}^2}$$

$$= 1.9906 \times 10^5 \text{ N/m}^2 \text{ abs}$$

This is equivalent to 199.06 kPa abs or 1.96 atm abs or 28.80 lb/in.² abs or 1.99 bar abs.

The pressure can be described as a gauge pressure by referencing it to atmospheric pressure. From Equation 9.1,

$$p(h) = p_{\text{abs}} - p_0 = \gamma h$$

$$= 9.7745 \times 10^4 \text{ N/m}^2$$

which is also equivalent to 97.7 kPa or 0.96 atm or 14.1 lb/in.² or 0.98 bar.

We can express this pressure as an equivalent column of liquid,

$$h = \frac{p_{\text{abs}} - p_0}{\rho g} = \frac{(1.9906 \times 10^5) - (1.0132 \times 10^5) \text{ N/m}^2}{(998.2 \text{ kg/m}^3)(9.8 \text{ m/s}^2)(1 \text{ N-s}^2/\text{kg-m})}$$

$$= 10 \text{ m H}_2\text{O}$$

9.3 PRESSURE REFERENCE INSTRUMENTS

The units of pressure can be defined through the standards of the fundamental dimensions of mass, length, and time. In practice, pressure transducers are calibrated by comparison against certain reference instruments, which also serve as pressure measuring instruments. This section discusses several basic pressure reference instruments that can serve either as working standards or as laboratory instruments.

McLeod Gauge

The McLeod gauge, originally devised by Herbert McLeod in 1874 (3), is a pressure-measuring instrument and laboratory reference standard used to establish gas pressures in the subatmospheric range of 1 mm Hg abs down to 0.1 mm Hg abs. A pressure that is below atmospheric pressure is also called a vacuum pressure. One variation of this instrument is sketched in Figure 9.3a, in which the gauge is connected directly to the low-pressure source. The glass tubing is arranged so that a sample of the gas at an unknown low pressure can be trapped by inverting the gauge from the sensing position, depicted as Figure 9.3a, to that of the measuring position, depicted as Figure 9.3b. In this way, the gas trapped within the capillary is isothermally compressed by a rising column of mercury. Boyle's law is then used to relate the two pressures on either side of the mercury to the distance of travel of the mercury within the capillary. Mercury is the preferred working fluid because of its high density and very low vapor pressure.

At the equilibrium and measuring position, the capillary pressure, p_2 , is related to the unknown gas pressure to be determined, p_1 , by $p_2 = p_1(\mathbb{V}_1/\mathbb{V}_2)$ where \mathbb{V}_1 is the gas volume of the gauge in Figure 9.3a (a constant for a gauge at any pressure), and \mathbb{V}_2 is the capillary volume in Figure 9.3b. But $\mathbb{V}_2 = Ay$, where A is the known cross-sectional area of the capillary and y is the vertical length of

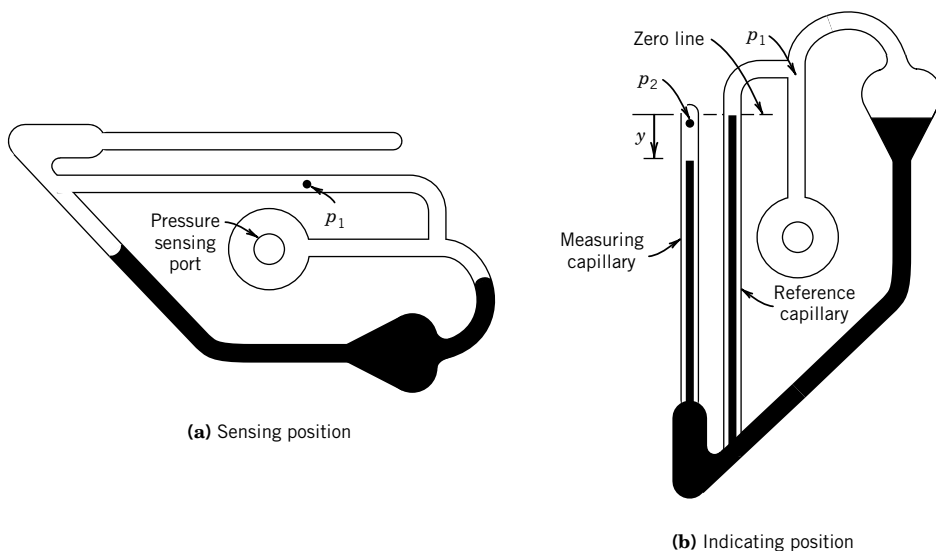


Figure 9.3 McLeod gauge.

the capillary occupied by the gas. With γ as the specific weight of the mercury, the difference in pressures is related by $p_2 - p_1 = \gamma y$ such that the unknown gas pressure is just a function of y :

$$p_1 = \gamma A y^2 / (\gamma A - Ay) \quad (9.4)$$

In practice, a commercial McLeod gauge has the capillary etched and calibrated to indicate either pressure, p_1 , or its equivalent head, p_1/γ , directly. The McLeod gauge generally does not require correction. The reference stem offsets capillary forces acting in the measuring capillary. Instrument systematic uncertainty is on the order of 0.5% (95%) at 1 mm Hg abs and increases to 3% (95%) at 0.1 mm Hg abs.

Barometer

A barometer consists of an inverted tube containing a fluid and is used to measure atmospheric pressure. To create the barometer, the tube, which is sealed at only one end, is evacuated to zero absolute pressure. The tube is immersed with the open end down within a liquid-filled reservoir as shown in the illustration of the Fortin barometer in Figure 9.4. The reservoir is open to atmospheric pressure, which forces the liquid to rise up the tube.

From Equations 9.2 and 9.3, the resulting height of the liquid column above the reservoir free surface is a measure of the absolute atmospheric pressure in the equivalent head (Eq. 9.3). Evangelista Torricelli (1608–1647), a colleague of Galileo, can be credited with developing and interpreting the working principles of the barometer in 1644.

As Figure 9.4 shows, the closed end of the tube is at the vapor pressure of the barometric liquid at room temperature. So the indicated pressure is the atmospheric pressure minus the liquid vapor pressure. Mercury is the most common liquid used because it has a very low vapor pressure, and so, for practical use, the indicated pressure can be taken as the local absolute barometric pressure. However, for very accurate work the barometer needs to be corrected for temperature effects, which

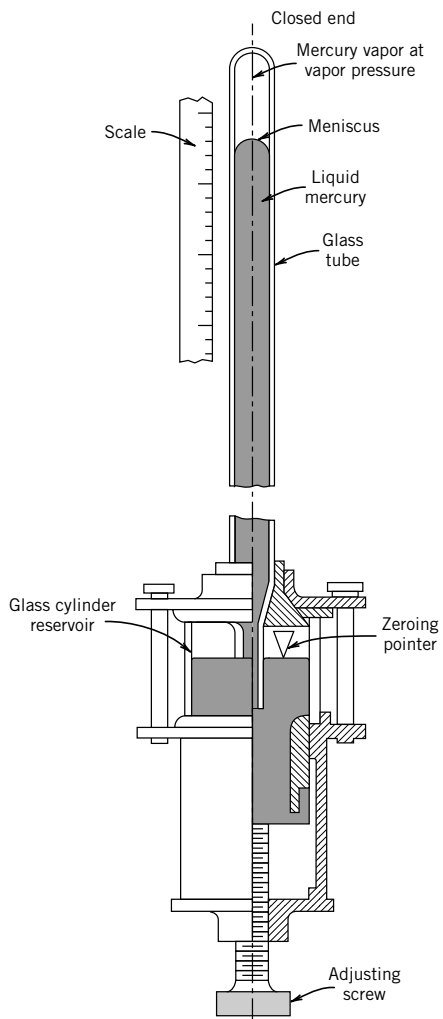


Figure 9.4 Fortin barometer.

change the vapor pressure, for temperature and altitude effects on the weight of mercury, and for deviations from standard gravity (9.80665 m/s^2 or 32.17405 ft/s^2). Correction curves are provided by instrument manufacturers.

Barometers are used as local standards for the measurement of absolute atmospheric pressure. Under standard conditions for pressure, temperature, and gravity, the mercury rises 760 mm (29.92 in.) above the reservoir surface. The U.S. National Weather Service always reports a barometric pressure that has been corrected to sea-level elevation.

Manometer

A manometer is an instrument used to measure differential pressure based on the relationship between pressure and the hydrostatic equivalent head of fluid. Several design variations are

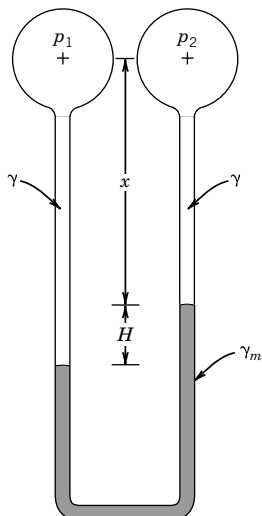


Figure 9.5 U-tube manometer.

available, allowing measurements ranging from the order of 0.001 mm of manometer fluid to several meters.

The U-tube manometer in Figure 9.5 consists of a transparent tube filled with an indicating liquid of specific weight γ_m . This forms two free surfaces of the manometer liquid. The difference in pressures p_1 and p_2 applied across the two free surfaces brings about a deflection, H , in the level of the manometer liquid. For a measured fluid of specific weight γ , the hydrostatic equation can be applied to the manometer of Figure 9.5 as

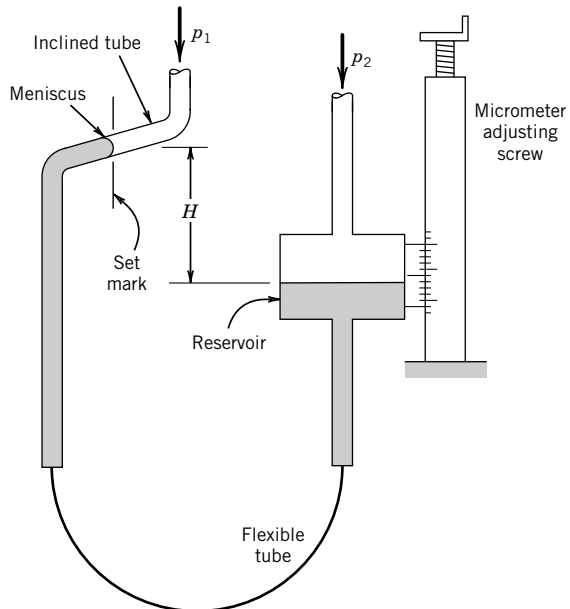
$$p_1 = p_2 + \gamma x + \gamma_m H - \gamma(H + x)$$

which yields the relation between the manometer deflection and applied differential pressure,

$$p_1 - p_2 = (\gamma_m - \gamma)H \quad (9.5)$$

From Equation 9.5, the static sensitivity of the U-tube manometer is given by $K = 1/(\gamma_m - \gamma)$. To maximize manometer sensitivity, we want to choose manometer liquids that minimize the value of $(\gamma_m - \gamma)$. From a practical standpoint the manometer fluid must not be soluble with the working fluid. The manometer fluid should be selected to provide a deflection that is measurable yet not so great that it becomes awkward to observe.

A variation in the U-tube manometer is the micromanometer shown in Figure 9.6. These special-purpose instruments are used to measure very small differential pressures, down to 0.005 mm H₂O (0.0002 in. H₂O). In the micromanometer, the manometer reservoir is moved up or down until the level of the manometer fluid within the reservoir is at the same level as a set mark within a magnifying sight glass. At that point the manometer meniscus is at the set mark, and this serves as a reference position. Changes in pressure bring about fluid displacement so that the reservoir must be moved up or down to bring the meniscus back to the set mark. The amount of this repositioning is equal to the change in the equivalent pressure head. The position of the reservoir is controlled by a micrometer or other calibrated displacement measuring device so that relative changes in pressure can be measured with high resolution.

**Figure 9.6** Micromanometer.

The inclined tube manometer is also used to measure small changes in pressure. It is essentially a U-tube manometer with one leg inclined at an angle θ , typically from 10 to 30 degrees relative to the horizontal. As indicated in Figure 9.7, a change in pressure equivalent to a deflection of height H in a U-tube manometer would bring about a change in position of the meniscus in the inclined leg of $L = H/\sin \theta$. This provides an increased sensitivity over the conventional U-tube by the factor of $1/\sin \theta$.

A number of elemental errors affect the instrument uncertainty of all types of manometers. These include scale and alignment errors, zero error, temperature error, gravity error, and capillary and meniscus errors. The specific weight of the manometer fluid varies with temperature but can be corrected. For example, the common manometer fluid of mercury has a temperature dependence approximated by

$$\gamma_{\text{Hg}} = \frac{133.084}{1 + 0.00006T} [\text{N/m}^3] = \frac{848.707}{1 + 0.000101(T - 32)} [\text{lb/ft}^3]$$

with T in $^{\circ}\text{C}$ or $^{\circ}\text{F}$, respectively. A gravity correction for elevation z and latitude ϕ corrects for gravity error effects using the dimensionless correction,

$$e_1 = -(2.637 \times 10^{-3} \cos 2\phi + 9.6 \times 10^{-8} z + 5 \times 10^{-5})_{US} \quad (9.6a)$$

$$= -(2.637 \times 10^{-3} \cos 2\phi + 2.9 \times 10^{-8} z + 5 \times 10^{-5})_{metric} \quad (9.6b)$$

where ϕ is in degrees and z is in feet for Equation 9.6a and meters in Equation 9.6b. Tube-to-liquid capillary forces lead to the development of a meniscus. Although the actual effect varies with purity of the manometer liquid, these effects can be minimized by using manometer tube bores of greater than about 6 mm (0.25 in.). In general, the instrument uncertainty in measuring pressure can be as low as 0.02% to 0.2% of the reading.

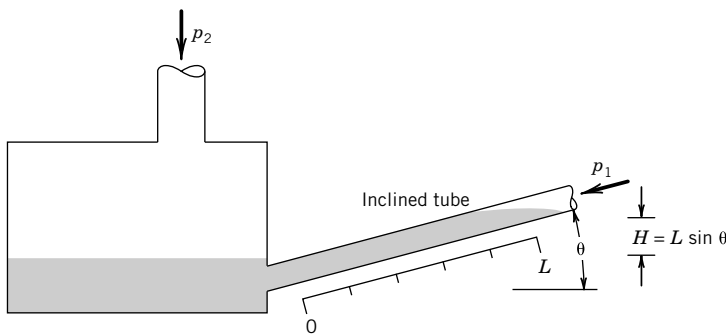


Figure 9.7 Inclined tube manometer.

Example 9.2

A high-quality U-tube manometer is a remarkably simple instrument to make. It requires only a transparent U-shaped tube, manometer fluid, and a scale to measure deflection. While a U-shaped glass tube of 6 mm or greater internal bore is preferred, a length of 6-mm i.d. (inside diameter) thick-walled clear tubing from the hardware store and bent to a U-shape works fine for many purposes. Water, alcohol, or mineral oil are all readily available nontoxic manometer fluids with tabulated properties. A sheet of graph paper or a ruler serves to measure meniscus deflection. There is a limit to the magnitude of pressure differential that can be measured, although use of a step stool extends this range. Tack the components to a board and the resulting instrument is accurate for measuring manometer deflections down to one-half the resolution of the scale in terms of fluid used!

The U-tube manometer is a practical tool useful for calibrating other forms of pressure transducers in the pressure range spanning atmospheric pressure levels. As one example, the ad-hoc U-tube described is convenient for calibrating surgical pressure transducers over the physiological pressure ranges.

Example 9.3

An inclined manometer with the inclined tube set at 30 degrees is to be used at 20°C to measure an air pressure of nominal magnitude of 100 N/m² relative to ambient. Manometer “unity” oil ($S = 1$) is to be used. The specific weight of the oil is $9770 \pm 0.5\% \text{ N/m}^2$ (95%) at 20°C, the angle of inclination can be set to within 1 degree using a bubble level, and the manometer resolution is 1 mm with a manometer zero error equal to its interpolation error. Estimate the uncertainty in indicated differential pressure at the design stage.

KNOWN $p = 100 \text{ N/m}^2$ (nominal)

Manometer

Resolution: 1 mm

Zero error: 0.5 mm

$\theta = 30 \pm 1^\circ$ (95% assumed)

$\gamma_m = 9770 \pm 0.5\% \text{ N/m}^3$ (95%)

ASSUMPTIONS Temperature and capillary effects in the manometer and gravity error in the specific weights of the fluids are negligible. The degrees of freedom in the stated uncertainties are large.

FIND u_d

SOLUTION The relation between pressure and manometer deflection is given by Equation 9.5 with $H = L \sin \theta$:

$$\Delta p = p_1 - p_2 = L(\gamma_m - \gamma) \sin \theta$$

where p_2 is the ambient pressure so that Δp is the nominal pressure relative to the ambient. For a nominal $\Delta p = 100 \text{ N/m}^2$, the nominal manometer rise L would be

$$L = \frac{\Delta p}{(\gamma_m - \gamma) \sin \theta} \approx \frac{\Delta p}{\gamma_m \sin \theta} = 21 \text{ mm}$$

where $\gamma_m \gg \gamma$ and the value for γ and its uncertainty are neglected. For the design stage analysis, $p = f(\gamma_m, L, \theta)$, so that the uncertainty in pressure, Δp , is estimated by

$$(u_d)_p = \pm \sqrt{\left[\frac{\partial \Delta p}{\partial \gamma_m} (u_d)_{\gamma_m} \right]^2 + \left[\frac{\partial \Delta p}{\partial L} (u_d)_L \right]^2 + \left[\frac{\partial \Delta p}{\partial \theta} (u_d)_{\theta} \right]^2}$$

At assumed 95% confidence levels, the manometer specific weight uncertainty and angle uncertainty are estimated from the problem as

$$\begin{aligned} (u_d)_{\gamma_m} &= (9770 \text{ N/m}^3)(0.005) \approx 49 \text{ N/m}^3 \\ (u_d)_{\theta} &= 1 \text{ degree} = 0.0175 \text{ rad} \end{aligned}$$

The uncertainty in estimating the pressure from the indicated deflection is due both to the manometer resolution, u_o , and the zero point offset error, which we take as its instrument error, u_c . Using the uncertainties associated with these errors,

$$(u_d)_L = \sqrt{u_o^2 + u_c^2} = \sqrt{(0.5 \text{ mm})^2 + (0.5 \text{ mm})^2} = 0.7 \text{ mm}$$

Evaluating the derivatives and substituting values gives a design-stage uncertainty interval of a measured Δp of

$$(u_d)_{\Delta p} = \sqrt{(0.26)^2 + (3.42)^2 + (3.10)^2} = \pm 4.6 \text{ N/m}^2 \quad (95\%)$$

COMMENT At a 30-degree inclination and for this pressure, the uncertainty in pressure is affected almost equally by the instrument inclination and the deflection uncertainties. As the manometer inclination is increased to a more vertical orientation, that is, toward the U-tube manometer, inclination uncertainty becomes less important and is negligible near 90 degrees. However, for a U-tube manometer, the deflection is reduced to less than 11 mm, a 50% reduction in manometer sensitivity, with an associated design-stage uncertainty of 6.8 N/m^2 (95%).

Deadweight Testers

The deadweight tester makes direct use of the fundamental definition of pressure as a force per unit area to create and to determine the pressure within a sealed chamber. These devices are a

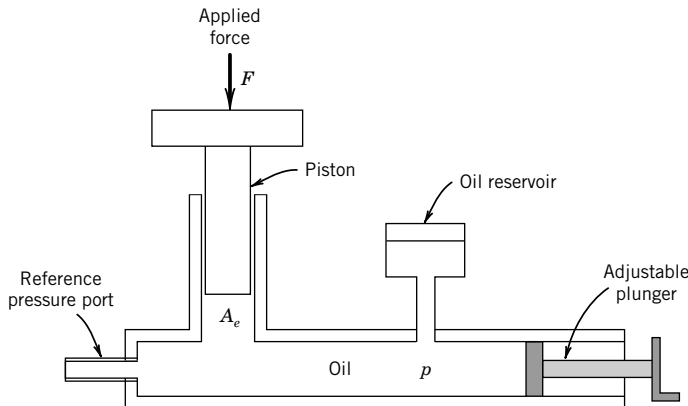


Figure 9.8 Deadweight tester.

common laboratory standard for the calibration of pressure-measuring devices over the pressure range from 70 to $7 \times 10^7 \text{ N/m}^2$ (0.01 to 10,000 psi). A deadweight tester, such as that shown in Figure 9.8, consists of an internal chamber filled with an oil and a close-fitting piston and cylinder. Chamber pressure acts on the end of the carefully machined piston. A static equilibrium exists when the external pressure exerted by the piston on the fluid balances the chamber pressure. This external piston pressure is created by a downward force acting over the equivalent area A_e of the piston. The weight of the piston plus the additional weight of calibrated masses are used to provide this external force F . At static equilibrium the piston floats and the chamber pressure can be deduced as

$$p = \frac{F}{A_e} + \sum \text{error corrections} \quad (9.7)$$

A pressure transducer can be connected to a reference port and calibrated by comparison to the chamber pressure. For most calibrations, the error corrections can be ignored.

When error corrections are applied, the instrument uncertainty in the chamber pressure using a deadweight tester can be as low as 0.005% to 0.01% of the reading. A number of elemental errors contribute to Equation 9.7, including air buoyancy effects, variations in local gravity, uncertainty in the known mass of the piston and added masses, shear effects, thermal expansion of the piston area, and elastic deformation of the piston (1).

An indicated pressure, p_i , can be corrected for gravity effects, e_1 , from Equation 9.6a or 9.6b, and for air buoyancy effects, e_2 , by

$$p = p_i(1 + e_1 + e_2) \quad (9.8)$$

where

$$e_2 = -\gamma_{\text{air}}/\gamma_{\text{masses}} \quad (9.9)$$

The tester fluid lubricates the piston so that the piston is partially supported by the shear forces in the oil in the gap separating the piston and the cylinder. This error varies inversely with the tester fluid viscosity, so high-viscosity fluids are preferred. In a typical tester, the uncertainty due to this error is less than 0.01% of the reading. At high pressures, elastic deformation of the piston affects the actual piston area. For this reason, the effective area is based on the average of the piston and cylinder diameters.

Example 9.4

A deadweight tester indicates 100.00 lb/in.^2 (i.e., 100.00 psi), at 70°F in Clemson, SC ($\phi = 34^\circ$, $z = 841 \text{ ft}$). Manufacturer specifications for the effective piston area were stated at 72°F so that thermal expansion effects remain negligible. Take $\gamma_{\text{air}} = 0.076 \text{ lb/ft}^3$ and $\gamma_{\text{mass}} = 496 \text{ lb/ft}^3$. Correct the indicated reading for known errors.

KNOWN $p_i = 100.00 \text{ psi}$; $z = 841 \text{ ft}$; $\phi = 34^\circ$

ASSUMPTION Systematic error corrections for altitude and latitude apply

FIND p

SOLUTION The corrected pressure is found using Equation 9.8. From Equation 9.9, the correction for buoyancy effects is

$$e_2 = -\gamma_{\text{air}}/\gamma_{\text{masses}} = -0.076/496 = -0.000154$$

The correction for gravity effects is from Equation 9.6a:

$$\begin{aligned} e_1 &= -(2.637 \times 10^{-3} \cos 2\phi + 9.6 \times 10^{-8} z + 5 \times 10^{-5}) \\ &= -(0.0010 + 8 \times 10^{-5} + 5 \times 10^{-5}) = -0.001119 \end{aligned}$$

From Equation 9.8, the corrected pressure becomes

$$p = 100.00 \times (1 - 0.000154 - 0.001119) \text{ lb/in.}^2 = 99.87 \text{ lb/in.}^2$$

COMMENT This amounts to correcting an indicated signal for known systematic errors. Here that correction is $\approx 0.13\%$.

9.4 PRESSURE TRANSDUCERS

A pressure transducer is a device that converts a measured pressure into a mechanical or electrical signal. The transducer is actually a hybrid sensor-transducer. The primary sensor is usually an elastic element that deforms or deflects under the measured pressure relative to a reference pressure. Several common elastic elements used, as shown in Figure 9.9, include the Bourdon tube, bellows, capsule, and diaphragm. A secondary transducer element converts the elastic element deflection into a readily measurable signal such as an electrical voltage or mechanical rotation of a pointer. There are many methods available to perform this transducer function, and we examine a few common ones.

General categories for pressure transducers are absolute, gauge, vacuum, and differential. These categories reflect the application and reference pressure used. Absolute transducers have a sealed reference cavity held at a pressure of absolute zero, enabling absolute pressure measurements. Gauge transducers have the reference cavity open to atmospheric pressure and are intended to measure above or below atmospheric pressure or both. Differential transducers measure the difference between two applied pressures. Vacuum transducers are a special form of absolute transducer for low-pressure measurements.

Pressure transducers are subject to some or all of the following elemental errors: resolution, zero shift error, linearity error, sensitivity error, hysteresis, noise, and drift due to environmental temperature changes. Electrical transducers are also subject to loading error between the transducer output and its indicating device (see Chapter 6). Loading errors increase the transducer nonlinearity

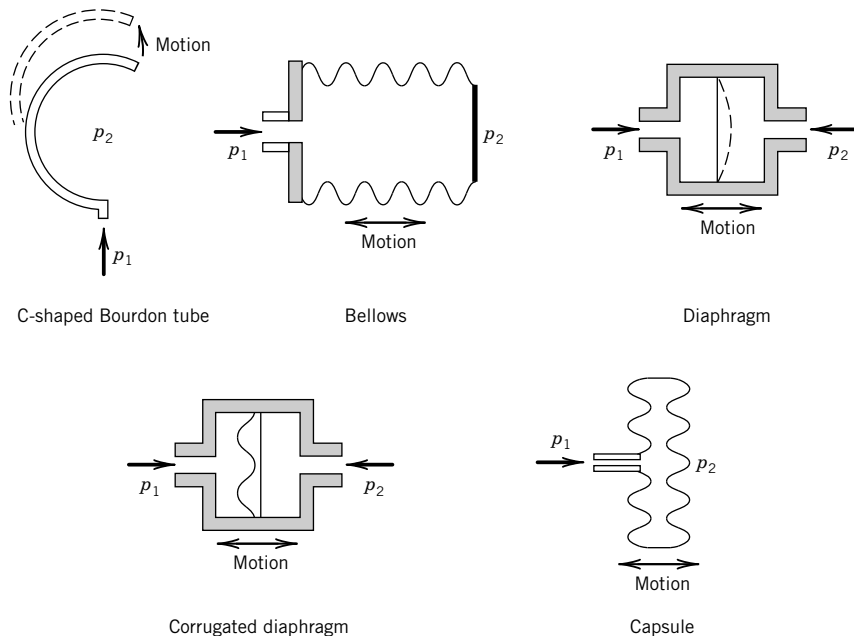


Figure 9.9 Elastic elements used as pressure sensors.

over its operating range. When this is a consideration, a voltage follower (see Chapter 6) can be inserted at the output of the transducer to isolate transducer load.

Bourdon Tube

The Bourdon tube is a curved metal tube having an elliptical cross section that mechanically deforms under pressure. In practice, one end of the tube is held fixed and the input pressure applied internally. A pressure difference between the outside of the tube and the inside of the tube brings about tube deformation and a deflection of the tube free end. This action of the tube under pressure can be likened to the action of a deflated balloon that is subsequently inflated. The magnitude of the deflection of the tube end is proportional to the magnitude of the pressure difference. Several variations exist, such as the C shape (Fig. 9.9), the spiral, and the twisted tube. The exterior of the tube is usually open to atmosphere (hence, the origin of the term “gauge” pressure referring to pressure referenced to atmospheric pressure), but in some variations the tube may be placed within a sealed housing and the tube exterior exposed to some other reference pressure, allowing for absolute and for differential designs.

The Bourdon tube mechanical dial gauge is a commonly used pressure transducer. A typical design is shown in Figure 9.10, in which the secondary element is a mechanical linkage that converts the tube displacement into a rotation of a pointer. Designs exist for low or high pressures, including vacuum pressures, and selections span a wide choice in range. The best Bourdon tube gauges have instrument uncertainties as low as 0.1% of the full-scale deflection of the gauge, with values of 0.5% to 2% more common. But the attractiveness of this device is that it is simple, portable, and robust, lasting for years of use.

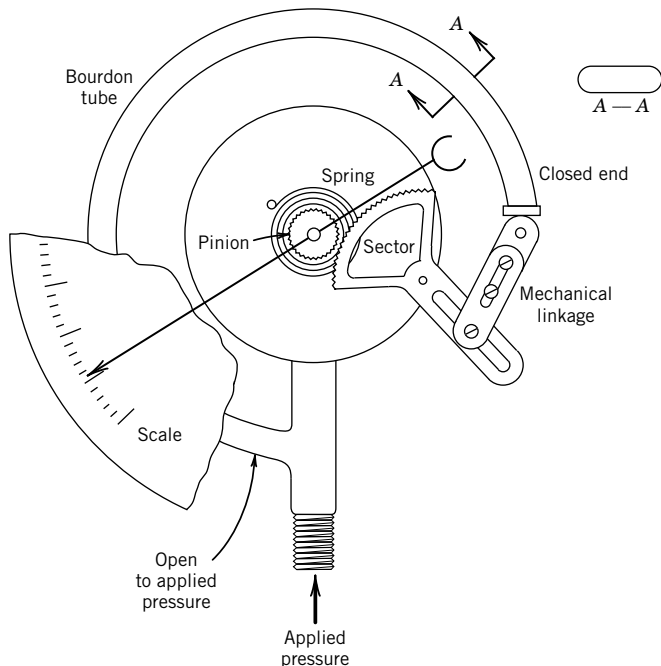


Figure 9.10 Bourdon tube pressure gauge.

Bellows and Capsule Elements

A bellows sensing element is a thin-walled, flexible metal tube formed into deep convolutions and sealed at one end (Fig. 9.9). One end is held fixed and pressure is applied internally. A difference between the internal and external pressures causes the bellows to change in length. The bellows is housed within a chamber that can be sealed and evacuated for absolute measurements, vented through a reference pressure port for differential measurements, or opened to atmosphere for gauge pressure measurements. A similar design, the capsule sensing element, is also a thin-walled, flexible metal tube whose length changes with pressure, but its shape tends to be wider in diameter and shorter in length (Fig. 9.9).

A mechanical linkage is used to convert the translational displacement of the bellows or capsule sensors into a measurable form. A common transducer is the sliding arm potentiometer (voltage-divider, Chapter 6) found in the potentiometric pressure transducer shown in Figure 9.11. Another type uses a linear variable displacement transducer (LVDT; see Chapter 12) to measure the bellows

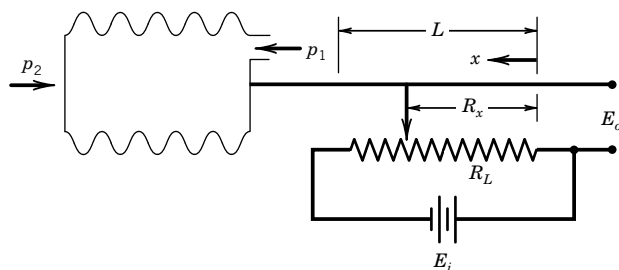


Figure 9.11 Potentiometer pressure transducer.

or capsule displacement. The LVDT design has a high sensitivity and is commonly found in pressure transducers rated for low pressures and for small pressure ranges, such as zero to several hundred mm Hg absolute, gauge, or differential.

Diaphragms

An effective primary pressure element is a diaphragm (Figure 9.9), which is a thin elastic circular plate supported about its circumference. The action of a diaphragm within a pressure transducer is similar to the action of a trampoline; a pressure differential on the top and bottom diaphragm faces acts to deform it. The magnitude of the deformation is proportional to the pressure difference. Both membrane and corrugated designs are used. Membranes are made of metal or nonmetallic material, such as plastic or neoprene. The material chosen depends on the pressure range anticipated and the fluid in contact with it. Corrugated diaphragms contain a number of corrugations that serve to increase diaphragm stiffness and to increase the diaphragm effective surface area.

Pressure transducers that use a diaphragm sensor are well suited for either static or dynamic pressure measurements. They have good linearity and resolution over their useful range. An advantage of the diaphragm sensor is that the very low mass and relative stiffness of the thin diaphragm give the sensor a very high natural frequency with a small damping ratio. Hence, these transducers can have a very wide frequency response and very short 90% rise and settling times. The natural frequency (rad/s) of a circular diaphragm can be estimated by (4)

$$\omega_n = 10.21 \sqrt{\frac{E_m t^2}{12(1 - \nu_p^2) \rho r^4}} \quad (9.10)$$

where E_m is the material bulk modulus (psi or N/m²), t the thickness (in. or m), r the radius (in. or m), ρ the material density (lb_m/in.³ or kg/m³), and ν_p the Poisson's ratio for the diaphragm material. The maximum elastic deflection of a uniformly loaded, circular diaphragm supported about its circumference occurs at its center and can be estimated by

$$y_{\max} = \frac{3(p_1 - p_2)(1 - \nu_p^2)r^4}{16E_m t^3} \quad (9.11)$$

provided that the deflection does not exceed one-third the diaphragm thickness. Diaphragms should be selected so as to not exceed this maximum deflection over the anticipated operating range.

Various secondary elements are available to translate this displacement of the diaphragm into a measurable signal. Several methods are discussed below.

Strain Gauge Elements

A common method for converting diaphragm displacement into a measurable signal is to sense the strain induced on the diaphragm surface as it is displaced. Strain gauges, devices whose measurable resistance is proportional to their sensed strain (see Chapter 11), can be bonded directly onto the diaphragm, integrated within the diaphragm material or onto a deforming element (such as a thin beam) attached to the diaphragm so as to deform with the diaphragm and to sense strain. Metal strain gauges can be used with liquids. Strain gauge resistance is reasonably linear over a wide range of strain and can be directly related to the sensed pressure (5). A diaphragm transducer using strain gauge detection is depicted in Figure 9.12.

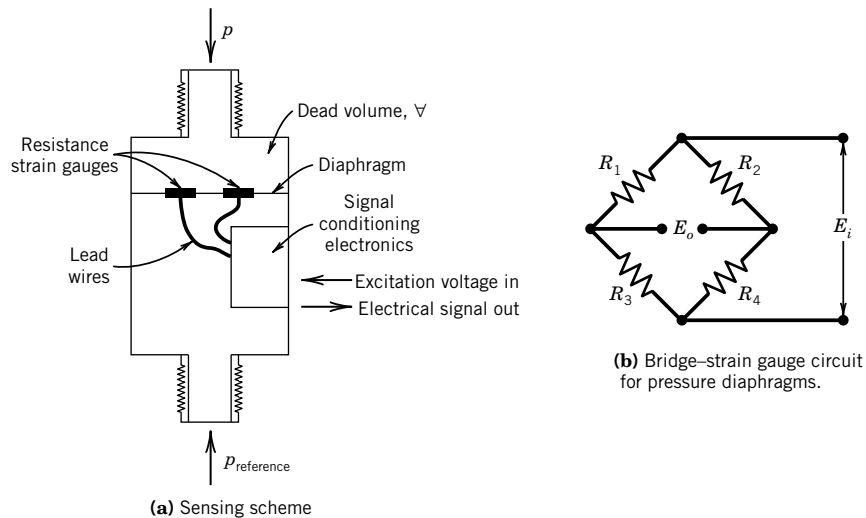


Figure 9.12 Diaphragm pressure transducer.

By using semiconductor technology in pressure transducer construction, we now have a variety of very fast, very small, highly sensitive strain gauge diaphragm transducers. Silicone piezoresistive strain gauges can be diffused into a single crystal of silicone wafer, which forms the diaphragm. Semiconductor strain gauges have a static sensitivity that is 50 times greater than conventional metallic strain gauges. Because the piezoresistive gauges are integral to the diaphragm, they are relatively immune to the thermoelastic strains prevalent in conventional metallic strain gauge-diaphragm constructions. Furthermore, a silicone diaphragm does not creep with age (as does a metallic gauge), thus minimizing calibration drift over time. However, uncoated silicone does not tolerate liquids.

Capacitance Elements

Another common method to convert diaphragm displacement to a measurable signal is a capacitance sensor. One version uses a thin metallic diaphragm as one plate of a capacitor paired with a fixed plate to complete the capacitor. The diaphragm is exposed to the process pressure on one side and to a reference pressure on the other or to a differential pressure. When pressure changes, so as to deflect the diaphragm, the gap between the plates changes, which causes a change in capacitance.

To illustrate this, a transducer using this method is depicted in Figure 9.13. The capacitance C developed between two parallel plates separated by average gap t is determined by

$$C = c \epsilon A / t \quad (9.12)$$

where the product $c\epsilon$ is the permittivity of the material between the plates relative to a vacuum ($\epsilon = 8.85 \times 10^{-12} \text{ F/m}$; c = dielectric constant), and A is the overlapping area of the two plates. The dielectric constant depends on the material in the gap, which for air is $c=1$ but for water is $c=80$. The capacitance responds to an instantaneous change in the area-averaged plate gap separation from which the time-dependent pressure is determined. However, the capacitance change is small relative

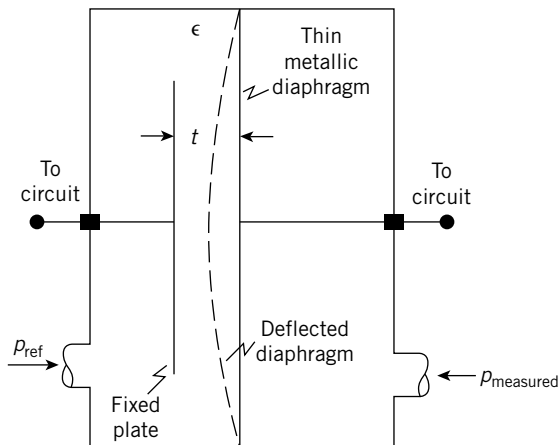


Figure 9.13 Capacitance pressure transducer. In this schematic, the diaphragm is conductive and its deflection exaggerated.

to the absolute capacitance. Oscillator and bridge circuits are commonly used to operate the circuit and to measure the small capacitance change providing an output voltage E_0 .

Example 9.5

Estimate the theoretical capacitance of a sensor similar to that of Figure 9.13 if the plate area is 1 mm^2 and the instantaneous plate separation is 1 mm. What is the sensor sensitivity? Assume the plates are separated by air.

SOLUTION With $A = 1 \text{ mm}^2$, $t = 1 \text{ mm}$, $\epsilon = 8.85 \times 10^{-15} \text{ F/mm}$, $c = 1$:

$$C = c\epsilon A/t = (1)(8.85 \times 10^{15} \text{ F/mm})(1 \text{ mm}^2)/(1 \text{ mm}) = 8.85 \times 10^{-15} \text{ F}$$

or $C = 8.85 \times 10^{-3}$ pF (picofarads). For small pressure changes, the diaphragm curvature has a negligible effect on the area-averaged plate gap so that pressure can be treated as linear with the area-average gap value.

The sensor sensitivity is $K_s = \partial C / \partial t = -8.85 \times 10^{-3} \times (cA/t^2) \text{ pF/mm}$.

The capacitance pressure transducer has the attractive features of other diaphragm transducers, including small size and a wide operating range. Many common and inexpensive pressure transducers use this measuring principle and are suitable for many engineering measurement demands, including a niche as the on-board car tire pressure sensor of choice. However, the principle is sensitive to temperature changes and has a relatively high impedance output. If attention is paid to these shortcomings, an accurate and stable transducer can be made.

Piezoelectric Crystal Elements

Piezoelectric crystals form effective secondary elements for dynamic (transient) pressure measurements. Under the action of compression, tension, or shear, a piezoelectric crystal deforms and develops a surface charge q , which is proportional to the force acting to bring about the deformation. In a piezoelectric pressure transducer, a preloaded crystal is mounted to the diaphragm sensor, as

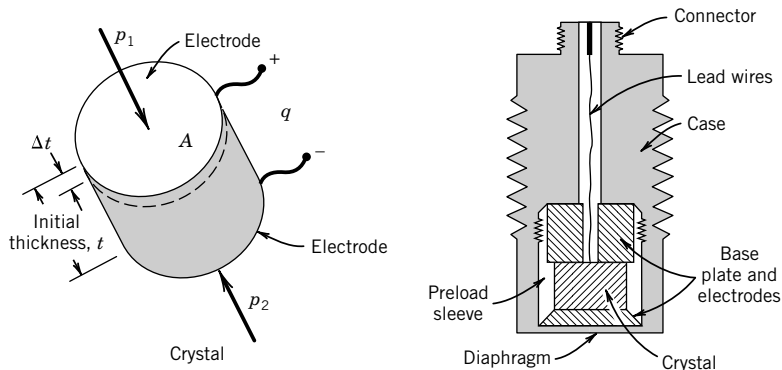


Figure 9.14 Piezoelectric pressure transducer.

indicated in Figure 9.14. Pressure acts normal to the crystal axis and changes the crystal thickness t by a small amount Δt . This sets up a charge, $q = K_q p A$, where p is the pressure acting over the electrode area A and K_q is the crystal charge sensitivity, a material property. A charge amplifier (see Chapter 6) is used to convert charge to voltage so that the voltage developed across the electrodes is

$$E_o = q/C \quad (9.13)$$

where C is the capacitance of the crystal-electrode combination, again given by Equation 9.12. The operating equation becomes

$$E_o = K_q t p / c \epsilon = K p \quad (9.14)$$

where K is the overall transducer gain. The crystal sensitivity for quartz, the most common material used, is $K_q = 2.2 \times 10^{-9}$ coulombs/N.

9.5 PRESSURE TRANSDUCER CALIBRATION

Static Calibration

A static calibration of a pressure transducer is usually accomplished either by direct comparison against any of the pressure reference instruments discussed (Section 9.3) or against the output from a certified laboratory standard transducer. For the low-pressure range, the McLeod gauge or the appropriate manometric instruments along with the laboratory barometer serve as convenient working standards. The approach is to pressurize (or evacuate) a chamber and expose both the reference instrument, which serves as the standard, and the candidate transducer to the same pressure for a side-by-side measurement. For the high-pressure range, the deadweight tester is a commonly used pressure reference standard.

Dynamic Calibration

The rise time and frequency response of a pressure transducer are found by dynamic calibration, and there are a number of clever ways to accomplish this (6). As discussed in Chapter 3, the rise time of an instrument is found through a step change in input. For under-damped systems, natural frequency and damping ratio can be measured based on the ringing behavior (see Chapter 3), giving the

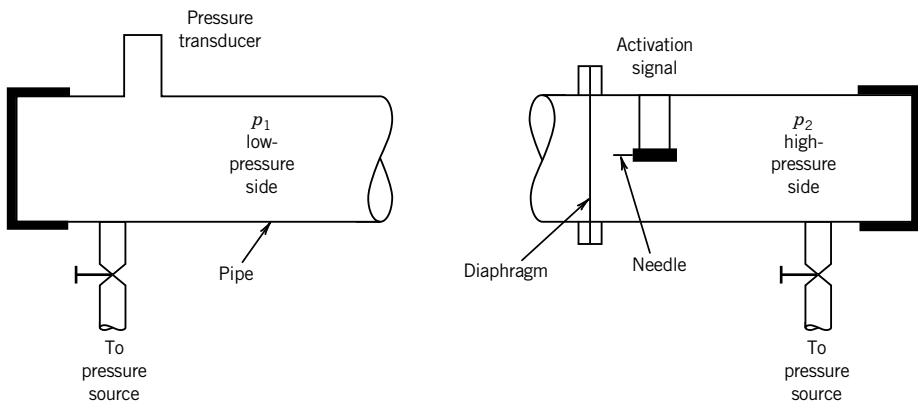


Figure 9.15 Schematic of a shock tube facility.

frequency response. The frequency response can be found directly by applying a constant amplitude periodic input signal and varying its frequency. A flush-mounted transducer places the sensor in direct contact with the fluid at the measurement site. Because pressure transducers could also be attached by means of a pressure tap or by connecting tubing to the tap, this length (called the transmission line) affects the overall response and should be included as part of the dynamic calibration.

An electrical switching valve or flow control valve can create a step change in pressure. But the mechanical lag of the valve limits its use to transducers having an expected rise time of 50 ms or more. Faster applications might use a shock tube calibration or some equivalent diaphragm burst test.

As shown in Figure 9.15, the shock tube consists of a long pipe separated into two chambers by a thin diaphragm. The transducer is mounted into the pipe wall of one chamber, the expansion section, at pressure p_1 . The pressure in the other chamber, the driver section, is raised from p_1 to p_2 . Some mechanism, such as a mechanically controlled needle, is used to burst the diaphragm on command. Upon bursting, the pressure differential causes a pressure shock wave to move down the low-pressure chamber. A shock wave has a thickness on the order of 1 μm and moves at the speed of sound, a . So as the shock passes the transducer, the transducer experiences a change in pressure from p_1 to p_3 over a time $t = d/a$, where d is the diameter of the transducer pressure port, and pressure p_3 is

$$p_3 = p_1 [1 + (2k/k + 1)(M_1^2 - 1)] \quad (9.15)$$

where k is the gas-specific heat ratio and M_1 is the Mach number calculated using normal shock wave tables and absolute pressure p_1 . The velocity of the shock wave can also be deduced from the output of fast-acting standard pressure sensors mounted in the shock tube wall. Typical values of t are on the order of 1 to 10 μs , so this method is at least four orders of magnitude faster than a switching valve. The transducer rise time is calculated from the output record.

A common verification check for system response is the “pop test,” which is well suited for liquids or gases and systems needing just moderate response times. In this situation, the transducer and connecting tubing are pressurized to a steady value, perhaps by using a small syringe or hand pump. The system is suddenly vented to atmosphere. The recorded transducer response gives an indication of the system rise time and ringing behavior. One variation of this approach attaches a balloon or similar flexible material to one end of the connecting tubing/transducer system. After pressurizing, the balloon is popped to suddenly vent the system.

A reciprocating piston within a cylinder can generate a sinusoidal variation in pressure for frequency-response calibration. The piston can be driven by a variable speed motor and its displacement measured by a fast-responding transducer, such as an LVDT (see Chapter 12). Under properly controlled conditions (Ex. 1.2), the actual pressure variation can be estimated from the piston displacement. Other techniques include an encased loudspeaker or an acoustically resonant enclosure, which serves as a frequency driver instead of a piston, or using an oscillating flow control valve to vary system pressure with time (6).

Example 9.6

A surgical pressure transducer is attached to a stiff-walled catheter and a small balloon is attached at its other end. The catheter is filled with saline using a small syringe to pressurize the system to 80 mm Hg. At $t = 0$ s, the balloon is popped, forcing a step change in pressure from 80 to 0 mm Hg. The time-based signal is recorded (Fig. 9.16). From the data, the ringing period is measured to be 45.5 ms at second peak amplitude, $y(0.0455) = 5.152$ mV. Is this system suitable to measure physiological pressures that have frequency content up to 5 Hz? Static sensitivity, $K = 1$ mV/mm Hg.

KNOWN $A = 80$ mm Hg, $K = 1$ mV/mm Hg,
 $y(0) = KA = 80$ mV; $y(0.0455) = 5.152$ mV
 $T_d = 0.0455$ s

FIND $M(f = 5$ Hz)

SOLUTION We use methods developed in Chapter 3. The step-function response has the form

$$y(t) = Ce^{-\omega_n \zeta t} \cos\left(\omega_n \sqrt{1 - \zeta^2} + \phi\right)$$

where for $y(0) = 80$ mV, $C = 80$ mV, which is consistent with the recorded signal. The steady-state value is $y(\infty) = 0$. The first peak amplitude is at $t = 0$, $y_1 = y(0) = 80$ mV. The second peak amplitude is $y_2 = y(0.0455) = 5.152$ mV. Using logarithmic decrement,

$$\zeta = \frac{1}{\sqrt{1 + \left(\frac{2\pi}{\ln(y_1/y_2)}\right)^2}} = \frac{1}{\sqrt{1 + (2\pi/\ln(80/5.152))^2}} = 0.40$$

$$f_n = 1/T_d \sqrt{1 - \zeta^2} = 23.98 \text{ Hz} \quad (\text{i.e., } \omega_n = 150 \text{ rad/s})$$

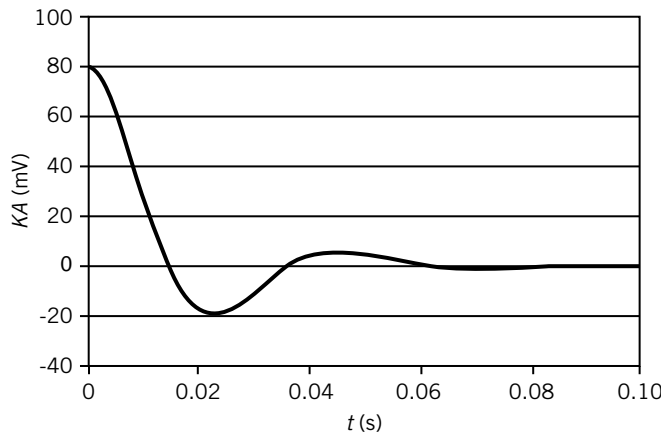


Figure 9.16 Recorded output signal from the pop test of Example 9.6.

Then,

$$M(f = 5) = \frac{1}{\sqrt{\left[1 - (f/f_n)^2\right]^2 + (2\zeta f/f_n)^2}} = 1.03$$

With a dynamic error of only about 3%, this system should be suitable for the intended measurements.

Example 9.7

A common method to estimate the data acquisition and reduction errors present in the pressure-measuring instrumentation of a test rig is to apply a series of replication tests on the M calibrated pressure transducers used on that rig (when the number of transducers installed is large, a few transducers can be selected at random and tested). In such a test each transducer is interconnected through a common manifold to the output of a single deadweight tester (or suitable standard) so that each transducer is exposed to exactly the same static pressure. Each transducer is operated at its normal excitation voltage. The test proceeds as follows: record applied test pressure (from the deadweight tester), record each transducer output N (e.g., $N \geq 10$) times, vent the manifold to local atmosphere, close the manifold to reapply test pressure, repeat the procedure at least K (e.g., $K \geq 5$) times. What information is available in such test data?

KNOWN $M(j = 1, 2, \dots, M)$ transducers

$N(i = 1, 2, \dots, N)$ repetitions at a test pressure

$K(k = 1, 2, \dots, K)$ replications of test pressure

SOLUTION The mean value for each transducer is given by the mean of the repetitions for that transducer,

$$\bar{p}_{jk} = \frac{1}{N} \sum_{i=1}^N p_{ijk}$$

The mean value for the replications of the j th transducer is given by

$$\langle \bar{p}_j \rangle = \frac{1}{K} \sum_{k=1}^K \bar{p}_{jk}$$

The difference between the pooled mean pressure and the known applied pressure would provide an estimate of the systematic error to be expected from any transducer during data acquisition. On the other hand, variations between \bar{p}_{jk} and $\langle \bar{p}_j \rangle$ are due to random errors in the data acquisition and reduction procedure. The variation of the test pressure mean, \bar{p}_{jk} , about the pooled mean, $\langle \bar{p}_j \rangle$, for each transducer is

$$\langle s_j \rangle = \sqrt{\frac{\sum_{k=1}^K (\bar{p}_{jk} - \langle \bar{p}_j \rangle)^2}{K - 1}}$$

The pooled standard deviation of the mean for the M transducers provides the estimate of the random

standard uncertainty of the data acquisition and reduction procedure:

$$\bar{s}_p = \frac{\langle s_p \rangle}{\sqrt{MK}} \quad \text{where} \quad \langle s_p \rangle = \sqrt{\sum_{j=1}^M \sum_{k=1}^K (\bar{p}_{jk} - \langle \bar{p}_j \rangle)^2 / M(K-1)}$$

with degrees of freedom, $v = M(K-1)$.

COMMENT The statistical estimate contains the effects of random error due to the pressure standard (applied pressure repeatability), pressure transducer repeatability (repetition and replication), excitation voltages, and the recording system. It does not contain the effects of instrument calibration errors, large deviations in environmental conditions, pressure tap design errors, or dynamic pressure effects. The systematic errors for these must be assigned by the engineer based on other available information. Note that if the above procedure were to be repeated over a range of different applied known pressures, then this calibration would allow instrument calibration errors and data reduction curve fit errors over the range to be entered into the analysis.

9.6 PRESSURE MEASUREMENTS IN MOVING FLUIDS

Pressure measurements in moving fluids warrant special consideration. Consider the flow over the bluff body shown in Figure 9.17. Assume that the upstream flow is uniform and steady with negligible losses. Along streamline A, the upstream flow moves with a velocity U_1 , such as at point 1. As the flow approaches point 2, it must slow down and finally stop at the front end of the body. Above streamline A, flow moves over the top of the bluff body, and below streamline A, flow moves under the body. Point 2 is known as the stagnation point and streamline A the stagnation streamline for this flow. Along streamline B, the velocity at point 3 is U_3 and because the upstream flow is considered to be uniform it follows that $U_1 = U_3$. As the flow along B approaches the body, it is deflected around the body. From the conservation of mass principles, $U_4 > U_3$. Application of conservation of energy between points 1 and 2 and between 3 and 4 yields

$$\begin{aligned} p_1 + \rho U_1^2/2 &= p_2 + \rho U_2^2 \\ p_3 + \rho U_3^2/2 &= p_4 + \rho U_4^2 \end{aligned} \tag{9.16}$$

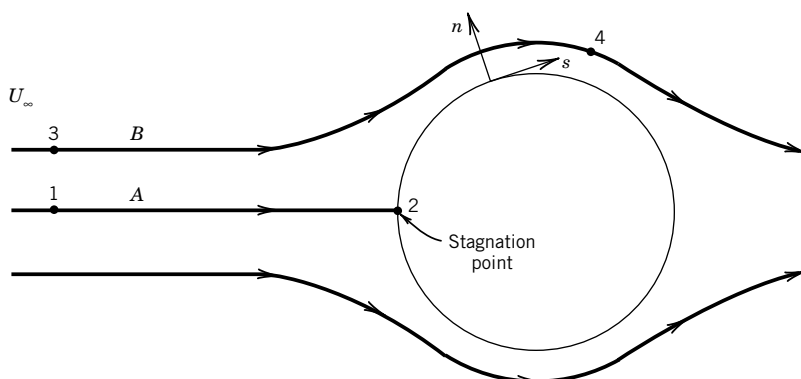


Figure 9.17 Streamline flow over a bluff body.

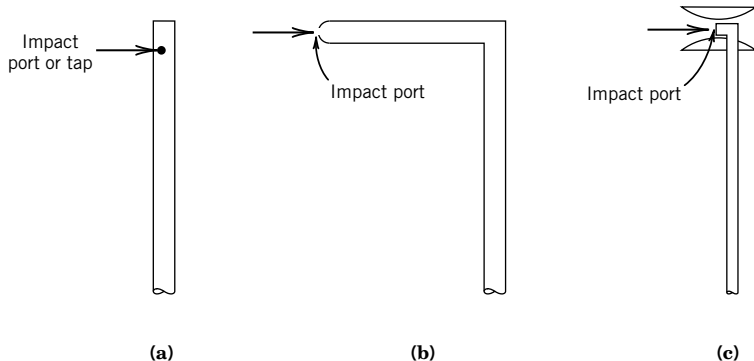


Figure 9.18 Total pressure measurement devices. (a) Impact cylinder. (b) Pitot tube. (c) Kiel probe.

However, because point 2 is the stagnation point, $U_2 = 0$, and

$$p_2 = p_t = p_1 + \rho U_1^2/2 \quad (9.17)$$

Hence, it follows that $p_2 > p_1$ by an amount equal to $p_v = \rho U_1^2/2$, called the *dynamic pressure*, an amount equivalent to the kinetic energy per unit mass of the flow as it moves along the streamline. If no energy is lost through irreversible processes, such as through a transfer of heat,¹ this translational kinetic energy is transferred completely into p_2 . The value of p_2 is known as the *stagnation* or the *total pressure* and is noted as p_t . The total pressure can be determined by bringing the flow to rest at a point in an isentropic manner.

The pressures at 1, 3, and 4 are known as static pressures² of the flow. The *static pressure* is that pressure sensed by a fluid particle as it moves with the same velocity as the local flow. The static pressure and velocity at points 1 and 3 are given the special names of the “freestream static pressure” and “freestream velocity.” Since $U_4 > U_3$, Equation 9.16 shows that $p_4 < p_3$. It follows from Equation 9.17 that the total pressure is the sum of the static and dynamic pressures anywhere in the flow.

Total Pressure Measurement

In practice, the total pressure is measured using an impact probe, such as those depicted in Figure 9.18. A small hole in the impact probe is aligned with the flow so as to cause the flow to come to rest at the hole. The sensed pressure is transferred through the impact probe to a pressure transducer or other pressure-sensing device such as a manometer. Alignment with the flow is somewhat critical, although the probes in Figure 9.18a,b are relatively insensitive (within $\sim 1\%$ error in indicated reading) to misalignment within a ± 7 degree angle (1). A special type of impact probe shown in Figure 9.18c, known as a Kiel probe, uses a shroud around the impact port. The effect of the shroud is to force the local flow to align itself with the shroud axis so as to impact directly onto the impact port. This effectively eliminates total pressure sensitivity to misalignment up to ± 40 degree (1).

¹This is a realistic assumption for subsonic flows. In supersonic flows, the assumption is not valid across a shock wave.

²The term “static pressure” is a misnomer in moving fluids, but its use here conforms to common expression. “Stream pressure” is more appropriate and is sometimes used.

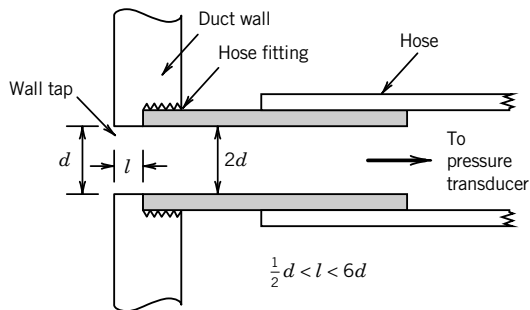


Figure 9.19 Anatomy of a static pressure wall tap.

Static Pressure Measurement

The local value of static pressure in a moving stream is measured by sensing the pressure in the direction that is normal to the flow streamline. Within ducted flows, static pressure is sensed by wall taps, which are small, burr-free, holes drilled into the duct wall perpendicular to the flow direction at the measurement point. The tap is fitted with a hose or tube, which is connected to a pressure gauge or transducer. A recommended design for a wall tap is shown in Figure 9.19. The tap hole diameter d is typically between 1% and 10% of the pipe diameter, with the smaller size preferred (7). The tap must be perpendicular to the local tangent to the wall with no drilling burrs (8).

Alternatively, a static pressure probe can be inserted into the flow to measure local stream pressure. It should be a streamlined design to minimize the disturbance of the flow. It should be physically small so as not to cause more than a negligible increase in velocity in the vicinity of measurement. As a rule, the frontal area of the probe should not exceed 5% of the pipe flow area. The static pressure sensing port should be located well downstream of the leading edge of the probe so as to allow the streamlines to realign themselves parallel with the probe. Such a concept is built into the improved Prandtl tube design shown in Figure 9.20a.

A Prandtl tube probe consists of eight holes arranged about the probe circumference and positioned 8 to 16 probe diameters downstream of the probe leading edge and 16 probe diameters upstream of its support stem. A pressure transducer or manometer is connected to the probe stem to measure the sensed pressure. The hole positions are chosen to minimize static pressure error caused by the disturbance to the flow streamlines due to the probe's leading edge and stem. This is illustrated in Figure 9.20b, where the relative static error, $p_e/p_v = (p_i - p)/(\frac{1}{2} \rho U^2)$, is plotted as a function of tap location along the probe body. Real viscous effects around the static probe cause a slight discrepancy between the actual static pressure and the indicated static pressure. To account for this, a correction factor, C_0 , is used with $p = C_0 p_i$ where $0.99 < C_0 < 0.995$ and p_i is the indicated (measured) pressure.

Example 9.8

An engineer is to measure rear aerodynamic downforce on a racing stock car as it moves on a race track. The pressure difference between the top and bottom surfaces of the car is responsible for this downward force, which allows the tires to adhere better at high speeds in turns. Pressure is measured using surface (wall) taps connected by 5-mm i.d. tubing to ± 25.4 cm H₂O, 0–5 V capacitance pressure transducers (accuracy: 0.25%), such as the connections of Figures 9.19. Transducer output is recorded on a portable data-acquisition system using a 12-bit, 5-V analog-to-

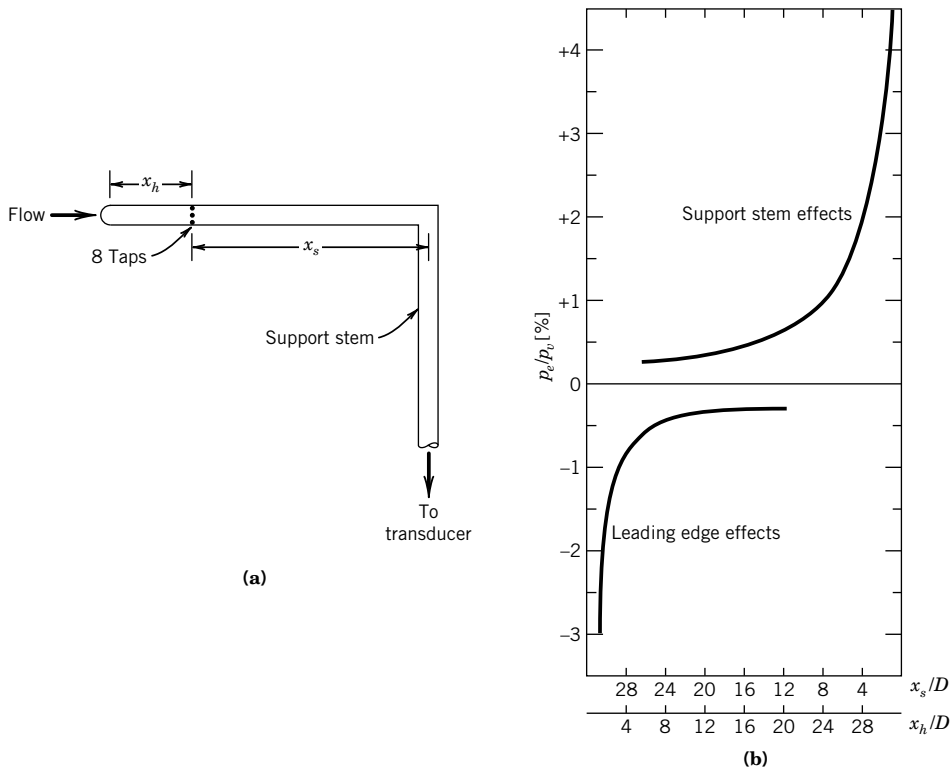


Figure 9.20 Improved Prandtl tube for static pressure. (a) Design. (b) Relative static error along tube length.

digital (A/D) converter (accuracy: 2 LSB). In testing at 180 km/hr, the maximum average pressure difference between the rear deck and underbody is about $8 \text{ cm H}_2\text{O} \pm 0.10 \text{ cm H}_2\text{O}$ (95%). The engineer is asked two questions: (1) Will increasing the resolution of the A/D conversion system reduce the measured uncertainty in pressure? (2) How well can rear downforce be measured on the track?

SOLUTION Aerodynamic downforce is determined by integrating the pressure over the surface area of the car. An approximation is to use average pressures acting on discrete effective areas on the car surface, such as on the upper and lower rear deck.

If we ignore installation errors and ambient influences and just look at direct measurement errors, the measurement system errors and data random errors are important. The resolution of the transducer and A/D system is limited to

$$\begin{aligned} Q_{\text{transducer}} &= 50.8 \text{ cm H}_2\text{O}/5 \text{ V} = 10.16 \text{ cm H}_2\text{O/V} \\ Q_{\text{A/D}} &= 5 \text{ V}/2^{12} = 0.00122 \text{ V/digit}, \end{aligned}$$

giving the total measuring system resolution of

$$Q = 0.00122 \times 10.16 = 0.0124 \text{ cm H}_2\text{O}$$

So we assign $u_o = 0.0124 \text{ cm H}_2\text{O}$. However, improving the data-acquisition system (DAS) to a 16-bit system improves Q and thereby u_o to $0.008 \text{ cm H}_2\text{O}$.

Pressure fluctuations occur as the flow fluctuates around the car. Statistical variations from average values give the stated random uncertainty, $u_{\Delta\bar{p}} = 0.10 \text{ cm H}_2\text{O}$ (95%), which we assign large degrees of freedom.

If we look at the rear deck of the car and use the instrument specifications as a measure of the instrument systematic uncertainty,

$$\begin{aligned} u_c \text{ transducer} &\approx (0.0025) (8 \text{ cm H}_2\text{O}) = 0.02 \text{ cm H}_2\text{O} \\ u_c \text{ A/D} &= (2 \text{ bits}) (0.0124 \text{ cm H}_2\text{O}/\text{bit}) = 0.025 \text{ cm H}_2\text{O} \end{aligned}$$

which, combined with u_o for the 12-bit system, gives the design-stage estimate

$$(u_d)_{\Delta\bar{p}} = \left[(0.02)^2 + (0.025)^2 + (0.0124)^2 \right]^{1/2} = 0.034 \text{ cm H}_2\text{O}$$

We can use this as an estimate of the systematic uncertainty at the 95% confidence level. Then, the combined uncertainty in mean pressure is

$$u_{\Delta\bar{p}} = \sqrt{0.034^2 + 0.10^2} = \pm 0.10 \text{ cm H}_2\text{O} \quad (95\%)$$

or about 1.25%. From this advanced design-stage analysis, a higher 16-bit resolution would not improve the measurement uncertainty.

The downforce is simply the downward component of force, $F_D = \Delta p A_{\text{eff}}$. The effective area on the rear deck, A_{eff} , can be estimated from carefully controlled calibration measurements within a wind tunnel using a highly accurate balance scale to measure downforce (i.e., N th order analysis, concomitant method). Suppose a value for the rear effective area is found to be $A_{\text{eff}} = 10832 \pm 147 \text{ cm}^2$ (95%). Combining uncertainties in pressure and area gives the percent uncertainty in rear downforce,

$$u_F/F_D = \pm \left[(u_{\Delta\bar{p}}/\Delta\bar{p})^2 + (u_A/A_{\text{eff}})^2 \right] = 0.019 \text{ or } 1.9\% \quad (95\%)$$

COMMENT Here we see that the dominant uncertainty is due to the measuring procedure and flow process and not the instrumentation.

9.7 MODELING PRESSURE AND FLUID SYSTEMS

Fluid systems can be modeled using lumped parameter ideal elements just as common resistor-inductor-capacitor electrical loops and mass-damper-spring mechanical systems are used. The common elements are inertance, resistance, and compliance.

Inertance describes the inertial properties of a mass in motion, such as that of a mass of fluid moving within a vessel. For a fluid of density ρ and a vessel of cross-sectional area A and length ℓ , the inertance is written

$$L_f = \rho\ell/A \quad (9.18)$$

When modeling inertial forces in laminar flows, this value should be increased by a factor of $\frac{4}{3}$. Inertance is the direct analog to electrical inductance.

Fluid *resistance* describes the opposition to motion. This is the pressure change required to move a volume of fluid per unit time, Q . It is written

$$R = \Delta p^n/Q = \Delta E/I \quad (9.19)$$

where $n = 1$ for laminar and $n = 0.5$ for turbulent flows. Hence, $Q = \frac{1}{R} \Delta p^n$.

The resistance of the laminar flow of a newtonian fluid through a circular pipe is $R = \frac{128\mu\ell}{\pi d^4}$, where μ is the fluid viscosity. In electrical systems, it has the analogous meaning as the opposition to current flow for an imposed voltage potential, such as an electrical resistor.

Compliance describes a measure of the volume change associated with a corresponding pressure change, such as

$$C_{vp} = \Delta V / \Delta p \quad (9.20)$$

It is a measure of the flexibility in a structure, component, or substance, and so it is the inverse of the system *stiffness*. Compliance is the direct analog to electrical capacitance.

9.8 DESIGN AND INSTALLATION: TRANSMISSION EFFECTS

Consider the configuration depicted in Figure 9.21 in which a tube of volume V , with length ℓ and diameter d is used to connect a pressure tap to a pressure transducer of internal dead volume V (e.g., Figure 9.12). Under static conditions, the pressure transducer indicates the static pressure at the tap. But if the pressure at the tap is a time-dependent pressure, $p_a(t)$, the response behavior of the tubing influences the time-indicated output from the transducer, $p(t)$.

By considering the one-dimensional pressure forces acting on a lumped mass of fluid within the connecting tube, balancing inertance, compliance, and resistance against forcing function, we can develop a model for the pressure system response. A network model is shown in Figure 9.22a in which the circuit is driven between two pressures, the applied pressure $p_a(t)$ at the tap and the measured pressure $p_m(t)$ at the transducer sensor. Using the electrical analog, inertance is modeled by the inductor, fluid resistance by a resistor, and compliance by a capacitor (Fig. 9.22b). The circuit analysis of the two loops gives

$$L\ddot{I} + RI + \frac{1}{C} \int Idt = E_a \quad \text{and} \quad \frac{1}{C} \int Idt = E_m \quad (9.21)$$

Taking the derivative of the second loop to get \dot{E}_m and \ddot{E}_m in terms of \dot{I} and \ddot{I} , then substituting these back into Equation 9.21 with $E_a = p_a$, $E_m = p_m$, $L = L_f$, and $C = C_{vp}$ gives

$$L_f C_{vp} \ddot{p}_m + R C_{vp} \dot{p}_m + p_m = p_a(t) \quad (9.22)$$

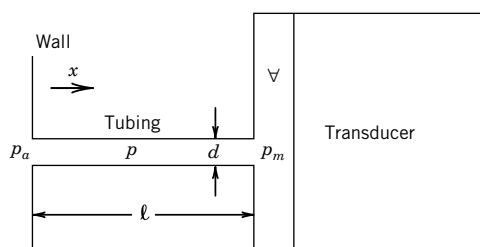


Figure 9.21 Wall tap to pressure transducer connection: the transmission line.

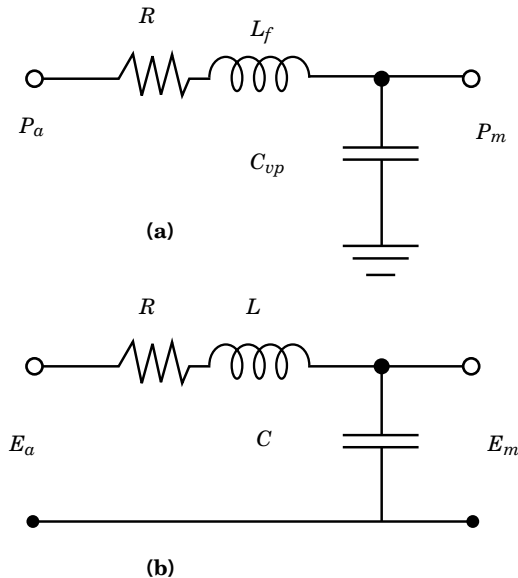


Figure 9.22 An equivalent lumped parameter network of the pressure transmission line model of Figure 9.21 using an electrical analogy.

Substituting Equations 9.18 to 9.20 into Equation 9.22 gives the working system response equation for the applied and measured pressures,

$$\frac{16\ell\rho C_{vp}}{3\pi d^2}\ddot{p}_m + \frac{128\mu\ell C_{vp}}{\pi d^4}\dot{p}_m + p_m = p_a(t) \quad (9.23)$$

in which we have augmented the fluid inertial force by $\frac{4}{3}$ (9).

In this simple model, the system compliance lumps the compliance of the fluid, tube walls, and transducer into a single value, C_{vp} . As these individual compliances could be modeled separately by using capacitors in parallel, the total capacitance is simply the sum of each. If one compliance dominates, the others can be neglected. Further, the inertance and resistance of the connecting tube and the transducer cavity are lumped into single values. Improved models use distributed, lumped parameters, such as are commonly used to model physiological vascular systems (10). A long-standing approach to modeling the transmission line (11) examines the forces acting on a fluid element. In this model, small pressure changes act on the element, moving it back and forth by a distance x within the tube. Summing the forces and substituting for p_m again results in Equation 9.23 (12). Be aware that models are based on simplifying assumptions and should be used only as a guide in the design of a system, not as a replacement for *in situ* calibration.

We can study the transient and frequency response of the system represented by Equation 9.23 by extracting values for ω_n and ζ ,

$$\omega_n = \frac{d}{4} \sqrt{3\pi/\rho\ell C_{vp}} \quad (9.24)$$

$$\zeta = \frac{16\mu}{d^3} \sqrt{3\ell C_{vp}/\pi\rho} \quad (9.25)$$

The total system compliance could be measured using Equation 9.20 by closing the pressure tap, increasing the fluid volume in the tubing by a small known amount, such as by syringe, and measuring the corresponding pressure change.

Liquids

Liquids are relatively incompressible, so that the compression-restoring force in the transmission line is due primarily to the compliance in the transducer, which is a transducer specification, for use in Equations 9.24 and 9.25. Connecting tubing can usually be considered rigid for the underlying assumptions of the above lumped parameter analysis. Thick-walled, flexible tubing is often used, but this is fairly rigid and its compliance can be ignored. If need be, the compliance can be measured.

Gases

For gases, we simplify by assuming that the system is rigid relative to the compressibility of the gas. Compliance is then modeled in terms of the fluid's adiabatic bulk modulus of elasticity, $E_m = \nabla/C_{vp}$. This gives

$$\omega_n = \frac{d}{4} \sqrt{3\pi E_m / \rho \ell \nabla} \quad (9.26)$$

$$\zeta = \frac{16\mu}{d^3} \sqrt{3\ell\nabla / \pi\rho E_m} \quad (9.27)$$

Equations 9.26 and 9.27 can also be written in terms of the speed of sound for the gas, a , which is related to its compressibility by $a = \sqrt{E_m/\rho}$ and for a perfect gas by $a = \sqrt{kRT}$, where T is the gas absolute temperature, giving

$$\omega_n = \frac{ad}{4} \sqrt{3\pi / \ell \nabla} \quad (9.28)$$

$$\zeta = \frac{16\mu}{apd^3} \sqrt{3\ell\nabla / \pi} \quad (9.29)$$

When the tube volume, $\nabla_t \gg \nabla$, then a series of standing pressure waves develop and we can expect $\omega \sim O(a/\ell)$. Hougen et al. (13) discuss an improved prediction as

$$\omega_n = \frac{a}{\ell \sqrt{0.5 + \nabla / \nabla_t}} \quad (9.30)$$

$$\zeta = \frac{16\mu\ell}{pad^2} \sqrt{0.5 + \nabla / \nabla_t} \quad (9.31)$$

Note that in all cases, larger diameter and shorter length tubes improve pressure system response.

Example 9.9

The pressure in a water-filled pipe varies with time. A pressure transducer is connected to a wall tap using a length of non-rigid plastic tubing to measure this pressure. To estimate the pressure system

compliance, the tubing is removed at the wall tap, filled with water, and purged of any residual air. The transducer output is noted. Using a syringe, 1 mL of water is then added to the system and the corresponding measured pressure increases by 100 mm Hg. Find the compliance.

SOLUTION Using Equation 9.20, the compliance of the transducer-tubing system is

$$C_{vp} = \Delta V / \Delta p = 1 \text{ mL} / 100 \text{ mm Hg} = 0.01 \text{ mL/mm Hg}$$

Example 9.10

A pressure transducer with a natural frequency of 100 kHz is connected to a 0.10-in. static wall pressure tap using a 0.10-in. i.d. rigid tube that is 5 in. long. The transducer dead volume is 1 in.³. Determine the system frequency response to fluctuating pressures of air at 72°F if the pressure fluctuates about an average value of 1 atm abs. Express the frequency response in terms of $M(\omega)$. $R_{\text{air}} = 53.3 \text{ ft-lb/lb}_m \cdot {}^\circ\text{R}$; $\mu = 4 \times 10^{-7} \text{ lb-s/ft}^2$; $E_m = 20.5 \text{ lb/in.}^2$

KNOWN $\ell = 5 \text{ in.}$ $k = 1.4$

$d = 0.1 \text{ in.}$ $T = 72^\circ\text{F} = 532^\circ\text{R}$

$\forall = 1 \text{ in.}^3$ $\rho = p/RT = 0.075 \text{ lb}_m/\text{ft}^3$

ASSUMPTION Air behaves as a perfect gas.

FIND $M(\omega)$

SOLUTION The frequency-dependent magnitude ratio is given by Equation 3.22

$$M(\omega) = \frac{1}{\sqrt{\left[1 - (\omega/\omega_n)^2\right]^2 + [2\zeta(\omega/\omega_n)]^2}}$$

We need ω_n and ζ to solve $M(\omega)$ for various frequencies.

With $\forall_t < \forall$, we use Equations 9.26 and 9.27, or alternately using Equations 9.28 and 9.29 with $a = 1130 \text{ ft/s}$, to find

$$\omega_n = \frac{d}{4} \sqrt{3\pi E_m / \rho \ell \forall} = 470 \text{ rad/s}$$

$$\zeta = \frac{16\mu}{d^3} \sqrt{3\ell\forall / \pi\rho E_m} = 0.06$$

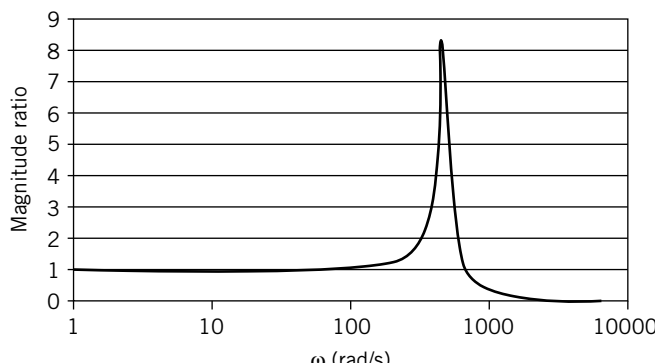


Figure 9.23 Magnitude response of the transmission line for Example 9.10.

This system is lightly damped. The magnitude frequency response, $M(\omega)$, is shown in Figure 9.23. The transmission line effects control the transducer response. In effect, the transmission line acts as a mechanical low-pass filter for the transducer.

Heavily Damped Systems

In systems in which we estimate a damping ratio greater than 1.5, the frequency response model can be simplified further. The behavior of the pressure-measuring system closely follows that of a first-order system. Again, the typical pressure transducer–tubing system has a compliance C_{vp} , which is a measure of the transducer and tubing volume change relative to an applied pressure change. The response of the first-order system is indicated through its time constant, which is estimated by neglecting the second-order term in Equation 9.23 so that (12)

$$\tau = \frac{128\mu\ell C_{vp}}{\pi d^4} \quad (9.32)$$

Equation 9.32 shows that the time constant is proportional to ℓ/d^4 . Long- and small-diameter connecting tubes promote a more sluggish system response to changes in pressure.

9.9 FLUID VELOCITY MEASURING SYSTEMS

Velocity measuring systems are used to measure the local velocity in a moving fluid. Desirable information can consist of the mean velocity, as well as any of the dynamic components of the velocity. Dynamic components are found in pulsating, phasic, or oscillating flows, or in turbulent flows. For most general engineering applications, information about the mean flow velocity is usually sufficient. The dynamic velocity information is often sought during applied and basic fluid mechanics research and development, such as in attempting to study airplane wing response to air turbulence, a complex periodic waveform as the wing sees it. In general, the instantaneous velocity can be written as

$$U(t) = \bar{U} + u \quad (9.33)$$

where \bar{U} is the mean velocity and u is the time-dependent dynamic (fluctuating) component of the velocity. The instantaneous velocity can also be expressed in terms of a Fourier series:

$$U(t) = \bar{U} + \sum_i C_i \sin(\omega_i t + \phi'_i) \quad (9.34)$$

so that the mean velocity and the amplitude and frequency information concerning the dynamic velocity component can be resolved with a Fourier analysis of the time-dependent velocity signal.

Pitot-Static Pressure Probe

For a steady, incompressible, isentropic flow, Equation 9.16 can be written at any arbitrary point x in the flow field as

$$p_t = p_x + \frac{1}{2}\rho U_x^2 \quad (9.35)$$

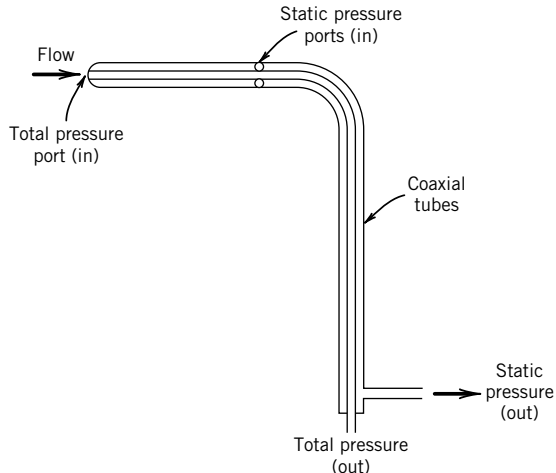


Figure 9.24 Pitot-static pressure probe.

or, rearranging,

$$p_v = p_t - p_x = \frac{1}{2} \rho U_x^2 \quad (9.36)$$

Again p_v , the difference between the total and static pressures at any point in the flow, is the *dynamic pressure*. Hence, measuring the dynamic pressure of a moving fluid at a point provides a method for estimating the local velocity,

$$U_x = \sqrt{\frac{2p_v}{\rho}} = \sqrt{\frac{2(p_t - p_x)}{\rho}} \quad (9.37)$$

In practice, Equation 9.37 is utilized through a device known as a *pitot-static pressure probe*. Such an instrument has an outward appearance similar to that of an improved Prandtl static pressure probe (Fig. 9.20a), except that the pitot-static probe contains an interior pressure tube attached to an impact port at the leading edge of the probe, as shown in Figure 9.24. This creates two coaxial internal cavities within the probe, one exposed to the total pressure and the second exposed to the static pressure. The two pressures are typically measured using a differential pressure transducer so as to indicate p_v directly.

The pitot-static pressure probe is relatively insensitive to misalignment over the yaw angle range of ± 15 degrees (1). When possible, the probe can be rotated until a maximum signal is measured, a condition that indicates that it is aligned with the mean flow direction. However, the probes have a lower velocity limit of use that is brought about by strong viscous effects in the entry regions of the pressure ports. In general, viscous effects should not be a concern, provided that the Reynolds number based on the probe radius, $Re_r = \bar{U}r/v$, is greater than 500, where v is the kinematic viscosity of the fluid. For $10 < Re_r < 500$, a correction to the dynamic pressure should be applied, $p_v = C_v p_i$, where

$$C_v = 1 + (4/Re_r) \quad (9.38)$$

and p_i is the indicated dynamic pressure from the probe. However, even with this correction, the measured dynamic pressure has a systematic uncertainty on the order of 40% at $Re_r \approx 10$ but decreases to 1% for $Re_r \geq 500$.

In high-speed gas flows, compressibility effects near the probe leading edge require a closer inspection of the governing equation for a pitot-static pressure probe. An energy balance along a streamline for a perfect gas between any point x and the stagnation point can be written as

$$\frac{U^2}{2} = c_p(T_t - T_\infty) \quad (8.34)$$

For an isentropic process, the relationship between temperature and pressure can be stated as

$$\frac{T_x}{T_t} = \left(\frac{p_x}{p_t} \right)^{(k-1)/k} \quad (9.39)$$

where k is the ratio of specific heats for the gas, $k = c_p/c_v$. The Mach number of a moving fluid relates its local velocity to the local speed of sound,

$$M = U/a \quad (9.40)$$

where the speed of sound, also called the acoustic wave speed, for a perfect gas is $a = \sqrt{kRT_x}$ where T_x is the absolute temperature of the gas at the point of interest. Combining these equations and using a binomial expansion gives a relationship between total pressure and static pressure at any point x in a moving compressible flow,

$$p_v = p_t - p_x = \frac{1}{2}\rho U_x^2 [1 + M^2/4 + (2 - k)M^4/24 + \dots] \quad (9.41)$$

Equation 9.41 reduces to Equation 9.36 when $M \ll 1$. The error in the estimate of p_v , based on the use of Equation 9.36 relative to the true dynamic pressure, becomes significant for $M > 0.3$, as shown in Figure 9.25. Thus, $M \sim 0.3$ is used as the incompressible limit for perfect gas flows.

For $M > 1$, the local velocity is found through iteration using the Rayleigh relation:

$$p_t/p = \left(\frac{(k+1)^2 M^2}{4kM^2 - 2(k-1)} \right)^{k/k-1} \left(\frac{1 - k + 2kM^2}{k+1} \right) \quad (9.42)$$

and Equation 9.40 where both p and p_t are the measured values.

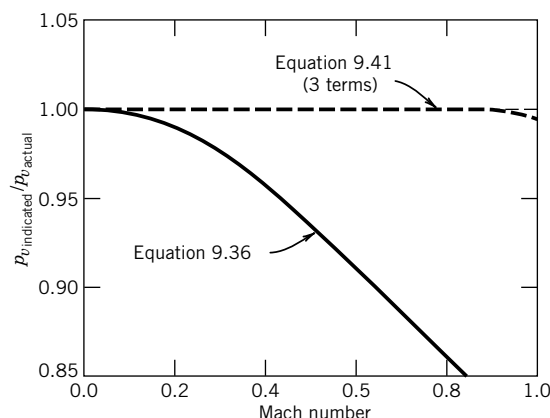


Figure 9.25 Relative error in the dynamic pressure between using Equations 9.36 and 9.41 at increasing flow speeds.

Thermal Anemometry

The rate at which energy, \dot{Q} , is transferred between a warm body at T_s and a cooler moving fluid at T_f is proportional both to the temperature difference between them and to the thermal conductance of the heat transfer path, hA . This thermal conductance increases with fluid velocity, thereby increasing the rate of heat transfer at any given temperature difference. Hence, a relationship between the rate of heat transfer and velocity exists forming the working basis of a thermal anemometer.

A thermal anemometer utilizes a sensor, a metallic resistance temperature detector (RTD) element, that makes up one active leg of a Wheatstone bridge circuit, as indicated in Figure 9.26. The resistance–temperature relation for such a sensor was shown in Chapter 8 to be well represented by

$$R_s = R_0[1 + \alpha(T_s - T_0)] \quad (9.43)$$

so that sensor temperature T_s can be inferred through a resistance measurement. A current is passed through the sensor to heat it to some desired temperature above that of the host fluid. The relationship between the rate of heat transfer from the sensor and the cooling fluid velocity is given by King's law (14) as

$$\dot{Q} = I^2 R = A + BU^n \quad (9.44)$$

where A and B are constants that depend on the fluid and sensor physical properties and operating temperatures, and n is a constant that depends on sensor dimensions (15). Typically, $0.45 \leq n \leq 0.52$ (16). A , B , and n are found through calibration.

Two types of sensors are common: the hot wire and the hot film. As shown in Figure 9.27, the hot-wire sensor consists of a tungsten or platinum wire ranging from 1 to 4 mm in length and from 1.5 to 15 μm in diameter. The wire is supported between two rigid needles that protrude from a

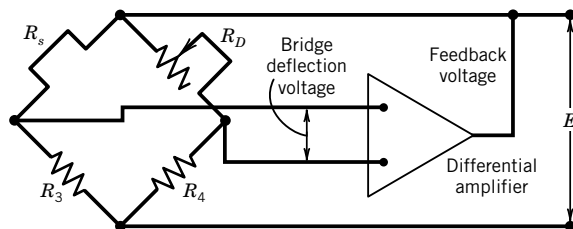


Figure 9.26 Thermal anemometer circuit, shown in constant resistance mode.

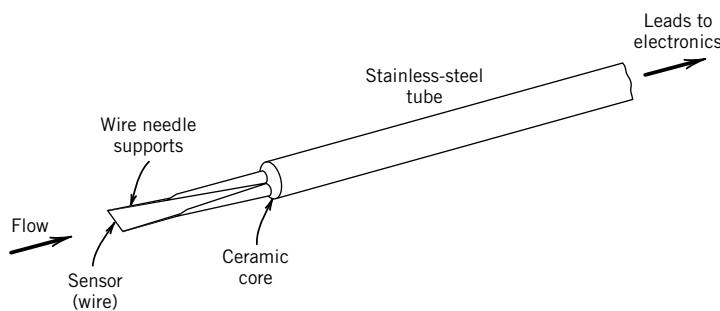


Figure 9.27 Schematic of a hot-wire probe.

ceramic tube that houses the lead wires. A hot-film sensor usually consists of a thin ($2 \mu\text{m}$) platinum or gold film deposited onto a glass substrate and covered with a high thermal conductivity coating. The coating acts to electrically insulate the film and offers some mechanical protection. Hot wires are generally used in electrically nonconducting fluids, while hot films can be used in conducting fluids or in nonconducting fluids when a more rugged sensor is needed.

Two anemometer bridge operating modes are possible: (1) constant current and (2) constant resistance. In constant-current operation, a fixed current is passed through the sensor to heat it. The sensor resistance and therefore its temperature, based on Equation 9.43, are permitted to vary with the rate of heat transfer between the sensor and its environment. Bridge-deflection voltage provides a measure of the cooling velocity. The more common mode of operation for velocity measurements is constant resistance. In constant-resistance operation, the sensor resistance of Equation 9.43 is originally set by adjusting the bridge balance. The sensor resistance is then maintained constant by using a differential feedback amplifier to sense small changes in bridge balance, which would be equivalent to sensing changes in the sensor set-point resistance; that is, the circuit acts as a closed loop controller using the bridge balance as the error signal. The feedback amplifier rapidly readjusts the bridge applied voltage, thereby adjusting the sensor current to bring the sensor back to its set-point resistance and corresponding temperature. Because the current through the sensor varies with changes in the velocity, the instantaneous power (I^2R_s) required to maintain this constant temperature is equivalent to the instantaneous rate of heat transfer from the sensor (\dot{Q}). In terms of the instantaneous applied bridge voltage, E , required to maintain a constant sensor resistance, the velocity is found by the general correlation

$$E^2 = C + DU^n \quad (9.45)$$

where the values of C , D , and n are found by calibration under a fixed sensor and fluid temperature condition. An electronic or digital linearizing scheme is usually employed to condition the signal by performing the transformation

$$E_l = K \left(\frac{E^2 - C}{D} \right)^{1/n} \quad (9.46)$$

such that the measured output from the linearizer, E_l , is

$$E_l = KU \quad (9.47)$$

where K is found through a static calibration.

For mean velocity measurements, the thermal anemometer is a straightforward device to use. It has a better usable sensitivity than the pitot-static tube at lower velocities. Multiple velocity components can be measured by using multiple sensors, each sensor aligned differently to the mean flow direction and operated by independent anemometer circuits (15,17). Because it has a high-frequency response, fluctuating (dynamic) velocities can be measured. In highly turbulent flows with root-mean-square (rms) fluctuations of $\sqrt{\bar{u}^2} \geq 0.1\bar{U}$, signal interpretation can become complicated, but it has been well investigated (17). Low-frequency fluid temperature fluctuations can be compensated for by placing resistor R_3 directly adjacent to the sensor and exposed to the flow. An extensive bibliography of thermal anemometry theory and signal interpretation can be found elsewhere (18).

In constant temperature mode using a fast-responding differential feedback amplifier, a hot-wire system can attain a frequency response that is flat up to 100,000 Hz, which makes it particularly useful in fluid mechanics turbulence research. However, less expensive and more rugged systems

are commonly used for industrial flow monitoring, where a fast dynamic response is desirable. There is a natural upper frequency limit on a cylindrical sensor of diameter d that is brought about by the natural oscillation in the flow immediately downstream of a body. This vibrates the sensor. The frequency of this oscillation, known as the Strouhal frequency (and explained further in Section 10.6 in Chapter 10), occurs at approximately

$$f \approx 0.22 [\overline{U}/d] \quad (10^2 < \text{Re}_d < 10^7) \quad (9.48)$$

The heated sensor warms the fluid within its proximity. Under flowing conditions this does not cause any measurable problems so long as the condition

$$\text{Re}_d \geq Gr^{1/3} \quad (9.49)$$

is met where $\text{Re}_d = \overline{U}d/v$, $Gr = d^3 g \beta (T_s - T_{\text{fluid}})/v^2$, and β is the coefficient of thermal expansion of the fluid. Equation 9.49 ensures that the inertial forces of the moving fluid dominate over the buoyant forces brought on by the heated sensor. This forms a lower velocity limit on the order of 0.6 m/s for using hot-wire sensors in air.

Doppler Anemometry

The Doppler effect describes the phenomenon experienced by an observer whereby the frequency of light or sound waves emitted from a source that is traveling away from or toward the observer is shifted from its original value and by an amount proportional to its speed. Most readers are familiar with the change in pitch of a train as heard by an observer as the train changes from approaching to receding. Any radiant energy wave, such as a sound or light wave, experiences a Doppler effect. The effect was recognized and modeled by Christian Johann Doppler (1803–1853). The observed shift in frequency, called the Doppler shift, is directly related to the speed of the emitter relative to the observer. To an independent observer, the frequency of emission is perceived to be higher than actual if the emitter is moving toward the observer and lower if moving away, because the arrival of the emission at the observer location is affected by the relative velocity of the emission source. The Doppler effect is used in astrophysics to measure the velocity of distant objects by monitoring the frequency of light emitted from a particular gas, usually hydrogen. Since, in the visible light spectrum, frequency is related to color, the common terms of red shift or blue shift refer to frequency shifts toward the red side of the spectrum or toward the blue side.

Doppler anemometry refers to a class of techniques that utilize the Doppler effect to measure the local velocity in a moving fluid. In these techniques, the emission source and the observer remain stationary. However, small scattering particles suspended in and moving with the fluid can be used to generate the Doppler effect. The emission source is a coherent narrow incident wave. Either acoustic waves or light waves are used.

When a laser beam is used as the incident wave source, the velocity measuring device is called a laser Doppler anemometer (LDA). LDA measures the time-dependent velocity at a point in the flow. Yeh and Cummins (19) in 1964 discussed the first practical laser Doppler anemometer system. A laser beam provides a ready emission source that is monochromatic and remains coherent over long distances. As a moving particle suspended in the fluid passes through the laser beam, it scatters light in all directions. An observer viewing this encounter between the particle and the beam perceives the scattered light at a frequency, f_s :

$$f_s = f_i \pm f_D \quad (9.50)$$

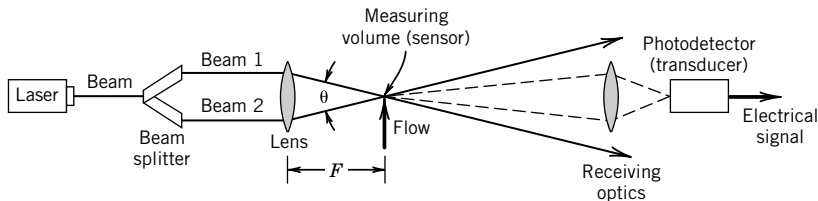


Figure 9.28 Laser Doppler anemometer, shown here in the dual-beam mode of operation.

where f_i is the frequency of the incident laser beam and f_D is the Doppler shift frequency. Using visible light, an incident laser beam frequency is on the order of 10^{14} Hz. For most engineering applications, the velocities are such that the Doppler shift frequency, f_D , is on the order of 10^3 to 10^7 Hz. Such a small shift in the incident frequency can be difficult to detect in a practical instrument. An operating mode that overcomes this difficulty is the dual-beam mode shown in Figure 9.28. In this mode, a single laser beam is divided into two coherent beams of equal intensity using an optical beam splitter. These incident beams are passed through a focusing lens that focuses the beams to a point in the flow. The focal point forms the effective measuring volume (sensor) of the instrument. Particles suspended in and moving with the fluid scatter light as they pass through the beams. The frequency of the scattered light is that given by Equation 9.50 everywhere but at the measuring volume. There, the two beams cross and the incident information from the two beams mix, a process known as optical heterodyne. The outcome of this mixing is a separation of the incident frequency from the Doppler frequency. A stationary observer, such as an optical photodiode, focused on the measuring volume, sees two distinct frequencies, the Doppler shift frequency and the unshifted incident frequency, instead of seeing their sum. It is a simple matter to separate the much smaller Doppler frequency from the incident frequency by filtering.

For the setup shown in Figure 9.28, the velocity is related directly to the Doppler shift by

$$U = \frac{\lambda}{2 \sin \theta/2} f_D = d_f f_D \quad (9.51)$$

where the component of the velocity measured is that which is in the plane of and bisector to the crossing beams. In theory, by using beams of different color or polarization, different velocity components can be measured simultaneously. However, the dependence of the lens focal length on color causes a small displacement between the different measuring volumes formed by the different colors. For most applications this can be corrected. The LDA technique requires no direct calibration beyond explicit determination of the parameters in d_f and the ability to measure f_D .

In dual-beam mode, the output from the photodiode transducer is a current of a magnitude proportional to the square of the amplitude of the scattered light seen and of a frequency equal to f_D . This effect is seen as a Doppler “burst” shown in the typical oscilloscope trace of Figure 9.29. The Doppler burst is the frequency signal created by a particle moving through the measuring volume. If the instantaneous velocity of a dynamic flow varies with time, the Doppler shift from successive scatters will vary with time. This time-dependent frequency information can be extracted by any variety of processing equipment that can interpret the signal current. The most common is the burst analyzer.

Burst analyzers extract Doppler frequency information by performing a Fourier analysis (see Chapter 2) on the input signal. This is done by first discretizing the photodetector analog signal at a high sample rate and then analyzing the signal.



Figure 9.29 Oscilloscope trace of a photodiode output showing the Doppler frequency from a single particle moving through the measuring volume.

The analysis can work in one of two ways. In the first approach, the analyzer performs the fast Fourier transform (FFT) continuously on small blocks of data from which the Doppler frequency is directly determined. In the second mode, the correlation mode, the sampled signal is correlated with itself through a mathematical transformation of the form

$$R_j = \sum_{i=1}^n x(i)x(i+j) \quad (9.52)$$

where i refers to the sample value at time t and j to the sample value at time delay Δt . This operation improves the signal-to-noise ratio (SNR) of the signal; the frequency is determined from the correlation function and the sample rate. From Equation 9.51, the Doppler frequency can be converted to a velocity and provided as an output signal. The acquisition and analysis occur rapidly so that the signal appears nearly continuous in time and with only a short time lag.

All methods output a voltage that is proportional to the instantaneous velocity, which makes their signal easy to process, or a digital output path to a digital file for signal analysis. At very low light levels and very few scattering particles, the signal level to noise level can be very low. In such cases, photon correlation techniques are successful (20,21).

The LDA technique measures velocity at a point. Thus, its probe volume needs to be moved around to map out the flow field. If the SNR and seeding is good, the LDA can measure time-dependent velocities well. The LDA technique is particularly useful where probe blockage effects render other methods unsuitable, where fluid density and temperature fluctuations occur, or where environments hostile to physical sensors exist. An extended discussion of LDA techniques can be found elsewhere (21,22).

Example 9.11

A laser Doppler anemometer made up of a He-Ne laser ($\lambda = 632.8$ nm) is used to measure the velocity of water at a point in a flow. A 150-mm lens, with $\theta = 11$ degrees, is used to operate the LDA in a dual-beam mode. If an average Doppler frequency of 1.41 MHz is measured, estimate the velocity of water.

KNOWN $\bar{f}_D = 1.41$ MHz
 $\lambda = 632.8$ nm $\theta = 11$ degrees

ASSUMPTIONS Scattering particles follow the water exactly.

FIND \bar{U}

SOLUTION Using Equation 9.51,

$$\bar{U} = \frac{\lambda}{2 \sin \theta/2} \bar{f}_D = \left(\frac{632.8 \times 10^{-9} \text{ m}}{2 \sin(11^\circ/2)} \right) (1.41 \times 10^6 \text{ Hz}) = 4.655 \text{ m/s}$$

Particle Image Velocimetry

Particle image velocimetry (PIV) measures the full-field instantaneous velocities in a planar cross section of a flow. The technique tracks the time displacement of particles, which are assumed to follow the flow. Principle components for the technique are a coherent light source (laser beam), optics, a CCD-camera, and dedicated signal interrogation software.

In a simple overview, the image of particles suspended in the flow are illuminated and recorded during very-short-duration repetitive flashes of a laser beam. These images are recorded and compared. The distance traveled by any particle during the period between flashes is a measure of its velocity. By repeatedly flashing the laser, in the manner of a strobe light, the particle positions can be tracked and velocity as a function of time obtained.

In a typical layout, such as shown in Figure 9.30, a pulsed flash laser beam is passed through a cylindrical lens, which converts the beam into a two-dimensional (2-D) sheet of light. This laser sheet is mechanically situated to illuminate an appropriate cross section of the flow field. The camera is positioned and focused to record the view of the illuminated field. The laser flash and camera shutter are synchronized to capture the flow image. The acquired digital image is stored and processed by interrogation software, resulting in a full-field instantaneous velocity mapping of the flow.

The operating principle is based on particle displacement with time

$$\vec{U} = \Delta \vec{x} / \Delta t \quad (9.53)$$

where \vec{U} is the instantaneous particle velocity vector based on its spatial position $\vec{x}(x, y, z, t)$. The camera records particle position at each flash into separate image frames. To obtain velocity data in a rapid manner, each image is divided into small areas, called interrogation areas. The corresponding interrogation areas between two images, I_1 and I_2 , are cross-correlated with each other, on a pixel-by-pixel basis. A particular particle movement from position \vec{x}_1 to \vec{x}_2 shows up as a signal peak in

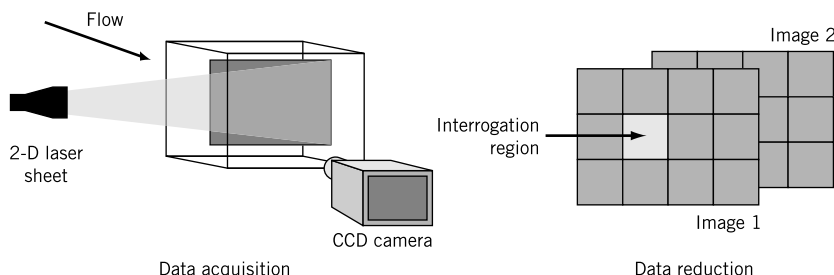


Figure 9.30 Basic layout of a digital particle image velocimeter.

the correlation $R_{12}(\Delta\vec{x})$, where

$$R_{12}(\Delta\vec{x}) = \int_A \int I_1(\Delta\vec{x})I_2(\vec{x} + \Delta\vec{x})d\vec{x} \quad (9.54)$$

so identifying the common particle and allowing the estimate of the particle displacement $\Delta\vec{x}$. By repeating the cross-correlation between images for each interrogation area, a velocity vector map of the full area results.

A number of variations of this process have been developed but the concept remains the same. The technique works in gases or liquids. Three-dimensional information can be obtained by using two cameras. As with LDA, particle size and properties should be chosen relative to the fluid and flow velocities expected so that the particles move with the fluid, but large enough relative to camera pixel size to avoid peak-locking errors (23). The maximum flow speed measurable is limited by the interrogation area size. The resolution depends on laser flash width and separation time, flow velocity, camera recording time, and image magnification. Raffel et al. (23) discuss the technique, its variations, and error estimates.

Selection of Velocity Measuring Methods

Selecting the best velocity measuring system for a particular application involves a number of factors that an engineer needs to weight accordingly:

1. Required spatial resolution
2. Required velocity range
3. Sensitivity to velocity changes only
4. Required need to quantify dynamic velocity
5. Acceptable probe blockage of flow
6. Ability to be used in hostile environments
7. Calibration requirements
8. Low cost and ease of use

When used under appropriate conditions, the uncertainty in velocity determined by any of the discussed methods can be as low as 1% of the measured velocity, although under special conditions LDA methods can have an uncertainty one order of magnitude lower (24).

Pitot-Static Pressure Methods

The pressure probe methods are best suited for finding the mean velocity in fluids of constant density. Relative to other methods, they are the simplest and cheapest method available to measure velocity at a point. Probe blockage of the flow is not a problem in large ducts and away from walls. Fluid particulate blocks the impact ports, but aspirating models are available for such situations. They are subject to mean flow misalignment errors. They require no calibration and are frequently used in the field and laboratory alike.

Thermal Anemometer

Thermal anemometers are best suited for use in clean fluids of constant temperature and density. They are well suited for measuring dynamic velocities with very high resolution. However, signal

interpretation in strongly dynamic flows can be complicated (17,25). Hot-film sensors are less fragile and less susceptible to contamination than hot-wire sensors. Probe blockage is not significant in large ducts and away from walls. Thermal anemometers are 180 degrees directionally ambiguous (i.e., flows from the left or right directions give the same output signal), an important factor in flows that may contain flow reversal regions. An industrial-grade system can be built rather inexpensively. The thermal anemometer is usually calibrated against either pressure probes or an LDA.

Laser Doppler Anemometer

The laser Doppler anemometer (LDA) is a relatively expensive and technically advanced point velocity measuring technique that can be used for most types of flows but is also well suited to hostile, combusting, or highly dynamic (unsteady, pulsatile, or highly turbulent) flow environments. It offers good frequency response, small spatial resolution, no probe blockage, and simple signal interpretation, but requires optical access and the presence of scattering particles. This method provides very good temporal resolution for time-accurate measurements in turbulent flows. The method measures the velocity of particles suspended in the moving fluid, not the fluid velocity, so careful planning is required in particle selection to ensure that the particle velocities represent the fluid velocity exactly. The size and concentration of the particles govern the system frequency response (26,27).

Particle Image Velocimetry

Particle image velocimetry (PIV) is a relatively expensive and technically advanced full-field velocity measuring technique that can be used for most types of flows, including hostile and combusting flows. There is no probe blockage of the flow, but it requires optical access and the presence of scattering particles. The method provides an instantaneous snapshot of the flow, providing excellent views of flow structures. Time-dependent quantification of such dynamic flows is possible, but frequency bandwidth is limited to camera frame rate and spatial resolution. As with LDA, this method measures the velocity of particles suspended in the moving fluid, not the fluid velocity, so careful planning is required in particle selection to ensure that the particle velocities represent the fluid velocity exactly.

9.10 SUMMARY

Several reference pressure instruments have been presented that form the working standards for pressure transducer calibration. Pressure transducers convert sensed pressure into an output form that is readily quantifiable. These transducers come in many forms but tend to operate on hydrostatic principles, expansion techniques, or force-displacement methods.

In moving fluids, special care must be taken when measuring pressure to delineate between static and total pressure. Methods for the separate measurement of static and total pressure or for the measurement of the dynamic pressure are readily available and well documented. But improper measuring technique causes errors, lowering the total pressure or increasing the static pressure.

Measuring the local velocity within a moving fluid can be accomplished in a number of ways. Selecting the proper tool requires assessment of the need: mean or fluctuating velocity, point or full field measurement, optical access or opaque boundaries or fluid. Specifically, dynamic pressure, thermal anemometry, Doppler anemometry, and particle velocimetry methods have been presented. As discussed, each method offers advantages over the others, and the best technique must be carefully weighed against the needs and constraints of a particular application.

REFERENCES

1. American Society of Mechanical Engineers (ASME), *PTC 19.2–1987: Pressure Measurement*, ASME International, New York, 1987.
2. Brombacher, W. G., D. P. Johnson, and J. L. Cross, Mercury Barometers and Manometers, *National Bureau Standards Monograph* 8, 1960.
3. McLeod, H. G., Vacuum Gauge, *Philosophical Magazine*, 48, 110, 1874. Reprinted in *History of Vacuum Science and Technology*, edited by T. E. Madey and W. C. Brown, American Vacuum Society, New York, 1984, pp. 102–105.
4. M. Hetenyi, ed., *Handbook of Experimental Stress Analysis*, Wiley, New York, 1950.
5. Way, S., Bending of circular plates with large deflection, *Transactions of the ASME* 56, 1934.
6. Instrument Society of America (ISA), *A Guide for the Dynamic Calibration of Pressure Transducers*, ISA-37.16.01-2002, Instrument Society of America, 2002.
7. Franklin, R. E., and J. M. Wallace, Absolute measurements of static-hole error using flush transducers, *Journal of Fluid Mechanics* 42, 1970.
8. Rayle, R. E., Influence of orifice geometry on static pressure measurements, ASME Paper No. 59-A-234, 1959.
9. Munson, B., D. Young, T. Okishi, *Fundamentals of Fluid Mechanics*, 6th ed., Wiley, New York, 2009.
10. Migliavacca, F., et al., Multiscale modelling in an Biofluidynamics: Application to reconstructive paediatric cardiac surgery, *Journal of Biomechanics*, 39, 6, 2006.
11. Delio, G., G. Schwent, and R. Cesaro, Transient behavior of lumped-constant systems for sensing gas pressures, National Advisory Council on Aeronautics (NACA) TN-1988, 1949.
12. Doebelin, E. O., *Measurement Systems: Application and Design*, 5th ed., McGraw-Hill Science/Engineering/Math, New York, 2003.
13. Hougen, J., O. Martin, and R. Walsh, Dynamics of pneumatic transmission lines, *Control Engr.*, September 1963.
14. King, L. V., On the convection from small cylinders in a stream of fluid: Determination of the convection constants of small platinum wires with application to hot-wire anemometry, *Proceedings of the Royal Society, London* 90, 1914.
15. Hinze, J. O., *Turbulence*, McGraw-Hill, New York, 1959.
16. Collis, D. C., and M. J. Williams, Two-dimensional convection from heated wires at low Reynolds numbers, *Journal of Fluid Mechanics* 6, 1959.
17. Rodi, W., A new method for analyzing hot-wire signals in a highly turbulent flow and its evaluation in a round jet, *DISA Information*, Dantek Electronics, Denmark, 1975. See also, Bruun, H. H., Interpretation of X-wire signals, *DISA Information*, Dantek Electronics, Denmark, 1975.
18. Freymuth, P., A bibliography of thermal anemometry, *TSI Quarterly* 4, 1978.
19. Yeh, Y., and H. Cummins, Localized fluid flow measurement with a He-Ne laser spectrometer, *Applied Physics Letters* 4, 1964.
20. Photon correlation and light beating spectroscopy, H. Z. Cummins and E. R. Pike, eds., *Proceedings of the NATO ASI*, Plenum, New York, 1973.
21. Durst, F., A. Melling, and J. H. Whitelaw, *Principles and Practice of Laser Doppler Anemometry*, Academic Press, New York, 1976.
22. R. J. Goldstein, ed., *Fluid Mechanics Measurements*, 2nd ed., CRC Press, New York, 1996.

23. Raffel, M., Willert, C.E., Wereley, S.T., Kompenhans, J., *Particle Image Velocimetry*, 2nd ed, Springer, Heidelberg, 2007.
24. Goldstein, R. J., and D. Kried, Measurement of laminar flow development in a square duct using a laser doppler flowmeter, *Journal of Applied Mechanics* 34, 1967.
25. Yavuzkurt, S., A guide to uncertainty analysis of hot-wire data, *Transactions of the ASME, Journal of Fluids Engineering* 106, 1984.
26. Maxwell, B. R., and R. G. Seaholtz, Velocity lag of solid particles in oscillating gases and in gases passing through normal shock waves, National Aeronautics and Space Administration TN-D-7490.
27. Dring, R. P., and Suo, M. Particle trajectories in swirling flows, *Transactions of the ASME, Journal of Fluids Engineering* 104, 1982.

NOMENCLATURE

d	diameter (l)	ω_n	natural frequency (t^{-1})
e_i	elemental errors	z	altitude (l)
d_f	fringe spacing (l)	C	capacitance (F)
f_D	doppler frequency (Hz)	E	voltage (V)
h	depth (l)	E_m	bulk modulus of elasticity ($m^{-1}lt^{-2}$)
h_0	reference depth (l)	Gr	Grashof number
k	ratio of specific heats	H	manometer deflection height (l)
p	pressure ($m^{-1}lt^{-2}$)	K	static sensitivity
p_a	applied pressure ($m^{-1}lt^{-2}$)	K_q	charge sensitivity ($m^{-1}lt^{-2}$)
p_{abs}	absolute pressure ($m^{-1}lt^{-2}$)	K_E	voltage sensitivity ($Vm^{-1}t^{-2}$)
p_e	relative static pressure error ($m^{-1}lt^{-2}$)	M	Mach number
p_i	indicated pressure ($m^{-1}lt^{-2}$)	Re_d	Reynolds number, $Re = Vd/\nu$
p_m	measured pressure ($m^{-1}lt^{-2}$)	S	specific gravity
p_t	total or stagnation pressure ($m^{-1}lt^{-2}$)	U	velocity (lt^{-1})
p_v	dynamic pressure ($m^{-1}lt^{-2}$)	\forall	volume (l^3)
q	charge (C)	γ	specific weight ($ml^{-2}t^{-2}$)
r	radius (l)	ϵ	dielectric constant
t	thickness (l)	λ	wavelength (l)
y	displacement (l)	μ	absolute viscosity ($mt^{-1}l^{-1}$)
ρ	density (ml^{-3})	ν	kinematic viscosity (l^2/t)
τ	time constant (t)	ν_p	Poisson ratio
ϕ	latitude		

PROBLEMS

- 9.1** Convert the following absolute pressures to gauge pressure units of N/m²:
- 12.2 psia
 - 2.0 bar abs
 - 29.92 in. H₂O absolute
 - 760 mm Hg abs

- 9.2** Convert the following gauge pressures into absolute pressure relative to one standard atmosphere:
- 12.0 psi
 - 200 mm Hg
 - 10.0 kPa
 - 7.62 cm H₂O
- 9.3** A water-filled manometer is used to measure the pressure in an air-filled tank. One leg of the manometer is open to atmosphere. For a measured manometer deflection of 250 cm water, determine the tank static pressure. Barometric pressure is 101.3 kPa abs.
- 9.4** A deadweight tester is used to provide a standard reference pressure for the calibration of a pressure transducer. A combination of 25.3 kg_f of 7.62-cm-diameter stainless steel disks is needed to balance the tester piston against its internal pressure. For an effective piston area of 5.065 cm² and a piston weight of 5.35 kg_f, determine the standard reference pressure in bars, N/m², and Pa abs. Barometric pressure is 770 mm Hg abs, elevation is 20 m, and latitude is 42 degrees.
- 9.5** The pressure differential across an orifice plate meter is measured using an inclined tube manometer with one pressure attached to each end of the manometer. Under no flow conditions, the manometer deflection is zero. For a set flow rate, the manometer deflects 10 cm H₂O. With a manometer inclination of 30 degrees relative to horizontal, determine the pressure differential across the orifice meter.
- 9.6** Show that the static sensitivity of an inclined tube manometer is a factor of $1/\sin\theta$ higher than for a U-tube manometer.
- 9.7** Determine the static sensitivity of an inclined tube manometer set at an angle of 30 degrees. The manometer tube measures the pressure difference of air using mercury as the manometer fluid.
- 9.8** Show that the instrument (systematic) uncertainty in an inclined tube manometer in Example 9.3 increases to 6.8 N/m² as θ goes to 90 degrees.
- 9.9** Determine the maximum deflection and the natural frequency of a 0.1-in.-thick diaphragm made of steel ($E_m = 30 \text{ Mpsi}$, $v_p = 0.32$, $\rho = 0.28 \text{ lb}_m/\text{in.}^3$) if the diaphragm must be 0.75 in. in diameter. Determine its differential pressure limit.
- 9.10** A strain gauge, diaphragm pressure transducer (accuracy: <0.1% reading) is subjected to a pressure differential of 10 kPa. If the output is measured using a voltmeter having a resolution of 10 mV and accuracy of better than 0.1% of the reading, estimate the uncertainty in pressure at the design stage. How does this change at 100 and 1000 kPa?
- 9.11** Select a practical fluid to use in a manometer to measure pressures up to 69 kPa of an inert gas ($\gamma = 10.4 \text{ N/m}^3$), if water ($\gamma = 9800 \text{ N/m}^3$), oil ($S = 0.82$), and mercury ($S = 13.57$) are available. Discuss the rationale for your choice(s).
- 9.12** An air pressure over the 200- to 400-N/m² range is to be measured relative to atmosphere using a U-tube manometer with mercury ($S = 13.57$). Manometer resolution is 1 mm with a zero error uncertainty of 0.5 mm. Estimate the design-stage uncertainty in gauge pressure based on the manometer indication at 20°C. Would an inclined manometer ($\theta = 30$ degrees) be a better choice if the inclination could be set to within 0.5 degree?
- 9.13** Calculate the design-stage uncertainty in estimating a nominal pressure of 10,000 N/m² using an inclined manometer (resolution: 1 mm; zero error uncertainty: 0.5 mm) with water at 20°C for inclination angles of 10 to 90 degree (using 10-degree increments). The inclination angle can be set to within 1 degree.

- 9.14** The pressure drop across a valve through which air flows is expected to be 10 kPa. If this differential were applied to the two legs of a U-tube manometer filled with mercury, estimate the manometer deflection. What is the deflection if a 30-degree inclined tube manometer were used? $S_{Hg} = 13.6$.
- 9.15** Estimate the sensitivity (pF/mm) of a capacitance transducer, such as in Figure 9.13, using water as the dielectric medium. The transducer plates have an overlap area of $8.1 \pm 0.01 \text{ mm}^2$ with an average gap separation of 1 mm.
- 9.16** A diaphragm pressure transducer is calibrated against a pressure standard that has been certified by the National Institute of Standards and Technology (NIST) ($b = 0.25 \text{ psi}$). Both the standard and pressure transducer output a voltage signal, which is to be measured by a voltmeter ($b = 5 \mu\text{V}$; resolution: $1 \mu\text{V}$). A calibration curve fit yields: $p = 0.564 + 24.0E \pm 0.5 \text{ psi}$ (68%) based on 35 points over the 0- to 100-psi range. When the transducer is installed for its intended purpose, installation effects are estimated to affect its reading by 0.25 psi (68%). Estimate the uncertainty associated with a pressure measurement using the installed transducer-voltmeter system.
- 9.17** A diaphragm pressure transducer is coupled with a water-cooled sensor for high-temperature environments. Its manufacturer claims that it has a rise time of 10 ms, a ringing frequency of 200 Hz, and damping ratio of 0.8. Describe a test plan to verify the manufacturer's specifications. Would this transducer have a suitable frequency response to measure the pressure variations in a typical four-cylinder engine? Show your reasoning.
- 9.18** Find the natural frequency of a 1-mm-thick, 6-mm-diameter steel diaphragm to be used for high-frequency pressure measurements near atmospheric pressure. What would be the maximum operating pressure difference that could be applied? What is the effect of a larger diameter for this application?
- 9.19** Estimate the differential pressure limit for a 0.5-mm-thick, 25-mm-diameter steel diaphragm pressure transducer. $v_p = 0.32$, $E_m = 200 \text{ GPa}$.
- 9.20** The pressure fluctuations in a pipe filled with air at 20°C at about 1 atm is to be measured using a static wall tap, rigid connecting tubing, and a diaphragm pressure transducer. The transducer has a natural frequency of 100,000 Hz. For a tap and tubing diameter of 3.5 mm, a tube length of 0.25 m, and a transducer dead volume of 1600 mm^3 , estimate the resonance frequency of the system. What is the maximum frequency that this system can measure with no more than a 10% dynamic error? Plot the frequency response of the system.
- 9.21** What is the sensitivity of a pitot-static tube pressure relative to velocity?
- 9.22** A pitot-static pressure probe inserted within a large duct indicates a differential pressure of 20.3 cm H_2O . What is the velocity measured?
- 9.23** A tall pitot-static tube is mounted through and 1.5-m above the roof of a performance car such that it senses the freestream flow. Estimate the static, stagnation, and dynamic pressure sensed at 325 kph, if (a) the car is moving on a long, straight section of road; and (b) the car is stationary within an open-circuit wind tunnel where the flow is blown over the car.
- 9.24** The pressure transmission line response equation of Equation 9.23 can be derived by considering the forces acting on a fluid element within the connecting tubing. Develop a model for the system measured pressure response based on an applied pressure force, shear resistance force, and restoring compliance related force through Newton's momentum (second law) principles. Refer to Figure 9.31.

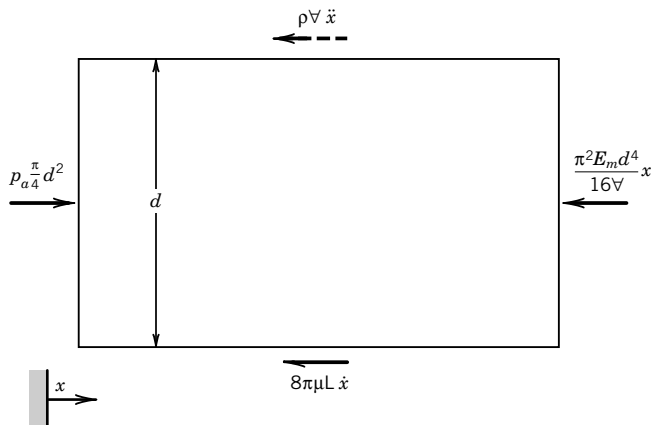


Figure 9.31 Freebody diagram for Problem 9.24.

- 9.25** A 1.5-mm i.d., 1-m-long catheter filled with saline is attached to a diaphragm pressure transducer. The system has a compliance of 2×10^{-4} mL/mm Hg. Estimate the natural frequency and damping ratio of the system. Use water for your calculations.
- 9.26** Compare the inertance of water in a 0.2-m-long tube to that of a 1-m-long tube each of 25-mm and then of 12.5-mm diameter.
- 9.27** The output from a resting healthy human adult heart is about 5 L/min. We can estimate that the mean systemic pressure is 95 mm Hg with a mean atrial pressure of 4 mm Hg. The mean pulmonary pressure is 15 mm Hg with an atrial pressure of 2 mm Hg. Compare the vascular resistance of the left (systemic) circulation to that of the right (pulmonary) circulation. Assume that the flow remains laminar.
- 9.28** The left ventricle of a healthy man ejects 80 mL of blood into the aorta each heart beat. The pressure of the corresponding circulation varies between 120 and 80 mm Hg during each beat, known as the blood pressure, for a change of 40 mm Hg. Estimate the average compliance of the left circulation.
- 9.29** A system similar to that described in Example 9.8 is used to measure surface pressures on a car during a wind tunnel test. Estimate the overall uncertainty of the measurements using the 12-bit A/D converter. Typical wind tunnel measurements of a stock race car at 180 km/hr based on $N = 100$ are:

Position	Pressure (cm H ₂ O)	
	p _{avr}	s _p
Hood	0.8	0.025
Roof	3.3	0.0025
Rear deck	8.0	0.05

- 9.30** Wall pressure taps (e.g., Figs. 9.19 and 9.21) are often used to sense surface pressure and are connected to transducers by connecting tubing. Two race engineers discuss the preferred diameter of the tubing to measure pressure changes on a car as it moves along a track. The tubing length may be

up to 2 m. Engineer A suggests very small 2-mm-diameter tubing to reduce air volume so as to increase response time. Engineer B disagrees and suggests 5-mm tubing to balance air friction with air volume to increase response time. Offer your opinion and its basis. (Hint: Look at length-to-diameter effects.)

- 9.31** Show that Equation 9.23 can be reduced to the fundamental form of Equation 9.22 in terms of system inertance, resistance, and compliance.
- 9.32** Apply a circuit analysis to an RLC analog of Figure 9.22 showing the steps to achieve Equations 9.21 through 9.23. Use the direct analogy equating E_a , E_m with p_a , p_m , respectively.
- 9.33** Determine the resolution of a manometer required to measure the velocity of air from 5 to 50 m/s using a pitot-static tube and a manometer fluid of mercury ($S = 13.57$) to achieve a zero-order uncertainty of 5% and 1%.
- 9.34** A long cylinder is placed into a wind tunnel and aligned perpendicular to an oncoming freestream. Static wall pressure taps are located circumferentially about the centerline of the cylinder at 45-degree increments with 0 degrees at the impact (stagnation) position. Each tap is connected to a separate manometer referenced to atmosphere. A pitot-static tube indicates an upstream dynamic pressure of 20.3 cm H₂O, which is used to determine the freestream velocity. The following static pressures are measured:

Tap (degrees)	p (cm H ₂ O)	Tap (degrees)	p (cm H ₂ O)
0	0.0	135	5.0
30	20.3	180	5.2
90	81.3		

Compute the local velocities around the cylinder if the total pressure in the flow remains constant. $p_{\text{atm}} = 101.3 \text{ kPa abs}$, $T_{\text{atm}} = 16^\circ\text{C}$.

- 9.35** A 6-mm-diameter pitot-static tube is used as a working standard to calibrate a hot-wire anemometer in 20°C air. If dynamic pressure is measured using a water-filled micromanometer, determine the smallest manometer deflection for which the pitot-static tube can be considered as accurate without correction for viscous effects.
- 9.36** For the thermal anemometer in Figures 9.26 and 9.27, determine the decade resistance setting required to set a platinum sensor at 40°C above ambient if the sensor ambient resistance is 110 Ω and $R_3 = 500 \Omega$ and $R_4 = 500 \Omega$, $\alpha = 0.00395^\circ\text{C}^{-1}$.
- 9.37** Determine the static sensitivity of the output from a constant resistance anemometer as a function of velocity. Is it more sensitive at high or at low velocities?
- 9.38** A laser Doppler anemometer setup in a dual-beam mode uses a 600-mm focal length lens ($\theta = 5.5$ degrees) and an argon-ion laser ($\lambda = 514.4 \text{ nm}$). Compute the Doppler shift frequency, f_D , expected at 1, 10, and 100 m/s. Repeat for a 300-mm lens ($\theta = 7.3$ degrees).
- 9.39** A set of 5000 measurements of velocity at a point in a flow using a dual-beam LDA gives the following results:

$$\bar{U} = 21.37 \text{ m/s} \quad s_U = 0.43 \text{ m/s}$$

For the system, $\theta = 6$ degrees and $\lambda = 623.8 \text{ nm}$, what is the mean Doppler frequency measured?

- 9.40** In order to measure the flow rate in a $2\text{ m} \times 2\text{ m}$ air conditioning duct, an engineer uses a pitot-static probe to measure dynamic head. The duct is divided into nine equal rectangular areas with the pressure measured at the center of each. Based on the results below, estimate the flow rate for air at 15°C and 1 atm.

Position	1	2	3	4	5	6	7	8	9
$H\text{ (mm H}_2\text{O)}$	5.0	6.0	6.5	6.0	5.0	6.5	7.5	7.0	5.0

Chapter 10

Flow Measurements

10.1 INTRODUCTION

The rate at which a fluid moves through a conduit is measured in terms of the quantity known as the flow rate. This chapter discusses some of the most common and accepted methods for measuring flow rate. Flow rate can be expressed in terms of a flow volume per unit time, known as the *volume flow rate*, or as a mass flow per unit time, known as the *mass flow rate*. Flow rate devices, called flow meters, are used to quantify, totalize, or monitor flowing processes. Type, accuracy, size, pressure drop, pressure losses, capital and operating costs, and compatibility with the fluid are important engineering design considerations for choosing a flow metering device. All methods have both desirable and undesirable features that necessitate compromise in the selection of the best method for the particular application, and many such considerations are discussed in this chapter. Inherent uncertainties in fluid properties, such as density, viscosity, or specific heat, can affect the accuracy of a flow measurement. However, some techniques, such as those incorporated into coriolis mass flow meters, do not require knowledge of exact fluid properties, allowing for highly accurate mass flow measurements in demanding engineering applications. The chapter objective is to present both an overview of basic flow metering techniques for proper meter selection, as well as those design considerations important in the integration of a flow rate device with the process system it will meter.

Upon completion of this chapter, the reader will be able to

- relate velocity distribution to flow rate within conduits,
- use engineering test standards to select and specify size, specify installation considerations, and use common obstruction meters,
- understand the differences between volume flow rate and mass flow rate and the means required to measure each,
- describe the physical principles employed in various commercially available types of flow meters and the engineering terms common to their use, and
- clearly describe primary and secondary calibration methods for flow meters.

10.2 HISTORICAL BACKGROUND

The importance to engineered systems give flow measurement methods their rich history. The earliest available accounts of flow metering were recorded by Hero of Alexandria (ca. 150 b.c.) who proposed a scheme to regulate water flow using a siphon pipe attached to a constant head reservoir.

The early Romans developed elaborate water systems to supply public baths and private homes. In fact, Sextus Frontinius (A.D. 40–103), commissioner of water works for Rome, authored a treatise on design methods for urban water distribution systems. Evidence suggests that Roman designers understood correlation between volume flow rate and pipe flow area. Weirs were used to regulate bulk flow through aqueducts, and the cross-sectional area of terra-cotta pipe was used to regulate fresh running water supplies to individual buildings.

Following a number of experiments conducted using olive oil and water, Leonardo da Vinci (1452–1519) first formally proposed the modern continuity principle: that duct area and fluid velocity were related to flow rate. However, most of his writings were lost until centuries later, and Benedetto Castelli (ca. 1577–1644), a student of Galileo, has been credited in some texts with developing the same steady, incompressible continuity concepts in his day. Isaac Newton (1642–1727), Daniel Bernoulli (1700–1782), and Leonhard Euler (1707–1783) built the mathematical and physical bases on which modern flow meters would later be developed. By the nineteenth century, the concepts of continuity, energy, and momentum were sufficiently understood for practical exploitation. Relations between flow rate and pressure losses were developed that would permit the tabulation of the hydraulic coefficients necessary for the quantitative engineering design of many modern flow meters.

10.3 FLOW RATE CONCEPTS

The flow rate through a conduit, be it a pipeline, duct, or channel, depends on fluid density, average fluid velocity, and conduit cross-sectional area. Consider fluid flow through a circular pipe of radius r_1 and having a velocity profile at some axial pipe cross section given by $u(r, \theta)$. The mass flow rate depends on the average mass flux flowing through a cross-sectional area; that is, it is the average product of fluid density times fluid velocity and area, as given by

$$\dot{m} = \iint_A \rho u(r, \theta) dA = \bar{\rho} \bar{U} A \quad (10.1)$$

The pipe area is simply $A = \pi r_1^2$. We see that to directly make a mass flow rate measurement, the device must be sensitive to the area-averaged mass flux per unit volume, $\bar{\rho} \bar{U}$, or to the fluid mass passing through it per unit time. Mass flow rate has the dimensions of mass per unit of time (e.g., units of kg/s, lb_m/s, etc.).

The volume flow rate depends only on the area-averaged velocity over a cross section of flow as given by

$$Q = \iint_A u dA = \bar{U} A \quad (10.2)$$

So to directly measure volume flow rate requires a device that is sensitive either to the average velocity, \bar{U} , or to the fluid volume passing through it per unit time. Volume flow rate has dimensions of volume per unit time (e.g., units of m³/s, ft³/s, etc.).

The difference between Equations 10.1 and 10.2 is quite significant, in that either requires a very different approach to its measurement: one sensitive to the product of density and velocity or to mass rate, and the other sensitive only to the average velocity or to volume rate. In the simplest case, where density is a constant, the mass flow rate can be inferred by multiplying the measured volume flow rate by the density. But in the metering of many fluids, this assumption may not be good enough

to achieve necessary accuracy. This can be because the density changes or it may not be well known, such as in the transport of polymers or petrochemicals, or because small errors in density accumulate into large errors, such as in the transport of millions of cubic meters of product per day.

The flow character can affect the accuracy of a flow meter. The flow through a pipe or duct can be characterized as being laminar, turbulent, or a transition between the two. Flow character is determined through the nondimensional parameter known as the Reynolds number, defined by

$$\text{Re}_{d_1} = \frac{\overline{U}d_1}{v} = \frac{4Q}{\pi d_1 v} \quad (10.3)$$

where v is the fluid kinematic viscosity and d_1 is the diameter for circular pipes. In pipes, the flow is laminar when $\text{Re}_{d_1} < 2000$ and turbulent at higher Reynolds number. The Reynolds number is a necessary parameter in estimating flow rate when using several of the types of flow meters discussed. In estimating the Reynolds number in noncircular conduits, the hydraulic diameter, $4r_H$, is used in place of diameter d_1 , where r_H is the wetted conduit area divided by its wetted perimeter.

10.4 VOLUME FLOW RATE THROUGH VELOCITY DETERMINATION

Volume flow rate can be determined with direct knowledge of the velocity profile as indicated by Equation 10.2. This requires measuring the velocity at multiple points along a cross section of a conduit to estimate the velocity profile. For highest accuracy, several traverses should be made at differing circumferential locations to account for flow nonsymmetry. Methods for determining the velocity at a point include any of those previously discussed in Chapter 9. Because it is a tedious method, this procedure is most often used for the one-time verification or calibration of system flow rates. For example, the procedure is often used in ventilation system setup and problem diagnosis, where the installation of an in-line flow meter is not necessary because operation does not require continuous monitoring.

When using this technique in circular pipes, a number of discrete measuring positions n are chosen along each of m flow cross sections spaced at $360/m$ degrees apart, such as shown in Figure 10.1. A velocity probe is traversed along each flow cross section, with readings taken at each

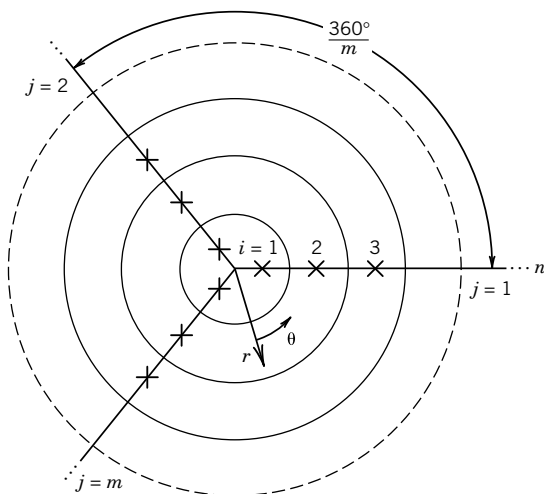


Figure 10.1 Location of n measurements along m radial lines in a pipe.

measurement position. There are several options in selecting measuring positions for different-shaped ducts, and such details are specified in available engineering test standards (1, 2, 4, 15). The simplest method is to divide the flow area into smaller equal areas, making measurements at the centroid of each small area and assigning the measured velocity to that area. Regardless of the option selected, the average flow rate is estimated along each cross section traversed using Equation 10.2 and the pooled mean of the flow rates for the m cross sections calculated to yield the best estimate of the duct flow rate. Uncertainty is assessed both by repeating the measurements and by analyzing for spatial variation effects. Example 10.1 illustrates this method for estimating volume flow rate.

Example 10.1

A steady flow of air at 20°C passes through a 25.4-cm inside diameter (i.d.) circular pipe. A velocity-measuring probe is traversed along three cross-sectional lines ($j = 1, 2, 3$) of the pipe, and measurements are made at four radial positions ($i = 1, 2, 3, 4$) along each traverse line, such that $m = 3$ and $n = 4$. The locations for each measurement are selected at the centroids of equally spaced areal increments as indicated below (1, 3). Determine the volume flow rate in the pipe.

Radial Location, i	r/r_1	U_{ij} (m/s)		
		Line 1 ($j = 1$)	Line 2 ($j = 2$)	Line 3 ($j = 3$)
1	0.3536	8.71	8.62	8.78
2	0.6124	6.26	6.31	6.20
3	0.7906	3.69	3.74	3.79
4	0.9354	1.24	1.20	1.28

KNOWN $U_{ij}(r/r_1)$ for $i = 1, 2, 3, 4; j = 1, 2, 3$

$$d_1 = 25.4 \text{ cm} (A = \pi d_1^2 / 4 = 0.051 \text{ m}^2)$$

ASSUMPTIONS Constant and steady pipe flow during all measurements; Incompressible flow

FIND Volume flow rate, Q

SOLUTION The flow rate is found by integrating the velocity profile across the duct along each line and subsequently averaging the three values. For discrete velocity data, Equation 10.2 is written along each line, $m = 1, 2, 3$, as

$$Q_j = 2\pi \int_0^{r_1} Ur dr \approx 2\pi \sum_{i=1}^4 U_{ij} r \Delta r$$

where Δr is the radial distance separating each position of measurement. This can be further simplified since the velocities are located at positions that make up the centroids of equal areas:

$$Q_j = \frac{A}{4} \sum_{i=1}^4 U_{ij}$$

Then, the mean flow rate along each line of traverse is

$$Q_1 = 0.252 \text{ m}^3/\text{s} \quad Q_2 = 0.252 \text{ m}^3/\text{s} \quad Q_3 = 0.254 \text{ m}^3/\text{s}$$

The average pipe flow rate \bar{Q} is the pooled mean of the individual flow rates

$$\bar{Q} = \langle Q \rangle = \frac{1}{3} \sum_{j=1}^3 Q_j = 0.253 \text{ m}^3/\text{s}$$

Example 10.2

Referring to Example 10.1, determine a value of the systematic standard uncertainty in mean flow rate due to the measured spatial variation.

KNOWN Data of Example 10.1 over three ($m = 3$) traverse sections.

SOLUTION The systematic standard uncertainty in mean flow rate due to error introduced by the measured spatial variations is estimated by

$$b_{\bar{Q}} = \frac{s_{\langle Q \rangle}}{\sqrt{m}} = \frac{\sqrt{\sum_{j=1}^3 (Q_j - \langle Q \rangle)^2 / 2}}{\sqrt{3}} = \frac{0.0012}{\sqrt{3}} = 0.0007 \text{ m}^3/\text{s} \quad \text{with } v = 2$$

10.5 PRESSURE DIFFERENTIAL METERS

The operating principle of a pressure differential flow rate meter is based on the relationship between volume flow rate and the pressure drop $\Delta p = p_1 - p_2$, between two locations along the flow path,

$$Q \propto (p_1 - p_2)^n \quad (10.4)$$

where $n = 1$ for laminar flow occurring between the pressure measurement locations and $n = 1/2$ for fully turbulent flow. Under steady flow conditions, an intentional reduction in flow area between locations 1 and 2 causes a measurable local pressure drop across this flow path. This reduced flow area leads to a concurrent local increase in velocity due to flow continuity (conservation of mass) principles. The pressure drop is in part due to the so-called Bernoulli effect, the inverse relationship between local velocity and pressure, but is also due to flow energy losses. Pressure differential flow rate meters that use area reduction methods are commonly called *obstruction meters*.

Obstruction Meters

Three common obstruction meters are the *orifice plate*, the *venturi*, and the *flow nozzle*. Flow area profiles of each are shown in Figure 10.2. These meters are usually inserted in-line with a pipe, such as between pipe flanges. This class of meters as a whole operates using similar physical reasoning to relate volume flow rate to pressure drop. Referring to Figure 10.3, consider an energy balance between two control surfaces for an incompressible fluid flow through the arbitrary control volume

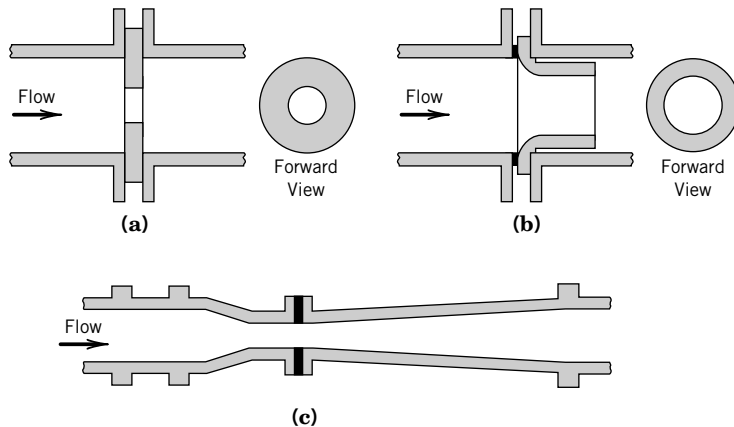


Figure 10.2 Flow area profiles of common obstruction meters. (a) Square-edged orifice plate meter. (b) American Society of Mechanical Engineers (ASME) long radius nozzle. (c) ASME Herschel venturi meter.

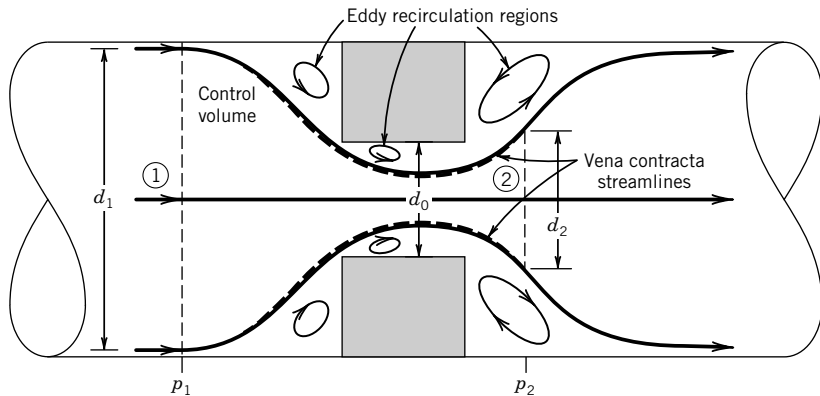


Figure 10.3 Control volume concept as applied between two streamlines for flow through an obstruction meter.

shown. Under the assumptions of incompressible, steady and one-dimensional flow with no external energy transfer, the energy equation is

$$\frac{p_1}{\gamma} + \frac{\bar{U}_1^2}{2g} = \frac{p_2}{\gamma} + \frac{\bar{U}_2^2}{2g} + h_{L_{1-2}} \quad (10.5)$$

where $h_{L_{1-2}}$ denotes the head losses occurring between control surfaces 1 and 2.

For incompressible flows, conservation of mass between cross-sectional areas 1 and 2 gives

$$\bar{U}_1 = \bar{U}_2 \frac{A_2}{A_1} \quad (10.6)$$

Then, substituting Equation 10.6 into Equation 10.5 and rearranging yields the incompressible volume flow rate,

$$Q_I = \bar{U}_2 A_2 = \frac{A_2}{\sqrt{1 - (A_2/A_1)^2}} \sqrt{\frac{2(p_1 - p_2)}{\rho}} + 2gh_{L_{1-2}} \quad (10.7)$$

where the subscript I emphasizes that Equation 10.7 gives an incompressible flow rate. Later we drop the subscript.

When the flow area changes abruptly, the effective flow area immediately downstream of the area reduction is not necessarily the same as the pipe flow area. This was originally investigated by Jean Borda (1733–1799) and illustrated in Figure 10.3. When a fluid cannot exactly follow a sudden area expansion due to its own inertia, a central core flow called the vena contracta forms that is bounded by regions of slower moving recirculating eddies. The pressure sensed with pipe wall taps corresponds to the higher moving velocity within the vena contracta with its unknown flow area, A_2 . To account for this unknown, we introduce a contraction coefficient C_c , where $C_c = A_2/A_0$, with A_0 based on the meter throat diameter, into Equation 10.7. This gives

$$Q_I = \frac{C_c A_0}{\sqrt{1 - (C_c A_0 / A_1)^2}} \sqrt{\frac{2(p_1 - p_2)}{\rho}} + 2gh_{L_{1-2}} \quad (10.8)$$

Furthermore the frictional head losses can be incorporated into a friction coefficient, C_f , such that Equation 10.8 becomes

$$Q_I = \frac{C_f C_c A_0}{\sqrt{1 - (C_c A_0 / A_1)^2}} \sqrt{\frac{2(p_1 - p_2)}{\rho}} \quad (10.9)$$

For convenience, the coefficients are factored out of Equation 10.9 and replaced by a single coefficient known as the *discharge coefficient*, C . Keeping in mind that the ideal flow rate would have no losses and no vena contracta, the discharge coefficient represents the ratio of the actual flow rate through a meter to the ideal flow rate possible for the pressure drop measured, that is, $C = Q_{I_{\text{actual}}} / Q_{I_{\text{ideal}}}$. Reworking Equation 10.9 leads to the incompressible operating equation

$$Q_I = C E A_0 \sqrt{\frac{2\Delta p}{\rho}} = K_0 A_0 \sqrt{\frac{2\Delta p}{\rho}} \quad (10.10)$$

where E , known as the velocity of approach factor, is defined by

$$E = \frac{1}{\sqrt{1 - (A_0 / A_1)^2}} = \frac{1}{\sqrt{1 - \beta^4}} \quad (10.11)$$

with the beta ratio defined as $\beta = d_0/d_1$, and where $K_0 = CE$ is called the *flow coefficient*.

The discharge coefficient and the flow coefficient are tabulated quantities found in test standards (1, 3, 4). Each is a function of the flow Reynolds number and the β ratio for each particular obstruction flow meter design, $C = f(\text{Re}_d, \beta)$ and $K_0 = f(\text{Re}_d, \beta)$.

Compressibility Effects

In compressible gas flows, compressibility effects in obstruction meters can be accounted for by introducing the compressible adiabatic expansion factor, Y . Here Y is defined as the ratio of the actual compressible volume flow rate, Q , divided by the assumed incompressible flow rate Q_I . Combining with Equation 10.10 yields

$$Q = Y Q_I = C E A_0 Y \sqrt{2\Delta p / \rho_1} \quad (10.12)$$

where ρ_1 is the upstream fluid density. When $Y = 1$, the flow is incompressible, and Equation 10.12 reduces to Equation 10.10. *Equation 10.12 represents the most general form of the working equation for volume flow rate determination when using an obstruction meter.*

The expansion factor, Y , depends on several values: the β ratio, the gas specific heat ratio, k , and the relative pressure drop across the meter, $(p_1 - p_2)p_1$, for a particular meter type, that is, $Y = f[\beta, k, (p_1 - p_2)/p_1]$. As a general rule, compressibility effects should be considered if $(p_1 - p_2)/p_1 \geq 0.1$.

Standards

The flow behaviors of the most common obstruction meters, namely the orifice plate, venturi, and flow nozzle, have been studied to such an extent that these meters are used extensively without calibration. Values for the discharge coefficients, flow coefficients, and expansion factors are tabulated and available in standard U.S. and international flow handbooks along with standardized construction, installation, and operation techniques (1, 3, 4, 16). Equations 10.10 and 10.12 are very sensitive to pressure tap location. For steam or gas flows, pressure taps should be oriented on the top or side of the pipe; for liquids, pressure taps should be oriented on the side. We discuss the recommended standard tap locations with each meter (1, 4). A nonstandard installation or design requires an *in situ* calibration.

Orifice Meter

An orifice meter consists of a circular plate having a central hole (orifice). The plate is inserted into a pipe so as to effect a flow area change. The orifice hole is smaller than the pipe diameter and arranged to be concentric with the pipe's i.d. The common square-edged orifice plate is shown in Figure 10.4. Installation is simplified by housing the orifice plate between two pipe flanges. With this installation technique any particular orifice plate is interchangeable with others of different β value. The simplicity of the design allows for a range of β values to be maintained on hand at modest expense.

For an orifice meter, plate dimensions and use are specified by engineering standards (1, 4). Equation 10.12 is used with values of A_0 and β based on the orifice (hole) diameter, d_o . The plate thickness should be between 0.005 d_1 and 0.02 d_1 , otherwise a taper must be added to the downstream side (1, 4). The exact placement of pressure taps is crucial to use standard coefficients. Standard pressure tap locations include (1) flange taps where pressure tap centers are located 25.4 mm (1 in.) upstream and 25.4 mm (1 in.) downstream of the nearest orifice face, (2) d and $d/2$ taps located one pipe diameter upstream and one-half diameter downstream of the upstream orifice face, and (3) vena contracta taps. Nonstandard tap locations always require *in situ* meter calibration.

Values for the flow coefficient, $K_0 = (\text{Re}_{d_1}, \beta)$ and for the expansion factor, $Y = f[\beta, k, (p_1 - p_2)/p_1]$ for a square-edged orifice plate are given in Figures 10.5 and 10.6 based on the use of flange taps. The relative instrument systematic uncertainty in the discharge coefficient (3) is $\sim 0.6\%$ of C for $0.2 \leq \beta \leq 0.6$ and $\beta\%$ of C for all $\beta > 0.6$. The relative instrument systematic uncertainty for the expansion factor is about $[4(p_1 - p_2)/p_1]\%$ of Y . Realistic estimates of the overall systematic uncertainty in estimating Q using an orifice meter are between 1% (high β) and 3% (low β) at high Reynolds numbers when using standard tables. Although the orifice plate represents a relatively inexpensive flow meter solution with an easily measurable pressure drop,

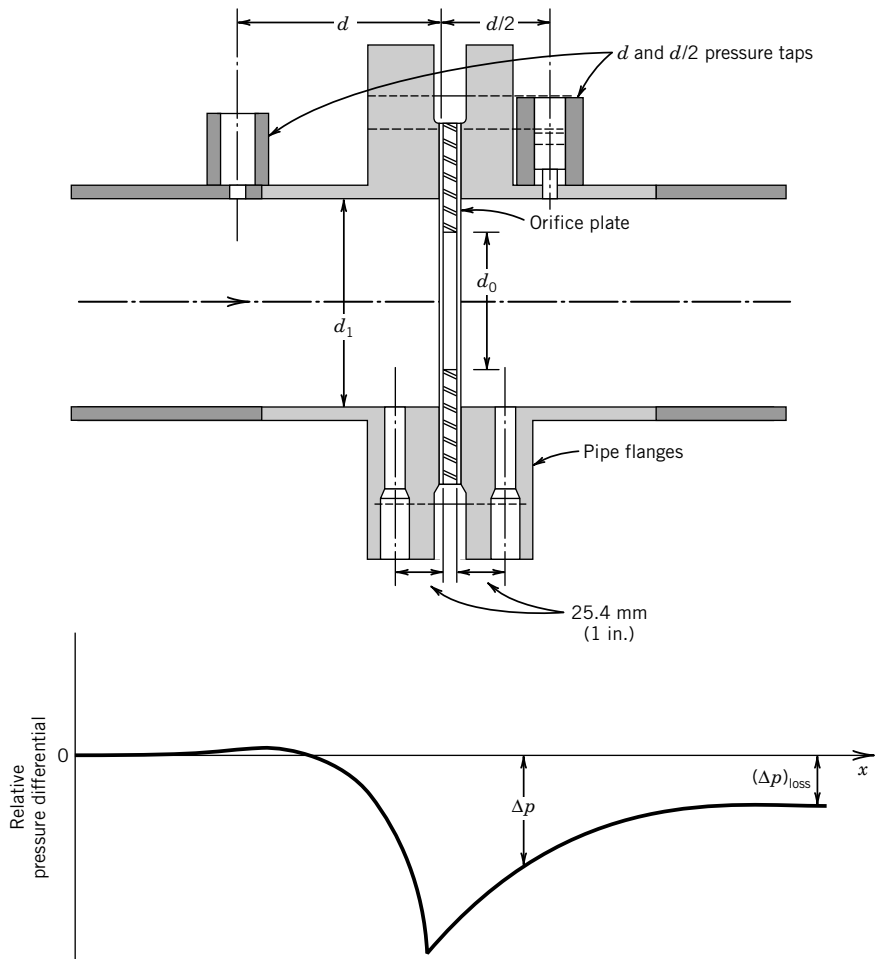


Figure 10.4 Square-edged orifice meter installed in a pipeline with optional 1 d and $\frac{1}{2} d$, and flange pressure taps shown. Relative flow pressure drop along pipe axis is shown.

it introduces a large permanent pressure loss, $(\Delta p)_{loss} = \rho g h_L$, into the flow system. The pressure drop is illustrated in Figure 10.4 with the pressure loss estimated from Figure 10.7.

Rudimentary versions of the orifice plate meter have existed for several centuries. Both Torricelli and Newton used orifice plates to study the relation between pressure head and efflux from reservoirs, although neither ever got the discharge coefficients quite right (5).

Venturi Meter

A venturi meter consists of a smooth converging ($21^\circ \pm 1^\circ$) conical contraction to a narrow throat followed by a shallow diverging conical section, as shown in Figure 10.8. The engineering standard venturi meter design uses either a 15-degree or 7-degree divergent

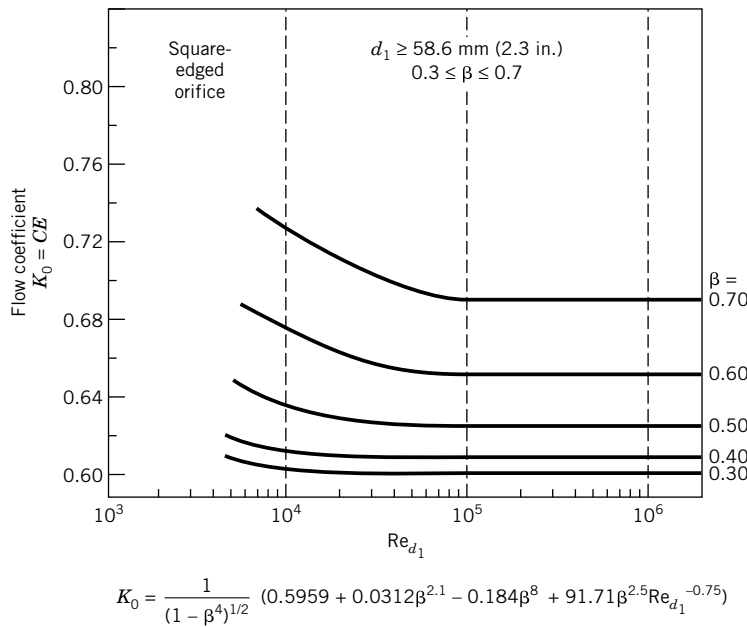


Figure 10.5 Flow coefficients for a square-edged orifice meter having flange pressure taps. (Courtesy of American Society of Mechanical Engineers, New York, NY; compiled from data in reference 1.)

section (1, 4). The meter is installed between two flanges intended for this purpose. Pressure taps are located just ahead of the upstream contraction and at the throat. Equation 10.12 is used with values for both A and β based on the throat diameter, d_0 .

The quality of a venturi meter ranges from cast to precision-machined units. The discharge coefficient varies little for pipe diameters above 7.6 cm (3 in.). In the operating range $2 \times 10^5 \leq Re_{d_1} \leq 2 \times 10^6$ and $0.4 \leq \beta \leq 0.75$, a value of $C = 0.984$ with a systematic uncertainty of 0.7% (95%) for cast units and $C = 0.995$ with a systematic uncertainty of 1% (95%) for machined units should be used (1, 3, 4). Values for expansion factor are shown in Figure 10.6 and have an instrument systematic uncertainty of $[(4 + 100\beta^2)(p_1 - p_2)/p_1]\%$ of Y (3). Although a venturi meter presents a much higher initial cost over an orifice plate, Figure 10.7 demonstrates that the meter shows a much smaller permanent pressure loss for a given installation. This translates into lower system operating costs for the pump or blower used to move the flow.

The modern venturi meter was first proposed by Clemens Herschel (1842–1930). Herschel's design was based on his understanding of the principles developed by several men, most notably those of Daniel Bernoulli. However, he cited the studies of contraction/expansion angles and their corresponding resistance losses by Giovanni Venturi (1746–1822) and later those by James Francis (1815–1892) as being instrumental to his design of a practical flow meter.

Flow Nozzles

A flow nozzle consists of a gradual contraction from the pipe's inside diameter down to a narrow throat. It needs less installation space than a venturi meter and has about 80% of the initial cost. Common forms are the ISO 1932 nozzle and the ASME long radius nozzle (1, 4). The long radius

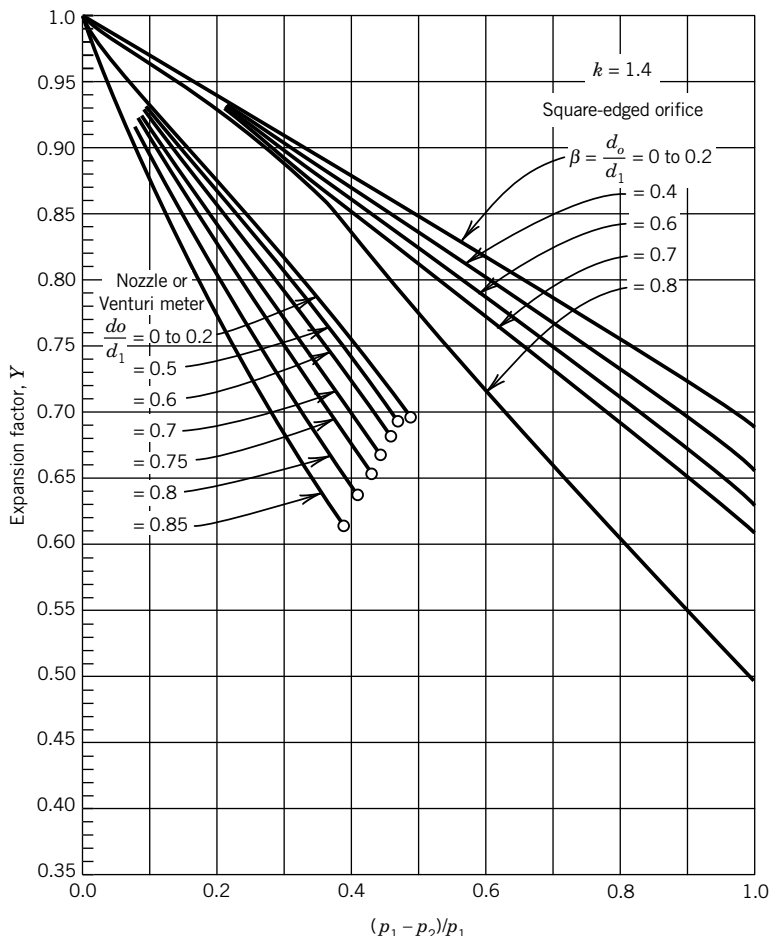


Figure 10.6 Expansion factors for common obstruction meters with $k = c_p/c_v = 1.4$. (Courtesy of American Society of Mechanical Engineers, New York, NY; compiled and reprinted from reference 1.)

nozzle contraction is that of the quadrant of an ellipse, with the major axis aligned with the flow axis, as shown in Figure 10.9. The nozzle is typically installed inline, but can also be used at the inlet to and the outlet from a plenum or reservoir or at the outlet of a pipe. Pressure taps are usually located (1) at one pipe diameter upstream of the nozzle inlet and at the nozzle throat using either wall or throat taps, or (2) d and $d/2$ wall taps located one pipe diameter upstream and one-half diameter downstream of the upstream nozzle face. The flow rate is determined from Equation 10.12 with values for A_o and β based on the throat diameter. Typical values for the flow coefficient and expansion factor are given in Figures 10.10 and 10.6. The relative instrument systematic uncertainty at 95% confidence for the discharge coefficient is about 2% of C and for the expansion factor is about $[2(p_1 - p_2)/p_1]\%$ of Y (3). The permanent loss associated with a flow nozzle is larger than for a comparable venturi but significantly smaller than for an orifice (Fig. 10.7) for the same pressure drop.

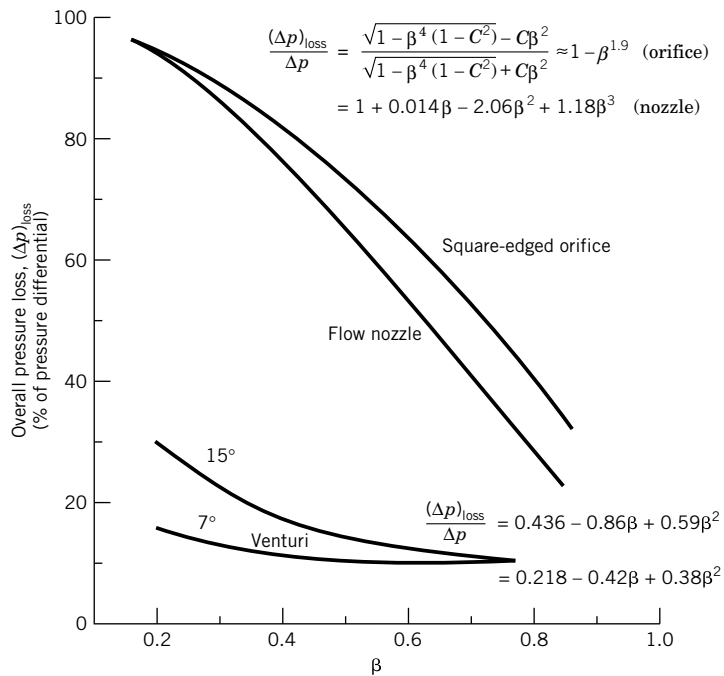


Figure 10.7 The permanent pressure loss associated with flow through common obstruction meters. (Courtesy of American Society of Mechanical Engineers, New York, NY; compiled and reprinted from reference 1.)

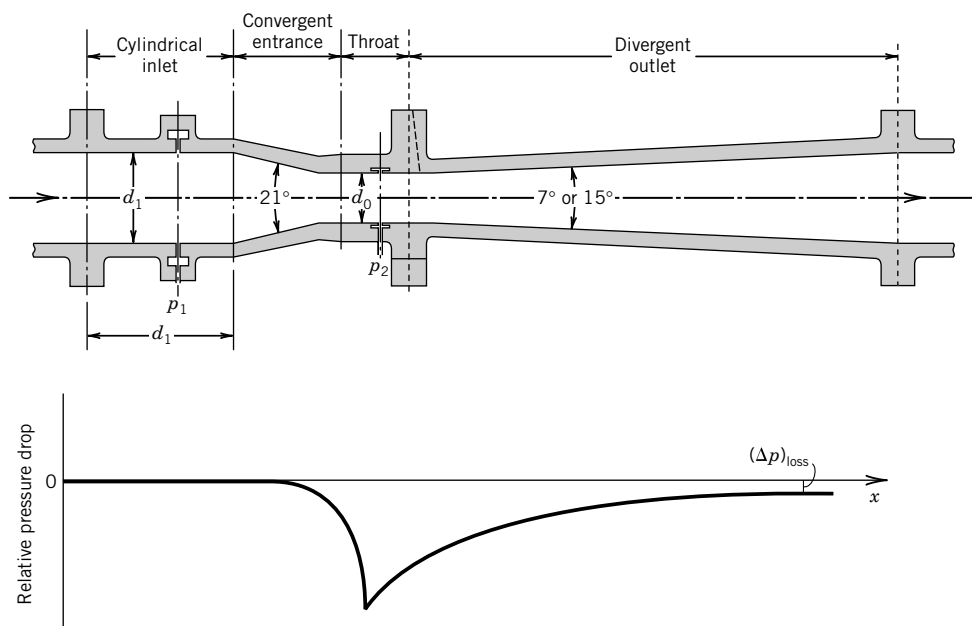


Figure 10.8 The Herschel venturi meter with the associated flow pressure drop along its axis.

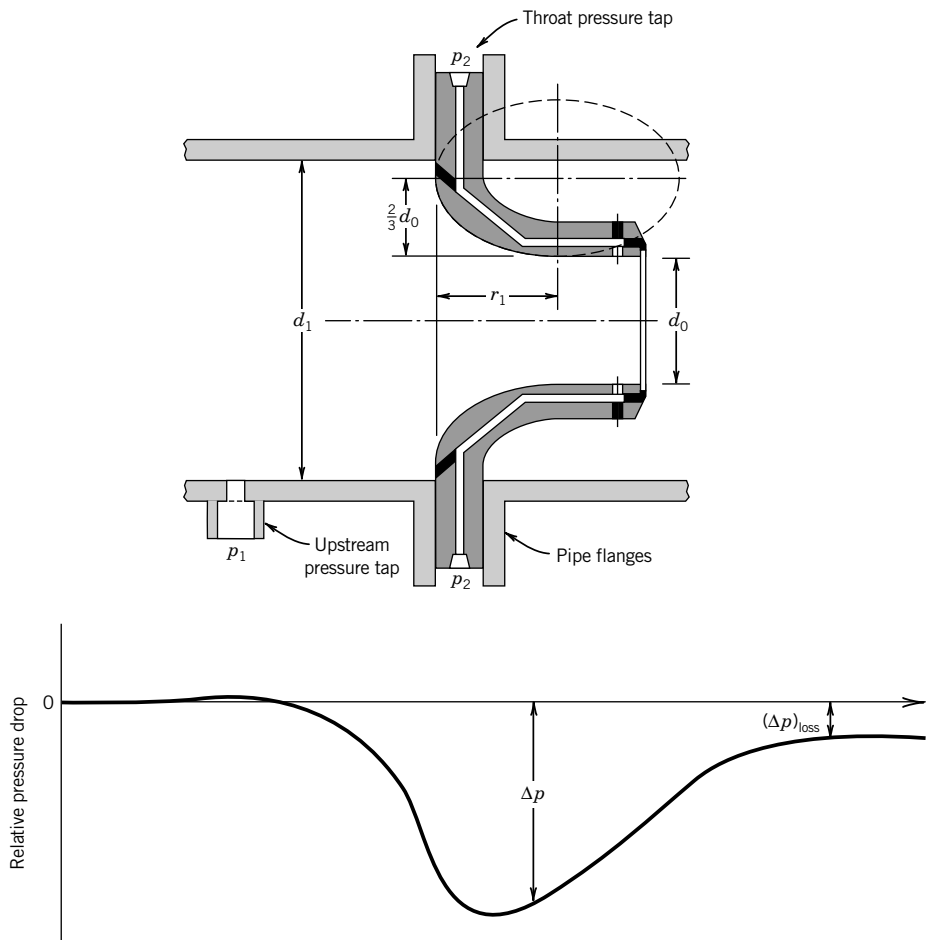


Figure 10.9 The ASME long-radius nozzle with the associated flow pressure drop along its axis.

The idea of using a nozzle as a flow meter was first proposed in 1891 by John Ripley Freeman (1855–1932), an inspector and engineer employed by a fire insurance firm. His work required tedious tests to quantify pressure losses in pipes, hoses, and fittings. He noted a consistent relationship between pressure drop and flow rate through fire nozzles at higher flow rates.

Example 10.3

The U-tube manometer filled with manometer fluid (of specific gravity S_m) of Figure 10.11 is used to measure the pressure drop across an obstruction meter. A fluid having specific gravity S flows through the meter. Determine a relationship between the meter flow rate and the measured manometer deflection, H .

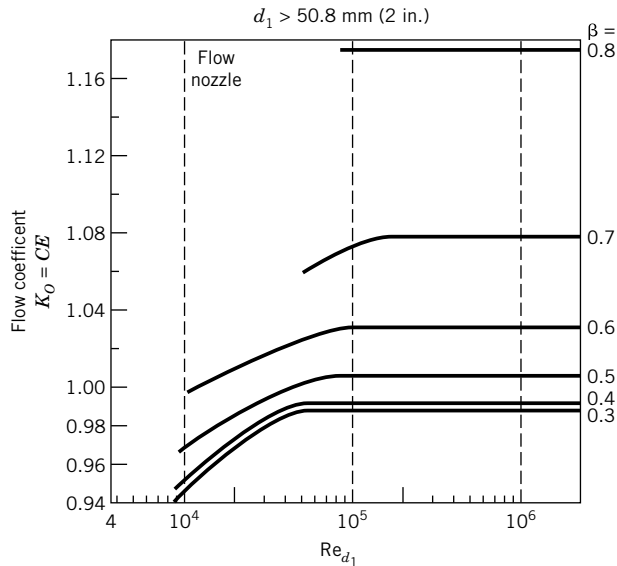


Figure 10.10 Flow coefficients for an ASME long-radius nozzle with a throat pressure tap. (Courtesy of American Society of Mechanical Engineers, New York, NY; compiled from reference 1.)

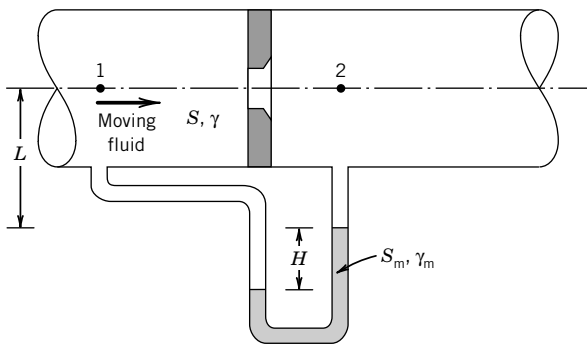


Figure 10.11 Manometer and flow meter of Example 10.3. A taper must be added to the downstream side of the orifice hole when the plate thickness exceeds $0.02d_1$ (1).

KNOWN Fluid (of specific gravity S and specific weight γ)
Manometer fluid (of specific gravity S_m and specific weight γ_m)

ASSUMPTION Densities of the fluids remain constant.

FIND $Q = f(H)$

SOLUTION Equation 10.12 provides a relationship between flow rate and flow pressure drop. From Figure 10.11 and hydrostatic principles, (see Chapter 9) the pressure drop measured by the manometer is

$$\Delta p = p_1 - p_2 = \gamma_m H - \gamma H = (\gamma_m - \gamma)H = \gamma H[(S_m/S) - 1]$$

Substituting this relation into Equation 10.12 yields the working equation based on the equivalent pressure head:

$$Q = CEA_o Y \sqrt{2gH[(S_m/S) - 1]} \quad (10.13)$$

Example 10.4

A 10-cm-diameter, square-edged orifice plate is used to meter the steady flow of 16°C water through a 20-cm pipe. Flange taps are used and the pressure drop measured is 50 cm Hg. Determine the pipe flow rate. The specific gravity of mercury is 13.5.

KNOWN $d_1 = 20 \text{ cm}$ $H = 50 \text{ cm Hg}$ $d_0 = 10 \text{ cm}$
Water properties (properties are from Appendix B)

$$\mu = 1.08 \times 10^{-3} \text{ N-s/m}^2 \quad \rho = 999 \text{ kg/m}^3$$

ASSUMPTIONS Incompressible flow of a liquid ($Y = 1$)

FIND Volume flow rate, Q

SOLUTION Equation 10.12 is used with an orifice plate, and it requires knowledge of the product CE . The beta ratio is $\beta = d_0/d_1 = 0.5$, so the velocity of approach factor is calculated from Equation 10.11:

$$E = \frac{1}{\sqrt{1 - \beta^4}} = \frac{1}{\sqrt{1 - 0.5^4}} = 1.0328$$

We know that $C = f(\text{Re}_{d_1}, \beta)$. The flow Reynolds number is estimated using Equation 10.3, which can be modified with the relation, $v = \mu/\rho$,

$$\text{Re}_{d_1} = \frac{4Q}{\pi d_1 v} = \frac{4\rho Q}{\pi d_1 \mu}$$

We see that without information concerning Q , we cannot determine the Reynolds number, and so C cannot be determined explicitly.

Instead, a trial-and-error iteration is undertaken: Guess a value for K_0 (or for C) and iterate. A good start is to guess a value at a high value of Re_{d_1} . This is the flat region of Figure 10.5, so choose a value of $K_0 = CE = 0.625$.

Based on the manometer deflection and Equation 10.13 (see Ex. 10.2),

$$\begin{aligned} Q &= CEA_0 Y \sqrt{2gH[(S_m/S) - 1]} = K_0 A_0 Y \sqrt{2gH[(S_m/S) - 1]} \\ &= (0.625)(\pi/4)(0.10 \text{ m})^2(1) \sqrt{2(9.8 \text{ m/s}^2)(0.50 \text{ m})[(13.5/1) - 1]} \\ &= 0.054 \text{ m}^3/\text{s} \end{aligned}$$

Next we have to test the guessed value for K_0 to determine if it was correct. For this value of Q ,

$$\text{Re}_{d_1} = \frac{4\rho Q}{\pi d_1 \mu} = \frac{4(999 \text{ kg/m}^3)(0.054 \text{ m}^3/\text{s})}{\pi(0.20 \text{ m})(1.08 \times 10^{-3} \text{ N-s/m}^2)} = 3.2 \times 10^5$$

From Figure 10.5, at this Reynolds number, $K_0 \approx 0.625$. The solution is converged, so we conclude that $Q = 0.054 \text{ m}^3/\text{s}$.

Example 10.5

Air flows at 20°C through a 6-cm pipe. A square-edged orifice plate with $\beta = 0.4$ is chosen to meter the flow rate. A pressure drop of 250 cm H₂O is measured at the flange taps with an upstream pressure of 93.7 kPa abs. Find the flow rate.

KNOWN $d_1 = 6 \text{ cm}$ $p_1 = 93.7 \text{ kPa abs}$
 $\beta = 0.4$ $T_1 = 20^\circ\text{C} = 293 \text{ K}$
 $H = 250 \text{ cm H}_2\text{O}$

Properties (found in Appendix B)

Air: $v = 1.0 \times 10^{-5} \text{ m}^2/\text{s}$

Water: $\rho_{\text{H}_2\text{O}} = 999 \text{ kg/m}^3$

ASSUMPTIONS Treat air behavior as an ideal gas ($p = \rho RT$)

FIND Volume flow rate, Q

SOLUTION The orifice flow rate is found from Equation 10.12, which requires information about E , C , and Y . From the given information, we calculate both the orifice area, $A_{d_0} = 4.52 \times 10^{-4} \text{ m}^2$, and, from Equation 10.11, the velocity of approach factor, $E = 1.013$. The air density is found from the ideal gas equation of state:

$$\rho_1 = \frac{p_1}{RT_1} = \frac{93,700 \text{ N/m}^2}{(287 \text{ N-m/kg})(293 \text{ K})} = 1.114 \text{ kg/m}^3$$

or use air-property tables. The pressure drop is $p_1 - p_2 = \rho_{\text{H}_2\text{O}}gH = 24,500 \text{ N/m}^2$.

The pressure ratio for this gas flow, $(p_1 - p_2)/p_1 = 0.26$. For pressure ratios greater than 0.1 the compressibility of the air should be considered. From Figure 10.6, $Y = 0.92$ for $k = 1.4$ (air) and a pressure ratio of 0.26.

As in the previous example, the discharge coefficient cannot be found explicitly unless the flow rate is known, since $C = f(\text{Re}_{d_1}, \beta)$. So a trial-and-error iterative approach is used. From Figure 10.5, we start with a guess of $K_0 = CE \approx 0.61$ (or $C = 0.60$). Then,

$$Q = CEY A_o \sqrt{\frac{2\Delta p}{\rho_1}} = (0.60)(1.013)(0.92)(4.52 \times 10^{-4} \text{ m}^2) \sqrt{\frac{(2)(24,500 \text{ N/m}^2)}{1.114 \text{ kg/m}^3}}$$

$$= 0.053 \text{ m}^3/\text{s}$$

Check: For this flow rate, $\text{Re}_{d_1} = 4 Q/\pi d_1 v = 7.4 \times 10^4$ and from Figure 10.5, $K_0 \approx 0.61$ as assumed. The flow rate through the orifice is taken to be $0.053 \text{ m}^3/\text{s}$.

Example 10.6

A pump can often impose pressure oscillations into a pipe flow that affect pressure measurements. Figure 10.12 plots separate pressure measurements taken upstream, p_1 , and downstream, p_2 , of an orifice meter, as well as pressure differential measurements, $\Delta p = p_1 - p_2$, taken across the meter. The systematic effect of the oscillations on the internal pipe pressure is seen in comparing p_1 and p_2 , which rise and fall together with a correlation coefficient of $r_{p_1,p_2} = 0.998$. Estimate the contribution to random standard uncertainty in estimating pressure differential due to the data scatter. The following information is known:

$$\bar{p}_1 = 9.25 \text{ kPa} \quad s_{p_1} = 2.813 \text{ kPa} \quad N = 20$$

$$\bar{p}_2 = 7.80 \text{ kPa} \quad s_{p_2} = 2.870 \text{ kPa} \quad N = 20$$

$$\overline{\Delta p} = 1.45 \text{ kPa} \quad s_{\Delta p} = 0.188 \text{ kPa} \quad N = 20$$

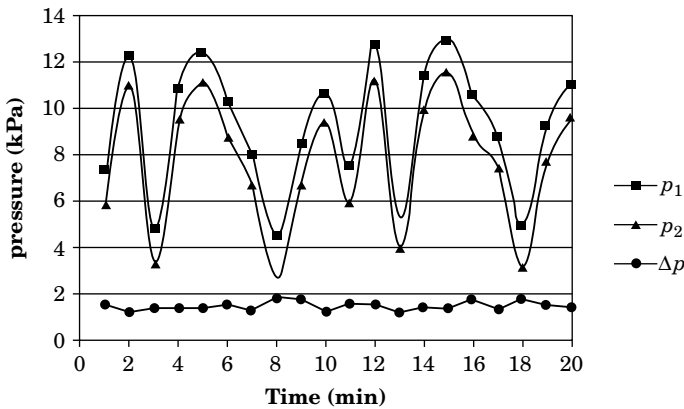


Figure 10.12 Upstream and downstream pressures and differential pressures across an orifice meter for Example 10.6.

SOLUTION As seen in Figure 10.12, pump-induced oscillations impose a trend on the individual pressure measurements. This is confirmed by the high correlation coefficient (see Chapter 4) between p_1 and p_2 . Notably, the pressure differential signal is unaffected by this periodicity because while the pressure within the pipe may rise and fall with time, the pressure difference across the orifice plate remains unaffected. Hence, analyzing the individual pressure data directly without accounting for this systematic effect would overstate the random uncertainty, which should be due only to the data scatter; analyzing the pressure differential data eliminates the systematic effect. We address these issues here and show a way to compensate for them.

The measured pressure differential is $\overline{\Delta p} = 1.47 \text{ kPa}$, or, alternately, when calculated from the individual pressure measurements, $\bar{p}_1 - \bar{p}_2 = 1.47 \text{ kPa}$.

We can estimate the random standard uncertainty in pressure differential directly from the data variation in Δp as

$$s_{\overline{\Delta p}} = \frac{s_{\Delta p}}{\sqrt{20}} = 0.042 \text{ kPa} \quad \text{with } v = 19.$$

Alternatively, we could analyze the individual pressure data and use these to estimate the random standard uncertainty in $\overline{\Delta p}$. With $\Delta p = p_1 - p_2$, the sensitivities are

$$\frac{\partial \Delta p}{\partial p_1} = 1 \quad \frac{\partial \Delta p}{\partial p_2} = -1$$

The elemental random standard uncertainties are

$$s_{\bar{p}_1} = \frac{s_{p_1}}{\sqrt{20}} = 0.629 \text{ kPa} \quad s_{\bar{p}_2} = \frac{s_{p_2}}{\sqrt{20}} = 0.642 \text{ kPa}$$

Then, accounting for the correlated error influence on the pressures, we write

$$s_{\overline{\Delta p}} = \left[\left(\frac{\partial \Delta p}{\partial p_1} s_{\bar{p}_1} \right)^2 + \left(\frac{\partial \Delta p}{\partial p_2} s_{\bar{p}_2} \right)^2 + 2 \frac{\partial \Delta p}{\partial p_1} \frac{\partial \Delta p}{\partial p_2} r_{p_1 p_2} s_{\bar{p}_1} s_{\bar{p}_2} \right]^{1/2} = 0.042 \text{ kPa} \quad (10.14)$$

with $v = 19$. Here the last term under the radical corrects for the correlated error between p_1 and p_2 .

Thus, either method gives the same result for $\overline{\Delta p}$ and for $s_{\overline{\Delta p}}$. However, the first method is preferred because it directly estimates the desired measured variable, Δp , and its random uncertainty is unaffected by the systematic effect.

If we neglected the correlated effect of the pump oscillation, we would instead be tempted to calculate

$$s_{\overline{\Delta p}} = \left[\left(\frac{\partial \Delta p}{\partial p_1} s_{\bar{p}_1} \right)^2 + \left(\frac{\partial \Delta p}{\partial p_2} s_{\bar{p}_2} \right)^2 \right]^{1/2} = 0.899 \text{ kPa}$$

which overstates the random standard uncertainty significantly and is wrong.

COMMENT Equation 10.14 revisits a method to correct for imposed correlated effects on random uncertainty estimates first discussed in Chapter 4. This example shows the importance of reviewing data and data trends in a measurement to uncover test procedure tendencies that affect test interpretation.

Sonic Nozzles

Sonic nozzles are used to meter and to control the flow rate of compressible gases (6). They may take the form of any of the previously described obstruction meters. If the gas flow rate through an obstruction meter becomes sufficiently high, the sonic condition will be reached at the meter throat. At the sonic condition, the gas velocity equals the speed of sound of the gas. At that point the throat is considered to be choked, that is, the mass flow rate through the throat is at a maximum for the given inlet conditions. Any further increase in pressure drop across the meter does not increase the mass flow rate. The theoretical basis for such a meter stems from the early work of Bernoulli, Venturi, and Saint-Venant (1797–1886). In 1866, Julius Weisbach (1806–1871) developed a direct relation between pressure drop and a maximum mass flow rate.

For a perfect gas undergoing an isentropic process, the pressure drop corresponding to the onset of the choked flow condition at the meter minimum area, the meter throat, is given by the *critical pressure ratio*:

$$\left(\frac{p_0}{p_1} \right)_{\text{critical}} = \left(\frac{2}{k+1} \right)^{k/(k-1)} \quad (10.15)$$

where p_0 is the throat pressure. If $(p_0/p_1) \leq (p_0/p_1)_{\text{critical}}$ the meter throat is choked and the gas flows at the sonic condition mass flow rate.

The steady-state energy equation written for a perfect gas is given by

$$c_p T_1 + \frac{2\bar{U}_1^2}{2} = c_p T_0 + 2\bar{U}_0^2 \quad (10.16)$$

where c_p is the constant pressure specific heat, which is assumed constant. Combining Equations 10.1, 10.15, and 10.16 with the ideal gas equation of state, $p = \rho RT$, yields the mass flow for at and below the critical pressure ratio:

$$\dot{m}_{\text{max}} = \rho_1 A_0 \sqrt{2RT_1} \sqrt{\frac{k}{k+1} \left(\frac{2}{k+1} \right)^{2/(k-1)}} \quad (10.17)$$

where k is the specific heat ratio of the gas. Equation 10.17 provides a measure of the ideal mass flow rate for a perfect gas. As with all obstruction meters, this ideal rate must be modified using a discharge coefficient to account for losses. However, the ideal and actual flow rates tend to differ by no more than 3%. When calibrations cannot be run, a $C = 0.98 \pm 2\%$ (95%) is assumed (1).

The sonic nozzle provides a very convenient method to meter and regulate a gas flow. The judicious selection of throat diameter can establish any desired fluid flow rate provided that the flow is sonic at the throat. This capability makes the sonic nozzle attractive as a local calibration standard for gases. Special orifice plate designs exist for metering at very low flow rates (1). Both large pressure drops and system pressure losses must be tolerated with the technique (1).

Example 10.7

A flow nozzle is to be used at choked conditions to regulate the flow of nitrogen N_2 at 1.3 kg/s through a 6-cm-i.d. pipe. The pipe is pressurized at 690 kPa abs and gas flows at 20°C. Determine the maximum β ratio nozzle that can be used. $R_{N_2} = 297 \text{ N}\cdot\text{m/kg}\cdot\text{K}$.

$$\begin{array}{lll} \text{KNOWN} & N_2(k = 1.4) & p_1 = 690 \text{ kPa abs} \\ & d_1 = 6 \text{ cm} & \dot{m} = 1.3 \text{ kg/s} \\ & T_1 = 293 \text{ K} & \rho = 7.93 \text{ kg/m}^3 \end{array}$$

ASSUMPTIONS Perfect gas (ideal gas with constant specific heats)
Steady, choked flow

FIND Find $\beta_{\max} = d_{0_{\max}}/d_1$

SOLUTION Equation 10.17 can be rewritten in terms of nozzle throat area, A :

$$\begin{aligned} A_{\max} &= \frac{\dot{m}}{\rho_1 \sqrt{2RT} \sqrt{[k/(k+1)][2/(k+1)]^{2/(k-1)}}} \\ &= 8.12 \times 10^{-4} \text{ m}^2 \end{aligned}$$

Since $A_o = \pi d_0^2/4$, this yields a maximum nozzle throat diameter, d_0 :

$$d_{0_{\max}} = 3.22 \text{ cm}$$

Hence, $\beta = d_0/d_1 \leq 0.536$ is required to maintain the specified mass flow rate.

Obstruction Meter Selection

Selecting between obstruction meter types depends on a number of factors and engineering compromises. Primary considerations include meter placement, overall pressure loss, overall (capital and operating) costs, accuracy, and operating range (turndown).

Placement

It is important to provide sufficient straight pipe lengths on each side of a flow meter to allow for proper flow development. The flow development dissipates swirl, promotes a symmetric velocity distribution, and allows for proper pressure recovery downstream of the meter so as to reduce systematic error. Installation effects can be minimized by placing the flow meter outlined in Figure 10.13. However, the engineer needs to be wary that installation effects are difficult to predict, particularly downstream of elbows (out-of-plane double elbow turns are notoriously difficult), and Figure 10.13 is a guide for best practice (3, 7). Even with recommended lengths, an additional 0.5%

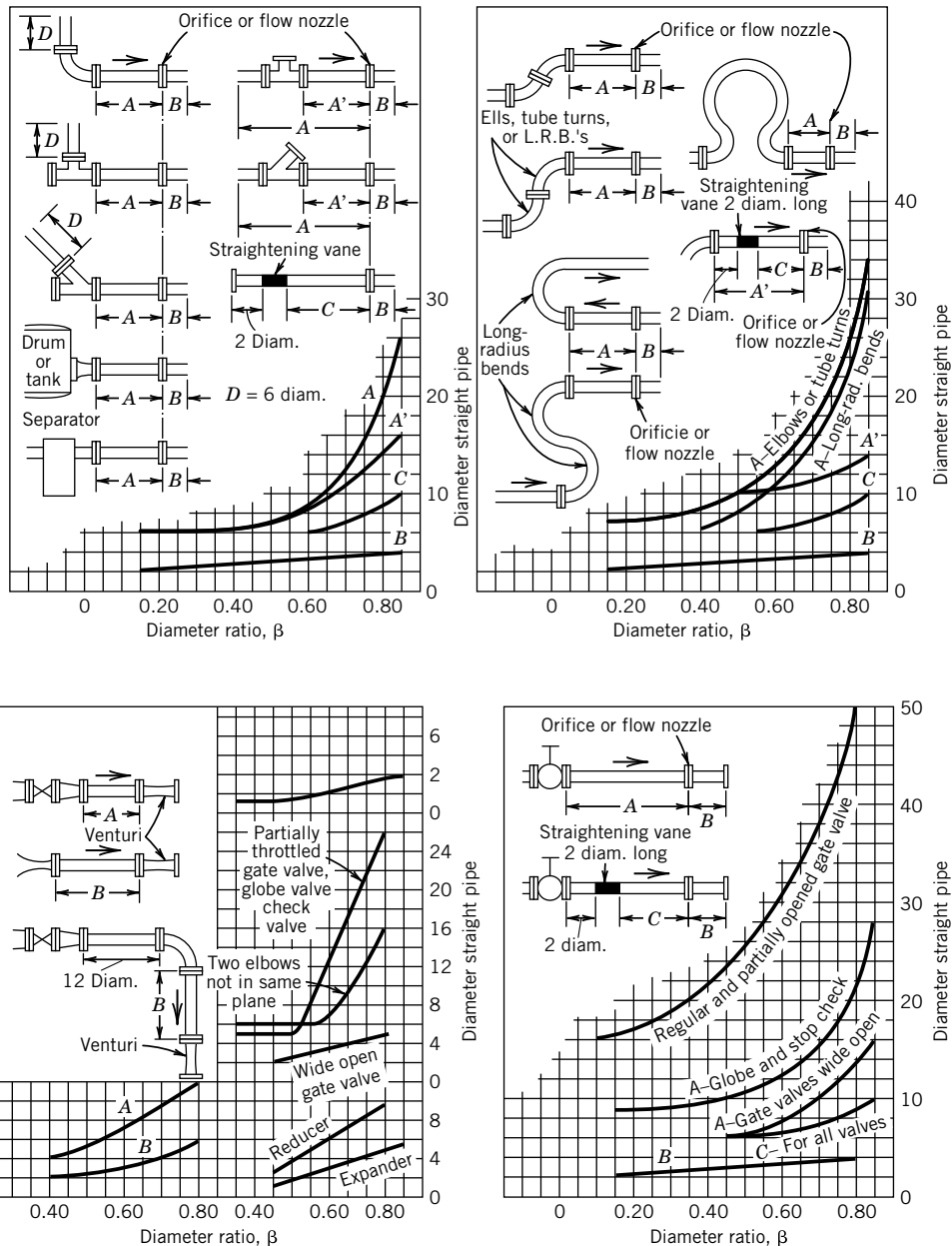


Figure 10.13 Recommended placements for flow meters in a pipeline. (Courtesy of American Society of Mechanical Engineers, New York, NY; reprinted from reference 1.)

systematic uncertainty should be added to the uncertainty in the discharge coefficient to account for swirl effects downstream of turns (3). Unorthodox installations require meter calibration to determine flow coefficients or the use of special correction procedures (3, 7). The physical size of a meter may become an important consideration in itself, since in large-diameter pipelines, venturi and nozzle meters can take up a considerable length of pipe.

Pressure Loss

The unrecoverable overall pressure loss, Δp_{loss} , associated with a flow meter depends on the β ratio and flow rate (Fig. 10.7). These losses must be overcome by the system prime mover (e.g., a pump, fan, or compressor driven by a motor) in addition to any other pipe system losses. In established systems, flow meters must be chosen on the basis of the pressure loss that the prime mover can accommodate and still maintain a desired system flow rate. The power, \dot{W} , required to overcome any loss in a system for flow rate Q is given by

$$\dot{W} = Q \frac{\Delta p_{\text{loss}}}{\eta} \quad (10.18)$$

where η is the prime mover efficiency.

Costs

The actual cost of a meter depends on its initial capital cost, the costs of installing it (including system down time), calibration costs, and the added capital and operating costs associated with flow meter pressure losses to the system. Indirect costs may include product losses due to the meter flow rate uncertainty.

Accuracy

The ability of an obstruction flow meter to accurately estimate the volume flow rate in a pipeline depends on both the method used to calculate flow rate and factors inherent to the meter. If standard tabulated values for meter coefficients are used, factors that contribute to the overall uncertainty of the measurement enter through the following data-acquisition elemental errors: (1) actual β ratio error and pipe eccentricity, (2) pressure and tap position errors, (3) temperature effects leading to relative thermal expansion of components, and (4) actual upstream flow profile. These errors are in addition to the errors inherent in the coefficients themselves and errors associated with the estimation of the upstream fluid density (1). Direct *in situ* calibration of any flow meter installation can assess these effects and their contributions to overall uncertainty. For example, the actual β ratio value, pressure tap locations, and other installation effects would be included in a system calibration and accommodated in the computed flow coefficient.

Turndown

The range over which a meter can be used is known as the meter *turndown*. The selection of a meter should consider whether the system into which the meter is to be installed will be used at more than one flow rate, and its effect on system performance over the entire anticipated flow rate range should be included.

Example 10.8

For the orifice meter in Example 10.3 with $\beta = 0.5$ and a pressure drop of 50 cm Hg, calculate the permanent pressure loss due to the meter that must be overcome by a pump.

KNOWN $H = 50 \text{ cm Hg}$
 $\beta = 0.5$

ASSUMPTION Steady flow

FIND Δp_{loss}

SOLUTION For a properly designed and installed orifice meter, the permanent pressure loss of the meter is about 75% of the pressure drop across the meter (Fig. 10.7). Hence,

$$\Delta p_{\text{loss}} = 0.75 \times \gamma_{\text{Hg}} H = 49.9 \text{ kPa} \quad (\text{or } H_{\text{loss}} = 38 \text{ cm Hg})$$

COMMENT In comparison, for $Q = 0.053 \text{ m}^3/\text{s}$ a typical venturi (say a 15-degree outlet) with a $\beta = 0.5$ would provide a pressure drop equivalent to 19.6 cm Hg with a permanent loss of only 3.1 cm Hg. Since the pump needs to supply enough power to create the flow rate and to overcome losses, a smaller pump could be used with the venturi.

Example 10.9

For the orifice of Example 10.8, estimate the operating costs required to overcome these permanent losses if electricity is available at \$0.08/kW-h, the pump is used 6000 h/year, and the pump-motor efficiency is 60%.

KNOWN Water at 16°C $Q = 0.053 \text{ m}^3/\text{s}$
 $\Delta p_{\text{loss}} = 49.9 \text{ kPa}$ $\eta = 0.60$

ASSUMPTIONS Meter installed according to standards (1)

FIND Annual cost due to Δp_{loss} alone

SOLUTION The pump power required to overcome the orifice meter permanent pressure loss is estimated from Equation 10.18,

$$\begin{aligned}\dot{W} &= Q \frac{\Delta p_{\text{loss}}}{\eta} \\ &= \frac{(0.55 \text{ m}^3/\text{s})(49,900 \text{ Pa})(3600 \text{ s/h})(1 \text{ N/m}^2/\text{Pa})(1 \text{ W/N-m/s})}{0.6} = 4530 \text{ W} = 4.53 \text{ kW}\end{aligned}$$

The additional annual pump operating cost required to overcome this is

$$\text{Cost} = (4.53 \text{ kW})(6000 \text{ h/year})(\$0.08/\text{kW-h}) = \$2175/\text{year}$$

COMMENT In comparison, the venturi discussed in the Comment to Example 10.7 would cost about \$180/year to operate. If installation space allows, the venturi meter may be the less expensive long-term solution.

Example 10.10

An ASME long radius nozzle ($\beta = 0.5$) is to be installed into a horizontal section of 12-in. (ANSI schedule 40) diameter (304.8 mm) pipe. A long, straight length of pipe exists just downstream of a fully open gate valve but upstream of an in-plane 90-degree elbow. Determine the minimum lengths of straight unobstructed piping that should exist upstream and downstream of the meter.

KNOWN $d_1 = 11.938 \text{ in. } (303.28 \text{ mm})$

$\beta = 0.5$

Installation layout

FIND Meter placement

SOLUTION From Figure 10.13, the meter should be placed a minimum of eight pipe diameters ($A = 8$) downstream of the valve and a minimum of three pipe diameters ($B = 3$) upstream of any flow fitting. Note that since a typical flow nozzle has a length of about 1.5 pipe diameters, this installation requires a straight pipe section of at least $8 + 3 + 1.5 = 12.5$ pipe diameters.

COMMENT A 12-in. diameter (Schedule 40) pipe has an inside diameter of 11.938 in. and an outside diameter of 12.75 in. The equivalent metric pipe is DN 300 with outside diameter of 323.9 mm and inside diameter of 303.3 mm.

Laminar Flow Elements

Laminar flow meters take advantage of the linear relationship between volume flow rate and the pressure drop over a length for laminar pipe flow ($\text{Re}_d < 2000$). For a pipe of diameter d with pressure drop over a length L , the governing equations of motion lead to

$$Q = \frac{\pi d^4}{128 \mu} \frac{p_1 - p_2}{L} \quad \text{where } \text{Re}_d < 2000 \quad (10.19)$$

This relation was first demonstrated by Jean Poiseulle (1799–1869), who conducted meticulous tests documenting the resistance of flow through capillary tubes.

The simplest type of laminar flow meter consists of two pressure taps separated by a length of piping.¹ However, because the Reynolds number must remain low, this restricts either the pipe diameter or the flow rate to which Equation 10.19 applies for a given fluid. This limitation is overcome in commercial units by using bundles of small-diameter tubes or passages placed in parallel and called laminar flow elements (Figure 10.14). The strategy of a laminar flow element is to divide the flow by passing it through the tube bundle so as to reduce the flow rate in each tube such that $\text{Re} < 2000$. Pressure drop is measured between the entrance and the exit of the laminar flow element, and a flow coefficient is used to account for inefficiency, such that

$$Q = K_1 \Delta p \quad (10.20)$$

where coefficient K_1 is the meter static sensitivity and is called its *K-factor*. Commercial units come calibrated with K_1 a constant over the useful meter range.

A laminar flow element has an upper limit on usable flow rate. Various meter sizes and designs are available to accommodate user needs. Turndowns of up to 100:1 are available.

¹ Alternately, if flow rate can be measured or is known, Equation 10.19 provides the basis for a capillary tube viscometer. The method also achieves a linear resistance.

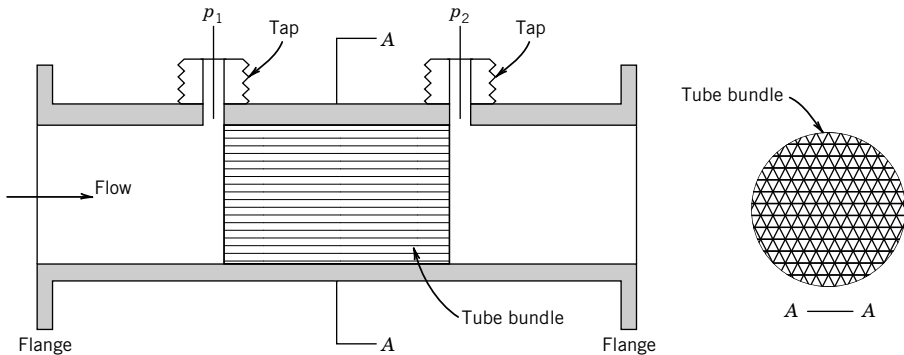


Figure 10.14 Laminar flow element flow meter concept using pipe flanges for installation. For noncircular tubes, Reynolds number is based on $d = 4r_H$.

Laminar flow elements offer some distinct advantages over other pressure differential meters. These include (1) a high sensitivity even at low flow rates, (2) an ability to measure flow from either meter direction, (3) a wide usable flow range, and (4) the ability to indicate an average flow rate in pulsating flows. The instrument systematic uncertainty in flow rate determination is as low as 0.25% (95%) of the flow rate. However, these meters are limited to clean fluids due to clogging potential. All of the measured pressure drop remains a system pressure loss.

10.6 INSERTION VOLUME FLOW METERS

Dozens of volume flow meter types based on a number of different principles have been proposed, developed, and sold commercially. A large group of meters is based on some phenomenon that is actually sensitive to the average velocity across a control surface of known area, that is, $Q = f(\bar{U}, A) = \bar{U}A$. Several of these designs are included in the discussion below. Another common group, called *positive displacement meters*, actually measure parcels of a volume of fluid per unit time, that is, $Q = f(\forall, t) = \forall/t$.

Electromagnetic Flow Meters

The operating principle of an *electromagnetic flow meter* (8) is based on the fundamental principle that an electromotive force (emf) of electric potential, E , is induced in a conductor of length, L , which moves with a velocity, \mathbf{U} , through a magnetic field of magnetic flux, \mathbf{B} . Simply, when an electrically conductive liquid moves through a magnetic field, a voltage is induced in the liquid at a right angle to the field. The voltage is detected by metal electrode sensors with the voltage magnitude and polarity directly proportional to the volume flow rate and the flow direction, respectively. This physical behavior was first recorded by Michael Faraday (1791–1867). In principle,

$$\mathbf{E} = \mathbf{U} \times \mathbf{B} \cdot \mathbf{L} \quad (10.21)$$

where symbols in bold face are vector quantities.

A practical utilization of the principle is shown in Figure 10.15. From Equation 10.21 the magnitude of E is affected by the average velocity, \bar{U} , as

$$E = \bar{U}BL \sin \alpha = f(\bar{U})$$

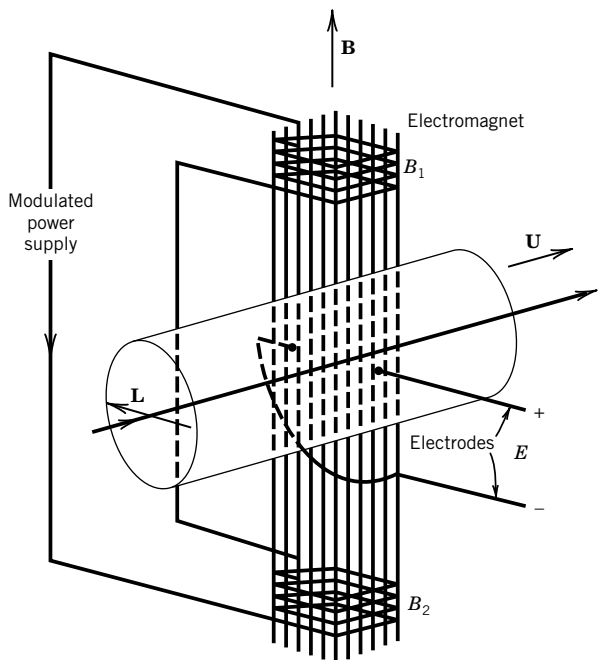


Figure 10.15 Electromagnetic principle as applied to a working flow meter.

where α is the angle between the mean velocity vector and the magnetic flux vector, usually at 90 degrees. In general, electrodes are located either in or mounted on the pipe wall in a diametrical plane that is normal to the known magnetic field. The electrodes are separated by a scalar length, L . The average magnitude of the velocity, \bar{U} , across the pipe is thus inferred through the measured emf. The flow rate is found by

$$Q = \bar{U} \frac{\pi d_1^2}{4} = \frac{E}{BL} \frac{\pi d_1^2}{4} = K_1 E \quad (10.22)$$

The value of L is on the order of the pipe diameter, the exact value depending on the meter construction and magnetic flux lines. The static sensitivity (or meter K -factor) K_1 is found by calibration and supplied by a manufacturer such that the relationship between the flow rate and the measured potential is linear.

The electromagnetic flow meter comes commercially as a packaged flow device, which is installed directly in-line and connected to an external electronic output unit. Special designs include an independent flow sensor unit that can clamp over a nonmagnetic pipe, a design favored to monitor blood flow rate through major arteries during surgery. The sensor is connected to a control unit by wiring. External sensors are also available as an in-line union, which can measure flow rate in either direction with instantaneous changes (Figure 10.16).

The electromagnetic flow meter has a very low pressure loss associated with its use due to its open tube, no obstruction design, and is suitable for installations that can tolerate only a small pressure drop. It can be used for either steady or unsteady flow measurements, providing either time-averaged or instantaneous data in the latter. This absence of internal parts is very attractive for metering corrosive and “dirty” fluids. The operating principle is independent of fluid density and viscosity, responding only to average velocity, and there is no difficulty with measurements in either

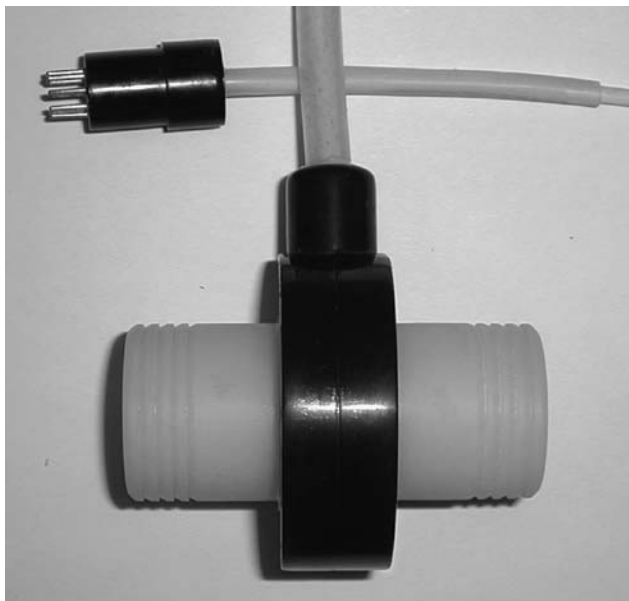


Figure 10.16 Example of an in-line electromagnetic flow probe. The black housing contains the electromagnet and two electrodes. The connecting plug has wires for power and electrode signals to/from an external control box. (Courtesy of Carolina Medical Electronics, East Bend, NC.)

laminar or turbulent flows, provided that the velocity profile is reasonably symmetrical. Uncertainty down to 0.25% (95%) of the measured flow rate can be attained, although values from 1% to 5% (95%) are more common for these meters in industrial settings. The fluid must be conductive, but the minimum conductivity required depends on a particular meter's design. Fluids with values as low as 0.1 microsieman (μ sieman)/cm have been metered. Adding salts to a fluid increases its conductivity. Stray electronic noise is perhaps the most significant barrier in applying this type of meter. Grounding close to the electrodes and increasing fluid conductivity reduce noise.

Vortex Shedding Meters

An oscillating street sign and the “singing” of power lines on a windy day are examples of the effects induced by vortex shedding from bluff-shaped bodies, a natural phenomenon in which alternating vortices are shed in the wake of the body. The vortices formed on opposite sides of the body are carried downstream in the body’s wake, forming a “vortex street,” with each vortex having an opposite sign of rotation. This behavior is seen in Figure 10.17, a photograph that captures the vortex shedding downstream of a section of an aircraft wing. The aerodynamicist Theodore von Karman (1881–1963) first deduced the existence of a vortex street, although Leonardo da Vinci appears to have been the first to actually record the phenomenon (9).

A *vortex flow meter* operates on the principle that the frequency of vortex shedding depends on the average velocity of the flow past the body and the body shape. The basic relationship between shedding frequency, f , where $f[\text{Hz}] = \omega/2\pi$, and average velocity, \bar{U} , for a given shape is given by the Strouhal number,

$$\text{St} = \frac{fd}{\bar{U}} \quad (10.23)$$

where d is a characteristic length for the body.

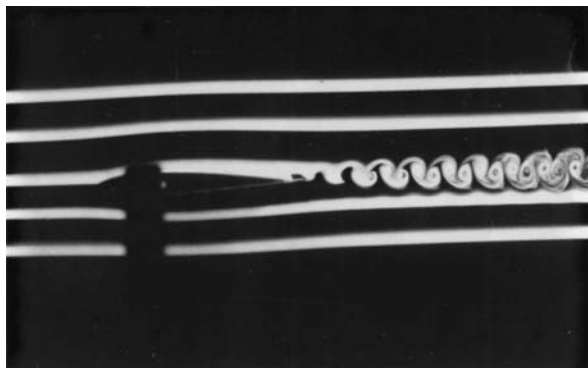


Figure 10.17 Smoke lines in this photograph reveal the vortex shedding behind a streamlined wing-shaped body in a moving flow. (Photograph by R. Figliola.)

A typical design is shown in Figure 10.18. The shedder spans the pipe, so its length $\ell \approx d_1$, and $d/\ell \approx 0.3$, so as to provide for strong, stable vortex strength. Although the Strouhal number is a function of the Reynolds number, various geometrical shapes, known as shedders, can produce a stable vortex flow that has a constant Strouhal number over a broad range of flow Reynolds numbers (for $Re_d > 10^4$). The oscillation stability, quality, and strength of the shedding is improved over common circular cylinders by using abrupt edges on the rear end of the shape and by providing a slightly concave upstream body face that traps the stagnation streamline at a point. Examples are given in Table 10.1.

For a fixed body and constant Strouhal number, the flow rate for a pipe of inside diameter d_1 is

$$Q = \overline{U}A = c \frac{\pi d_1^2}{4St} fd = K_1 f \quad (10.24)$$

where the constant c accounts for shedder blockage effects that tend to increase the average velocity sensed. The value of K_1 , known as the K -factor, is the meter static sensitivity and remains essentially constant for $10^4 < Re_d < 10^7$. Shedding frequency can be measured in many ways. The shedder strut can be instrumented to detect the force oscillation by using strut-mounted strain gauges or capacitance sensor, for example, or a piezoelectric crystal wall sensor can be used to detect the pressure oscillations in the flow.

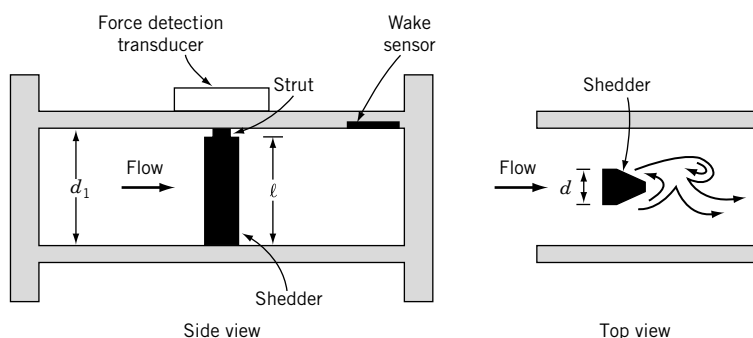
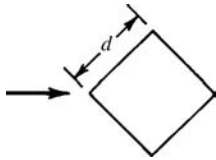
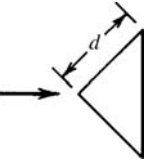
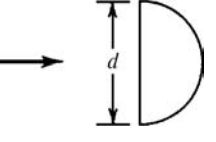
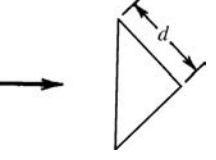
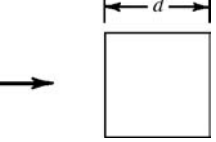


Figure 10.18 Vortex shedding flow meter. Different shedder shapes are available.

Table 10.1 Sheddor Shape and Strouhal Number

Cross Section	Strouhal Number ^a
	0.16
	0.19
	0.16
	0.15
	0.12

^aFor Reynolds number $\text{Re}_d \geq 10^4$. Strouhal number $\text{St} = fd/\bar{U}$.

The lower flow rate limit on vortex meters is at Reynolds numbers (Re based on d in Fig. 10.18) near 10,000, below which the Strouhal number can vary nonlinearly with flow rate and shedding becomes unstable. This can be a limitation in metering high-viscosity pipe flows ($\mu > 20$ centipoise). The upper flow bound is limited either by the onset of cavitation in liquids or by the onset of compressibility effects in gases at Mach numbers exceeding 0.2. Property variations affect meter performance only indirectly. Density variations affect the strength of the shed vortex, and this places a lower limit on fluid density, which is based on the sensitivity of the vortex-shedding detection equipment. Viscosity affects the operating Reynolds number. Otherwise, within bounds, the meter is insensitive to property variations.

The meter has no moving parts and relatively low pressure losses compared to obstruction meters. A single meter can operate over a flow range of up to 20:1 above its minimum with a linearity in K_1 of 0.5%. Because d can be replaced by a constant times d_1 in Equation 10.24, we see that the strength of the shedding frequency sensed over the pipe area decreases as the pipe diameter

cubed. This indicates that a meter's accuracy drops off as pipe diameter increases, placing an upper limit on the meter size.

Rotameters

The rotameter is a widely used insertion meter for volume flow rate indication. As depicted in Figure 10.19, the meter consists of a float within a vertical tube, tapered to an increasing cross-sectional area at its outlet. Flow entering through the bottom passes over the float, which is free to move. The equilibrium height of the float indicates the flow rate.

The operating principle of a rotameter is based on the balance between the drag force, F_D , and the weight, W , and buoyancy forces, F_B , acting on the float in the moving fluid. It is the drag force that varies with the average velocity over the float.

The force balance in the vertical direction y yields

$$\sum F_y = 0 = +F_D - W + F_B$$

with $F_D = \frac{1}{2} C_D \rho \overline{U^2} A_x$, $W = \rho_b g V_b$, and $F_B = \rho g V_b$. The average velocity sensed by the float depends on its height in the tube and is given by

$$\overline{U} = \overline{U}(y) = \sqrt{2(\rho_b - \rho)gV_b/C_D\rho A_x} \quad (10.25)$$

where

ρ_b = density of float (body)

ρ = density of fluid

C_D = drag coefficient of the float

A_x = tube cross-sectional area

\overline{U} = average velocity past the float

V_b = volume of float (body)

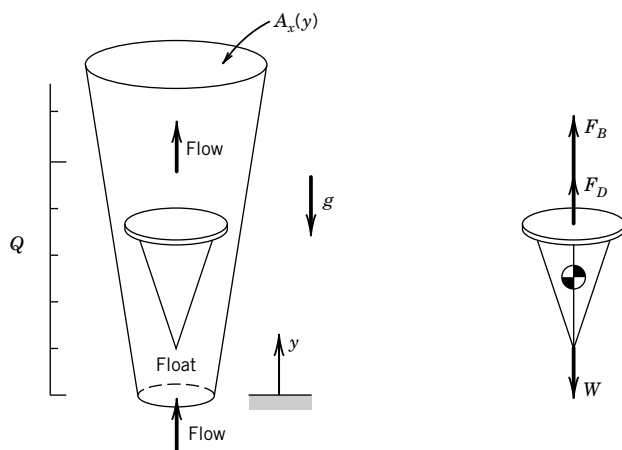


Figure 10.19 Concept of a rotameter.

In operation, the float rises to an equilibrium position. The height of this position increases with flow velocity and, hence, flow rate. This flow rate is found by

$$Q = \bar{U}A_a(y) = K_1A_a(y) \quad (10.26)$$

where $A_a(y)$ is the annular area between the float and the tube, and K_1 is a meter constant. Both the average velocity and the annular area depend on the height of the float in the tube. So the float's vertical position is a direct measure of flow rate, which can be read from a graduated scale, electronically sensed with an optical cell, or detected magnetically. Floats with sharp edges are less sensitive to fluid viscosity changes with temperature. A typical meter turndown is 10:1 with an instrument systematic uncertainty of $\sim 2\%$ (95%) of flow rate.

Turbine Meters

Turbine meters make use of angular momentum principles to meter flow rate. In a typical design (Fig. 10.20), a rotor is encased within a bored housing through which the fluid to be metered is passed. Its housing contains flanges or threads for direct insertion into a pipeline. In principle, the exchange of momentum within the flow turns the rotor at a rotational speed that is proportional to the flow rate. Rotor rotation can be measured in a number of ways. For example, a reluctance pickup coil can sense the passage of magnetic rotor blades, producing a pulse train signal at a frequency that is directly related to rotational speed. This can be directly output as a TTL pulse train, or the frequency can be converted to an analog voltage.

The rotor angular velocity, ω , depends on the average flow velocity, \bar{U} , and the fluid kinematic viscosity, ν , through the meter bore of diameter, d_1 . Dimensionless analysis of these parameters (10) yields

$$Q = K_1\omega \quad (10.27)$$

where K_1 is the meter's K -factor but the relation is a function of Reynolds number. In practice, there is a region in which the rotor angular velocity varies linearly with flow rate, and this region becomes the meter operating range.

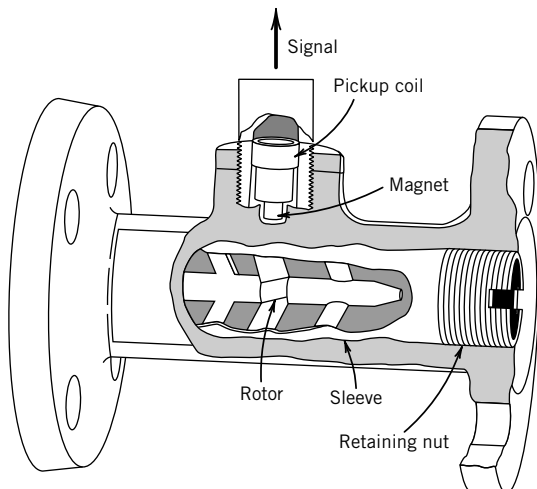


Figure 10.20 Cutaway view of a turbine flow meter. (Courtesy of Actaris Gas Division, Owenton, KY.)

Turbine meters offer a low-pressure drop and very good accuracy. A typical instrument's systematic uncertainty in flow rate is $\sim 0.25\%$ (95%) with a turndown of 20:1. The measurements are exceptionally repeatable making the meters good candidates for local flow rate standards. However, their use must be restricted to clean fluids because of possible fouling of their rotating parts. The turbine meter rotational speed is sensitive to temperature changes, which affect fluid viscosity and density and therefore K_1 . Some compensation for viscosity variations can be made electronically (11). The turbine meter is very susceptible to installation errors caused by pipe flow swirl (7), and a careful selection of installation position must be made.

Transit Time and Doppler (Ultrasonic) Flow Meters

Ultrasonic meters use sound waves to determine flow rate. *Transit time flow meters* use the travel time of ultrasonic waves to estimate average flow velocity. Figure 10.21 shows a pair of transducers, separated by some distance, fixed to the outside of a pipe wall. A reflector applied to the opposite outside wall of the pipe increases the signal-to-noise ratio. Each transducer acts as a transmitter and a receiver for ultrasonic waves. An ultrasonic wave emitted by one transducer passes through the fluid, reflects off the pipe wall, and is received by the other transducer. The difference in transit time for a wave to travel from transducer 1 to transducer 2 and from transducer 2 to transducer 1 is directly related to the average velocity of flow in the pipe. For a fluid with speed of sound a , for flow with average velocity \bar{U} based on a flow rate Q , and for a beam oriented at angle θ relative to the pipe flow axis,

$$t_1 = \frac{2L}{a + \bar{U} \cos \theta} \quad t_2 = \frac{2L}{a - \bar{U} \cos \theta}$$

with $L = d_1 / \sin \theta$. When $\bar{U} \ll a$, $\bar{U} = (a^2 / 4d_1 \cot \theta)(t_2 - t_1)$. Or, eliminating a we obtain $\bar{U} = (L / \cos \theta)(t_2 - t_1) / t_2 t_1$. The flow rate is

$$Q = \bar{U}A = K_1 A(t_2 - t_1) \quad (10.28)$$

where K_1 is a constant called the meter K -factor. The method requires accurate measurements of t_1 and t_2 .

Transit time meters are noninvasive and thus offer no pressure drop. Portable models are strapped to the outside of the pipe, making them useful for field diagnostics. They can be set up to measure time-dependent velocity, including flow direction with time. Instrument relative systematic uncertainty ranges from $\sim 1\%$ to 5% (95%) of the flow rate.

Doppler flowmeters use the Doppler effect to measure the average velocity of fluid particles (contaminants, particulate, or small bubbles) suspended in the pipe flow. In one approach, a single

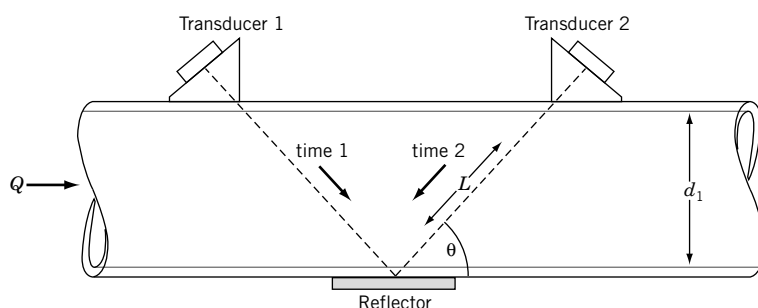


Figure 10.21 Principle of a transit time (ultrasonic) flow meter.

ultrasonic transducer is mounted to the outside of a pipe wall. A wave of frequency f on the order of 100 kHz to 1 MHz is emitted. The emitted wave is bounced back by particles suspended in the moving fluid, and this scattered wave is detected by the transducer. The scattered waves travel at a slightly different frequency, the difference being the Doppler frequency f_D . The flow rate is

$$Q = \overline{U}A = \frac{\pi d_1^2 a f_D}{8f \cos \theta} = K_1 f_D \quad (10.29)$$

These devices can measure time-dependent flow rates. Instrument systematic uncertainty is $\sim 2\%$ (95%) of the flow rate.

Positive Displacement Meters

Positive displacement meters contain mechanical elements that define a known volume filled with the fluid being metered. The free-moving elements are displaced or rotated by the action of the moving fluid. A geared counting mechanism counts the number of element displacements to provide a direct reading of the volume of fluid passed through the meter, ∇ . This metering method is common to water, gasoline, and natural gas meters.

To be used as volume flow rate meters, volume measurement can be used in conjunction with a timer, so that

$$Q = \nabla/t \quad (10.30)$$

These units serve applications needing ruggedness and accuracy in steady flow metering. Common applications are metering related to domestic water and natural gas consumption.

Diaphragm meters contain two opposing flexible bellows coupled by linkages to exhaust valves that alternately displace a known volume of fluid through the meter. Through the coupled linkage, the flow of fluid through one bellows drives the motion of the opposite bellows. Thus, as entering gas causes one bellows to expand within its chamber sealed by a closed valve, the gas in the opposite bellows exhausts through an open valve to allow its bellows to collapse; this alternating motion cycles the gears of its counter register (output display). Such “dry gas” meters are common to natural gas or propane lines for volume measurement. Thomas Glover invented the first diaphragm meter in 1843, and modern meters retain the major elements of his design.

Wobble meters contain a disk that is seated in a chamber. The flow of liquid through the chamber causes the disk to oscillate so that a known volume of fluid moves through the chamber with each oscillation. The disk is connected to a counter that records each oscillation as volume is displaced. Wobble meters are used for domestic water applications, where they must have an uncertainty of no greater than 1% of actual delivery.

Frequently found on oil trucks and at the gasoline pump, *rotating vane meters* use rotating cups or vanes that move about an annular opening, displacing a known volume with each rotation.

With any of these meters, uncertainty can be as low as 0.2% (95%) of actual delivery. Because of the good accuracy of these meters, they are often used as local working standards to calibrate other types of volume flow meters.

10.7 MASS FLOW METERS

There are many situations in which the mass flow rate is the quantity of interest. Mass flow rate demands measuring the mass flux per unit volume, $\overline{\rho U}$, to yield $\dot{m} = \overline{\rho U}A$.

If the density of the metered fluid is known under the exact conditions of measurement, then a direct estimate can be made based on volume flow rate measurements. But not all fluids have a constant, known value of density (e.g., petroleum products, polymers, and cocoa butter), and many processes are subject to significant changes in density. The direct measurement of mass flow rate is desirable because it eliminates the uncertainties associated with estimating or measuring actual density.

The difference between a meter that is sensitive to Q as opposed to \dot{m} is not trivial. Prior to the 1970s, reliable commercial mass flow meters with sufficient accuracy to circumvent volume flow rate corrections were generally not available, even though the basic principles and implementation schemes for such meters had been understood in theory for several decades. United States patents dating back to the 1940s record schemes for using heat transfer, Coriolis forces, and momentum methods to infer mass flow rate directly.

Thermal Flow Meter

The rate at which energy, \dot{E} , must be added to a flowing fluid to raise its temperature between two control surfaces is directly related to the mass flow rate by

$$\dot{E} = \dot{m}c_p\Delta T \quad (10.31)$$

where c_p is the fluid specific heat. Methods to utilize this effect to directly measure mass flow rate incorporate an in-line meter having some means to input energy to the fluid over the meter length. The passing of a current through an immersed filament is a common method. Fluid temperatures are measured at the upstream and downstream locations of the meter. This type of meter is quite easy to use and appears to be reliable. It is widely used for gas flow applications. In fact, in the 1980s, the technique was adapted for use in automobile fuel injection systems to provide an exact air-fuel mixture to the engine cylinders despite short-term altitude, barometric, and seasonal environmental temperature changes.

The operating principle of this meter assumes that c_p is known and remains constant over the length of the meter. For common gases, such as air, this assumption is quite good. Flow rate turndown of up to 100:1 is possible with uncertainties of 0.5% (95%) of flow rate with very little pressure drop. But the assumptions become restrictive for liquids and for gases for which c_p may be a strong function of temperature.

A second type of thermal mass flow meter is a velocity-sensing meter and thermal sensor together in one direct insertion unit. The meter uses both hot-film anemometry methods to sense fluid velocity through a conduit of known diameter and an adjacent resistance temperature detector (RTD) sensor for temperature measurement. For sensor and fluid temperatures, T_s and T_f , respectively, mass flow rate is inferred from the correlation

$$\dot{E} = \left[C + B(\rho\overline{U})^{1/n} \right] (T_s - T_f) \quad (10.32)$$

where C , B , and n are constants that depend on fluid properties (12) and are determined through calibration. In a scheme to reduce the fluid property sensitivity of the meter, the RTD may be used as an adjacent resistor leg of the anemometer Wheatstone bridge circuit to provide a temperature-compensated velocity output over a wide range of fluid temperatures with excellent repeatability (0.25%). Gas velocities of up to 12,000 ft/min and flow rate turndown of 50:1 are possible with uncertainties down to 2% of the flow rate and very little pressure drop.

Coriolis Flow Meter

The term “Coriolis flow meter” refers to the family of insertion meters that meter mass flow rate by inducing a Coriolis acceleration on the flowing fluid and measuring the resulting developed force (13). The developed force is directly related to the mass flow rate independent of the fluid properties. The Coriolis effect was proposed by Gaspard de Coriolis (1792–1843) following his studies of accelerations in rotating systems. Coriolis meters pass a fluid through a rotating or vibrating pipe system to develop the Coriolis force. A number of methods to utilize this effect have been proposed since the first U.S. patent for a Coriolis effect meter was issued in 1947. This family of meters has seen steady growth in market share since the mid-1980s.

In the most common scheme for commercially available units, the pipe flow is diverted from the main pipe and divided between two bent, parallel, adjacent tubes of equal diameter, such as shown for the device in Figure 10.22, a device developed in part by the first author of this text.² The tubes themselves are mechanically vibrated in a relative out-of-phase sinusoidal oscillation by an electromagnetic driver. In general, a fluid particle passing through the meter tube, which is rotating (due to the oscillating tube) relative to the fixed pipe, experiences an acceleration at any arbitrary position S . The total acceleration at S , $\ddot{\mathbf{r}}$, is composed of several components (Fig. 10.23),

$$\ddot{\mathbf{r}} = \ddot{\mathbf{R}}_{O'} + \dot{\boldsymbol{\omega}} \times \mathbf{r}_{S/O'} + \boldsymbol{\omega} \times \boldsymbol{\omega} \times \mathbf{r}_{S/O'} + \ddot{\mathbf{r}}_{S/O'} + 2\boldsymbol{\omega} \times \dot{\mathbf{r}}_{S/O'} \quad (10.33)$$

where boldface refers to vector quantities and

$\ddot{\mathbf{R}}_{O'}$ = translation acceleration of rotating origin O' relative to fixed origin O

$\boldsymbol{\omega} \times \boldsymbol{\omega} \times \mathbf{r}_{S/O'}$ = centripetal acceleration of S relative to O'

$\dot{\boldsymbol{\omega}} \times \mathbf{r}_{S/O'}$ = tangential acceleration of S relative to O'

$\ddot{\mathbf{r}}_{S/O'}$ = translational acceleration of S relative to O'

$2\boldsymbol{\omega} \times \dot{\mathbf{r}}_{S/O'}$ = Coriolis acceleration at S relative to O'

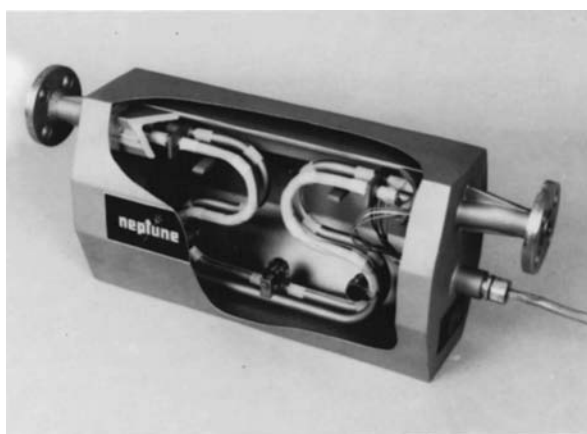


Figure 10.22 Cutaway view of a Coriolis mass flow meter. (Courtesy of Actaris Neptune Liquid Measurement Division, Greenwood, SC.)

² In its beta test, the unit shown in Figure 10.22 was first installed in a chocolate factory to meter the mass flow of cocoa butter. It was next installed at a fiber factory to discern the trace presence of ink dye in the wastewater.

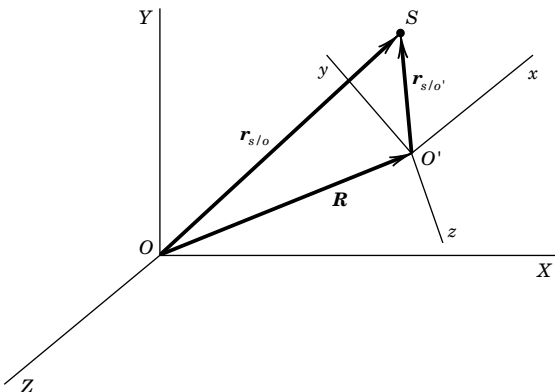


Figure 10.23 Fixed and rotating reference frames.

with ω the angular velocity of point S relative to O' . In these meters, the tubes are rotated but not translated, so that the translational accelerations are zero. A fluid particle experiences forces due to the remaining accelerations that cause equal and opposite reactions on the meter tube walls. The Coriolis acceleration distinguishes itself by acting in a plane perpendicular to the tube axes and develops a force gradient that creates a twisting motion or oscillating rotation about the tube plane.

The utilization of the Coriolis force depends on the shape of the meter. However, the basic principle is illustrated in Figure 10.24. Rather than rotating the tubes a complete 360 degrees about the pipe axis, the meter tubes are vibrated continuously at a drive frequency, ω , with amplitude displacement, z , about the pipe axis. This eliminates rotational seal problems. The driving frequency is selected at the tube resonant frequency that places the driven tube into what is called a limit cycle, a continuous, single-frequency oscillation. This configuration is essentially a self-sustaining tuning fork because the meter naturally responds to any disturbance at this frequency with a minimum in input energy. By driving the tube up and down, the mass flow causes the tube to wobble. The magnitude of wobble is directly related to the mass flow rate.

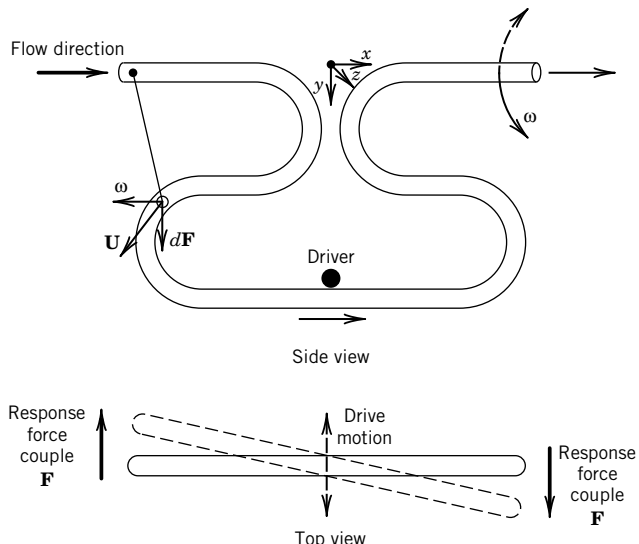


Figure 10.24 Concept of the operating principle of a Coriolis mass flow meter. Use the right hand rule to relate the vectors of ω , \mathbf{U} , and $d\mathbf{F}$.

As a fluid particle of elemental mass, dm , flows through a section of the flow meter, it experiences the Coriolis acceleration, $2\omega \times \dot{\mathbf{r}}_{S/O'}$, and an inertial Coriolis force

$$d\mathbf{F} = (2\omega \times \dot{\mathbf{r}}_{S/O'}) dm \quad (10.34)$$

acting in the z direction. For the flow meter design of Figure 10.22 and as depicted in Figure 10.24, as the particle travels along the meter the direction of the velocity vector changes. This results, using the right-hand rule, in a change in direction of vector force, $d\mathbf{F}$, between the left and right sides. The resultant forces experienced by the tube are of equal magnitude but the opposite sign of those experienced by the particle. Each tube segment senses a corresponding differential torque, $d\mathbf{T}$, a rotation about the y axis at a frequency ω_c ,

$$d\mathbf{T} = x' \times d\mathbf{F} = x' \times (2\omega \times \dot{\mathbf{r}}_{S/O'}) dm \quad (10.35)$$

where x' refers to the x distance between the elemental mass and the y axis, $\mathbf{x}' = \mathbf{x}'\hat{e}_x$. The total magnitude of torque experienced by each tube is found by integration along the total path length of the tube, L ,

$$\mathbf{T} = \int_0^L d\mathbf{T} \quad (10.36)$$

A differential element of fluid has mass $dm = \rho A dl$, for an elemental cross section of fluid A , of differential length dl , and of density ρ . If this mass moves with an average velocity, \bar{U} , then the differential mass can be written as

$$dm = \rho A dl = \dot{m}(dl/\bar{U}) \quad (10.37)$$

The Coriolis cross-product can be expressed as

$$2\omega \times \dot{\mathbf{r}}_{S/O'} = (2\omega \times \dot{\mathbf{r}}_{S/O'} \sin \theta) \hat{e}_z = (2\omega_c \bar{U} \sin \theta) \hat{e}_z \quad (10.38)$$

where θ is the angle between the Coriolis rotation and the velocity vector. Then,

$$\dot{m} = \frac{T}{2 \int_0^L (\rho x' \omega_c \sin \theta) dl} \hat{e}_y \quad (10.39)$$

Since the velocity direction changes by 180 degrees, the Coriolis-developed torque acts in opposite directions on each side of the tube.³ The meter tubes twist about the y axis of the tube (i.e., wobbles) at an angle δ . For small angles of rotation the twist angle is related to torque by

$$\delta = k_s T = \text{constant} \times \dot{m} \quad (10.40)$$

where k_s is related to the stiffness of the tube. The objective becomes to measure the twist angle, which can be accomplished in many ways. For example, by driving the two meter tubes 180 degrees out of phase, the relative phase at any time between the two tubes is directly related to the mass flow rate. The exact relationship is linear over a wide flow range and determined by calibration with any fluid (14).

³ We can envision a design in which the velocity does not reverse direction along the flow path but ω does. In fact, after the first publication of this footnote, one vendor adopted this approach in a commercial product.

The tangential and centripetal accelerations remain of minor consequence due to the tube stiffness in the directions in which they act. However, at high mass flow rates they can excite modes of vibration in addition to the driving mode, ω , and response mode, ω_c . In doing so, they affect the meter linearity and zero error (drift), which affects mass flow uncertainty and meter turndown. Essentially, the magnitude of these undesirable effects is inherent to the particular meter shape and is controlled, if necessary, through tube-stiffening members.

Another interesting problem occurs mostly in meters of small tube diameter where the tube mass may approach the mass of the fluid in the tube. At flow rates that correspond to flow transition from a laminar to turbulent regime, the driving frequency can excite the flow instabilities responsible for the flow transition. The fluid and tube can go out of phase, reducing the response amplitude and its corresponding torque. This affects the meter's calibration linearity, but a good design can contain this effect to within 0.5% of the meter reading.

The meter principle is unaffected by changing fluid properties, but temperature changes affect the overall meter stiffness, an effect that can be compensated for electronically. A very desirable feature is an apparent insensitivity to installation position. Commercially available Coriolis flow meters can measure flow rate with an instrument systematic uncertainty to 0.25% (95%) of mass flow rate, but 0.10% is achievable. Turndown is about 20:1. The meter is also used as an effective densitometer.

10.8 FLOW METER CALIBRATION AND STANDARDS

While a fundamental primary standard for flow rate does not exist per se, there are a number of calibration test code procedures in place, and government and private bureaus that perform calibrations. The general procedure for the calibration of in-line flow meters requires establishing a steady flow in a calibration flow loop and then determining the volume or mass of flowing fluid passing through the flow meter in an accurately determined time interval. Such flow loop calibration systems are known as *provers*. Often calibration is by comparison to a meter of proven accuracy. Several methods to establish the flow rate are discussed.

In liquids, variations of a “catch-and-weigh” technique are often employed in flow provers. One variation of the technique consists of a calibration loop with a catch tank as depicted in Figure 10.25. Tank A is a large tank from which fluid is pumped back to a constant head reservoir, which supplies the loop with a steady flow. Tank B is the catch-and-weigh tank into which liquid can be diverted for an accurately determined period of time. The liquid volume is measured, either directly using a positive displacement meter, or indirectly through its weight, and the flow rate deduced through time. The ability to determine the volume and the uncertainty in the initial and final time of the event are fundamental limitations to the accuracy of this technique. Neglecting installation effects, the ultimate limits of uncertainty (at 95%) in the flow rate of liquids are on the order of 0.03%, a number based on $u_{\text{meter}} \sim 0.02\%$, $u_V \sim 0.02\%$, and $u_t \sim 0.01\%$.

Flow meter calibration by determining the pipe velocity profile is particularly effective for *in situ* calibration in both liquids and gases, provided that the gas velocity does not exceed about 70% of the sonic velocity. Velocity traverses at any cross-sectional location some 20 to 40 pipe diameters downstream of any pipe fitting in a long section of straight pipe are preferred.

Comparison calibration against a local standard flow meter is another common means of establishing the flow rate through a prover. Flow meters are installed in tandem with the standard and directly calibrated against it. Turbine and vortex meters and Coriolis mass flow meters have consistent, highly accurate calibration curves and are often used as local standards. Other provers

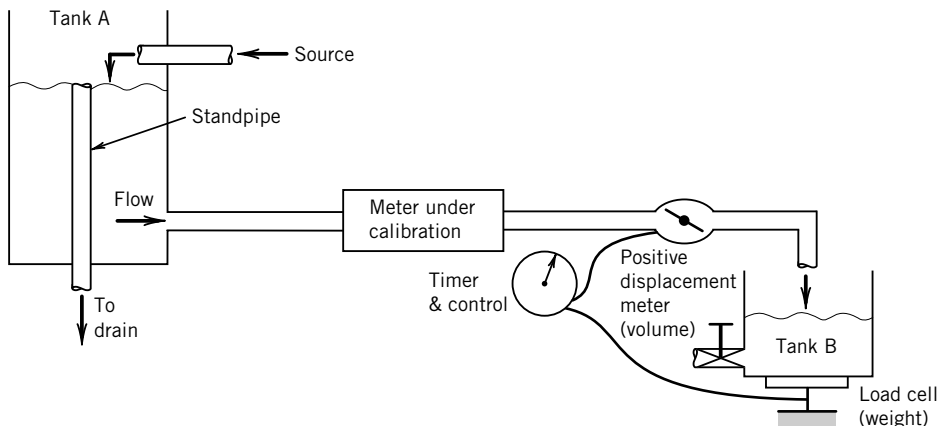


Figure 10.25 Flow diagram of a flow meter prover for liquids.

use an accurate positive displacement meter to determine flow volume over time. Of course, these standards must be periodically recalibrated. In the United States, the National Institute of Standards and Technology (NIST) maintains flow meter calibration facilities for this purpose. However, installation effects in the end-user facility are not accounted for in an NIST calibration. This last point accounts for much of the uncertainty in a flow meter calibration and use. Lastly, a sonic nozzle can also be used as a standard to establish the flow rate of a gas in a comparison calibration.

In any of these methods, the calibration uncertainty is limited by the standard used, installation effects, end-use variations, and the inherent limitations of the flow meter calibrated.

10.9 ESTIMATING STANDARD FLOW RATE

When the range of pressures and temperatures for flow processes vary in use, the measured “actual” flow rates can be adjusted to a standard temperature and pressure for comparison. This adjusted flow rate is called the *standard flow rate*. Standard flow rates are often reported in units such as standard cubic meters per minute (SCMM) or standard cubic feet per minute (SCFM). They are found by converting from the actual conditions at the measurement point, with the actual flow rate noted with corresponding units, such as ACMM or ACFM, in which A stand for “actual.” The mass flow rate remains the same regardless of conditions, so using subscript *s* for the standard conditions and *a* for the actual measured conditions, we have $\dot{m}_s = \dot{m}_a$, so that

$$Q_s = Q_a \frac{\rho_a}{\rho_s} \quad (10.41)$$

For example, the actual flow rates of common gases are “standardized” to 760 mm Hg absolute and 20°C. Assuming ideal gas behavior, $\rho = p/RT$, the standard flow rate is found from Equation 10.41 as

$$Q_s = Q_a \frac{T_s p_a}{T_a p_s} = Q_a \left(\frac{293}{273 + T_a} \right) \left(\frac{760 + p_a}{760} \right) \quad (10.42)$$

10.10 SUMMARY

Flow quantification has been an important engineering task for well over two millennia. This chapter presents methods to determine the volume rate of flow and the mass rate of flow. The engineering decision involving the selection of a particular meter depends on a number of constraining factors. In general, flow rate can be determined to within about 0.25% of actual flow rate with the best of present technology but practical values for industrial installations are more nearly 3–6% for obstruction meters and 1–3% for insertion meters. However, new methods may push these lower limits even further, provided that calibration standards can be developed to document method uncertainties and the effects of installation.

REFERENCES

1. American Society of Mechanical Engineers, *PTC 19.5 - Flow Measurements*, ASME International, New York, 2005.
2. American Society of Heating, Refrigeration and Air Conditioning Engineers (ASHRAE), *ASHRAE Fundamentals*, Rev. ed., ASHRAE, Atlanta, 2009.
3. American Society of Mechanical Engineers, *Measurement of Fluid Flow in Pipes Using Orifice, Nozzle and Venturi*, ASME Standard MFC-3M-1985, ASME International, New York, 1985.
4. International Organization for Standardization (ISO), *Measurement of fluid flow by means of pressure differential devices inserted in circular cross-section conduits: Parts 1 through 4*, ISO 5167, ISO, Geneva, 2003.
5. Rouse, H., and S. Ince, *History of Hydraulics*, Dover, New York, 1957.
6. Amberg, B. T., A review of critical flowmeters for gas flow measurements, *Transactions of the ASME*, 84, 1962, pp. 447–460.
7. Mattingly, G., *Fluid measurements: Standards, Calibrations and Traceabilities*, Proceedings of the ASME/AIChE National Heat Transfer Conference, Philadelphia, PA, 1989.
8. Shercliff, J. A., *Theory of Electromagnetic Flow Measurement*, Cambridge University Press, New York, 1962.
9. da Vinci, L., *Del Moto e Misura Dell'Aqua* (English translation), E. Carusi and A. Favaro, eds., Zanichelli, Bologna, 1923.
10. Hochreiter, H. M., Dimensionless correlation of coefficients of turbine-type flow-meters, *Transactions of the ASME*, 80; 1958, pp. 1363–1368.
11. Lee, W. F., and H. Karlby, A study of viscosity effects and its compensation on turbine flow meters, *Journal of Basic Engineering*, 82, 1960, pp. 717–728.
12. Hinze, J. O., *Turbulence*, McGraw-Hill, New York, 1953.
13. American Society of Mechanical Engineers, *Measurement of Fluid Flow by Means of Coriolis Mass Flow Meters*, MFC-11M, ASME International, 2003.
14. Corwon, M., and R. Oliver, Omega-shaped Coriolis-type Mass Flow Meter System, U.S. Patent 4,852,410, 1989.
15. Jorgensen, R. (ed), *Fan Engineering*, 8th edition, Buffalo Forge Co., Buffalo, New York, 1983.
16. Crane Company, *Flow of Fluids through Valves and Fittings*, Technical Paper No. 410, Spiral Edition, Crane Co., Chicago, 2009.

NOMENCLATURE

c_p, c_v	specific heats ($J^2/t^2\circ$)	\dot{m}	mass flow rate (mt^{-1})
d	diameter (l)	p	pressure ($ml^{-1}t^{-2}$)
d_0	flow meter throat or minimum diameter (l)	$p_1 - p_2, \Delta p$	pressure differential ($ml^{-1}t^{-2}$)
d_1	pipe diameter (l)	Δp_{loss}	permanent pressure loss ($ml^{-1}t^{-2}$)
d_2	vena contracta diameter (see Fig. 10.3) (l)	r	radial coordinate (l)
f	cyclical frequency ($\omega/2\pi$) (t^{-1})	r_1	pipe radius (l)
g	gravitational acceleration constant (lt^{-2})	r_H	hydraulic radius (l)
$h_{L_{1-2}}$	energy head loss between points 1 and 2 (l)	A	area (l^2)
k	ratio of specific heats, c_p/c_v	A_0	area based on d_0 (l^2)
C	discharge coefficient	A_1	area based on pipe diameter d_1 (l^2)
C_D	drag coefficient	\mathbf{B}	vena contracta area (l^2)
E	velocity of approach factor; voltage	S	magnetic field flux vector
Gr	Grashof number	T	specific gravity
H	manometer deflection (l)	U	temperature ($^\circ$); torque (ml^2t^{-2})
K_0	flow coefficient ($= CE$)	∇	velocity (lt^{-1})
K_1	flow meter constant; K -factor; static sensitivity	Y	volume (l^3)
L	length (l)	β	expansion factor
Q	volume flow rate (l^3t^{-1})	ρ	diameter ratio
R	gas constant	δ	density (ml^{-3})
Re_{d_1}	Reynolds number (based on d_1)	ω	twist angle
		μ	frequency (t^{-1}); angular velocity (t^{-1})
		v	absolute viscosity ($ml^{-1}t^{-1}$)
			kinematic viscosity ($= \mu/\rho$) (l^2t^{-1})

PROBLEMS

- 10.1** Determine the average mass flow rate of 5°C air at 1 bar abs through a 5-cm-i.d. pipe whose velocity profile is found to be symmetric and described by $U(r) = 25[1 - (r/r_1)^2]$ cm/s
- 10.2** A 10-cm-i.d. pipe of flowing 10°C air is traversed along three radial lines with measurements taken at five equidistant stations along each radial. Determine the average pipe flow rate.

Radial		$U(r)$ (cm/s)		
Location	r (cm)	Line 1	Line 2	Line 3
1	1.0	25.31	24.75	25.10
2	3.0	22.48	22.20	22.68
3	5.0	21.66	21.53	21.79
4	7.0	15.24	13.20	14.28
5	9.0	5.12	6.72	5.35

- 10.3** What is the best estimate of the pipe flow rate for Problem 10.2, accounting for spatial variation and if the systematic standard uncertainty of the instrument is 1% of the reading?
- 10.4** A manometer is used in a 5.1-cm water line to measure the pressure drop across a flow meter. Mercury is used as the manometric fluid ($S = 13.57$). If the manometer deflection is 10.16 cm Hg, determine the pressure drop in N/m².
- 10.5** A capacitance pressure transducer is used to measure the pressure differential across an orifice meter located in a 25.4-cm pipe. For air flowing at 32°C, if the pressure differential is 69 kPa, find the pressure head in cm H₂O.
- 10.6** Estimate the expansion factor in measuring the flow of O₂ at 16°C through a 100-mm-i.d. pipe using a square-edged orifice plate. The upstream pressure is 6.9 bar and the downstream pressure is 5.24 bar. The orifice diameter is 50 mm. $R_{O_2} = 260 \text{ J/kg-K}$.
- 10.7** The Reynolds number of a fluid flowing through a 5-cm-diameter, square-edged orifice plate meter within a 15-cm pipe is 250,000. Find the discharge coefficient for flange taps.
- 10.8** At what flow rate of 20°C water through a 10-cm-i.d. pipe would the discharge coefficient of a square-edged orifice plate ($\beta = 0.4$) become essentially independent of the Reynolds number?
- 10.9** Water (25°C) flows through a square-edged orifice plate ($\beta = 0.5$) housed within a 12-cm-i.d. pipe at 50 L/s. Estimate the power required to overcome the orifice plate's permanent pressure loss. Assume flange taps.
- 10.10** Determine the flow rate of 38°C air through a 6-cm pipe if an ASME flow nozzle with a 3-cm throat and throat taps are used, the pressure drop measured is 75 cm H₂O, and the upstream pressure is 94.4 kPa abs.
- 10.11** A square-edged orifice ($\beta = 0.5$) is used to meter N₂ at 520°F through a 4-in. pipe. If the upstream pressure is 20 psia and the downstream pressure is 15 psia, determine the flow rate through the pipe. Flange taps are used. $R_{N_2} = 55.13 \text{ ft-lb/lbm-R}$.
- 10.12** Size a suitable orifice plate to meter the steady flow of water at 20°C flowing through a 38-cm pipe if the nominal flow rate expected is 200 kg/s and the pressure drop must not exceed 15 cm Hg.
- 10.13** A cast venturi meter is to be used to meter the flow of 15°C water through a 10-cm pipe. For a maximum differential pressure of 76 cm H₂O and a nominal 0.5-m³/min flow rate, select a suitable throat size.
- 10.14** For 120 ft³/m of 60°F water flowing through a 6-in. pipe, size a suitable orifice, venturi, and nozzle flow meter if the maximum pressure drop cannot exceed 20 in. Hg. Estimate the permanent losses associated with each meter. Compare the annual operating cost associated with each if the power cost is \$0.10/kW-h, a 60% efficient pump motor is used, and the meter is operated 6000 hr/year.
- 10.15** Estimate the flow rate of water through a 15-cm-i.d. pipe that contains an ASME long radius nozzle ($\beta = 0.6$) if the pressure drop across the nozzle is 25.4 cm Hg. Water temperature is 27°C.
- 10.16** Locate a suitable position for a 10-cm square-edged orifice along a 2-m straight run of 20-cm i.d. pipe if the orifice must be situated downstream but in-plane of a 90-degree elbow using ASME codes.
- 10.17** An orifice ($\beta = 0.4$) is used as a sonic nozzle to meter a 40°C air flow in a 5-cm pipe. If upstream pressure is 695 mm Hg abs and downstream pressure is 330 mm Hg abs, estimate the mass flow rate through the meter. $R = 287 \text{ N-m/kg-K}$, $k = 1.4$.
- 10.18** Compute the flow rate of 20°C air through a 0.5-m square-edged orifice plate that is situated in a 1.0-m-i.d. pipe. The pressure drop across the plate is 90 mm H₂O, and upstream pressure is 2 atm.

- 10.19** An ASME long radius nozzle ($\beta = 0.5$) is to be used to meter the flow of 20°C water through a 8-cm-i.d. pipe. If flow rates range from 0.6 to 1.6 L/s, select the range required of a single pressure transducer if that transducer is used to measure pressure drop over the flow rate range. If the transducer to be used has a typical error of 0.25% of full scale, estimate the uncertainty in flow rate at the design stage.
- 10.20** A square-edged orifice plate is selected to meter the flow of water through a 2.3-in.-i.d. pipe over the range of 10 to 50 gal/min at 60°F. It is desired to operate the orifice in the range where C is independent of the Reynolds number for all flow rates. A pressure transducer having accuracy to within 0.5% of reading is to be used. Select a suitable orifice plate and estimate the design-stage uncertainty in the measured flow rate at 10, 25, and 50 gal/min. Assume flange pressure taps and reasonable values for the systematic uncertainty on pertinent parameters.
- 10.21** Estimate the error contribution to the uncertainty in flow rate due to the effect of the relative humidity of air on air density. Consider the case of using an orifice plate to meter air flow if the relative humidity of the 70°F air can vary from 10% to 80% but a density equivalent to 45% relative humidity is used in the computations.
- 10.22** For Problem 10.21, suppose the air flow rate is 17 m³/hr at 20°C through a 6-cm-i.d. pipe, a square-edged orifice ($\beta = 0.4$) is used with flange taps, and the pressure drop can be measured to within 0.5% of reading for all pressures above 5 cm H₂O using a manometer. If basic dimensions are maintained to within 0.1 mm, estimate a design-stage uncertainty in the flow rate. Use $p_1 = 96.5$ kPa abs, $R = 287$ N·m/kg·K.
- 10.23** An application uses water flowing at up to 0.2 m³/min of 20°C through a 10-cm-diameter pipe. The engineer wants to select from a set of orifice plates using flange taps to measure and monitor the flow. It is desired that the meter develop a nominal 250 mm Hg pressure head. Specify an appropriate size (d_o) for the orifice meter. $S_{Hg} = 13.6$.
- 10.24** A sonic nozzle can be used to regulate air flow by intentionally designing it to choke the flow at the throat. Consider the case where we use an ASME long radius nozzle to regulate air at 70°F (20°C) to 45 ft³/min (1.27 m³/s). Determine the downstream pressure required to choke the nozzle if air is supplied at 14.1 psia (97.2 kPa abs). Select a suitable nozzle throat diameter. $k = 1.4$, $R = 53.3$ (ft-lb)/(lb_m·°R) = 287 N·m/kg·K.
- 10.25** Select an appropriate range for a differential pressure transducer to be used with an ASME long radius nozzle with $\beta = 0.5$. This system is to be used to measure the flow of 20°C water through a 20-cm diameter pipe. The operating flow rate expected is between 5000 cm³/s and 50,000 cm³/s. Estimate the permanent pressure loss associated with this nozzle. As an optional assignment, go to a vendor catalog or Web site and select an appropriate pressure transducer from its listings that has a 0- to 5-V DC output.
- 10.26** From a vendor catalog or online site, select a differential pressure transducer to measure between 203 Pa and 20,100 Pa across an obstruction meter. The transducer must be compatible with water. The output signal is to be measured using a data-acquisition system with 0 to 5 V, 12-bit analog-to-digital converter. Estimate the percent relative quantization error at the low and high flow rates. Based on your selection, do you recommend any signal conditioning?
- 10.27** A vortex flow meter uses a shedder having a Strouhal number of 0.20. Estimate the mean duct velocity if the shedding frequency indicated is 77 Hz and the shedder characteristic length is 1.27 cm.

- 10.28** A thermal mass flow meter is used to meter 30°C air flow through a 2-cm-i.d. pipe. If 25 W of power are required to maintain a 1°C temperature rise across the meter, estimate the mass flow rate through the meter. Clearly state any assumptions. $c_p = 1.006 \text{ kJ/kg}\cdot\text{K}$.
- 10.29** Research available thermal mass flow meters. Discuss the assumptions necessary for their use. Describe situations where they would be appropriate and not appropriate.
- 10.30** When used with air (or any perfect gas), a sonic nozzle can be used to regulate volume flow rate. However, uncertainty arises due to variations in density brought on by local atmospheric pressure and temperature changes. For a range of $101.3 \pm 7 \text{ kPa abs}$ and $10^\circ \pm 5^\circ\text{C}$, estimate the error in regulating a $1.4\text{-m}^3/\text{min}$ flow rate at critical pressure ratio due to these variations alone.
- 10.31** Estimate an uncertainty in the determined flow rate in Example 10.5, assuming that dimensions are known to within 0.025 mm, the systematic uncertainty in pressure is 0.25 cm H₂O, and the pressure drop shows a standard deviation of 0.5 cm H₂O in 31 readings. Upstream pressure is constant. State your reasonable assumptions.
- 10.32** A thermal mass flow meter is used to meter air in a 1-cm-i.d. tube. The meter adds 10 W of energy to the air passing through the meter, from which the meter senses a 3°C temperature gain. What is the mass flow rate? $c_p = 1.006 \text{ kJ/kg}\cdot\text{K}$.
- 10.33** A vortex meter is to use a shedder having a profile of a forward facing equilateral triangle (Table 10.1) with a characteristic length of 10 mm. Estimate the shedding frequency developed for 20°C air at 30 m/s in a 10-cm-i.d. pipe. Estimate the meter constant and measured flow rate.
- 10.34** The flow of air is measured to be $30 \text{ m}^3/\text{min}$ at 50 mm Hg and 15°C. What is the flow rate in SCMM?
- 10.35** A 6 in. \times 4 in. i.d. cast venturi is used to measure the flow rate of water. Estimate the flow rate and its uncertainty at 95%. The following values are known from a large sample:

x	Value	$b_{\bar{x}}$	$s_{\bar{x}}$
C	0.984	0.00375	0
d_o	3.995 in.	0.0005	0
d_i	6.011 in.	0.001	0
ρ	$62.369 \text{ lb}_m/\text{ft}^3$	0.002	0.002
H	100 in H ₂ O @ 68°F	0.15	0.4

- 10.36** A 60-mm-i.d. pipe will be used to transport alcohol ($\rho = 790 \text{ kg/m}^3$; $\mu = 1.2 \times 10^{-3} \text{ N}\cdot\text{s/m}^2$) from storage to its point of use in a manufacturing process. A flow nozzle with flange taps is selected to meter the flow. If a pressure drop of 4kPa is desired at $0.003 \text{ m}^3/\text{s}$, specify the nozzle diameter, d_o .

Chapter 11

Strain Measurement

11.1 INTRODUCTION

The design of load-carrying components for machines and structures requires information concerning the distribution of forces within the particular component. Proper design of devices such as shafts, pressure vessels, and support structures must consider load-carrying capacity and allowable deflections. Mechanics of materials provides a basis for predicting these essential characteristics of a mechanical design, and provides the fundamental understanding of the behavior of load-carrying parts. However, theoretical analysis is often not sufficient, and experimental measurements are required to achieve a final design.

Engineering designs are based on a safe level of stress within a material. In an object that is subject to loads, forces within the object act to balance the external loads.

As a simple example, consider a slender rod that is placed in uniaxial tension, as shown in Figure 11.1. If the rod is sectioned at B–B, a force within the material at B–B is necessary to maintain static equilibrium for the sectioned rod. Such a force within the rod, acting per unit area, is called *stress*. Design criteria are based on stress levels within a part. In most cases stress cannot be measured directly. But the length of the rod in Figure 11.1 changes when the load is applied, and such changes in length or shape of a material can be measured. This chapter discusses the measurement of physical displacements in engineering components. The stress is calculated from these measured deflections.

Upon completion of this chapter, the reader will be able to

- define strain and delineate the difficulty in measuring stress,
- state the physical principles underlying mechanical strain gauges,
- analyze strain gauge bridge circuits, and
- describe methods for optical strain measurement.

11.2 STRESS AND STRAIN

Before we proceed to develop techniques for strain measurements, we briefly review the relationship between deflections and stress. The experimental analysis of stress is accomplished by measuring the deformation of a part under load, and inferring the existing state of stress from the measured deflections. Again, consider the rod in Figure 11.1. If the rod has a cross-sectional area of A_c , and the

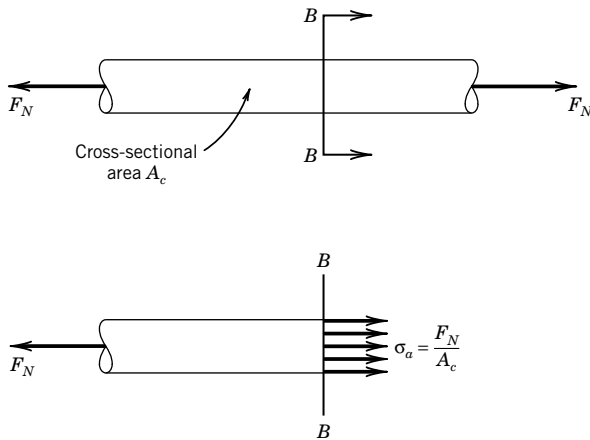


Figure 11.1 Free-body diagram illustrating internal forces for a rod in uniaxial tension.

load is applied only along the axis of the rod, the normal stress is defined as

$$\sigma_a = F_N / A_c \quad (11.1)$$

where A_c is the cross-sectional area and F_N is the tension force applied to the rod normal to the area A_c . The ratio of the change in length of the rod (which results from applying the load) to the original length is the *axial strain*, defined as

$$\varepsilon_a = \delta L / L \quad (11.2)$$

where ε_a is the average strain over the length L , δL is the change in length, and L is the original unloaded length. For most engineering materials, strain is a small quantity; strain is usually reported in units of 10^{-6} in./in. or 10^{-6} m/m. These units are equivalent to a dimensionless unit called a microstrain ($\mu\epsilon$).

Stress-strain diagrams are very important in understanding the behavior of a material under load. Figure 11.2 is such a diagram for mild steel (a ductile material). For loads less than that required to permanently deform the material, most engineering materials display a linear relationship between stress and strain. The range of stress over which this linear relationship holds is called the *elastic region*. The relationship between uniaxial stress and strain for this elastic behavior is expressed as

$$\sigma_a = E_m \varepsilon_a \quad (11.3)$$

where E_m is the modulus of elasticity, or Young's modulus, and the relationship is called Hooke's law. Hooke's law applies only over the range of applied stress where the relationship between stress and strain is linear. Different materials respond in a variety of ways to loads beyond the linear range, largely depending on whether the material is ductile or brittle. For almost all engineering components, stress levels are designed to remain well below the elastic limit of the material; thus, a direct linear relationship may be established between stress and strain. Under this assumption, Hooke's law forms the basis for experimental stress analysis through the measurement of strain.

Lateral Strains

Consider the elongation of the rod shown in Figure 11.1 that occurs as a result of the load F_N . As the rod is stretched in the axial direction, the cross-sectional area must decrease since the total mass (or

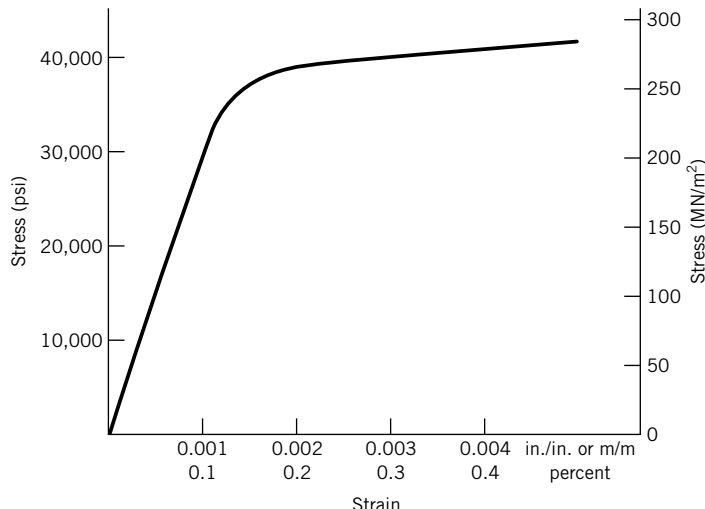


Figure 11.2 A typical stress–strain curve for mild steel.

volume for constant density) must be conserved. Similarly, if the rod were compressed in the axial direction, the cross-sectional area would increase. This change in cross-sectional area is most conveniently expressed in terms of a lateral (transverse) strain. For a circular rod, the lateral strain is defined as the change in the diameter divided by the original diameter. In the elastic range, there is a constant rate of change in the lateral strain as the axial strain increases. In the same sense that the modulus of elasticity is a property of a given material, the ratio of lateral strain to axial strain is also a material property. This property is called Poisson's ratio, defined as

$$\nu_p = \frac{|\text{Lateral strain}|}{|\text{Axial strain}|} = \frac{\varepsilon_L}{\varepsilon_a} \quad (11.4)$$

Engineering components are seldom subject to one-dimensional axial loading. The relationship between stress and strain must be generalized to a multidimensional case. Consider a two-dimensional geometry, as shown in Figure 11.3, subject to tensile loads in both the x and y directions, resulting in normal stresses σ_x and σ_y . In this case, for a biaxial state of stress, the stresses and strains are

$$\begin{aligned} \varepsilon_y &= \frac{\sigma_y}{E_m} - \nu_p \frac{\sigma_x}{E_m} & \varepsilon_x &= \frac{\sigma_x}{E_m} - \nu_p \frac{\sigma_y}{E_m} \\ \sigma_x &= \frac{E_m(\varepsilon_x + \nu_p \varepsilon_y)}{1 - \nu_p^2} & \sigma_y &= \frac{E_m(\varepsilon_y + \nu_p \varepsilon_x)}{1 - \nu_p^2} \end{aligned} \quad (11.5)$$

$$\tau_{xy} = G\gamma_{xy}$$

In this case, all of the stress and strain components lie in the same plane. The state of stress in the elastic condition for a material is similarly related to the strains in a complete three-dimensional situation (1, 2). Since stress and strain are related, it is possible to determine stress from measured strains under appropriate conditions. However, strain measurements are made at the surface of an engineering component. The measurement yields information about the state of stress on the surface

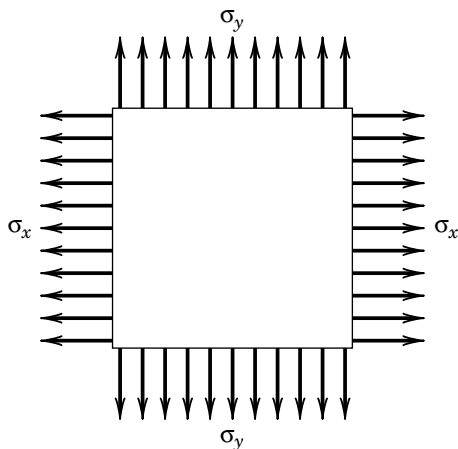


Figure 11.3 Biaxial state of stress.

of the part. The analysis of measured strains requires application of the relationship between stress and strain at a surface. Such analysis of strain data is described elsewhere (3), and an example provided in this chapter.

11.3 RESISTANCE STRAIN GAUGES

The measurement of the small displacements that occur in a material or object under mechanical load can be accomplished by methods as simple as observing the change in the distance between two scribe marks on the surface of a load-carrying member, or as advanced as optical holography. In any case, the ideal sensor for the measurement of strain would (1) have good spatial resolution, implying that the sensor would measure strain at a point; (2) be unaffected by changes in ambient conditions; and (3) have a high-frequency response for dynamic (time-resolved) strain measurements. A sensor that closely meets these characteristics is the *bonded resistance strain gauge*.

In practical application, the bonded resistance strain gauge is secured to the surface of the test object by an adhesive so that it deforms as the test object deforms. The resistance of a strain gauge changes when it is deformed, and this is easily related to the local strain. Both metallic and semiconductor materials experience a change in electrical resistance when they are subjected to a strain. The amount that the resistance changes depends on how the gauge is deformed, the material from which it is made, and the design of the gauge. Gauges can be made quite small for good resolution and with a low mass to provide a high-frequency response. With some ingenuity, ambient effects can be minimized or eliminated.

In an 1856 publication in the *Philosophical Transactions of the Royal Society* in England, Lord Kelvin (William Thomson) (4) laid the foundations for understanding the changes in electrical resistance that metals undergo when subjected to loads, which eventually led to the strain gauge concept. Two individuals began the modern development of strain measurement in the late 1930s—Edward Simmons at the California Institute of Technology and Arthur Ruge at the Massachusetts Institute of Technology. Their development of the bonded metallic wire strain gauge led to commercially available strain gauges. The resistance strain gauge also forms the basis for a variety of other transducers, such as load cells, pressure transducers, and torque meters.

Metallic Gauges

To understand how metallic strain gauges work, consider a conductor having a uniform cross-sectional area A_c and length L made of a material having an electrical resistivity, ρ_e . For this electrical conductor, the resistance, R , is given by

$$R = \rho_e L / A_c \quad (11.6)$$

If the conductor is subjected to a normal stress along the axis of the wire, the cross-sectional area and the length change resulting in a change in the total electrical resistance, R . The total change in R is due to several effects, as illustrated in the total differential:

$$dR = \frac{A_c(\rho_e dL + L d\rho_e) - \rho_e L dA_c}{A_c^2} \quad (11.7)$$

which may be expressed in terms of Poisson's ratio as

$$\frac{dR}{R} = \frac{dL}{L} (1 + 2v_p) + \frac{d\rho_e}{\rho_e} \quad (11.8)$$

Hence, the changes in resistance are caused by two basic effects: the change in geometry as the length and cross-sectional area change, and the change in the value of the resistivity, ρ_e . The dependence of resistivity on mechanical strain is called piezoresistance, and may be expressed in terms of a *piezoresistance coefficient*, π_1 defined by

$$\pi_1 = \frac{1}{E_m} \frac{d\rho_e / \rho_e}{dL / L} \quad (11.9)$$

With this definition, the change in resistance may be expressed

$$dR/R = dL/L (1 + 2v_p + \pi_1 E_m) \quad (11.10)$$

Example 11.1

Determine the total resistance of a copper wire having a diameter of 1 mm and a length of 5 cm. The resistivity of copper is $1.7 \times 10^{-8} \Omega \text{ m}$.

KNOWN

$D = 1 \text{ mm}$
$L = 5 \text{ cm}$
$\rho_e = 1.7 \times 10^{-8} \Omega \text{ m}$

FIND The total electrical resistance

SOLUTION The resistance may be calculated from Equation 11.6 as

$$R = \rho_e L / A_c$$

where

$$A_c = \frac{\pi}{4} D^2 = \frac{\pi}{4} (1 \times 10^{-3})^2 = 7.85 \times 10^{-7} \text{ m}^2$$

The resistance is then

$$R = \frac{(1.7 \times 10^{-8} \Omega \text{ m})(5 \times 10^{-2} \text{ m})}{7.85 \times 10^{-7} \text{ m}^2} = 1.08 \times 10^{-3} \Omega$$

COMMENT If the material were nickel ($\rho_e = 7.8 \times 10^{-8} \Omega \text{ m}$) instead of copper, the resistance would be $5 \times 10^{-3} \Omega$ for the same diameter and length of wire.

Example 11.2

A very common material for the construction of strain gauges is the alloy constantan (55% copper with 45% nickel), having a resistivity of $49 \times 10^{-8} \Omega \text{ m}$. A typical strain gauge might have a resistance of 120Ω . What length of constantan wire of diameter 0.025 mm would yield a resistance of 120Ω ?

KNOWN The resistivity of constantan is $49 \times 10^{-8} \Omega \text{ m}$.

FIND The length of constantan wire needed to produce a total resistance of 120Ω

SOLUTION From Equation 11.6, we may solve for the length, which yields in this case

$$L = \frac{RA_c}{\rho_e} = \frac{(120 \Omega)(4.91 \times 10^{-10} \text{ m}^2)}{49 \times 10^{-8} \Omega \text{ m}} = 0.12 \text{ m}$$

The wire would then be 12 cm in length to achieve a resistance of 120Ω .

COMMENT As shown by this example, a single straight conductor is normally not practical for a local strain measurement with meaningful resolution. Instead, a simple solution is to bend the wire conductor so that several lengths of wire are oriented along the axis of the strain gauge, as shown in Figure 11.4.

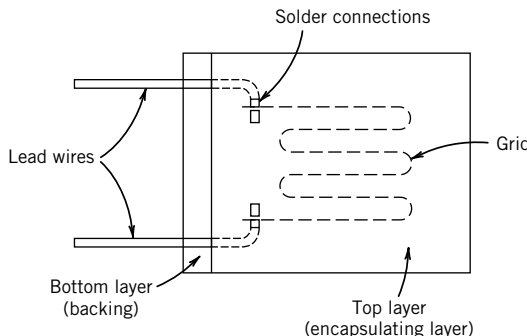


Figure 11.4 Detail of a basic strain gauge construction. (Courtesy of Micro-Measurements Division, Measurements Group, Inc., Raleigh, NC.)

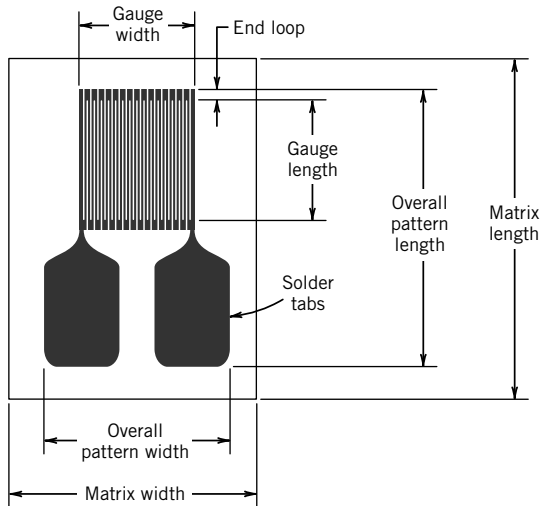


Figure 11.5 Construction of a typical metallic foil strain gauge. (Courtesy of Micro-Measurements Division, Measurements Group, Inc., Raleigh, NC.)

Strain Gauge Construction and Bonding

Figure 11.5 illustrates the construction of a typical metallic-foil bonded strain gauge. Such a strain gauge consists of a metallic foil pattern that is formed in a manner similar to the process used to produce printed circuits. This photoetched metal foil pattern is mounted on a plastic backing material. The *gauge length*, as illustrated in Figure 11.5, is an important specification for a particular application. Since strain is usually measured at the location on a component where the stress is a maximum and the stress gradients are high, the strain gauge averages the measured strain over the gauge length. Because the maximum strain is the quantity of interest and the gauge length is the resolution, errors due to averaging can result from improper choice of a gauge length (5).

The variety of conditions encountered in particular applications require special construction and mounting techniques, including design variations in the backing material, the grid configuration, bonding techniques, and total gauge electrical resistance. Figure 11.6 shows a variety of strain gauge configurations. The adhesives used in the bonding process and the mounting techniques for a particular gauge and manufacturer vary according to the specific application. However, there are some fundamental aspects that are common to all bonded resistance gauges.

The strain gauge backing serves several important functions. It electrically isolates the metallic gauge from the test specimen, and transmits the applied strain to the sensor. A bonded resistance strain gauge must be appropriately mounted to the specimen for which the strain is to be measured. The backing provides the surface used for bonding with an appropriate adhesive. Backing materials are available that are useful over temperatures that range from -270° to 290°C .

The adhesive bond serves as a mechanical and thermal coupling between the metallic gauge and the test specimen. As such, the strength of the adhesive should be sufficient to accurately transmit the strain experienced by the test specimen, and should have thermal conduction and expansion

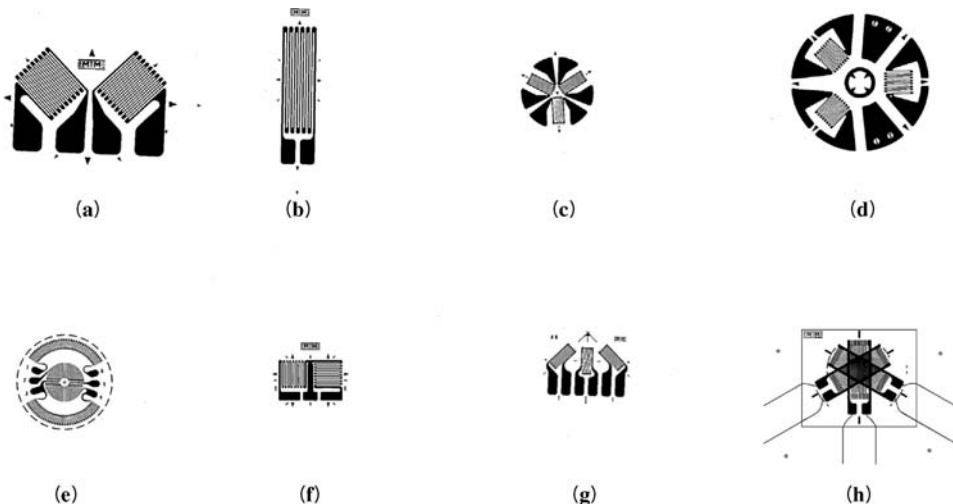


Figure 11.6 Strain gauge configurations. (a) Torque Rosette; (b) Linear Pattern; (c) Delta Rosette; (d) Residual Stress Pattern; (e) Diaphragm Pattern; (f) Tee Pattern; (g) Rectangular Rosette; (h) Stacked Rosette. (Courtesy of Micro-Measurements Division, Measurements Group, Inc., Raleigh, NC.)

characteristics suitable for the application. If the adhesive shrinks or expands during the curing process, apparent strain can be created in the gauge. A wide array of adhesives are available for bonding strain gauges to a test specimen. Among these are epoxies, cellulose nitrate cement, and ceramic-based cements.

Gauge Factor

The change in resistance of a strain gauge is normally expressed in terms of an empirically determined parameter called the *gauge factor* (GF). For a particular strain gauge, the gauge factor is supplied by the manufacturer. The gauge factor is defined as

$$GF \equiv \frac{\delta R/R}{\delta L/L} = \frac{\delta R/R}{\varepsilon_a} \quad (11.11)$$

Relating this definition to Equation 11.10, we see that the gauge factor is dependent on the Poisson ratio for the gauge material and its piezoresistivity. For metallic strain gauges, the Poisson ratio is approximately 0.3 and the resulting gauge factor is ~ 2 .

The gauge factor represents the total change in resistance for a strain gauge, under a calibration loading condition. The calibration loading condition generally creates a biaxial strain field, and the lateral sensitivity of the gauge influences the measured result. Strictly speaking then, the sensitivity to normal strain of the material used in the gauge and the gauge factor are not the same. Generally gauge factors are measured in a biaxial strain field that results from the deflection of a beam having a value of Poisson's ratio of 0.285. Thus, for any other strain field there is an error in strain indication due to the transverse sensitivity of the strain gauge. The

percentage error due to transverse sensitivity for a strain gauge mounted on any material at any orientation in the strain field is

$$e_L = \frac{K_t(\varepsilon_L/\varepsilon_a + v_{p0})}{1 - v_{p0}K_t} \times 100 \quad (11.12)$$

where

$\varepsilon_a, \varepsilon_L$ = axial and lateral strains, respectively (with respect to the axis of the gauge)

v_{p0} = Poisson's ratio of the material on which the manufacturer measured GF
(usually 0.285 for steel)

e_L = error as a percentage of axial strain (with respect to the axis of the gauge)

K_t = lateral (transverse) sensitivity of the strain gauge

The uncorrected estimate can be used as the uncertainty.

Typical values of the transverse sensitivity for commercial strain gauges range from -0.19 to 0.05 . Figure 11.7 shows a plot of the percentage error for a strain gauge as a function of the ratio of lateral loading to axial loading and the lateral sensitivity. It is possible to correct for the lateral sensitivity effects (6).

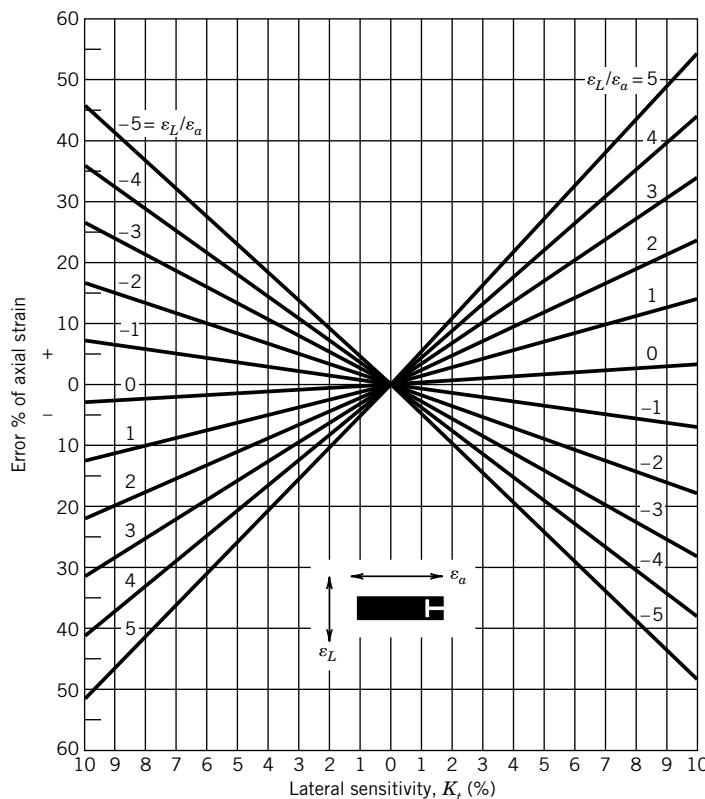


Figure 11.7 Strain measurement error due to strain gauge transverse sensitivity.
(Courtesy of Measurements Group, Inc., Raleigh, NC.)

Semiconductor Strain Gauges

When subjected to a load, a semiconductor material exhibits a change in resistance, and therefore can be used for the measurement of strain. Silicon crystals are the basic material for semiconductor strain gauges; the crystals are sliced into very thin sections to form strain gauges. Mounting such gauges in a transducer, such as a pressure transducer, or on a test specimen requires backing and adhesive techniques similar to those used for metallic gauges. Because of the large piezoresistance coefficient, the semiconductor gauge exhibits a very large gauge factor, as large as 200 for some gauges. These gauges also exhibit higher resistance, longer fatigue life, and lower hysteresis under some conditions than metallic gauges. However, the output of the semiconductor strain gauge is nonlinear with strain, and the strain sensitivity or gauge factor may be markedly dependent on temperature.

Semiconductor materials for strain gauge applications have resistivities ranging from 10^{-6} to $10^{-2} \Omega\text{-m}$. Semiconductor strain gauges may have a relatively high or low density of charge carriers (3, 7). Semiconductor strain gauges made of materials having a relatively high density of charge carriers ($\sim 10^{20}$ carriers/cm 3) exhibit little variation of their gauge factor with strain or temperature. On the other hand, for the case where the crystal contains a low number of charge carriers ($< 10^{17}$ carriers/cm 3), the gauge factor may be approximated as

$$GF = \frac{T_0}{T} GF_0 + C_1 \left(\frac{T_0}{T} \right)^2 \quad (11.13)$$

where GF_0 is the gauge factor at the reference temperature T_0 , under conditions of zero strain (8), and C_1 is a constant for a particular gauge. The behavior with temperature of a high-resistivity P-type semiconductor is shown in Figure 11.8.

Semiconductor strain gauges find their primary application in the construction of transducers, such as load cells and pressure transducers. Because of the capability for producing small gauge

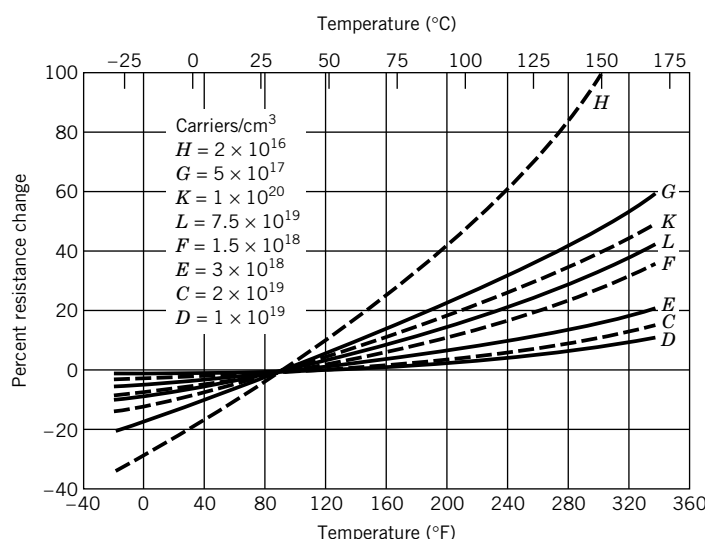


Figure 11.8 Temperature effect on resistance for various impurity concentrations for P-type semiconductors (reference resistance at 81°F). (Courtesy of Kulite Semiconductor Products, Inc.)

lengths, silicon semiconductor strain gauge technology provides for the construction of very small transducers. For example, flush-mount pressure transducers having diameters of less than 8 mm provide pressure measurements up to 15,000 psi, with excellent frequency response characteristics. However, silicone diaphragm pressure transducers require special procedures for measuring in liquid environments such as deposition of a thin film of next material over the silicone diaphragm. Semiconductor strain gauges are somewhat limited in the maximum strain that they can measure, approximately $5000 \mu\epsilon$ for tension, but larger in compression. Because of the possibility of an inherent sensitivity to temperature, careful consideration must be given to each application to provide appropriate temperature compensation or correction. Temperature effects can result, for a particular measurement, in zero drift for the duration of a measurement.

11.4 STRAIN GAUGE ELECTRICAL CIRCUITS

A Wheatstone bridge is generally used to detect the small changes in resistance that are the output of a strain gauge measurement circuit. A typical strain gauge measuring installation on a steel specimen has a sensitivity of $10^{-6} \Omega/(kN m^2)$. As such, a high-sensitivity device such as a Wheatstone bridge is desirable for measuring resistance changes for strain gauges. The fundamental relationships for the analysis of such bridge circuits are discussed in Chapter 6. Equipment is commercially available that can measure changes in gauge resistance of less than 0.0005Ω ($0.000001 \mu\epsilon$).

A simple strain gauge Wheatstone bridge circuit is shown in Figure 11.9. The bridge output under these conditions is given by Equation 6.15:

$$E_0 + \delta E_0 = E_i \frac{(R_1 + \delta R)R_4 - R_3R_2}{(R_1 + \delta R + R_2)(R_3 + R_4)} \quad (6.15)$$

where E_0 is the bridge output at initial conditions, δE_0 is the bridge deflection associated with the change in the strain gauge resistance δR . Consider the case where all the fixed resistors and the strain gauge resistance are initially equal, and the bridge is balanced such that $E_0 = 0$. If the strain gauge is then subjected to a state of strain, the change in the output voltage, δE_0 , from Equation 6.15

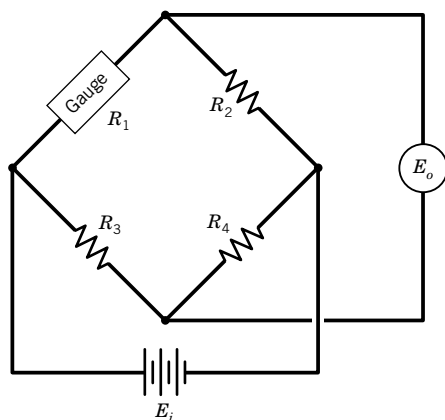
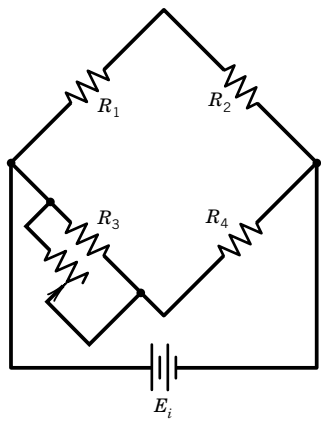
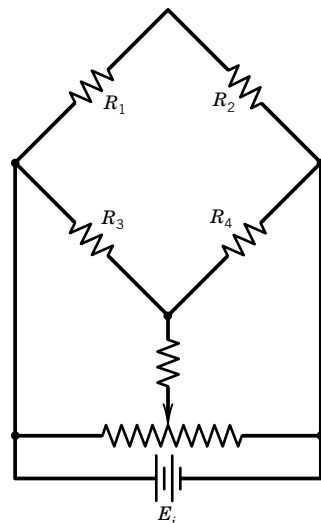


Figure 11.9 Basic strain gauge Wheatstone bridge circuit.

Circuit arrangement for shunt balance



Differential shunt balance arrangement

**Figure 11.10** Balancing schemes for bridge circuits.

reduces to

$$\frac{\delta E_o}{E_i} = \frac{\delta R/R}{4 + 2(\delta R/R)} \approx \frac{\delta R/R}{4} \quad (11.14)$$

under the assumption that $\delta R/R \ll 1$. This simplified form of Equation 6.15 is suitable for all but those measurements that demand the highest accuracy, and is valid for values of $\delta R/R \ll 1$. Using the relationship from Equation 11.11 that $\delta R/R = GF\epsilon$,

$$\frac{\delta E_o}{E_i} = \frac{GF\epsilon}{4 + 2GF\epsilon} \approx \frac{GF\epsilon}{4} \quad (11.15)$$

Equations 11.14 and 11.15 yield two practical equations for strain gauge measurements using a single gauge in a Wheatstone bridge.

The Wheatstone bridge has several distinct advantages for use with electrical resistance strain gauges. The bridge may be balanced by changing the resistance of one arm of the bridge. Therefore, once the gauge is mounted in place on the test specimen under a condition of zero loading, the output from the bridge may be zeroed. Two schemes for circuits to accomplish this balancing are shown in Figure 11.10. Shunt balancing provides the best arrangement for strain gauge applications, since the changes in resistance for a strain gauge are small. Also, the strategic placement of multiple gauges in a Wheatstone bridge can both increase the bridge output and cancel out certain ambient effects and unwanted components of strain as discussed in the next two sections.

Example 11.3

A strain gauge, having a gauge factor of 2, is mounted on a rectangular steel bar ($E_m = 200 \times 10^6 \text{ kN/m}^2$), as shown in Figure 11.11. The bar is 3 cm wide and 1 cm high, and is subjected

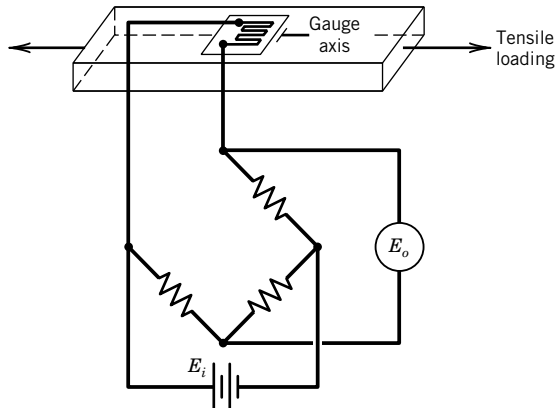


Figure 11.11 Strain gauge circuit subject to uniaxial tension.

to a tensile force of 30 kN. Determine the resistance change of the strain gauge if the resistance of the gauge was $120\ \Omega$ in the absence of the axial load.

$$\text{KNOWN} \quad GF = 2 \quad E_m = 200 \times 10^6 \text{ kN/m}^2 \quad F_N = 30 \text{ kN}$$

$$R = 120\ \Omega \quad A_c = 0.03 \text{ m} \times 0.01 \text{ m}$$

FIND The resistance change of the strain gauge for a tensile force of 30 kN

SOLUTION The stress in the bar under this loading condition is

$$\sigma_a = \frac{F_N}{A_c} = \frac{30 \text{ kN}}{(0.03 \text{ m})(0.01 \text{ m})} = 1 \times 10^5 \text{ kN/m}^2$$

and the resulting strain is

$$\varepsilon_a = \frac{\sigma_a}{E_m} = \frac{1 \times 10^5 \text{ kN/m}^2}{200 \times 10^6 \text{ kN/m}^2} = 5 \times 10^{-4} \text{ m/m} \quad (11.16)$$

For strain along the axis of the strain gauge, the change in resistance from Equation 11.11 is

$$\delta R/R = \varepsilon GF$$

or

$$\delta R = R\varepsilon GF = (120\Omega)(5 \times 10^{-4})(2) = 0.12\ \Omega$$

Example 11.4

Suppose the strain gauge described in Example 11.3 is to be connected to a measurement device capable of determining a change in resistance with a stated uncertainty of $\pm 0.005\ \Omega$ (95%). This stated uncertainty includes a resolution of $0.001\ \Omega$. What uncertainty in stress would result when using this resistance measurement device?

KNOWN A stress is to be inferred from a strain measurement using a strain gauge having a gauge factor of 2 and a zero load resistance of $120\ \Omega$. The measurement of resistance has a stated uncertainty of $\pm 0.005\ \Omega$ (95%).

FIND The design-stage uncertainty in stress

SOLUTION The design-stage uncertainty in stress, $(u_d)_\sigma$, is given by

$$(u_d)_\sigma = \frac{\partial \sigma}{\partial (\delta R)} (u_d)_{\delta R}$$

with

$$\sigma = \varepsilon E_m = \frac{\delta R/R}{GF} E_m$$

Then with $(u_d)_{\delta R} = 0.005 \Omega$ and

$$\frac{\partial \sigma}{\partial (\delta R)} = \frac{E_m}{R(GF)}$$

we can express the uncertainty as

$$(u_d)_\sigma = \frac{E_m}{R(GF)} (u_d)_{\delta R} = \frac{200 \times 10^6 \text{ kN/m}^2}{120 \Omega (2)} (0.005 \Omega)$$

This results in a design-stage uncertainty in stress of $(u_d)_\sigma = \pm 4.17 \times 10^3 \text{ kN/m}^2$ (95%) or $\sim 2.4\%$ of the expected stress.

11.5 PRACTICAL CONSIDERATIONS FOR STRAIN MEASUREMENT

This section describes some characteristics of strain gauge applications that allow practical implementation of strain measurement.

The Multiple Gauge Bridge

The output from a bridge circuit can be increased by the appropriate use of more than one strain gauge. This increase can be quantified by employing a *bridge constant* as illustrated in the following discussion. In addition, multiple gauges can be used to compensate for unwanted effects, such as temperature or specific strain components. Consider the case when all four resistances in the bridge circuit of Figure 11.9 represent strain gauges. In general, the bridge output is given by

$$E_0 = E_i \left[\frac{R_1}{R_1 + R_2} - \frac{R_3}{R_3 + R_4} \right] \quad (11.17)$$

The strain gauges R_1 , R_2 , R_3 , and R_4 are assumed initially to be in a state of zero strain. If these gauges are now subjected to strains such that the resistances change by dR_i , where $i = 1, 2, 3$, and 4, then the change in the bridge output voltage can be expressed as

$$dE_0 = \sum_{i=1}^4 \frac{\partial E_0}{\partial R_i} dR_i \quad (11.18)$$

Evaluating the appropriate partial derivatives from Equation 11.17 yields

$$dE_0 = E_i \left[\frac{R_2 dR_1 - R_1 dR_2}{(R_1 + R_2)^2} + \frac{R_3 dR_4 - R_4 dR_3}{(R_3 + R_4)^2} \right] \quad (11.19)$$

Then from Equations 11.2 and 11.11, $dR_i = R_i \varepsilon_i GF_i$, and the value of dE_0 can be determined. Assuming that $dR_i \ll R_i$, the resulting change in the output voltage, δE_0 , may now be expressed as

$$\delta E_0 = E_i \left[\frac{R_1 R_2}{(R_1 + R_2)^2} (\varepsilon_1 GF_1 - \varepsilon_2 GF_2) + \frac{R_3 R_4}{(R_3 + R_4)^2} (\varepsilon_4 GF_4 - \varepsilon_3 GF_3) \right] \quad (11.20)$$

If $R_1 = R_2 = R_3 = R_4$, then

$$\frac{\delta E_0}{E_i} = \frac{1}{4} (\varepsilon_1 GF_1 - \varepsilon_2 GF_2 + \varepsilon_4 GF_4 - \varepsilon_3 GF_3) \quad (11.21)$$

It is possible and desirable to purchase matched sets of strain gauges for a particular application, so that $GF_1 = GF_2 = GF_3 = GF_4$, and

$$\frac{\delta E_0}{E_i} = \frac{GF}{4} (\varepsilon_1 - \varepsilon_2 + \varepsilon_4 - \varepsilon_3) \quad (11.22)$$

Equation 11.22 is important and forms the basic working equation for a strain gauge bridge circuit using multiple gauges (compare this equation with Eq. 11.15).

Equation 11.22 shows that for a bridge containing one or more strain gauges, equal strains on opposite bridge arms sum, whereas equal strains on adjacent arms of the bridge cancel. These characteristics can be used to increase the output of the bridge, to provide temperature compensation, or to cancel unwanted components of strain. Practical means of achieving these desirable characteristics will be explored further, after the concept of the bridge constant is developed.

Bridge Constant

Commonly used strain gauge bridge arrangements may be characterized by a *bridge constant*, κ , defined as the ratio of the actual bridge output to the output that would result from a single gauge sensing the maximum strain, ε_{\max} . The output for a single gauge experiencing the maximum strain may be expressed as

$$\frac{\delta R}{R} = \varepsilon_{\max} GF \quad (11.23)$$

So that, again for a single gauge,

$$\frac{\delta E_0}{E_i} \approx \frac{\varepsilon_{\max} GF}{4} \quad (11.24)$$

The bridge constant, κ , is found from the ratio of the actual bridge output given by Equation 11.22 to the output for a single gauge given by Equation 11.24. When more than one gauge is used in the bridge circuit, Equation 11.15 becomes

$$\frac{\delta E_0}{E_i} = \frac{\kappa \delta R / R}{4 + 2 \delta R / R} = \frac{\kappa GF \varepsilon}{4 + 2 GF \varepsilon} \approx \frac{\kappa GF \varepsilon}{4} \quad (11.25)$$

The simplified form of Equation 11.25 is suitable for all but those measurements demanding the greatest accuracy possible, and remains valid for values of $\delta R/R \ll 1$. The bridge constant concept is illustrated in Example 11.5.

Example 11.5

Determine the bridge constant for two strain gauges mounted on a structural member, as shown in Figure 11.12. The member is subject to uniaxial tension, which produces an axial strain ε_a and a lateral strain $\varepsilon_L = -\nu_p \varepsilon_a$. Assume that all the resistances in Figure 11.12 are initially equal, so that the bridge is initially balanced. Let $(GF)_1 = (GF)_2$.

KNOWN Strain gauge installation shown in Figure 11.12

FIND The bridge constant for this installation

ASSUMPTION The change in the strain gauge resistances are small compared to the initial resistance (see explanation as follows).

SOLUTION The gauges are mounted so that gauge 1 is aligned with the axial tension and gauge 2 is mounted transversely on the member. The changes in resistance for the gauges may be expressed

$$\frac{\delta R_1}{R_1} = \varepsilon_a (GF)_1 \quad (11.26)$$

and

$$\frac{\delta R_2}{R_2} = -\nu_p \varepsilon_a (GF)_2 = -\nu_p \frac{\delta R_1}{R_1} \quad (11.27)$$

With only one gauge active, Equation 11.14 would be applicable, and yields

$$\frac{\delta E_0}{E_i} = \frac{\delta R_1/R_1}{4 + 2(\delta R_1/R_1)} \approx \frac{\delta R_1/R_1}{4} \quad (11.14)$$

But with both gauges installed and active, as shown in Figure 11.12, the output of the bridge is determined from an analysis of the bridge response, which results in

$$\frac{\delta E_0}{E_i} = \frac{(\delta R_1/R_1)(1 + \nu_p)}{4 + 2(\delta R_1/R_1)(1 + \nu_p)}$$

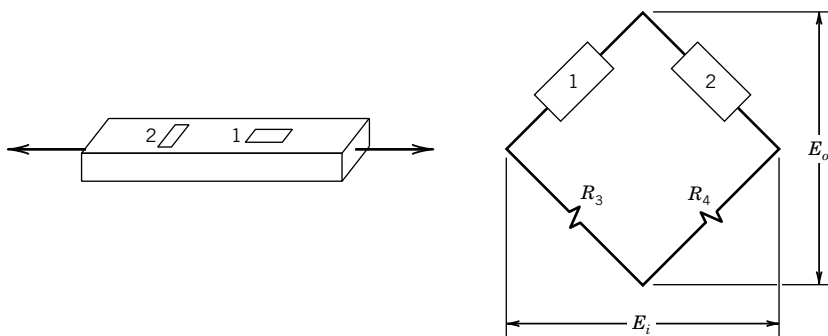


Figure 11.12 Bridge circuit with two arms active; strain gauge installation for increased sensitivity.

In practical applications, it is most often the case that changes in resistance are small in comparison to the resistance values, that is, $\delta R/R \ll 1$; thus

$$\frac{\delta E_0}{E_i} = \frac{(\delta R_1/R_1)(1 + v_p)}{4} \quad (11.28)$$

Therefore the bridge constant is the ratio of Equation 11.28 to Equation 11.14:

$$\frac{(\delta R_1/R_1)(1 + v_p)/4}{(\delta R_1/R_1)/4} \quad (11.29)$$

And the bridge constant is

$$\kappa = 1 + v_p$$

Comparing Equation 11.28 to Equation 11.14 shows that the use of two gauges oriented as described has increased the output of the bridge by a factor of $1 + v_p$ over that of using a single gauge.

11.6 APPARENT STRAIN AND TEMPERATURE COMPENSATION

Apparent strain is manifested as any change in gauge resistance that is not due to the component of strain being measured. Techniques for accomplishing temperature compensation, eliminating certain components of strain, and increasing the value of the bridge constant can be devised by examining more closely Equation 11.22. The bridge constant is influenced by (1) the location of strain gauges on the test specimen and (2) the gauge connection positions in the bridge circuit. The combined effect of these two factors is determined by examining the existing strain field and using Equation 11.22 to determine the resulting bridge output.

Let us examine how a component of strain can be removed (compensation) from the measured signal. Consider a beam having a rectangular cross section and subject to the loading condition shown in Figure 11.13, where the beam is subject to an axial load F_N and a bending moment M . The stress distribution in this cross section is given by

$$\sigma_x = \frac{-12My}{bh^3} + \frac{F_N}{bh} \quad (11.30)$$

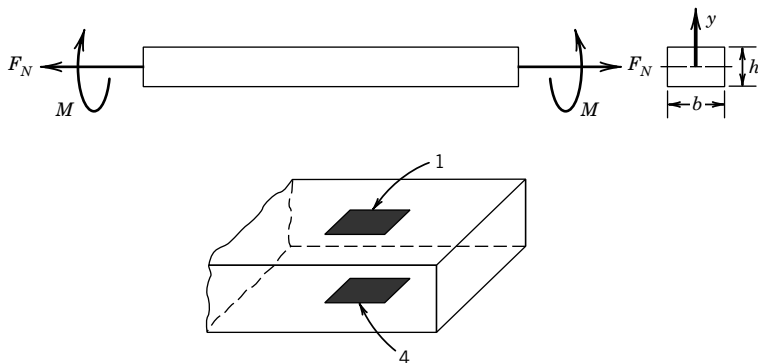


Figure 11.13 Strain gauge installation for bending compensation.

To remove the effects of bending strain, identical strain gauges are mounted to the top and bottom of the beam as shown in Figure 11.13, and they are connected to bridge locations 1 and 4 (opposite bridge arms). The gauges experience equal but opposite bending strains (Eq. 11.30), and both strain gauges are subject to the same axial strain caused by F_N . The bridge output under these conditions is

$$\frac{\delta E_0}{E_i} = \frac{GF}{4} (\varepsilon_1 + \varepsilon_4) \quad (11.31)$$

where $\varepsilon_1 = \varepsilon_{a1} + \varepsilon_{b1}$ and $\varepsilon_4 = \varepsilon_{a4} - \varepsilon_{b4}$, with subscripts a and b referring to axial and bending strain, respectively. Hence, because $|\varepsilon_{a1}| = |\varepsilon_{a4}|$ and $|\varepsilon_{b1}| = |\varepsilon_{b4}|$, the bending strains cancel but the axial strains sum, giving

$$\frac{\delta E_0}{E_i} = \frac{GF}{2} \varepsilon_a \quad (11.32)$$

For a single gauge experiencing the maximum strain,

$$\frac{\delta E_0}{E_i} = \frac{GF}{4} \varepsilon_a \quad (11.33)$$

The ratio of the output represented in Equation 11.32 to that represented in Equation 11.33 has a value of 2. This is the bridge constant ($\kappa = 2$) for the strain gauge arrangement in Figure 11.12. The bending strain cancels from Equation 11.32 indicating that this arrangement compensates for the bending strain.

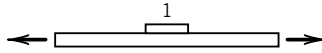
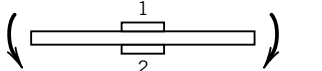
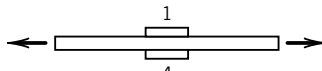
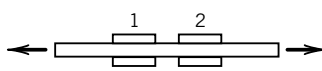
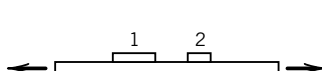
A guide for some practical bridge-gauge configurations is provided in Table 11.1.

Temperature Compensation

Differential thermal expansion between the gauge and the specimen on which it is mounted creates an apparent strain in the strain gauge. So, temperature sensitivity of strain gauges is caused by temperature changes in the gauge itself and the strain experienced by the gauge as a result of differential thermal expansion between the gauge and the material on which it is mounted. Using gauges of identical alloy composition as the specimen minimizes this latter effect. However, even keeping the specimen at a constant temperature may not be enough to eliminate the effect of gauge thermal expansion. Heating of the strain gauge as a result of current flow from the measuring device may be a source of significant error since the gauge is also a temperature-sensitive element. The temperature sensitivity of a strain gauge is an obstacle to accurate mechanical strain measurement that must be considered. Fortunately, there are effective ways to deal with it.

Figure 11.14 shows two circuit arrangements that provide temperature compensation for a strain measurement. The strain gauge mounted on the test specimen experiences changes in resistance caused by temperature changes and by applied strain, whereas the compensating gauge experiences resistance changes caused only by temperature changes. As long as the compensating gauge, as shown in Figure 11.14, experiences an identical thermal environment as the measuring gauge, temperature effects will be eliminated from the circuit. To show this, consider the case when all the bridge resistances are initially equal and the bridge is therefore balanced. If the temperature of the strain gauges now changes, their resistance changes as a result of thermal expansion, creating an apparent thermal strain. Under an applied axial load, the output of the bridge is derived from

Table 11.1 Common Gauge Mountings

Arrangement	Compensation Provided	Bridge Constant κ	
	Single gauge in uniaxial stress	None	$\kappa = 1$
	Two gauges sensing equal and opposite strain—typical bending arrangement	Temperature	$\kappa = 2$
	Two gauges in uniaxial stress	Bending only	$\kappa = 2$
	Four gauges with pairs sensing equal and opposite strains	Temperature and bending	$\kappa = 4$
	One axial gauge and one Poisson gauge		$\kappa = 1 + \nu$
	Four gauges with pairs sensing equal and opposite strains—sensitive to torsion only; typical shaft arrangement.	Temperature and axial	$\kappa = 4$

Equation 11.22,

$$\delta E_0 = E_i \frac{GF(\varepsilon_1 - \varepsilon_2)}{4} = E_i \frac{GF\varepsilon_a}{4} \quad (11.34)$$

where $\varepsilon_1 = \varepsilon_a + \varepsilon_T$ and $\varepsilon_2 = \varepsilon_T$ (ε_T refers to the temperature-induced apparent strain). Under this condition, the output value is not affected by changes in temperature. The result is the same if the compensating gauge is mounted in arm 3 instead, as shown in Figure 11.14b. Furthermore, any two active gauges mounted on adjacent bridge arms compensate for temperature changes.

Since this relationship holds in general, we can state that as long as two gauges, which are mounted to a specimen or to similar specimens, remain at the same temperature and are connected

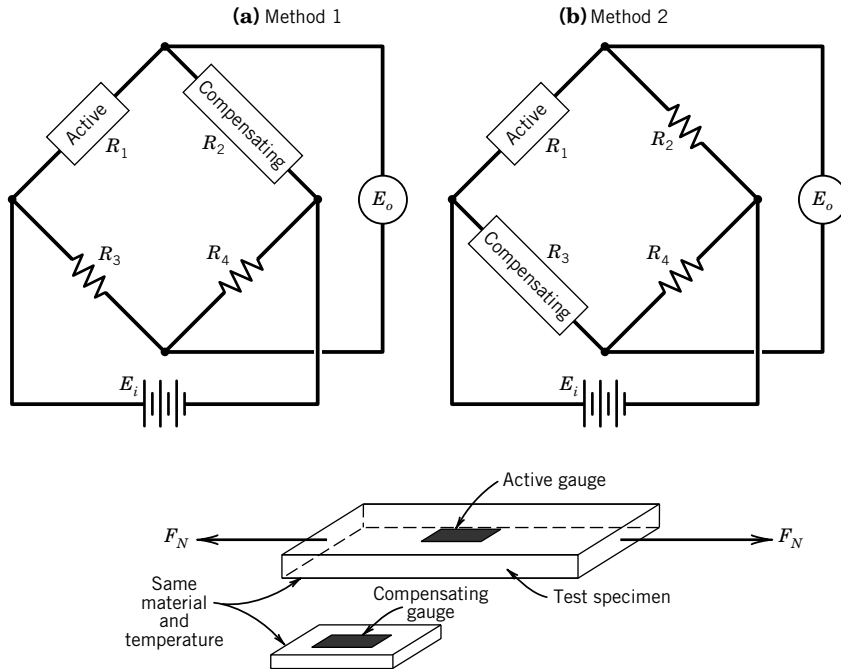


Figure 11.14 Bridge arrangements for temperature compensation.

to adjacent arms of a Wheatstone bridge, they will provide temperature compensation for each other.

Looking back, the arrangement in Figure 11.13 does not provide temperature compensation, as gauges 1 and 4 are on opposite bridge arms. However, temperature compensation could be provided for that installation by having two additional strain gauges that are at the same temperature as gauges 1 and 4 and occupy arms 2 and 3 of the bridge.

Bridge Static Sensitivity

The static sensitivity of the bridge arrangement in Figure 11.14a (method 1) is

$$K_B = \frac{E_0}{\varepsilon} = E_i \frac{R_1 R_2}{(R_1 + R_2)^2} GF \quad (11.35)$$

and with $E_i = (2R_g)I_g$ and $R_g = R_1 = R_2$, the static sensitivity may be expressed in the terms of the current flowing through the gauge, (I_g), as

$$K_B = \frac{1}{2} GF \sqrt{(I_g^2 R_1) R_1} \quad (11.36)$$

Note that $I_g^2 R_g$ is the power dissipated in the strain gauge as a result of the bridge current. Excessive power dissipation in the gauge would cause temperature changes and introduce uncertainty into a strain measurement. These effects can be minimized by good thermal coupling

between the strain gauge and the object to which it is bonded to allow effective dissipation of thermal energy.

Consider the static sensitivity of the bridge arrangement in Figure 11.14b. With identical gauges at positions R_1 and R_3 and equal resistance changes for the two gauges, no change in bridge output would occur. However, the static sensitivity for this arrangement is not the same as for method 1, but is given by

$$K_B = \frac{R_1/R_2}{1 + R_1/R_2} GF \sqrt{\left(I_g^2 R_1\right) R_1} \quad (11.37)$$

Here the sensitivity is the same as for a bridge having a single active gauge and without temperature compensation. However, the sensitivity depends on the choice of the fixed resistor R_2 . If $R_1 = R_2$, the resulting sensitivity is the same as for method 1. However, resistor R_2 can be chosen to provide the desired static sensitivity for the circuit, within the limitations of measurement capability and allowable bridge current.

Practical Considerations

An assumption in the definition of the gauge factor is that the change in resistance of the gauge is linear with applied strain for a particular gauge. However, a strain gauge can exhibit some nonlinearity. Also, in cycling between a loaded and unloaded condition, there is some degree of hysteresis and a shift in the resistance for a state of zero strain. A typical cycle of loading and unloading is shown in Figure 11.15. The strain gauge typically indicates lower values of strain during unloading than are measured as the load is increased. The extent of these behaviors is determined not only by the strain gauge characteristics but also by the characteristics of the adhesive and by the previous strains that the gauge has experienced. For properly installed gauges, the deviation from linearity should be on the order of 0.1% (3). On the other hand, first-cycle hysteresis and zero shift are difficult to predict. The effects of first-cycle hysteresis and zero shift can be minimized by cycling the strain gauge between zero strain and a value of strain above the maximum value to be measured prior to taking measurements.

In dynamic measurements of strain, the dynamic response of the strain gauge itself is generally not the limiting factor for such dynamic measurements. The rise time (90%) of a bonded resistance strain gauge may be approximated as (9)

$$t_{90} \approx 0.8(L/a) + 0.5\mu s \quad (11.38)$$

where L is the gauge length and a is the speed of sound in the material on which the gauge is mounted. Typical response times for gauges mounted on steel specimens are on the order of 1 μs .

Analysis of Strain Gauge Data

Strain gauges mounted on the surface of a test specimen respond only to the strains that occur at the surface of the test specimen. As such, the results from strain gauge measurements must be analyzed to determine the state of stress occurring at the strain gauge locations. The complete determination of the stress at a point on the surface of a particular test specimen generally requires the measurement of three strains at the point under consideration. The result of these measurements yields the principal strains and allows determination of the maximum stress (3).

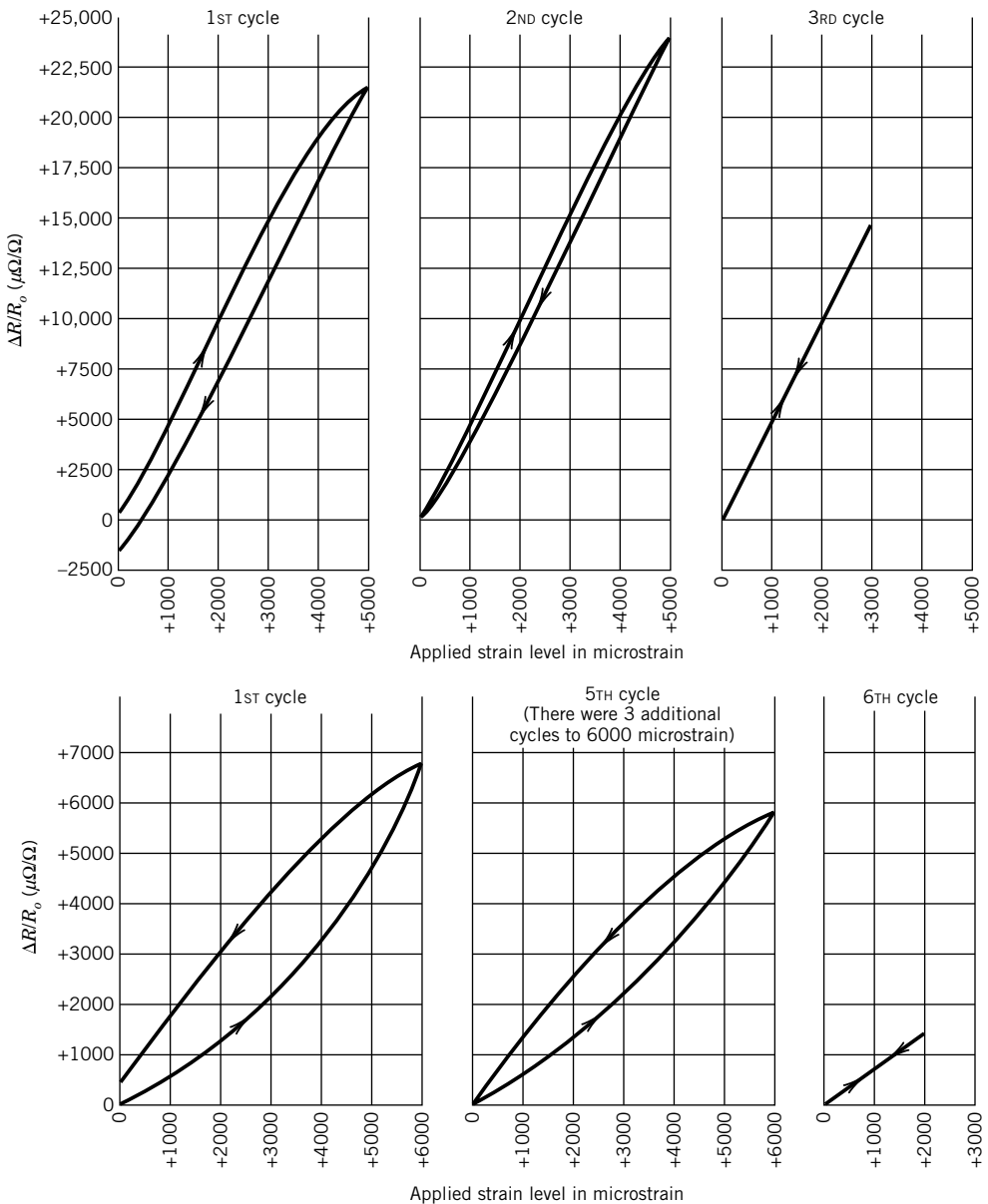


Figure 11.15 Hysteresis in initial loading cycles for two strain gauge materials. (Courtesy of Micro-Measurements Division, Measurements Group, Inc., Raleigh, NC.)

The multiple-element strain gauges used to measure more than one strain at a point are called *strain gauge rosettes*. An example of a two-element rosette is shown in Figure 11.16. For general measurements of strain and stress, commercially available strain rosettes can be chosen that have a pattern of multiple-direction gauges that is compatible with the specific nature of the particular

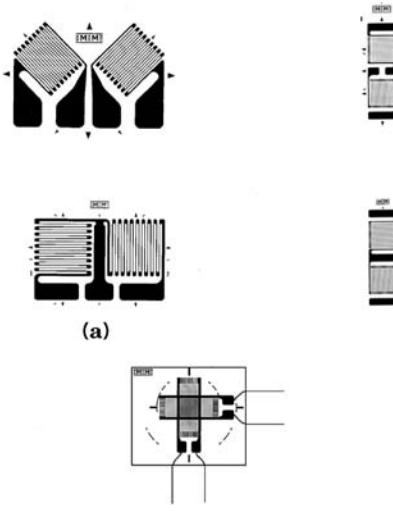


Figure 11.16 Biaxial strain gauge rosettes. (a) Single-plane type. (b) Stacked type. (Courtesy of Micro-Measurements Division, Measurements Group, Inc., Raleigh, NC.)

application (5). In practice, the applicability of the single-axis strain gauge is extremely limited, and improper use can result in large errors in the measured stress.

Strain gauge rosettes are commercially available in a variety of configurations, including gauges placed at angles of 0, 45, 90 degrees and 60, 60, 60 degrees. Consider the rectangular rosettes with angles of 0, 45, 90 degrees as shown in Figure 11.17. As we have emphasized, measuring surface strain allows calculation of the principal stresses. Assume that the measured strains from the stacked gauge in Figure 11.17b are ε_1 (from the 0-degree gauge, oriented with the x -axis) ε_2 (from the 45-degree gauge), and ε_3 (from the 90-degree gauge, oriented with the y -axis). From these measured strains, the principal stresses, σ_{\max} and σ_{\min} , and the maximum shear stress, τ_{\max} , may be calculated as

$$\begin{aligned}\sigma_{\max} &= \frac{E_m}{2} \left[\frac{\varepsilon_1 + \varepsilon_3}{1 - v_p} + \frac{1}{1 + v_p} \sqrt{(\varepsilon_1 - \varepsilon_3)^2 + [2\varepsilon_2 - (\varepsilon_1 + \varepsilon_3)]^2} \right] \\ \sigma_{\min} &= \frac{E_m}{2} \left[\frac{\varepsilon_1 + \varepsilon_3}{1 - v_p} - \frac{1}{1 + v_p} \sqrt{(\varepsilon_1 - \varepsilon_3)^2 + [2\varepsilon_2 - (\varepsilon_1 + \varepsilon_3)]^2} \right] \\ \tau_{\max} &= \frac{E_m}{2(1 + v_p)} \sqrt{(\varepsilon_1 - \varepsilon_3)^2 + [2\varepsilon_2 - (\varepsilon_1 + \varepsilon_3)]^2}\end{aligned}\quad (11.39)$$

The angle between the x -axis and the maximum principal stress is given by

$$\phi = \frac{1}{2} \tan^{-1} \frac{2\varepsilon_2 - (\varepsilon_1 + \varepsilon_3)}{\varepsilon_1 - \varepsilon_3} \quad (11.40)$$

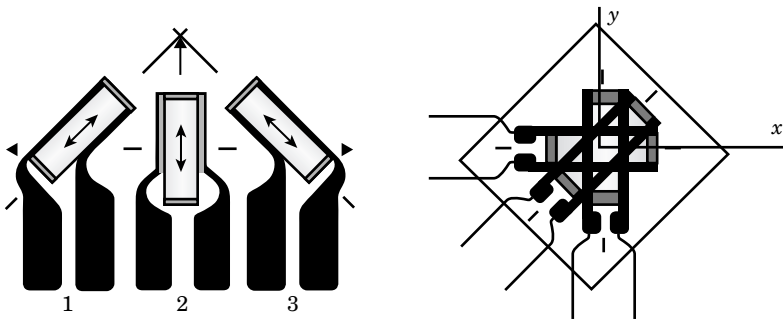


Figure 11.17 Rectangular (0, 45, 90 degree) strain gauge rosettes; (a) planar configuration, (b) stacked configuration.

Example 11.6

A rectangular strain gauge rosette is composed of strain gauges oriented at relative angles of 0, 45, and 90 degrees, as shown in Figure 11.17b. The rosette is used to measure strain on an aluminum structural member ($E_m = 69 \text{ MPa}$, $\nu_p = 0.334$). The measured values of strain are

$$\begin{aligned}\varepsilon_1 &= 20,000 \mu\epsilon \\ \varepsilon_2 &= 5,000 \mu\epsilon \\ \varepsilon_3 &= 10,000 \mu\epsilon\end{aligned}$$

Determine the principal stresses and the angle of the maximum principle stress relative to the x -axis.

KNOWN $\varepsilon_1 = 20,000 \mu\epsilon$
 $\varepsilon_2 = 5,000 \mu\epsilon$
 $\varepsilon_3 = 10,000 \mu\epsilon$

ASSUMPTIONS Strain gauge 1 is oriented along the x -axis. The material behaves in a homogeneous, isotropic manner and the loads are below the elastic limit.

FIND The values and direction of the principal stresses

SOLUTION Equation 11.39 can be applied directly to compute the stresses. For the maximum principal stress,

$$\sigma_{\max} = \frac{E_m}{2} \left[\frac{\varepsilon_1 + \varepsilon_3}{1 - \nu_p} + \frac{1}{1 + \nu_p} \sqrt{(\varepsilon_1 - \varepsilon_3)^2 + [2\varepsilon_2 - (\varepsilon_1 + \varepsilon_3)]^2} \right]$$

$$\sigma_{\max} = \frac{69 \text{ MPa}}{2} \left[\frac{(0.02 + 0.01)}{1 - 0.334} + \frac{1}{1 + 0.334} \sqrt{(0.02 - 0.01)^2 + [2 \times 0.005 - (0.02 + 0.01)]^2} \right]$$

$$= 2.13 \text{ MPa}$$

Equation 11.39 and Equation 11.40 yield the remaining values

$$\begin{aligned}\sigma_{\min} &= -0.976 \text{ MPa} \\ \tau_{\max} &= 0.578 \text{ MPa} \\ \phi &= -63.4^\circ\end{aligned}$$

COMMENT Other orientations of strain gauge rosettes result in different equations relating stress and measured strain.

Signal Conditioning

The most common form of signal conditioning in strain gauge bridge circuits is amplifying the signal using a low noise amplifier. For an amplifier of gain G_A , Equation 11.25 becomes

$$\frac{\delta E_0}{E_i} = \frac{G_A \kappa (\delta R/R)}{4 + 2(\delta R/R)} = \frac{G_A \kappa G F \varepsilon}{4 + 2(\delta R/R)} \approx \frac{G_A \kappa G F \varepsilon}{4} \quad (11.41)$$

The simplified form of Equation 11.41 is suitable for all but those measurements that demand the highest accuracy, and remains valid when $\delta R/R \ll 1$. A common means of recording strain gauge bridge circuit signals is the automated data acquisition system. A schematic diagram of such a setup is shown in Figure 11.18.

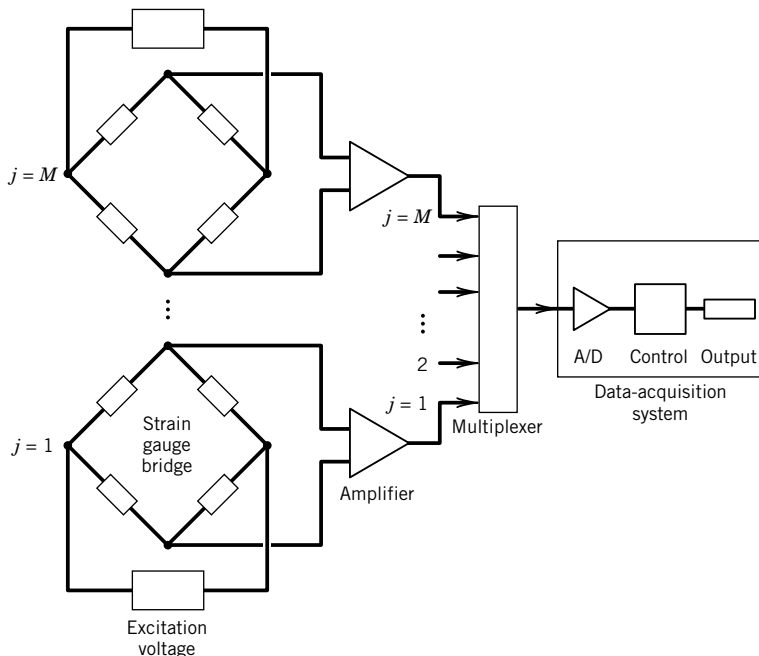


Figure 11.18 Data acquisition and reduction system for Example 11.7.

Uncertainties in Multichannel Measurements

Uncertainties caused by an automated multichannel strain measurement system can be estimated in a system calibration. Example 11.7 describes an initial test of such a system, often called a shakedown test, and discusses the information that results from this test.

Example 11.7

The strain developed at M different locations about a large test specimen is to be measured at each location using a setup similar to that shown in Figure 11.18. At each location similar strain gauges are appropriately mounted and connected to a Wheatstone bridge that is powered by an external supply. The bridge deflection voltage is to be amplified and measured. A similar setup is used at all M locations. The output from each amplifier is input through an M -channel multiplexer to an automated data acquisition system. If N (say 30) readings for each of the M setups are taken while the test specimen is maintained in a condition of uniform zero strain, what information is obtained?

KNOWN Strain setup of Figure 11.18

M ($j = 1, 2, \dots, M$) setups

N ($i = 1, 2, \dots, N$) readings per setup

ASSUMPTIONS All setups are to be operated in a similar manner. Gauges are operated in their linear regimes.

SOLUTION Consider the data that will become available. First, each setup is exposed to a similar strain. Hence, each setup should indicate the same strain. We can calculate the pooled mean value of the $M \times N$ readings to obtain

$$\langle \bar{\varepsilon} \rangle = \frac{1}{MN} \sum_{j=1}^M \sum_{i=1}^N \varepsilon_{ij} = \frac{1}{M} \sum_{j=1}^M \bar{\varepsilon}_j$$

The difference between the pooled mean strain and the applied strain (zero here) is an estimate of the systematic uncertainty that can be expected from any channel during data acquisition.

Random errors manifest themselves through scatter in the data set. The pooled standard deviation of the means

$$\langle \bar{s}_{\varepsilon} \rangle = \sqrt{\frac{\sum_{j=1}^M \sum_{i=1}^N (\varepsilon_{ij} - \bar{\varepsilon}_j)^2}{M(N-1)}} / \sqrt{MN}$$

provides a representative estimate of the uncertainty due to random error to be expected in any channel that is due to the data acquisition and reduction instrumentation.

COMMENT This test yields an estimate of the uncertainties in systematic and random error due to propagation of the elemental errors amid M setups due to

- excitation voltage errors (differences in settings, variations),
- amplifier error (differences in gain, noise),
- analog-to-digital (A/D) converter, multiplexer, and conversion errors,
- computer errors (noise and roundoff),

- bridge null errors,
- apparent strain error during the test, and
- variations in gauge factors and gauge heating.

The test data do not include uncertainties resulting from temporal variation of the measurands or procedural variations under loading, instrument calibration errors, temperature variation effects, and electrical noise induced by operation of the loading test of the specimen, dynamic effects on the gauges, including differences in creep and fatigue, or reduction curve fit errors.

11.7 OPTICAL STRAIN MEASURING TECHNIQUES

Optical methods for experimental stress analysis can provide fundamental information concerning directions and magnitudes of the stresses in parts under design loading conditions. Optical techniques have been developed for the measurement of stress and strain fields, either in models made of materials having appropriate optical properties, or through coating techniques for existing specimens. Photoelasticity takes advantage of the changes in optical properties of certain materials that occur when these materials are strained. For example, some plastics display a change in optical properties when strained that causes an incident beam of polarized light to be split into two polarized beams that travel with different speeds and that vibrate along the principal axes of stress. Since the two light beams are out of phase, they can be made to interfere; measuring the resulting light intensity yields information concerning applied stress. To implement this method, a model is constructed of an appropriate material, or a coating is applied to an existing part.

A second optical method of stress analysis is based on the development of a moiré pattern, which is an optical effect resulting from the transmission or reflection of light from two overlaid grid patterns. The fringes that result from relative displacement of the two grid patterns can be used to measure strain; each fringe corresponds to the locus of points of equal displacement.

Recent developments in strain measurement include the use of lasers and holography to very accurately determine whole field displacements for complex geometries.

Basic Characteristics of Light

To utilize optical strain measurement techniques, we must first examine some basic characteristics of light. Electromagnetic radiation, such as light, may be thought of as a transverse wave with sinusoidally oscillating electric and magnetic field vectors that are at right angles to the direction of propagation. In general, a light source emits a series of waves containing vibrations in all perpendicular planes, as illustrated in Figure 11.19. A light wave is said to be plane-polarized if the transverse oscillations of the electric field are parallel to each other at all points along the direction of propagation of the wave.

Figure 11.19 illustrates the effect of a polarizing filter on an incident light wave; the transmitted light is plane polarized, with a known direction of polarization. Complete extinction of the light beam could be achieved by introduction of a second polarizing filter, with the axis of polarization at 90 degrees to the first filter (labeled an Analyzer in Fig. 11.19). These behaviors of light are employed to measure direction and magnitude of strain in photoelastic materials.

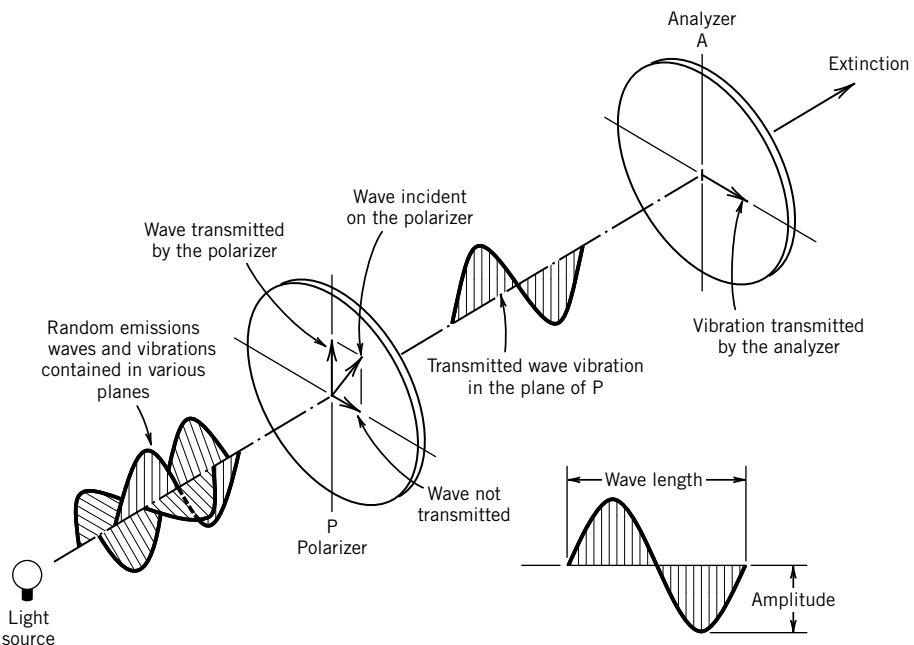


Figure 11.19 Polarization of light. (Courtesy of Measurements Group, Inc., Raleigh, NC.)

Photoelastic Measurement

Photoelastic methods of stress analysis take advantage of the anisotropic optical characteristics of some materials, notably plastics, when subject to an applied load to determine the strain field. Stress analysis may be accomplished either by constructing a model of the part to be analyzed from a material selected for its optical properties, or by coating the actual part or prototype with a photoelastic coating. If a model is constructed from a suitable plastic, the required loads for the model are significantly less than the service loads of the actual part, which reduces effort and expense in testing.

The changes in optical properties, known as artificial birefringence, which occur in certain materials subject to a load or loads was first observed by Sir David Brewster (10) in 1815. He observed that when light passes through glass that is subject to uniaxial tension, such that the stress is perpendicular to the direction of propagation of the light, the glass becomes doubly refracting, with the axes of polarization in the glass aligned with and perpendicular to the stress. Maxwell (11) and Neumann (12) first put forward the mathematical observation that the relationship between artificial birefringence and applied stress or strain is linear. These relations are known as the stress-optic law.

The anisotropy that occurs in photoelastic materials results in two refracted beams of light and one reflected beam, produced for a single incident beam of appropriately polarized light. The two refracted beams propagate at different velocities through the material because of an anisotropy in the index of refraction. In an appropriately designed photoelastic (two-dimensional) model, these two refracted components of the incident light travel in the same direction and can be examined in a polariscope. The degree to which the two light waves are out of phase is related to the stress by the

stress-optic law:

$$\delta \propto n_x - n_y \quad (11.42)$$

where

δ = relative retardation between the two light beams

n_x, n_y = indices of refraction in the directions of the principal strains

The index of refraction changes in direct proportion to the amount the material is strained, such that

$$n_x - n_y = K(\varepsilon_x - \varepsilon_y) \quad (11.43)$$

The strain optical coefficient, K , is generally assumed to be a material property that is independent of the wavelength of the incident light. However, if the photoelastic material is strained beyond the elastic limit, this constant may become wavelength dependent, a phenomenon known as photoelastic dispersion.

Figure 11.20 shows the use of a plane polariscope to examine the strain in a photoelastic model. Plane polarized light enters the specimen and emerges with two planes of polarization along the principal strain axes. This light beam is then passed through a polarizing filter, called the analyzer, which transmits only the component of each of the light waves that is parallel to the plane of polarization. The transmitted waves interfere, since they are out of phase, and the resulting light intensity is a function of the angle between the analyzer and the principal strain direction and the

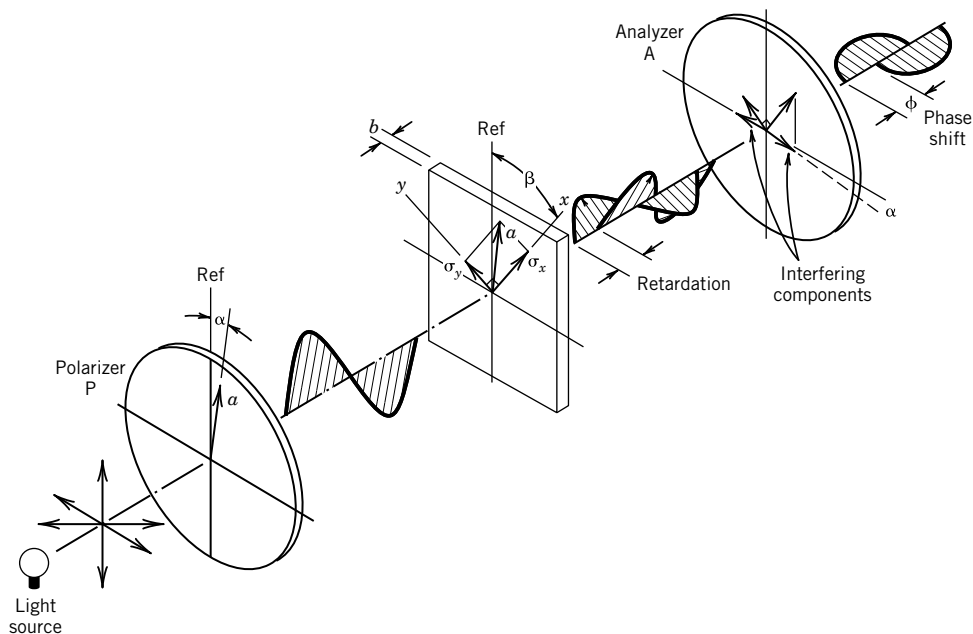


Figure 11.20 Construction of a plane polariscope. (Courtesy of Measurements Group, Inc., Raleigh, NC.)

phase shift between the beams. The variations in strain in the specimen produce a pattern of fringes, which can be related to the strain field through the strain optic relation.

When a photoelastic model is observed in a plane polariscope, a series of fringes is observed. The complete extinction of light occurs at locations where the principal strain directions coincide with the axes of the analyzer or where either the strain is zero or $\varepsilon_x - \varepsilon_y = 0$. These fringes are termed *isoclinics*, and are used to determine the principal strain directions at all points in the photoelastic model. Figure 11.21 shows the isoclinics in a ring subject to a compression load (as shown in the figure). A reference direction is selected along the horizontal compression load and labeled 0 degrees. For each measurement angle, one of the principal strains at a point on an isoclinic is parallel to the specified angle and the other is perpendicular. For the 0-degree isoclinics, the principal strains are oriented at 0 and 90 degrees.

Using the fact that the direction of the principal axes is known at a free surface and the fact that the shear stress is zero on a free surface, the magnitude of the stress on the boundary can be determined. The primary applications for photoelasticity, especially in a historical sense, have been in the study of stress concentrations around holes or reentrant corners. In these cases, the maximum stress is at the boundary and corresponds to one of the principal stresses. This maximum stress can be obtained directly by the optical method, since the shear stress is zero on the boundary.

Optical methods provide information about the strain and stress at every point in the object being examined, in contrast to a strain gauge that supplies information about the strain at a single location on the object. The optical methods provide the possibility of identifying stress concentration locations and may allow for an improvement in design or guide detailed measurements with strain gauges.

Moiré Methods

A moiré pattern results from two overlaid, relatively dense patterns that are displaced relative to each other. This observable optical effect occurs, for example, in color printing, where patterns of dots form an image. If the printing is slightly out of register, a moiré pattern results. Another common example is the striking shimmering effect that occurs with some patterned clothing on television. This effect results when the size of the pattern in the fabric is essentially the same as the resolution of the television image.

In experimental mechanics, moiré patterns are used to measure surface displacements, typically in a model constructed specifically for this purpose. The technique uses two gratings, or patterns of parallel lines spaced equally apart. Figure 11.22 shows two line gratings. There are two important properties of line gratings for moiré techniques. The pitch is defined as the distance between the centers of adjacent lines in the grating, and for typical gratings has a value of from 1 to 40 lines/mm. The second characteristic of gratings is the ratio of the open, transparent area of the grating to the total area, or, for a line grating the ratio of the distance between adjacent lines to the center-to-center distance, as illustrated in Figure 11.22. Clearly, a greater density of lines per unit width allows a greater sensitivity of strain measurement; however, as line densities increase, coherent light is required for practical measurement.

To determine strain using the moiré technique, a grating is fixed directly to the surface to be studied. This can be accomplished through photoengraving, cementing film copies of a grating to the surface, or interferometric techniques. The master or reference grating is next placed in contact with the surface, forming a reference for determining the relative displacements under loaded conditions. A series of fringes result when the gratings are displaced relative to each other; the bright fringes are

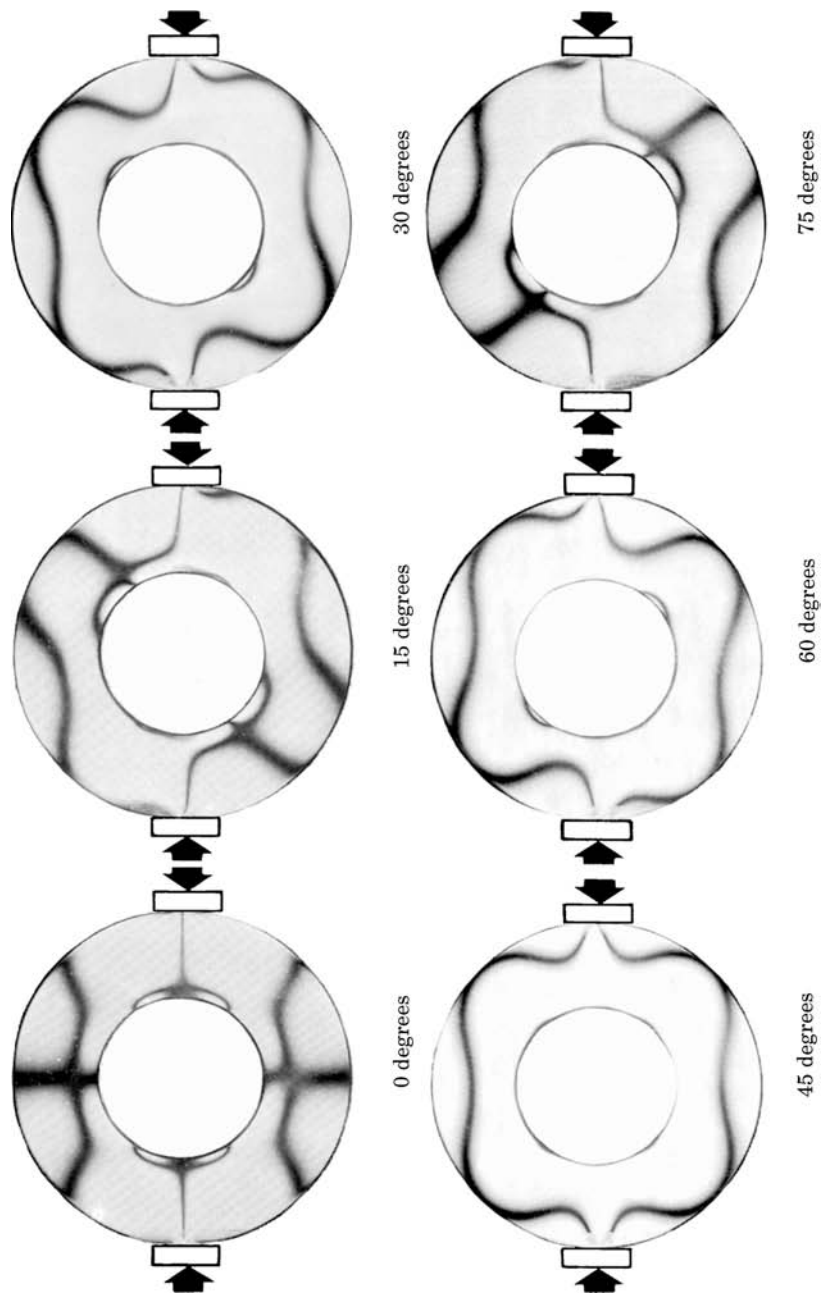
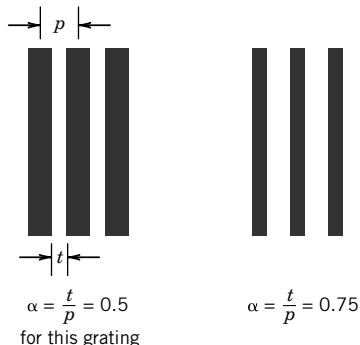


Figure 11.21 Construction of a plane polariscope. (Courtesy of Measurements Group, Inc., Raleigh, NC.)

**Figure 11.22** Moiré gratings.

the loci of points where the projected displacements of the surface are integer multiples of the pitch. The technique then is two-dimensional, providing information concerning the projection of the displacements into the plane of the master grating. Once a fringe pattern is recorded, data reduction techniques are employed to determine the stress and strain field. Graphical techniques exist that allow the strain components in two orthogonal directions to be determined. Further information on moiré techniques, and additional references may be found in the review article by Sciammarella (13).

Recently, techniques such as moiré-fringe multiplication have greatly increased the sensitivity of moiré techniques, with possible grating density of 1200 lines/mm. Moiré interferometry is an extension of moiré-fringe multiplication that uses coherent light and has sensitivities on the order of 0.5 mm/fringe (14). A reflective grating is applied to the specimen, which experiences deformation under load conditions. The technique provides whole field readings of in-plane strain, with a four-beam optical arrangement currently in use (15).

11.8 SUMMARY

Experimental stress analysis can be accomplished through several practical techniques, including electrical resistance, photoelastic, and moiré strain measurement techniques. Each of these methods yields information concerning the surface strains for a test specimen. The design and selection of an appropriate strain measurement system begins with the choice of a measurement technique.

The bonded electrical resistance strain gauge provides a versatile means of measuring strain at a specific location on a test specimen. Strain gauge selection involves the specification of strain gauge material, the backing or carrier material, and the adhesive used to bond the strain gauge to the test specimen, as well as the total electrical resistance of the gauge. Other considerations include the orientation and pattern for a strain gauge rosette, and the temperature limit and maximum allowable elongation. In addition, for electrical resistance strain gauges, appropriate arrangement of the gauges in a bridge circuit can provide temperature compensation and elimination of specific components of strain.

Optical methods are useful in the initial determination of a stress field for complex geometries, and the determination of whole-field information in model studies. Such whole-field methods provide the basis for design, and establish information necessary to make detailed local strain measurements.

The techniques for strain measurement described in this chapter provide the basis for determining surface strains for a test specimen. While the focus here has been the measurement

techniques, the proper placement of strain gauges and the interpretation of the measured results requires further analysis. The inference of load-carrying capability and safety for a particular component is a result of the overall experimental program.

REFERENCES

1. Hibbeler, R.C., *Mechanics of Materials*, 5th ed., Prentice-Hall, Upper Saddle River, NJ, 2002.
2. Timoshenko, S. P., and J. M. Goodier, *Theory of Elasticity*, Engineering Society Monographs, McGraw-Hill, New York, 1970.
3. Dally, J. W., and W. F. Riley, *Experimental Stress Analysis*, 3rd ed., McGraw-Hill, New York, 1991.
4. Thomson, W. (Lord Kelvin), On the electrodynamic qualities of metals, *Philosophical Transactions of the Royal Society* (London) 146: 649–751, 1856.
5. Micro-Measurements Division, Measurements Group, Inc., Strain Gauge Selection: Criteria, Procedures, Recommendations, Technical Note 505-1, Raleigh, NC, 1989.
6. Micro-Measurements Division, Measurements Group, Inc., Strain Gauge Technical Data, Catalog 500, Part B, and TN-509: Errors Due to Transverse Sensitivity in Strain Gauges, Raleigh, NC, 1982.
7. Kulite Semiconductor Products, Inc, Bulletin KSG-5E: *Semiconductor Strain Gauges*, Leonia, NJ.
8. Weymouth, L. J., J. E. Starr, and J. Dorsey, Bonded resistance strain gauges, *Experimental Mechanics* 6(4): 19A, 1966.
9. Oi, K., Transient response of bonded strain gauges, *Experimental Mechanics* 6(9): 463, 1966.
10. Brewster, D., On the effects of simple pressure in producing that species of crystallization which forms two oppositely polarized images and exhibits the complementary colours by polarized light, *Philosophical Transactions A* 105: 60, 1815.
11. Maxwell, J. C., On the equilibrium of elastic solids, *Transactions of the Royal Society* 20 (Part I): 87, 1853.
12. Neumann, F. E., Über Gesetze der Doppelbrechung des Lichtes in comprimierten oder ungleichformig Erwachten unkristallischen Körpern, *Abh. Akad. Wiss. Berlin, Part II*: 1, 1841 (in German).
13. Sciammarella, C. A., The moiré method—a review, *Experimental Mechanics* 22(11): 418, 1982.
14. Post, D., Moiré interferometry at VPI & SU, *Experimental Mechanics* 23(2): 203, 1983.
15. Post, D., Moiré interferometry for deformation and strain studies, *Optical Engineering* 24(4): 663, 1985.

NOMENCLATURE

b	width (l)	D	diameter (l)
c	speed of sound ($l \ t^{-1}$)	E_m	modulus of elasticity ($ml^{-1}t^{-2}$)
h	height (l)	E_i	input voltage (V)
n_i	index of refraction in the direction of the principal strain in the i direction	E_o	output voltage (V)
$(u_d)_x$	design-stage uncertainty in the variable x	e_i	strain gauge lateral sensitivity error as a percentage of axial strain
A_c	cross-sectional area (l^2)	F_N	force normal to A_c ($m \ l \ t^{-2}$)

G	shear modulus ($m t^{-2}$)	δ	relative retardation between two light beams in a photoelastic material
G_A	amplifier gain	ε_a	axial strain
GF	gauge factor	ε_b	bending strain
K	strain optical coefficient	ε_r	strain in the i coordinate direction (i.e., x direction)
K_B	bridge sensitivity (V)	ε_l	lateral or transverse strain
K_I	strain gauge lateral sensitivity	ε_t	apparent strain due to temperature
L	length (l)	κ	bridge constant
δE_o	voltage change (V)	ν_p	Poisson ratio
δL	change in length (l)	ν_{po}	Poisson ratio for gauge factor calibration test
δR	resistance change (Ω)	π_1	piezoresistance coefficient ($t^2 l m^{-1}$)
M	bending moment ($m l^2 t^{-2}$)	ρ_e	electrical resistivity ($\Omega \cdot l$)
R	electrical resistance (Ω)	σ	stress ($m l^{-1} t^{-2}$)
T	temperature ($^\circ$)	σ_a	axial stress ($m l^{-1} t^{-2}$)
T_0	reference temperature ($^\circ$)	τ_{xy}	shear stress in the xy plane ($m l^{-1} t^{-2}$)
α	moiré grating width to spacing parameter		
γ_{xy}	shear strain in the xy plane ($m l^{-1} t^{-2}$)		

PROBLEMS

- 11.1** Calculate the change in length of a steel rod ($E_m = 30 \times 10^6$ psi) that has a circular cross section, a length of 10 in., and a diameter of 1/4 in. The rod supports a mass of 50 lbm in such a way that a state of uniaxial tension is created in the rod.
- 11.2** Calculate the change in length of a steel rod ($E_m = 20 \times 10^{10}$ Pa) that has a length of 0.3 m and a diameter of 5 mm. The rod supports a mass of 60 kg in a standard gravitation field in such a way that a state of uniaxial tension is created in the rod. Make the same calculation for a rod made of aluminum ($E_m = 70$ GPa).
- 11.3** An electrical coil is made by winding copper wire around a core. What is the resistance of 20,000 turns of 16-gauge wire (0.051 in. diameter) at an average radius of 2.0 in.?
- 11.4** Compare the resistance of a volume of $\pi \times 10^{-5}$ m³ of aluminum wire having a diameter of 2 mm, with the same volume of aluminum formed into 1-mm-diameter wire. (The resistivity of aluminum is 2.66×10^{-8} $\Omega \cdot m$.)
- 11.5** A conductor made of nickel ($\rho_e = 6.8 \times 10^{-8}$ $\Omega \cdot m$) has a rectangular cross section 5×2 mm and is 5 m long. Determine the total resistance of this conductor. Calculate the diameter of a 5-m-long copper wire that has a circular cross section that yields the same total resistance.
- 11.6** Consider a Wheatstone bridge circuit that has all resistances equal to 100 Ω . The resistance R_1 is a strain gauge that cannot sustain a power dissipation of more than 0.25 W. What is the maximum applied voltage that can be used for this bridge circuit? At this level of bridge excitation, what is the bridge sensitivity?
- 11.7** A resistance strain gauge with $R = 120 \Omega$ and a gauge factor of 2 is placed in an equal-arm Wheatstone bridge in which all the resistances are equal to 120 Ω . If the maximum gauge current is to be 0.05 A, what is the maximum allowable bridge excitation voltage?
- 11.8** A strain gauge that has a nominal resistance of 350 Ω and a gauge factor of 1.8 is mounted in an equal-arm bridge, which is balanced at a zero applied strain condition. The gauge is mounted on a

1-cm² aluminum rod, with $E_m = 70$ GPa. The gauge senses axial strain. The bridge output is 1 mV for a bridge input of 5 V. What is the applied load, assuming the rod is in uniaxial tension?

- 11.9** Suppose the bridge in Problem 11.8 was operated in balanced mode. What change in resistance would be required to balance the bridge? Assume the loading conditions are the same.
- 11.10** Consider a structural member subject to loads that produce both axial and bending stresses, as shown in Figure 11.13. Two strain gauges are to be mounted on the member and connected in a Wheatstone bridge in such a way that the bridge output indicates the axial component of strain only (the installation is bending compensated). Show that the installation of the gauges shown in Figure 11.13 will not be sensitive to bending.
- 11.11** A steel beam member ($\nu_p = 0.3$) is subjected to simple axial tensile loading. One strain gauge aligned with the axial load is mounted on the top and center of the beam. A second gauge is similarly mounted on the bottom of the beam. If the gauges are connected as arms 1 and 4 in a Wheatstone bridge (Fig. 11.12), determine the bridge constant for this installation. Is the measurement system temperature compensated? (explain why or why not.) If $\delta E_0 = 10 \mu\text{V}$ and $E_i = 10$ V, determine the axial and transverse strains. The gauge factor for each gauge is 2, and all resistances are initially equal to 120Ω .
- 11.12** An axial strain gauge and a transverse strain gauge are mounted to the top surface of a steel beam that experiences a uniaxial stress of 2222 psi. The gauges are connected to arms 1 and 2 (Fig. 11.12) of a Wheatstone bridge. With a purely axial load applied, determine the bridge constant for the measurement system. If $\delta E_0 = 250 \mu\text{V}$ and $E_i = 10$ V, estimate the average gauge factor of the strain gauges. For this material, Poisson's ratio is 0.3 and the modulus of elasticity is 29.4×10^6 psi.
- 11.13** A strain gauge is mounted on a steel cantilever beam of rectangular cross section. The gauge is connected in a Wheatstone bridge; initially $R_{\text{gauge}} = R_2 = R_3 = R_4 = 120 \Omega$. A gauge resistance change of 0.1Ω is measured for the loading condition and gauge orientation shown in Figure 11.23. If the gauge factor is $2.05 \pm 1\%$ (95%) estimate the strain. Suppose the uncertainty in each resistor value is 1% (95%). Estimate an uncertainty in the measured strain due to the uncertainties in the bridge resistances and gauge factor. Assume that the bridge operates in a null mode, which is detected by a galvanometer. Also assume reasonable values for other necessary uncertainties and parameters, such as input voltage or galvanometer sensitivity.

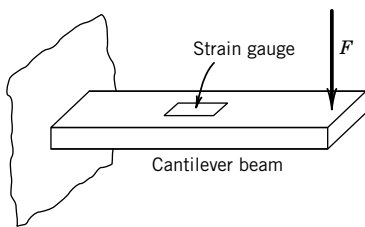


Figure 11.23 Loading for Problem 11.13.

- 11.14** Two strain gauges are mounted so that they sense axial strain on a steel member in uniaxial tension. The 120Ω gauges form two legs of a Wheatstone bridge, and are mounted on opposite arms. For a bridge excitation voltage of 4 V and a bridge output voltage of $120 \mu\text{V}$ under load, estimate the strain in the member. What is the resistance change experienced by each gauge? The gauge factor for each of the strain gauges is 2 and E_m for this steel is 29×10^6 psi.

- 11.15** A rectangular bar is instrumented with strain gauges and subjected to a state of uniaxial tension. The bar has a cross-sectional area of 2 in.^2 , and the bar is 12 in. long. The two strain gauges are mounted such that one senses the axial strain, while the other senses the lateral strain. For an axial load of 1500 lb, the axial strain is measured as $1500 \mu\epsilon$ ($\mu\text{in./in.}$), and the lateral gauge indicates a strain of $-465 \mu\epsilon$. Determine the modulus of elasticity and Poisson's ratio for this material.
- 11.16** A round member having a cross-sectional area of 3 cm^2 experiences an axial load of 10 kN. Two strain gauges are mounted on the member, one measuring an axial strain of $600 \mu\epsilon$ (m/m), and the other measuring a lateral strain of $-163 \mu\epsilon$. Determine the modulus of elasticity and Poisson's ratio for this material.
- 11.17** Show that the use of a dummy gauge together with a single active gauge compensates for temperature but not for bending. Consider the case in which the active gauge is subjected to axial loading with minimal bending and both gauges experience the same temperature.
- 11.18** Show that four strain gauges mounted to a shaft such that the gauge pairs measure equal and opposite strain can be used to measure torsional twist (as suggested in Table 11.1). Show that this method compensates for axial and bending strains and for temperature.
- 11.19** For each bridge configuration described below, determine the bridge constant. Assume that all of the active gauges are identical, and that all of the fixed resistances are equal. The locations of the gauges in the bridge are shown in Figure 11.24.

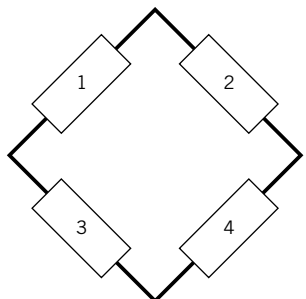


Figure 11.24 Bridge arrangement for Problems 11.19 to 11.21.

Bridge Configuration	Description
(a) 1: active gauge; 2–4: fixed resistors	Single gauge in uniaxial tension
(b) 1: active gauge; 2: Poisson gauge; 3, 4: fixed resistors	Two active gauges in uniaxial stress field
(c) 1: active gauge; 3: active gauge; 2, 4: fixed resistors	Gauge 1 aligned with maximum axial stress; gauge 2 lateral Equal and opposite strains applied to the active gauges (bending compensation)
(d) Four active gauges	Gauges 1 and 4 aligned with uniaxial stress; gauges 2 and 3 transverse
(e) Four active gauges	Gauges 1 and 2 subject to equal and opposite strains; gauges 3 and 4 subject to the same equal but opposite strains

- 11.20** A bathroom scale uses four internal strain gauges to measure the displacement of its diaphragm as a means for determining load. Four active gauges are used in a bridge circuit. The gauge factor is 2, and gauge resistance is 120Ω for each gauge. If an applied load to the diaphragm causes a compression strain on R_1 and R_4 of $20 \mu\epsilon$, while gauges R_2 and R_3 experience a tensile strain of $20 \mu\epsilon$, estimate the bridge deflection voltage. The supply voltage is 9 V. Refer to Figure 11.24 for gauge position.
- 11.21** Suppose in Problem 11.20 that the lead wires of two gauges (R_2 and R_4) are accidentally interchanged on the assembly line such that a compression strain is now sensed on R_1 and R_2 of $20 \mu\epsilon$, while gauges R_4 and R_3 experience a tensile strain of $20 \mu\epsilon$. Should this really matter? Explain. Estimate the bridge deflection voltage. Refer to Figure 11.24 for gauge position.

Problems 11.22 through 11.24 address measuring strains associated with a thin-walled pressure vessel. The pressure vessel is constructed of steel and has a circular cross-section. The tangential and longitudinal stresses in the wall of the pressure vessel are:

$$\sigma_t = pD/2t \quad \sigma_l = pD/4t$$

where

σ_t = tangential stress

σ_l = longitudinal stress

p = pressure

t = wall thickness

- 11.22** A single-strain gauge is mounted on the surface of a thin-walled pressure vessel that has a diameter of 1 m. For a strain gauge oriented along the tangential stress direction, determine the percentage error in tangential strain measurement caused by lateral sensitivity as a function of pressure and vessel wall thickness. The lateral sensitivity is 0.03.
- 11.23** Consider a Wheatstone bridge circuit that has all fixed resistances equal to 100Ω and with a strain gauge located at the R_1 position, which has a value of 100Ω under conditions of zero strain. The strain gauge is mounted so as to sense longitudinal strain for a thin-walled pressure vessel made of steel that has a wall thickness of 2 cm and a diameter of 2 m. The strain gauge has a gauge factor of 2 and cannot sustain a power dissipation of more than 0.25 W. What is the maximum static sensitivity that can be achieved with this proposed measurement system? Is this static sensitivity constant with input pressure? If not, under what conditions would it be reasonable to assume a constant static sensitivity? The static sensitivity should be expressed in units of V/kPa.
- 11.24** Design a Wheatstone bridge measurement system to measure the tangential strain in the wall of the pressure vessel described above, and develop a reasonable estimate of the resulting uncertainty. You may assume that the strain does not vary with time, and that the bridge is operated in a balanced mode. Your selection of specified values for the input voltage, the fixed resistances in the bridge and the galvanometer sensitivity, and their associated uncertainties will allow completion of this design.
- 11.25** A steel cantilever beam is fixed at one end and free to move at the other. A load F of 980 N is applied to the free end. Four axially aligned strain gauges ($GF = 2$) are mounted to the beam a distance L from the applied load, two on the upper surface, R_1 and R_4 , and two on the lower surface, R_2 and R_3 . The bridge deflection output is passed through an amplifier (gain, $G_A = 1000$) and measured. For a

cantilever, the relationship between applied load and strain is

$$F = \frac{2E_m I \varepsilon}{Lt}$$

where I is the beam moment of inertia ($= bt^3/12$), t is the beam thickness, and b is the beam width. Estimate the measured output for the applied load if $L = 0.1$ m, $b = 0.03$ m, $t = 0.01$ m, and the bridge excitation voltage is 5 V. $E_m = 200$ GPa.

- 11.26** A cantilever beam is to be used as a scale. The beam, made of 2024-T4 aluminum, is 21 cm long, 0.4 cm thick, and 2 cm wide. The scale load of between 0 and 200 g is to be concentrated at a point along the beam centerline 20 cm from its fixed end. Strain gauges are to be used to measure beam deflection and mounted to a Wheatstone bridge to provide an electrical signal that is proportional to load. Either 1/4-, 1/2-, or full-bridge gauge arrangements can be used. Design the sensor arrangement and its location on the beam. Specify appropriate signal conditioning to excite the bridge and to measure its output on a data acquisition system using a ± 5 V, 12-bit A/D converter. Can the system achieve a 4% uncertainty at the design-stage? The following specifications and system choices are stated at the 95% confidence level:

Sensors: one, two, or four axial gauges at $120 \Omega \pm 0.2\%$ (selectable)

Gauge factor of $2.0 \pm 1\%$

Bridge excitation: 1, 3, 5 V $\pm 0.5\%$ (selectable)

Bridge null: within 5 mV

Signal conditioning:

Amplifier gain: 1X, 10X, 100X, 1000X $\pm 1\%$ (selectable)

Low-pass filter: f_c at 0.5, 5, 50, 500 Hz @ -12dB/octave (selectable)

Data acquisition system:

Conversion errors: $< 0.1\%$ reading

Sample rate: 1, 10, 100, 1000 Hz (selectable)

- 11.27** A rectangular strain gauge rosette is composed of strain gauges oriented at relative angles of 0, 45, and 90 degrees, as shown in Figure 11.17b. The rosette is used to measure strain on a steel structural member having $E_m = 200$ GPa and $\nu_p = 0.3$. The measured values of strain are

$$\varepsilon_1 = 10000 \mu\varepsilon$$

$$\varepsilon_2 = 5000 \mu\varepsilon$$

$$\varepsilon_3 = 50000 \mu\varepsilon$$

Determine the principal stresses and the angle that the maximum principal stress makes with the 0-degree gauge.

- 11.28** Research the equivalent of Equation 11.39 for a 60-60-60 degree strain rosette.

Chapter 12

Mechatronics¹: Sensors, Actuators, and Controls

12.1 INTRODUCTION

Rapid advances in microprocessors have led to a dramatic increase in electronically controlled devices and systems. All of these systems require sensors and actuators to be interfaced with the electronics. Understanding the operating principles and limitations of sensors is essential to selecting and interfacing sensors for linear motion, rotary motion, and engineering variables such as force torque and power. *Actuators* are required to produce motion, such as to move an electric car seat, for a fly-by-wire throttle for automotive applications, or for positioning a precision laser welder. This chapter discusses sensors and actuators, and provides a brief introduction to linear control theory.

Upon completion of this chapter, the reader will be able to

- describe and analyze methods for displacement measurement,
- state the physical principles underlying velocity and acceleration measurements,
- describe various load cells and their appropriate applications,
- describe various methods for measuring torque and power,
- describe various actuators and their role in mechatronic systems, and
- analyze proportional-integral-derivative (PID) control schemes as part of a mechatronic system.

12.2 SENSORS

The previous chapters described a wide variety of measurement sensors and the fundamentals of their operation. Thermocouples, strain gauges, flow meters, and pressure sensors represent the means to measure the very important engineering process variables of temperature, strain, flow rate, and pressure. In this chapter we add to this base by introducing methods and sensors for the measurement of linear and rotary displacement, acceleration and vibration, velocity measurement, force or load, torque, and mechanical power.

¹The term “mechatronics” is derived from the terms “mechanical” and “electronic,” and refers to the integration of mechanical and electronic devices.

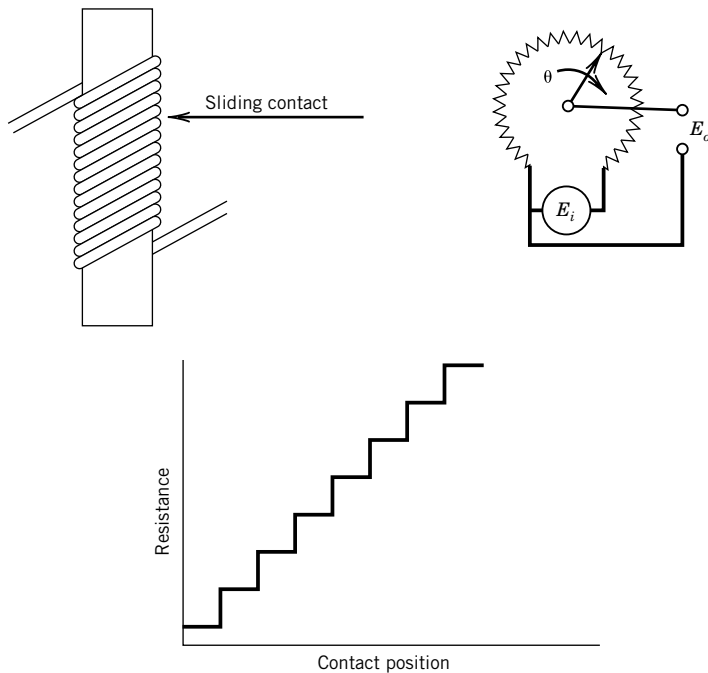


Figure 12.1 Potentiometer construction.

Displacement Sensors

Methods to measure position or displacement are a key element in many mechatronic systems. Often potentiometric or linear variable differential transformer (LVDT) transducers are employed in these applications.

Potentiometers

A potentiometer is a device employed to measure linear or rotary displacement. The principle of operation relies on an increase in electrical resistance with displacement.

A wire-wound potentiometer² or variable electrical resistance transducer is depicted in Figure 12.1. This transducer is composed of a sliding contact and a winding. The winding is made of many turns of wire wrapped around a nonconducting substrate. Output signals from such a device can be realized by imposing a known voltage across the total resistance of the winding and measuring the output voltage, which is proportional to the fraction of the distance the contact point has moved along the winding. Potentiometers can also be configured in a rotary form, with numerous total revolutions of the contact possible in a helical arrangement. The output from the sliding contact as it moves along the winding is actually discrete, as illustrated in Figure 12.1; the resolution is limited by the number of turns per unit distance. The loading errors associated with voltage-dividing circuits, discussed in Chapter 6, should be considered in choosing a measuring device for the output voltage.

² The potentiometer-transducer should not be confused with the potentiometer-instrument. Although both are based on voltage-divider principles, the latter measures low-level voltages (10^{-6} to 10^{-3} V) as described in Chapter 6.

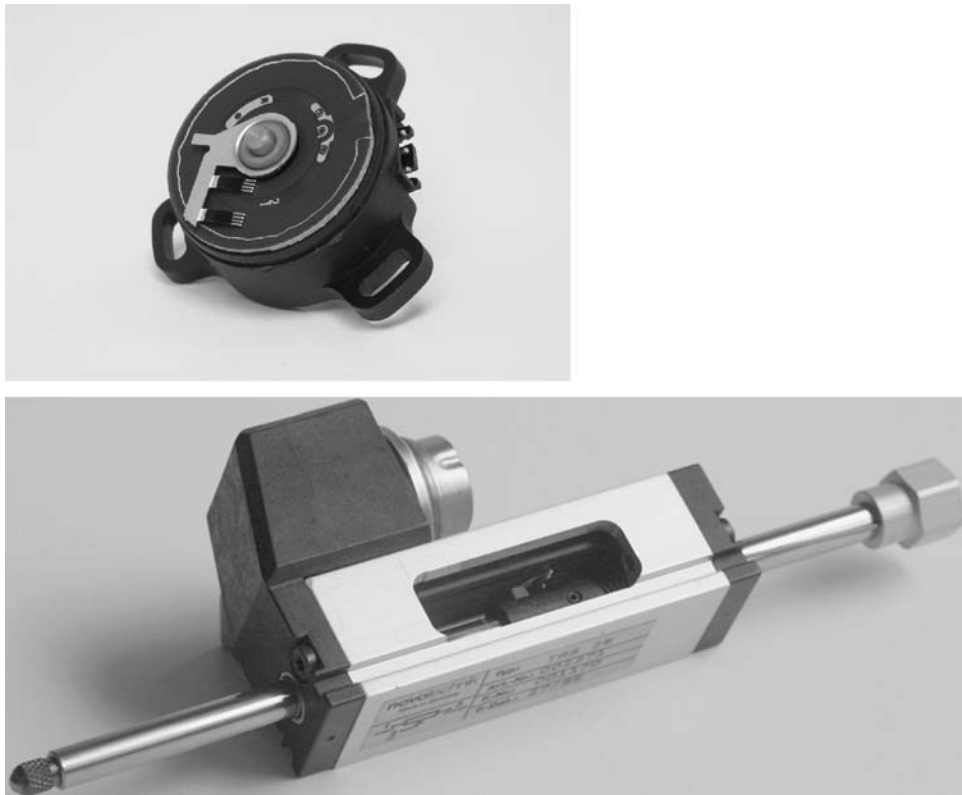


Figure 12.2 Conductive plastic potentiometer. (Courtesy of Novotechnic U.S., Inc.).

Wire-wound potentiometers display a stepwise output as the wiper contacts successive turns of the wire winding. Conductive plastic potentiometers were developed to eliminate this stepwise output, and are now widely employed in mechatronic systems. Two such potentiometers are shown in Figure 12.2. The key components are the structural support and mechanical interface, the conductive plastic resistor, and the wiper where electrical contact occurs. A linear output with displacement is most often the design objective for these sensors. Typical linearity errors introduce instrument uncertainty from 0.2% to 0.02% of the reading.

Linear Variable Differential Transformers

The LVDT, as shown in Figure 12.3, produces an AC output with an amplitude that is proportional to the displacement of a movable core. The movement of the core causes a mutual inductance in the secondary coils for an AC voltage applied to the primary coil. The waveform of the output from the LVDT is sinusoidal; the amplitude of the sine wave is proportional to the displacement of the core for a limited range of core motion.

In 1831, the English physicist Michael Faraday (1791–1867) demonstrated that a current could be induced in a conductor by a changing magnetic field. An interesting account of the development of the transformer may be found elsewhere (1). Recall that for two coils in close proximity, a change

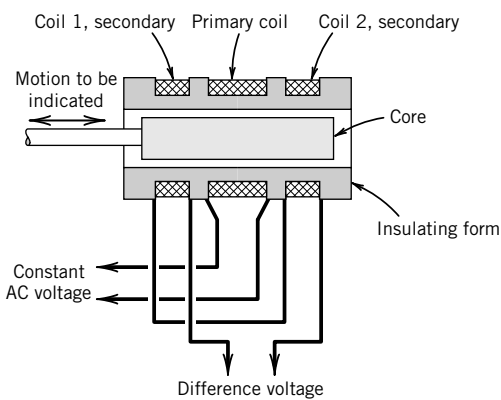
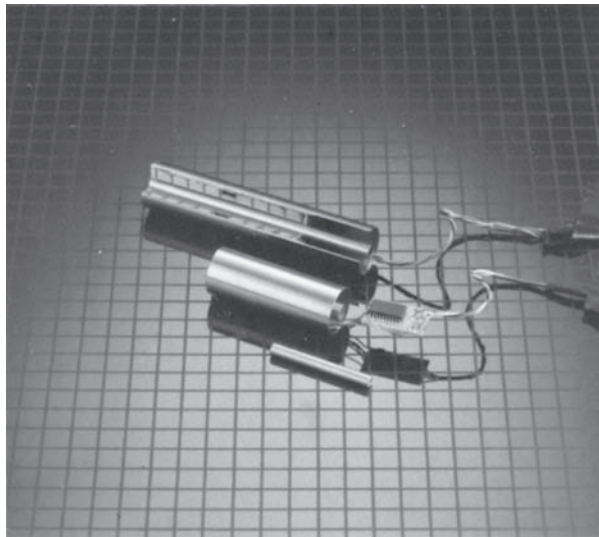


Figure 12.3 Construction of a linear variable differential transformer (LVDT). (Courtesy of Schaevitz Engineering; from reference 2.)

in the current in one coil induces an electromotive force (emf) in the second coil according to Faraday's law. The application of this inductance principle to the measurement of distance begins by applying an AC voltage to the primary coil of the LVDT. The two secondary coils are connected in a series circuit, such that when the iron core is centered between the two secondary coils the output voltage amplitude is zero (Fig. 12.3). Motion of the magnetic core changes the mutual inductance of the coils, which causes a different emf to be induced in each of the two secondary coils. Over a limited range of operation, the output amplitude is essentially linear with core displacement, as first noted in a U.S. patent by G. B. Hoadley in 1940 (2). The output of a differential transformer is illustrated in Figure 12.4, in which both the linear range and nonlinear behavior are observed. Beyond the linear range, the output amplitude rises in a nonlinear manner to a maximum, and eventually falls to zero. The output voltages on either side of the zero displacement position are 180 degrees out of phase. Thus with appropriate phase measurement it is possible to determine positive or negative displacement of the core. However, note that due to harmonic distortion in the supply voltage and the fact that the two secondary coils are not identical, the output voltage with the coil

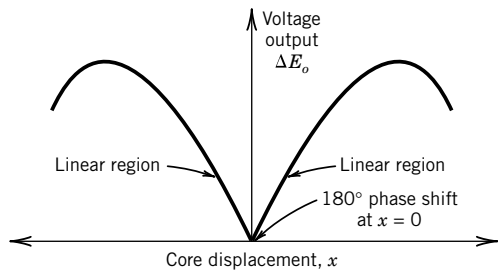


Figure 12.4 LVDT output as a function of core position.

centered is not zero but instead reaches a minimum. Resolution of an LVDT strongly depends on the resolution of the measurement system used to determine its output. Resolutions down to the nanometer range are available.

The differential voltage output of an LVDT, as shown in Figure 12.4, may be analyzed by assuming that the magnetic field strengths are uniform along the axis of the coils, neglecting end effects, and limiting the analysis to the case where the core does not move beyond the ends of the coils (2). Under these conditions the differential voltage may be expressed in terms of the core displacement. The sensitivity of the LVDT in the linear range is a function of the number of turns in the primary and secondary coils, the root-mean-square (rms) current in the primary coil, and the physical size of the LVDT.

Excitation Voltage and Frequency

The dynamic response of an LVDT is directly related to the frequency of the applied AC voltage, since the output voltage of the secondary coil is induced by the variation of the magnetic field induced by the primary coil. For this reason the excitation voltage should have a frequency at least 10 times the maximum frequency in the measured input. An LVDT can be designed to operate with input frequencies ranging from 60 Hz up to 25 kHz (for specialized applications, frequencies in the megahertz range can be used).

The maximum allowable applied voltage for an LVDT is determined by the current-carrying capacity of the primary coil, typically in the 1- to 10-V range. A constant current source is preferable for an LVDT to limit temperature effects. For other than a sine wave input voltage form, harmonics in the input signal increase the voltage output at the null position of the core. The appropriate means of measuring and recording the output signal from an LVDT and the AC frequency applied to the primary coil should be chosen based on the highest frequencies present in the input signal to the LVDT. For example, for static measurements and signals having frequency content much lower than the excitation frequency of the primary coil, an AC voltmeter may be an appropriate choice for measuring the output signal. In this case, it is likely that the frequency response of the measuring system would be limited by the averaging effects of the AC voltmeter. For higher frequency signals, it is possible to create a DC voltage output that follows the input motion to the LVDT through demodulation and amplification of the resulting signal using a dedicated electronic circuit. Alternatively, the output signal can be sampled at a sufficiently high frequency using a computer data acquisition system to allow signal processing for a variety of purposes.

The measurement of distance using an LVDT is accomplished using an assembly known as an LVDT gauge head. Such devices are widely used in machine tools and various types of gauging equipment. Control applications have similar transducer designs. The basic construction is shown in

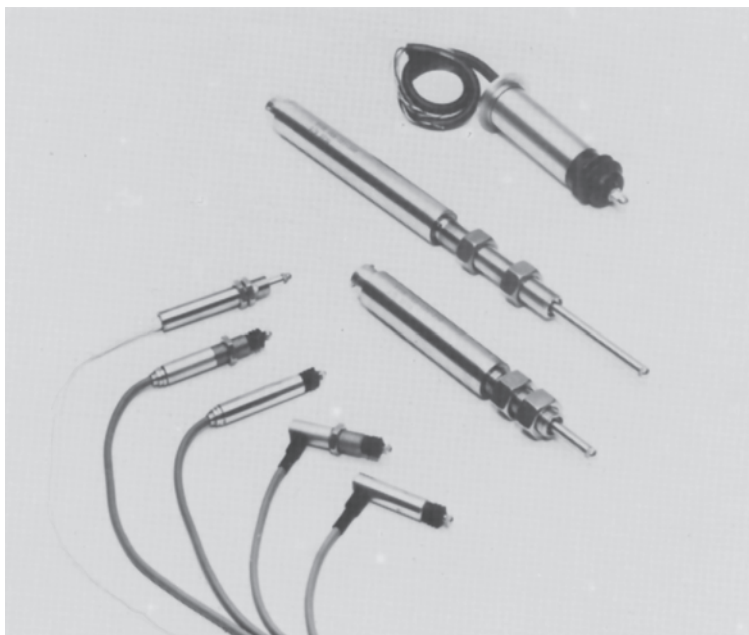
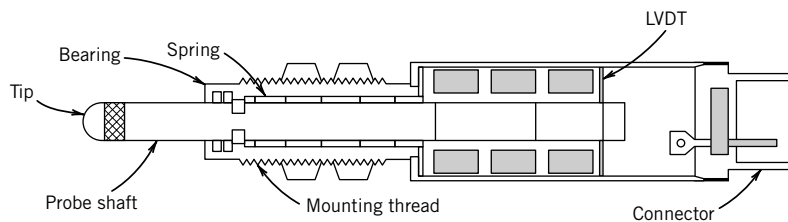


Figure 12.5 LVDT gauge head. Top: Cross section of a typical LVDT gauge head. (Courtesy of Schaevitz Engineering; from reference 2.)

Figure 12.5. The gauge head can reduce instrument errors to as low as 0.05% with repeatability of 0.0001 mm.

Angular displacement can also be measured using inductance techniques employing a rotary variable differential transformer (RVDT). The output curve of an RVDT and a typical construction are shown in Figure 12.6, in which the linear output range is approximately ± 40 degrees.

Measurement of Acceleration and Vibration

The measurement of acceleration is required for a variety of purposes, ranging from machine design to guidance systems. Because of the range of applications for acceleration and vibration measurements, there exists a wide variety of transducers and measurement techniques, each associated with a particular application. This section addresses some fundamental aspects of these measurements along with some common applications.

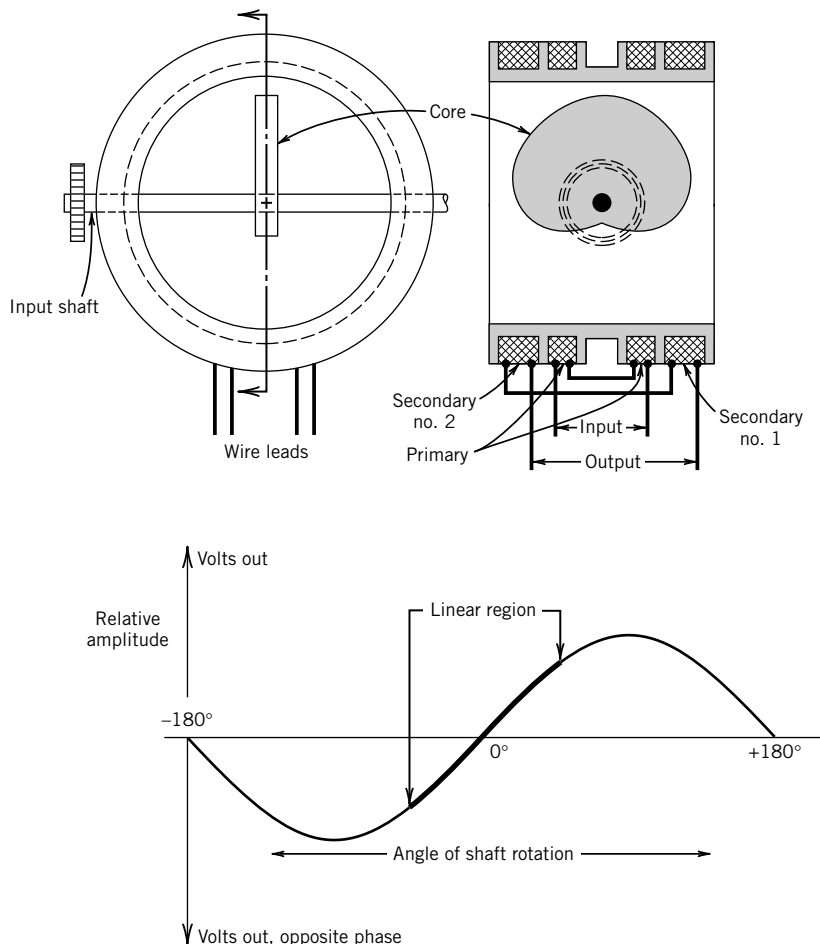


Figure 12.6 Rotary variable differential transformer. (Courtesy of Schaevitz Engineering; from reference 6.)

Displacement, velocity, and acceleration measurements are also referred to as shock or vibration measurements depending on the waveform of the forcing function that causes the acceleration. A forcing function that is periodic in nature generally results in accelerations that are analyzed as vibrations. On the other hand, a force input having a short duration and a large amplitude would be classified a shock load.

The fundamental aspects of acceleration, velocity, and displacement measurements can be discerned through examination of the most basic device for measuring acceleration and velocity, a seismic transducer.

Seismic Transducer

A seismic transducer consists of three basic elements, as shown in Figure 12.7: a spring-mass-damper system, a protective housing, and an appropriate output transducer. Through the appropriate

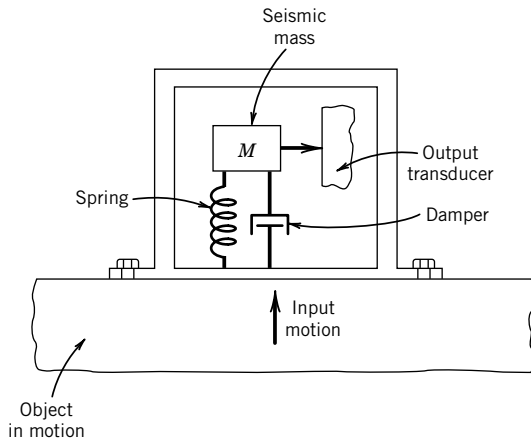


Figure 12.7 Seismic transducer.

design of the characteristics of this spring-mass-damper system, the output is a direct indication of either displacement or acceleration. To accomplish a specific measurement, this basic seismic transducer is rigidly attached to the object experiencing the motion that is to be measured.

Consider the case where the output transducer senses the position of the seismic mass; a variety of transducers could serve this function. Under some conditions, the displacement of the seismic mass serves as a direct measure of the acceleration of the housing and the object to which it is attached. To illustrate the relation between the relative displacement of the seismic mass and acceleration, consider the case in which the input to the seismic instrument is a constant acceleration. The response of the instrument is illustrated in Figure 12.8. At steady-state conditions, under this constant acceleration, the mass is at rest with respect to the housing. The spring deflects an amount proportional to the force required to accelerate the seismic mass, and since the mass is known, Newton's second law yields the corresponding acceleration. The relationship between a constant acceleration and the displacement of the seismic mass is linear for a linear spring (where $F = kx$).

We might want to measure not only constant accelerations but also complex acceleration waveforms. Recall from Chapter 2 that a complex waveform can be represented as a series of sine or

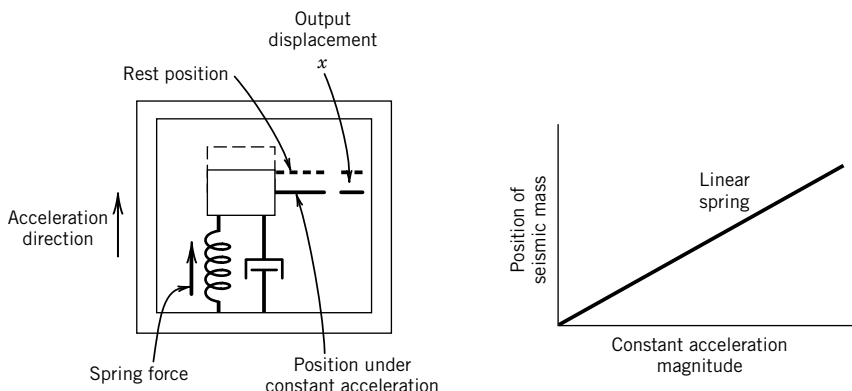


Figure 12.8 Response of a seismic transducer to a constant acceleration.

cosine functions, and that by analyzing a measuring system response to a periodic waveform input we can discern the allowable range of frequency inputs.

Consider an input to our seismic instrument such that the displacement of the housing is a sine wave, $y_{hs} = A \sin \omega t$, and the absolute value of the resulting acceleration of the housing is $A\omega^2 \sin \omega t$. If we consider a free-body diagram of the seismic mass, the spring force and the damping force must balance the inertial force for the mass. (Notice that gravitational effects could play an important role in the analysis of this instrument, for instance, if the instrument were installed in an aircraft.) The spring force and damping force are proportional to the relative displacement and velocity between the housing and the mass, whereas the inertial force is dependent only on the absolute acceleration of the seismic mass.

We define a relative displacement, y_r , as the difference between the housing displacement, y_{hs} , and the displacement of the seismic mass, y_m , given by

$$y_r = y_m - y_{hs} \quad (12.1)$$

Newton's second law may then be expressed

$$m \frac{d^2 y_m}{dt^2} + c \frac{dy_r}{dt} + ky_r = 0 \quad (12.2)$$

Substituting Equation 12.1 into Equation 12.2 yields

$$m \left(\frac{d^2 y_{hs}}{dt^2} + \frac{d^2 y_r}{dt^2} \right) + c \frac{dy_r}{dt} + ky_r = 0 \quad (12.3)$$

But we know that $y_{hs} = A \sin \omega t$ and

$$\frac{d^2 y_{hs}}{dt^2} = -A\omega^2 \sin \omega t \quad (12.4)$$

Thus,

$$m \frac{d^2 y_r}{dt^2} + c \frac{dy_r}{dt} + ky_r = mA\omega^2 \sin \omega t \quad (12.5)$$

This equation is identical in form to Equation 3.12. As in the development for a second-order system response, we examine the steady-state solution to this governing equation. The transducer senses the relative motion between the seismic mass and the instrument housing. Thus, for the instrument to be effective, the value of y_r must provide indication of the desired output.

For the input function $y_{hs} = A \sin \omega t$, the steady-state solution for y_r is

$$(y_r)_{\text{steady}} = \frac{(\omega/\omega_n)^2 A \cos(\omega t - \phi)}{\left\{ [1 - (\omega/\omega_n)^2]^2 + [2\zeta(\omega/\omega_n)]^2 \right\}} \quad (12.6)$$

where

$$\omega_n = \sqrt{\frac{k}{m}} \quad \zeta = \frac{c}{2\sqrt{km}} \quad \phi = \tan^{-1} - \frac{2\zeta(\omega/\omega_n)}{1 - (\omega/\omega_n)^2} \quad (12.7)$$

The characteristics of this seismic instrument can now be discerned by examining Equations 12.6 and 12.7. The natural frequency and damping are fixed for a particular design. We wish to examine the motion of the seismic mass and the resulting output for a range of input frequencies.

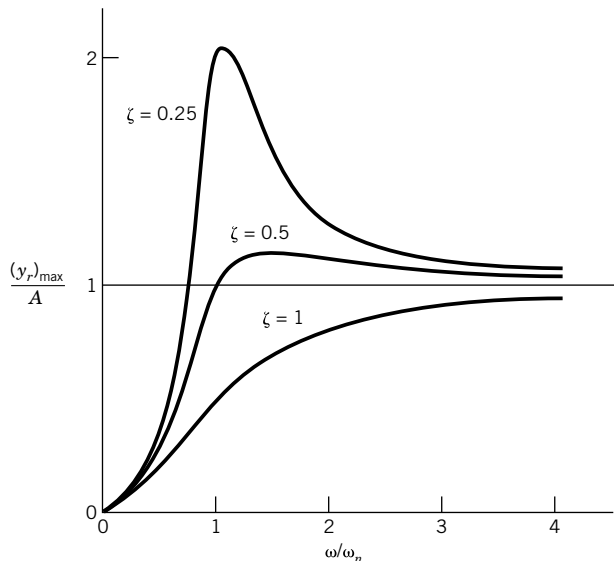


Figure 12.9 Displacement amplitude at steady state as a function of input frequency for a seismic transducer.

For vibration measurements, it is desirable to measure the amplitude of the displacements associated with the vibrations; thus, the desired behavior of the seismic instrument would be to have an output that gives a direct indication of y_{hs} . For this to occur, the seismic mass should remain stationary in an absolute frame of reference, and the housing and output transducer should move with the vibrating object. To determine the conditions under which this behavior would occur, the amplitude of y_r at steady state can be examined. The ratio of the maximum amplitude of the output divided by the equivalent static output is $(y_r)_{\max}/A$. For vibration measurements, this ratio should have a value of 1. Figure 12.9 shows $(y_r)_{\max}/A$ as a function of the ratio of the input frequency to the natural frequency as determined from Equation 12.6. Clearly, as the input frequency increases, the output amplitude, y_r , approaches the input amplitude, A , as desired. Thus, a seismic instrument that is used to measure vibration displacements should have a natural frequency smaller than the expected input frequency. Damping ratios near 0.7 are common for such an instrument. The seismic instrument designed for this application is called a *vibrometer*.

Example 12.1

A seismic instrument like the one shown in Figure 12.7 is to be used to measure a periodic vibration having an amplitude of 0.05 in. and a frequency of 15 Hz.

1. Specify an appropriate combination of natural frequency and damping ratio such that the dynamic error in the output is less than 5%.
2. What spring constant and damping coefficient would yield these values of natural frequency and damping ratio?
3. Determine the phase lag for the output signal. Would the phase lag change if the input frequency were changed?

KNOWN Input function $y_{hs} = 0.05 \sin 30\pi t$

FIND Values of ω_n , ζ , k , m , and c to yield a measurement with less than 5% dynamic error. Examine the phase response of the system.

SOLUTION Numerous combinations of the mass, spring constant, and damping coefficient would yield a workable design. Let's choose $m = 0.05 \text{ lb}_m$ (22.7 g) and $\zeta = 0.7$. We know that for a spring-mass-damper system

$$\omega = \sqrt{\frac{k}{m}} \quad c_c = 2\sqrt{km}$$

where c_c is the critical damping coefficient. With $\zeta = c/c_c = 0.7$, the damping coefficient, c , is found as

$$c = 2(0.7)\sqrt{km}$$

We can now examine the values of $(y_r)_{\max}/A$ and the phase angle, ϕ , for $\zeta = 0.7$. The largest magnitude in Equation 12.6 occurs when $\cos(\omega t - \phi) = 1$, so

$$(y_r)_{\max}/A = \frac{(\omega/\omega_n)^2}{\left\{[1 - (\omega/\omega_n)^2]^2 + [2\zeta(\omega/\omega_n)]^2\right\}^{1/2}}$$

and ϕ is found from Equation 12.7. Here is sample of the results:

$\frac{\omega}{\omega_n}$	$\frac{(y_r)_{\max}}{A}$	ϕ (degrees)
10	1.000	172
8	1.000	169.9
6	1.000	166.5
4	0.999	159.5
3	0.996	152.3
2	0.975	137.0
1.7	0.951	128.5

Using the dynamic error as $\left|\frac{(y_r)_{\max}}{A} - 1\right|$, acceptable behavior is achieved for values of $\omega/\omega_n \geq 1.7$ for $\zeta = 0.7$, and an acceptable maximum value of the natural frequency is

$$\omega_n = \omega/1.7 = 30\pi/1.7 = 55.4 \text{ rad/s}$$

with³

$$\omega_n = \sqrt{k/m}$$

³ Note: 1 lb = 32.2 lb_m-ft/s² whereas 1 N = 1 kg-m/s².

for $m = 0.05 \text{ lb}_m$ (22.7 g), then the value of k is 4.8 lb/ft (70 N/m). So the value of the damping coefficient is

$$c = 2(0.7)\sqrt{km} = 0.12 \text{ lb-s/ft} = 1.76 \text{ N-s/m}$$

COMMENTS We should consider other constraints, including size, cost, and operating environment. The phase shift–frequency behavior for this combination of design parameters could allow distortion of complex waveform signals, so if that is important, another set of parameters may be preferable. This and other issues can be explored using the program file *seismic_transducer.vi*.

Acceleration Measurement with a Seismic Instrument

If it is desired to measure acceleration, the behavior of the seismic mass must be quite different from that in Example 12.1. The amplitude of the acceleration input signal is $A\omega^2$. To have the output value y_r represent the acceleration, it is clear from Equation 12.6 that the value of $y_r/A(\omega/\omega_n)^2$ must be a constant over the design range of input frequencies. If this is true, the output will be proportional to the acceleration. The amplitude of $y_r/A(\omega/\omega_n)^2$ is

$$\frac{(y_r)_{\text{steady}}}{A(\omega/\omega_n)^2} = \frac{\cos(\omega t - \phi)}{\left\{ [1 - (\omega/\omega_n)^2]^2 + [2\zeta(\omega/\omega_n)]^2 \right\}^{1/2}} \quad (12.8)$$

and

$$M(\omega) = \frac{1}{\left\{ [1 - (\omega/\omega_n)^2]^2 + [2\zeta(\omega/\omega_n)]^2 \right\}^{1/2}} \quad (12.9)$$

where $M(\omega)$ is the magnitude ratio as given by Equation 3.22 in Chapter 3. The magnitude ratio is plotted as a function of input frequency and damping ratio in Figure 3.16.

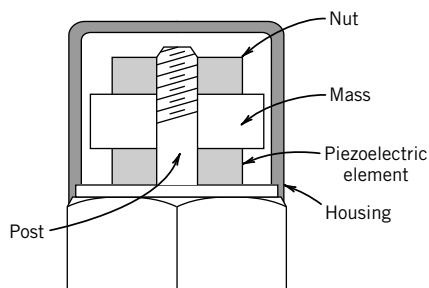
From Figure 3.16, we find that the desired flat magnitude response is achieved over a range of input frequency ratios from $0 \leq \omega/\omega_n \leq 0.4$. Typically, in an accelerometer the damping ratio is designed to be near 0.7, so that the phase shift is linear with frequency such that distortion is minimized.

In summary, the seismic instrument can be designed so that the output can be interpreted in terms of either the input displacement or the input acceleration. Acceleration measurements may be integrated to yield velocity information; the differentiation of displacement data to determine velocity or acceleration introduces significantly more difficulties than the integration process.

Transducers for Shock and Vibration Measurement

In general, the destructive forces generated by vibration and shock are best quantified through the measurement of acceleration. Although a variety of accelerometers are available, strain gauge and piezoelectric transducers are widely employed for the measurement of shock and vibration (3).

A piezoelectric accelerometer employs the principles of a seismic transducer through the use of a piezoelectric element to provide a portion of the spring force. Figure 12.10 illustrates one basic construction of a piezoelectric accelerometer. A preload is applied to the piezoelectric element

**Figure 12.10** Basic piezoelectric accelerometer.

simply by tightening the nut that holds the mass and piezoelectric element in place. Upward or downward motion of the housing changes the compressive forces in the piezoelectric element, resulting in an appropriate output signal. Instruments are available with a range of frequency response from 0.03 to 10,000 Hz. Depending on the piezoelectric material used in the transducer construction, the static sensitivity can range from 1 to 100 mV/g. Steady accelerations cannot be effectively measured with such a piezoelectric transducer.

Strain gauge accelerometers are generally constructed using a mass supported by a flexure member, with the strain gauge sensing the deflection that results from an acceleration of the mass. The frequency response and range of acceleration of these instruments are related, such that instruments designed for higher accelerations have a wider bandwidth but significantly lower static sensitivity. Table 12.1 provides typical performance characteristics for two strain gauge accelerometers that employ semiconductor strain gauges.

Many other accelerometer designs are available, including potentiometric, reductive, or accelerometers that use closed loop servo systems to provide a high output level. Piezoelectric transducers have the highest frequency response and range of acceleration, but have relatively lower sensitivity. Amplification can overcome this drawback to some degree. Semiconductor strain gauge transducers have a lower frequency response limit than do piezoelectric transducers, but they can be used to measure steady accelerations.

Velocity Measurements

Linear and angular velocity measurements utilize a variety of approaches ranging from radar and laser systems for speed measurement to mechanical counters to provide an indication of a shaft rotational speed. For many applications, the sensors employed provide a scalar output of speed. However, sensors and methods exist that can provide indication of both speed and direction,

Table 12.1 Representative Performance Characteristics for Piezoresistive Accelerometers^a

Characteristic	25-g Range	2500-g Range
Sensitivity [mV/g]	50	0.1
Resonance frequency [Hz]	2700	30,000
Damping ratio	0.4–0.7	0.03
Resistance [Ω]	1500	500

^aAdapted from reference 7.

when properly employed. Here we consider techniques for the measurement of linear and angular speed.

Displacement, velocity, and acceleration measurements are made with respect to some frame of reference. Consider the case of a game of billiards in a moving railway car. Observers on the platform and on the train would assign different velocity vectors to the balls during play. The velocity vectors would differ by the relative velocity of the two observers. Simply differentiating the vector velocity equation, however, shows that the accelerations of the balls are the same in all reference frames moving relative to one another with constant relative velocity.

Linear Velocity Measurements

As previously discussed, measurements of velocity require a frame of reference. For example, the velocity of a conveyor belt might be measured relative to the floor of the building where it is housed. On the other hand, advantages may be realized in a control system if the velocity of a robotic arm, which “picks” parts from this same conveyor belt, is measured relative to the moving conveyor. In the present discussion, it is assumed that velocity is measured relative to a ground state, which is generally defined by the mounting point of a transducer.

Consider the measurement of velocity relative to a fixed frame of reference. Typically, if the measurement of linear velocity is to be made on a continuous basis, an equivalent angular rotational speed is measured, and the data is analyzed in such a way so as to produce a measured linear velocity. For example, a speedometer on an automobile provides a continuous record of the speed of the car, but the output is derived from measuring the rotational speed of the drive shaft or transmission.

Velocity from Displacement or Acceleration

Velocity, in general, can be directly measured by mechanical means only over very short times or small displacements, due to limitations in transducers. However, if the displacement of a rigid body is measured at identifiable time intervals, the velocity can be determined through differentiation of the time-dependent displacement. Alternatively, if acceleration is measured, the velocity may be determined from integration of the acceleration signal. The following example demonstrates the effect of integration and differentiation on the uncertainty of velocities computed from acceleration or displacement.

Example 12.2

Suppose our goal is to assess the merits of measuring velocity through the integration of an acceleration signal as compared to differentiating a displacement signal. The following conditions are assumed to apply.

For both $y(t)$ and $y''(t)$ the data acquisition system and transducers have the characteristics described in Table 12.2. Note that the uncertainties are derived directly from the analog-to-digital (A/D) resolution error and accuracy statements. Assume that the signals for both acceleration and displacement are sampled at 10 Hz and numerical techniques are used to differentiate or integrate the resulting signals.

SOLUTION Consider first determining the velocity through differentiation of the displacement signal. Displacement is measured digitally by the data acquisition system, with a digitized

Table 12.2 Specification and Uncertainty Analyses for Displacement and Acceleration

Measured Variable	Functional Form	Full-Scale Output Range
Displacement (cm)	$y(t) = 20 \sin 2t$	0 to 10 V
Acceleration (cm/s ²)	$y'' = -\frac{20}{4} \sin 2t$	-5 to 5 V
Uncertainty Values for Displacement and Acceleration		
Measured Variable	Uncertainty	
Displacement	Accuracy: 1% full scale = 0.2 cm A/D 8 bit (0.04 V) = 0.08 cm Total uncertainty = ±0.22 cm	
Acceleration	Accuracy: 1% full scale = 0.05 cm/s ² A/D 8 bit (0.04 V) = 0.04 cm/s ² Total uncertainty = ±0.064 cm/s ²	

value of displacement recorded at time intervals δt . The velocity at any time $n\delta t$ can be approximated as

$$v(t) = y'(t) = \frac{y_{n+1} - y_n}{\delta t} \quad (12.10)$$

where

y_{n+1} = the $(n+1)$ measurement of displacement at time $(n + 1)\delta t$

y_n = the n th measurement of displacement at time $n\delta t$

$v(t)$ = velocity at time t

If the signal is sampled at 10 Hz, δt is 0.1 s. For the present, we assume that the uncertainty in time is negligible, so that the uncertainty in v, u_v can be expressed as

$$u_v = \left\{ \left[\frac{\partial v}{\partial y_{n+1}} u_{y_{n+1}} \right]^2 + \left[\frac{\partial v}{\partial y_n} u_{y_n} \right]^2 \right\}^{1/2} \quad (12.11)$$

The uncertainties in the measured displacements, y_n and y_{n+1} , will be equal, and are listed in Table 12.2. Substituting these values for uncertainty in Equation 12.11 yields an uncertainty of ± 3 cm/s in the velocity measurement. Notice that this uncertainty magnitude is not a function of time or the measured velocity. This corresponds to a minimum uncertainty of 30% in the velocity measurement.

To determine velocity from acceleration, the measured values of acceleration must be integrated. Since we have a digital signal, the integration can be accomplished numerically as

$$v(t) = y'(t) = \sum_i y_i'' \delta t \quad (12.12)$$

Assuming the uncertainty in time is negligible, the uncertainty in velocity at any time t is simply

$$u_v = u_{y''} t \quad (12.13)$$

Clearly, the integration process tends to accumulate error as the calculation of velocity proceeds in time, as illustrated in Figure 12.11, but for very short time periods can produce acceptable results.

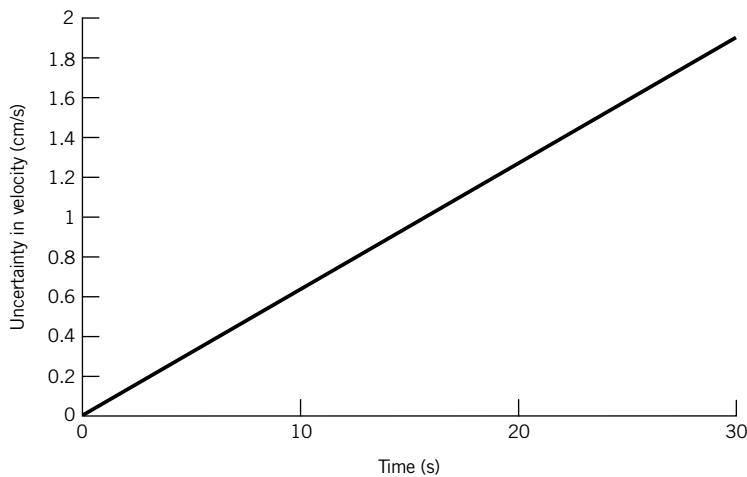


Figure 12.11 Uncertainty in velocity as a function of time.

COMMENT This example can be used to illustrate several useful principles for data analysis. Consider the effects of adding noise, or a degree of random error, to measured data; such a signal is shown in Figure 12.12. In general, noise tends to be minimized through a process of integration and amplified through differentiation. Figure 12.13 shows the result of integrating the noisy data from

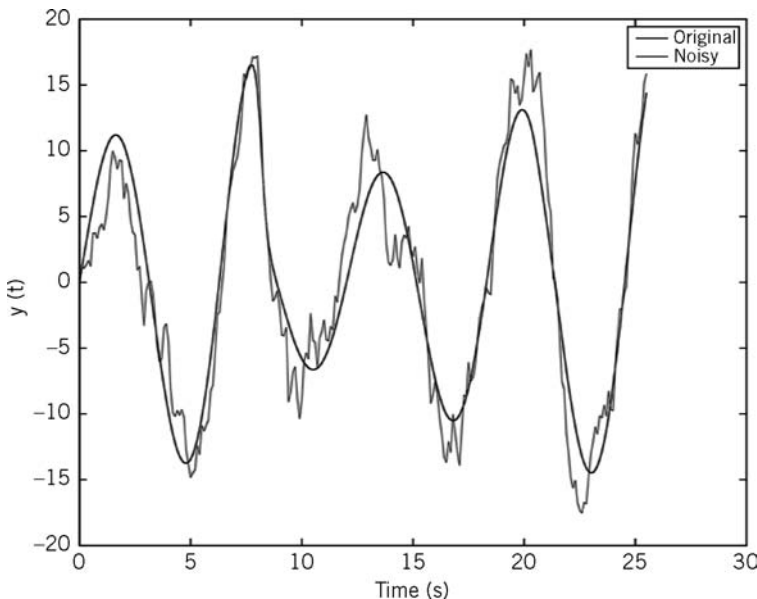


Figure 12.12 Deterministic signal with added noise.

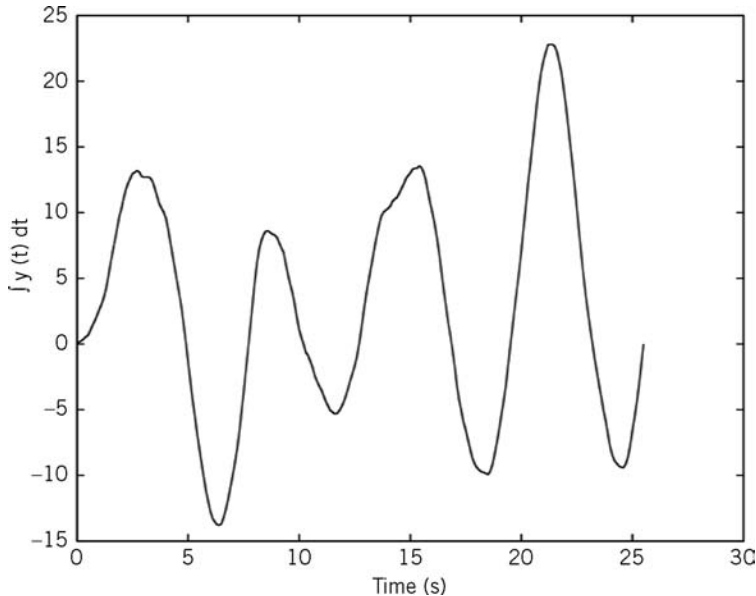


Figure 12.13 Result of integrating the noisy signal from Figure 12.12.

Figure 12.12, with the result that the effects of noise are reduced. However, because of the accumulation of error, the technique must balance the integration period against error accumulation. Differentiation tends to be extremely sensitive to low amplitude, high-frequency noise, which can create very large errors in derivatives, especially at high sampling frequencies. This is apparent in Figure 12.14, in which the signal in Figure 12.12 has been differentiated numerically. Appropriate filtering or smoothing techniques are generally effective at reducing errors associated with noise in derivatives in cases where the noise has low amplitude.

Moving Coil Transducers

Moving coil transducers take advantage of the voltage generated when a conductor experiences a displacement in a magnetic field. This is the same phenomenon used to generate electric power in generators and alternators. An illustration of a moving coil velocity pickup is provided in Figure 12.15. Recall that a current carrying conductor experiences a force in a magnetic field, and that a force is required to move a conductor in a magnetic field. For the latter case, an emf is induced in the conductor. Consider the case in which the magnetic field strength is at right angles to the conductor. The induced emf is given by

$$\text{emf} = \pi B D_c l N \frac{dy}{dt} \quad (12.14)$$

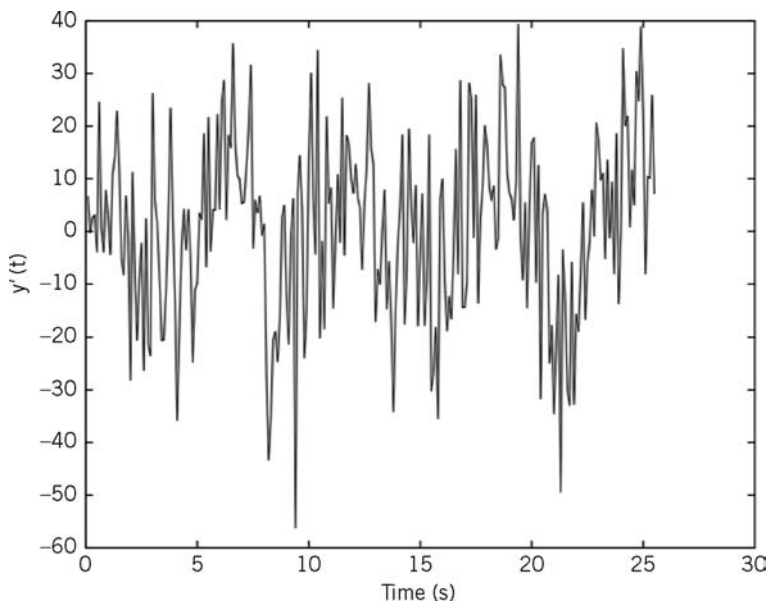


Figure 12.14 Result of numerical differentiation of the noisy signal from Figure 12.12.

where

B = magnetic field strength

D_c = coil diameter

emf = induced electromotive force

N = number of turns in coil

dy/dt = velocity of coil linear motion

l = coil length

A moving coil transducer is appropriate for vibration applications in which the velocities of small amplitude motions are measured. The output voltage is proportional to the coil velocity, and the output polarity indicates the velocity direction. Static sensitivities on the order of 2 V/s/m are

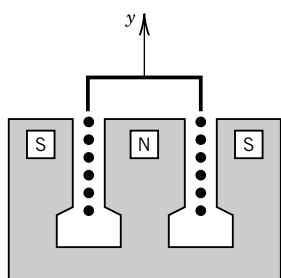


Figure 12.15 Moving coil transducer.

typical. Moving coil transducers find application in seismic measurements as well as in vibration applications.

Angular Velocity Measurements

The measurement of angular velocity finds a wide range of applications, including such familiar examples as speedometers on automobiles. We consider a variety of applications and measurement techniques.

Mechanical Measurement Techniques

Mechanical means of measuring angular velocity or rotational speed were developed primarily to provide feedback for control of engines and steam turbines. Mechanical governors and centrifugal tachometers (4) operate on the principle illustrated in Figure 12.16. Here the centripetal acceleration of the flyball masses result in a steady-state displacement of the spring, which provides a control signal or is a direct indication of rotational speed. For this arrangement, the spring force is proportional to the square of the angular velocity.

Stroboscopic Angular Velocity Measurements

A stroboscopic light source provides high-intensity flashes of light, which can be caused to occur at a precise frequency. A stroboscope is illustrated in Figure 12.17. Stroboscopes permit the intermittent observation of a periodic motion in a manner that appears to stop or slow the motion. Advances in electronics in the mid-1930s allowed the development of a stroboscope with a very well defined flashing rate and led to the use of stroboscopic tachometers. Figure 12.18 illustrates the use of a strobe to measure rotational speed. A timing mark on the rotating object is illuminated with the strobe, and the strobe frequency is adjusted such that the mark appears to remain motionless, as shown in Figure 12.18a. Thus, the highest synchronous speed is the actual rotational speed. At this speed, the output value is available from a calibration of the stroboscopic lamp flash frequency, with uncertainties to less than 0.1%. Clearly,

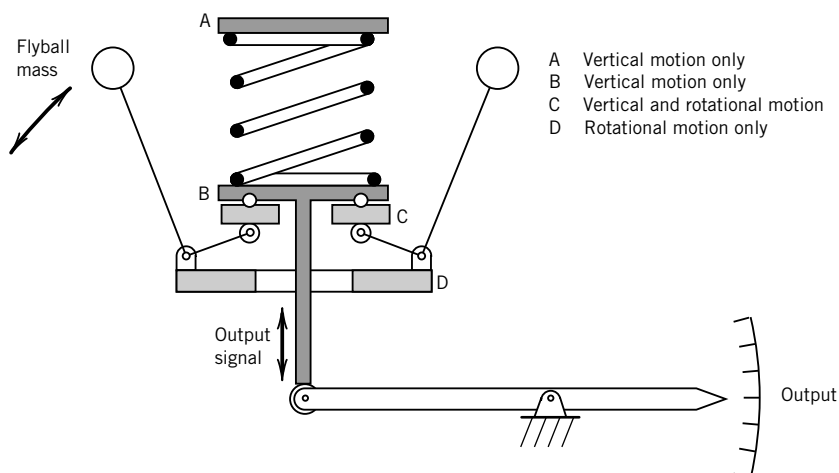


Figure 12.16 Mechanical angular velocity sensor.

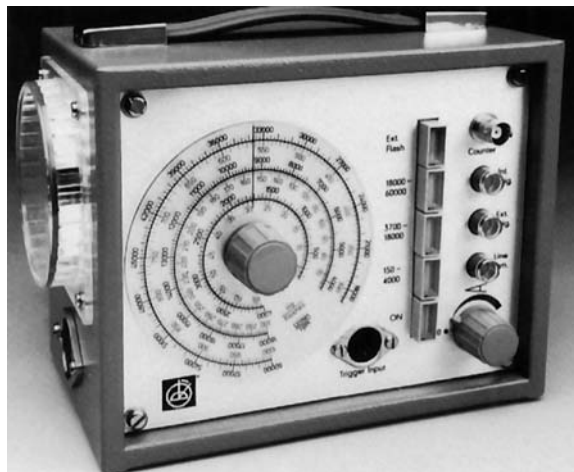


Figure 12.17 Stroboscope. (Courtesy of Mill Devices Co., a division of A. B. Carter Inc.)

a timing mark would appear motionless for integer multiples of the actual rotational speed and for integral submultiples, as illustrated in Figure 12.18b–e.

The synchronization of images at flashing rates other than the actual speed requires some practical approaches to ensuring the accurate determination of speed. Spurious images can easily result for symmetrical objects, and some asymmetric marking is necessary to prevent misinterpretation of stroboscopic data. To distinguish the actual speed from a submultiple, the flashing

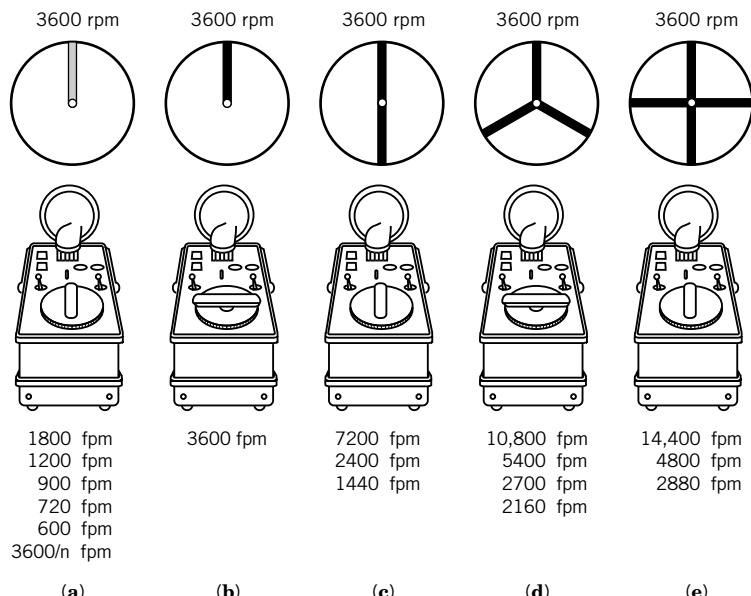


Figure 12.18 Images resulting from harmonic and subharmonic flashing rates for stroboscopic angular speed measurement. (Courtesy of Mill Devices Co., a division of A.B. Carter Inc.)

rate can be decreased until another single synchronous image appears. If this flashing rate corresponds to one-half the original rate, then the original rate is the actual speed. If it does not occur at one-half the original value, then the original value is a submultiple.

The upper limit of the flash rate of the strobe does not limit the ability of the stroboscope to measure rotational speed. For high speeds, synchronization can be achieved N times, with ω_1 representing the maximum achievable synchronization speed, and $\omega_2, \omega_3, \dots$ representing successively lower synchronization speeds. The measured rotational speed is then calculated as

$$\omega = \frac{\omega_1 \omega_N (N - 1)}{\omega_1 - \omega_N} \quad (12.15)$$

The program file *stroboscope.vi* on the companion software disk illustrates the basic operation and interesting stroboscopic effects.

Electromagnetic Techniques

Several measurement techniques for rotational velocity utilize transducers that generate electrical signals, which are indicative of angular velocity. One of the most basic is illustrated in Figure 12.19. This transducer consists of a toothed wheel and a magnetic pickup; the pickup consists of a magnet and a coil. As the toothed wheel rotates, an emf is induced in the coil as a result of changes in the magnetic field. As each ferromagnetic tooth passes the pickup, the reluctance of the magnetic circuit changes in time, yielding a voltage in the coil given by

$$E = C_B N_t \omega \sin N_t \omega t \quad (12.16)$$

where

E = output voltage

C_B = proportionality constant

N_t = number of teeth

ω = angular velocity of the wheel

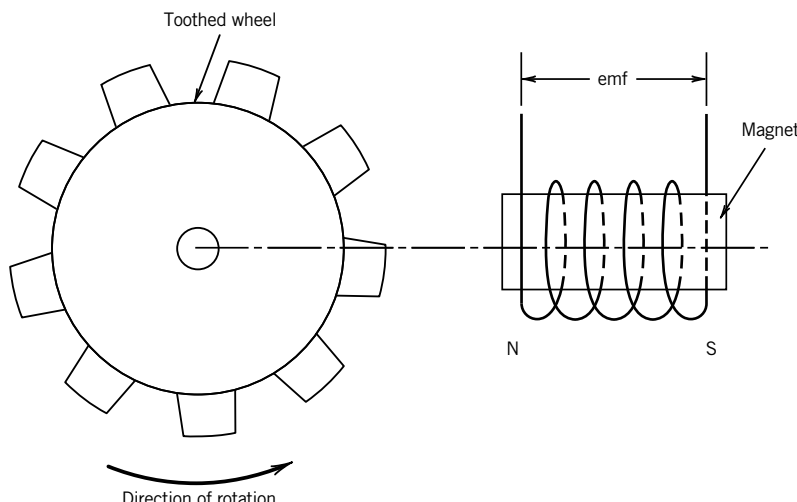


Figure 12.19 Angular velocity measurement employing a toothed wheel and magnetic pickup.

The angular velocity can be found either from the amplitude or the frequency of the output signal. The voltage amplitude signal is susceptible to noise and loading errors. Thus, less error is introduced if the frequency is used to determine the angular velocity; typically, some means of counting the pulses electronically is employed. This frequency information can be transmitted digitally for recording, which eliminates the noise and loading error problems associated with voltage signals.

Force Measurement

The measurement of force is most familiar as the process of weighing, ranging from weighing micrograms of a medicine to weighing trucks on the highway. Force is a quantity derived from the fundamental dimensions of mass, length, and time. Standards and units of measure for these quantities are defined in Chapter 1. The most common techniques for force measurement are described in this section.

Load Cells

“Load cell” is a term used to describe a transducer that generates a voltage signal as a result of an applied force, usually along a particular direction. Such force transducers often consist of an elastic member and a deflection sensor. These deflection sensors may employ changes in capacitance, resistance, or the piezoelectric effect to sense deflection. A technology overview for such devices is provided elsewhere (5). Consider first load cells that are designed using a linearly elastic member instrumented with strain gauges.

Strain Gauge Load Cells Strain gauge load cells are most often constructed of a metal, and have a shape such that the range of forces to be measured results in a measurable output voltage over the desired operating range. The shape of the linearly elastic member is designed to meet the following goals: (1) provide an appropriate range of force-measuring capability with necessary accuracy, (2) provide sensitivity to forces in a particular direction, and (3) have low sensitivity to force components in other directions.

A variety of designs of linearly elastic load cells are shown in Figure 12.20. In general, load cells may be characterized as beam-type load cells, proving rings, or columnar-type designs. Beam-type load cells may be characterized as bending beam load cells or shear beam load cells.

A bending beam load cell, as shown in Figure 12.21, is configured such that the sensing element of the load cell functions as a cantilever beam. Strain gauges are mounted on the top and bottom of the beam to measure normal or bending stresses. Figure 12.21 provides qualitative indication of the shear and normal stress distributions in a cantilever beam. In the linear elastic range of the load cell, the bending stresses are linearly related to the applied load.

In a shear beam load cell the beam cross section is that of an I-beam. The resulting shear stress in the web is nearly constant, allowing placement of a strain gauge essentially anywhere in the web with reasonable accuracy. Such a load cell is illustrated schematically in Figure 12.22, along with the shear stress distribution in the beam. In general, bending beam load cells are less costly due to their construction; however, the shear beam load cells have several advantages, including lower creep and faster response times. Typical load cells for industrial applications are illustrated in Figure 12.23.

Piezoelectric Load Cells Piezoelectric materials are characterized by their ability to develop a charge when subject to a mechanical strain. The most common piezoelectric material is single-crystal quartz. The

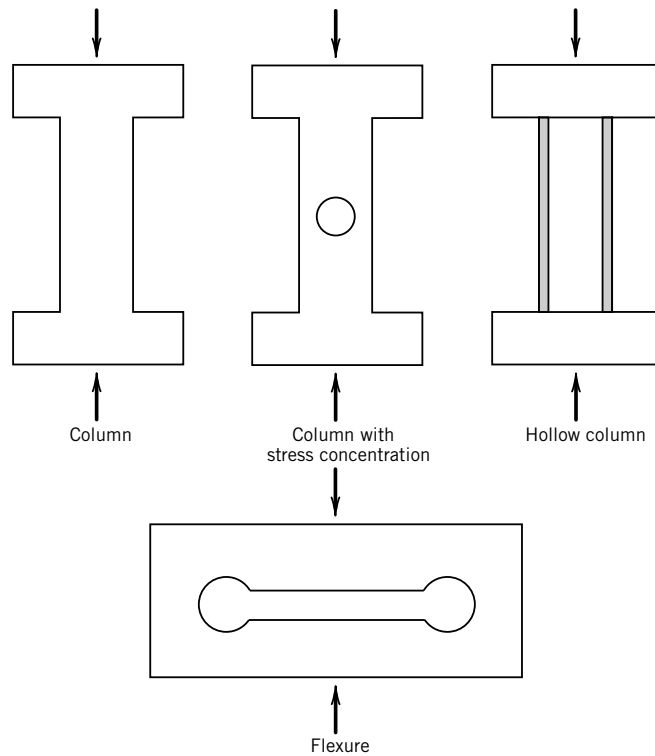


Figure 12.20 Elastic load cell designs.

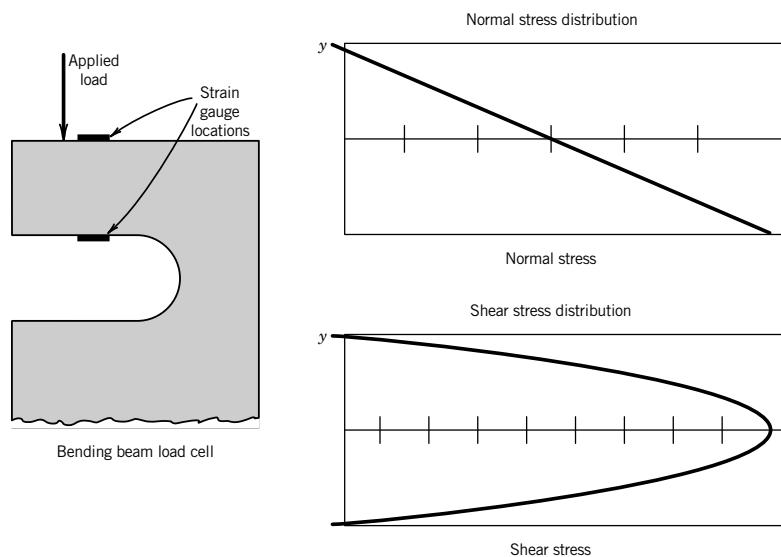


Figure 12.21 Bending beam load cell and stress distributions.

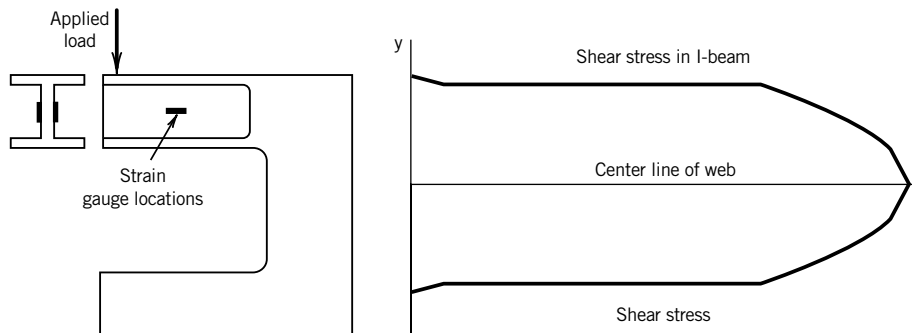


Figure 12.22 Shear beam load cell and shear stress distribution.



Figure 12.23 Typical load cells. (Courtesy of Transducer Techniques, Inc.)

basic principle of transduction that occurs in a piezoelectric element may best be thought of as a charge generator and a capacitor. The frequency response of piezoelectric transducers is very high, since the frequency response is determined primarily by the size and material properties of the quartz crystal. The modulus of elasticity of quartz is approximately 85 GPa, yielding load cells with typical static sensitivities ranging from 0.05 to 10 mV/N, and a frequency response up to 15,000 Hz. A typical piezoelectric load cell construction is shown in Figure 12.24.

Proving Ring A ring-type load cell can be employed as a local force standard. Such a ring-type load cell, as shown in Figure 12.25, is often employed in the calibration of materials testing machines because of the high degree of precision and accuracy possible with this arrangement of

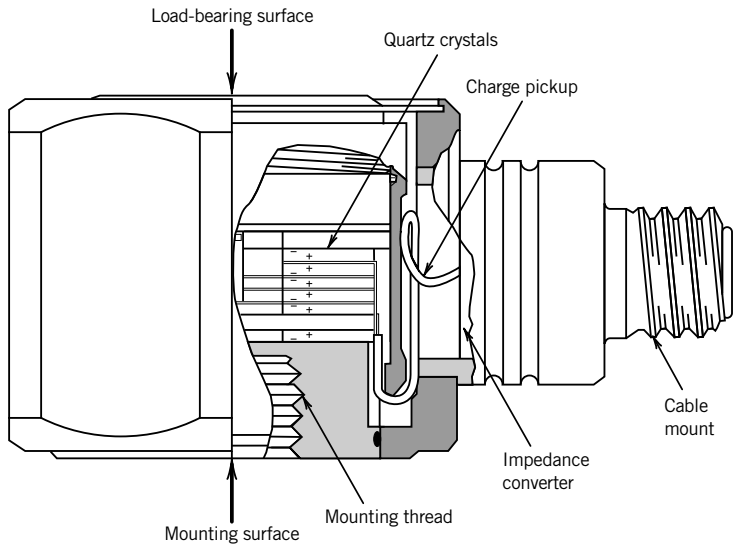


Figure 12.24 Piezoelectric load cell design. (Courtesy of the Kistler Instrument Co.)

transducer and sensor. If the sensor is approximated as a circular right cylinder, the relationship between applied force and deflection is given by

$$\delta y = \left(\frac{\pi}{2} - \frac{4}{\pi} \right) \frac{F_n D^3}{16EI} \quad (12.17)$$

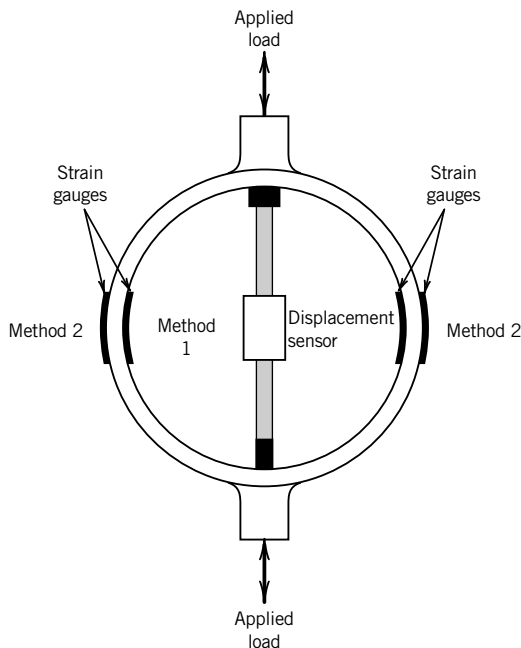


Figure 12.25 Ring type load cell, or proving ring.

where

δy = deflection along the applied force

F_n = applied force

D = diameter

E = modulus of elasticity

I = moment of inertia

The application of the proving ring involves measuring the deflection of the proving ring in the direction of the applied force. Typical methods for this displacement measurement include displacement transducers, which measure overall displacement, and strain gauges. These methods are illustrated in Figure 12.25.

Torque Measurements

Torque and mechanical power measurements are often associated with the energy conversion processes that serve to provide mechanical and electrical power to our industrial world. Such energy conversion processes are largely characterized by the mechanical transmission of power produced by prime movers such as internal combustion engines. From automobiles to turbine-generator sets, mechanical power transmission occurs through torque acting through a rotating shaft.

The measurement of torque is important in a variety of applications, including sizing of load-carrying shafts. This measurement is also a crucial aspect of the measurement of shaft power, such as in an engine dynamometer. Strain-gauge-based torque cells are constructed in a manner similar to load cells, in which a torsional strain in an elastic element is sensed by strain gauges appropriately placed on the elastic element. Figure 12.26 shows a circular shaft instrumented with strain gauges for the purpose of measuring torque, and a commercially available torque sensor.

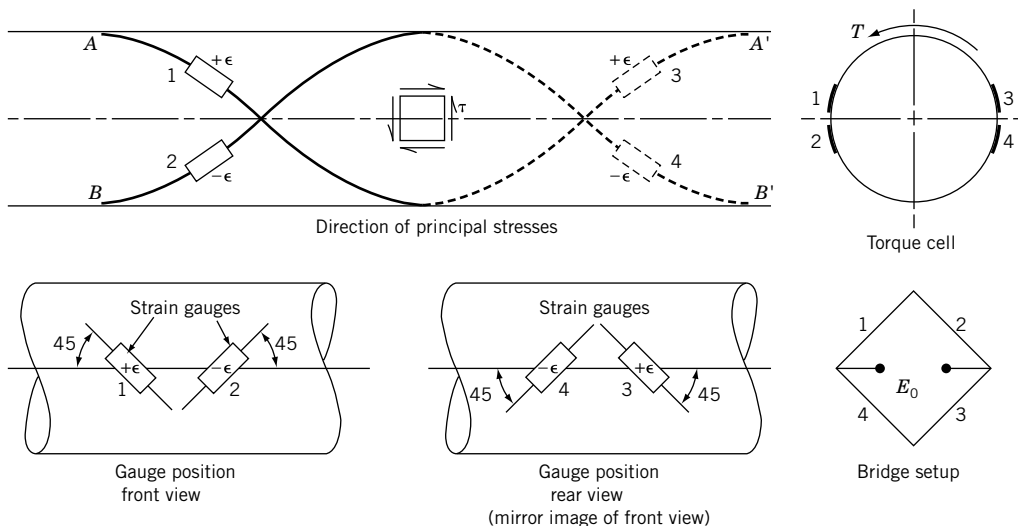


Figure 12.26 Shaft instrumented for torque measurement.

Consider the stresses created in a shaft of radius R_0 subject to a torque T . The maximum shearing stress in a circular shaft occurs on the surface and may be calculated from the torsion formula⁴

$$\tau_{\max} = TR_0/J \quad (12.18)$$

where

τ_{\max} = maximum shearing stress

T = applied torque

J = polar moment of inertia ($\pi R_0^2/2$ for a solid circular shaft)

For a shaft in pure torsion, there are no normal stresses, σ_x , σ_y , or σ_z . The principal stresses lie along a line that makes a 45-degree angle with the axis of the shaft, as illustrated in Figure 12.26, and have a value equal to τ_{\max} . Strains that occur along the curve labeled A-A' are opposite in sign from those that occur along B-B'. These locations allow placement of four active strain gauges in a Wheatstone bridge arrangement, and the direct measurement of torque in terms of bridge output voltage.

Mechanical Power Measurements

Almost universally, prime movers such as internal combustion (IC) engines and gas turbines convert chemical energy in a fuel to thermodynamic work transmitted by a shaft to the end use. In automotive applications, the pistons create a torque on the crankshaft, which is ultimately transmitted to the driving wheels. In each case, the power is transmitted through a mechanical coupling. This section discusses the measurement of such mechanical power transmission.

Rotational Speed, Torque, and Shaft Power

Shaft power is related to rotational speed and torque as

$$\vec{P}_s = \vec{\omega} \times \vec{T} \quad (12.19)$$

where P_s is the shaft power, ω is the rotational velocity vector, and T is the torque vector. In general, the orientation of the torque and rotational velocity vectors are such that the equation may be written in scalar form as

$$P_s = \omega T \quad (12.20)$$

Table 12.3 provides a summary of useful equations related to shaft power, torque, and speed as employed in mechanical measurements. Historically, a device called a Prony brake was used to measure shaft power. A typical Prony brake arrangement is shown in Figure 12.27. Consider using the Prony brake to measure power output for an IC engine. The Prony brake serves to provide a well-defined load for the engine, with the power output of the engine dissipated as thermal energy in the braking material. By adjusting the load, the power output over a range of speeds and throttle settings can be realized. The power is measured by recording the torque acting on the torque arm and the rotational speed of the engine. Clearly, this device is limited in speed and power, but does serve to demonstrate the operating principles of power measurement, and is historically significant as the first technique for measuring power.

⁴ Coulomb developed the torsion formula in 1775 in connection with electrical instruments.

Table 12.3 Shaft Power, Torque, and Speed Relationships

	SI	U.S. Customary
Shaft power, P	$P = \omega T$	$P = \frac{2\pi nT}{550}$
Power	P (W)	P (hp)
Rotational speed	ω (rad/s)	n (rev/s)
Torque	T (N m)	T (ft lb)

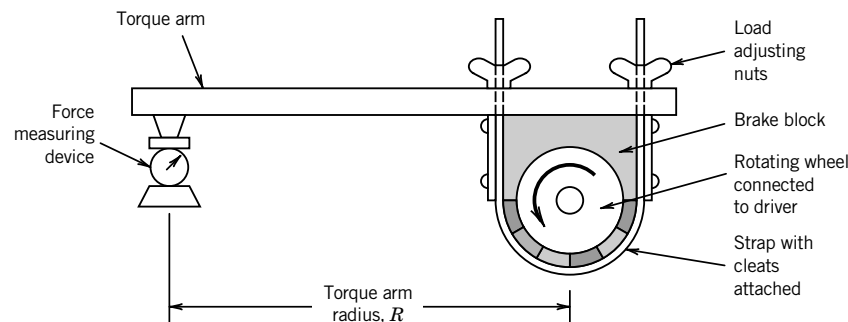


Figure 12.27 Prony brake. (Courtesy of the American Society of Mechanical Engineers, New York, NY. Reprinted from PTC 19.7-1980 6.)

Cradled Dynamometers

A Prony brake is an example of an absorbing dynamometer. The term “dynamometer” refers to a device that absorbs and measures the power output of a prime mover. Prime movers are large mechanical power-producing devices such as gasoline or diesel engines or gas turbines. Several methods of energy dissipation are utilized in various ranges of power, but the measurement techniques are governed by the same underlying principles. Thus, we consider first the measurement of power, and then discuss means for dissipating the sometimes large amounts of power generated by prime movers.

The cradled dynamometer measures mechanical power by measuring the rotational speed of the shaft, which transmits the power, and the reaction torque required to prevent movement of the stationary part of the prime mover. This reaction torque is impressively illustrated by so-called wheelies by motorcycle riders. A cradled dynamometer is supported in bearings, which are called trunion bearings, such that the reaction torque is transmitted to a torque or force-measuring device. The state-of-the-art dynamometer shown in Figure 12.28 is designed for emissions testing, with power absorption ratings above 200 HP and a top speed of 120 MPH.

In principle, the operation of the dynamometer involves the steady-state measurement of the load F_r created by the reaction torque and the measurement of shaft speed. From Equation 12.19 the transmitted shaft power can be calculated directly.

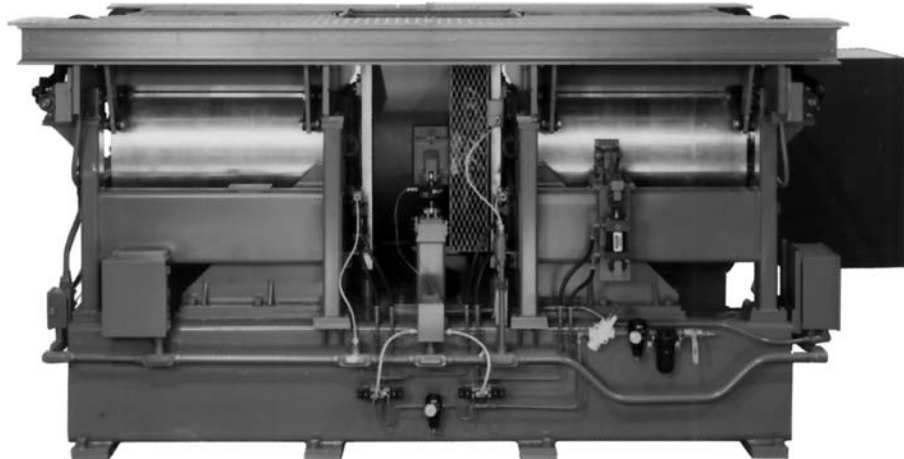


Figure 12.28 Dynamometer. (Courtesy of Burke E. Porter Machinery Co., Grand Rapids, MI)

The American Society of Mechanical Engineers (ASME) Performance Test Code (PTC) 19.7 (6) provides guidelines for the measurement of shaft power. According to PTC 19.7, overall uncertainty in the measurement of shaft power by a cradled dynamometer results from (1) trunnion-bearing friction error uncertainty, (2) force measurement uncertainty (F_r), (3) moment arm length uncertainty (L_r), (4) static unbalance of dynamometer error uncertainty and, (5) uncertainty in rotational speed measurement.

A means of supplying a controllable load to the prime mover, and dissipating the energy absorbed in the dynamometer, are an integral part of the design of any dynamometer. Several techniques are described for providing an appropriate load.

Eddy Current Dynamometers: A direct current field coil and a rotor allow shaft power to be dissipated by eddy currents in the stator winding. The resulting conversion to thermal energy by joulian heating of the eddy currents necessitates some cooling be supplied, typically using cooling water.

Alternating Current and DC Generators: Cradled AC and DC machines are employed as power absorbing elements in dynamometers. The AC applications require variable frequency capabilities to allow a wide range of power and speed measurements. The power produced in such dynamometers may be dissipated as thermal energy using resistive loads.

Waterbrake Dynamometers: A waterbrake dynamometer employs fluid friction and momentum transport to create a means of energy dissipation. Two representative designs are provided in Figure 12.29. The viscous shear type brake is useful for high rotational speeds, and the agitator type unit is used over a range of speeds and loads. Waterbrakes may be employed for applications up to 10,000 HP (7450 kW). The load absorbed by waterbrakes can be adjusted using water level and flow rates in the brake.

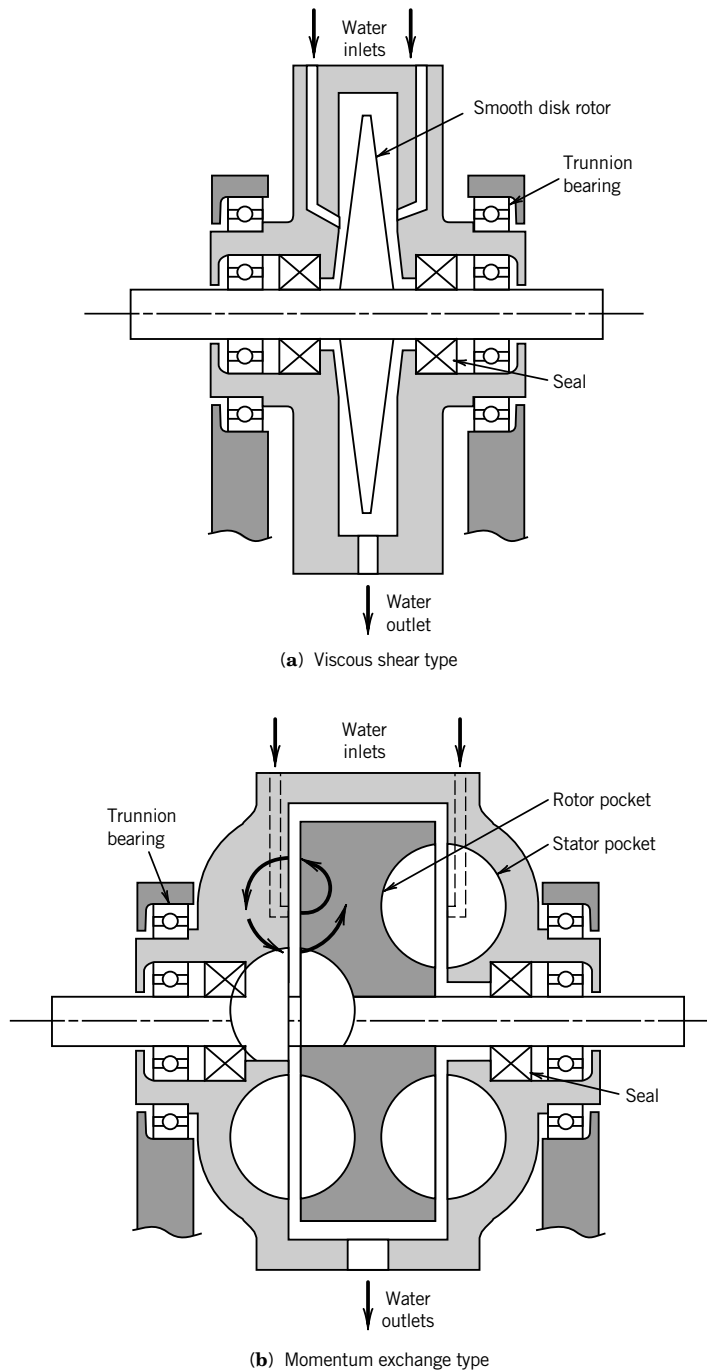


Figure 12.29 Waterbrake dynamometers. (Courtesy of the American Society of Mechanical Engineers, New York, NY. Reprinted from PTC 19.7-1980 6.)

12.3 ACTUATORS

Linear Actuators

The task of a linear actuator is to provide motion in a straight line. We discuss three ways to achieve linear motion:

1. Conversion of rotary motion into linear motion. This can be accomplished using a linkage, as in the slider-crank mechanism, or using screw threads coupled to a rotary motion source.
2. Use of a fluid pressure to move a piston in a cylinder. When air or another gas is used as the working fluid, the system is called a pneumatic system. When a fluid such as oil is used as the working fluid, the system is termed hydraulic.
3. Electromagnetic

Slider–Crank Mechanism

A common means of generating a reciprocating linear motion, or converting linear motion to rotary motion, is the slider–crank mechanism, as illustrated in Figure 12.30. Such a mechanism is the basis of transforming the reciprocating motion of the piston in an internal combustion engine. This or similar linkages could also be applied in pick-and-place operations, or in a variety of automation applications.

Screw-drive linear motion

A common means for translating rotary motion into linear motion is a lead screw. A lead screw has helical threads that are designed for minimum backlash to allow precise positioning. Numerous designs exist for such actuating threads. The basic principle is illustrated in Figure 12.31. The rotary motion of the lead screw is translated into linear motion of the nut, with the torque required to drive the lead screw directly related to the thrust the particular application requires.

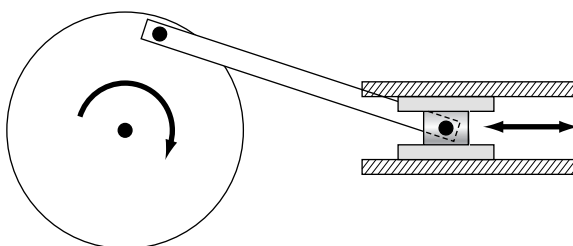


Figure 12.30 Slider–crank mechanism.

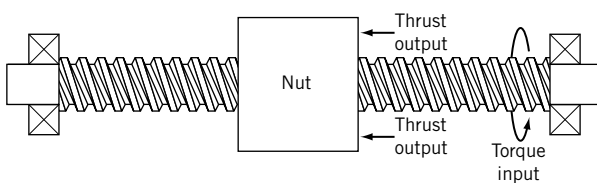


Figure 12.31 Linear actuation using a lead screw.

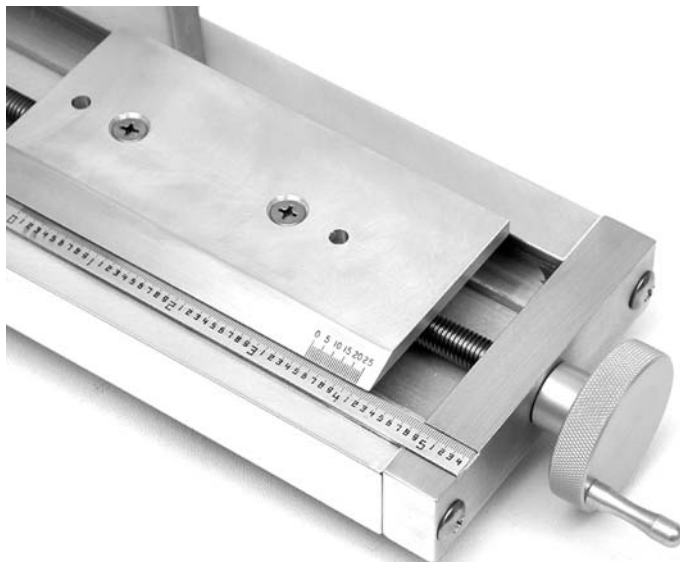


Figure 12.32 Precision translation table. (UniSlide® from Velmex, Inc).

Common applications that employ a lead screw include the worktable for a mill, and a variety of other precision positioning translation tables, such as the one shown in Figure 12.32.

Pneumatic and Hydraulic Actuators

The term “pneumatic” implies a component or system that uses compressed air as the energy source. On the other hand, a hydraulic system or component uses incompressible oil as the working fluid. An example of a hydraulic system is the power steering on an automobile; such a system is illustrated in Figure 12.33. Hydraulic fluid is supplied at an elevated pressure from the power steering pump. When a steering input is made from the driver, the rotary valve allows high-pressure fluid to enter the appropriate side of the piston, and aid in turning the wheels. By maintaining a direct connection between the steering column and the rack and pinion, the car can be steered even if the hydraulic system fails.

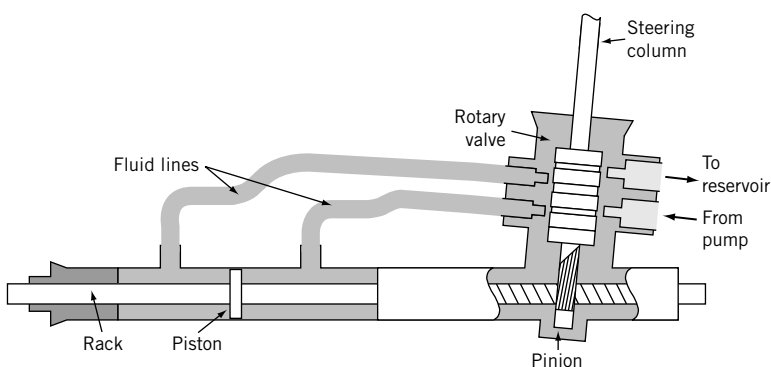


Figure 12.33 Schematic diagram of a power steering system.

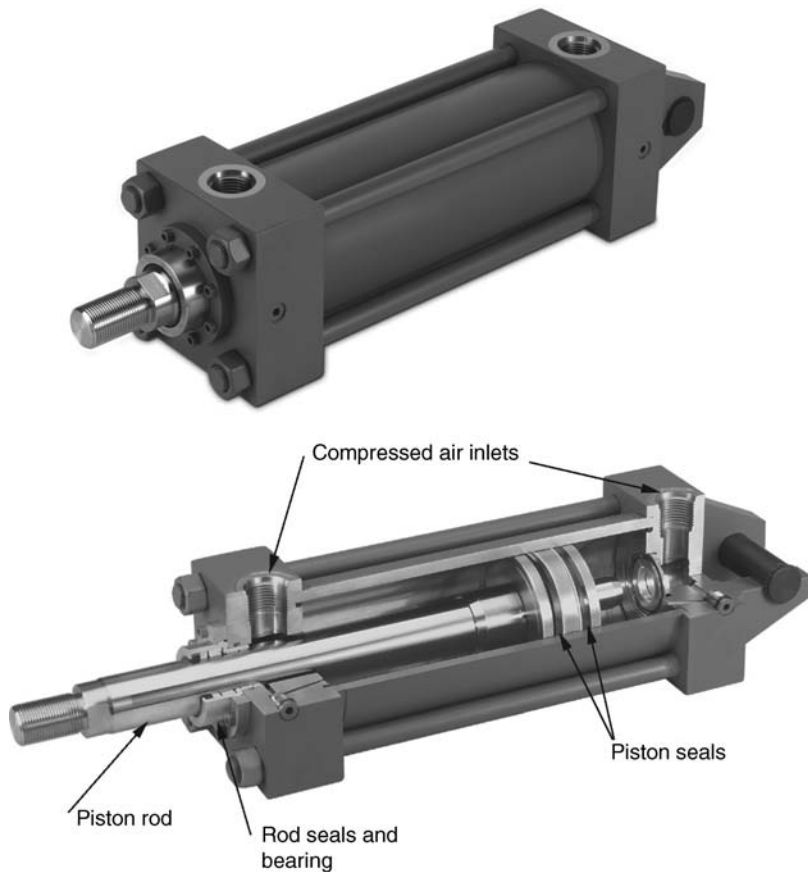


Figure 12.34 Construction of a pneumatic cylinder. (Courtesy of Parker Hannifin, Inc.)

Pneumatic Actuators

When compressed air is the energy source of choice, a pneumatic cylinder can create linear motion. In general, the purpose of a pneumatic cylinder is to provide linear motion between two fixed locations. Figure 12.34 shows a pneumatic cylinder and a cutaway of such a cylinder. By applying high-pressure compressed air to either side of the piston, linear actuation between two defined positions can easily be accomplished.

Solenoids

“Solenoid” is a term used to describe an electromagnetic device that is employed to create linear motion of a plunger, as shown in Figure 12.35. The initial force available from a solenoid can be determined from

$$F = \frac{1}{2} (NI)^2 \frac{\mu A}{\delta^2} \quad (12.21)$$

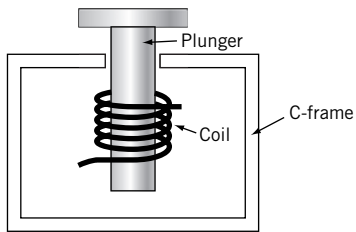


Figure 12.35 Construction of a solenoid linear actuator.

where

F = force on plunger

N = number of turns of wire in the electromagnetic

I = current

μ = magnetic permeability of air ($4\pi \times 10^{-7}$ H/m)

δ = size of the air gap

A = plunger cross-sectional area

When the electromagnet is actuated, the resulting magnetic force pulls the plunger into the C-frame. Because the air gap is largest when the electromagnet is actuated, the minimum force occurs at actuation and the force increases as the air gap decreases.

Rotary Actuators

Stepper Motors

There is a class of electric motors that has the primary purpose of providing power to a process. An example would be the electric motor that drives an elevator, an escalator, or a centrifugal blower. In these applications the electric motor serves as a prime mover, with clear and specific requirements for rotational speed, torque, and power. However, some applications have stringent requirements for positioning.

Rotary positioning presents a significant engineering challenge, but one that is so ubiquitous that it has been addressed through a variety of design strategies. One design strategy is to employ a free-rotating DC motor to supply the motive power and impose precise control on the resulting motion through gearing and some control scheme. DC motors that are subject to feedback control are generally described as servo-motors. While this may be appropriate and necessary for some applications, the stepper motor has found wide-ranging applications in precision rotary motion control, and is a better choice for many applications.

Stepper or stepping motors, as their name implies, are capable of moving a fraction of a rotation with a great degree of precision. This is accomplished by the design of a rotor that aligns with the magnetic field generated by energized coils. The step size can range from 90 degrees to as little as 0.5 degrees or less. Two common types of stepper motors are variable reluctance and unipolar designs. The design of a variable reluctance stepping motor is illustrated in Figure 12.36. Let's consider the operation of this motor. There are three sets of windings, labeled 1, 2, and 3 in the figure, and there are two sets of teeth on the rotor, labeled X and Y. With the windings labeled 1 energized, the rotor snaps to a position where one set of the teeth are aligned with the windings. This motion is a result of the magnetic field generated by the windings. Suppose that winding 1 is

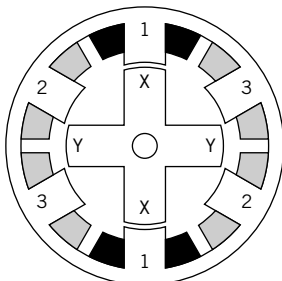


Figure 12.36 Variable reluctance stepper motor design.

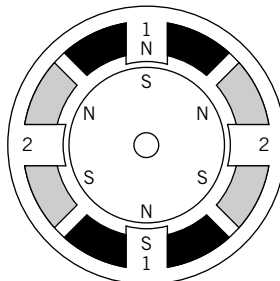


Figure 12.37 Variable reluctance stepper motor design having six poles and two windings.

de-energized and winding 2 is energized. The rotor will turn until the teeth marked Y are aligned with winding 2. This produces a 30-degree step.

A useful characteristic of stepper motors is holding torque. As long as one of the windings is energized, the rotor resists motion, until the torque produced by the winding to rotor interaction is overcome.

The motor shown in Figure 12.37 is a variable reluctance design. Unipolar motors incorporate permanent magnets as the rotor. Figure 12.37 shows a rotor having six magnetic poles and two sets of windings. The motor moves in 30-degree increments as the windings are alternately energized.

Flow-Control Valves

Valves are mechanical devices intended to allow, restrict, throttle, or meter fluid flow through pipes or conduits. Flow-control valves are used to regulate either the flow or the pressure of a fluid by their electronic actuation. They generally function by allowing flow while in their open position, stopping flow when closed, and metering flow or fluid pressure to a desired value with a position that is somewhere between these settings, which is called proportional control. These valves contain a valve positioning element that is driven by an actuator, such as a solenoid. Any valve type can be controlled. The common control valve design offers either a single chamber body containing a poppet with valve seat or a multichamber body containing a sliding spool with multiple poppets. Flow-control valves are used to transfer gases, liquids, and hydraulic fluids. The application ratings are as follows: general service, for working with common liquids and gases; cryogenic service, for fluids such as liquid oxygen; vacuum service, for low pressure applications; and oxygen service, for contamination-free flow of oxygen.

The control valve can respond to signals from any type of process variable transducer. The signal determines the position of the actuating solenoid. A specific characteristic of any control valve refers to whether its nonenergized operating state is open or closed. This is referred to as its “fail position.” The fail position of a control valve is determined by the nonenergized solenoid plunger position. This position is an important consideration for process safety.

These valves come in various configurations reflecting their number of ports. A two-way valve has two ports. Two-way position control takes on one of two values: open or closed. A two-way valve has two connections: supply port (P) and service port (A). Most common household valves fall

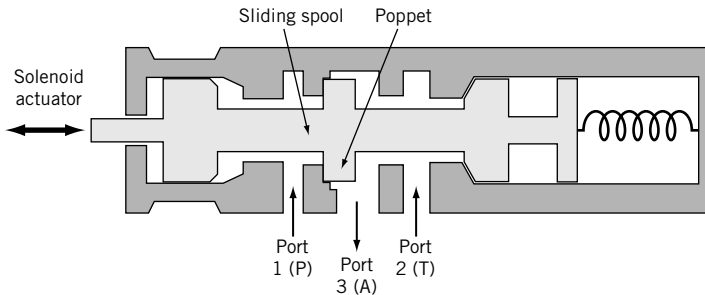


Figure 12.38 Three-way flow control valve (deactivated position shown).

into this category. A three-way valve has three port connections: supply (P), exhaust (T), and service (A). The service port may be switched between the supply and the exhaust. A four-way has four connections: supply (P), exhaust (T), and two service ports (A and B). The valve connects either P to A and B to T, or P to B and A to T. In general, an N -way valve has N -ports with N number of flow directions available. An example of a three-port sliding spool control valve is shown in Figure 12.38. The solenoid drives the spool, which contains two valve seats. In the fully activated position, port P is open to service port A. When the solenoid is deactivated, port T is open to service port A (shown). For example, in one application this valve can be used to pressurize a system (open the system to port P) for a period of time and then adjust the system pressure to another value (open the system to port A) for a period of time.

All valve ports offer some level of flow resistance, and this is specified through a flow coefficient, C_v . Flow resistance can be adjusted in design by varying the internal dimensions of the valve chamber and can be set operationally by varying the element position within the chamber. The flow coefficient is found based on the formulation detailed in Chapter 10 or simply as

$$Q = C_v \sqrt{\Delta p} \quad (12.22)$$

where Q is the steady flow rate through the valve and Δp is the corresponding pressure drop. This loss is also expressed in terms of a K -factor based on the average velocity through the ports,

$$\Delta p = K \rho \bar{U}^2 / 2 \quad (12.23)$$

Flow-control valves are classified in a number of ways: the type of control, the number of ports in the valve housing, the specific function of the valve, and the type of valve element used in the construction of the valve. Directional control valves allow or prevent the flow of fluid through designated ports. Flow can move in either direction. Check valves are a special class of directional valve that allow flow in only one direction. Proportional valves can be infinitely positioned to control the amount, pressure, and direction of fluid flow. In a proportional valve, the valve is opened by an amount proportional to the applied current. The valves are termed proportional because their output flow is not exactly linear in relation to the input signal. These valves provide a way to control pressure or flow rate with a high response rate.

In the simplest application, a solenoid is used to turn a valve either on or off. In a more demanding application, the solenoid is expected to cycle rapidly to open and close the valve. The

time between each signal cycle coupled with the internal flow loss character of the valve determines the average flow. Valve response time can be defined in several ways but all are consistent with the methods used in Chapter 3. The 90% response time, t_{90} , is the time required to either fill or exhaust a target device chamber through a valve port, in effect a step function response. There is a separate response time for filling or exhausting. Either way,

$$t_{90} = m + F\forall \quad (12.24)$$

where m is the valve lag time between when the signal is applied and steady flow is established at the designated port, F is the reciprocal of the average flow rate through the port, and \forall is the volume of the target device chamber. For example, a valve having an F of 0.54 ms/cc and a lag time of 20 ms requires $t_{90} = 155$ ms to fill a 250-cc chamber. Alternatively, the valve frequency response can be found by cycling the valve with a sine wave electrical signal and measuring the flow rate through the valve. The valve frequency bandwidth is thus established by its -3 dB point.

12.4 CONTROLS

Control of a process or system can be exerted in a wide variety of ways. Suppose our goal is to create a healthy lawn by appropriate watering. Each day we could monitor the weather forecast, take into account the probability of precipitation, and choose whether to water and for how long. We could choose to water all of the lawn or just those parts most subject to stress from heat and lack of moisture. If we choose to water, we could place the sprinklers and turn on the faucet (remembering to shut off the flow at an appropriate later time)!

All of the functions described above for lawn care are completely reasonable for a person to accomplish, and they represent the functioning of an intelligent controller. Suppose we wish to introduce some automation into the process.

At the simplest level, a timer-based control system could be implemented, as shown in Figure 12.39. The functioning of this system would be to open and close the faucet at predetermined times of the day. At the simplest level, this could be a mechanical timer that watered the lawn once each 24-hour period for a predetermined length of time. This type of control is called an *open loop control*. For this control

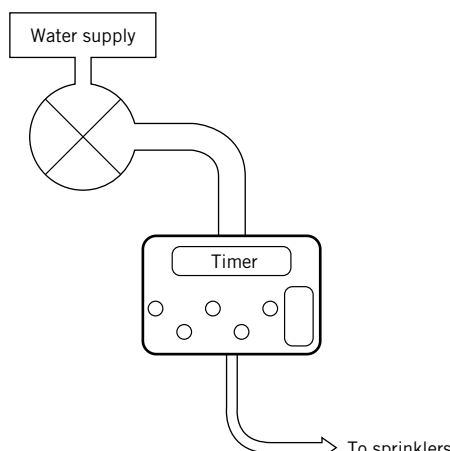
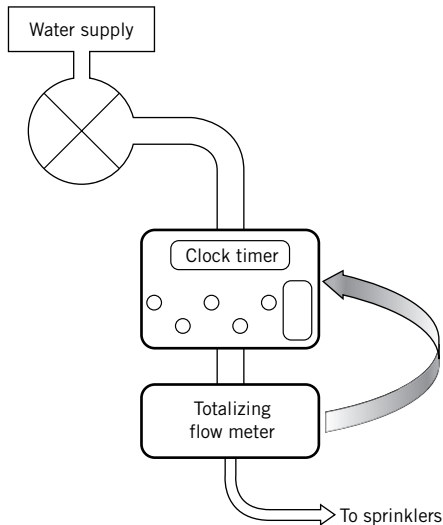


Figure 12.39 Open-loop control of a sprinkler system.

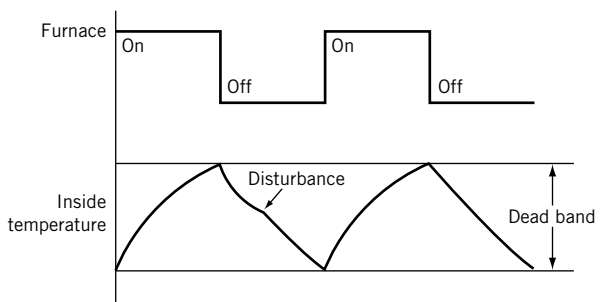
**Figure 12.40** Feedback control of a sprinkler system.

system there are no sensors to monitor the amount of water applied to the lawn; in fact, all that the control system is accomplishing is to open and, later, to close the faucet.

More advanced automatic control systems implement a *closed-loop control*. For the present example, it might be desired to apply 100 gallons (379 liters) of water to the lawn. A flow meter that sensed the total water flow that had occurred could be used to provide feedback to the control system to allow the faucet to be closed when the flow totaled 100 gallons. Such flow meters are common and serve as water meters. The term *closed-loop* or *feedback control* simply means that the variable that is to be controlled is being measured, and that the control system in some way uses this measurement to exert the control.

Figure 12.40 illustrates a control system designed to apply 100 gallons of water to the lawn. There are two inputs to the controller: the time of day and the output of the totalizing flow meter. At the appropriate time of day, the controller opens the valve. The totalizing flow meter output is used by the controller to close the valve after the total flow reaches 100 gallons. This type of binary control scheme is termed *on-off control*. The valve controlling the water flow is either fully open or fully closed.

Probably the most familiar form of a binary on-off control system is the thermostat for a home furnace or air conditioner. Figure 12.41 shows the status of a home furnace and a time trace of the inside temperature during a winter day. A schematic representation of this control system is shown

**Figure 12.41** Operation of on-off controller with a dead band.

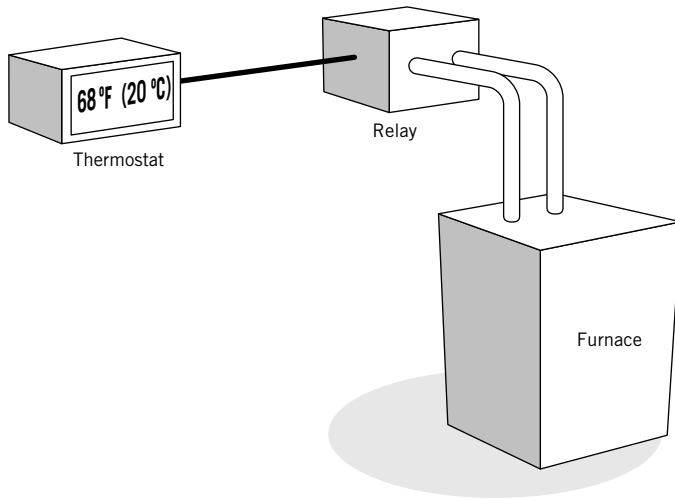


Figure 12.42 Components of a thermostatic control for a home furnace.

in Figure 12.42. A key element here is that there is the possibility of a *disturbance* that would influence the rate of change of the inside temperature. Suppose a delivery arrives and the door remains open for a period of time. The thermostat must then respond to this disturbance and attempt to maintain the inside temperature at the set point.

Essentially all practical implementations of on-off control systems require a dead band that creates a hysteresis loop in the control action. This is illustrated in Figure 12.43. The dead band is centered around zero error, and the action of the controller depends on the magnitude of the error. Here the error is defined as

$$e = T_{\text{setpoint}} - T_{\text{room}}$$

Recall that we are considering a furnace thermostat under winter conditions. As the room temperature falls relative to the set point, the error becomes a larger positive number. When the error reaches the value corresponding to “Furnace ON” in Figure 12.43, the furnace begins to add heat to the conditioned space. Room temperature begins to rise and the error decreases towards zero. The furnace remains on until the room temperature reaches a predetermined value that is greater than the set point. Here the error is negative. At this temperature, the furnace is turned off and room temperature begins once again to decrease. Because of the dead band in the controller, no further control action occurs until the error reaches the “Furnace ON” error magnitude.

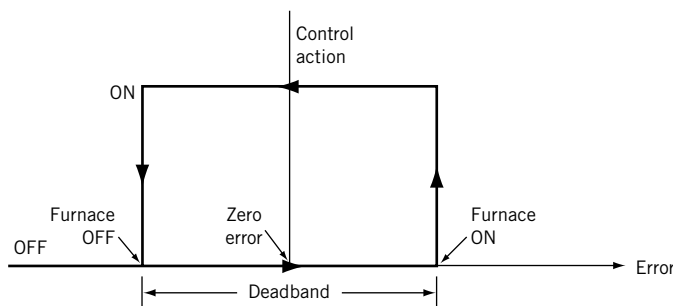


Figure 12.43 Control action and hysteresis loop of a binary on-off controller with a dead band.

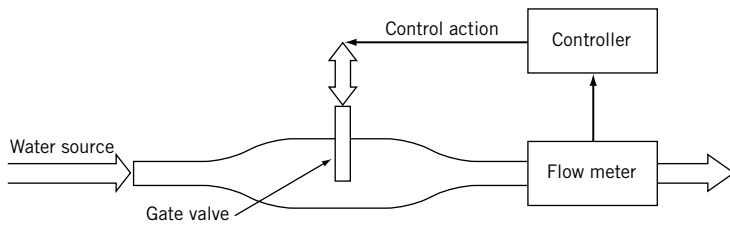


Figure 12.44 Flow rate control system.

Many control systems are designed to maintain a specified set point without a dead band; clearly this is not possible using on–off control. Consider again watering a lawn. Suppose that due to varying water pressure the lawn was being watered nonuniformly. We might choose to control both the water flow rate and the total water flow applied to the lawn. A scheme for accomplishing this is shown in Figure 12.44. The key components of the control system are a flow meter, the controller, and an actuator that can control the position of a gate valve. Here a desired flow rate is set, say, to 2 gallons per minute. The task of the controller is to vary the position of the gate valve in order to maintain the flow rate at the set point.

Dynamic Response

As another example of closed-loop control, consider the cruise-control system on an automobile. Once a desired speed is set, the system varies the throttle position to ensure that the set point is maintained. Another issue in the analysis and design of control systems lies in the dynamic response of the physical process, the controller, and the actuators. An automobile does not respond instantaneously to changes in the throttle position and time is required for a stepper motor to change the position of a valve. The complexities of the combined responses of the physical and control systems, especially in the presence of disturbances, are the subject of the remainder of this section.

Laplace Transforms

In Chapter 3, we used Laplace transforms to model the response of simple systems. Now let us apply Laplace transforms to understand how control systems function. The fundamental basis of the application of Laplace transforms to control systems is the solution of a mathematically well-posed initial value problem.

Consider an initial-value problem (here time is the independent variable) that is described by an ordinary differential equation. If we apply the Laplace transform to a differential equation, we convert the differential equation to an algebraic equation. For partial differential equations in time and one spatial variable, the Laplace transform converts the partial differential equation into an ordinary differential equation in the space variable. Appendix C reviews the application of Laplace transforms and provides a table of Laplace transform pairs.

We illustrate the application of the Laplace transform through solution of first-order and second-order differential equations, which are important for control systems.

Example 12.3

Consider the response of a first-order system to a unit step input forcing function, which we have previously modeled by Equation 3.4. The governing equation is

$$\tau \dot{y} + y = U_s(t) \quad (12.25)$$

Applying the Laplace transform (Table C.1 can be used as a reference) yields

$$\tau s Y(s) - y(0) + Y(s) = \frac{1}{s} \quad (12.26)$$

where we have employed the property of the Laplace transform that

$$\mathcal{L}\left[\tau \frac{dy(t)}{dt}\right] = \tau \mathcal{L}\left[\frac{dy(t)}{dt}\right]$$

The process of solving the differential equation involves the following steps:

1. Apply the Laplace transform to the governing differential equation, in this case Equation 12.25.
2. Solve the resulting equation for $Y(s)$, Equation 12.26.
3. Employ the table of Laplace transform pairs, (e.g., Table C.1), to determine $y(t)$.

We assume that $y(0) = 0$. Solving Equation 12.26 for $Y(s)$ yields

$$Y(s) = \frac{1}{s(\tau s + 1)} \quad (12.27)$$

An important tool for the inversion of Laplace transforms is partial fractions. To accomplish the inversion of Equation 12.27, we start from the assumption

$$\frac{1}{s(\tau s + 1)} = \frac{A}{s} + \frac{B}{(\tau s + 1)} \quad (12.28)$$

Next we find a common denominator for the right-hand side of Equation 12.28:

$$\frac{1}{s(\tau s + 1)} = \frac{A(\tau s + 1)}{s(\tau s + 1)} + \frac{Bs}{s(\tau s + 1)}$$

In this form we see that

$$1 = A(\tau s + 1) + Bs$$

Equating powers of s yields

$$\begin{aligned} 1 &= A \\ 0 &= A\tau + B \Rightarrow B = -\tau \end{aligned}$$

We can now express $Y(s)$ as

$$Y(s) = \frac{1}{s} + \frac{-\tau}{(\tau s + 1)} = \frac{1}{s} + \frac{-1}{(s + 1/\tau)} \quad (12.29)$$

We find that (e.g., from transform pairs 1 and 5 in Table C.1)

$$y(t) = 1 - e^{-t/\tau} \quad (12.30)$$

With the appropriate initial condition and steady-state output value, this can be written as Equation 3.6:

$$\Gamma(t) = \frac{y(t) - y_\infty}{y_0 - y_\infty} = e^{-t/\tau}$$

where τ is the time constant for a first-order system and $\Gamma(t)$ is the error fraction

Example 12.4

Employing Laplace transforms, determine the solution of the second-order, ordinary linear differential equation,

$$y'' + 4y' - 5y = 0 \quad (12.31)$$

with the initial conditions

$$\begin{aligned} y(0) &= -1 \\ y'(0) &= 4 \end{aligned}$$

SOLUTION We recall that

$$\mathcal{L}[y^{(n)}] = s^n \mathcal{L}[y] - s^{n-1}y(0) - s^{n-2}y'(0) - \dots - y^{(n-1)}(0)$$

If we apply this relationship to Equation 12.31, we find that the Laplace transform is

$$s^2Y(s) - sy(0) - y'(0) + 4[sY(s) - y(0)] - 5Y(s) = 0$$

Substituting the initial conditions yields

$$s^2Y(s) - s - 4 + 4[sY(s) + 1] - 5Y(s) = 0$$

Solving for $Y(s)$ yields

$$Y(s) = \frac{-s}{s^2 + 4s - 5} \quad (12.32)$$

Now we are faced with the task of determining the inverse Laplace transform of this expression. Factoring the denominator yields

$$Y(s) = \frac{-s}{(s+5)(s-1)} \quad (12.33)$$

Applying partial fractions allows Equation 12.33 to be expressed

$$\frac{-s}{(s+5)(s-1)} = \frac{-5/6}{s+5} + \frac{-1/6}{s-1} \quad (12.34)$$

Finding the inverse Laplace transform (e.g., from Table C.1) provides the solution for Equation 12.34 as

$$y(t) = -\frac{5}{6}e^{-5t} - \frac{1}{6}e^t \quad (12.35)$$

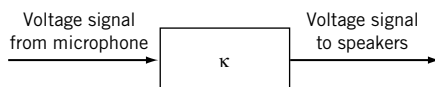


Figure 12.45 Single-input, single-output amplifier block.

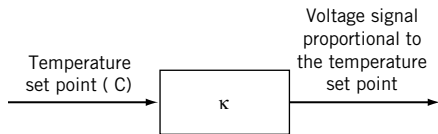


Figure 12.46 Temperature-input, voltage-output amplifier block.

Block Diagrams

A very useful representation of feedback control systems is accomplished using block diagrams. We first describe the basic elements of a block diagram.

Operational Blocks

An operational block performs a defined operation on a signal. Consider a public-address system consisting of a microphone, an amplifier, and speakers. Figure 12.45 provides a single-input, single-output block representing the amplifier. An ideal amplifier would follow exactly the waveform of the input signal from the microphone, and simply multiply the voltage signal by a constant value, κ . This constant value represents a *gain* and so it is called a gain block.

In Figure 12.46 a gain block is shown that supplies a reference voltage signal based on a temperature set point. In most practical applications, signals are transmitted in control systems as voltage or current. The gain represented in Figure 12.46 would have units of volts/ $^{\circ}\text{C}$. We note that a pure linear gain is equivalent to the static sensitivity of a zero-order system.

An important type of block used to represent a control system is a comparator. Figure 12.47 illustrates the operation of a comparator. Two voltage signals are either added or subtracted by the comparator. Figure 12.47 uses a furnace thermostat as an example. The signals represent the desired temperature set point and the measured temperature, in terms of voltages. The difference in these two values represents the error in the temperature value, the difference between the measured and set-point values.

We can now construct a block diagram of the thermostat for the home furnace described in Figures 12.41 and 12.42. Figure 12.48 shows the block diagram of the controller, the furnace, and the house. Together the furnace and the house are usually referred to as the plant or the process.

The detailed design of a control system requires that we consider the time-dependent behavior of both the controller and the process. We propose a process and derive the governing equation for the process. Then a controller is implemented and the dynamic response of the system to a

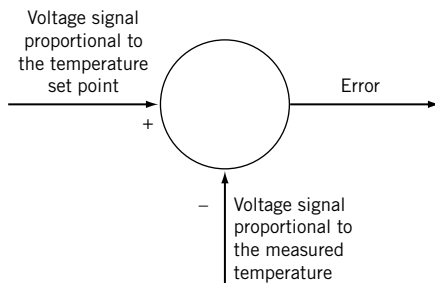


Figure 12.47 Comparator.

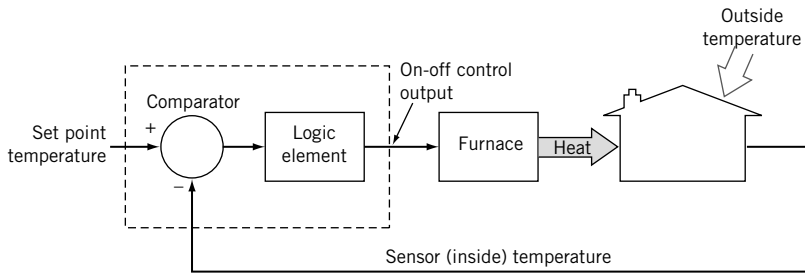


Figure 12.48 Block diagram representation of a furnace thermostat.

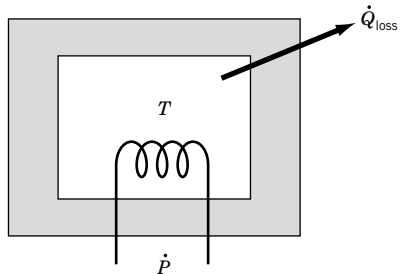


Figure 12.49 Energy flows for an oven.

step-change in the set point is derived. A key point in this model is the use of a stationary operating set point.

Model for Oven Control

Plant Model

The system we wish to control is illustrated in Figure 12.49. An oven is maintained at a temperature above the ambient temperature by power input \dot{P} from an electric heater. The controller is implemented to maintain a desired oven temperature.

A first law analysis of the oven at steady-state conditions yields

$$\dot{P} = \dot{Q}_{\text{loss}}$$

The energy loss from the oven \dot{Q}_{loss} may be expressed in terms of the oven temperature, T , the ambient temperature, T_{∞} , the surface area, A_s , and an overall loss coefficient, U , as

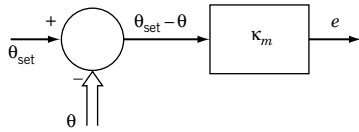
$$\dot{Q}_{\text{loss}} = UA_s(T - T_{\infty}) \quad (12.36)$$

Consider a steady-state operating point for the oven, designated by the subscript “o.” At steady state the power supplied by the heater is exactly balanced by the energy lost to the ambient,

$$\dot{P}_o = UA_s(T_o - T_{\infty}) \quad (12.37)$$

To aid in the mathematical analysis, we define a new temperature variable as

$$\theta = T - T_{\infty} \quad (12.38)$$

**Figure 12.50** Proportional Control.

so that Equation 12.37 can be expressed as

$$\dot{P}_o = UA_s \theta_o \quad (12.39)$$

The first law for the oven for a transient condition, one where the power input is changed, is

$$\dot{P} - UA_s \theta = mc \frac{d\theta}{dt} \quad (12.40)$$

where m is the mass of the oven and c is the average specific heat. This product represents the total heat capacity of the oven. Equation 12.40 now provides the governing equation for the plant in this example.

Controller Model

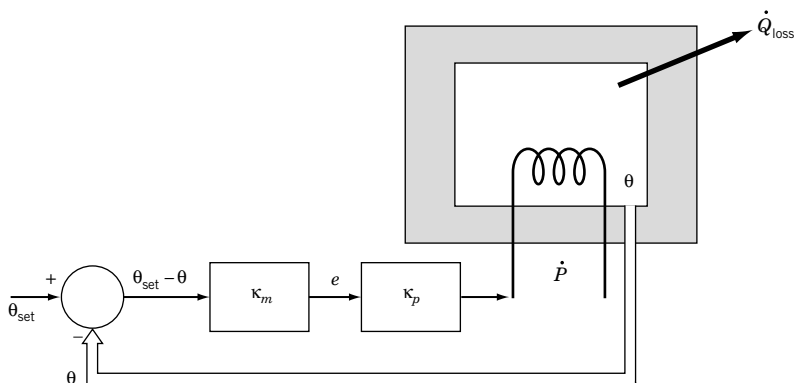
We now wish to implement a controller. The first controller we implement is termed a proportional controller and is illustrated in Figure 12.50. The error between the set point temperature and the actual temperature of the oven is multiplied by a constant value to determine the power input to the heater. A block diagram of the controller and plant combined system is shown in Figure 12.51; two proportional gains are shown in this figure to emphasize that the error signal will most likely be a voltage.

The governing equation for the temperature of the oven may be expressed

$$\frac{mc}{[UA_s + \kappa_p \kappa_m]} \frac{d\theta}{dt} + \theta = \frac{\kappa_p \kappa_m}{[UA_s + \kappa_p \kappa_m]} \theta_{set} \quad (12.41)$$

By comparison with Equation 3.4,

$$\tau \dot{y} + y = KF(t)$$

**Figure 12.51** Proportional Control of an oven.

it is clear that this represents the response of a first-order system having a time constant of

$$\tau = \frac{mc}{[UA_s + \kappa_p \kappa_m]} \quad (12.42)$$

The analysis for this step change is best accomplished by using Laplace transforms.

Laplace Transform Analysis

Taking the Laplace transform of Equation 12.41 yields

$$\frac{mc}{[UA_s + \kappa_p \kappa_m]} s \Theta(s) + \Theta(s) = \frac{\kappa_p \kappa_m \Theta_{set}(s)}{[UA_s + \kappa_p \kappa_m]} \quad (12.43)$$

which is of the form

$$(\tau s + 1)\Theta(s) = KF(s)$$

Solving Equation 12.43 for the ratio $\Theta(s)/\Theta_{set}(s)$ yields

$$\frac{\Theta(s)}{\Theta_{set}(s)} = \frac{\frac{\kappa_p \kappa_m}{[UA_s + \kappa_p \kappa_m]}}{\left[\frac{mc}{[UA_s + \kappa_p \kappa_m]} s + 1 \right]} = KG(s) \quad (12.44)$$

For convenience, define

$$\begin{aligned} C_1 &= \frac{mc}{UA_s + \kappa_p \kappa_m} \\ C_2 &= \frac{\kappa_p \kappa_m}{UA_s + \kappa_p \kappa_m} \end{aligned} \quad (12.45)$$

With these definitions, Equation 12.44 becomes

$$\frac{\Theta(s)}{\Theta_{set}(s)} = \frac{C_2}{[C_1 s + 1]} = G(s) \quad (12.46)$$

Equation 12.46 represents the transfer function, $G(s)$, for the system consisting of the oven and the proportional controller. For the linear system consisting of the oven and controller, the transfer function represents the ratio of the Laplace transforms of the output to the input assuming a zero initial condition.

Step Response

Suppose we consider the startup of the furnace, with an initial temperature equal to the ambient, or $\theta = 0$. From this condition we impose a value of θ_{set} that is larger than the ambient temperature, say θ_1 ; this represents a step-change input that is expressed in Laplace transform space as

$$\Theta_{set}(s) = \frac{\theta_1}{s} \quad (12.47)$$

The transform of the governing differential equation becomes

$$\Theta(s) = \frac{\theta_1 C_2}{s[C_1 s + 1]} \quad (12.48)$$

Employing partial fractions yields

$$\Theta(s) = \theta_1 C_2 \left[\frac{1}{s} - \frac{1}{s + 1/C_1} \right] \quad (12.49)$$

From Table C.1 we can determine the time-domain solution corresponding to this Laplace transform as

$$\theta(t) = \theta_1 C_2 \left[1 - e^{-t/C_1} \right] \quad (12.50)$$

Recall that we have assumed $\theta(0) = 0$. In the limit as $t \rightarrow \infty$

$$\theta(t) = \theta_1 C_2 = \frac{\kappa_p \kappa_m \theta_1}{U A_s + \kappa_p \kappa_m}$$

For a step change input, we have found that $\theta(t) \neq \theta_1$ unless $\frac{\kappa_p \kappa_m}{U A_s + \kappa_p \kappa_m} = 1$. This will not in general be the case. Thus we find that a proportional controller, in general, is characterized by a nonzero steady-state error.

Example 12.5

Consider the proportional control of an oven that has a total mass of 20 kg, with an average specific heat of 800 J/kg-K. The oven is initially at room temperature. A step input is supplied to the controller, changing the set-point temperature to 100°C above the ambient. Plot the temperature of the oven and the power supplied to the oven as a function of time, and determine the steady-state error if the values of the gains in the system are $\kappa_m = 20$ and $\kappa_p = 12$.

SOLUTION Equation 12.50 provides the solution for oven temperature as a function of time, for the case where there is a step change in the set-point temperature. By examining Figure 12.51, we see that our controller provides a power to the oven given by

$$\kappa_p \kappa_m (\theta_1 - \theta)$$

The temperature response and the supplied power are provided in Figure 12.52.

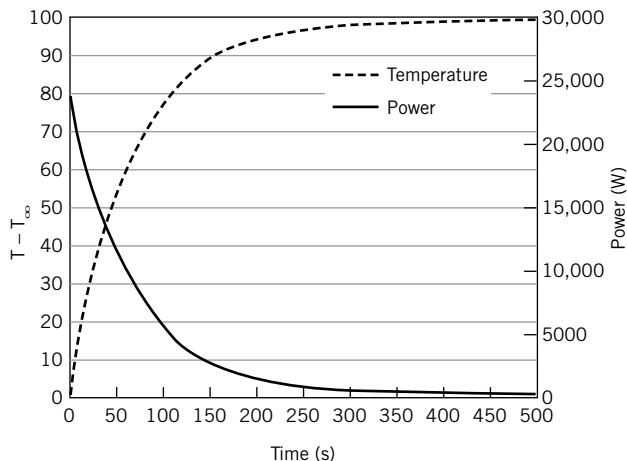
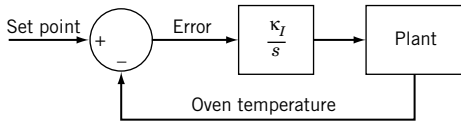


Figure 12.52 Response of oven-controller system.

**Figure 12.53** Block diagram for an integral controller.

COMMENT The values of the gains in this problem are directly tied to the power required for the oven. The physical arrangement of heaters and the required electrical service are a strong consideration in a practical implementation of this conceptual design. The effect of the controller gains and the system parameters can be further explored using the program file *First Order PID.vi*.

Proportional-Integral (PI) Control

The steady-state error that exists for a proportional controller is not acceptable in many applications. Adding a control signal that is proportional to the time integral of the error improves the performance of the proportional controller. Let's first examine the behavior of a pure integral controller.

Integral Control

Figure 12.53 provides a block diagram in the Laplace transform domain for an integral controller applied to control the temperature of our oven. In the time domain, this results in

$$\dot{P}(t) = \kappa_I \int_0^t e(t) dt + \dot{P}(0) \quad (12.51)$$

We immediately see that as long as the error remains finite and positive, the power will continue to increase. Clearly a pure integral controller would have very limited application.

Proportional-Integral (PI) Control

Suppose the actions of the proportional and integral controllers are combined, as shown in Figure 12.54. In Laplace transform space this may be expressed

$$P(s) = \kappa_p \kappa_m E(s) + \frac{\kappa_I \kappa_m}{s} E(s) = \left[\kappa_p \kappa_m + \frac{\kappa_I \kappa_m}{s} \right] E(s) \quad (12.52)$$

Expressed in terms of the set point, the closed loop transfer function is

$$\frac{\Theta(s)}{\Theta_{set}(s)} = \frac{\kappa_m \left(\kappa_p + \frac{\kappa_I}{s} \right) \left(\frac{C_2}{C_1 s + 1} \right)}{1 + \kappa_m \left(\kappa_p + \frac{\kappa_I}{s} \right) \left(\frac{C_2}{C_1 s + 1} \right)} \quad (12.53)$$

Clearing fractions yields a form of the transfer function that allows the inverse transform to be determined,

$$\frac{\Theta(s)}{\Theta_{set}(s)} = \frac{\kappa_m (\kappa_p s + \kappa_I) C_2}{C_1 s^2 + s (1 + C_2 \kappa_m \kappa_p) + C_2 \kappa_m \kappa_I} \quad (12.54)$$

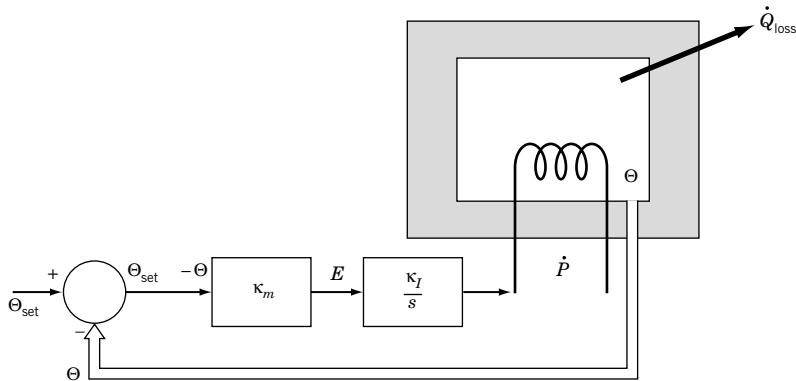


Figure 12.54 Block diagram for PI control of an oven.

Once again we impose a step change in the set-point temperature so that $\Theta_{set}(s) = \frac{\theta_1}{s}$, and

$$\Theta(s) = \frac{\theta_1 [\kappa_m(\kappa_p s + \kappa_I) C_2]}{s [C_1 s^2 + s(1 + C_2 \kappa_m \kappa_p) + C_2 \kappa_m \kappa_I]} \quad (12.55)$$

Employing the final value theorem, we multiply by s and take the limit as $s \rightarrow 0$

$$\lim_{s \rightarrow 0} \Theta(s) = \lim_{s \rightarrow 0} \frac{s [\kappa_m(\kappa_p s + \kappa_I) C_2] \theta_1}{s [C_1 s^2 + s(1 + C_2 \kappa_m \kappa_p) + C_2 \kappa_m \kappa_I]} = \frac{C_2 \kappa_m \kappa_I}{C_2 \kappa_m \kappa_I} \theta_1 = \theta_1 \quad (12.56)$$

Clearly, the steady-state error for this PI controller is zero. This is a general result for PI control.

Time Response

The time response of this system to a step-change input could be determined by finding the inverse Laplace transform of Equation 12.57:

$$\frac{\Theta(s)}{\Theta_{set}(s)} = \frac{\kappa_m(\kappa_p s + \kappa_I) C_2}{C_1 s^2 + s(1 + C_2 \kappa_m \kappa_p) + C_2 \kappa_m \kappa_I} \quad (12.57)$$

However, by comparison with the Laplace transform of the governing differential equation for a second-order system, as provided in Equation 3.13, Palm (7) shows that

$$\varsigma = \frac{1 + C_2 \kappa_m \kappa_p}{2\sqrt{C_1 C_2 \kappa_m \kappa_I}} \quad (12.58)$$

and that for $\varsigma < 1$ the equivalent time constant is

$$\tau = \frac{2C_1}{1 + C_2 \kappa_m \kappa_p} \quad (12.59)$$

The behavior of the oven-controller system can be further explored using the program file *First Order PID.vi*.

Proportional Integral-Derivative Control of a Second-Order System

Consider a spring-mass-damper system such as the one described in Figure 3.3. The governing equation describing the position of the mass as a function of time for a given forcing function $f(t)$ is

$$\frac{1}{\omega_n^2} \frac{d^2y}{dt^2} + \frac{2\xi}{\omega_n} \frac{dy}{dt} + y = f(t) \quad (12.60)$$

This system and the governing equation serve as a model to demonstrate the properties of proportional integral-derivative (PID) control when applied to a second-order system.

The goal is to apply a step change in input to the system, and have the mass move to the new equilibrium position; in other words, the ideal response of the system would be a step-change. Our first objective is to review the response of the second-order system without a controller in place. The behavior of the system is examined in two examples.

Example 12.6

A spring-mass-damper system has mass of 2 kg, a spring constant of 7900 N/m, and a damping coefficient of 176 kg/s. Plot the open loop time response of this system to a step-change input in force.

ASSUMPTIONS The initial conditions for velocity, $\frac{dy}{dt}$, and position, y , are zero.

SOLUTION Although, the solution to this example could be determined from the results in Chapter 3, we will determine the response using Laplace transforms. Taking the Laplace transform of Equation 12.60 yields

$$\frac{1}{\omega_n^2} s^2 Y(s) + \frac{2\xi}{\omega_n} s Y(s) + Y(s) = KF(s) \quad (12.61)$$

For the mass, spring constant, and damping ratio given in the problem statement, we compute the natural frequency and damping ratio as

$$\omega_n = \sqrt{\frac{k}{m}} = \sqrt{\frac{7900}{2}} = 62.85 \text{ rad/s} \quad \text{and} \quad \xi = \frac{c}{2\sqrt{km}} = \frac{176}{2\sqrt{7900 \times 2}} = 0.7$$

The open-loop transfer function defines the dynamic response of the system, and is defined as

$$\frac{Y(s)}{KF(s)} = \left[\frac{1}{\frac{1}{\omega_n^2} s^2 + \frac{2\xi}{\omega_n} s + 1} \right] = \left[\frac{1}{\frac{1}{3950} s^2 + 0.02235s + 1} \right] \quad (12.62)$$

where K is one for the present case. Options exist for calculating and plotting the open-loop response of this system. The program file *Second order PID.vi* can be used. Figure 12.55 shows the response of this system to a step input; the output has been normalized so that the displacement, as characterized by the amplitude, is from 0 to 1.

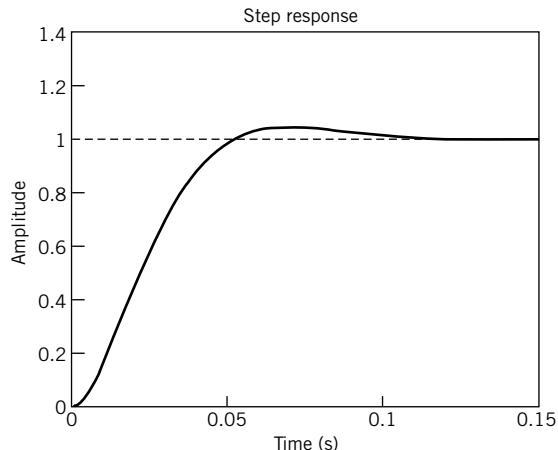


Figure 12.55 Second-order system response to a step-change input with a damping ratio of 0.7. Other parameters are described in Example 12.6.

Example 12.7

Consider the second-order system described in Example 12.6. Plot the open loop response of the system to a step-change in input for damping ratios of 0.3 and 1.3.

SOLUTION Figures 12.56 and 12.57 show the response of the system to a step-change input for values of the damping coefficient of 0.3 and 1.3, respectively. By comparing Figures 12.55 through 12.57, we can learn some important characteristics of second-order systems. Suppose our goal is to have the system respond quickly to the input, but without oscillation and without exceeding the equilibrium value excessively. Let's characterize the response of the system having a damping ratio of 1.3 as being comparatively slow. This system requires 0.2 s to approach the equilibrium value of 1. The system having a damping coefficient of 0.3 first reaches 1 in a time less than 0.05 s, but there is both overshoot and oscillations. The system having a damping ratio of 0.7 has no oscillations, and minimal overshoot. The system with $\zeta = 0.3$ has a shorter rise time but longer settling time than with $\zeta = 0.7$.

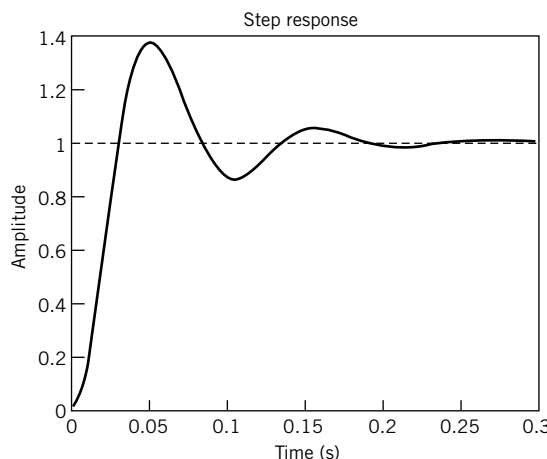


Figure 12.56 Second-order system response to a step-change input with a damping ratio of 0.3. Other parameters are described in Example 12.7.

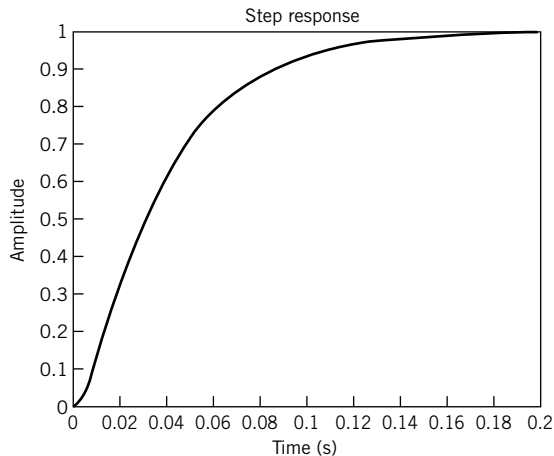


Figure 12.57 Second-order system response to a step-change input with a damping ratio of 1.3. Other parameters are described in Example 12.7.

In the previous example, the response for a damping ratio of 0.7 appears to be the most likely candidate to meet our needs. But can we improve the situation by implementing a controller?

Proportional Control

Consider the application of a proportional controller to the second-order system described in Example 12.7 for the case where the damping coefficient is 0.3. The block diagram for the control system is shown in Figure 12.58.

The transfer function for this system when the damping ratio is 0.3 is

$$\frac{Y(s)}{KF(s)} = \left[\frac{\kappa_p}{\frac{1}{\omega_n^2} s^2 + \frac{2\zeta}{\omega_n} s + 1} \right] = \left[\frac{\kappa_p}{\frac{1}{3950} s^2 + 0.02235s + 1} \right] \quad (12.63)$$

We implement a proportional controller having a proportional gain of 10, and examine the step response of the system. Figure 12.59 shows the resulting response of the system. Clearly, we have not eliminated the overshoot and oscillations in this system. On the other hand, if we implement the same controller for the system having a damping ratio of 1.3, the response is shown in Figure 12.60. Here the proportional controller is helpful for the performance of the system. Let's explore whether a more sophisticated control scheme improves the response of the system having a damping ratio of 0.3.

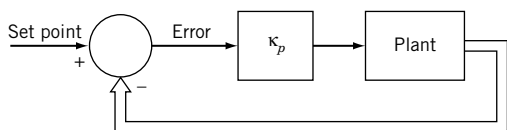


Figure 12.58 Block diagram for proportional control of a second-order plant.

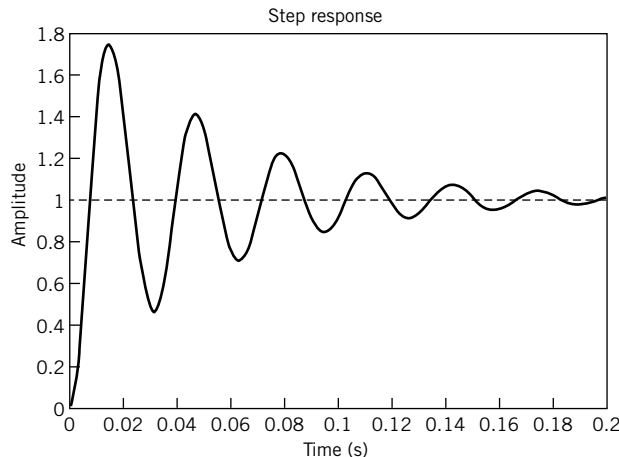


Figure 12.59 Response of a second-order system with a proportional controller having a gain of 10. The system has a damping ratio of 0.3 and the other parameters as described in Example 12.6.

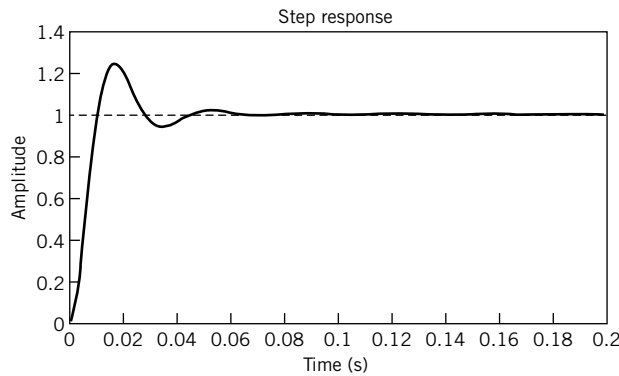


Figure 12.60 Proportional control of second-order system with a controller gain of 10, with damping 1.3.

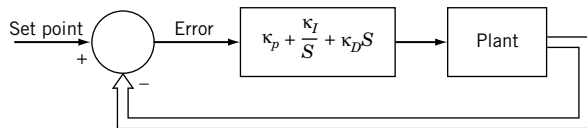


Figure 12.61 Block diagram for proportional integral-derivative (PID) control of a second-order system.

Proportional Integral-Derivative Control

A block diagram representing a PID control for our spring-mass-damper system is shown in Figure 12.61. The transfer function for this system is

$$\frac{Y(s)}{Kf(s)} = \left[\frac{\kappa_D s^2 + \kappa_p s + \kappa_I}{\frac{1}{\omega_n^2} s^3 + \left(\frac{2\zeta}{\omega_n} + \kappa_D \right) s^2 + \kappa_p s + \kappa_I} \right] \quad (12.64)$$

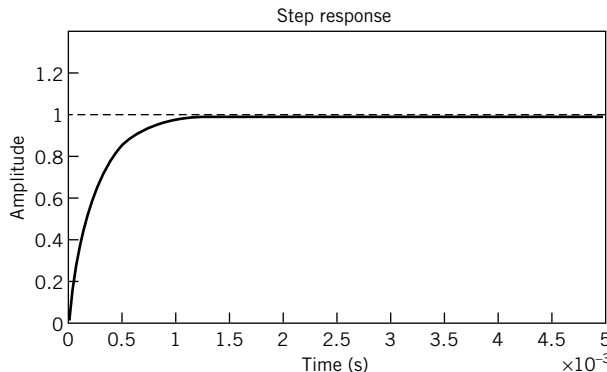


Figure 12.62 Response of a second-order system having a damping ratio of 0.3 when subject to PID control.

Table 12.4 Effect of Increasing Gain on Rise Time, Overshoot, and Steady-State Error for a PID Controller

Control Action	Rise Time	Overshoot	Steady-State Error
Proportional	↓	↑	↓
Integral	↓	↑	Eliminate
Derivative	↓	↓	

Recall that taking a derivative in time space is multiplying by s in Laplace transform space, and integrating in time space is dividing by s in Laplace transform space. The choice of gains for the control actions, κ_p , κ_I , and κ_D , is a challenging task and one for which much theory has been established (7). However, for our purposes we only wish to demonstrate the possible improvement in the system performance.

We select gains for the controllers of unity and just test the performance. For our second-order system having a damping ratio of 0.3, the result is shown in Figure 12.62. We compare this figure with Figures 12.55 and 12.57 and clearly see that this control scheme has improved the performance of the system. The system behavior with a variety of parameters and control gains can be explored using the program file *Second order PID.vi*. Although there are interactions among the proportional, integral, and derivative actions in a PID controller, the basic trends with increasing gain are provided in Table 12.4

12.5 SUMMARY

The integration of mechanical and electrical systems with advanced electronics is increasingly required for the design of systems as complex as an aircraft or as simple as a coffee maker that grinds beans and makes coffee at a set time each morning. Mechatronic systems require sensors, actuators, and control schemes to function as an integrated system. This chapter presented the operating principles and designs of those sensors used most often for linear and rotary displacement in mechatronic systems. “Actuators” is a term that represents a broad range of mechanical, electrical, pneumatic, and hydraulic devices designed to create motion. Selection of an actuator should be done through a system integration approach, so that the sensors and control scheme are appropriate for the actuator chosen.

We have provided an introduction to block-diagram representation of dynamic systems based on Laplace transforms, and have provided a review of the application of Laplace transforms to the solution of ordinary, linear differential equations. A discussion of open- and closed-loop control methods provided examples of proportional, proportional-integral, and proportional-integral-derivative control.

NOMENCLATURE

a	acceleration ($l t^{-2}$)	D_c	coil diameter for magnetic pickup (l)
c	damping coefficient ($m t^{-1}$)	E_i	input voltage (V)
c_c	critical damping coefficient ($m t^{-1}$)	E_o	output voltage (V)
g	acceleration of gravity ($l t^{-2}$)	F	force, vector ($m l t^{-2}$)
k	spring constant ($m t^{-2}$)	J	polar moment of inertia (l^4)
m	mass (m)	L	length (l)
p	pressure ($m l^{-1} t^{-2}$)	M	magnitude ratio
r	radius, vector (l)	M	moment, vector ($m l^2 t^{-2}$)
t	time (t)	P	power ($m l^2 t$)
δt	time interval for data sampling (t)	Q	volumetric flow rate ($l^3 t^{-1}$)
u	uncertainty	R_o	outer radius (l)
v	linear velocity ($l t^{-1}$)	T	temperature ($^\circ$)
y	displacement (l)	T	torque ($m l^2 t^{-2}$)
y_{hs}	displacement of housing, seismic instrument (l)	\forall	volume (l^3)
y_m	displacement of seismic mass (l)	ζ	damping ratio
y_r	relative displacement between seismic mass and housing in a seismic instrument (l)	τ	time constant (t)
δy	deflection (l)	τ_{\max}	maximum shearing stress ($m t^2 l^{-1}$)
A	amplitude	ϕ	phase angle
B	magnetic field strength ($m C^{-1} t^{-1}$)	κ	controller gain
C_v	discharge coefficient	ω	rotational speed (t^{-1})
		ω_n	natural frequency (t^{-1})

REFERENCES

1. Coltman, J. W., The transformer, *Scientific American*, 86, January 1988.
2. Herceg, E. E., *Schaevitz Handbook of Measurement and Control*, Schaevitz Engineering, Pennsauken, NJ, 1976.
3. Bredin, H., Measuring shock and vibration, *Mechanical Engineering*, February: 30, 1983.
4. Measurement of Rotary Speed, ASME Performance Test Codes, ANSI/ASME PTC 19.13-1961, American Society of Mechanical Engineers, New York, 1961.
5. Gindy, S. S., Force and torque measurement, a technology overview, *Experimental Techniques*, 9: 28, 1985.
6. *Measurement of Shaft Power*, ASME Performance Test Codes, ASME PTC 19.7-1980, (Reaffirmed Date: 1988), American Society of Mechanical Engineers, New York, 1980.
7. Palm, William J., *Modeling Analysis and Control of Dynamic Systems*, 2nd ed., John Wiley and Sons, New York, 1999.

PROBLEMS

- 12.1** Consider a linear potentiometer as shown in Figure 12.1. The potentiometer consists of 0.1-mm copper wire ($\rho_e = 1.7 \times 10^{-8} \Omega\text{-m}$) wrapped around a core to form a total resistance of $1 \text{ k}\Omega$. The sliding contact surface area is very small.
- Estimate the range of displacement that could be measured with this potentiometer for a 1.5-cm core.
 - The circuit shown in Figure 12.63 is used to record position. On a single plot, show the loading error in an indicated displacement as a function of displacement, over the range found in (a), for values of the meter resistance, R_m , of 1, 10, and 100 kW . For practical meters, would the loading error be significant?

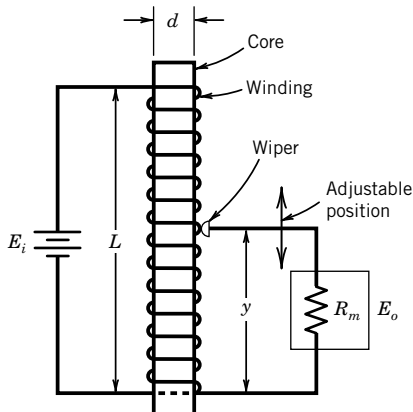


Figure 12.63 Circuit for Problem 12.1.

- 12.2** Mechatronic applications for linear displacement sensors are numerous. Select a particular application and develop specifications that would be required for a linear displacement sensor. Possible applications include automotive seat position, pick-and-place operations, and throttle position sensors.
- 12.3** Compare and contrast wire-wound and conductive-plastic potentiometers. Are there advantages and disadvantages for either linear or rotary applications?
- 12.4** Compare and contrast the use of an LVDT and a resistance-based potentiometer for position measurement.
- 12.5** A seismic instrument, as shown in Figure 12.7, is used to measure a vibration given by

$$y(t) = 0.2\cos 10t + 0.3\cos 20t$$

where

y = displacement in in.

t = time in s

The seismic instrument is to have a damping ratio of 0.7 and a spring constant of 1.2 lb/ft .

- Select a combination of seismic mass and damping coefficient to yield less than a 10% amplitude error in measuring the input signal. Under what conditions would the output signal experience significant distortion?
- Plot and describe the phase response of the system, either in a plot or tabular form.

- 12.6** A seismic instrument is to measure motion given by

$$y(t) = 0.5\cos 15t + 0.8\cos 30t$$

where

y = displacement in cm

t = time in s

The seismic instrument is to have a damping ratio of 0.7.

- a. Select a combination of seismic mass, spring constant, and damping coefficient to yield less than a 6% amplitude error in measuring the input signal. Under what conditions would the output signal experience significant distortion?

- b. Plot and describe the phase response of the system, either in a plot or tabular form.

- 12.7** A seismic instrument has a natural frequency of 20 Hz and a damping ratio of 0.65. Determine the maximum input frequency for a vibration such that the amplitude error in the indicated displacement is less than 5%.
- 12.8** A seismic instrument consists of a housing and a seismic mass. To measure vibration, the seismic mass should remain stationary in an absolute frame of reference. To measure acceleration, the magnitude ratio should be unity. Explain in detail the requirements for mass, spring constant, and damping ratio to satisfy these requirements.
- 12.9** A seismic instrument consists of a housing and a seismic mass. To measure vibration, the seismic mass should remain stationary in an absolute frame of reference. To measure acceleration, the magnitude ratio should be unity. Using Labview, develop a model of the seismic instrument for both vibration and acceleration measurement.
- 12.10** Determine the bandwidth for a seismic instrument employed as an accelerometer having a seismic mass of 0.2 g and a spring constant of 20,000 N/m, with very low damping. Discuss the advantages of a high natural frequency and a low damping ratio. Piezoelectric sensors are well suited for the construction of accelerometers, since they possess these characteristics.
- 12.11** In Example 12.2, integration is identified as a method for reducing the effects of noise in a signal. Discuss how a moving average can be used to reduce the effects of noise in a velocity measurement, through the integration of an acceleration signal. Discuss the effects of averaging time on the elimination of noise. Assume that the noise has significant amplitude, but higher frequency content than the velocity being measured.
- 12.12** Consider a moving coil transducer having a coil diameter D_c of 0.8 cm and a coil length of 2 cm. The nominal range of velocities to be measured is from 1 to 10 cm/s. The resulting emf is measured by a PC-based data acquisition system with an 8-bit A/D converter and a range of -1 to 1 V. The accuracy is 0.1% full-scale. Plot the number of turns as a function of magnetic field strength to provide an accuracy of 1% in the resulting velocity measurement.
- 12.13** Consider measuring a rotational speed using a stroboscope. The rotational speed is higher than the flash rate of the stroboscope. The stroboscope is observed to synchronize at 10,000, 18,000, and 22,000 flashes/s. Determine the rotational speed.
- 12.14** Research the state-of-the art specifications for load cells designed to measure the smallest possible forces. What applications exist for such precise measurements of small forces?
- 12.15** Design a proving ring load cell appropriate to serve as a laboratory calibration standard in the range of 250 to 1000 N. The proving ring material is steel.
- 12.16** Power transmitted through the drive shaft of a car results in a rotational speed of 1800 rpm with a power transmission of 40 horsepower. Determine the torque that the driveshaft must support.
- 12.17** Discuss the importance of a dynamometer for automotive emissions testing.
- 12.18** Research applications for linear actuators. For each application that you identify suggest the most appropriate linear actuator. Why was the actuator chosen for the particular application? For many applications, a choice is made to convert rotary motion to linear motion.

- 12.19** Pneumatic actuators span a very large range of size and force. Research the range of commercially available pneumatic cylinders.
- 12.20** Estimate the flow coefficient for a flow control valve if the rating corresponds to 32 SCFM (0.906 SCMM) with a $\Delta p = 10$ psi (0.69 bar). The test is conducted using air with a line pressure of 100 psi (6.7 bar), $T = 68^\circ\text{F}$ (20°C), and a relative humidity of 36% at the supply port. What is the pressure at the exhaust port? Base your answer on standard conditions.
- 12.21** A low profile three-port control valve with 6-mm port diameters has an F value of 0.82 ms/cc and a lag time of 8 ms to pressurize through ports P to A . The exhaust path through ports T to A has an F value of 0.70 ms/cc with an 8 ms lag time. The valve is connected to a 500 mL vessel. Supply pressure is 1 bar; exhaust pressure is 0 bar. Estimate the time needed to pressurize this vessel to 0.9 bar. Estimate the time to exhaust this vessel to 0.1 bar.
- 12.22** Research the design of a totalizing flow meter, with particular emphasis on the meters used to generate water bills.
- 12.23** The companion software includes a program *stroboscope.vi* that models the behavior of a stroboscope.
- Set the bar rotation frequency to 40 rps, and then set the strobe frequency to 20 and 40 Hz. Explain your results.
 - Set the bar rotation frequency to 100 rps. Using $f_1 = 50$ Hz and $f_N = 10$ Hz, apply Equation 12.15 to show that we can measure rotation frequencies larger than the maximum frequency of the stroboscope. Be careful to find all N of the synchronous frequencies.
- 12.24** Describe the operating principle of a thermostat for residential applications, and the design of a bimetallic sensor for measuring the temperature. How is a dead-band created in such an instrument?
- 12.25** Show that a proportional controller has a steady-state error. How would you quantify the steady-state error for a controller and a first-order system?
- 12.26** Using *First order PID.vi*, develop a model of the oven described in Example 12.5 coupled with a PI controller. Vary the proportional and integral gains and discuss the resulting behavior of this first-order system.
- 12.27** Using *Second order PID.vi*, develop a model for PID control of the oven described in Example 12.5. Vary the gains and discuss the resulting behavior of the system. Quantify the power input required to achieve a given response.
- 12.28** Consider the block diagram for an automotive speed control system shown in Figure 12.64.
- Find the transfer function from $V(s)$ to $Y(s)$, where V is the desired speed and Y is the actual speed.
 - Assume that the desired speed is a constant, and in Laplace space is v_o/s . Determine values of the gains such that

$$\lim_{t \rightarrow \infty} y(t) = v_o$$

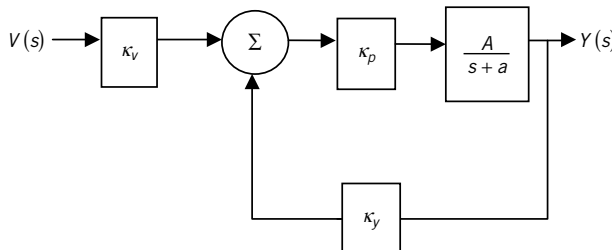


Figure 12.64 Block diagram for an automotive speed control.

Appendix A

A Guide For Technical Writing

A technical report is the most common way to communicate and to archive engineering test results. Depending on the intended audience, papers usually take on one of three formats, with wording and purpose directed towards that audience: (1) Executive (or Extended) summary, (2) Laboratory report, (3) Technical report. All reports share a common theme: Background - *Why* did you do the test, Approach - *How* did you do the test, Results - *What* did you find, and Conclusions - *So what* do we now know. The reports differ in purpose, and consequently, in length and detail.

The executive summary is intended typically either for upper level management who will plan decisions around the input from the report or to communicate to the engineering community a synopsis of a study. These consist of a one- or two-page (under 500 word) brief stating the reasons for the tests conducted (*why*), the approach and important results (*how*), and the conclusions (*so what*). The document composition is subdivided into *Objectives*, *Results*, and *Conclusions* although these heading may not be used explicitly. A summary may include a key figure and/or chart and references, as needed. Because of its brevity and readership, the strategic use of words and clearly directed and meaningful conclusions are crucial.

A laboratory report is an internal report usually accessed by members of your engineering group. These reports communicate information in a way that educates the reader and archives useful information. The format stresses methods and results in detail. These reports should include the reasons for the tests, the pretest planning, the methods and test conditions used, with an emphasis on the discussion of the results, quality of results (uncertainty), and conclusions. The document can be subdivided into headings of *Objectives*, *Approach*, *Results and Discussion*, *Conclusion*. Related and prior works are clearly referenced. Data in the form of tables and graphs are cited and discussed within the report. A laboratory report may contain an *Abstract* as a brief snapshot of the report contents. Appendices containing supporting information, such as raw data and data analysis programs, may be attached but must be independent from the main body of the report. Because these reports document test methods and findings, laboratory reports may become legal evidence to justify device performance or test outcome should performance or function ever be challenged.

A technical report is used to disseminate new engineering information to a broader technical audience outside of the immediate work group. Common forms can be found as a technical conference paper or journal article. They are written at a level and style that is appropriate for the receiving audience. Accordingly, these reports should include and/or cite sufficient background information so that the reader can understand the purpose of and the history behind the tests, the hypothesis or question being tested, the manner in which the tests were analyzed, the discussion of the test result and their implications, and a conclusion. A technical report must present enough information for the reader to justify the author's conclusions. Data should be presented only in the form of well-prepared tables and graphs cited from within the report. The report ends with a concise conclusion.

Each company, agency, or test laboratory has its own format for these reports. However, we provide suggested guidelines for the preparation of a technical report below. Regardless of format or length, a report must communicate the purpose and the outcome of a test to the intended audience. Further information concerning technical reporting may be found in numerous guides for technical writing (1,2).

A.1 A GUIDE FOR TECHNICAL WRITING³

Competent engineers can communicate their ideas in both oral and written formats to both technical and non-technical audiences. This primer is intended as a brief guide to constructing a technical report intended for a technical audience. The organization of this section is itself representative of most

technical reporting formats. The major headings, such as Abstract and Introduction, are typical, but are not meant to be exclusive.

Abstract

Effective technical communication abilities are important traits for an engineer in a technologically advancing society. A technical report provides a means to document and to disseminate relevant technical information, such as test or modeling results. The purpose of this article is both to provide specific procedures and ideas for generating sound technical reports and to serve as a format example of a technical report. Guidelines for preparing each section of a report and detailed ideas for presentation of results in plots and tables are provided. The reader can draw from this outline to prepare a technical report on a chosen subject.

Introduction

In a 2002 report, the U.S. National Academy of Engineering concluded that the majority of Americans “are not able to make well-considered decisions . . . about technology (4).” Our ability to communicate effectively with both technical and nontechnical segments of society is essential for addressing the myriads of technological problems and decisions facing our society. On a more personal level, career advancement in any profession is largely based on how well a person communicates among peers. The primary form of written communication used by practicing engineers and engineering managers, as well as researchers, is the technical report or one of its variations, the executive summary or the laboratory report. Technical codes and standards would fall into one of these categories, as well. Collectively speaking, these communications are directed toward a technically knowledgeable audience. The purpose of this guide is to provide reasonable ideas and suggestions for producing clear and concise technical manuscripts.

The following steps may help you prepare an effective document:

1. Always clearly define the question, the question being the objective or the hypothesis tested in the study described by the report!
2. Your report should flow from what you sought to show and why it is important, to how you tried to answer it, to what you found, and finally to what those findings mean relative to the question asked. Start with a detailed outline using this logic flow. Then expand your outline to at least the level where topics and some sentences have been formulated. The outline will help you avoid making a chronological or “stream of consciousness” presentation, which is not desirable. This will enable you to develop the rationale for your question and how you attempted to answer it in a logical manner.
3. Analyze your data, creating meaningful figures and tables. Then, organize your discussion on what this information shows. In terms of answering your question, which figures and tables are important and which are not? Use what is important. When deciding on just what to present, keep the particular audience for whom you are writing in mind.
4. Set your format or headings using the format or style guide for a specific publication, workplace template, or use this Guide. Organize around those headings.
5. Write a first draft in which you add meaningful sentences to your outline under each heading.
6. Read the draft, then rewrite it for presentation clarity and accuracy. Remember that you are telling a technical story, so think clarity as from the reader’s point of view. Edit as needed. Proofread the manuscript. Remember: Your audience cannot read your mind, just your report – put what you want to say in writing. If possible, have a peer read the draft and ask for effective feedback on clarity and content.
7. Use a typography that is easy to read. If not specified, try a 12-point serif font, such as Times or Arial. Maintain margins of at least 1.25 inches (32 mm). Number all pages (exception: page one may be left unnumbered).

Approach

The supporting blocks for constructing an effective technical document are the written text, well-prepared figures, and clear tables, and an organized structure that communicates the story. Present the report from the standpoint of your current knowledge. You do not need to report on bad data, failed trials, blunders, and so on

unless these are vital to your conclusions. Instead, take a fresh look at the results and organize the flow of your document to present the work in an effective way. In most technical documents, figures and tables provide the substance for the purpose, results, and conclusion of the study and so these should comprise a good bit of your discussion. The following guidelines for preparing each section of a technical document provide some basics necessary for sound reporting procedures. *Just a note: these sections are not absolutes, just a guide. The important thing is to communicate effectively.*

The Abstract—A Summary of the Entire Report

An Abstract is a complete, concise distillation of the full report. It provides a brief (one sentence) introduction to the subject, a statement of the problem and question studied, highlights of the results (quantitative, if possible), and the conclusion. It must stand alone without citing figures, tables, or references. A concise, clear approach is essential. It is usually written after the main body of the report is complete. Most abstracts are rarely exceed 150 words.

Similar in organization but using more like 500 words as a common length, an Executive Summary does not need an abstract. It may include a critical figure, table, or chart, and references.

The Introduction—Why Did You Do What You Did?

An Introduction provides the necessary background information, including appropriate literature review, develops for the reader a clear rationale for the work, and clearly states the objective of the report. This is where you develop and then state the hypothesis or question tested. The Introduction does not contain results, and generally would not contain equations. It could contain a figure or table as needed to develop the rationale.

Approach – What was done and how?

The Approach section contains the methodology used in the study. This might include separate sections describing descriptive analytical, experimental and/or numerical models, as appropriate.

Analysis—Is There A Model? An Analysis section develops a descriptive model used in the study. Sufficient detail (mathematical or otherwise) should be provided for the reader to clearly understand the physical assumptions associated with a theory or model. This will help explain what information was needed from any supporting experimental or numerical tests.

Experimental Program—What Did You Measure and How? The Experimental Program section is intended to describe how the experimental model was developed to support the analysis and so test the hypothesis, and to detail how the results were obtained. Provide an overview of the approach, test facilities, verification studies, and range of measurements in just sufficient detail that the reader understands what was done and how. Do not give instructions, this is not a recipe. If a list of equipment is included in the report, it should be a table in the body of the report, or cited and placed in an appendix. In cases where both an analysis and experiment are described, these two sections of the report should complement and support each other. The relationship of the analysis to the experiment should be clearly stated. Often, the experiment provides the values used to complete the analysis.

Numerical Model—What Did You Simulate and How? If a numerical simulation was performed, it should be described under a separate heading using the same guidelines as presented for the Experimental Program.

Results and Discussion—So What Did You Find?

Here you present and discuss your test results and tie them back to your original hypothesis. For technical or laboratory reports, this section will usually be the longest section of the document. Describe the operation conditions and range of tests done and then present your findings. When presenting your results remember that even though you are usually writing to an experienced technical audience, what may be clear to you may not be obvious to the reader. Guide the reader towards your interpretation. Tell the story.

Data must be interpreted to be useful and this section is where you transform the raw data in your notes into useful results within the report. For any experimental or numerical study, you should include a synopsis of your uncertainty analysis culminating in a statement about the quality of the results presented. Often the most important vehicles for the clear presentation of results are figures and tables. Each figure and table should be numbered, labeled with a caption, and cited by number within the text. Since you have spent significant time in preparing the plots and tables and you are intimately familiar with their trends and implications; the reader needs your insight to understand the results as well as you. *As a good rule, spend at least one paragraph discussing each figure or table.*

Figure A.1 shows an example of an appropriately prepared plot. Note that this plot has a figure number and a descriptive caption, and clearly labeled axes. As an example of what to write: your report might start with, “*the measured temperature as a function of position within the heated, packed particle bed is shown in Figure A.1. Two curves are shown, one taken along the centerline ($R/R_0 = 0.0$) and the other along the bed wall ($R/R_0 = 1.0$). Also shown are the corresponding model predictions. The measured bed temperature is essentially uniform from the centerline to the wall for $X/L > 0.5$ but shows spatial gradients elsewhere. Error bars represent the 95% confidence intervals.*” Be sure to cite any corresponding equations used. Then the extended discussion of this figure might focus on the differences in the curves, why they are different, how they relate to a model or prediction, and assess whether their shape and magnitudes make sense.

The visual impact of a plot conveys considerable information about the relationship between the plotted dependent and independent variables. Suggestions for creating effective plots:

1. The independent parameter is always plotted on the x axis; the dependent parameter is always plotted on the y axis.
2. Try to use at least four tics or increments for each axis. Multiples of 1, 2, or 5 are good increments because they make it easy to interpolate. Watch out for automatic scaling features from software: it is hard to justify strange increments such as 0, 7, 14.
3. In drawing smooth curves through experimental data points, try to follow these rules:
 - (a) Show the data points as symbols, such as open or filled squares, circles, or triangles.
 - (b) Do not extend a curve beyond the ends of the data points. If you need to extrapolate, then use a dashed line outside the known range. If appropriate, indicate the curve-fit equations.

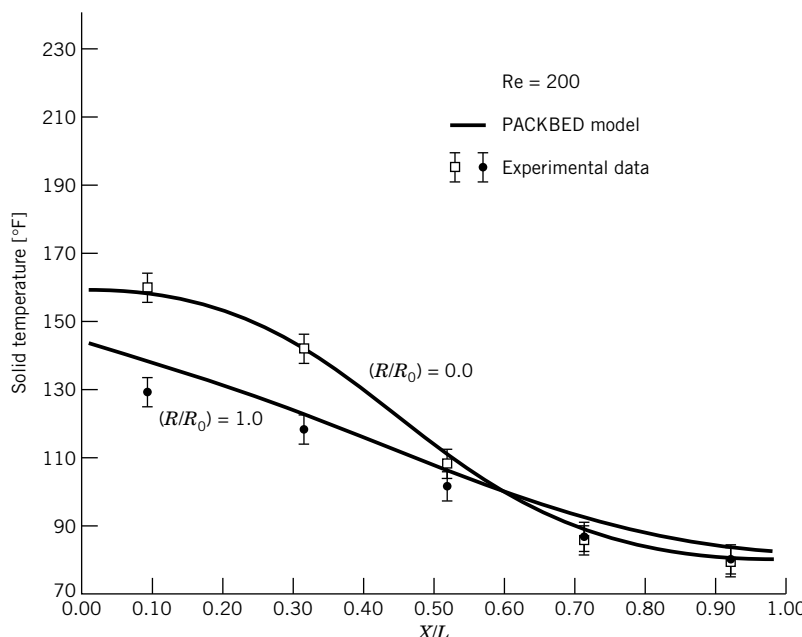


Figure A.1 Comparison of experimentally measured and computed results for axial temperature distributions in a thermal energy storage bed.

- (c) If you are certain that $y = 0$ when $x = 0$, put the curve through the origin. But if you are uncertain, don't use the origin; stop the line at the lowest point (see 3b).
- 4. Use a minimum variety of symbols for your data. Always include a symbol legend. Consistently use the same symbols for the same variables between graphs. Pick a symbol font that will be legible.
- 5. To compare experimentally determined data with model predictions, show the experimental points as symbols and the model as a smooth curve. Similarly, show numerical predictions as a smooth curve. Clear labeling is essential for this kind of plot.
- 6. The figure should contain enough information to stand alone, especially if there's a chance it will later be used by itself (e.g., as a slide).
- 7. Always provide axes quantities with units. Use axes font sizes that are readable.
- 8. Adjust the graph scales so that the curves are not bunched near the top, bottom, or one of the sides.
- 9. Uncertainty limits should be indicated for a number of measured points on a given plot using interval bands about the mean value, as shown in Figure A.1

Table A.1 is an example of results presented in a tabular form. The table has a number and a descriptive caption. As an example of how to describe a table, your report could start with, “*Table A.1 lists the measured thermistor voltage output as a function of an applied velocity.*” The extended discussion of this table might focus on its range, curve fit, how it relates to a model or prediction and how it is used.

Conclusions—What Do I Now Know and So What?

The Conclusions section is where you should concisely restate your answer to the questions: “What do I know now?” and “Why is that important?” Your answer must support or refute your hypothesis and provide a useful closure to the report. In a short summary, restate why the work was done, how it was done and why these results are significant. This is not the place to offer new facts or discussion. A conclusion will normally have a quantified outcome. An example might be: “*The temperature measuring system was calibrated against a laboratory standard RTD. The system was found to indicate the correct temperature over the range of 0 to 150°C with no more than ± 0.5°C uncertainty at 95% confidence. This is acceptable for the intended use in our product.*” It would not normally be appropriate to conclude simply, “The temperature measuring system was tested and worked well enough.” Conclusions should be clear and concise statements of the important findings of a particular study; most conclusions require some quantitative statement to be useful.

Table A.1 Characteristics of a Thermistor Anemometer in a Uniform Flow Field

Velocity [m/s]	[V]
0.467	3.137
0.950	3.240
2.13	3.617
3.20	3.811
3.33	3.876
4.25	3.985
5.00	4.141
6.67	4.299
8.33	4.484
10.0	4.635
12.0	4.780

Appendices

Appendices are places to place non-critical, supplemental or supporting information, such as raw data, lengthy derivations, or sample programs. Appendices are independent from the report; they are often misused by a new engineer. Uncertain as to whether or not some information should be in an Appendix? Ask yourself: If I place this material in the Appendix and the reader did not read the Appendix, would the main body of the report still be sufficient? It should be!

References

The references cited within a report should be detailed in a formal list at the end of the report. Use references that provide credit for prior work but also to provide more information for the reader. For example, did the test program follow an established engineering standard? Then provide a citation so the reader can go to this standard for reading. If you used an internet webpage or web document, cite the URL and the date used. References for this document provide an acceptable general format.

Some Writing Tips

1. Communicate! You are telling a story, albeit a highly technical one. Proofread, and then rewrite it!
Have someone else read it, and then rewrite it as needed!
2. Do not overdo significant figures. See the discussion in Chapter 1.

On Writing Style

Engineers often write reports in the third person in deference to impartiality and to focus attention on the subject matter at hand. The idea is to disassociate the writer from the action and make the equipment/model/test the “doer of the action (5).” This is a notable goal but one that takes time and practice to do effectively. But achieving this goal does not require extensive use of the passive voice, despite traditional beliefs to the contrary. Do use the active voice where possible to liven up your report. The occasional impersonal construction in the first person is fine if it improves readability. Frankly, we find it difficult to write extensively in the third person, passive voice without the writing coming off as clumsy . . . and long. But choose the style that suits your writing best. The important thing is to communicate effectively!

Conclusions

Technical authors must be cognizant of coupling the intended audience with the test goals when presenting the results of their writing. This report has outlined the essential features germane to technical report writing and it serves as an example of both style and format. We describe the purpose and content for each section of a report. We also pass along some useful advice drawn from our experience in helping young engineers learn to write technically. We conclude that an effective, polished, and professional product can be produced only through careful revision of manuscript, by incorporating effective figures and tables, and by targeting the intended audience.

References

1. Tichy, H.S., and S. Foudrinier, “Effective Writing for Engineers, Managers, and Scientists,” 2d ed., Wiley Interscience, New York, 1988.
2. Donnell, J. and S. Jeter, *Writing Style and Standards in Undergraduate Reports*, College Pub., 2003.
3. Henry, M. H., and H. K. Lonsdale, “The researcher’s writing guide”, *Journal of Membrane Science* 13: 101–107, 1983. (adapted with permission)
4. Committee on Technological Literacy, “Technically Speaking, why All Americans need to know more about technology,” G. Pearson and A. Young, Ed., National Academy of Engineering, National Academy Press, Washington, D.C., 2002.
5. Daniell, B., R. Figliola, A. Young, D. Moline, “Learning to Write: Experiences with Technical Writing Pedagogy Within the Mechanical Engineering Laboratories,” Proc. ASEE, Paper 1141, 2003.

Appendix B

Property Data and Conversion Factors

Table B.1 Properties of Pure Metals and Selected Alloys

	Density (kg/m ³)	Modulus of Elasticity (GPa)	Coefficient of Thermal Expansion (10 ⁻⁶ m/m-K)	Thermal Conductivity (W/m-K)	Electrical Resistivity (10 ⁻⁶ Ω-cm)
<i>Pure Metals</i>					
Aluminum	2 698.9	62	23.6	247	2.655
Beryllium	1 848	275	11.6	190	4.0
Chromium	7 190	248	6.2	67	13.0
Copper	8 930	125	16.5	398	1.673
Gold	19 302	78	14.2	317.9	2.01
Iron	7 870	208.2	15.0	80	9.7
Lead	11 350	12.4	26.5	33.6	20.6
Magnesium	1 738	40	25.2	418	4.45
Molybdenum	10 220	312	5.0	142	8.0
Nickel	8 902	207	13.3	82.9	6.84
Palladium	12 020	—	11.76	70	10.8
Platinum	21 450	130.2	9.1	71.1	10.6
Rhodium	12 410	293	8.3	150.0	4.51
Silicon	2 330	112.7	5.0	83.68	1 × 10 ⁵
Silver	10 490	71	19.0	428	1.47
Tin	5 765	41.6	20.0	60	11.0
Titanium	4 507	99.2	8.41	11.4	42.0
Zinc	7 133	74.4	15.0	113	5.9
<i>Alloys</i>					
Aluminum (2024, T6)	2 770	72.4	22.9	151	4.5
Brass (C36000)	8 500	97	20.5	115	6.6
Brass (C86500)	8 300	105	21.6	87	8.3
Bronze (C90700)	8 770	105	18	71	1.5
Constantan annealed (55%					
Cu 45% Ni)	8 920	—	—	19	44.1
Steel (AISI 1010)	7 832	200	12.6	60.2	20
Stainless Steel (Type 316)	8 238	190	—	14.7	—

Source: Complied from *Metals Handbook*, 9th ed., American Society for Metals, Metals Park, OH, 1978, and other sources.

Table B.2 Thermophysical Properties of Selected Metallic Solids

Composition	Melting point (K)	Properties at 300 K						Properties at various temperatures (K)					
		ρ (kg/m ³)	c_p (J/kg · K)	k (W/m · K)	$\alpha \times 10^4$ (m ² /s)	k (W/m · K)			c_p (J/kg · K)				
						100	200	400	600	100	200	400	600
Aluminum	933	2702	903	237	97.1	302	237	240	231	482	796	949	1033
Pure	775	2770	875	177	73.0	65	163	186	186	473	787	925	1042
Alloy 2024-T6 (4.5% Cu, 1.5% Mg, 0.6% Mn)	—	2790	883	168	68.2	—	—	174	185	—	—	—	—
Alloy 195, cast (4.5% Cu)	2118	7160	449	93.7	29.1	159	111	90.9	80.7	192	384	484	542
Chromium	1358	8933	385	401	117	482	413	393	379	252	356	397	417
Copper	1293	8800	420	52	14	—	42	52	59	—	785	460	545
Pure	Commercial bronze (90% Cu, 10% Al)	1104	8780	355	54	17	—	41	65	74	—	—	—
Phosphor gear bronze (89% Cu, 11% Sn)	Cartridge brass (70% Cu, 30% Zn)	1188	8530	380	110	33.9	75	95	137	149	—	360	395
Constantan (55% Cu, 45% Ni)	1493	8920	384	23	6.71	17	19	—	—	237	362	—	—
Iron	Pure	1810	7870	447	80.2	23.1	134	94.0	69.5	54.7	216	384	490
Armco (99.75%)	—	7870	447	72.7	20.7	95.6	80.6	65.7	53.1	215	384	490	574
Carbon steels	Plain carbon (Mn $\leq 1\%$, Si $\leq 0.1\%$)	—	7854	434	60.5	17.7	—	—	56.7	48.0	—	—	487
AISI 1010	—	7832	434	63.9	18.8	—	—	58.7	48.8	—	—	487	559

Carbon-silicon (Mn \leq 1%, 0.1% Si \leq 0.6%)	—	7817	446	51.9	14.9	—	—	49.8	44.0	—	—	501	582
Carbon-manganese- silicon (1% $<$ Mn \leq 1.65%, 0.1% Si \leq 0.6%)	—	8131	434	41.0	11.6	—	—	42.2	39.7	—	—	487	559
Chromium (low) steels 1/2 Cr-1/4 Mo-Si (0.18% C, 0.65% Cr, 0.23% Mo, 0.6% Si)	—	7822	444	37.7	10.9	—	—	38.2	36.7	—	—	492	575
1 Cr-1/2 Mo (0.16% C, 1% Cr, 0.54% Mo, 0.39% Si)	—	7858	442	42.3	12.2	—	—	42.0	39.1	—	—	492	575
1 Cr-V (0.2% C, 1.02% Cr, 0.15% V)	—	7836	443	48.9	14.1	—	—	46.8	42.1	—	—	492	575
Stainless steels													
AISI 302	—	8055	480	15.1	3.91	—	—	17.3	20.0	—	—	512	559
AISI 304	1670	7900	477	14.9	3.95	9.2	12.6	16.6	19.8	272	402	515	559
AISI 316	—	8238	468	13.4	3.48	—	—	15.2	18.3	—	—	504	550
AISI 347	—	7979	480	14.2	3.71	—	—	15.8	18.9	—	—	513	559
Lead	601	11 340	129	35.3	24.1	39.7	36.7	34.0	31.4	118	125	132	142
Magnesium	923	1740	1024	156	87.6	169	159	153	149	649	934	1074	1170
Molybdenum	2894	10 240	251	138	53.7	179	143	134	126	141	224	261	275
Nickel	Pure	1728	8900	444	90.7	23.0	164	107	80.2	65.6	232	383	485
Nichrome (80% Ni, 20% Cr)	1672	8400	420	12	3.4	—	—	14	16	—	—	480	525
Inconel X-750 (73% Ni, 15% Cr, 6.7% Fe)	1665	8510	439	11.7	3.1	8.7	10.3	13.5	17.0	—	372	473	510

Table B.3 Thermophysical Properties of Saturated Water (Liquid)

<i>T</i> (K)	ρ (kg/m ³)	c_p (kJ/kg·K)	$\mu \times 10^6$ (N·s/m ²)	k (W/m·K)	Pr	$\beta \times 10^6$ (K ⁻¹)
273.15	1000	4.217	1750	0.569	12.97	-68.05
275.0	1000	4.211	1652	0.574	12.12	-32.74
280	1000	4.198	1422	0.582	10.26	46.04
285	1000	4.189	1225	0.590	8.70	114.1
290	999	4.184	1080	0.598	7.56	174.0
295	998	4.181	959	0.606	6.62	227.5
300	997	4.179	855	0.613	5.83	276.1
305	995	4.178	769	0.620	5.18	320.6
310	993	4.178	695	0.628	4.62	361.9
315	991	4.179	631	0.634	4.16	400.4
320	989	4.180	577	0.640	3.77	436.7
325	987	4.182	528	0.645	3.42	471.2
330	984	4.184	489	0.650	3.15	504.0
335	982	4.186	453	0.656	2.89	535.5
340	979	4.188	420	0.660	2.66	566.0
345	977	4.191	389	0.664	2.46	595.4
350	974	4.195	365	0.668	2.29	624.2
355	971	4.199	343	0.671	2.15	652.3
360	967	4.203	324	0.674	2.02	679.9
365	963	4.209	306	0.677	1.90	707.1
370	961	4.214	289	0.679	1.79	728.7
373.15	958	4.217	279	0.680	1.73	750.1
400	937	4.256	217	0.688	1.34	896
450	890	4.40	152	0.678	0.99	
500	831	4.66	118	0.642	0.86	
550	756	5.24	97	0.580	0.88	
600	649	7.00	81	0.497	1.14	
647.3	315	0	45	0.238	∞	

Formulas for interpolation (*T* = absolute temperature)

$$f(T) = A + BT + CT^2 + DT^3$$

<i>f(T)</i>	<i>A</i>	<i>B</i>	<i>C</i>	<i>D</i>	Standard Deviation, σ
$273.15 < T < 373.15 \text{ K}$					
ρ	766.17	1.80396	-3.4589×10^{-3}		0.5868
c_p	5.6158	-9.0277×10^{-3}	14.177×10^{-6}		4.142×10^{-3}
k	-0.4806	5.84704×10^{-3}	-0.733188×10^{-5}		0.481×10^{-3}
$273.15 < T < 320 \text{ K}$					
$\mu \times 10^6$	0.239179×10^6	-2.23748×10^3	7.03318	-7.40993×10^{-3}	4.0534×10^{-6}
$\beta \times 10^6$	-57.2544×10^3	530.421	-1.64882	1.73329×10^{-3}	1.1498×10^{-6}
$320 < T < 373.15 \text{ K}$					
$\mu \times 10^6$	35.6602×10^3	-272.757	0.707777	-0.618833×10^{-3}	1.0194×10^{-6}
$\beta \times 10^6$	-11.1377×10^3	84.0903	-0.208544	0.183714×10^{-3}	1.2651×10^{-6}

Source: From Incropera, F. P., and D. P. DeWitt, *Fundamentals of Heat and Mass Transfer*, Wiley, New York, 1985.

Table B.4 Thermophysical Properties of Air

<i>T</i> [K]	ρ [kg/m ³]	c_p [kJ/kg · K]	$\mu \times 10^7$ [N · s/m ²]	$\nu \times 10^6$ [m ² /s]	$k \times 10^3$ [W/m · K]	$\alpha \times 10^5$ [m ² /s]	Pr
200	1.7458	1.007	132.5	7.590	18.1	10.3	0.737
250	1.3947	1.006	159.6	11.44	22.3	15.9	0.720
300	1.1614	1.007	184.6	15.89	26.3	22.5	0.707
350	0.9950	1.009	208.2	20.92	30.0	29.9	0.700
400	0.8711	1.014	230.1	26.41	33.8	38.3	0.690
450	0.7740	1.021	250.7	32.39	37.3	47.2	0.686
500	0.6964	1.030	270.1	38.79	40.7	56.7	0.684
550	0.6329	1.040	288.4	45.57	43.9	66.7	0.683
600	0.5804	1.051	305.8	52.69	46.9	76.9	0.685
650	0.5356	1.063	322.5	60.21	49.7	87.3	0.690
700	0.4975	1.075	338.8	68.10	52.4	98.0	0.695
750	0.4643	1.087	354.6	76.37	54.9	109.	0.702
800	0.4354	1.099	369.8	84.93	57.3	120.	0.709
850	0.4097	1.110	384.3	93.80	59.6	131.	0.716
900	0.3868	1.121	398.1	102.9	62.0	143.	0.720
950	0.3666	1.131	411.3	112.2	64.3	155.	0.723
1000	0.3482	1.141	424.4	121.9	66.7	168.	0.726

Formulas for Interpolation (*T* = absolute temperature)

$$\rho = \frac{348.59}{T} \quad (\sigma = 9 \times 10^4)$$

$$f(T) = A + BT + CT^2 + DT^3$$

<i>f</i> (<i>T</i>)	<i>A</i>	<i>B</i>	<i>C</i>	<i>D</i>	Standard Deviation, σ
c_p	1.0507	-3.645×10^{-4}	8.388×10^{-7}	-3.848×10^{-10}	4×10^{-4}
$\mu \times 10^7$	13.554	0.6738	-3.808×10^{-4}	1.183×10^{-7}	0.4192×10^{-7}
$k \times 10^3$	-2.450	0.1130	-6.287×10^{-5}	1.891×10^{-8}	0.1198×10^{-3}
$\alpha \times 10^8$	-11.064	7.04×10^{-2}	1.528×10^{-4}	-4.476×10^{-8}	0.4417×10^{-8}
Pr	0.8650	-8.488×10^{-4}	1.234×10^{-6}	-5.232×10^{-10}	1.623×10^{-3}

Source: From F. P. Incropera and D. P. DeWitt, *Fundamentals of Heat and Mass Transfer*. Wiley, New York, 1985.

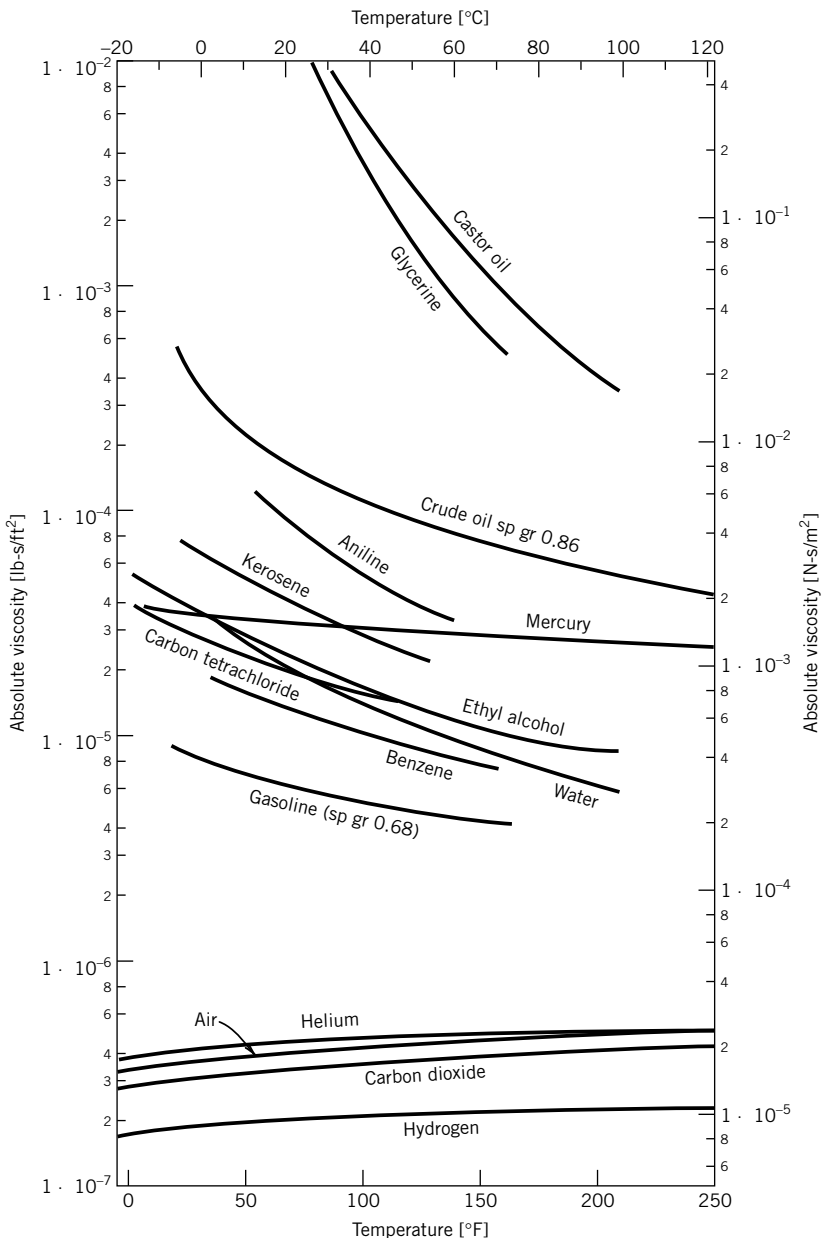


Figure B.1 Absolute viscosities of certain gases and liquids. (From Streeter, V. L., and E. B. Wylie, *Fluid Mechanics*, 8th ed., McGraw-Hill, New York, 1985.)

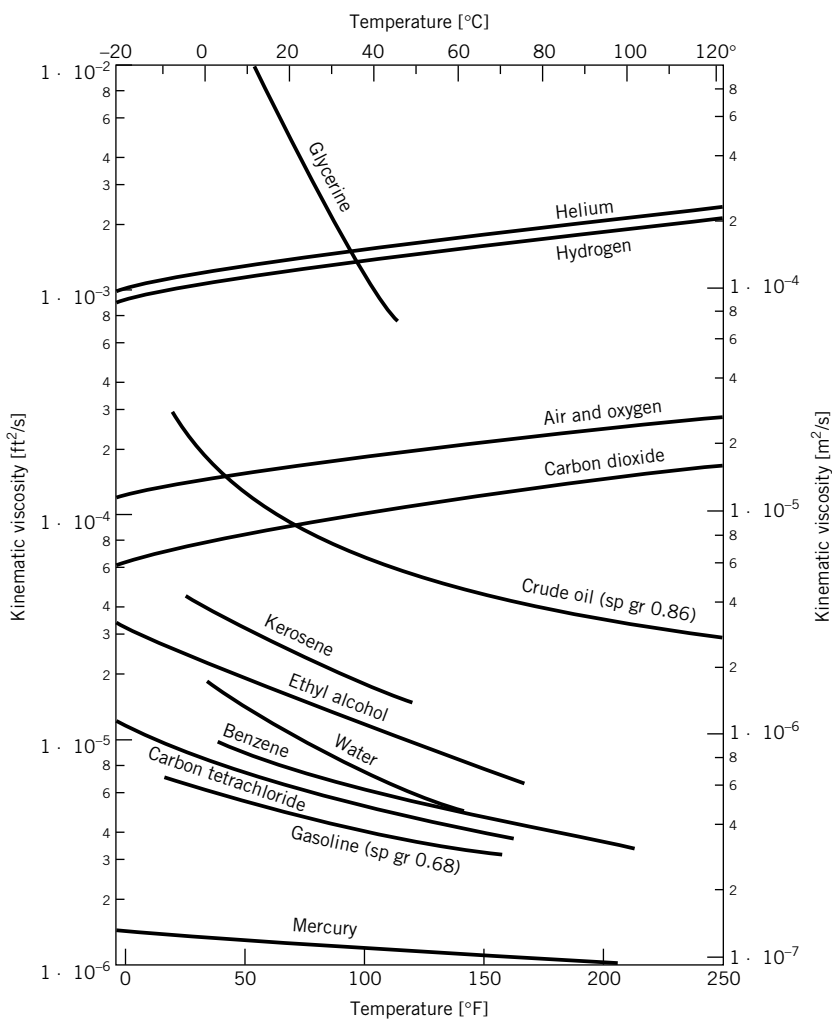


Figure B.2 Kinematic viscosities of certain gases and liquids. The gases are at standard pressure. (From Streeter, V. L., and E. B. Wylie, *Fluid Mechanics*, 8th ed., McGraw-Hill, New York, 1985.)

Laplace Transform Basics

We offer the following primer of Laplace transforms for review purposes to meet the needs of this text. Extensive treatment of this subject is available elsewhere [1]. The Laplace transform of a function $y(t)$ is defined as

$$Y(s) = \mathcal{L}[Y(t)] = \int_0^\infty y(t)e^{-st}dt \quad (\text{C.1})$$

There are many functions that are useful in modeling linear systems that have analytical forms for their Laplace transforms. Consider the unit step function, defined by

$$U(t) = \begin{cases} 0 & t < 0 \\ 1 & t > 0 \end{cases} \quad (\text{C.2})$$

Applying the definition of the Laplace transform yields

$$\mathcal{L}[U(t)] = \int_0^\infty e^{-st}dt = \frac{1}{s} \quad (\text{C.3})$$

The unit step function and its Laplace transform form a Laplace transform pair. Table C.1 provides a list of common Laplace transform pairs.

One of the most important properties of the Laplace transform results from the application of the Laplace transform to a derivative, as

$$\mathcal{L}\left[\frac{dy(t)}{dt}\right] = sY(s) - y(0) \quad (\text{C.4})$$

Differentiation in the time domain is the same as multiplication in the Laplace transform domain. This relationship is derived through application of integration by parts of the definition of the Laplace transform, and can be generalized as

$$\mathcal{L}\left[\frac{d^n y(t)}{dt^n}\right] = s^n Y(s) - s^{n-1}y(0) - s^{n-2}\frac{dy(0)}{dt} - \dots - \frac{d^{n-1}y(0)}{dt^{n-1}} \quad (\text{C.5})$$

Table C.1 Laplace Transform Pairs

	$f(t)$	$\mathcal{L}(f)$
1	1	$\frac{1}{s}$
2	t	$\frac{1}{s^2}$
3	t^2	$\frac{2!}{s^3}$
4	t^n	$\frac{n!}{s^{n+1}}$
where n is integer		
5	e^{-at}	$\frac{1}{s+a}$
6	te^{-at}	$\frac{1}{(s+a)^2}$
6	$\frac{e^{-at} - e^{-bt}}{b-a}$	$\frac{1}{(s+a)(s+b)}$
7	$\sin at$	$\frac{a}{s^2 + a^2}$
8	$\cos at$	$\frac{s}{s^2 + a^2}$

C.1 FINAL VALUE THEOREM

A useful property of the Laplace transform allows us to determine the value of the function $y(t)$ knowing only the Laplace transform of the function. The final value theorem states

$$\lim_{t \rightarrow \infty} y(t) = \lim_{s \rightarrow \infty} [sY(s)] \quad (\text{C.6})$$

Let's apply this to the unit step function

$$\lim_{s \rightarrow 0} sY(s) = \lim_{s \rightarrow 0} s \frac{1}{s} = 1 \quad (\text{C.7})$$

Clearly this is the correct limit!

C.2 LAPLACE TRANSFORM PAIRS

Table C.1 provides Laplace transform pairs for a variety of important engineering functions. More extensive lists and methods for more complex transformations may be found in most advanced engineering mathematics texts.

Reference

1. Schiff, J. L., *The Laplace Transform: Theory and Applications*, Springer, New York, 1999.

Glossary

A/D converter A device that converts analog voltages into a digital numbers.

absolute temperature scale A temperature scale referenced to the absolute zero of temperature; equivalent to thermodynamic temperature.

accelerometer An instrument for measuring acceleration.

accuracy The closeness of agreement between the measured value and the true value.

actual flow rate Flow rate specified under the actual temperature and pressure conditions of the measurement. See standard flow rate.

actuator Device that creates a desired linear or rotary motion; classes generally include electrical, mechanical, hydraulic or pneumatic.

advanced-stage uncertainty The uncertainty estimate beyond the design-stage that includes the uncertainty due to measurement system, measurement procedure, and measured variable variation.

alias frequency A false frequency appearing in a discrete data set that is not in the original signal.

amplitude Characteristic of a signal or component frequency of a signal that expresses a range of time-dependent magnitude variations.

apparent strain A false output from a strain gauge as a result of input from extraneous variables such as temperature.

astable multivibrator Switching circuit that toggles on or off continuously in response to an applied voltage command.

band-pass filter A device that allows a range of signal frequencies to pass unaltered, while frequencies outside this range, both higher and lower, are attenuated.

Bessel filter Filter design having a maximally linear phase response over its passband.

bias An offset value.

bias error See systematic error. Archaic term no longer used in measurements.

bimetallic thermometer A temperature measuring device that utilizes differential thermal expansion of two materials.

bistable multivibrator See flip-flop.

bit The smallest unit in binary representation.

bit number The number of bits used to represent a word in a digital device.

bonded resistance strain gauge A strain sensor that exhibits an electrical resistance change indicative of strain. The sensor is bonded to the test specimen in

such a way that the gauge accurately measures the strain at the surface of the test specimen.

bridge constant The ratio of the actual bridge voltage to the output of a single strain gauge sensing the maximum strain.

buffer Memory set aside to be accessed by a specific I/O device, such as to temporarily store data.

bus A major computer line used to transmit information.

Butterworth filter Filter design having a maximally flat magnitude ratio over its passband.

byte A collection of 8 bits.

calibration Act of applying a known input value to a system so as to observe the system output value.

calibration curve Plot of the input values versus the output values resulting from a calibration.

central tendency Tendency of data scatter to group about a central (mean or most expected) value.

charge amplifier Amplifier used to convert a high impedance charge into a voltage.

circular frequency Frequency specified in radians per second; angular frequency.

closed-loop control Type of control action that is based on the output value from a sensor relative to a set-point.

combined standard uncertainty Uncertainty estimate that includes both systematic and random standard uncertainties.

common-mode voltage Voltage difference between two different ground points. See ground loop.

concomitant method An alternate method to assess a value of a variable.

conduction error Error in temperature measurement caused by the diffusion of heat through a temperature sensor either to or away from the measuring environment so as to change the sensor temperature.

confidence interval Interval that defines the limits about a mean value within which the true value is expected to fall.

confidence level Probability that the true value falls within the stated confidence interval.

control A means to set and maintain a value during a test.

control parameter Parameter whose value is set during a test and that has a direct effect on the value of the measured variable.

conversion error The errors associated with converting an analog value into a digital number.

conversion time The duration associated with converting an analog value into a digital number.

coupled system The combined effect of interconnected instruments used to form a measurement system.

critical pressure ratio The pressure ratio necessary to accelerate a fluid to a velocity equal to its speed of sound.

cut-off frequency The 3 dB design point frequency of a filter.

d'Arsonval movement Device that senses the flow of current through torque on a current carrying loop; it is the basis for most analog electrical meters.

D/A converter A device that converts a digital number into an analog voltage.

damping ratio A measure of system damping—a measure of a system's ability to absorb or dissipate energy.

data acquisition board A device that contains a minimum of components required for data acquisition; usually connected to a computer.

data acquisition system A system that quantifies and stores data.

deflection mode Measuring method that uses signal energy to cause a deflection in the output indicator. See loading error.

dependent variable A variable whose value depends on the value of one or more other variables.

design-stage uncertainty The uncertainty due only to instrument error and instrument resolution; an uncertainty value based on the minimum amount of information that is known at the early stage of test design.

deterministic signal A signal that is predictable in time or in space, such as a sine wave or ramp function.

diaphragm meter A type of positive displacement flow meter that measures gas volume flow rate by alternately passing isolated but known volumes of the gas between two chambers.

differential-ended connection Dual-wire connection scheme that measures the difference between two signals with no regard to ground.

digital signal Representation of an analog signal that is quantized in both magnitude and time.

deviation plot Graphical representation of the difference between a reference and expected value.

direct memory access Transfer protocol that allows a direct transmission path between a device and computer memory.

discharge coefficient Coefficient equating the ratio of actual flow rate across a flow meter to the ideal flow rate if no losses or flow separation occurred.

discrete random variable Random variable whose value is not continuous.

distortion Any undesirable change in the shape of a waveform that occurs during signal conditioning or measurement.

dispersion The scattering of values of a variable around a mean value.

disturbance An effect that changes the operating condition of a control system away from its set-point. Requires controller action to maintain or re-establish the set point.

Doppler anemometry Refers to various techniques that use the Doppler shift to measure velocity.

Doppler flowmeter Flowmeter that uses the Doppler shift in the frequency of ultrasonic waves passing through the fluid flow to indicate volume flow rate.

dynamic calibration Process of calibration such that the input variable is time-varying.

dynamic pressure Difference between the total and static pressures at any point.

dynamic response Response of a system to a well-defined sine wave input.

dynamometer Device for measuring shaft power.

earth ground A ground path whose voltage level is zero.

elastic region An operating range of strain versus load wherein a material returns to its initial length when the load is removed.

error Difference between a measured value and its true (actual) value. In controls, it is the difference between a sensor value and a set-point.

error fraction A measure of the time-dependent error in the time response of a first-order system.

expanded uncertainty Uncertainty interval with the combined effects of random and systematic uncertainties at a stated confidence level (typically 95%) other than one standard deviation.

electromagnetic flow meter Device that bases fluid flow rate on the magnitude of the current induced in a magnetic field caused by the velocity of the fluid passing through that magnetic field.

end standard Length standard described the distance between two flat square ends of a bar.

expansion factor Coefficient used to account for compressibility effects in obstruction flow meters.

extraneous variable A variable that is not or cannot be controlled during a measurement, but that affects the measured value.

feedback-control stage Stage of a measurement system that interprets the measured signal and exerts control over the process.

firewire A serial method for data transmission between a computer and peripherals using a thin cable and based on the IEEE 1394 standard.

first-order system A system characterized as having time-dependent storage or dissipative ability but having no inertia.

fixed point temperature Temperatures specified through a reproducible physical behavior, such as a melting or boiling point.

flip-flop A switching circuit that toggles either on or off on command. Also called a bistable multivibrator.

- flow coefficient** Product of the discharge coefficient and the velocity of approach factor; used in a flow meter calculation.
- flow nozzle** Flow meter consisting of a gradual concentric contraction from a larger diameter to a smaller throat diameter that is inserted into a pipe to create a measurable pressure drop proportional to flow rate.
- Fourier transform** Mathematical function that allows a complex signal to be decomposed into its frequency components.
- frequency bandwidth** The range of frequencies in which the magnitude ratio remains within 3 db of unity.
- frequency response** The magnitude ratio and phase shift of a system as a function of applied input frequency.
- full-scale output (FSO)** The arithmetic difference between the end points (range) of a calibration expressed in units of the output variable.
- fundamental frequency** Smallest frequency component of a signal.
- gain** Result of amplification or some multiplier of a signal magnitude; also used to refer to a constant multiplier for a transfer function block.
- galvanometer** Instrument that is sensitive to current flow through torque on a current loop; typically used to detect a state of zero current flow.
- gauge blocks** Working length standard for machining and calibration.
- gauge factor** Property of a strain gauge that relates changes in electrical resistance to strain.
- gauge length** Effective length over which a strain gauge averages strain during a measurement.
- ground** Signal return path to earth.
- ground loop** A signal circuit formed by grounding a signal at more than one point with the ground points having different voltage potentials.
- Hall effect** Voltage induced across a current-carrying conductor situated within a magnetic field. The magnetic field exerts a transverse force pushing the charged electrons to one side of the conductor.
- handshake** An interface procedure to control data flow between different devices that includes start and stop (hello and goodbye) signals.
- high-pass filter** A device that allows signal frequencies above the cut-off frequency to pass unaltered, while lower frequencies are attenuated.
- Hooke's law** The fundamental linear relation between stress and strain. The proportionality constant is the modulus of elasticity.
- hysteresis** A difference in the indicated value for any particular input value when approached going upscale as opposed to going downscale.
- immersion errors** Temperature measurement errors due to the measuring environment leading to differences between sensor temperature and the temperature being measured.
- impedance matching** Process of setting either the input impedance or the output impedance in a way to keep signal loading errors to an acceptable level.
- independent variable** A variable whose value is changed directly to cause a change in the value of a dependent variable.
- indicated value** The value displayed or indicated by the measurement system.
- input value** Process information sensed by the measurement system.
- insertion error** Any error brought on by the interaction between a sensor and the immediate environment in which it is installed.
- in situ** In measurements, this means installed in the system as intended for use.
- interference** Extraneous effect that imposes a deterministic trend on the measured signal.
- interferometer** Device for measuring length that uses interference patterns of light sources; provides very high resolution.
- interrupt** A signal to initiate a different procedure; analogous to raising one's hand.
- junction** For thermocouples, an electrical connection between two dissimilar materials.
- laminar flow element** Device that measures flow rate by the linear pressure drop versus flow rate relationship occurring when fluid travels through a tube or cluster of tubes under laminar flow conditions.
- least squares regression** Analysis tool used to generate a curve fit equation that minimizes the sum of the squares of the deviations between the predicted values of the curve fit and the data set on which the curve fit is based.
- line standard** Standard for length made by scribing two marks on a dimensionally stable material.
- linearity** The closeness of a calibration curve to a straight line.
- load cell** Sensor for measuring force or load.
- loading error** Error due to energy being extracted from the variable being measured by the very act of measurement so as to change the value measured.
- low-pass filter** A device that allows signal frequencies below the cut-off frequency to pass unaltered, while higher frequencies are attenuated.
- linear variable differential transformer (LVDT)** A sensor/transducer that provides a voltage output as a function of core displacement.
- Mach number** Ratio of the local speed to the speed of sound in the medium.
- magnitude ratio** The ratio of the values of output amplitude to the input amplitude of a dynamic signal.
- mass flow rate** Mass flow per unit time.
- measurand** Measured variable.

measured value A number assigned to the variable measured.

measured variable A variable whose value is measured; also known as the measurand.

mechatronics Subject area focused on the interaction between electrical and mechanical components of devices and the control of such devices.

measurement The act of assigning a specific value to the variable being measured.

metrology The science of weights and measures.

moiré patterns An optical effect resulting from overlaying two dense grids that are displaced slightly in space from one another.

monostable One-shot device that toggles on and then off on a single voltage command.

moving coil transducer A sensor that uses a displacement of a conductor in a magnetic field to sense velocity.

multiplexer An input/output (I/O) switch having multiple input signal lines but only one output signal line.

natural frequency The frequency of the free oscillations of an undamped system.

noise An extraneous effect that imposes random variations on the measured signal.

null mode Measuring method that balances a known amount against an unknown amount to determine the measured value.

Nyquist frequency One-half of the sample rate or sampling frequency.

obstruction flow meter Device that measures flow rate by the magnitude of the pressure drop arising by purposefully creating an abrupt area change in the flow.

ohmmeter An instrument for measuring resistance.

open-loop control Type of control action that does not use a sensor to measure the variable being controlled, such as by controlling room lights using a light switch timer.

operating conditions Conditions of the test, including all equipment settings, sensor locations, and environmental conditions.

optical pyrometer Nonintrusive temperature measurement device. Measurement is made through an optical comparison.

orifice meter Flow meter consisting of a flat plate with a hole in its center that fits between a pipe flange to create a pressure drop proportional to flow rate; also known as an orifice plate.

oscilloscope An instrument for measuring a time-varying voltage signal and displaying a trace; very high frequency signals can be examined.

outlier A measured data point whose value falls outside the range of reasonable probability.

output value The value indicated by the measurement system.

output stage Stage of a measurement system that indicates or records the measured value.

overall error Instrument uncertainty estimate based on the square root of the sum of the squares (RSS) of the uncertainties of all known instrument errors.

parallel communication Technique that transmits information in groups of bits simultaneously.

parameter The value defined by some functional relationship between variables related to the measurement.

particle image velocimetry Optical method that measures flow velocity by observing the distance traveled by fluid particles per unit time suspended within the fluid.

passband Range of frequencies over which the signal amplitude is attenuated by no more than 3 dB. See stopband.

Peltier effect Describes the reversible conversion of energy from electrical to thermal when a current flows through a junction of dissimilar materials.

phase shift A shift or offset between the input signal and the output signal representing the measured signal; may be expressed in terms of an angle.

photoelastic Describes a change in optical properties with strain.

pitot-static pressure probe Device used to measure dynamic pressure.

piezoresistance coefficient Constant that describes the change in electrical resistance with applied strain.

Poisson's ratio Ratio of lateral strain to axial strain.

pooled value Statistical value determined from separate data sets, such as replications, that are subsequently grouped together.

population The set representing all possible values for a variable.

potentiometer Refers either to a variable resistor or to an instrument for measuring small voltages with high accuracy.

potentiometer transducer Variable electrical resistance transducer for measurement of length or rotation angle.

precision The amount of dispersion expected with repeated measurements; archaic term used to describe the random uncertainty.

precision (instrument specification) Ultimate performance claim of instrument repeatability based on multiple tests conducted at multiple labs and on multiple units.

precision error See random error. Archaic term no longer used in measurements.

precision indicator Statistical measure that quantifies the dispersion in a reported value.

precision interval Interval evaluated from data scatter that defines the probable range of a statistical value and ignoring the effects of systematic errors.

primary standard The defining value of a unit.

prover Flow meter calibration device using some method placed in series with the candidate flow meter

- that accurately measures the volume of fluid passing per unit time.
- Prony brake** A historically significant dynamometer design that uses mechanical friction to dissipate and measure power.
- proving ring** An elastic load cell, which may be used as a local calibration standard.
- pyranometer** Optical instrument used to measure irradiation on a plane.
- quantization** Process of converting an analog value into a digital number.
- quantization error** An error brought on by the resolution of an A/D converter.
- radiation error** Temperature measurement insertion error caused by a radiative heat exchange between a temperature sensor and portions of its immediate environment not at the same temperature as the variable being measured.
- radiation shield** A device which reduces radiative heat transfer to a temperature sensor, to reduce insertion errors associated with radiation.
- radiometer** Device for measuring radiative source temperature using a thermopile detector.
- random error** The portion of error that varies randomly on repeated measurements of the same variable.
- random standard uncertainty** The random uncertainty estimated at the one standard deviation level or at the 68% probability level for a normal distribution.
- random uncertainty** Uncertainty assigned to a random error; contribution to combined uncertainty due to random errors.
- random test** Measurement strategy that sets a random order to the changes in the independent variable.
- randomization methods** Test methods used to break up the interference effects from extraneous variables by strategies that randomize the effects of those variables on the data set.
- range** The lower to upper limits of an instrument or test.
- recovery errors** Temperature measurement error in a high speed flowing gas stream related to the conversion of kinetic energy into a temperature rise at the sensor.
- reference junction** In reference to a thermocouple, it is the junction at which the temperature is known.
- repeatability** Instrument specification estimating the expected random uncertainty based on multiple tests within a given lab on a single unit.
- repetition** Repeating measurements during the same test.
- replication** Duplicating a test under similar operating conditions using similar instruments.
- reproducibility** Random uncertainty estimate based on multiple tests performed in different labs on a single unit.
- resistivity** Material property describing the basic electrical resistance of a material.
- resolution** The smallest detectable change in a measured value as indicated by the measuring system.
- resonance frequency** The frequency at which the magnitude ratio reaches a maximum value greater than unity.
- result** The final value determined from a set or sets of measurements.
- resultant** A variable calculated from the values of other variables.
- ringing frequency** The frequency of the free oscillations of a damped system; a function of the natural frequency and damping ratio.
- rise time** The time required for a first-order system to respond to 90% of a step change in input signal.
- rms value** Root-mean-square value.
- roll-off slope** Decay rate of a filter stopband.
- RTD** Resistance temperature detector; senses temperature through changes in electrical resistance of a conductor.
- root-sum-square value (RSS)** The value obtained by taking the square root of the sum of a series of squared values.
- rotating cusp meter** A type of positive displacement flow meter that measures volume flow rate by the rate at which fluid is displaced within alternating rotating cusps.
- sample** A data point or single value of a population.
- sample rate** The rate or frequency at which data points are acquired; reciprocal of sample time increment.
- sample statistics** Statistics of a variable determined from a set of data points whose set size is less than the population of that variable.
- sample time increment** The time interval between two successive data measurements. Reciprocal of sample rate.
- saturation error** Error due to an input value exceeding the device maximum.
- second-order system** A dynamic system model whose behavior includes inertia.
- Seebeck effect** Source of open circuit electromotive force in thermocouple circuits.
- seismic transducer** Instrument for measuring displacement in time, velocity, or acceleration; based on a spring-mass-damper system.
- sensitivity** The rate of change of a variable (y) relative to a change in some other variable (x), for example, dy/dx .
- sensitivity index** The sensitivity between two variables evaluated at some operating point and used to weight individual uncertainties in uncertainty propagation.
- serial communication** Technique that transmits information 1 bit at a time.
- sensor** The portion of the measurement system that senses or responds directly to the process variable being measured.

settling time The time required for a second-order system to settle to within $\pm 10\%$ of the final value of a step change in input value.

shielded twisted pair Describes electrical wiring that reduces mutual induction between conductors through twisting the conductors around each other, and which reduces noise through shielding.

signal Information in transit through a measurement system; often exists in electrical or mechanical form.

single-ended connection Two-wire connection scheme that measures the signal relative to ground.

signal conditioning stage Stage of a measurement system that modifies the signal to a desired magnitude and form.

signal-to-noise ratio Ratio of signal power to noise power.

single-sample uncertainty analysis Method of uncertainty analysis used to evaluate uncertainty when very few repeated measurements are made.

span The difference between the maximum and minimum values of operating range of an instrument.

stage Refers to a general component in a measurement signal flow that has a specific purpose.

standard The known or reference value used as the basis of a calibration. Also, a test method set by international agreement for quantifying some outcome or device performance.

static calibration Calibration method where the input value is held constant while the output value is measured.

static pressure Pressure sensed by a fluid particle as it moves with the flow.

static sensitivity The rate of change of the output signal relative to a change in a static input signal. The slope of the static calibration curve at a point. Also called the static gain. See sensitivity.

steady response A portion of the time-dependent system response that either remains constant with time or repeats its waveform with time.

step response System time response to a step change in input value.

stagnation pressure Pressure at the point where a flow is brought to rest. See total pressure.

stopband Range of frequencies over which the signal amplitude is attenuated by 3 dB or more. See passband.

strain Elongation per unit length of a member subject to an applied force.

strain gauge Sensor used to measure the strain on the surface of a part when under load.

strain gauge rosette Two or more strain gauges arranged at precise angles and locations relative to each other so as to measure differing components of strain.

stress Internal force per unit area.

stroboscope High-intensity source of light that can be made to flash at a precise rate. It is used to measure the frequency of rotation.

Student's t-distribution Sampling distribution that arises when estimating the mean of a population when the sample size is small.

systematic error The portion of error that remains constant in repeated measurements of the same variable. A constant offset between the indicated value and the actual value measured.

systematic uncertainty Uncertainty assigned to a systematic error. The uncertainty due to all the systematic errors affecting the result.

systematic standard uncertainty The systematic uncertainty estimated at the one standard deviation level or at the 68% probability level for a normal distribution. This value is often taken as being one-half the estimated systematic uncertainty.

temperature scale Establishes a universal means of assigning a quantitative value to temperatures.

theristor Temperature-sensitive semiconductor resistor.

thermocouple Wire sensor consisting of at least two junctions of two dissimilar conductors and used to measure temperature.

thermoelectric Refers to a type of device that indicates a thermally induced voltage.

thermopile A multiple junction thermocouple circuit designed to measure a particular temperature, an average temperature, or a temperature difference.

Thomson effect Describes the presence of a voltage arising through a temperature difference in a homogeneous conductor.

time constant System property defining the time required for a first-order system to respond to 63.2% of a step input.

time delay The lag time between an applied input signal and the measured output signal.

time response The complete time-dependent system response to an input signal.

total pressure Pressure sensed at a point where the flow is brought to rest without losses; sum of the static and dynamic pressures; isentropic value of stagnation pressure.

total sample period Duration of the measured signal as represented by the data set.

transducer The portion of measurement system that transforms the sensed information into a different form. Also, loosely refers to a device that houses the sensor, transducer and, often, signal conditioning stages of a measurement system.

transient response Portion of the time-dependent system response that decays to zero with time.

transit time flow meter Device that determines flow rate by measuring the time it takes for an ultrasonic

- wave to travel through the moving flow along a well-defined path.
- trigonometric series** Infinite series of trigonometric functions; applications include representing complex waveforms in terms of frequency content.
- true rms** Data-reduction technique that can correctly provide the rms value for a nonsinusoidal signal; a signal conditioning method that integrates the signal.
- true value** The actual or exact value of the measured variable.
- TTL (true-transistor-logic)** Switched signal that toggles between a high (e.g., 5 V) and a low (e.g., 0 V) state.
- turndown** Ratio of the highest flow rate to the lowest flow rate that a particular flow meter can measure within specification.
- type A uncertainty** An uncertainty value estimated from the statistics of a variable.
- type B uncertainty** An uncertainty value estimated by other than statistical methods.
- uncertainty** An estimate of probable error in a reported value.
- uncertainty analysis** A process of identifying the errors in a measurement and quantifying their effects on the value of a stated result.
- uncertainty interval** An interval about a variable or result that is expected to contain the true value.
- USB (universal serial bus)** A serial method of data transmission between a computer and peripherals using a four-wire cable.
- validation** Process or test to assess if test model data behave in the same way as the physical process the test simulates; can be used to assign uncertainty in the model.
- velocity of approach factor** A coefficient used in obstruction flow meter calculations that depends on the ratio of flow meter throat diameter to pipe diameter.
- venturi meter** In-line flow meter whose internal diameter narrows from the pipe diameter to a smaller diameter throat and then expands back to the pipe diameter so as to create a pressure drop proportional to flow rate.
- verification** Test designed to ensure that a measurement system as a whole or some portion of the system is working correctly; can be used to assign uncertainty values to aspects of a measurement system.
- vernier calipers** Tool for measuring both inside and outside dimensions.
- vernier scale** Technique that allows increased resolution in reading a length scale.
- volume flow rate** Flow volume per unit time.
- VOM** Acronym for volt-ohm meter.
- vortex flow meter** Device that measures flow rate by measuring the frequency of vortex shedding from a body placed within the flow.
- wheatstone bridge** Electrical circuit for measuring resistance with a high measure of accuracy and sensitivity.
- wobble meter** A type of positive displacement flow meter that measures fluid volume flow rate by the rate of fluid displaced within alternating known volumes created by oscillating disks.
- word** A collection of bits used to represent a number.
- zero drift** A shift away from a zero output value under a zero input value condition.
- zero-order system** A system whose behavior is independent of the time-dependent characteristics of storage or inertia.
- zero-order uncertainty** Random uncertainty estimate based only on a measurement system's resolution or finest increment of measure.

Index

A

Acceleration measurement, 504, 510, 515, 517
Accelerometer, 82, 83, 96, 98, 99, 103, 515, 516
 piezoelectric, 82, 515, 516
 vibrometer, 513
Accuracy, 17–18, 443
Acoustic wave speed, 407
Advanced-stage uncertainty, 176–182
 Nth-order analysis, 178–182
Aliasing, 260, 265, 266, 268, 284
Alloys, properties of, 315, 333, 336
Ammeter, 211, 212, 219, 324
Amontons, Guillaume, 309
Amplifier, 230–234, 236–237, 240, 247, 248, 253, 272, 284, 285, 288, 297, 408, 409, 490, 491, 546
bias, 235
charge, 236–237, 392
differential, 231–233, 235
feedback, 409
inverting, 233
linear scaling, 231
logarithmic, 231
noninverting, 233
operational, 231–234, 236, 237, 240, 247, 248, 272
Amplitude ambiguity, 266–268, 303
Analog-to-digital, 43, 217, 235, 260, 271, 273, 279, 348, 491, 517
 conversion, 217, 235, 271, 273–274, 279
 conversion error, 274–277, 279
 converter, 217, 235, 271, 273–274, 279
 dual slope, 280
 quantization error, 274–275
 ramp, 279–281
 saturation error, 275
 signal-to-noise, 275, 412
 successive approximation, 277–279, 287, 288
Angular velocity, 452, 522–524
 mechanical measurement, 522
 stroboscopic measurement, 522–524
Aperiodic, 44, 268
Apparent strain, 482–492
American Society of Mechanical Engineers. *See* ASME
ASME, 30, 162, 375, 428, 432, 435, 436, 532
Average value, 46, 118
 analog signal, 46, 47
 digital signal, 47

discrete time signal, 47
error, 18
moving, 72, 284

B

Balance
 null, 217, 218, 226, 282
Band-pass filter. *See* Filters, band-pass
Barometer, 379–380
Bernoulli, Daniel, 424, 432
Bernoulli effect, 427
Bessel filter. *See* Filter, Bessel
Best estimate, 173–174, 187, 188, 328
Beta ratio, 429, 437
Bias, 222, 231, 232, 235, 274, 347
Bias error, 170
Bimetallic thermometer. *See* Thermometer, bimetallic
Binary coded decimal, 270
Binary codes, 270, 271
Binary numbers, 44, 269–271, 273, 277
BIOS. *See* Basic input/Output system
Birefringence, 493
Bit, 239, 269, 271–283
Block, 10, 12
 diagrams, 546–547
 jumper, 285
Boltzmann's constant, 352, 360
Borda, Jean, 429
Brewster, Sir David, 493
Bridge circuits, 219–221, 229, 319–323, 476, 477, 480–482, 490
 balanced, 221
Callendar–Griffiths, 319, 320
deflection, 222–226
four-wire, 319, 320
loading error, 225
Mueller, 319, 320
null, 221–222
three-wire, 319
uncertainty, 221
Wheatstone, 219, 221–224, 226, 229, 319, 320, 325, 408, 455, 476, 477, 485, 491, 530
Bridge constant, 479. *See also* Bridge circuits, Wheatstone
Buffer, 294
Bus, 284, 288–289, 295–297
Butterworth filter. *See* Filter, Butterworth
Byte, 269

C

Calibration, 5, 11, 15–23
 curve, 15–17, 20–22, 84, 144, 459

deviation, 17
dynamic, 16, 392–393
error, 168–169, 177, 180
random, 21
sequential, 20
static, 15, 22, 392
temperature. *See* Temperature, calibration
Capillary tube viscometer, 445
Castelli, Benedetto, 424
Catch and weigh flow measurement, 459
Celsius, Anders, 310
Celsius scale, 311
Central tendency, 120–122, 125, 126
Charge amplifier, 236–237
Chauvenet's criterion. *See* Outlier
Chi-square distribution, 135–139
Coaxial cable, 252
Common mode voltage (CMV), 251, 290, 292
Compact disk player, 44
Complex periodic waveform, 44, 266, 405
Compliance, 401–405
Concomitant methods, 14, 19, 171
Conduction errors, 357–360
Confidence interval, 118, 119, 133, 142, 144–149, 184, 198
Conservation of mass, 396, 427, 428
Continuous variable, 42
Control of variables, 7
Control surface, 427, 428, 446, 455
Control volume, 427, 428
Coriolis, 455
 flow meter, 456–459
 turndown, 459
 uncertainty, 459
Coriolis, Gaspard de, 456
Correlation, 15
 coefficient, 144, 197, 438, 439
 function, 412
 photon, for LDA, 412
Coupled systems, 109–111
Critical pressure ratio, 440
Critically damped system, 96
Current:
 alternating, ac, 61, 212–214
 ammeter, 211, 212
 analog measurement, 210
 direct, dc, 48–49, 210–212
Current loop: 4–20 mA, 237

D

D/A converter. *See* Digital-to-analog converter

- D'Arsonval movement, 210–212, 214
 Data acquisition, 260
 controller, 287
 plug-in board, 288–289
 Data-acquisition error, 169, 190
 Data-acquisition system, 260, 283–288
 Data-reduction error, 169–170, 186
 dc component, 46
 dc offset, 46, 48
 da Vinci, Leonardo, 424, 448
 Dead volume, 401, 404
 Deadweight tester, 384–386, 392, 395
 Deflection mode, 211, 212, 323
 Degree, 310
 Degrees of freedom, 130, 131, 134–136,
 138, 139, 141, 145, 148, 170, 184,
 185, 188, 189, 191, 192, 194. *See also* Welch–Satterwaite estimate
 Derived units, 26, 28
 Design-stage uncertainty, 164–168, 176,
 180, 322, 323, 479
 Design of experiments, 6, 10, 14
 Deviation plot, 17
 DFT. *See* Fourier transform-discrete
 Differential-ended connection, 290–292,
 297, 347
 Digital:
 signals, 43, 44, 47, 260, 287, 518
 voltmeter, 217, 220, 222, 282
 Digital-to-Analog converter (D/A),
 271–273, 287
 Dimension, 23
 base, 24–26
 derived, 27
 electrical, 27–28
 length, 25
 mass, 24
 temperature, 25
 time, 24–25
 Direct memory access, 579
 Discharge coefficient, 429–433, 443
 Discrete Fourier transform, 65–69, 261
 amplitude ambiguity, 266–268
 leakage, 268
 resolution, 66, 268
 Discrete time signal, 42, 65, 263, 266
 Displacement measurement, 510, 529
 LVDT, 508
 potentiometer, 505
 Distortion, 106, 215, 515
 Doppler
 anemometry. *See* laser Doppler
 anemometer
 effect, 410, 453
 flow meters, 453–454
 shift, 410, 411
 Doppler, Johann, 410
 Dynamic calibration, 16, 392, 393
 Dynamic error, 94, 95, 103, 242, 244, 245,
 514
 Dynamic pressure. *See* Pressure, dynamic
 Dynamometer, 529, 531
 absorbing, 531
 ac and dc generators, 532
 cradled, 531–533
 eddy current, 532
 engine, 529
 waterbrake, 532–533
E
 Earth ground, 250, 251
 Elastic behavior of materials, 467
 Electrodynamometer, 212, 214
 Electromagnetic flow meter, 446–448
 uncertainty, 448
 Electromotive force (emf), 27, 213, 331,
 446, 507
 Electronic reference junction, 334
 Emissive power, 351–352
 End standard. *See* Standard, end
 Error:
 bias. *See* Error, systematic
 correlated, 195–197
 random, 197
 systematic, 195–197
 hysteresis, 20
 instrument, 23, 165, 171
 linearity, 21–22
 loading, 212, 226
 overall instrument, 23
 precision. *See* Error, random
 random, 18–20, 31, 88, 118, 119, 132,
 142, 144, 161–164, 171–172, 183,
 184
 repeatability, 22
 reproducibility, 23
 sensitivity, 22
 systematic, 18–20, 125, 126, 132–134,
 152, 162, 163, 170–171, 183, 184,
 186, 192, 194
 temperature measurement, 309
 zero shift, 22, 386
 Error fraction, 86–88, 98
 Euler formulas, 56, 61
 Euler, Leonhard, 424
 Expansion factor, 429–430, 432, 433
 Experimental design, 6, 10, 14
 External memory, 239
 Extraneous variable, 7–13, 177, 314, 356
F
 Fahrenheit, Gabriel D., 310
 Faraday, Michael, 446, 506
 Feedback control, 5, 288, 537, 541, 546
 FFT. *See* Fourier transform, fast
 Filter:
 active, 240, 247–250
 analog, 240, 284
 anti-alias, 298
 band, 102
 bandpass, 239–241, 248, 249
 Bessel, 241, 247, 249, 250
 Butterworth, 240–250
 design, 240, 241, 243
 high-pass, 239–241, 244, 246–250
 Linkwitz–Riley, 246
 low-pass, 239, 240, 242, 244, 246,
 248–250, 264
 multiple, 241
 notch, 239, 240
 passive, 240, 241
 roll-off, 241
 Sallen–Key, 249, 250
 Finite statistics, 130
 sample mean, 130, 132
 sample standard deviation, 130
 standard deviation of the means,
 132–134
 First-order systems, 85–88, 90–95, 97,
 104, 105, 111, 241, 405, 541
 First-order uncertainty, 178, 179, 181
 Flip-flop, 237–239
 Flow coefficient, 8, 429
 Flow meter. *See also* listings by type.
 accuracy, 423
 placement, 442
 pressure loss, 443
 prover, 459
 selection, 443
 Flow nozzle, 427, 432
 ASME long radius, 432
 discharge coefficient, 433
 expansion factor, 433
 pressure loss, 431
 pressure taps, 433
 uncertainty, 433
 Flow rate.
 actual, 460
 mass, 423, 454
 standard, 460
 volume, 423
 Folding diagram, 264, 265
 Force measurement, 525–529
 Forcing function, 82, 107, 401, 510, 544,
 553
 Fourier:
 analysis, 50
 coefficients, 56, 68
 cosine series, 58
 frequency content, 16, 53
 harmonics, 53
 series, 53, 56
 sine series, 58
 Fourier transform, 63, 65
 amplitudes, 63, 65
 amplitude spectrum, 65
 discrete. *See* Discrete Fourier
 inverse, 64
 power spectrum, 65
 transform fast, 66
 Francis, James, 432
 Freeman, John Ripley, 435
 Frequency, 16, 24, 41, 49, 52, 56, 63, 69

- alias, 263
 bandwidth, 94, 102, 415
 circular, 25, 51
 cut-off, 239, 241
 cyclical, 25
 distribution, 121
 fundamental, 53
 natural, 98, 392
 Nyquist, 264
 response, 93
 determination of, 95
 Frontinius, Sextus, 424
Function:
 aperiodic, 44
 even, 57
 odd, 57
 periodic, 52
- G**
 Galvanometer, 211
 Gauge blocks, 192
 Gauge factor, 473, 475
 Gauge length, 472
 Gaussian distribution. *See* Normal distribution
 General purpose interface bus (GPIB), 295
 Goodness-of-fit test, 138
 Gosset, William, 131
 Ground loops, 250, 251, 356
 common-mode voltage, 251
- H**
 Handshake, 293, 294
 Harmonics, 53, 70, 264, 507
 Harmonization, 53, 56
 Hero of Alexandria, 423
 Herschel, Clemens, 432
 Higher-order uncertainty, 177
 High-pass filter. *See* Filter, high-pass
 Histogram, 121
 Hooke's law, 467
 Hot-film sensor, 409, 415
 Hot-wire sensor, 408, 410, 415
 Hypsometer, 370
 Hysteresis, 20
- I**
 Impedance matching, 226
 Inertance, 400
 Infinite statistics, 130
 Input, 4, 15
 Insertion error, 356–357
 Instrument error. *See* Error, instrument
 Instrument precision (specification), 23
 Instrument uncertainty, 23, 164–166, 178
 Interference, 9–12, 14
 Interferometer, 497
 Interlaboratory comparison, 170, 171
 International Temperature Scale of 1990 (ITS-90), 312
- Interpolation. *See* Temperature, interpolation
 Interrupt, 289
 Invar, 315
 Isoclinics, 495
 International Standards Organization. *See* ISO
 ISO, 30, 432
 guide to uncertainty in measurements, 162
 ITS-90. *See* International Temperature Scale of 1990
- K**
 Kiel probe, 397
 King's law, 408
- L**
 Laboratory reports, 563
 Laminar flow meter, 445
 turndown, 445
 uncertainty, 446
 Laser Doppler anemometer, 410–412, 415
 Least squares method, 91n, 140–143, 147
 Leibniz, Gottfried Wilhelm, 61n
 Linear variable differential transformer, 505, 506
 excitation, 508
 Linkwitz–Riley filter. *See* Filter, Linkwitz–Riley
 Linnaeus, Carolis, 310
 Liquid-in-glass thermometer. *See* Thermometer, liquid-in-glass
 Load cell, 475, 525–529
 piezoelectric, 525–526
 strain gauge, 475, 525
 Loading error, 212, 217, 221, 226–230, 282, 298, 319, 338, 386, 525
 interstage, 226, 228–230
 voltage dividing circuit, 226–228
 Low-pass filter. *See* Filter, low-pass
 Lumped parameter, 80–82, 84, 89, 400, 402, 403
 LVDT. *See* Linear variable differential transformer
- M**
 Mach number, 364–365, 407, 450
 Magnitude ratio, 93–95, 100–101, 104, 105, 110, 111, 239–242, 244, 245, 249, 515
 Magnitude, signal, 5, 42–44, 80, 214, 230
 Manometer, 380
 inclined, 382, 383
 micromanometer, 381, 382
 uncertainty, 382
 U-tube, 381–383
 Mass, 24
 Mass flow meter, 454–459
 Coriolis, 456–459
 thermal, 455–456
- Mass flow rate, 423, 424, 440, 454–455, 457–460
 McLeod gauge, 378–379, 392
 uncertainty, 379
 Mean value, 46, 47, 118–120, 125, 126, 130, 132–135, 140, 147, 149, 152, 171–174, 185, 190
 digital signal, 47
 discrete time signal, 47
 sample mean, 119
 true mean, 120
 Measurand, 119
 Measured variable, 2, 119–120
 Measurement system, 2, 187
 first-order, 85, 241
 general model, 81
 second-order, 95
 zero-order, 83
 Measurement uncertainty:
 random, 182
 systematic, 183
 Memory, 269
 Metals, properties of, 569
 Method of least squares. *See* Least squares
 Metrology, standard, 162
 Modem, 293
 Modified three-sigma test, 147
 Modulus of elasticity, 403, 467, 468, 527
 Moire strain measurement. *See* Strain measurement, Moire
 Monostable circuit, 238
 Monte Carlo, 150
 method, 176
 numerical tolerance, 176
 simulations, 119, 150–152, 176
 Moving coil transducer, 520–522
 Mueller bridge. *See* Bridge circuits, Mueller
 Multiple measurement uncertainty, 182–195
 Multiplexer, 286
 Multivibrator, 237–239
- N**
 National Institute of Standards and Technology. *See* NIST
 Network model, 401
 Newton, Sir Isaac, 424
 NIST, 313, 319, 336, 337, 348, 349, 460
 NIST-RTD, 319
 NIST-temperature, 314
 Noise, 7, 9, 11, 234, 237, 251, 280, 290, 300, 348, 448, 519, 525
 Nondeterministic signal, 45
 Normal distribution, 126, 129, 130, 132, 136, 138, 139, 151
 Normal error function, 126
 Nth-order uncertainty, 178, 179, 181
 Nyquist frequency. *See* Frequency, Nyquist

O

Obstruction meter, 427
selection, 441
standards, 430

Ohmmeter, 219

On-track effects, 406

Optical cable, 252

Optical fiber thermometer, 355–356

Optical pyrometer, 355

Optical strain measurements, 492

Orifice meter, 430

discharge coefficient, 430

expansion factor, 430

pressure loss, 431

tap location, 430

uncertainty, 430

Oscilloscope, 215–217

Outlier, 147

Chauvenet's criterion, 147, 148

three-sigma test, 147

Output, 15, 41

Output stage, 4

Overall instrument error, 23

Overdamped system, 96

P

Parallel communication, 284, 293, 296

Parameter, 8

Parity, 294

Particle image velocimetry, 413, 415

Peltier coefficient, 332

Peltier effect, 331, 332

Peltier, Jean Charles Athanase, 332

Pendulum scale, 44

Period, 9, 24, 27, 46, 47

Periodic function, 50, 52, 53, 59

Perturbation, sequential, 174–176

Phase

angle, 50, 57

linearity, 106

shift, 66, 93, 100, 106, 110

Photoelastic strain measurements. *See*

Strain measurements, photoelastic

Piezoelectric, 82, 236, 391, 515, 516, 527, 528

Piezoresistance coefficient, 470, 475

Pitot-static tube, 405

uncertainty, 406

Pitot tube (Prandtl), 397

Planck's constant, 352

Platinum resistance thermometer. *See*

Thermometer, platinum resistance

Poiseulle, Jean, 445

Poisson's ratio, 389, 468, 470

Polariscope, 493–495

Polarization, 411, 492, 493

Pooled sample mean, 134–135

Pooled standard deviation, of the means, 135

Pooled statistics, 134–135

Pop test, 393, 394

Population, 125, 129, 130, 161, 172

Positive displacement flow meter, 446, 454, 459, 460
uncertainty, 454, 459

Potentiometer, 217–218. *See also*
Displacement measurement,
potentiometer

Power measurement, 529–530

Power spectrum, 65

Prandtl tube, 398, 399

Precision error, 171n

Precision estimate
of the slope, 144
of the zero intercept, 144

Precision interval, 130, 131, 136, 137

Pressure

absolute, 84, 376, 378

differential, 376, 380, 381, 383, 390, 439

dynamic, 389, 396, 397, 406, 407

freestream, 397

gauges, 179, 237, 292, 390, 449, 469, 471, 475, 479, 482, 483, 485, 488, 525, 529. *See also* Pressure, transducer

head, 377

reference instruments, 378

reference standards, 28

static, 395, 398–399, 401

total, 397, 406

Pressure transducer

Bourdon tube, 386, 387

calibration, 11, 15–18, 28, 378, 392

capacitance, 390

compliance, 404

dead volume, 401

diaphragm, 389

linear variable displacement, 388

piezoelectric, 391, 392

piezoresistive, 390

potentiometric, 388

uncertainty, 396

Pressure elements

bellows, 388

Bourdon tube, 386

capacitance, 390

capsule, 388

diaphragm, 389

strain gauge, 389–390

Primary standards, 23–24

Probability, 118

density, 119

function, 120–122

Prony brake, 530, 531

Propagation of error, 172

Propagation of uncertainty, 188

root-sum-square (RSS) method, 174

uncertainty in the result, 188

Proving ring, 525, 527–529

Pyranometer, 354

Q

Quantization, 43–44, 273–274
error, 274–275

R

Radiation

blackbody, 355

detectors, 353

emissive power, 351, 352

shield, 362

temperature measurement, 351, 352

wavelength distribution, 352
Radiative temperature measurement, 351, 352

Radiometer, 353, 354

RAM. *See* Random access memory

Random access memory (RAM), 294

Random calibration, 21

Randomization methods, 9

Random test, 10, 20

Random uncertainty. *See* Uncertainty, random

Random variable, 120

Range, 16, 20

full-scale-operating (FSO), 16, 20

Rayleigh relation, 407

Recovery factor, 363, 364

Rectangular distribution, 150, 151, 177, 198
standard uncertainty, 177

Reference junction, 333–335

compensation, 335

Register, 269

Regression analysis, 139–140

Repeatability, 18, 20, 22, 168, 171

Repetition, 13

Replication, 13, 14, 134

Replication-level analysis, 171

Reproducibility, 23

Resistance

analog measurement, 219–226

dimensions, 27

fluid, 313, 314

temperature detector, 315, 316

construction, 316

platinum, 317

thin-film, 323

Resistivity electrical, 470

temperature coefficient of, 315

Resolution, 16–18, 164, 171, 177, 180, 274, 275, 282, 344

Resonance, 101–102

band, 101–102

frequency, 101–102, 111, 516

Reynolds number, 8, 364, 406, 425, 429, 430, 437, 445, 446, 449, 450, 452

Ringing frequency, 97–99, 102

Rise time, determination of, 98–99

ROM. *See* Read-only memory

Root-mean-square

analog signal, 47

- digital signal, 47
 discrete time signal, 47
 value, 47
 Root-sum-square method, 164, 321
 Rotameter, 451
 turndown, 452
 uncertainty, 452
 Rotating vane flowmeter, 454
 RTD. *See* Resistance temperature detector
 Ruge, Arthur, 469
- S**
- Sample, 119, 120
 mean value, 130
 standard deviation, 130
 standard deviation of the mean, 132
 variance, 130
 Sample and hold circuit, 235, 279
 Sampling, 42, 43, 47, 119, 130, 260, 261
 rate, 42, 43, 236
 theorem, 262, 263, 266
 time period, 261
 Sampling convolution, 47
 Second-order systems, 95
 Second power law, 175
 Seebeck coefficient, 331
 Seebeck effect, 331
 Seebeck, Thomas Johann, 331
 Seismic transducer, 510
 Sensitivity error, 21–23, 165
 Sensitivity index, 174, 175, 189
 Sensor, 3, 4
 Sequential perturbation, 174, 176
 Sequential test, 20
 Serial communication, 293, 294
 Settling time, 98
 determination of, 98, 99
 Shaft power, 529–531
 Shielding, 250
 Shock measurement, 516
 piezoelectric, 516
 Shock tube, 393
 Shunt balancing, 477
 Shunt circuit, 285
 Signal, 41
 ac component, 46, 48
 analog signal, 42, 43, 47, 65, 230, 234,
 239, 261, 263, 290
 averaging period, 284
 conditioning, 4, 5, 209, 215,
 230, 234, 239, 275, 285,
 290, 292
 dc component, 46, 47
 digital, 43, 47, 239, 260, 274, 287, 303
 discrete time, 42, 43, 47, 65, 260, 261,
 263, 266
 frequency, 25, 42, 49, 64, 69, 92, 93,
 246, 252, 411
 input, 41–46
 magnitude or amplitude, 41
 output, 41–46
- sampling, 42, 261
 waveform, 41–42, 106, 269
 Signal classification
 analog, 42
 aperiodic, 43
 complex periodic, 44
 deterministic, 44
 digital, 42
 discrete time, 42–43
 dynamic, 42
 nondeterministic, 45
 static, 44
 steady periodic, 44
 Simmons, Edward, 469
 Single-ended connection, 290
 Single-measurement uncertainty analysis, 177
 Sonic nozzle, 440
 discharge coefficient, 441
 uncertainty, 441
 Source
 random limit, 171
 systematic limit, 170
 Span, 16
 Spectrum
 amplitude, 65
 power, 65
 Stagnation streamline, 396, 449
 Standard atmosphere, 311, 377
 Standard deviation, 22, 125, 130, 132
 of the means, 132
 Standard error of the fit, 141, 144–146,
 186
 Standards, 23
 hierarchy, 28
 primary, 23
 temperature, 310
 test, 30
 Standardized normal variate, 126
 Static calibration, 15, 84, 392
 Static pressure. *See* Pressure, static
 Static sensitivity, 16, 83
 determination of, 16, 84, 110, 381,
 447
 Static temperature. *See* Temperature,
 static
 Steady response, 86, 88, 92, 93, 98
 Steady signal, 117
 Step function, 85, 97
 Strain, 466
 apparent, 482
 axial, 467, 468, 474, 488
 lateral, 467–469
 Strain gauge, 469
 bonded resistance, 469
 bonding, 473
 bridge constant, 479
 circuits, 476
 configurations, 483
 construction, 472
 dynamic response, 492
 foil, 472
 gauge factor, 473
 gauge length, 472, 486
 hysteresis, 487
 load cell, 525
 metallic, 470
 multiple, 390
 resistance, 389, 390
 rosettes, 487–489
 semiconductor, 475
 temperature compensation, 485
 transverse sensitivity, 473, 474
- Strain measurement
 Moire, 495
 photoelastic, 493
 resistance, 469
 Strain optical coefficient, 494
 Stress, 468
 biaxial, 469
 Stroboscope, 522
 harmonic techniques, 523
 Strouhal number, 448–450
 Student's t distribution, 131
 Superposition, 12, 44, 63, 107
 Systematic uncertainty. *See* Uncertainty,
 systematic
 System response, 79
 frequency, 92, 98
 steady, 83, 512
 time, 83
 transient, 86, 92, 96, 97, 402
- T**
- Technical writing, 30, 163
 Temperature, 25
 absolute, 25, 312, 360
 calibration, 314, 324, 337, 351
 compensation, 292, 335, 482
 dynamic, 363
 fixed points, 311
 interpolation, 25
 radiative, 351
 scales, 312
 stagnation, 363
 standards, 25, 460
 static, 363, 364
 thermal expansion, 4, 313, 314
 thermodynamic, 25, 312
 thermoelectric, 330–350
 total, 363, 365
 t estimator, 131, 145
 Test plan. *See* Measurement plan
 Thermal anemometer, 408, 409, 414,
 415
 Thermal flow meter, 455
 turndown, 455
 uncertainty, 455
 Thermistor, 323
 circuit, 324
 dissipation constant, 325, 327
 zero-power resistance, 325

- Thermocouple, 330
 applications, 346
 circuit, 333
 data acquisition, 347
 laws, 333
 parallel, 346
 reference functions, 342
 standards, 336, 337, 339
 tolerance limits, 337
 type, 337
 voltage measurement, 346, 347
- Thermoelectric temperature measurement, 330–350
- Thermometer
 bimetallic, 313
 complete immersion, 314
 electrical resistance, 315
 liquid-in glass, 311, 313
 optical fiber, 355, 356
 partial immersion, 314
 platinum resistance, 313, 318
 radiation, 351
 total immersion, 314
- Thermophysical properties (table), 570–573
- Thermopile, 345, 346, 353, 354
- Thomson coefficient, 333
- Thomson effect, 331, 332
- Thomson, William (Lord Kelvin), 25
- Three sigma test, 147
- Time constant, 87, 90
 determination of, 87
- Time delay, 93, 94, 107, 247, 412
- Time response, 80, 86, 87, 92, 97, 99, 105, 112, 113, 115, 353, 552, 553
- Torque measurement, 529, 530
 rotating shaft, 529
- Torricelli, Evangelista, 379, 431
- Total pressure. *See* Pressure, total
- Transducer, 3, 4
- Transfer function, 104
- Transient response, 86, 92, 96, 97, 105, 110
- Transit-time flowmeter, 453
- Transmission line effect on pressure measurement, 401
 gases, 403
 liquids, 403
 lumped parameter, 80–82, 84, 89, 213, 401–403
- Triangular distribution, 123
- Trigonometric series, 52, 53, 56, 57, 61
- True value, 17, 118, 119
- Turbine meter, 452
 turndown, 453
 uncertainty, 453
- Turndown, 443
- Twisted pair wiring, 252, 291, 297
- U**
- Uncertainty, 18, 19, 23, 142, 161
 advanced-stage. *See* Advanced-stage uncertainty
 combined standard, 184, 188, 189, 195, 198
 design-stage. *See* Design-stage uncertainty
 elemental, 184
 expanded, 184–186, 188, 189, 192
 instrument, 23, 164–166, 382, 385, 506
*N*th order. *See* *N*th order uncertainty
 overall, 19, 179, 443, 532
 standard
 random standard, 133, 171, 183–189, 191–195, 197, 438–440
 systematic standard, 170, 183, 184, 186, 188, 189, 191, 194–196, 203, 427
 random, 19, 23, 31, 118, 134, 145, 172, 186, 190, 204
 systematic, 19, 163, 164, 170, 185, 186, 189, 196, 197
- nonsymmetric interval, 197
- Uncertainty analysis, 161–198
- Under-damped system, 97, 98, 102, 392
- Unit, 23
- Universal serial bus (USB), 288, 295
- USB. *See* Universal serial bus
- U.S. Engineering Unit System, 24
- V**
- Variable
 controlled, 7
 dependent, 7
 extraneous, 7, 9, 177
 independent, 7
- Variance, 125, 126
- Velocity
 fluid, measurement, 363, 401, 405, 424
 freestream, 397
 linear, 517
 uncertainty, 406
- Velocity of approach factor, 429, 437, 438
- Vena contracta, 428–430
- Venturi, Giovanni, 432
- Venturi meter, 431
 discharge coefficient, 432
 expansion factor, 432
 uncertainty, 432
- Vibration measurement, 509, 510, 513, 515
- Vibrometer, 213
- Viscosity
 absolute, 574
 kinematic, 406, 425, 452, 575
- Voltage
 analog comparator, 279
 analog measurement, 273–277
 digital measurement, 271
 follower, 232
 oscilloscope. *See* Oscilloscope
 potentiometer. *See* Potentiometer
- Voltage divider, 217
 loading error, 226–228
- Volume flow rate, 425, 426, 428, 437, 451, 455
- von Karman, Theodore, 448
- Vortex flow meter, 448
 shedder shape, 450
 turndown, 452
 uncertainty, 452
- W**
- Water, thermophysical properties, 572
- Waveform, 41
 analog, 42, 268
 classification, 42, 45
 complex periodic, 44, 45, 266
 digital, 44
 discrete time, 43
 Fourier analysis, 63
- Weisbach, Julius, 440
- Welch-Satterwaite estimate, 184, 189
- Wheatstone bridge. *See* Bridge circuits
- Wires, connecting, 250
- Wobble flow meter, 454, 457
- Word (digital), 270
- Y**
- Young's modulus, 467
- Z**
- Zero-order system, 83, 546
- Zero-order uncertainty, 164, 165, 177, 179, 277, 421
- z variable, 126, 130, 131

CONVERSION FACTORS*

MASS

$$1 \text{ lb}_m = 0.4536 \text{ kg}$$
$$1 \text{ slug} = 14.5939 \text{ kg}$$

LENGTH

$$1 \text{ inch} = 0.0254 \text{ m}$$
$$1 \text{ ft} = 0.3048 \text{ m}$$
$$1 \text{ km} = 1000 \text{ m} = 1 \times 10^3 \text{ m}$$
$$1 \text{ cm} = 0.01 \text{ m} = 0.3937 \text{ in.} = 0.0328 \text{ ft}$$
$$1 \text{ mm} = 0.001 \text{ m} = 1 \times 10^{-3} \text{ m}$$
$$1 \mu\text{m} = 0.000001 \text{ m} = 1 \times 10^{-6} \text{ m}$$
$$1 \text{ nm} = 0.000000001 \text{ m} = 1 \times 10^{-9} \text{ m}$$
$$1 \text{ mi} = 5280 \text{ ft} = 1.6093 \text{ km}$$
$$1 \text{ l.y.} = 9.4605 \times 10^{15} \text{ m}$$

AREA

$$1 \text{ ft}^2 = 0.0929 \text{ m}^2$$
$$1 \text{ cm}^2 = 1 \times 10^{-4} \text{ m}^2 = 0.155 \text{ in.}^2$$

VOLUME

$$1 \text{ L} = 1000 \text{ cm}^3 = 0.2642 \text{ gal} = 1 \times 10^{-3} \text{ m}^3$$
$$1 \text{ gal} = 231.0 \text{ in.}^3 = 0.1337 \text{ ft}^3$$
$$1 \text{ gal} = 3.7854 \text{ L} = 0.003785 \text{ m}^3$$
$$1 \text{ ft}^3 = 28.3168 \text{ L} = 0.0283 \text{ m}^3$$

TIME

$$1 \text{ min} = 60 \text{ s}$$
$$1 \text{ h} = 60 \text{ min} = 3600 \text{ s}$$
$$1 \text{ day} = 8.640 \times 10^4 \text{ s}$$

FORCE

$$1 \text{ N} = 1 \text{ kg}\cdot\text{m/s}^2 = 1 \times 10^5 \text{ dynes}$$
$$1 \text{ lb} = 4.4482 \text{ N}$$
$$1 \text{ kg}_f = 9.8067 \text{ N}$$

PRESSURE OR STRESS

$$1 \text{ Pa} = 1 \text{ N/m}^2$$
$$1 \text{ lb/in}^2 = 6894.757 \text{ Pa}$$
$$1 \text{ atm} = 14.6959 \text{ lb/in.}^2 = 760 \text{ Torr}$$
$$= 101,325 \text{ Pa}$$
$$1 \text{ bar} = 14.5038 \text{ lb/in.}^2 = 1 \times 10^5 \text{ Pa}$$
$$= 750 \text{ Torr}$$
$$1 \text{ dyn/cm}^2 = 0.10 \text{ Pa}$$
$$1 \text{ inch Hg} = 3386.388 \text{ N/m}^2$$
$$1 \text{ inch H}_2\text{O} = 2.54 \text{ cm H}_2\text{O} = 249.089 \text{ Pa}$$
$$= 0.0361 \text{ lb/in.}^2$$
$$1 \text{ Torr} = 1 \text{ mm Hg} = 133.322 \text{ Pa}$$
$$1 \mu\text{strain} = 10^{-6} \text{ m/m} = 10^{-6} \text{ in/in}$$

TEMPERATURE

$$\text{K} = ^\circ\text{C} + 273.15$$
$$1^\circ\text{C} = 1.8^\circ\text{F} = 1 \text{ K}$$
$$^\circ\text{F} = 1.8^\circ\text{C} + 32$$
$$^\circ\text{R} = ^\circ\text{F} + 459.67$$

VOLUME FLOW RATE

$$1 \text{ gal/min} = 0.00223 \text{ ft}^3/\text{s} = 0.06309 \text{ L/s}$$
$$1 \text{ m}^3/\text{min} = 35.315 \text{ ft}^3/\text{min} = 1 \times 10^6 \text{ cm}^3/\text{min}$$

ANGLE

$$1^\circ = 0.01745 \text{ rad}$$
$$1' = 2.909 \times 10^{-4} \text{ rad}$$
$$1 \text{ rad} = 0.1592 \text{ revolutions}$$

ROTATION

$$1 \text{ rev/s} = 2\pi \text{ rad/s} = 6.2832 \text{ rad/s}$$
$$1 \text{ rpm} = 1 \text{ rev/min} = 0.1047 \text{ rad/s}$$

FREQUENCY

$$1 \text{ Hz} = 2\pi \text{ rad/s}$$

*Many of these conversion factors have been rounded off.

MOMENT OR TORQUE

$$1 \text{ lb-ft} = 1.3558 \text{ N-m}$$

POWER

$$\begin{aligned}1 \text{ W} &= 1.0 \text{ J/s} = 860.42 \text{ cal/hr} \\1 \text{ hp} &= 550.0 \text{ ft-lb/s} = 745.6998 \text{ W} \\1 \text{ kW} &= 1 \times 10^3 \text{ W} \\1 \text{ Btu/hr} &= 778.1692 \text{ ft-lb/hr} = 0.2931 \text{ W}\end{aligned}$$

ENERGY

$$\begin{aligned}1 \text{ J} &= 1.0 \text{ N-m} = 1 \times 10^7 \text{ ergs} \\1 \text{ erg} &= 1 \text{ dyne-cm} \\1 \text{ cal} &= 4.1868 \text{ J} \\1 \text{ ft-lb} &= 1.3558 \text{ J} \\1 \text{ Btu} &= 1055.0558 \text{ J}\end{aligned}$$

VISCOSITY

$$\begin{aligned}1 \text{ lb-s/ft}^2 &= 47.8790 \text{ N-s/m}^2 \\1 \text{ centipoise} &= 0.01 \text{ dyne-s/cm}^2 = 0.001 \text{ Pa-s}\end{aligned}$$

SPECIFIC HEAT

$$1 \text{ Btu/lb}_m \cdot {}^\circ\text{F} = 4.1868 \text{ kJ/kg} \cdot {}^\circ\text{C}$$

GAS CONSTANT

$$1 \text{ ft-lb/lb}_m \cdot {}^\circ\text{R} = 5.382 \text{ J/kg-K}$$

THERMAL CONDUCTIVITY

$$1 \text{ Btu/hr-ft} \cdot {}^\circ\text{F} = 1.7295 \text{ W/m} \cdot {}^\circ\text{C}$$

HEAT TRANSFER COEFFICIENT

$$1 \text{ Btu/hr-ft}^2 \cdot {}^\circ\text{F} = 5.6786 \text{ W/m}^2 \cdot {}^\circ\text{C}$$

BULK MODULUS

$$1 \times 10^6 \text{ psi} = 6.895 \times 10^9 \text{ Pa}$$

PHYSICAL CONSTANTS

$$\begin{aligned}\text{Standard Acceleration of Gravity} \\g &= 9.80665 \text{ m/s}^2 = 32.1742 \text{ ft/s}^2\end{aligned}$$

$$\begin{aligned}\text{Speed of Light} \\c &= 2.998 \times 10^8 \text{ m/s}\end{aligned}$$

$$\begin{aligned}\text{Planck's Constant} \\h_p &= 6.6261 \times 10^{-34} \text{ J-s}\end{aligned}$$

$$\begin{aligned}\text{Stefan-Boltzmann Constant} \\\sigma &= 5.6704 \times 10^{-8} \text{ W/m}^2 \cdot \text{K}^4 \\&= 0.1712 \times 10^{-8} \text{ Btu/h-ft}^2 \cdot {}^\circ\text{R}^4\end{aligned}$$

$$\begin{aligned}\text{Universal Gas Constant} \\R &= 8.3143 \text{ J/gmole-K} \\&= 1.9859 \text{ Btu/lbmole-}^\circ\text{R}\end{aligned}$$

PREFIXES FOR QUANTITY STATEMENTS

10^{18}	exa	E	1,000,000,000,000,000,000
10^{15}	peta	P	1,000,000,000,000,000
10^{12}	tera	T	1,000,000,000,000
10^9	giga	G	1,000,000,000
10^6	mega	M	1,000,000
10^3	kilo	k	1,000
10^2	hecto	h	100
10^1	deca	da	10
1			1
10^{-1}	deci	d	0.1
10^{-2}	centi	c	0.01
10^{-3}	milli	m	0.001
10^{-6}	micro	μ	0.000001
10^{-9}	nano	n	0.000000001
10^{-12}	pico	p	0.000000000001
10^{-15}	femto	f	0.00000000000001
10^{-18}	atto	a	0.0000000000000001